

**Multi-Class Liquid Chromatography-High Resolution Mass Spectrometry  
Methods for Monitoring of Mycotoxins and Metabolites in Human Plasma  
for Exposure Studies**

Irina Slobodchikova

A Thesis

In the Department

of

Chemistry and Biochemistry

Presented in Partial Fulfillment of the Requirements

For the Degree of

Doctor of Philosophy (Chemistry) at

Concordia University

Montréal, Québec, Canada

June, 2020

© Irina Slobodchikova, 2020

CONCORDIA UNIVERSITY

SCHOOL OF GRADUATE STUDIES

This is to certify that the thesis prepared

By: Irina Slobodchikova

Entitled: Multi-Class Liquid Chromatography-High Resolution Mass Spectrometry Methods for Monitoring of Mycotoxins and Metabolites in Human Plasma for Exposure Studies

and submitted in partial fulfillment of the requirements for the degree of

DOCTOR OF PHILOSOPHY (Chemistry)

complies with the regulations of the University and meets the accepted standards with respect to originality and quality.

Signed by the final examining committee:

Dr.	Chair	_____
Dr. M. Sumarah	External Examiner	_____
Dr. V. Titorenko	External to Program	_____
Dr. Y. Gélinas	Examiner	_____
Dr. C. Skinner	Examiner	_____
Dr. D. Vuckovic	Thesis Supervisor	_____

Approved by \_\_\_\_\_

Chair of Department or Graduate Program Director

Dr. Y. Gélinas, Graduate Program Director

\_\_\_\_\_

Dr. Pascale Sicotte, Dean, Faculty of Arts and Science

## Abstract

### Multi-Class Liquid Chromatography-High Resolution Mass Spectrometry Methods for Monitoring of Mycotoxins and Metabolites in Human Plasma for Exposure Studies

Irina Slobodchikova, PhD candidate, Concordia University, 2020

Mycotoxins are secondary metabolites produced by fungi that can pose a serious threat to human and animal health due to their toxicity. The assessment of human chronic exposure to mycotoxins requires reliable and highly sensitive multi-analyte assay(s) enabling simultaneous measurements of common toxicologically important mycotoxins and their metabolites in human plasma.

The first goal of the thesis was to develop sensitive liquid chromatography – high-resolution mass spectrometry (LC-HRMS) multi-mycotoxin method(s) for the detection and quantification of common toxicologically important mycotoxins frequently occurring in Canada and emerging mycotoxins of interest. Based on the results of extraction recoveries and chromatographic separation, two LC-HRMS methods were required to cover the full mycotoxin panel of interest. The first method combined liquid-liquid extraction with pentafluorophenyl reversed-phase LC-HRMS for the quantification of 17 mycotoxins, aflatoxins B1, B2, G1 and G2, zearalenone, 7- $\alpha$ -hydroxy-zearalenol ( $\alpha$ -ZOL), 7- $\beta$ -hydroxy-zearalenol, zearalanone, 7- $\alpha$ -hydroxy-zearalanol, 7- $\beta$ -hydroxy-zearalanol, T-2 toxin, HT-2 toxin, deoxynivalenol, nivalenol, 15-acetyldeoxynivalenol, 3-acetyldeoxynivalenol and fusarenon X. The method was validated using procedures described in the Food and Drug Administration (FDA) guidance for Industry Bioanalytical Method Validation. Lower limits of quantification (LLOQs) ranged from 0.1 to 0.5 ng/ml, except for nivalenol (3 ng/ml). The method (intra-day and inter-day) accuracy and precision ranged from 85.6% to 116.4% and from 1.6% to 15.6% RSD, respectively, excluding  $\alpha$ -ZOL for which an accuracy of 72.9 % to 97.2% was observed. The second method covered ten mycotoxins, fumonisin B1, fumonisin B2, ochratoxin  $\alpha$  (OT $\alpha$ ), citrinin, ochratoxin A, beauvericin, enniatin A, enniatin A1 (ENNA1), enniatin B (ENNB) and enniatin B1, and combined methanol protein precipitation with C18 reversed-phase chromatography and polarity-switching LC-HRMS. LLOQs ranged from 1.25 to 4 ng/ml. Absolute recovery ranged from 86.6% to 127.7% in individual plasma samples. Significant matrix effects were observed for OT $\alpha$  (77.5%) in one out of ten individual plasma samples and fumonisins (134.8% to 167.8%), ENNB (69.7% to 79.4%) and ENNA (69.3% to 79.2%) in all individual

plasma samples. The rest of the mycotoxins showed negligible matrix effects ranging from 87.2% to 112.2% in all lots of plasma tested.

Excellent LLOQs, negligible matrix effects and accurate quantitation capability of the first method coupled with the lower cost of analysis per sample make the method suitable for large-scale analysis of human plasma samples. The second method is also simple and low cost but requires additional modification to further improve LLOQs and reduce the matrix effect before full validation and implementation. Both methods are versatile and can be applied for retrospective analysis and other applications such as metabolism studies due to the use of HRMS and superior chromatographic separation. To show this capability, the first method was successfully applied for the in-depth metabolism studies of 17 mycotoxins. The method showed excellent suitability and advantages for the detection of various mycotoxin metabolites from Phase I metabolism and glucuronidation obtained from human microsomal incubations. Two ppm mass accuracy with internal mass calibration reduced the number of possible elemental formulas for a measured  $m/z$  value. Data-dependent acquisition in combination with collision-induced dissociation or higher energy collisional dissociation was used to ensure adequate fragmentation and to study the structure of the mycotoxin metabolites. The Compound Discoverer 2.1 software, which contains extensive libraries of common metabolic pathways and mass spectral libraries, was used to streamline the identification and the characterization of the metabolites. In total, 188 mycotoxin metabolites were generated, characterized and used to build an extensive in-house library of human mycotoxin metabolites. One hundred metabolites were reported for the first time, showing the power and sensitivity of the approach. For these 17 mycotoxins, 92 metabolites were previously described in literature, and among these known metabolites only four could not be generated using our approach. Currently, this is the most comprehensive LC-MS library of human mycotoxin metabolites.

In conclusion, both LC-MS methods and the in-house mycotoxin metabolite library will allow the monitoring of 27 mycotoxins and their 188 metabolites in large-scale biomonitoring studies. In the long-term, this will help to prioritize metabolites that should be routinely included during exposure monitoring studies and will provide important new data on mycotoxin exposure of the Canadian population.

## Acknowledgement

I feel honored to be part of Concordia University and I would like to thank the staff of the Department of Chemistry and Biochemistry of Concordia University for giving me this opportunity.

A special note of thanks to my supervisor, Dr. Dajana Vuckovic for useful comments and criticism, for her professional guidance and assistance in the learning process.

I am grateful to graduate committee members consisting of Dr. Cameron Skinner and Dr. Yves Gélinas that pushed the boundaries of the scientific knowledges and helped me grow into more confident scientist.

I would like to express my sincere gratitude to Alain Tessier and Dr. Heng Jiang who are always close and ready to assist all students.

As well, I would like to thank all my current and previous lab mates, Dr. Shama Naz, Dmitri Sitnikov, Cian Monnin, Marianna Russo, Alexander Napylov, Ankita Gupta, Rosalynde Sonnenberg, Oluwatosin Kuteyi, Lise Cougnaud, Hamed Tahmasbi and Melika Mirabi.

Nobody has been more important to me in the pursuit of these studies than my family. I would like to thank my husband, Aleksey, for his support and patience and my children, Lada and Alex who always make me happy and inspire me so much.

## Contribution of Authors

### Chapter 2

Chapter 2 was published in an article entitled “Liquid chromatography - high resolution mass spectrometry method for monitoring of 17 mycotoxins in human plasma for exposure studies”, authored by I. Slobodchikova and D. Vuckovic and published in *Journal of Chromatography A*, 2018, 1548, 51-63.

I.S. performed all plasma sample preparation, LC-MS experiments, full method validation and analysis of the obtained data. I.S. and D.V. developed LC-MS and sample preparation methods. D.V supervised all work and conceptualized the study. I.S. and D.V. interpreted results and co-wrote the first draft of the manuscript prior to the manuscript submission.

### Chapter 3

Chapter 3 was published in an article entitled “Characterization of Phase I and glucuronide Phase II metabolites of 17 mycotoxins using liquid chromatography—high-resolution mass spectrometry” authored by I. Slobodchikova, R. Sivakumar, S. Rahman and D. Vuckovic, in *Toxins* 2019, 11(8), 433.

R. Sivakumar and S. Rahman performed microsomal incubation for *in vitro* metabolism study of HT-2 and aflatoxin B1 mycotoxin, respectively, and partial characterization of their metabolites. I.S. performed all other experimental work, structural interpretation and wrote the first of draft of the manuscript. D.V. designed the study, supervised all work and edited the manuscript.

### Chapter 4

Chapter 4 is the first draft of manuscript in preparation entitled “Development and validation of polarity-switching liquid chromatography high-resolution mass spectrometry method for ochratoxin, fumonisins and enniatins in human plasma”.

I.S. performed all method development of plasma sample preparation and LC-MS and analysis and interpretation of the obtained data. I.S wrote this first draft of this manuscript. D.V supervised all work and conceptualized the study.

# Table of Contents

List of Figures .....	xi
List of Figures Appendix A .....	xiii
List of Figures Appendix B.....	xv
List of Figures Appendix C.....	xvii
List of Tables .....	xx
List of Tables Appendix A.....	xxii
List of Tables Appendix B.....	xxiii
List of Tables Appendix C.....	xxiv
Abbreviations.....	xxv
1. Introduction .....	1
1.1 Occurrence of mycotoxins in food .....	1
1.2 Toxicity of mycotoxins .....	2
1.3 Current regulations and consumer safety .....	6
1.4 Co-exposure to mycotoxins.....	10
1.5 Assessment of dietary and long-term exposure to mycotoxins using biofluid monitoring .....	11
1.6 Current methods for mycotoxin determination in biological samples .....	14
1.6.1 Methods for the analysis of mycotoxins in urine samples .....	17
1.6.2 Methods for the analysis of mycotoxins in human blood-derived samples .....	22
1.6.3 Methods for analysis of mycotoxins in animal blood-derived samples .....	28
1.7 Mycotoxin metabolism.....	30
1.8 Objectives.....	36
2. Liquid chromatography – high-resolution mass spectrometry method for monitoring of 17 mycotoxins in human plasma for exposure studies .....	39

2.1 Introduction .....	39
2.2 Materials and methods .....	42
2.2.1 Chemicals .....	42
2.2.2 Mycotoxin standards .....	42
2.2.3 Method development of sample preparation: comparison of LLE, SPE and protein precipitation methods .....	43
2.2.4 Final optimized three-step LLE procedure with ethyl acetate used for method validation .....	46
2.2.5 LC–MS analysis .....	46
2.2.6 Method validation.....	48
2.3 Results and discussion.....	50
2.3.1 Development of a sensitive LC–MS method.....	50
2.3.2 Development of sample preparation method for multi-mycotoxin analysis .....	53
2.3.3 Results of method validation .....	57
2.4 Conclusions .....	64
3. Characterization of Phase I and glucuronide Phase II metabolites of 17 mycotoxins using liquid chromatography – high-resolution mass spectrometry.....	66
3.1 Introduction .....	66
3.2 Materials and methods .....	69
3.2.1 Chemicals .....	69
3.2.2 Mycotoxin standards .....	69
3.2.3 Experimental design and microsomal incubations .....	69
3.2.4 LC-HRMS analysis .....	70
3.3 Results .....	71
3.3.1 Trichothecene type A and B .....	72



3.3.2 Aflatoxins .....	79
3.3.3 Group of zearalenone .....	82
3.4 Conclusions .....	86
4. Development and validation of polarity-switching liquid chromatography high-resolution mass spectrometry method for ochratoxins, fumonisins and enniatins in human plasma .....	93
4.1 Introduction .....	93
4.2 Materials and methods .....	96
4.2.1 Chemicals .....	96
4.2.2 Mycotoxin standards .....	96
4.2.3 Sample preparation method development .....	97
4.2.4 Final protein precipitation with subsequent acidification used for the method validation .....	99
4.2.5 Evaluation of recovery and matrix effects using final protein precipitation with subsequent acidification .....	100
4.2.6 LC-HRMS analysis .....	100
4.3 Results and discussion.....	105
4.3.1 Development of a sensitive LC-HRMS method.....	105
4.3.2 Evaluation of method accuracy and precision.....	118
4.3.3 Evaluation of recovery and matrix effects of finalized method using 10 individual lots of plasma.....	127
4.3.4 Comparison of current method to literature methods.....	129
4.4 Conclusion and future work for LC-HRMS method for 10 mycotoxins .....	131
5. Conclusions and future work.....	133
5.1 Conclusions .....	133
5.2 Future work .....	135

References.....	141
Appendix A.....	178
Appendix B.....	197
Appendix C.....	262

## List of Figures

Figure 1.1. Mycotoxin structures including (a) zearalenone group and aflatoxins, (b) type A and B trichothecenes, (c) ochratoxins and fumonisins, (d) enniatins and BEA	4
Figure 1.2. Overview of different techniques used for determination of mycotoxins and their metabolites in various human biological samples	14
Figure 1.3. Pie chart shows sample types most used for biomonitoring of mycotoxins and their metabolites	16
Figure 1.4. Overview of different techniques used for detection of mycotoxins and their metabolites in human urine samples	17
Figure 1.5. Pie chart shows the percent distribution of techniques and sample type used for the determination of mycotoxins and their metabolites	21
Figure 1.6. Phase I and Phase II biotransformations	32
Figure 2.1. Comparison of (a) process efficiency (PE%) and (b) absolute matrix effects evaluated for mycotoxins in human plasma samples	55
Figure 2.2. Inter-day accuracy and precision for mycotoxins detected in ESI(+) (a) and ESI(-) (b)	60
Figure 2.3. Investigation of absolute ionization matrix effect in 10 individual plasma samples using ESI(+) (a) and ESI(-) (b)	62
Figure 3.1. Scheme of microsomal incubation experiment to generate Phase I and glucuronide Phase II metabolites	72
Figure 3.2. Comparison of the amount of parent toxins remaining after incubation in Phase I and heated Phase I (a) and Phase II and heated Phase II (b) microsomal incubation samples	74
Figure 3.3. Microsomal biotransformation of T-2 in Phase I and Phase II reactions	75
Figure 3.4. Microsomal biotransformation of DON in Phase I and II reactions	78
Figure 3.5. Microsomal biotransformations of AFB1 in Phase I reactions	81
Figure 3.6. Microsomal biotransformation of ZEN in Phase I and II reactions	83

Figure 3.7. Summary of Phase I and Phase II metabolism of ZEN group	85
Figure 4.1. The scheme of experiment #1 (a) and experiment #2 (b) for the evaluation of the mycotoxin solubility and adsorption	102
Figure 4.2. Chromatographic separation of all mycotoxins obtained using optimized Cortecs T3 C <sub>18</sub> LC method and methanol/water/isopropanol/0.02% AA mobile phase	107
Figure 4.3. Evaluation of signal intensities of mycotoxins using different mobile phase additives	109
Figure 4.4. Evaluation of non-specific adsorption using plastic and glass inserts and different injection solvent compositions, 40% and 60% methanol	113
Figure 4.5. Evaluation of non-specific adsorption using plastic and glass inserts and different injection solvent compositions, 40% and 60% methanol	114
Figure 4.6. Evaluation of PEs% using different precipitation and reconstitution solvents, methanol and acetonitrile	116
Figure 4.7. Evaluation of absolute extraction recoveries using different sample preparation methods	117
Figure 4.8. Evaluation of matrix effects using protein precipitation with methanol	118
Figure 4.9. Summary of intra-day accuracy and precision results obtained in the first experiment	120
Figure 4.10. Summary of intra-day accuracy and precision results obtained in the second experiment	121
Figure 4.11. Summary of intra-day accuracy and precision results obtained in the third experiment	123
Figure 4.12. Evaluation of absolute ionization matrix effects (a) and absolute recoveries (b)	128
Figure 5.1. The workflow for LC-HRMS monitoring of 215 mycotoxins and their metabolites to enable extensive exposure studies	138
Figure 5.2. Current and future research objectives to enable mycotoxin human biomonitoring	139

## List of Figures Appendix A

Supplementary Figure A1. The comparison of the process efficiencies (PE%) for the mycotoxins in human plasma using different sample preparation techniques	181
Supplementary Figure A2. Overview of sample preparation methods tested during method development	182
Supplementary Figure A3. Chromatographic separation of all mycotoxins obtained using optimized PFP LC method using (a) ESI(+) and (b) ESI(-)	183
Supplementary Figure A4. Extracted ion chromatograms of all mycotoxins obtained using optimized PFP LC method using (a) ESI(+) and (b) ESI(-)	184
Supplementary Figure A5. Retention time stability of $\alpha$ -ZOL, ZAN, and ZEN on F5 (a) and PFP (b) columns over long analytical run	185
Supplementary Figure A6. Effect of different additives, formic (0.1% v/v) and acetic acid (0.1% v/v) in mobile phase, on signal intensity of mycotoxins in ESI(+) and ESI(-)	186
Supplementary Figure A7. Effect of acetic acid concentration on signal intensity of 100 ng/mL mycotoxin standard (n=3) in ESI(-) mode	187
Supplementary Figure A8. Effect of sample pH (a) and solvent selection (b) on the process efficiency of mycotoxins using LLE	188
Supplementary Figure A9. Effect of multi-step extraction with ethyl acetate on the process efficiency of mycotoxins	189
Supplementary Figure A10. Effect of salting out and acidification on the process efficiency of mycotoxins using multi-step LLE with ethyl acetate	190
Supplementary Figure A11. Investigation of absolute mycotoxin recovery in plasma samples using ESI(+) (a) and ESI(-) (b)	191
Supplementary Figure A12. Intra-day accuracy and precision for mycotoxins detected in ESI(+) (a) and ESI(-) (b)	192
Supplementary Figure A13. Effect of using two internal standards	193
Supplementary Figure A14. Evaluation of mycotoxin stability in ESI(+) (a) and in ESI(-) (b)	194

Supplementary Figure A15. Evaluation of mycotoxin stability in autosampler in ESI(+) (a) and ESI(-) (b) 196

## List of Figures Appendix B

Supplementary Figure B1. Chromatographic separation of T-2 and its metabolites	235
Supplementary Figure B2. Extracted ion chromatograms of T-2 hydroxyl metabolites	236
Supplementary Figure B3. Product ion spectra of T-2 hydroxy metabolites	237
Supplementary Figure B4. Product ion mass spectra of the T-2 hydrolyzed metabolites	238
Supplementary Figure B5. Chromatographic separation of T-2 and HT-2 glucuronides	239
Supplementary Figure B6. Product ion spectra of T-2 and HT-2 glucuronides	240
Supplementary Figure B7. Chromatographic separation of HT-2 and its metabolites	241
Supplementary Figure B8. Extracted ion chromatogram of HT-2 hydroxyl-metabolites	242
Supplementary Figure B9. Product ion mass spectra of HT-2 hydroxy metabolites	243
Supplementary Figure B10. Chromatographic separation of 3-AcDON and its metabolites	244
Supplementary Figure B11. Product ion mass spectra of 3-AcDON and its glucuronide	245
Supplementary Figure B12. Chromatographic separation of 15-AcDON and its metabolites	246
Supplementary Figure B13. Product mass spectra of 15-AcDON and its glucuronide	247
Supplementary Figure B14. Chromatographic separation of DON and its metabolites	248
Supplementary Figure B15. Product mass spectra of DON and NIV	249
Supplementary Figure B16. Product ion mass spectra of DON Phase I metabolites	250
Supplementary Figure B17. Product mass spectra of DON glucuronides	251
Supplementary Figure B18. Extracted ion chromatogram of FUS-X and its metabolites	252
Supplementary Figure B19. Product ion mass spectra of FUS-X and its glucuronide	253
Supplementary Figure B20. Extracted ion chromatogram of NIV and its metabolites	254
Supplementary Figure B21. Product ion mass spectra of NIV metabolites	255
Supplementary Figure B22. Chromatographic separation of AFB1 metabolites	256
Supplementary Figure B23. Product mass spectra of AFB1 and its metabolites	257

Supplementary Figure B24. Product mass spectra of AFB1 O-demethylated metabolites	258
Supplementary Figure B25. Product mass spectra of AFG1 and its hydroxyl metabolite	259
Supplementary Figure B26. Product mass spectra of AFB2 and its hydroxyl metabolites	260
Supplementary Figure B27. Product mass spectra of AFG2	261



## List of Figures Appendix C

Supplementary Figure C1. Chromatographic separation of all mycotoxins	268
Supplementary Figure C2. Total ion chromatograms of the blank samples	269
Supplementary Figure C3. Ionization patterns of emerging mycotoxins	270
Supplementary Figure C4. Comparison of four calibration curves of OT $\alpha$ (a) and CIT (b)	271
Supplementary Figure C5. Comparison of four calibration curves of FB1 (a) and OTA (b)	272
Supplementary Figure C6. Comparison of four calibration curves of FB2 (a) and ENNB (b)	273
Supplementary Figure C7. Comparison of four calibration curves of ENNB1 (a) and BEA (b)	274
Supplementary Figure C8. Comparison of four calibration curves of ENNA1 (a) and ENNA (b)	275
Supplementary Figure C9. Evaluation of OT $\alpha$ , CIT and OTA signal intensities at different fragmentor values (from 50 to 250 V)	276
Supplementary Figure C10. Evaluation of FB1, FB2 and FB3 signal intensities at different fragmentor values (from 50 to 250 V)	277
Supplementary Figure C11. Evaluation of ENNB, BEA and ENNB1 signal intensities at different fragmentor values (from 50 to 250 V)	278
Supplementary Figure C12. Evaluation of ENNA1 and ENNA signal intensities at different fragmentor values (from 50 to 250 V)	279
Supplementary Figure C13. Evaluation of signal intensities of mycotoxins at different calibration instrument mass ranges (50-1700 and 50-750 m/z)	280
Supplementary Figure C14. Comparison of two calibration curves of (a) CIT and (b) OT $\alpha$ in plasma using extended dynamic range mode (2 GHz) vs. high resolution mode (4 GHz)	281
Supplementary Figure C15. Comparison of two calibration curves of (a) FB1 and (b) OTA in plasma using extended dynamic range mode (2 GHz) vs. high resolution mode (4 GHz)	282
Supplementary Figure C16. Comparison of two calibration curves of (a) FB2 and (b) ENNB1 in plasma using extended dynamic range mode (2 GHz) vs. high resolution mode (4 GHz)	283

Supplementary Figure C17. Comparison of two calibration curves of (a) BEA and (b) ENNB in plasma using extended dynamic range mode (2 GHz) vs. high resolution mode (4 GHz)	284
Supplementary Figure C18. Comparison of two calibration curves of (a) ENNA and (b) ENNA1 in plasma using extended dynamic range mode (2 GHz) vs. high resolution mode (4 GHz)	285
Supplementary Figure C19. Evaluation of signal intensities of mycotoxins using different acquisition rate time, 3 and 2 spectra per second	286
Supplementary Figure C20. Evaluation of signal stability during the analytical run	287
Supplementary Figure C21. Comparison of peak shapes of OT $\alpha$ and CIT in different solvents, 40%, 60% and 80% methanol	288
Supplementary Figure C22. Evaluation of signal stability during the analytical run	289
Supplementary Figure C23. Evaluation of signal stability during the analytical run	290
Supplementary Figure C24. Internal standard areas of FB3 and OTAd <sub>5</sub> over long analytical run	291
Supplementary Figure C25. TICs of validation samples	292
Supplementary Figure C26. Extracted ion chromatogram of OT $\alpha$ and S/N determination	293
Supplementary Figure C27. Extracted ion chromatogram of OTA and S/N determination	294
Supplementary Figure C28. Extracted ion chromatogram of FB2 and S/N determination	295
Supplementary Figure C29. Extracted ion chromatogram of ENNA and S/N determination	296
Supplementary Figure C30. Ionization patterns of emerging mycotoxins are shown for (a) experiment 1, (b) experiment 2 and (c) experiment 3	297
Supplementary Figure C31. Ionization patterns of emerging mycotoxins are shown for 10 individual lots of plasma	298
Supplementary Figure C32. Signal intensities (expressed as peak area) of the protonated ions of emerging mycotoxins are shown for 10 individual lots of plasma	299
Supplementary Figure C33. Signal intensities (expressed as peak area) of the ammonium ions of emerging mycotoxins are shown for 10 individual lots of plasma	300

Supplementary Figure C34. Signal intensities (expressed as peak area) of the sodium ions of emerging mycotoxins are shown for 10 individual lots of plasma 301

Supplementary Figure C35. Sum of signal intensities (expressed as peak area) of the protonated, ammonium ions and sodium ions of emerging mycotoxins 302

## List of Tables

Table 1.1. Established tolerable daily intake levels of some mycotoxins	6
Table 1.2. Legislated maximum tolerated levels and recommended tolerance levels of mycotoxins in some human foods	7
Table 1.3. Legislated maximum tolerated levels and recommended tolerance levels of mycotoxins in some feedstuffs	8
Table 1.4. Chemical properties of mycotoxins	18
Table 1.5. Summary of all LC-MS methods for the measurement of mycotoxins in human blood-derived products	23
Table 1.6. Binding constants (K) of mycotoxins to human serum albumin, expressed as logK	26
Table 1.7. Summary of LLOQ methods for analysis of mycotoxins in animal blood-derived samples	29
Table 2.1. LOD and LLOQs of all mycotoxins and inter- and intra-day accuracy and precision obtained at LLOQ level	58
Table 3.1. Summary of Phase I oxidation metabolites observed for ZEN group	84
Table 3.2. Number of glucuronides observed in ZEN group	84
Table 3.3. Summary of metabolic pathways of 17 mycotoxins	86
Table 3.4. Comparison of expected metabolites known in literature and metabolites generated in this assay	87
Table 4.1. MS settings, time segments, ionization mode and fragmentor voltage	104
Table 4.2. Validation sample concentrations prepared to evaluate method accuracy and precision in the first intra-day experiment	119
Table 4.3. Validation sample concentrations prepared to evaluate method accuracy and precision in the second experiment	121
Table 4.4. Validation sample concentrations prepared to evaluate method accuracy and precision in the third experiment	122

Table 4.5. Summary of LLOQ values obtained for three intra-day accuracy and precision experiments	124
Table 4.6. Summary of matrix-matched calibration curves for all mycotoxins across three experiments	124
Table 4.7. Internal standard mean peak area and %RSD across all three experiments	124
Table 4.8. Summary of matrix-matched calibration curves for all mycotoxins across three experiments normalized to internal standards	125
Table 4.9. Quality control (QC) standard sample %RSD across three experiments	125
Table 4.10. Comparison of our method and class-specific and multi-class method LLOQs	130
Table 4.11. Mean measured concentrations of FB1, CIT, OTA, OT $\alpha$ , ENNB in human blood-derived samples	131
Table 5.1. Comparison of LLOQs obtained in our method presented in Chapter 2 and published methods	136

## List of Tables Appendix A

Supplementary Table A1. Monoisotopic masses of the most intense ions and retention times of all mycotoxins and internal standards	179
Supplementary Table A2. Inter-day accuracy and precision for mycotoxins detected in ESI(+) and ESI(-)	180

## List of Tables Appendix B

Supplementary Table B1. Microsomal incubation protocol for Phase I and II reactions	198
Supplementary Table B2. T-2 and its metabolites generated in Phase I and Phase II	199
Supplementary Table B3. HT-2 and its metabolites, detected in ESI(+), as [M+Na] <sup>+</sup> ions	201
Supplementary Table B4. Metabolites of 3-AcDON generated in Phase I and Phase II	204
Supplementary Table B5. Metabolites of 15-AcDON generated in Phase I and Phase II	205
Supplementary Table B6. Metabolites of DON generated in Phase I and Phase II	206
Supplementary Table B7. Metabolites of FUS-X generated in Phase I and Phase II	208
Supplementary Table B8. Metabolites of NIV generated in Phase I and Phase II	209
Supplementary Table B9. AFB1 and its metabolites of Phase I reactions	210
Supplementary Table B10. AFB2 and its metabolites of Phase I reactions	212
Supplementary Table B11. AFG1 and its metabolite (OH-AFG1)	213
Supplementary Table B12. AFG2 and its metabolites of Phase I reactions	214
Supplementary Table B13. Metabolites of ZEN generated in Phase I and Phase II	215
Supplementary Table B14. Metabolites of $\alpha$ -ZOL generated in Phase I and Phase II	218
Supplementary Table B15. Metabolites of $\beta$ -ZOL generated in Phase I and Phase II	222
Supplementary Table B16. Metabolites of ZAN generated in Phase I and Phase II	224
Supplementary Table B17. Metabolites of $\alpha$ -ZAL generated in Phase I and Phase II	229
Supplementary Table B18. Metabolites of $\beta$ -ZAL generated in Phase I and Phase II	232

## List of Tables Appendix C

Supplementary Table C1. Monoisotopic masses of the most intense ions and retention times of all mycotoxins and internal standards	263
Supplementary Table C2. Comparison of S/N ratio and the number of points per peak at two MS settings, 2 scans/s and 3 scans/s	264
Supplementary Table C3. Concentrations of matrix-matched calibration curves prepared for the first intra-day accuracy and precision experiment	265
Supplementary Table C4. Concentrations of matrix-matched calibration curves for all mycotoxins prepared for the second intra-day accuracy and precision experiment	266
Supplementary Table C5. Evaluation of RSD% using validation samples for the experiment 3, low concentration, 4 ng/ml.	267



## Abbreviations

Acetic acid	AA
15-AcDON-glucuronide	Gluc-15-AcDON
15-acetyldeoxynivalenol	15-AcDON
15-deacetyl-T-2	15-de-Ac-T-2
3-AcDON-glucuronide	Gluc-3-AcDON
3-acetyldeoxynivalenol	3-AcDON
3-glucuronide-HT-2	3-Gluc-HT-2
3-glucuronide-T-2	3-Gluc-T-2
4-deacetyl-neosolaniol	4-de-Ac-NEO
4-OH-ochratoxin A	4-OH-OTA
7- $\alpha$ -hydroxy-zearalanol	$\alpha$ -ZAL
7- $\alpha$ -hydroxy-zearalenol	$\alpha$ -ZOL
7- $\beta$ -hydroxy-zearalanol	$\beta$ -ZAL
7- $\beta$ -hydroxy-zearalenol	$\beta$ -ZOL
AFB1 8,9 endo/exo-epoxide	AFBO
Aflatoxicol	AFL
Aflatoxin B1	AFB1
Aflatoxin B1 di-hydrodiol	AFB1-diol
aflatoxin B1 N7-guanine	AFB1-N7-guanine
Aflatoxin B2	AFB2
Aflatoxin G1	AFG1
Aflatoxin G2	AFG2
Aflatoxin G2A	AFG2A
Aflatoxin GM1	AFGM1
Aflatoxin GM2	AFGM2
Aflatoxin M1	AFM1
Aflatoxin M2	AFM2
Aflatoxin P1	AFP1
Aflatoxin P2	AFP2
Aflatoxin Q1	AFQ1
Aflatoxin Q2	AFQ2
Beauvericin	BEA
Canadian Food Inspection Agency	CFIA
Collision-induced dissociation	CID
Data-dependent acquisition	DDA
De-epoxy-deoxynivalenol	DOM-1
De-epoxy-nivalenol	DNIV

Deoxynivalenol	DON
Dilute-and-shoot	DAS
Dilute-evaporate-and-shoot	DES
Dispersive liquid–liquid microextraction	DLLME
DON-15-glucuronide	15-Gluc-DON
DON-3-glucuronide	3-Gluc-DON
Dried blood spot	DBS
Dried serum spot	DSS
Energy collisional dissociation	CID
Enniatin A	ENNA
Enniatin A1	ENNA1
Enniatin B	ENNB
Enniatin B2	ENNB1
Enzyme-linked immunosorbent assay	ELISA
Extracted-ion chromatogram	EIC
Flavin-containing monooxygenases	FMO
Food and Drug Administration	FDA
Formic acid	FA
Fumonisin B1	FB1
Fumonisin B2	FB2
Fumonisin B3	FB3
Fusarenon X	FUS-X
FUS-X-glucuronide	Gluc-FUS-X
Gas chromatography–mass spectrometry	GC-MS
Gluc-3-4-de-acetyl-neosolaniol	Gluc-3-4-de-Ac-NEO
Higher-energy collisional dissociation	HCD
High-performance liquid chromatography	HPLC
High-performance liquid chromatography coupled with fluorescence detection	HPLC–FD
High-resolution mass spectrometry	HRMS
HT-2 toxin	HT-2
Hybrid triple quadrupole linear ion trap mass spectrometer	QTrap
Hydrolysed fumonisin B1	HFB1
Hydrophilic-Lipophilic Balanced sorbent	Oasis HLB
Immuno-affinity columns	IAC
Lethal dose	LD <sub>50</sub>
Limit of detection	LOD
Liquid chromatography – mass spectrometry	LC-MS
Liquid-liquid extraction	LLE

Lower limit of quantification	LLOQ
Lowest-observed-adverse-effect level	LOAEL
Methyl tert-butyl ether	MTBE
Moniliformin	MON
Multiple-reaction monitoring mode	MRM
Negative electrospray ionization	ESI(-)
Neosolaniol	NEO
Nicotinamide adenine dinucleotide phosphate	NADPH
Nivalenol	NIV
NIV-glucuronide	Gluc-NIV
No-observed-adverse-effect level	NOAEL
Ochratoxin A	OTA
Ochratoxin A-d <sub>5</sub>	OTAd <sub>5</sub>
Ochratoxin $\alpha$	OT $\alpha$
Pentafluorophenyl column	PFP
Phosphate-buffered saline	PBS
Positive electrospray ionization	ESI(+)
Process efficiency, %	PE%
Quadrupole-time-of-flight mass spectrometer	QTOF
Quality control	QC
Quick, easy, cheap, effective, rugged, and safe	miniQuEChERS
Relative standard deviation	RSD%
Reversed-phase (liquid chromatography)	RP(LC)
Salting-out liquid-liquid extraction	SALLE
Signal-to-noise ratio	S/N
Solid-phase extraction	SPE
Strong anion-exchange solid-phase extraction	SAX SPE
T-2 toxin	T-2
Thin-layer chromatography	TLC
Tolerable daily intake	TDI
Total ion chromatogram	TIC
Triple quadrupole mass spectrometer	QQQ
Ultra-high performance liquid chromatography	UHPLC
Upper limit of quantification	ULOQ
Uridine 5'-diphospho-glucuronosyltransferases	UGT
Uridine diphosphate glucuronic acid	UDPGA
ZAN-14-glucuronide	14-Gluc-ZAN
ZAN-16-glucuronide	16-Gluc-ZAN
Zearalenone	ZEN
ZEN-14-glucuronide	14-Gluc-ZEN

ZEN-16-glucuronide	16-Gluc-ZEN
$\alpha$ -ZAL-14-glucuronide	14-Gluc- $\alpha$ -ZAL
$\alpha$ -ZAL-16-glucuronide	16-Gluc- $\alpha$ -ZAL
$\alpha$ -ZAL-7-glucuronide	7-Gluc- $\alpha$ -ZAL
$\alpha$ -ZOL-14-glucuronide	14-Gluc- $\alpha$ -ZOL
$\alpha$ -ZOL-16-glucuronide	16-Gluc- $\alpha$ -ZOL
$\alpha$ -ZOL-7-glucuronide	7-Gluc- $\alpha$ -ZOL
$\beta$ -ZAL-14-glucuronide	14-Gluc- $\beta$ -ZAL
$\beta$ -ZAL-16-glucuronide	16-Gluc- $\beta$ -ZAL
$\beta$ -ZAL-7-glucuronide	7-Gluc- $\beta$ -ZAL
$\beta$ -ZOL-14-glucuronide	14-Gluc- $\beta$ -ZOL
$\beta$ -ZOL-16-glucuronide	16-Gluc- $\beta$ -ZOL
$\beta$ -ZOL-7-glucuronide	7-Gluc- $\beta$ -ZOL

# 1. Introduction

## 1.1 Occurrence of mycotoxins in food

Mycotoxins are toxic secondary metabolites produced by filamentous fungi, such as *Fusarium*, *Aspergillus*, and *Penicillium* genera.<sup>1-3</sup> Studying mycotoxin contamination is of utmost importance today because they can have deleterious effects on animal and human health and have significant economic impact. According to the most recent estimations, detectable concentrations of mycotoxins have been measured in 60-80% of food crops across the world.<sup>4</sup> Human exposure to mycotoxins occurs via contaminated food intake, inhalation, and/or dermal contact. Usually, contaminated food is the primary source of human exposure to mycotoxins. The foods most commonly contaminated with mycotoxins include cereals, wine, coffee, dried fruits, meat, nuts, and dairy products.<sup>2,5,6</sup> Currently, about 300 mycotoxins are known, but only some of them are considered to be important for routine monitoring because of their toxicity and probability to find in foods.<sup>2</sup> Overall, toxicologically important mycotoxins can be divided in five classes: type A (T-2 toxin (T-2) and HT-2 toxin (HT-2)) and type B (nivalenol (NIV), deoxynivalenol (DON), fusarenon X (FUS-X), 15-acetyldeoxynivalenol (15-AcDON), 3-acetyldeoxynivalenol (3-AcDON)) trichothecenes (types A and B are differentiated based on the substitution at the C-8 position, isovaleric acid and carbonyl group, respectively) fumonisins (fumonisin B1 (FB1), fumonisin B2 (FB2), aflatoxins (aflatoxin B1 (AFB1), aflatoxin B2 (AFB2), aflatoxin G1 (AFG1), aflatoxin G2 (AFG2)), zearalenone group (zearalenone (ZEN), 7- $\alpha$ -hydroxy-zearalenol ( $\alpha$ -ZOL), 7- $\beta$ -hydroxy-zearalenol ( $\beta$ -ZOL), zearalanone (ZAN), 7- $\alpha$ -hydroxy-zearalanol ( $\alpha$ -ZAL), 7- $\beta$ -hydroxy-zearalanol ( $\beta$ -ZAL)), and ochratoxins (ochratoxin A (OTA) and citrinin (CIT)).<sup>7</sup>

Worldwide studies on the occurrence of mycotoxins in more than 19,000 cereal and oilseed samples showed that 72% were contaminated with at least one of the following mycotoxins aflatoxins (26%), DON (56%), OTA (25%), fumonisins (54%), and ZEN (37%)<sup>8</sup>. In agreement with these findings, the Canadian Food Inspection Agency (CFIA) Guidance for both feed and food has also prioritized similar mycotoxin groups: trichothecenes, ZEN, fumonisins, OTA, ergot, and aflatoxins for monitoring.<sup>9,10</sup> Although aflatoxins are common mycotoxins in tropical countries they can be found in Canada in the food imported from warmer climates.<sup>9</sup> The most recent extensive surveys of Canadian food supply conducted in 2013-2015 tested 2235 samples

and detected 21 out of 25 mycotoxins.<sup>9</sup> Fifty-nine percent of food samples were contaminated with at least one mycotoxin.<sup>9</sup> They also found that the most prevalent toxin was DON detected in 1044 samples (46.7%).<sup>9</sup> The survey of Canadian breakfast cereals in 2007 also showed similar results, whereby detectable levels of one or more mycotoxins were present in 75% of Canadian cereals, and DON was the most prevalent mycotoxin (>40%).<sup>11</sup> Fumonisin (>30%), OTA (>30%), and ZEN (>20%) were the next most frequently detected mycotoxins.<sup>11</sup> The occurrence of OTA was investigated in various Canadian retail food samples from Quebec City and Calgary (2008-2009).<sup>12</sup> The results showed the presence of OTA in 102 out of 140 samples (73%)<sup>12</sup>, while 100% prevalence was found in cocoa and chocolate products.<sup>13</sup> Similarly, fumonisins were detected in 57% of corn products.<sup>14</sup> Targeted surveys in 2012-2013 and 2015-2016 provided a snapshot of aflatoxin prevalence, 17% and 11% respectively, in foods sampled at Canadian retail stores which can be likely contaminated with these mycotoxins.<sup>15,16</sup>

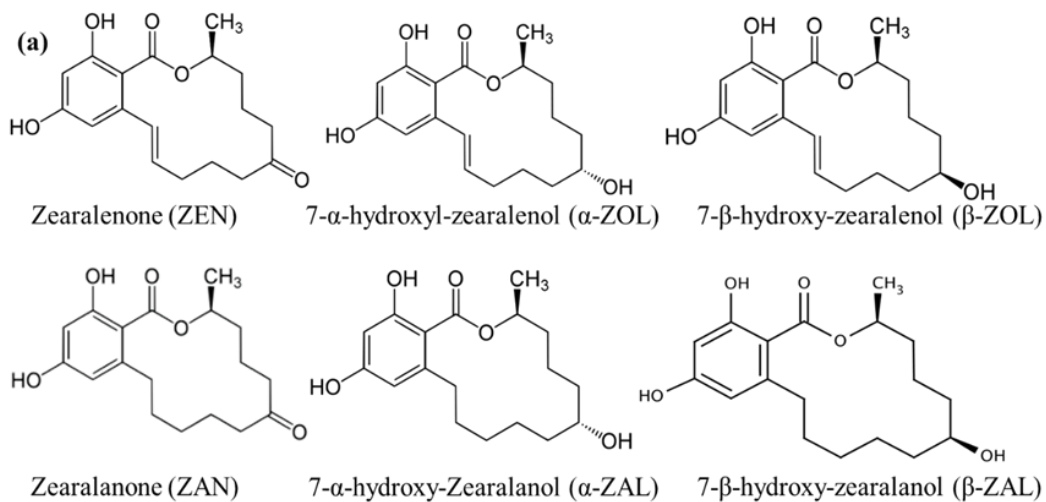
Besides common mycotoxins, there is a group of mycotoxins, enniatins (enniatin A1 (ENNA1), enniatin A (ENNA), enniatin B1 (ENNB1), enniatin B1 (ENNB1) and beauvericin (BEA) that are called “emerging”. They are less studied mycotoxins that caught attention because of their co-occurrence with other mycotoxins and potential risk to human health. These “emerging” mycotoxins are produced by *Fusarium* species and their presence greatly depends on the environmental conditions during the flowering period.<sup>17</sup> In 2010, due to excessive precipitation, the cereals from Western Canada were contaminated with *Fusarium* species<sup>17</sup> and enniatins were observed in all samples, whereas the other mycotoxins, including moniliformin (MON), DON and BEA contaminated 75% of tested samples.<sup>17</sup> Moreover, total concentration of emerging mycotoxins was about 10 times higher than DON.<sup>17</sup>

## 1.2 Toxicity of mycotoxins

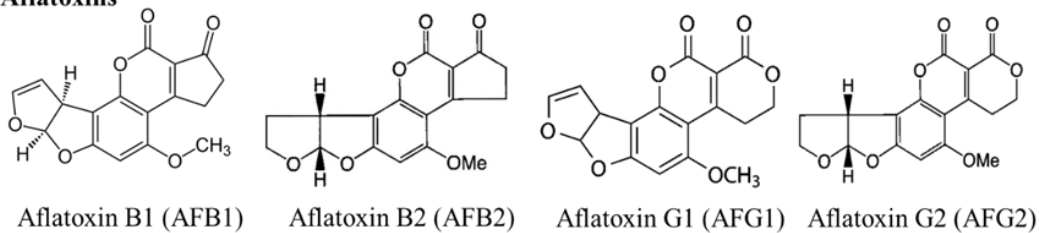
Mycotoxins can cause acute or/and chronic toxicity. Acute toxicity is described as single poisoning occurring to high exposure in a short period of time and chronic toxicity is a result of long-term poisoning with low levels of mycotoxins.<sup>18</sup> Acute poisoning is occasionally observed in developing countries rather than developed countries.<sup>2,18</sup> Acute symptoms are non-specific and described as sore throat, shortness of breath, vomiting and cough, headache and abdominal pain.<sup>19-</sup>

<sup>21</sup> Short-term exposure can cause death, but a complete recovery is also possible.

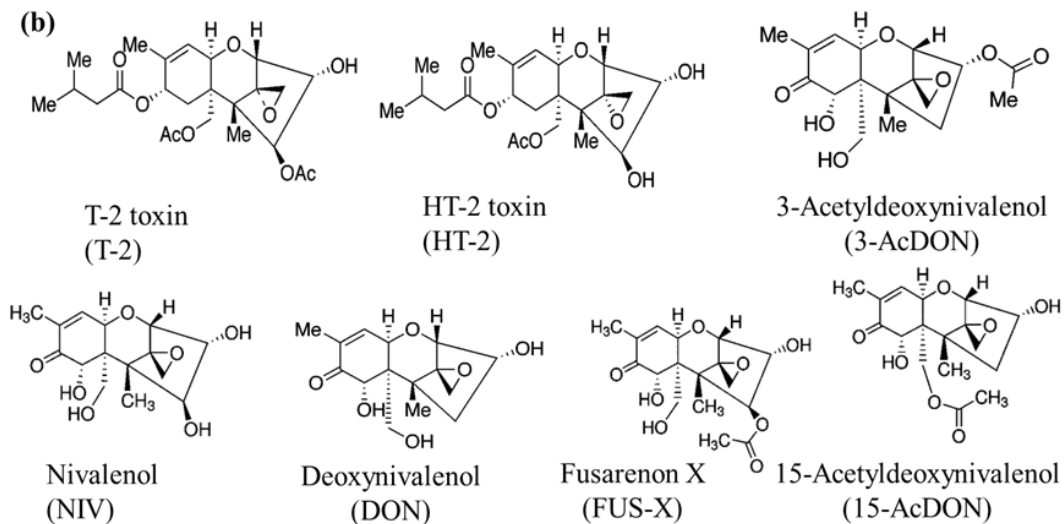
### Zearalenone group



### Aflatoxins



### Type A and B trichothecenes



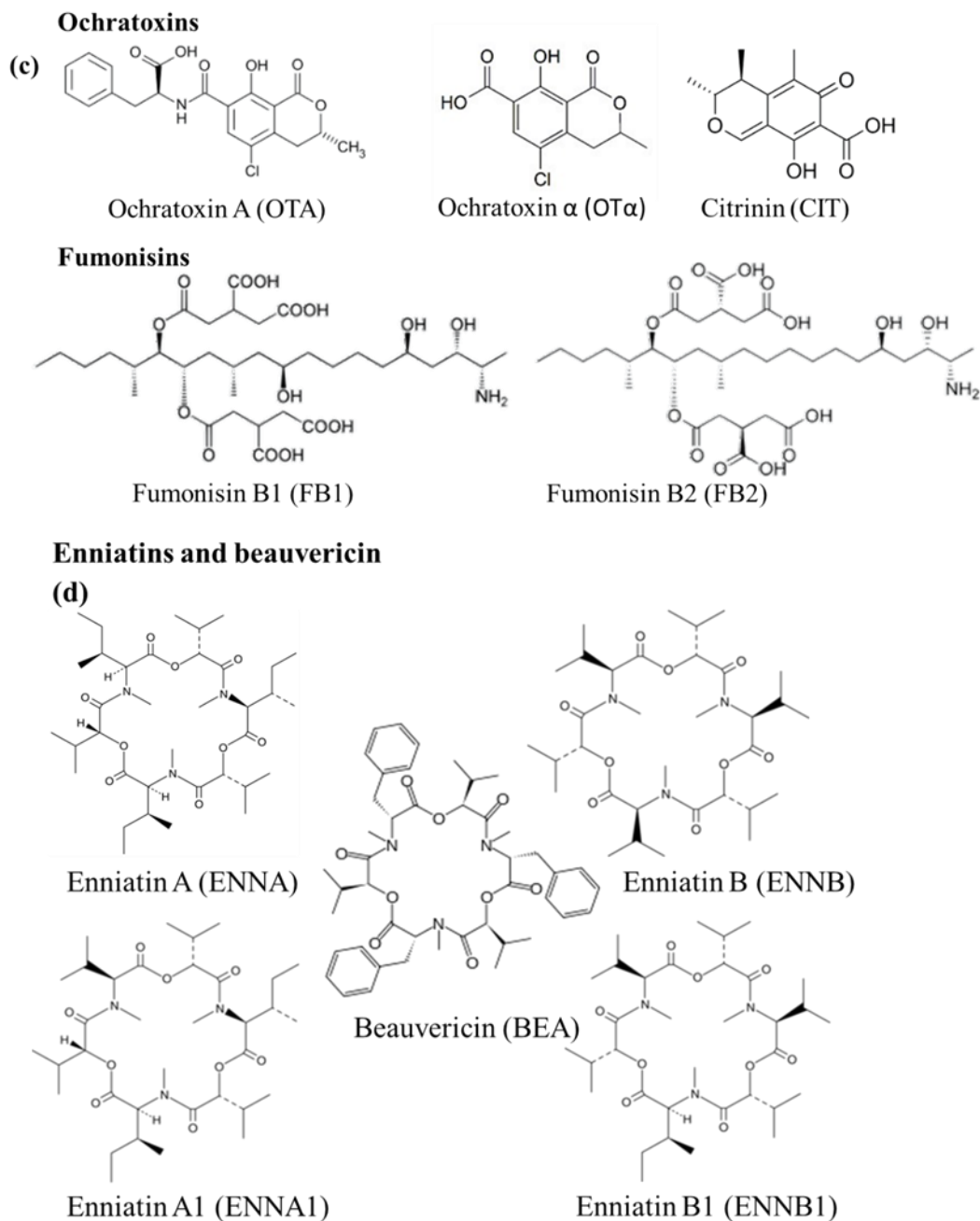


Figure 1.1. Mycotoxin structures including (a) zearalenone group and aflatoxins, (b) type A and B trichothecenes, (c) ochratoxins and fumonisins, (d) enniatins and BEA.

Mortality due to mycotoxin exposure depends on the toxin concentration, and nourishment of an individual.<sup>21</sup> Acute poisoning can be described using a lethal dose (LD<sub>50</sub>) which is the mycotoxin lethal concentration for 50% of a population and is usually expressed in milligrams of chemical



per kilogram of body weight (mg/kg).<sup>22</sup> Mycotoxin LD<sub>50</sub> values vary a lot and are available only for some species, for example OTA and FB1 have LD<sub>50</sub> values of 48 mg/kg and 787 mg/kg in rats, respectively.<sup>23</sup> LD<sub>50</sub> in mice ranged from 7.2-17.9 mg/kg for AFB1<sup>24</sup>, 46 mg/kg for OTA, 43-70 mg/kg for DON, 500-2000 mg/kg for ZEN.<sup>25</sup>

Beyond acute effects, mycotoxins can also contribute to immunosuppression, hepatotoxicity, carcinogenicity and nephrotoxicity, so chronic exposure to mycotoxins is of possible health concern.<sup>18</sup> The international Agency for Research on Cancer classified some naturally occurring mycotoxins, including FB1 and FB2, OTA as possible carcinogens to humans, Group 2B (limited evidence) and aflatoxins as Group 1 (sufficient data, carcinogenic to humans).<sup>26</sup> Aflatoxins are considered to be the most toxic mycotoxin group because of the strong evidence of carcinogenicity, but they are also mutagenic, immunosuppressive and hepatotoxic.<sup>27,28</sup> Nowadays, 4.6–28.2% of all hepatocellular carcinoma was associated with aflatoxin exposure.<sup>27,28</sup> OTA may be mutagenic, genotoxic and teratogenic, although it is primarily known as a nephrotoxin that is possibly involved in the etiology of Balkan endemic nephropathy.<sup>29,30</sup> The main targets of FB1 are the liver and kidneys in humans, although epidemiological studies have also shown that FB1 is highly associated with esophageal cancer and neural tube defects in humans<sup>31,32</sup>. Trichothecenes including DON can cause vomiting, digestive, immune, and reproductive problems.<sup>33</sup> The zearalenone group has low acute toxicity, but it has strong estrogenic activity and can result in a genotoxic effect, oxidative stress and reproductive disorders.<sup>34–36</sup>

In view of this, risk assessment of the human exposure to mycotoxins through the consumption of foods is important to provide adequate protections.<sup>37</sup> A tolerable daily intake (TDI) is usually established by World Health Organization experts, including the Expert Committee on Food Additives and the European Food Safety Authority<sup>37</sup>, for different mycotoxins to control or prevent contamination. TDI is defined as an estimated quantity of toxins that are not expected to cause adverse health effects in humans over a lifetime.<sup>37</sup> The calculation of TDI values is based on the no-observed-adverse-effect level (NOAEL) method. In turn the NOAEL is determined experimentally on the basis of laboratory toxicity, and if it is not available, the lowest-observed-adverse-effect level (LOAEL) is used instead.<sup>37</sup> Finally, TDI is calculated by dividing NOAEL or LOAEL by uncertainty factor(s).<sup>37</sup> The unit of TDI is mg per kg body weight per day, (mg/kg bw/d).<sup>37</sup> Established mycotoxin TDIs are summarized in Table 1.1.

Table 1.1. Established tolerable daily intake levels of some mycotoxins.

Mycotoxin	TDI, µg/kg bw/d	Reference
DON	1.0	38
FB1 or sum of FB1+FB2+FB3	2.0	38
ZEN	0.2	38
OTA	0.017	37
NIV	1.2	39
T-2	0.02	40
HT-2	0.02	40
AFB1	no established level because of the risk	38

### 1.3 Current regulations and consumer safety

About 100 countries have mycotoxin legislation to protect consumer safety.<sup>2</sup> Currently, mycotoxins are regulated by setting limits on the concentrations of specific mycotoxins in human foods and animal feeds. The CFIA has established maximum tolerable levels of aflatoxins, DON, and HT-2 in some foodstuffs and feedstuffs and recommended tolerance levels of T-2, diacetoxyscirpenol, ZEN, OTA and ergot in some feedstuffs, (Tables 1.2-1.3).<sup>10</sup> In addition, Canada regularly performs targeted surveys of whole grains and retail foods in order to minimize any health risks from mycotoxin exposure. For example, a multi-year survey of mycotoxins was conducted in Canadian oat, wheat and durum wheat samples collected in the years 2014-2017, 2010, 2011 and 2013–2016, respectively.<sup>41,42</sup> Foods in Canadian market were also examined for the presence of mycotoxins in various years, for instance breakfast cereals in 2008, corn products, nuts, nut products, raisins, cocoa powder, chili powder, and paprika in the years 2012-2013 and selected spices, oilseeds, rice and rice products<sup>11,15,16</sup>. As a result, routine mycotoxin monitoring programs showed that mycotoxin prevalence could vary and depend on agronomic and climatic factors.<sup>41,43</sup> For example, OTA, DON, ENN B, and ENN B1 contents were higher in shipment samples than in the harvest samples.<sup>41</sup> Canadian climatic conditions also favour more OTA production during storage rather than in the field.<sup>41</sup> Tittlemier *et al.* showed that the concentrations of studied mycotoxins fluctuated among years and provinces and within province in different years.<sup>41</sup> Among selected harvesting years and provinces, DON median concentrations fluctuated the most significantly and ranged from 68 to 1142 µg/kg.<sup>41</sup> Within one province, Québec, the highest prevalence of DON and depsipeptides was observed in 2014.<sup>41</sup>

Table 1.2. Legislated maximum tolerated levels and recommended tolerance levels of mycotoxins in some human foods. The table description is at the bottom.

<b>Mycotoxins</b>	<b>Foods</b>	<b>Legislated maximum tolerated levels, mg/kg</b>
Deoxynivalenol	Uncleaned soft wheat for human consumption	2
Aflatoxins	Nuts and nut products	0.015
<b>Mycotoxins</b>	<b>Foods</b>	<b>Recommended Health Canada maximum limits, mg/kg</b>
Ochratoxin A	Raw cereal grains	0.005
	Directly consumer grains (i.e. rice, oats, pearly barley):	0.003
	Derived cereal products (flour)	0.003
	Derived cereal products (wheat bran)	0.007
	Breakfast cereals	0.003
	Grape juice (and as ingredients in other beverages) and related products	0.002
	Dried vine fruit (currants, raisins, sultanas)	0.010
	Baby foods and processed cereal-based foods for infants and young children	0.0005
	Dietary foods for special medicinal purposes intended for infants	0.0005

This table is reproduced from the site: <https://www.inspection.gc.ca/animal-health/livestock-feeds/regulatory-guidance/rg-8/eng/1347383943203/1347384015909?chap=1>, accessed date 20200115 and <https://www.canada.ca/en/health-canada/services/food-nutrition/public-involvement-partnerships/information-document-proposed-maximum-limits-standards-presence-mycotoxin-ochratoxin-foods.html> accessed date 2020510.

The comparison of wheat samples harvested from 2003 to 2012 that were damaged with *Fusarium* species showed that the greatest contamination occurred in 2010, reaching an occurrence up to 60%.<sup>17</sup> In 2010, the precipitation level greatly exceeded the normal average and promoted *Fusarium* growth.<sup>17</sup>

Unexpectedly, recent biomonitoring studies in urine in several European countries, such as Spain, Italy, Belgium, and Sweden found that TDIs of DON and OTA were exceeded. For example, DON TDI of 1 µg/kg body weight/day was exceeded in Spain (8.1% of samples tested), Italy (40% of samples tested), Belgium (16 to 69% of samples tested), and Sweden (1.3% of samples tested).<sup>44-47</sup> For OTA, 94% samples collected in Italy and 1% samples collected in Belgium exceeded OTA TDI of 0.017 µg/kg body weight/day.<sup>45,46</sup> A logical question then arises: are we protected by measuring mycotoxins only in food samples?

Table 1.3. Legislated maximum tolerated levels and recommended tolerance levels of mycotoxins in some feedstuffs. The table description is at the bottom.

<b>Mycotoxin</b>	<b>Commodities</b>	<b>Legislated maximum tolerated levels, mg/kg</b>
Deoxynivalenol	Diets for cattle & poultry	5
Deoxynivalenol	Diets for swine, young calves, & lactating dairy animals	1
HT-2 toxin	Diets for cattle & poultry	0.1
HT-2 toxin	Diets for dairy animals	0.025
Aflatoxins	Animal feeding stuffs	20
<b>Mycotoxin</b>	<b>Commodities</b>	<b>Recommended tolerance levels, mg/kg</b>
Diacetoxyscirpenol	Swine feed	<2
	Poultry feed	<1
T-2 toxin	Swine and poultry feed	<1
Zearalenone	Gilt diets	<1-3
	Cow diets and Swine and sheep industry	10 (1.5 if other toxins present) 0.25 - 5
Ochratoxin A	Swine diets	0.2
	Swine diets	2
	Poultry diets	2
Ergot	In feed of:	
	Cattle, sheep, horses	2-3
	Swine	4-6
	Chicks	6-9

This table is reproduced from the site: <https://www.inspection.gc.ca/animal-health/livestock-feeds/regulatory-guidance/rg-8/eng/1347383943203/1347384015909?chap=1>, accessed date 20200115.

In general, a preventive/regulatory model that is based on the maximum tolerated mycotoxin levels in foodstuffs and feedstuffs has its drawbacks. The main drawback is that the maximum tolerable mycotoxin levels are calculated using the average daily dietary intake and do not take into account differences in individual uptake, distribution and metabolism.

It is well known that food preferences can differ a lot amongst individuals. For example, some factors such as age, gender, and preference for plant-based vs. animal-based food and geographical locations can determine eating patterns. For instance, comparative studies of the DON exposure in vegetarians and non-vegetarians in United Kingdom showed that only

vegetarians (32%) exceeded the TDI of DON.<sup>48</sup> Food origins will be also important since mycotoxin contamination can vary in different geographical regions. For example, DON worldwide incidence changes amongst different geographical regions and food commodities from 0% to 100%.<sup>49</sup> DON variations of mean concentrations were even observed within one region, Saskatchewan, from 0.017 mg/kg to 1.6 mg/kg in durum samples harvested in 2010.<sup>17</sup> Kuiper-Goodman *et al.* evaluated human exposure to OTA and concluded that people ingest OTA through food consumption on a daily basis.<sup>37</sup> Mean adjusted exposures of 1–4-year-olds vs. other age groups exceeded TDI because of their lower body weight.<sup>37</sup> Moreover, the consumption pattern of 1–4-year-olds relied on wheat-based foods, oats, rice, and raisins.<sup>37</sup> For adults, beer, coffee, and wine were the main contributors of OTA for these groups.<sup>37</sup> Food processing is another factor that can influence mycotoxin intake and can reduce the amount of mycotoxins in food samples or convert them into less toxic species.<sup>50</sup> Sakuma *et al.* evaluated the losses of aflatoxins and OTA during the process of cooking rice and pasta, respectively.<sup>51</sup> Aflatoxin recoveries ranged from 83% to 89% in cooked rice, whereas OTA recovery was 60% in pasta.<sup>51</sup> However, the evaluation of the effect of food processing on the OTA levels in the cocoa beans showed that the heating treatment of cocoa beans destroyed only 16.6% of OTA, whereas the most of the remaining OTA can be removed by winnowing.<sup>52</sup> Cooking may reduce levels of some mycotoxins, but the most toxic members are not fully eliminated during cooking.

Furthermore, surveillance data for mycotoxins in human biological samples, except for OTA is not available for any time period for Canada. The most recent OTA exposure data that is available for Canada was reported in 1998.<sup>53</sup> The comparison of the daily OTA intakes for Canadians ranged from 0.0006 to 0.0047 µg/kg body weight/day and the calculated TDI of 0.0037 µg/kg body weight/day showed that some individuals exceeded the established OTA TDI.<sup>53</sup> Moreover, the mean daily intake of OTA, 0.017 µg/kg body weight/day, is equal to the current OTA TDI, which was estimated by Food Additives and the European Food Safety Authority in 2006, as shown in Table 1.1.<sup>53</sup>

In conclusion, human biomonitoring and feed/food monitoring complement each other and are both needed in order to minimize human mycotoxin exposure. Human biomonitoring also has its limitations. Biomonitoring results only reflect the concentration of a mycotoxin in the body at the time of testing, which may differ from the original exposure. Tested samples can represent exposure from yesterday, last week, or last month. Mycotoxin levels may also vary depending on

their half-life, biofluids used for biomonitoring and inter-individual differences, for example sex.<sup>54</sup> However, human biomonitoring can verify if existing food and feed regulations are sufficiently stringent to protect consumer health by providing evidence of the actual exposure. In addition, human biomonitoring shows levels of total mycotoxin exposure from any exposure route, including contaminated food intake, inhalation and/or dermal contact.<sup>55</sup>

#### **1.4 Co-exposure to mycotoxins**

As long as mycotoxins are prevalent food and feed contaminants the risk to be exposed to multiple mycotoxins at the same time is relatively high, by eating different types of foods contaminated with one or multiple mycotoxins. Another possible route of co-exposure is due to their different half-lives such that mycotoxins from the previous exposure may still be circulating in the body by the time of the next mycotoxin intake.

Co-occurrence of mycotoxins can be frequently observed in food and feed commodities because some mycotoxins can be produced by more than one filamentous fungus species and one filamentous species can produce more than one mycotoxin. Moreover, food commodities can be contaminated with more than one filamentous fungus species at the same time. For example, CIT is produced by *Penicillium*, *Aspergillus* and *Monascus* species.<sup>56,57</sup> *Fusarium* species can produce fumonisins, BEA, enniatins, trichothecenes type A and B and zearalenones. western Canadian durum harvested in 2010 was contaminated with a variety of *Fusarium* species, such as *F. avenaceum*, *F. graminearum*, *F. culmorum*, *F. poae*, *F. acuminatum*, *F. sporotrichioides* and *Phaeosphaeria nodorum*. The analyzed samples contained DON, T-2, HT-2, MON, BEA, and enniatins.<sup>17</sup> In a global survey program of agricultural commodities, co-contamination with two or more mycotoxins was reported in 38% (n > 19,000) of samples.<sup>8</sup> Lee *et al.* reported that co-contamination varied from 41% to 48% from year to year according to Biomin's global mycotoxin occurrence analysis in agricultural commodities.<sup>49</sup> Cereal grain samples collected in 2016-2017 from the regions of Saskatchewan, Alberta, and Manitoba in Western Canada also showed that 70% of barley samples and 54% of wheat samples contained two mycotoxins.<sup>58</sup> However, co-occurrence of up to five mycotoxins was also observed in this study.<sup>58</sup> Mycotoxin co-exposure was also confirmed by analyzing biological samples. Sweden exposure studies revealed that 69% of adults (n=252) had more than two mycotoxins detected in urine samples.<sup>59</sup> Spain urine samples

from children and adults were evaluated for the presence of 15 mycotoxins and co-occurrence was documented in 20% of tested samples (n=54).<sup>44</sup>

Co-exposure to any two toxic compounds can cause antagonistic, additive, or synergistic effects on human and animal health. An antagonistic effect of toxins results in less damage than the sum of their individual toxicity. Additive effect is the sum of individual effects and thus can be accurately predicted. Synergism is the interaction of toxins that results in higher adverse effects than the sum of their individual toxic effects. Synergism cannot be predicted and demands special examination. Studies to date indicate that the combination of OTA and FB1 can cause additive or synergistic effects depending on cell type.<sup>23,60,61</sup> For instance, in human lymphocytes the combined exposure to OTA and FB1 reduced cell viability to 53% versus cell viability of 86 and 97% for the exposure to OTA and FB1 individually, indicating synergistic effects.<sup>61</sup> Logically, one can hypothesize that OTA with moderate toxicity may enhance cell susceptibility to the second mycotoxin, FB1 with weak toxicity, and thus results in more adverse damage of cells. Additional studies of low-dose exposure to multiple mycotoxins are needed to further understand their toxicity and possible health effects. To achieve this goal, first more information is needed including which mycotoxin co-occurrences are most frequently observed in a wider Canadian population.

### **1.5 Assessment of dietary and long-term exposure to mycotoxins using biofluid monitoring**

Human biomonitoring of 53 mycotoxins was recently performed in urine and serum from multiple European countries, such as Belgium, the Czech Republic, France, the Netherlands, and Norway.<sup>62</sup> All individuals (n=600) participated in dietary recall interviews, urine samples were first collected during 24 hours and repeated in one month from 188 participants, while single time-point serum samples were obtained from non-fasting participants (n=268).<sup>62</sup> Ninety-seven percent of serum samples and 99% of urine samples were contaminated at least with one mycotoxin.<sup>62</sup> The percent of contaminated urine and serum samples was similar for aflatoxins (serum 57%; urine 51%), fumonisins (serum 42%; urine 40%), ochratoxins (serum 42%; 48%), and type B trichothecenes (serum 42%; urine 52%).<sup>62</sup> The most frequent serum mycotoxin (70%), patulin, was not detected in urine samples, whereas some mycotoxins, such as ZAN, hydroxyl metabolites of T-2 and ENNB1 were not observed in serum samples<sup>62</sup>. The visualization of urine, serum and dietary mycotoxin occurrence as Kernel density plot to estimate participant exposure to multiple

mycotoxins showed similar distributions for urine and serum, but not for dietary recall data.<sup>62</sup> Biomonitoring data reflected better dietary exposure than dietary questionnaire data based on this study.<sup>62</sup> Urine and serum samples can provide information about individual exposures.<sup>63</sup> Fan *et al.* performed multi-mycotoxin analysis in both plasma and urine to evaluate individual exposure of 260 participants in China.<sup>64</sup> Out of 26 tested mycotoxins only 10 were detected and/or in urine and plasma.<sup>64</sup> OTA, FB1, DON, ZEN, ZAN were plasma and urine mycotoxins, T-2, AFM1, 3-Gluc-DON and 15-Gluc-DON and AFB1-lysine were detected in urine and plasma, respectively.<sup>64</sup> At least one mycotoxin was found in 36.5% of plasma samples and 55.4% of urine samples.<sup>64</sup> The most frequent mycotoxins in plasmas were OTA (27.7%) and AFB1-lysine (19.6%). The incidences of the other mycotoxins ranged from 1.2% to 6.5%.<sup>64</sup> The most prevalent mycotoxins in urine were 15-Gluc-DON (43.8%) followed by 3-Gluc-DON (15.8%), AFM1 (10.4%) and DON (10.0%). The other mycotoxins were found in 1.2%-7.7% samples.<sup>64</sup> FB1 and DON and T-2, 15-Gluc-DON, 3-Gluc-DON and ZEN concentrations were higher in male plasma and urine samples, respectively.<sup>64</sup> Swedish adolescent (1105) exposure to mycotoxins was evaluated in urine and plasma samples.<sup>65</sup> They found 2'R-ochratoxin A serum concentration dependence on gender and ages.<sup>65</sup> In urine, the differences between the concentrations of DON and its glucuronic metabolites were associated with the ages of students.<sup>65</sup> Muñoz *et al.* also analyzed simultaneously human urine and plasma of 13 volunteers to estimate OTA dietary exposure.<sup>66</sup> Their methods were developed and validated only for OTA and its metabolite, OT $\alpha$ .<sup>66</sup> OT $\alpha$  was the OTA predominant metabolite in both urine and plasma, and its concentration was 16-20 times higher than OTA in urine.<sup>66</sup>

Most current biomonitoring methods rely on urine analysis only, because urine is a non-invasive matrix that is easy to collect. Blood-derived products are examples of invasive samples due to incursion into the body. Compared to plasma, urine can be sampled in larger volumes. However, urine can vary in its composition, pH, and concentrations of urine components from sample to sample.<sup>67</sup> Physiological urine variability can be compensated by creatinine normalization strategy.<sup>68</sup> This strategy assumes that creatinine concentration is a constant value for individuals without kidney dysfunction and accounts for urine dilution effects. In addition to creatinine measurements, urine analysis requires a pH control/adjustment and a proper time point selection that, in turn, can influence on the recovery during sample preparation and the concentration profiles of the analytes of interest, respectively. The time since last exposure and the



properties of mycotoxins can also determine the choice of appropriate biological samples for dietary exposure studies.<sup>69</sup> Some mycotoxins, such as OTA and AFB1 can bind to plasma proteins and have long half-lives in the body.<sup>70,71</sup> For example, OTA half-life is 35.55 days in human plasma and about 90% of OTA can be found in plasma after administration.<sup>72</sup> Some mycotoxins that have short half-lives, from minutes to hours, can be detected more easily in urine than in plasma, since they are rapidly metabolized and mostly excreted via urine. For example, T-2, FB1 and DON have half-life of < 5 minutes, 6 minutes, and 1.53 hours, respectively in pig plasma making urine biomonitoring more suitable.<sup>73-75</sup> Whereas AFB1 half-life is about 90 hours in rats and it may be detected better in plasma than in urine.<sup>76</sup> For example, the DON ingested through the contaminated food is excreted up to 64% and 86%, respectively, via human and animal urine.<sup>54,77</sup> The majority of DON is eliminated from the body in the first ~8 hours.<sup>54,77</sup> An exposure experiment in piglets has demonstrated that ingested and excreted amounts of mycotoxins have linear dose-response correlation coefficients in the range of 0.68 and 0.78 for the administered mycotoxins, including DON, AFB1, ZEN, and OTA measured in 24-hour urine collection.<sup>78</sup> However, daily mycotoxin concentrations in urine can fluctuate significantly (~ 15 times), so 24-hour urine collection is preferred over a one-time spot collection for the appropriate assessment of exposure.<sup>54,77</sup> However, the 24-hour urine collection is unworkable and time-consuming from the participant point of view. Plasma is suitable for the analysis of mycotoxins with long and short half-lives, and the measured concentration will be a time-weighted average.<sup>63,69,79</sup> However, measurements of mycotoxins in plasma can be challenging because of their low concentrations and require methods with sub ng/ml limits of detection. Fumonisin B1 concentrations were measured during a 28-day exposure to low FB1 dietary levels in several piglet biological samples, including plasma, urine, feces and hair. The lowest concentration range of 0.15 to 1.08 ng/ml was measured in plasma versus 16.09-75.01 ng/ml in urine.<sup>63</sup> However, the evaluation of long-term exposure of piglets to FB1 during 28 days showed that only plasma had high correlation coefficient ( $r = 0.81-0.89$ ) between ingested FB1 and plasma FB1 levels.<sup>63</sup> Unlike plasma, the urinary levels of FB1 showed a high variability among pigs which might be a result of the physiological urinary fluctuation affected by food and water intake, differences in individual metabolism and the lack of normalization. In summary, it is important to measure mycotoxins in both urine and plasma to obtain a more complete picture of individual exposure.

## 1.6 Current methods for mycotoxin determination in biological samples

Nowadays, there are variety of techniques for the mycotoxin determination in biological samples, including enzyme-linked immunosorbent assay (ELISA), liquid chromatography–mass spectrometry (LC-MS), gas chromatography–mass spectrometry (GC-MS), high-performance liquid chromatography with fluorescence detection (HPLC-FD) or aptamers.<sup>80</sup> LC-MS (48%), ELISA (28%) and HPLC-FD (16%) are the most common techniques as shown in Figure 1.2.

In the last decade, LC-MS based methods have become the main methods for the assessment of combined exposures to multiple mycotoxins. LC-MS based methods are most relevant for this purpose, as they routinely can be applied for the simultaneous analysis of multiple mycotoxins and their metabolites.<sup>81</sup>

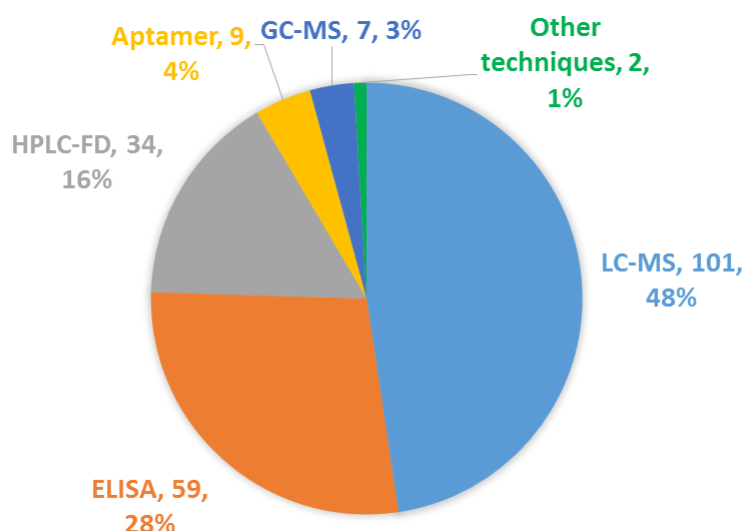


Figure 1.2. Overview of different techniques used for determination of mycotoxins and their metabolites in various human biological samples. Data from <https://www.ncbi.nlm.nih.gov/pubmed/>; filters: human samples, last 10 years, accessed date 20191211. Other techniques include immunosensor and thin-layer chromatography (TLC).

Current LC-MS methods usually cover more than one class of mycotoxin including some mycotoxin metabolites.<sup>82–84</sup> Besides LC-MS, GC-MS methods have also been developed for multi-class analysis of mycotoxins. The GC-MS methods usually provide good sensitivity and are less subjected to ion suppression or enhancement.<sup>85</sup> However, they are less preferred for mycotoxin analysis. The main disadvantage of GC-MS is that only thermally stable and volatile analytes can be analyzed. Volatility of compounds can be improved by derivatization procedures, such as trimethylchlorosilyl, trimethylsilyl, trimethylchlorosilane and trifluoroacetyl derivatization.<sup>85,86</sup>

Additional step in sample preparation makes GC-MS less amenable since this step also adds some uncertainties associated with the stability of derivatives and affect the method reproducibility.<sup>85,86</sup> Recently developed by Rodríguez-Carrasco *et al.*, GC-MS methods for 10 and 15 mycotoxins in urine demonstrated similar or worse sensitivity.<sup>44,87</sup> The comparison of the two validated methods, GC-MS and LC-MS for zearalenones in bovine urine also showed that LC-MS method had 4 times better LLOQs for  $\alpha/\beta$ -ZOLs.<sup>88</sup>

Techniques such as ELISA, HPLC-FD and aptamers, are used for the qualitative and quantitative analysis of a single mycotoxin or a few mycotoxins.<sup>89-91</sup> ELISA is commonly used in mycotoxin analysis due to its lower cost, speed, simplicity and simpler sample treatment compared to LC-MS enabling its successful implementation by less qualified technical personal.<sup>80</sup> However, ELISA methods can produce inaccurate quantitation in biological samples, as a result of antibody cross-reactivity to structurally similar molecules f.<sup>7,80,92</sup> Measurements of OTA levels in human serum by ELISA and HPLC-FD methods revealed that ELISA underestimated the OTA levels in serum at low concentrations.<sup>92</sup> The determination of DON was evaluated in a large international inter-laboratory study where it was reported that the ELISA method cannot distinguish DON and its acetylated metabolites, 3-AcDON and 15-AcDON.<sup>93</sup> Similarly, Cavaliere *et al.* reported that the ELISA kit designed for ZEN had cross-reactivity with ZEN group mycotoxins, such as  $\alpha$ -ZOL,  $\beta$ -ZOL and ZAN whereas the DON ELISA kit showed evidence of false positives and overestimated DON concentration due to cross-reactivity not only with 3-AcDON and 15-AcDON, but also with NIV and FUS-X.<sup>94</sup> Another investigation of five different DON ELISA kits for cross-reactions with main type A and B trichothecenes and their metabolites in food and feedstuffs showed that two kits had low to moderate cross-reactivity whereas three had high cross-reactivity.<sup>95</sup>

Methods using HPLC-FD and LC-MS are both considered to be gold standards in mycotoxin measurements and are used as reference methods.<sup>80,96,97</sup> Compared to LC-MS methods, HPLC-FD methods are less expensive and commonly used for the determination of a single mycotoxin or a few mycotoxins in biofluids.<sup>90,97-99</sup> Some mycotoxins, such as aflatoxins, OTA, CIT, ZEN have natural fluorescence whereas fumonisins, DON, NIV do not.<sup>85,96,100</sup> However, a derivatization step is generally necessary in the analysis by HPLC-FD to improve the sensitivity and selectivity for the detection of trace mycotoxin levels. Milićević *et al.* compared the performance of HPLC-FD, HPLC-FD with methylation and liquid chromatography-tandem mass

spectrometry (LC-MS/MS) methods for the OTA identification and quantification in pig serum and tissues.<sup>101</sup> Their results showed that the presence of OTA was confirmed by HPLC-FD, HPLC-FD with methylation and LC-MS/MS in 30%, 11% and 95% tissue samples (n=270).<sup>101</sup> They concluded that it was not possible to detect low OTA levels by HPLC-FD with methylation because of interfering co-extractive compounds.<sup>101</sup> LC-MS/MS was not able to detect OTA in only 5% of samples, since the OTA concentration was below LOD.<sup>101</sup> LC-MS/MS surpassed both HPLC-FD and HPLC-FD with methylation in specificity at trace level OTA analysis. Corcuera *et al.* developed HPLC-FD method for the simultaneous detection of OTA and AFB1 in rat plasma, liver and kidney.<sup>102</sup>

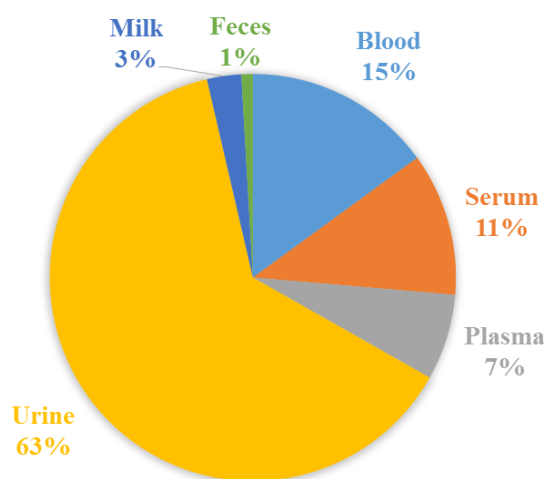


Figure 1.3. Pie chart shows sample types most used for biomonitoring of mycotoxins and their metabolites. Data from <https://www.ncbi.nlm.nih.gov/pubmed/>; filters: human samples, last 10 years, accessed date 20191211.

In order to be able to quantify AFB1 at low levels they had to use post-column iodine derivatization without affecting OTA intensity.<sup>102</sup> Overall, HPLC-FD can be used, but the derivatization step leads to additional method complexity, and LC-MS LODs and LLOQs generally outperform FD detection.

Recently, new sensor-based measurements have allowed mycotoxin analysis.<sup>103–105</sup> The advantages of these methods are low cost, small sample volume and ease of use. However, they are synthesized for one particular target molecule and cannot be used for multi-analysis.<sup>85</sup>

As shown in Figure 1.3 urine analysis is the most popular with a total of 63% of the methods for quantification of mycotoxin(s) in urine samples. Blood, serum and plasma methods compose 15%, 11% and 7% of the methods, respectively.

### 1.6.1 Methods for the analysis of mycotoxins in urine samples

Figure 1.4 shows that three frequently used techniques are LC-MS (63%), HPLC-FD (19%) and ELISA (11%), which is in line with Escrivá *et al.* review published in 2017.<sup>80</sup>

ELISA techniques were usually used for the detection of aflatoxins in urine with more than a half of the methods specifically for aflatoxin M1 (AFM1)<sup>89,106,107</sup> whereas ELISA methods were rarely used for OTA and ZEN analysis.<sup>108,109</sup> The aflatoxin ELISA kits were commonly used to investigate the association between urinary aflatoxins and dietary exposure in developing countries as a relatively low cost and easily operated technique.<sup>104</sup>

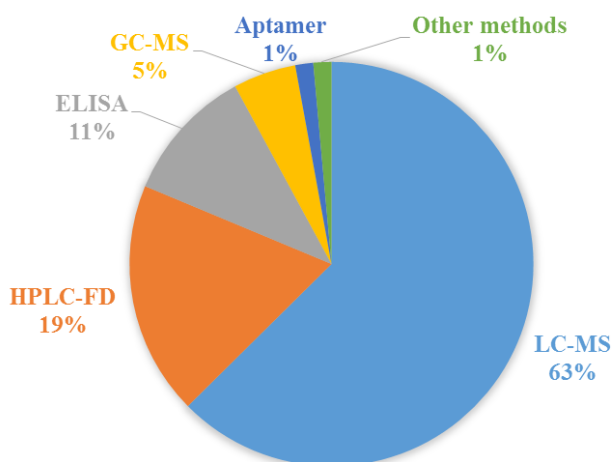


Figure 1.4. Overview of different techniques used for detection of mycotoxins and their metabolites in human urine samples. Data from <https://www.ncbi.nlm.nih.gov/pubmed/>; filters: human samples, last 10 years, accessed date 20191211. Other techniques are immunosensor and TLC.

On the other hand, HPLC-FD methods for urine samples are mostly used for the OTA detection, and much less for the aflatoxin class, CIT, ochratoxin  $\alpha$  (OT $\alpha$ ) and ZEN.<sup>111–113</sup>

There are several multi-mycotoxin methods developed using LC-MS.<sup>38,82–84,114,115</sup> However, LC-MS approaches also have some limitations and challenges in mycotoxin urine analysis, including recovery, matrix effect and sensitivity.<sup>80,116</sup> Mycotoxins are chemically diverse compounds, with partition coefficient, logP, and values ranging from -0.87 to 4.79 (ChemAxon calculator). The partition coefficient (P) is defined as the ratio of concentrations of a compound in

a mixture of two immiscible solvents. Some mycotoxins are acidic compounds such as ochratoxins and fumonisins. Others are basic, including all emerging mycotoxins, aflatoxins, and type A and B trichothecenes. Zearalenone mycotoxins are neutral. Table 1.4 summarizes the properties of mycotoxins of interest, including pK<sub>a</sub> which is the negative base-10 logarithm of the acid dissociation constant (K<sub>a</sub>).

Table 1.4. Chemical properties of mycotoxins.

Mycotoxin	LogP (ALOGPS, ChemAxon)	pK <sub>a</sub> (strongest acidic)	Accessed data 2020/01/14
Aflatoxins			
AFB1	1.73, 1.58	17.79	<a href="http://www.hmdb.ca/">http://www.hmdb.ca/</a>
AFB2	1.63, 1.57	17.79	<a href="http://www.hmdb.ca/">http://www.hmdb.ca/</a>
AFG1	1.81, 1.37	-4.4 (strongest basic)	<a href="http://www.t3db.ca/toxins/">http://www.t3db.ca/toxins/</a>
AFG2	1.59, 1.36	-4.1 (strongest basic)	<a href="http://www.hmdb.ca/">http://www.hmdb.ca/</a>
Trichothecenes type A and B			
T-2	1.95, 1.02	13.07	<a href="http://www.t3db.ca/toxins/">http://www.t3db.ca/toxins/</a>
HT-2	1.32, 0.58	12.98	<a href="http://www.t3db.ca/toxins/">http://www.t3db.ca/toxins/</a>
15-AcDON	-0.54, -0.53	12.74	<a href="http://www.t3db.ca/toxins/">http://www.t3db.ca/toxins/</a>
3-AcDON	-0.61, -0.53	12.75	<a href="http://www.t3db.ca/toxins/">http://www.t3db.ca/toxins/</a>
DON	-0.76, -0.97	12.68	<a href="http://www.hmdb.ca/">http://www.hmdb.ca/</a>
NIV	-0.79, -1.9	12.23	<a href="http://www.hmdb.ca/">http://www.hmdb.ca/</a>
FUS-X	-0.59, -1.4	12.49	<a href="http://www.t3db.ca/toxins/">http://www.t3db.ca/toxins/</a>
Zearalenone group			
ZEN	3.04, 4.37	8.54	<a href="http://www.t3db.ca/toxins/">http://www.t3db.ca/toxins/</a>
α-ZOL	3.27, 4.17	8.54	<a href="http://www.t3db.ca/toxins/">http://www.t3db.ca/toxins/</a>
β-ZOL	3.27, 4.17	8.54	<a href="http://www.t3db.ca/toxins/">http://www.t3db.ca/toxins/</a>
ZAN	-	-	
α-ZAL	3.23, 4.45	8.68	<a href="http://www.t3db.ca/toxins/">http://www.t3db.ca/toxins/</a>
β-ZAL	3.23, 4.45	8.68	The same as α-ZAL
Ochratoxins			
CIT	1.23, 0.81	3.55	<a href="http://www.hmdb.ca/">http://www.hmdb.ca/</a>
OTα	-	-	-
OTA	3.18, 4.61	3.17 (4.74 measured)	<a href="http://www.hmdb.ca/">http://www.hmdb.ca/</a>
Fumonisins			
FB1	-0.81, -0.67	3.16	<a href="http://www.hmdb.ca/">http://www.hmdb.ca/</a>
FB2	-0.28, 0.72	3.16	<a href="http://www.hmdb.ca/">http://www.hmdb.ca/</a>
Emerging mycotoxins			
ENNA	4.79, 6.46	18.8	<a href="http://www.t3db.ca/toxins/">http://www.t3db.ca/toxins/</a>
ENNA1	4.39, 5.93	18.8	<a href="http://www.t3db.ca/toxins/">http://www.t3db.ca/toxins/</a>
ENNB	3.81, 4.96	18.8	<a href="http://www.t3db.ca/toxins/">http://www.t3db.ca/toxins/</a>
ENNB1	4.06, 5.41	18.8	<a href="http://www.t3db.ca/toxins/">http://www.t3db.ca/toxins/</a>
BEA	5.25, 7.27	18.8	<a href="http://www.t3db.ca/toxins/">http://www.t3db.ca/toxins/</a>

Establishing a single method for such diverse compounds is challenging from both sample preparation and HPLC perspectives. It is difficult to find the appropriate sample preparation technique that could provide enough sample clean-up and efficiently recover all mycotoxins of interest from a urine matrix. For example, Song *et al.* examined three sample preparation techniques, including liquid–liquid extraction (LLE), urine dilution with methanol (1:1, “dilute-and-shoot” (DAS)) and urine dilution with methanol (1:1) with the subsequent evaporation of supernatant and the reconstitution step (“dilute-evaporate-and-shoot” (DES)) for the simultaneous extraction of the 12 mycotoxins and their metabolites in urine samples (DON, AFB1, AFM1, T-2, HT-2, neosolaniol (NEO), FB1, OTA, OT $\alpha$ , ZEN,  $\alpha$ -ZOL and  $\beta$ -ZOL).<sup>114</sup> Their findings showed the DES and DAS technique generated a higher matrix effect than LLE which in turn resulted in poor limits of detection (LOD) of up to 8-20 times higher with DES and DAS than with LLE.<sup>114</sup> DES and DAS samples also provide a less efficient clean-up, which led to a short column life.<sup>114</sup> However, in order to obtain satisfactory recovery for LLE across all mycotoxins, careful optimization of solvents and salt concentrations (MgSO<sub>4</sub>, NH<sub>4</sub>SO<sub>4</sub>, NH<sub>4</sub>Ac) were required to improve recovery of relatively polar mycotoxins (DON, NEO and FB1), which achieved method recoveries of 70–108%.<sup>114</sup> Escrivá *et al.* evaluated and optimized salting-out liquid–liquid extraction (SALLE), miniQuEChERS (abbreviation name originates from the first letters of quick, easy, cheap, effective, rugged, and safe), and dispersive liquid–liquid microextraction (DLLME) to extract 11 mycotoxins (AFB1, AFB2, AFG1, AFG2, OTA, ZEN, BEA, ENNA, ENNB, ENNA1 and ENNB1) from urine.<sup>115</sup> They compared these three techniques based on common validation parameters. The matrix effect and LLOQ results clearly demonstrated that SALLE had the worst matrix effect in the range of 76.3-143.8% compared to DLLME (70.6-109.9%) and miniQuEChERS (70.1-110.1%).<sup>115</sup> On the other hand, DLLME demonstrated 10-17x higher LLOQs than miniQuEChERS and SALLE.<sup>115</sup> These examples illustrate key difficulties in developing multi-mycotoxin methods with satisfactory LLOQs, recoveries and matrix effects.

Methods that would be appropriate for the analysis of a larger number of mycotoxins with various chemical and physical properties may need to combine complex sample preparation, by using multiple techniques. For example, Ediage *et al.* developed a method for the extraction of 18 mycotoxins and their metabolites, AFB1, aflatoxin B1 N7-guanine adduct (AFB1-N7-guanine),

AFM1, CIT, DON, DON-3-glucuronide (3-Gluc-DON), de-epoxy-deoxynivalenol (DOM-1), FB1, hydrolysed FB1 (HFB1), OTA, OT $\alpha$ , 4-OH-ochratoxin A (4-OH-OTA), T-2, HT-2, ZEN, ZEN-14-glucuronide (ZEN-14-Gluc),  $\alpha$ -ZOL and  $\beta$ -ZOL. The sample preparation included ethyl acetate LLE followed by a strong anion-exchange solid-phase extraction (SAX SPE) and finally hexane LLE.<sup>117</sup> Solfrizzo *et al.* used sequential SPE, first reversed-phase Hydrophilic-Lipophilic Balanced sorbent (Oasis HLB) followed by Myco6in1 immunoaffinity to extract AFM1, OTA, DOM-1,  $\alpha$ -ZOL,  $\beta$ -ZOL, and FB1.<sup>38</sup>

In summary, sample preparation techniques, such as SPE, LLE, “dilute-and-shoot”, QuEChERS, and immuno-affinity columns (IAC) are frequently used in urine LC-MS methods<sup>80,118</sup>. Simple and direct sample preparation techniques, such as “dilute-and-shoot” are generally utilized to combine a larger number of metabolites in one LC-MS method and for high-throughput. However, problems arise when the matrix effect is evaluated and when their sensitivity is compared to more selective techniques, such as with LLE.<sup>80,96,114,117,118</sup> To the best of my knowledge, a maximum of 32 mycotoxins can be analyzed by one LC-MS method which uses filtration as sample clean-up.<sup>119</sup> However, the study reported significant matrix effects that ranged from 13% to 335%. In fact, 10 out of 32 mycotoxins had matrix effects in the acceptable range of 80% to 120%.<sup>119</sup>

Most existing LC-MS urine methods to date rely on tandem mass spectrometry for qualitative and quantitative mycotoxin analysis, with triple quadrupole (QQQ) mass spectrometer as the most often used instrument.<sup>45,64,114,117,119–121</sup> Another common instrument is hybrid triple quadrupole linear ion trap spectrometers (QTrap).<sup>38,115,122,123</sup> Tandem mass spectrometry uses a targeted approach where only pre-selected mycotoxins can be detected, using a multiple-reaction monitoring (MRM) mode. It relies on recording precursor ion to product ion transitions, which provide great selectivity and sensitivity. Reported LODs and LLOQs in urine ranged from 0.000125 ng/ml - 12 ng/ml and 0.0005 ng/ml - 40 ng/ml, respectively.<sup>80</sup> To the best of my knowledge, the most sensitive methods have LLOQs, which ranged from 0.003–0.5 ng/ml, 0.0013–0.3125 ng/ml and 0.0005–0.9 ng/ml for the measured mycotoxins.<sup>83,119,123</sup>

Tandem mass spectrometry is coupled to high-performance liquid chromatography or ultra-high performance liquid chromatography (UHPLC).<sup>114,115,120,121,123</sup> The addition of HPLC or UHPLC separation reduces sample complexity prior MS analysis and allows simultaneous detection of a large number of targeted mycotoxins. Usually, a C<sub>18</sub> stationary phase is used and



provides acceptable separation for toxicologically important mycotoxins.<sup>38,117,119,122</sup> Other types of reversed-phase column are utilized less frequently for mycotoxins, for example phenyl columns.<sup>45</sup> As well, often mobile phases are water/methanol<sup>38,45,114,115,117,119,121</sup>, water/acetonitrile composition was less used.<sup>64,120,122</sup> However, there is no consensus about mobile phase additives and their concentrations. Song *et al.* and Ediage *et al.* the examined effect of mobile phase additives, such as ammonium acetate, ammonium formate, acetic acid and formic acid at different concentrations on mycotoxin signal intensities and a 0.3% FA and 5 mM ammonium formate in water/methanol mobile phase was chosen for their methods.<sup>114,117</sup> Huybrechts *et al.* stated that ammonium acetate/ acetic acid was more preferable in a water/methanol mobile phase, in positive electrospray ionization mode final additive concentrations were 5 mM ammonium acetate and 0.05% acetic acid, while in negative electrospray ionization mode, it was 0.1% acetic acid.<sup>119</sup> Warth *et al.* reported the choice of 0.1% acetic acid in water/acetonitrile mobile phase as compromise between signal intensity and matrix effect.<sup>122</sup>

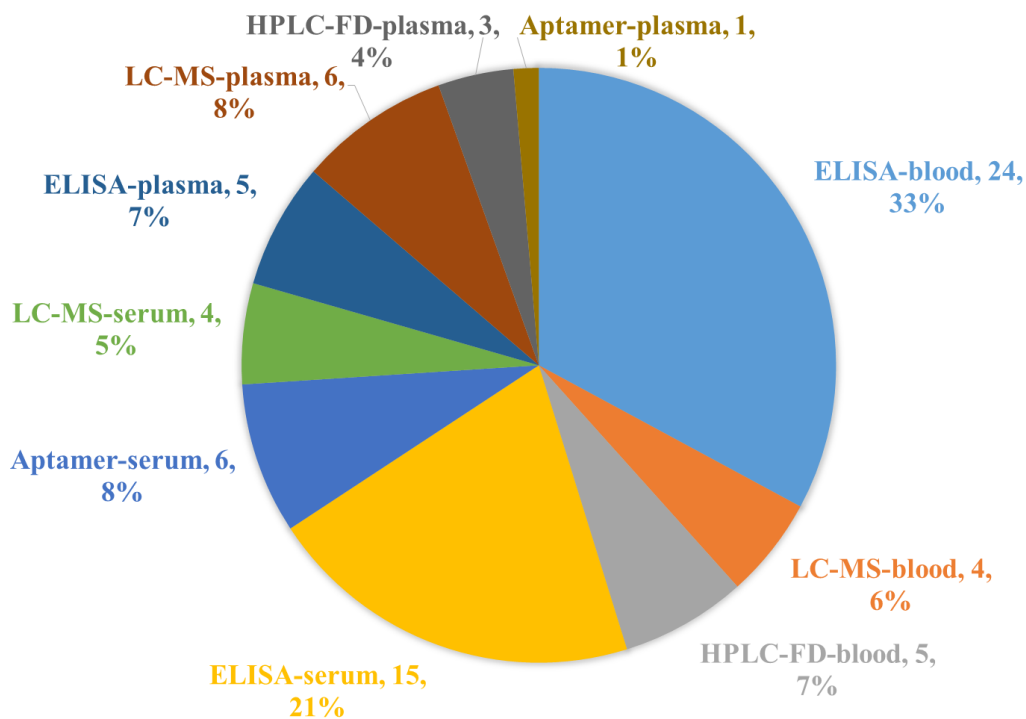


Figure 1.5. Pie chart shows the percent distribution of techniques and sample type used for the determination of mycotoxins and their metabolites. Data from <https://www.ncbi.nlm.nih.gov/pubmed/>; filters: human samples, last 10 years, accessed date 20191211.

After the examination of four mobile phase additives (ammonium acetate, ammonium formate, acetic acid and formic acid) Belhassen *et al.* chose 0.1% formic acid which resulted in optimal peak shapes in water/acetonitrile mobile phase.<sup>120</sup> Escrivá *et al.* and Solfrizzo *et al.* used 1% formic acid and 5 mM ammonium formate and 0.05% acetic acid, respectively in water/methanol mobile phase.<sup>38,45,115</sup>

In conclusion, there are a variety of methods developed to monitor mycotoxins in human urine to date. Published multi-mycotoxin methods focused on achieving a high mycotoxin coverage by applying simple and high-throughput sample preparation techniques. The increasing sensitivity of modern mass spectrometers allows us to obtain method LLOQs at sub ng /mL levels in combination with these simple sample preparation approaches such as “dilute-and-shoot”. However, almost all of the developed methods for urine suffer from matrix effects which can impact accurate quantitation of mycotoxins for urine biomonitoring, .

### **1.6.2 Methods for the analysis of mycotoxins in human blood-derived samples**

Compared to methods for the analysis of human urine there are significantly fewer methods developed for human blood-derived products. Among these, most were developed using ELISA techniques with 7, 21 and 33% of them targeting human plasma, serum, and blood samples, respectively, as seen in Figure 1.6. The other of analytical techniques, including LC-MS, have not been used frequently (1% to 8%), as seen in Figure 1.6. About 81% of ELISA methods were used for the detection of AFB1 and/or its metabolites, such as AFB1-lysine adduct and AFM1.<sup>121–125</sup> Sixteen percent of ELISA methods were used for the OTA detection and only one ELISA method was reported for ZEN detection.<sup>92,129</sup> HPLC-FD was used for the OTA measurement only.<sup>130–132</sup> In spite of the recent interest to develop multi-mycotoxin methods, LC-MS methods for various blood-derived products are still scarce.

There are total of 11 LC-MS methods developed for various blood-derived products (Table 1.5). Amongst these seven methods cover only one mycotoxin or one class of mycotoxins, and only four methods cover two or more mycotoxin classes. All methods used tandem mass spectrometry whereas Choe *et al.* used both HRMS and tandem mass spectrometry.<sup>133</sup> Tandem mass spectrometry was combined with chromatographic reversed-phase separations, such as C<sub>18</sub>, pentafluorophenyl and biphenyl, as shown in Table 1.5. Two commonly used mobile phases were water/methanol<sup>133–135</sup> and water/acetonitrile for mycotoxin chromatographic separation.<sup>64,136,137</sup>

Table 1.5. Summary of all LC-MS methods for the measurement of mycotoxins in human blood-derived products.

Human matrix	Mycotoxins	Column	LC-MS/MS detection	Sample preparation	Sample volume, $\mu$ l	LOD, ng/ml	LLOQ, ng/ml	Reference
blood	OTA and 2'R-OTA	Nucleodur C <sub>18</sub> ISIS, 5 $\mu$ m, 150 $\times$ 2 mm	QTRAP 6500 (Sciex)	Dried blood spot (DBS), extraction: water/acetone/acetonitrile (30:35:35 v/v/v)	100	0.005	0.021	134
blood	DON, HT-2, T-2, NIV, and other trichothecenes type mycotoxins	Kinetex F5, 2.6 $\mu$ m, 100 $\times$ 2.1 mm, 100 $\text{\AA}$	TripleTOF 6600 system (Sciex)	LLE (ethyl acetate)	1000	-	-	133
blood /serum/ plasma	OTA	Syneri Polar-RP 4 $\mu$ m 150 $\times$ 2 mm, 80 $\text{\AA}$	API 4000 QTrap (Applied Biosystems Inc.)	IAC	0.50 g	0.02	0.07	135
blood/ serum	AFB1, AFB2, AFG1, AFG2, AFM1, DON; DON-3-Gluc, T-2; HT-2; HT-2-4-Gluc, FB1, OTA, 2'R-OTA, OT $\alpha$ , 10-OH-OTA, CIT, DH-CIT, ZEN, ZAN, ALT, AOH, AME, ENNA1, ENNA, ENNB1, ENNB, BEA,	Nucleodur C <sub>18</sub> Gravity SB, 3 $\mu$ m, 100 $\times$ 2.0 mm	QTRAP 6500 (Sciex)	DBS/DSS, extraction: water/acetone/acetonitrile (30:35:35, v/v/v)	100	0.0013-1.396/ 0.0012-1.344	0.005-5/0.05-5	136

<b>Human matrix</b>	<b>Mycotoxins</b>	<b>Column</b>	<b>LC-MS/MS detection</b>	<b>Sample preparation</b>	<b>Sample volume, <math>\mu</math>l</b>	<b>LOD, ng/ml</b>	<b>LLOQ, ng/ml</b>	<b>Reference</b>
serum	AFB1, AFM1, DON, DOM-1, FB1, GLIO, OTA, ZEN	Biphenyl, Kinetex 2.6 $\mu$ m, 50 $\times$ 3 mm, 100 $\text{Å}$	Quattro Premier (Waters)	LLE (ethyl acetate), QuEChERS	1000	-	0.01-11	137
serum	OTA, AFB1, AFB2, AFG1, AFG2, AFM1, AFM2	Gemini 5 $\mu$ m C <sub>18</sub> , 150 $\times$ 2 mm, 110 $\text{Å}$	API 3000 QQQ (Sciex)	LLE (chloroform)	500	0.2-0.5	0.5-1	140
plasma	ENNA1, ENNA, ENNB1, ENNB, BEA	Hypersil Gold, 3 $\mu$ m, 150 $\times$ 2.1 mm	TSQ Vantage QQQ (Thermo Fisher Scientific)	Protein precipitation: MeOH/H <sub>2</sub> O (40/60, v/v), SPE (Carboglyph-4)	250	0.02 – 0.04	0.02 – 0.04	121
plasma	CIT and HO-CIT	Nucleosil 100–5 C <sub>18</sub> HD, 125 $\times$ 3 mm	1200-L Quadrupole (Varian)	Protein precipitation (acetonitrile)	1000	0.07-0.15	0.15-0.3	141
plasma	AFB1, AFB2, AFG1, AFG2, AFM1, ST, PAT, CIT, FB1, FB2, OTA	Kinetex 100 C <sub>18</sub> , 2.6 $\mu$ m 100 mm $\times$ 2.1 mm	API 4500 QQQ (Sciex)	Protein precipitation (acetonitrile/ acetic acid (99/1, v/v))	200	0.02 to 0.41 and 0.01 to 0.19	0.10 to 1.02 and 0.09 to 0.47	139
plasma	CIT	Nucleosil 100-5 C <sub>18</sub> HD, 3 $\mu$ m 125 x 3 mm	1200-L Quadrupole (Varian)	Protein precipitation (acetonitrile)	1000	0.07	0.15	138

Human matrix	Mycotoxins	Column	LC-MS/MS detection	Sample preparation	Sample volume, $\mu$ l	LOD, ng/ml	LLOQ, ng/ml	Reference
Plasma	AFB1, AFB2, AFG1, AFG2, AFM1, AFM2, OTA, OT $\alpha$ , FB1, T-2, HT-2, DON, 3-ADON, 15-ADON, FUS-X, ZEN, ZAN, $\alpha$ -ZOL, $\beta$ -ZOL, $\alpha$ -ZAL, $\beta$ -ZAL, DON-3-Gluc, ZEN-14-Gluc, ZAN-14-Gluc, AFB1-lysine	Poroshell 120 EC-C <sub>18</sub> , 2.7 $\mu$ m, 100 x 3.0 mm,	QTRAP® 5500 (Sciex)	Protein precipitation (acetonitrile/formic acid (99/1, v/v))	200	0.03-0.5	0.1 - 1	64

In published studies, positive- and negative-mode electrospray ionization (ESI(+)) for aflatoxins, fumonisins, emerging mycotoxins, OTA, CIT and trichothecenes and ESI(-) for zearalenones and CIT) were employed for the determination of mycotoxins.<sup>136,138,139</sup>

Achieving the optimal ionization efficiency of mycotoxins in the ESI ion source is still a challenge since mycotoxin physicochemical properties vary greatly. For example, aflatoxins and fumonisins ionize well in ESI(+) and form protonated ions, whereas emerging mycotoxins are detected as protonated, sodium, and ammonium ions.<sup>121,136,139</sup> It is known that mobile phase additives can influence ionization efficiency.<sup>85</sup> Similarly to trends observed in urine analysis there is no coherence in mobile phase additives, and their concentrations which vary from method to method, for example, 1% FA, 0.1% AA and 0.1% FA, 5 mM ammonium formate and 3% FA.<sup>133,134,137</sup> Multiple-reaction monitoring mode (MRM) data allowed using QQQ and QTrap frequently used in mycotoxin analysis.

The coupling of MS with liquid chromatography additionally helps to improve both sensitivity and confidence in quantification. LOD and LLOQ levels achieved in blood-derived samples ranged from 0.0013-1.396 ng/ml and 0.005-1 ng/ml, respectively, Table 1.5. The sensitivity of LC-MS methods can also be improved by efficient sample preparation by reducing sample complexity and/or adding an enrichment step. Blood-derived matrices usually require protein precipitation to provide protein removal, to remove chromatographic interferences, and to avoid protein aggregation and column clogging.<sup>142</sup> Protein precipitation can be performed with different organic solvents, such as methanol or acetonitrile, which are considered to be the most efficient methods of protein removal and typically provide >90% removal when blood : precipitant ratios higher than 1:2 are used.<sup>143</sup> In addition, a protein precipitation step also disrupts any protein binding between mycotoxins and highly abundant carrier proteins in blood. Most mycotoxins of interest, such as CIT, DON, OTA, ZEN,  $\alpha$ -ZOL,  $\beta$ -ZOL, and aflatoxins are able to form stable non-covalent complexes with human serum albumin.<sup>144-146</sup> Mycotoxin binding constants ( $\log K$ ) to human serum albumin range from 7.65 to 2.49, as shown in Table 1.6. Generally, non-covalent interactions in protein-mycotoxin complexes are driven by van der Waals interactions, hydrophobic forces, multiple hydrogen bonds, and/or electrostatic interactions. Hydrophobic interactions were determined as dominant in protein-mycotoxin complex.<sup>144-146</sup>

*Table 1.6. Binding constants (K) of mycotoxins to human serum albumin, expressed as logK.*

<b>Mycotoxins</b>	<b>logK (unit of K: L/mol)</b>	<b>Reference</b>
ZEN	5.5	145
$\alpha$ -ZOL	4.72	145
$\beta$ -ZOL	4.33	145
AFB1	4.65	144
AFB2	4.55	144
AFG1	4.58	144
AFG2	4.34	144
AFM1	4.52	144
OTA	7.65	146
CIT	5.3	148
DON	2.49	149

Thus the most hydrophobic mycotoxins show a high degree of binding in blood, for example 82.2 to 88.9% for OTA in avian species, around 70% for T-2 and HT-2 in dogs.<sup>70,147</sup> This binding must

be disrupted to ensure mycotoxins are not removed during the protein removal step and to accurately quantitate their total levels in blood-derived matrices.

To date, different sample preparation methods were used in blood samples, for example, protein precipitation, DBS, LLE, IAC, and SPE, as shown in Table 1.5. Evaluating all methods in terms of mycotoxin coverage of toxicologically important mycotoxins, high recovery, minimal matrix effects and reaching the best limit of detections, there was no method that could perfectly fit all these criteria. From the sample preparation point of view, extraction of all toxicologically important mycotoxins using one technique is challenging. The majority of published methods used a simple sample preparation, such as protein precipitation, DSS and DBS because it can provide a wide coverage of mycotoxins. For example, Osteresch *et al.* developed a method for 27 mycotoxins and their metabolites, covering aflatoxins, trichothecenes, ochratoxins, emerging mycotoxins and zearalenones in both blood and serum samples using DSS and DBS.<sup>136</sup> However, the main drawback of such sample clean-ups are huge matrix effects. Matrix effects are expressed as a ratio of the signal of an analyte in the matrix to the signal of the same analyte in standard solution, multiplied by 100. Usually, matrix effects are acceptable if they are in the range of 80% -120%. But the matrix effects in Osteresch *et al.* method ranged from 17%-939% and 13%-842% for serum and blood, respectively.<sup>136</sup> There were only two and one mycotoxins with a matrix effect in the range of 80%-120% in serum and blood samples, respectively.<sup>136</sup> Mycotoxin recoveries were in the range of 70%-120%, except for DON (< 70%), and FB1 (< 64%) in serum samples and 3-Gluc-DON (>194%), HT-2-4-Gluc (>130%) in human blood.<sup>136</sup> Fan *et al.* developed a method for the measurement of 26 mycotoxins, including aflatoxins, trichothecenes, ochratoxins, zearalenones and their metabolites in human plasma using acetonitrile protein precipitation with satisfactory recovery of 70.3% to 115.9%.<sup>64</sup> This method also had huge matrix effects, 28%-125% for 19 mycotoxins and only 9 mycotoxins showed matrix effects within the acceptable range of 80%-120%.<sup>64</sup> Multi-mycotoxin and analyte-specific methods were designed for 11 mycotoxins (aflatoxins, ochratoxins, fumonisins, patulin and sterigmatocystin) with the recovery of ranging from 60.1% to 109.8% by Cao *et al.*<sup>139</sup> However, a 60%-140% matrix effect was observed for five out of 11 mycotoxins.<sup>139</sup> Nine mycotoxins (AFB1, AFM1, DON, DOM-1, FB1, gliotoxin, OTA, and ZEN) were studied by De Santis *et al.* They also reported significant matrix effects of 54%-79% for four out of nine mycotoxins. However, clean-up combined ethyl acetate LLE and QuEChERS was used and resulted in a poor absolute recovery for almost all

mycotoxins, ranging between 50% and 63%, except for AFB1 (82%).<sup>137</sup> Osteresch *et al.* could reach sub ng/ml LLOQ for a majority of mycotoxins for human blood-derived samples.<sup>136</sup> Besides, the Fan *et al.* method also had low LLOQ levels, 0.1 – 1 ng/ml.<sup>64</sup>

To conclude, monitoring all toxicologically important mycotoxins with a single LC-MS method is currently extremely challenging and leads to many drawbacks and compromises, such as unacceptable matrix effects leading to poor method accuracy, poor recovery and/or poor LLOQs.

### 1.6.3 Methods for analysis of mycotoxins in animal blood-derived samples

The methods for analysis of mycotoxins in animal blood-derived samples are also important for consideration because they could also potentially be adopted for human exposure studies. The summary of methods for analysis of mycotoxins in animal blood-derived samples is shown in Table 1.7. All methods used tandem mass spectrometry and C<sub>18</sub> chromatographic separation. There is only one multi-mycotoxin method for the determination of 13 mycotoxins (DON, DOM-1, T-2, HT-2, ZEN, ZAN,  $\alpha/\beta$ -ZOLs,  $\alpha/\beta$ -ZALs, OTA, FB1 and AFB1) in pig plasma developed by Devreese. *et al.*<sup>75</sup> This method used universal and fast sample preparation, protein precipitation with acetonitrile, and showed an acceptable absolute recovery (78%-110%) and matrix effect (84 to 109%).<sup>75</sup> The main disadvantage of the method is the poor LLOQs ranging from 2 to 10 ng/ml. However, some class-specific methods could reach sub ng/ml LLOQ levels. For example, Han *et al.* developed a method for AFB1 and T-2 with LLOQs of 0.05 ng/ml for both mycotoxins.<sup>150</sup> They used a combined sample preparation, acetone protein precipitation and homemade SPE composed from silica gel and florisil.<sup>150</sup> Matrix effects ranged from 73.0 to 105.8% and from 74.9 to 88.6% for AFB1 and T-2, respectively.<sup>150</sup> Absolute recovery was in the range of 56-65% and 69-78% for AFB1 and T-2, respectively.<sup>150</sup> Broekaert *et al.* developed a method for type B trichothecenes, DON, DOM-1, 3-AcDON and 15-AcDON in chicken and pig plasma, using protein precipitation with acetonitrile in chicken and pig plasma. However, sub ng/ml LLOQs were reached only for DON (0.1 ng/ml) and DOM-1 (0.5 ng/ml) in pig plasma.<sup>151</sup> Absolute recovery and matrix effects ranged from 67 to 97% and from 73 to 97% in chicken plasma and from 28 to 88% and from 44 to 97% in pig plasma, showing an important matrix influence.<sup>151</sup> Brezina *et al.* developed a method for the determination of ZEN, ZAN,  $\alpha/\beta$ -ZOLs,  $\alpha/\beta$ -ZALs, DON and DOM-1 in pig serum.<sup>152</sup>



Table 1.7. Summary of LLOQ methods for analysis of mycotoxins in animal blood-derived samples.

Mycotoxins	Published <b>class-specific methods</b> and <b>multi-class methods</b>		
	LLOQ, ng/ml	Matrix	Author
AFB1 AFB1	0.05 2	Rat plasma Pig plasma	Han <i>et al.</i> <sup>150</sup> Devreese <i>et al.</i> <sup>75</sup>
T-2 and HT-2 T-2, HT-2, T-2 triol T-2 T-2 and HT-2	1 and 2.5 1-5 0.05 (T-2) 2 and 5	Pig and chicken plasma Pig plasma Rat plasma Pig plasma	De Baere <i>et al.</i> <sup>153</sup> Sun <i>et al.</i> <sup>154</sup> Han <i>et al.</i> <sup>150</sup> Devreese <i>et al.</i> <sup>75</sup>
3-AcDON, 15-AcDON, DON, DOM-1 DON, DOM-1 DON DON	0.1-1 and 1-2 1-2.5 and 1.25-2.5 0.45 (DON) 10 (DON)	Pig and chicken plasma Pig and chicken plasma Pig serum Pig plasma	Broekaert <i>et al.</i> <sup>151</sup> Baere <i>et al.</i> <sup>153</sup> Brezina <i>et al.</i> <sup>152</sup> Devreese <i>et al.</i> <sup>75</sup>
ZEN, ZAN, $\alpha/\beta$ -ZOLs, $\alpha/\beta$ - ZALs ZEN, ZAN, $\alpha/\beta$ -ZOLs, $\alpha/\beta$ - ZALs	0.5-0.6 0.08 -2.37 0.2- 1 and 1-5 5	Horse plasma Pig serum Pig and chicken plasma Pig plasma	Songsermsakul <i>et al.</i> <sup>155</sup> Brezina <i>et al.</i> <sup>152</sup> De Baere <i>et al.</i> <sup>156</sup> Devreese <i>et al.</i> <sup>75</sup>

They evaluated 14 sample preparation techniques and chose Oasis HLB SPE based on recovery which ranged from 82–131%.<sup>152</sup> All mycotoxin LLOQs were in the range of 0.08-0.78 ng/ml, except for  $\beta$ -ZOL with an LLOQ of 2.37 ng/ml.<sup>152</sup> Songsermsakul *et al.* developed a method for six zearalenones, ZEN, ZAN,  $\alpha/\beta$ -ZOLs, and  $\alpha/\beta$ -ZALs in horse plasma using one step IAC clean-up that resulted in recoveries of 84–100% with LLOQs ranging from 0.5–0.6 ng/ml.<sup>155</sup> Type A trichothecenes, T-2, HT-2 and T-2 metabolite, T-2 triol were analysed in pig plasma by Sun *et al.*<sup>154</sup> Protein precipitation with acetonitrile resulted in excellent recoveries (89-101%), but poor LLOQs (1 to 5 ng/ml).<sup>154</sup> De Baere *et al.* developed a method for pig and chicken plasma for DON, DOM-1, T-2 and HT-2. Sample preparation included the combination of protein precipitation with methanol followed by Oasis HLB.<sup>153</sup> LLOQ levels were 1-2.5 ng/ml and 1.25-2.5 ng/ml for pig and chicken plasma, respectively.<sup>153</sup> Absolute recoveries ranged from 69-92% and 39-115% for chicken and pig plasma, and a matrix effect of 96-106% and 46-130% for the chicken and pig plasma.<sup>153</sup> This demonstrates the method for one species may not easily transfer to another species or biofluid.

In conclusion, amongst all methods developed for mycotoxin detections in animal biofluids there is no method that would cover all toxicologically important mycotoxins and have ng/ml LLOQs. Either low recoveries or huge matrix effects or both were observed almost in all methods. There is no mycotoxin method that would be a good candidate to adopt for human blood-derived products. Various sample preparation techniques were used in class-specific methods; however, it is not possible to conclude which is better. Even the combination of two sequential clean-up steps can result in poor LLOQ levels or recovery and extending a class-specific method to multi-class analysis is not trivial.

## 1.7 Mycotoxin metabolism

After exposure, toxins are altered or metabolized by the human body in order for these substances to be effectively eliminated from the body. However, these toxin metabolites can in some instances become more toxic than the parent compounds.<sup>3,157,158</sup> Human metabolism of xenobiotics, such as mycotoxins, can be classified into two major types: Phase I and Phase II biotransformation reactions.<sup>159–161</sup> Phase I biotransformation reactions convert a parent toxin to a more polar molecule by increasing its hydrophilicity by adding one or more polar functional groups ( $-\text{OH}$ ,  $-\text{NH}_2$ ,  $-\text{SH}$  or  $-\text{COOH}$ ).<sup>161</sup> Common reactions of Phase I biotransformation are hydrolysis, reduction, and

oxidation, as shown in Figure 1.6. The role of Phase II biotransformation reactions is to produce significantly more hydrophilic metabolites than the parent toxin in order to promote renal excretion. In Phase II metabolism, parent toxins undergo covalent conjugation with small hydrophilic endogenous molecules such as glucuronic acid, sulfate, lysine, or glutathione (Figure 1.6). Thus major Phase II biotransformation reactions are glucuronidation, acetylation, sulfation, conjugation with glutathione and amino acids. After Phase I metabolism, toxins can undergo additional Phase II biotransformation reactions, for example T-2 is first rapidly hydrolyzed to HT-2 followed by glucuronidation.<sup>162</sup> They also can bypass Phase I metabolism and only undergo conjugation reactions directly.

Two models are commonly used to study mycotoxin metabolism, *in vitro* and *in vivo* animal models. Due to mycotoxin toxicity human *in vivo* studies are very rare. Animal models are used to study metabolic pathways and fate of mycotoxins, however, inter-species differences should be taken into consideration.<sup>163</sup> *In vitro* models have several major advantages. They are rapid, relatively inexpensive, easy to manipulate and require a small amount of chemicals. They eliminate the use of animals and avoid inter-species differences, such as differences in molecular pathways and metabolism. *In vitro* models that are most often used in mycotoxin studies are subcellular fractions of tissue homogenate and cell-based models. Both *in vitro* models are powerful tools to study toxin metabolism. However, cell-based models have wider application in toxicity studies. Cell-based models are also relevant for the assessment of genotoxic, estrogenic and immunotoxic activities of mycotoxins and acute lethality tests. Subcellular fractions are a good option for toxin metabolism studies and metabolite characterization, since they contain a rich variety of metabolic enzymes, such as cytochrome P450, flavin monooxygenases, uridine glucuronide transferases, sulfurotransferases and glutathione transferases. The primary subcellular fractions are human liver microsomes, S9 fraction and cytosol. They are obtained by the sequential centrifugation of liver homogenates. The first isolated fraction of liver homogenates is the S9 fraction which contains a wide variety of Phase I and Phase II enzymes involved in xenobiotic metabolism. The S9 fraction is further separated using ultracentrifugation into microsomes and a soluble fraction called cytosol. Human liver microsomes are a rich source of Phase I enzymes, including cytochrome P450 and flavine-containing monooxygenases and Phase II enzymes, uridine glucuronide transferases. The liver cytosolic fraction contains the soluble enzymes of Phase I and Phase II, such as epoxide hydrolases, esterases, sulfurtransferases and glutathione transferases.

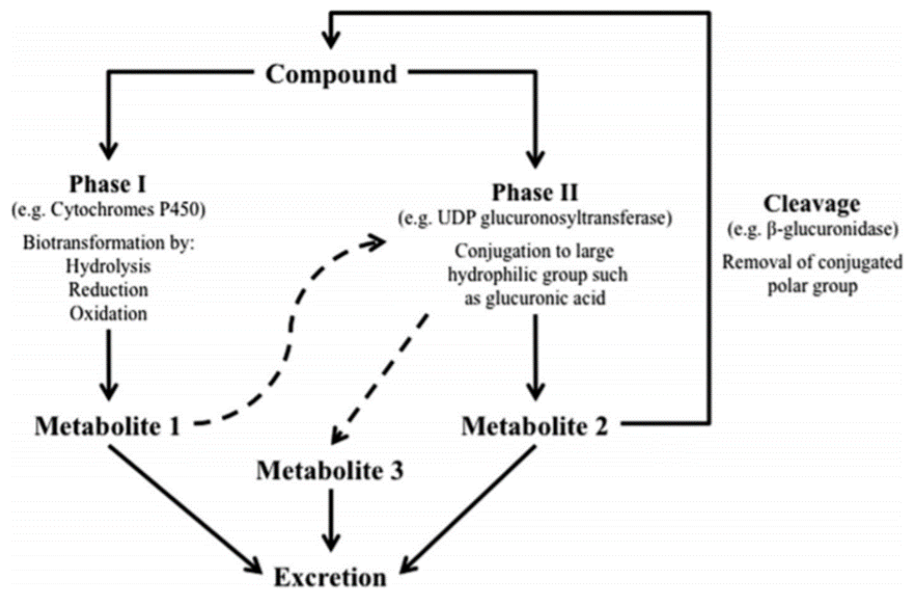


Figure 1.6. Phase I and Phase II biotransformations. This figure was reproduced with permission from reference <sup>164</sup>, license number 4773850578859.

To date, the metabolism of some mycotoxins (AFB1, DON, ZEN, FB1, OTA, CIT, ENNB, ENNB1 T-2 and HT-2) is well known and has been studied extensively using either *in vitro* and/or *in vivo* animal models. Toxin metabolism studies has identified the main Phase I and Phase II metabolites, which can be further used for the assessment of mycotoxin exposure in biofluids. Some of these biomarkers may become putative or validated biomarkers of exposure pending further studies. The major benefit of a biomarker-driven approach is that it can precisely evaluate an individual's exposure to mycotoxins. However, the biomarker-driven approach is only slowly emerging in mycotoxin analysis because of its limitations. Mycotoxin metabolites are not fully identified and characterized for many mycotoxins, and their commercial standards do not exist for all toxicologically important mycotoxins. In addition, the metabolites selected as biomarker(s) should be detectable, be predominant, and be stable metabolite(s) in urine and/or blood-derived products.

The era of mycotoxin biomarker analysis started in 1980s, from the evaluation of the carcinogenic aflatoxin effect.<sup>165</sup> To date, known aflatoxin metabolites were investigated to identify human biomarkers of aflatoxin B1. Out of six known Phase I metabolites (AFM1, aflatoxin Q1 (AFQ1), aflatoxicol (AFL), aflatoxin P1 (AFP1), AFB1 8,9 endo/exo-epoxide (AFBO) and aflatoxin B1 di-hydrodiol (AFB1-diol)), AFM1 was identified as the only aflatoxin present in

urine<sup>166</sup> while on the contrary Mykkänen *et al.* demonstrated that AFQ1 was present at higher concentration (10.4 ng/ml) than AFM1 (0.04 ng/ml).<sup>167</sup> They stated unexpectedly high AFQ1 incidences can be associated with the age of participants and their diet preferences showing the importance of inclusion of all AFB1 metabolites in biomonitoring.<sup>167</sup>

Deoxynivalenol metabolism was investigated *in vitro* using liver microsomes and *in vivo* human models.<sup>168</sup> Both models showed that most of the free DON was converted into glucuronides.<sup>168</sup> According to the *in vivo* model, urinary species of DON exposure were free DON (27%), DON-3-Gluc (14%) and DON-15-glucuronide (15-Gluc-DON, 58%) demonstrating the importance of including metabolites for the assessment of exposure.<sup>54</sup> The exposure can be underestimated about four times if mycotoxin monitoring relies on free DON only. 15-Gluc-DON (0.828-37.7 ng/ml), 3-Gluc-DON (0.583-5.84 ng/ml) and DON (1.39-14.7 ng/ml) were found in 43.8%, 15.8% and 10% of urine samples, showing agreement with *in vitro* and *in vivo* studies and showing their utility as urinary biomarkers.<sup>64</sup> Besides glucuronic forms, sulfates were also found in animal and human studies. However, they only accounted for 1.5% of the orally administered DON in mice and 4% of the DON quantity ingested through the contaminated food.<sup>77,169</sup>

Zearalenones are mycotoxin class prone to glucuronidation and/or sulfation mediated by families of glucuronide transferases and sulfotransferases, respectively. All zearalenones can be conjugated with glucuronic acid or sulfuric acid via the same aromatic hydroxyl groups and aliphatic hydroxyl group for  $\alpha/\beta$ -ZOLs and  $\alpha/\beta$ -ZALs. Sulfation and glucuronidation reactions can be in competition, but glucuronidation reactions imply that a lot of substrate must be present to saturate the enzyme, whereas sulfation is opposite.<sup>170,171</sup> At low doses of toxin, sulfation can be a preferred reaction. In addition, it is believed that the co-factor (3'-phosphoadenosine-5'-phosphosulfate) that assists in sulfation reactions can limit the reaction because its concentration can vary in different tissues.<sup>171</sup> Metabolic pathways also vary between species because of differences in the set of enzyme isoforms that catalyse reactions.<sup>172,173</sup> For example the glucuronide conjugation of ZEN was predominant in *in vivo* human and rat experiments whereas sulfation was principally identified in chickens.<sup>174,175</sup> Unfortunately, the percentage of glucuronidation and sulfation was not reported in these studies. Pfeiffer *et al.* reported the ratio of glucuronide-to-sulfate formation ranged from 0.9 to 2.1, depending on zearalenones, in *in vitro* studies using human Caco-2 cells.<sup>176</sup> ZEN, ZAN,  $\alpha/\beta$ -ZOLs and  $\alpha/\beta$ -ZALs glucuronides were generated *in vitro* using pig, rat, bovine and human liver microsomes.<sup>177</sup> Pfeiffer *et al.* demonstrated interspecies differences, up to

a factor of 10, for glucuronidation pathways. The highest activity for the glucuronidation pathway was observed in pig liver microsomes (28-36 nmolmin<sup>-1</sup>mgprotein<sup>-1</sup>) followed by bovine (11-15 nmolmin<sup>-1</sup>mgprotein<sup>-1</sup>), rat (8-10 nmolmin<sup>-1</sup>mgprotein<sup>-1</sup>) and human (4-7 nmolmin<sup>-1</sup>mgprotein<sup>-1</sup>) liver microsomes.<sup>177</sup> Two glucuronides were formed for ZEN and ZAN whereas three glucuronides were reported for  $\alpha/\beta$ -ZOLs and  $\alpha/\beta$ -ZALs.<sup>177</sup> The glucuronide formation preferred at C-14 over C-16 for all zearalenones.<sup>177</sup> C-7 glucuronides was preferent over the C-16 conjugation in  $\alpha/\beta$ -ZOLs and  $\alpha/\beta$ -ZALs except for  $\beta$ -ZAL in the rat liver microsomes.<sup>177</sup> Wu *et al.* depicted that enzyme substrate specificity determines the preferred glucuronide form over the others in compounds with multiple hydroxyl groups.<sup>178</sup> Regioselective properties enzymes depend on the size and shape of the substrate-binding pocket.<sup>178</sup> *In vivo* pig and *in vivo* human metabolism studies were in agreement about the predominant glucuronic species where only ZEN-14-Gluc were generated.<sup>175,179</sup> The results of the Portugal biomonitoring study agreed on both *in vivo* studies making it a suitable as urinary biomarker.<sup>180</sup> However, Ruyck *et al.* did not observe ZEN-14-Gluc in urine samples.<sup>62</sup> In order to explain the observed differences, additional studies are required using the broader panel of ZEN metabolites in both urine and plasma. Recently, Yang *et al.* studied ZEN metabolism using *in vivo* animal model and human liver microsomes and confirmed that ZEN-14-Gluc was the most observed glucuronide.<sup>174</sup> In addition, several animal studies showed that fecal elimination is the major route of ZEN excretion.<sup>181</sup> For example, the mean excretion rates of ZEN were 55% and 15-20% in rat feces and urine and 40% and 26% in pig feces and urine.<sup>179,182</sup> Warth *et al.* reported ZEN renal human excretion rate was 9.4%.<sup>175</sup>

Enniatin B and ENNB1 metabolism was investigated using *in vitro* and *in vivo* animal models. Human, rat, and dog liver microsomes were used for the generation of ENNB metabolites. Oxidation, dehydrogenation and N-demethylation Phase I reactions produced 12 metabolites.<sup>183</sup> Similar results were obtained for ENNB and ENNB1 when chickens were exposed to these mycotoxins.<sup>184</sup> Both toxins undergo only Phase I biotransformation, predominantly oxidation, and no Phase II metabolites were observed.<sup>184</sup> Biomonitoring studies of ENNB in urine samples reported that 83.7% urine samples contained ENNB and 87.7%, 96.3% and 6.7% of samples had the mono-oxygenated, N-demethylated and di-oxygenated metabolites, respectively, based on the putative identification by HRMS.<sup>184</sup> However, the lack of commercial metabolites does not allow us to routinely monitor and quantify them in biological samples.

Schertz *et al.* described toxicokinetics and detoxification of fumonisins in pigs.<sup>73</sup> Fumonisins are poorly metabolized, only minor metabolites were detected, partially hydrolyzed and fully hydrolyzed forms of fumonisins.<sup>73</sup> Current biomonitoring studies are based on the detection of fumonisins only.<sup>45,180</sup> Fumonisin B1 is mycotoxin with a short elimination half-life of 36 minutes in serum, so about 8% of FB1 is excreted unmetabolized in urine.<sup>73</sup> Bile was proposed as the main excretion route for elimination of FB1.<sup>73</sup>

The main metabolites of OTA are OT $\alpha$  and hydroxyl-metabolite.<sup>158</sup> OT $\alpha$  is a metabolite that is formed by the cleavage of the phenylalanine OTA moiety.<sup>158</sup> Muñoz *et al.* proposed to use OT $\alpha$  in OTA analysis in both urine and plasma, since OTA is extensively converted to OT $\alpha$ .<sup>66</sup> The importance of the OTA hydroxyl metabolite is not clear in the assessment of exposure to OTA since OTA hydroxyl metabolite is rarely included in the analysis. Therefore, further analyses are required to clarify its validity and/or importance in biomonitoring. The presence of OTA and OT $\alpha$  glucuronide species were confirmed by Solfrizzo *et al.*, Klapac *et al.*, Muñoz *et al.*<sup>38,99,185</sup> Currently, there is only one known metabolite of CIT, dihydro-CIT, which was detected with high frequency (>70%) in some urine analyses.<sup>186,187</sup> Dihydro-CIT concentration was at least three times higher than CIT indicating its importance for the assessment of exposure.<sup>186,187</sup> Based on Vidal *et al.* literature review, the detailed investigation of CIT metabolites has not been performed yet, so it is possible that human exposure to CIT is underestimated.<sup>168</sup>

T-2 and HT-2 are two type A trichothecene mycotoxins. T-2 is rapidly converted to HT-2 in 5 to 20 minutes according to *in vivo* animal models.<sup>75,188</sup> Metabolites of T-2 and HT-2 were studied recently in detail using animal and human liver microsomes and *in vivo* animal models.<sup>162,189</sup> Yang *et al.* generated 18 Phase I T-2 metabolites and three glucuronides in rats, chicken, goat, pigs, cows, and humans.<sup>162</sup> Additionally, they identified new T-2 sulfate metabolites in *in vivo* chicken experiment, however, sulfation was only a minor pathway.<sup>162</sup> HT-2, 3'-hydroxy-HT-2 and 3-glucuronide-HT-2 were predominant human metabolites.<sup>162</sup> Similarly, HT-2 metabolic pathways were studied and the same main metabolites, 3'-hydroxy-HT-2 and 3-glucuronide-HT-2 were observed.<sup>189</sup> *In vivo* animal and *in vitro* using liver microsomes models agreed that hydroxylation and glucuronidation were the main metabolic pathways of T-2 and HT-2.<sup>162,189</sup> These applications demonstrated that a human liver microsomal model provides a superior alternative to the use of an animal *in vivo* model. *In vitro* models are also able to generate similar numbers of metabolites with a lower cost and higher speed. Moreover, HRMS played an important

role in these studies allowing us to identify metabolites without having their commercial standards.<sup>162,189</sup>

In conclusion, Phase I metabolites and glucuronides are prioritized for the biomonitoring of mycotoxins since other Phase II metabolic pathways typically represent minor pathways in mycotoxin metabolism. In some cases, metabolites can reflect dietary exposure even better than parent mycotoxins since they are often the most predominant species in biofluids. However, the lack of commercial standards does not allow us to include them in routine analytical methods. To address this limitation, *in vitro* models using human microsomes can be used to generate mycotoxin metabolites. Finally, the generated metabolites can be used to build up LC-MS library allowing to identify metabolites and further include them in routine biomonitoring.<sup>62</sup>

## 1.8 Objectives

Human exposure to mycotoxins is minimized by strict regulation of foods and feed according to the maximum tolerated levels and modelling of daily intake values of different food commodities. However, many recent biomonitoring studies across the globe reported that there were incidences when individual TDIs were exceeded, showing that periodic surveillance is necessary in order to better understand and minimize the health risk posed by mycotoxins. Low-cost high-throughput methods capable of accurately measuring low levels of various mycotoxins still remain scarce thus impeding broader biomonitoring efforts and in fact no mycotoxin biomonitoring studies have been reported in Canada in the past two decades.

The goal of my project is to develop a multi-mycotoxin assay for the analysis of 27 toxicologically important mycotoxins, including the well-known mycotoxins, T-2, HT-2, NIV, DON, FUS-X, 15-AcDON, 3-AcDON, FB1, FB2, AFB1, AFB2, AFG1, AFG2, ZEN,  $\alpha$ -ZOL,  $\beta$ -ZOL, ZAN,  $\alpha$ -ZAL, ZAL, OTA, OT $\alpha$ , CIT, as well as emerging mycotoxins, BEA, ENNA, ENNA1, ENNB, and ENNB1, and their metabolites in human plasma for exposure studies. These mycotoxins were selected for their prevalence or possible emerging concern in Canada and their well-established toxicity profiles. In this thesis, I will report two reliable multi-mycotoxin liquid chromatography-high resolution mass spectrometry methods for the detection and quantification of these selected mycotoxins in human plasma. The first method covers 17 mycotoxins (T-2, HT-2, NIV, DON, FUS-X, 15-AcDON, 3-AcDON, AFB1, AFB2, AFG1, AFG2, ZEN,  $\alpha$ -ZOL,  $\beta$ -ZOL, ZAN,  $\alpha$ -ZAL, and ZAL) and the second method combines 10 mycotoxins (FB1, FB2, OTA, OT $\alpha$ ,



CIT and emerging mycotoxins). The two methods are required due to diverse physicochemical properties of mycotoxins. The first method covers basic and neutral mycotoxins whereas the second method covers acidic classes of mycotoxins, fumonisins and ochratoxins, and the most hydrophobic mycotoxins belonging to cyclic depsipeptides. Plasma is selected as the matrix for this analysis as it can provide a better readout of long-term exposure to mycotoxins, at least for mycotoxins that have long plasma half-life, and it has shown better correlation to food intake for other mycotoxins with short half-lives. For this application, sensitivity, selectivity, negligible matrix effects and high analyte recovery were prioritized during method development since mycotoxins are present at trace levels in plasma. Thus I have compared pentafluorophenyl and C<sub>18</sub> stationary phases and different mobile phase solvents as well as mobile phase additives, such as acetic acid, formic acid, ammonium formate and ammonium acetate in order to obtain a good separation of all mycotoxins. Particular attention was paid to the chromatographic separation of isomeric compounds, 3-AcDON and 15-AcDON,  $\alpha$ -ZOL,  $\beta$ -ZOL, and ZAN,  $\alpha$ -ZAL and ZAL. I have also performed a detailed comparison of sample preparation techniques, such as solvent precipitation with acetonitrile and methanol, solid-phase extraction and liquid-liquid extraction with ethyl acetate and MTBE, in terms of analyte recovery, selectivity, and matrix effects. The final choice of sample preparation for this application was made based on the prioritized method parameters with the specific focus to achieve sub ng/ml LLOQ levels without immunoaffinity enrichment. This work focuses on the LC-HRMS, which has been used to quantitate mycotoxins and further to evaluate for qualitative screening of metabolites not included in the test panel. The first method uses a LTQ Orbitrap Velos with 60000 resolution whereas the second method relies on the QTOF 6545 operating at 25000 resolution and time-segment polarity-switching. The finalized methods were validated according to the FDA guidance for Bioanalytical Method Validation<sup>190</sup> in order to ensure method reliability and accurate quantification. Chapter 2 describes the development and validation of the first method for 17 mycotoxins while Chapter 4 describes the second method for 10 mycotoxins.

In addition to the direct application of the first multi-mycotoxin method to measure 17 parent mycotoxins (T-2, HT-2, NIV, DON, FUS-X, 15-AcDON, 3-AcDON, AFB1, AFB2, AFG1, AFG2, ZEN,  $\alpha$ -ZOL,  $\beta$ -ZOL, ZAN,  $\alpha$ -ZAL and ZAL) in human plasma, I have expanded and examined the method and its suitability for the identification and characterization of mycotoxin metabolites using HRMS in combination with data-dependent acquisition and collision-induced

dissociation or higher energy collisional dissociation. I have focused on the generation of Phase I and Phase II glucuronide mycotoxin metabolites using human liver microsomes as these pathways are common to the mycotoxins of interest and generate some of the major known metabolites. The characterized metabolites were used to build the most extensive LC-MS library of mycotoxin metabolites. This study examines whether multiple existing literature LC-MS methods for mycotoxin metabolites can be replaced by one single LC-HRMS to increase its versatility. Moreover, the proposed metabolism studies and resulting metabolite library will allow the use of extended LC-HRMS method for simultaneous detection of both parent mycotoxins and their metabolites in order to more accurately estimate human exposure to multiple mycotoxins. These metabolism studies of 17 mycotoxins are described in Chapter 3.

## **2. Liquid chromatography – high-resolution mass spectrometry method for monitoring of 17 mycotoxins in human plasma for exposure studies**

Chapter 2 was published in an article entitled “Liquid chromatography - high resolution mass spectrometry method for monitoring of 17 mycotoxins in human plasma for exposure studies”, authored by I. Slobodchikova and D. Vuckovic and published in *Journal of Chromatography A*, 2018, 1548, 51-63.

### **2.1 Introduction**

Mycotoxins are fungal metabolites that can be toxic to animal and human populations. Mycotoxin exposure may contribute to a variety of adverse health effects, as specific mycotoxins may have hepatotoxic, nephrotoxic, carcinogenic, cytotoxic, immunosuppressive, inflammatory, neurological, estrogenic and/or teratogenic effects.<sup>191,192</sup> Direct contact and inhalation represent minor routes of exposure, while the majority of human exposure to mycotoxins occurs through diet via intake of contaminated food. In fact, 25% of grain supply worldwide is estimated to be contaminated with mycotoxins, and the contamination of Canadian food chain is well documented.<sup>11,193–196</sup> Although food contamination and consumption data can be used to estimate human exposure levels, such approaches raise concerns about the accuracy of the estimated levels especially for at risk populations such as infants and children. In addition, inter-individual variability in adsorption, distribution, metabolism, and excretion of mycotoxins can contribute to higher exposure of particular individuals or consumer groups. Thus, the direct monitoring of mycotoxin levels in biological fluids such as urine or blood is crucial for the most accurate estimate of human exposure to these toxins and for further refinement of diet-based models.

The majority of existing mycotoxin methods for biomonitoring studies focus on the quantitation of one or few mycotoxins of similar chemical properties, OTA being the most commonly studied in biological fluids due to its high toxicity, long lifetime in blood and high prevalence worldwide with 90–100% incidence in samples tested.<sup>66,197</sup> The use of such single analyte or class-specific methods<sup>96,198</sup> makes large scale studies of multiple mycotoxins cost prohibitive. Ideally, accurate methods for monitoring trace quantities of mycotoxins in both urine and plasma are required to obtain complementary information on both short-and medium-term

exposure, depending on the toxin half-life in plasma, as well as metabolism and excretion rates of these species. Depending on the mycotoxin of interest, monitoring of either plasma or urine specimens can provide different advantages. For example, for OTA, which has plasma life of 35 days<sup>82</sup>, monitoring of plasma is beneficial as it can provide evidence of medium-term and time-weighted average exposure. This mycotoxin is also present at higher concentrations in plasma versus urine which further supports use of this matrix.<sup>199</sup> For AFB1, analysis of plasma also reflects medium-term exposure due to AFB1 binding to plasma albumin<sup>200</sup>. On the other hand, monitoring of mycotoxins such as FB1 and T-2 in plasma provides evidence of short-term exposure due to their shorter lifetimes of 18 min and 8.1 h in rat blood, respectively.<sup>150,201</sup>

The importance of direct biomonitoring studies is illustrated by findings of higher prevalence than expected of some mycotoxins. For example, CIT and its main metabolite were detected in 90% of urine samples in a Belgian study.<sup>119</sup> Another study found that 16–69% and 1% of Belgian population may have exceeded tolerable daily intakes of DON and OTA, respectively.<sup>46</sup> Gerding *et al.*<sup>123</sup> also found 16% of urine samples collected in Germany exceeded tolerable daily intake of DON whereas 94% and 40% of study participants in southern Italy exceeded tolerable daily intakes for OTA and DON<sup>45</sup>. These studies clearly establish the need and the importance of direct biomonitoring of mycotoxins. To support multi-mycotoxin biomonitoring studies and reduce the cost of such studies, the availability of LC–MS assays that can measure as many species as possible simultaneously and without the need for immunoaffinity enrichment is critically needed. For example, Wallin *et al.* used extensive sample preparation including an enzymatic hydrolysis step, sequential immunoaffinity and reversed-phase SPE to quantitate 5–10 mycotoxins in human urine.<sup>59</sup> Although the method achieved good limits of detection for human biomonitoring, the use of immunoaffinity increases the cost per sample of the assay and/or restricts the method for analytes recognized by the antibodies utilized. To avoid these limitations, several LC–MS multi-mycotoxin methods that omit immunoaffinity enrichment have been reported and validated in urine.<sup>117,165,202</sup> These simple direct injection or dilute-and-shoot methods were recently further extended to enable (semi-)quantitation of total of 32 mycotoxins<sup>119</sup> or 23 mycotoxins<sup>123</sup>, respectively. Heyndrickx *et al.*<sup>46</sup> combined two LC–MS methods, one direct filter-and-shoot and one with extensive sample clean-up (LLE) with ethyl acetate/formic acid followed by strong ion exchange SPE to permit monitoring of a total of 33 mycotoxins, out of which 9 were detected in urine samples from children and adult Belgian population<sup>46</sup>. In addition, two methods combining QuEChERS extraction and

LC–MS for monitoring of 27 mycotoxins in human breast milk and 30 mycotoxins in animal milk were also developed.<sup>203,204</sup>

In contrast to urine and milk biomatrices, suitable multi-class LC–MS methods for biomonitoring of human plasma or serum are currently not available due to high matrix complexity, physicochemical diversity of mycotoxins of interest and the need for exceptional analytical sensitivity. Thus, for the determination of multiple mycotoxins in plasma, most methods to date focused on analysis of structurally-related mycotoxins belonging to a single family, for example ZEN and its metabolites<sup>156</sup> or enniatins and BEA.<sup>121</sup> To address these limitations, Devreese *et al.*<sup>75</sup> developed a simple acetonitrile solvent precipitation method in combination with LC–MS for the measurement of 13 mycotoxins in pig plasma suitable for toxicological studies, but the limits of quantitation (2–10 ng/ml)<sup>75</sup> do not make this method adaptable to human biomonitoring. Similarly, De Santis *et al.*<sup>137</sup> combined pronase treatment, acidified ethyl acetate LLE and QuEChERS with LC–MS detection for the analysis of 8 mycotoxins, but the method showed insufficient lower limit of quantifications (LLOQs) for accurate quantitation (mean values for positive samples below LLOQ) and significant susceptibility to matrix effects for several of the analytes despite extensive clean-up. Tolosa *et al.*<sup>205</sup> developed a dispersive liquid–liquid microextraction method using ethyl acetate in combination with LC–MS/MS for the measurement of 15 mycotoxins in fish plasma. However, the method LLOQs ranged from 1 to 17 ng/ml which is not sufficient for detection of mycotoxins in human plasma. Osteresch *et al.*<sup>136</sup> proposed a method that combines simple solvent extraction using water/acetone/acetonitrile (30:35:35, v/v/v), evaporation/reconstitution and LC–MS/MS analysis using multiple reaction monitoring mode for dried blood spots or dried serum spots. This method enables the quantitation of the largest panel of mycotoxins to date in blood (27 mycotoxins and their metabolites) with LLOQs ranging from 0.005–5.0 ng/ml which makes it suitable for human blood biomonitoring. However, significant stability and matrix effect issues were observed. For example, matrix effects ranged from 13 to 842% and from 14 to 939% for dried blood spot matrix and dried serum spot matrix, respectively, whereas the values of 80–120% indicate the absence of significant matrix effect. In summary, none of the existing methods adequately meet the needs for human biomonitoring in terms of sensitivity, coverage, accuracy, and matrix effects. Matrix effect is a complex and analyte-specific phenomenon that can be compensated by the addition of isotopically-labelled internal standards. These internal standards can compensate not only for the losses during the procedure, but also any changes in ionization

due to presence of matrix interferences. However, for the mycotoxins of interest in this work there are very few commercially available isotopically-labelled standards, and using multiple  $^{13}\text{C}$  isotopically labelled mycotoxin standards makes the method prohibitively expensive to implement for population monitoring studies. Therefore, one of the objectives of this study was to develop a sample preparation method that results in minimal absolute matrix effect while achieving high analyte recovery (>80% was preferable) for this application.

The mycotoxins selected for method development are those routinely monitored and detected in North American, and specifically, in Canadian food supply.<sup>8</sup> The effect of sample preparation (solvent precipitation, SPE and LLE) and LC separation on simultaneous analysis of all important/prevalent mycotoxin classes using a single small volume sample of human blood was investigated in detail. Special attention was also paid to minimizing matrix effects without the need for isotopically-labelled internal standards (especially if unavailable). The final method was validated for the quantitation of 17 mycotoxins of interest. Current methods do not cover a sufficiently wide range of such analytes in human plasma, and most still need immunoaffinity enrichment to obtain satisfactory limits of quantitation. The present work attempts to address the disadvantages of these current methods.

## **2.2 Materials and methods**

### **2.2.1 Chemicals**

LC-MS grade water, methanol and acetonitrile, and HPLC grade ethyl acetate were purchased from Fisher Scientific (Ottawa, Ontario, Canada). Acetic acid (AA, meets specifications of American Chemical Society grade, 99.7%), formic acid (FA, for mass spectrometry, 98%), and magnesium sulfate (anhydrous, ReagentPlus®,  $\geq 99.5\%$ ) were purchased from Sigma-Aldrich Canada (Oakville, Ontario, Canada). Pooled human plasma with sodium citrate as anti-coagulant was purchased from Bioreclamation Inc. (Baltimore, MD, USA).

### **2.2.2 Mycotoxin standards**

Nivalenol hydrate, DON, FUS-X, 3-AcDON, 15-AcDON, AFB1, AFB2, AFG2,  $\alpha$ -ZOL,  $\beta$ -ZOL, OTA and ZAN were purchased from Sigma-Aldrich Canada. AFG1, T-2, HT-2,  $\alpha$ -ZAL,  $\beta$ -ZAL, and ochratoxin A-d<sub>5</sub> (OTAd<sub>5</sub>) were purchased from Toronto Research Chemicals Inc. (Toronto,

ON, Canada). FB1, FB2 and ZEN were purchased from Cayman Chemicals (Ann Arbor, MI, USA). Individual standard stock solutions of all mycotoxins at 1 mg/ml concentration were prepared in 100% MeOH and kept at  $-80^{\circ}\text{C}$ . Fumonisin B3 (FB3, 50  $\mu\text{g}/\text{ml}$  in 50% acetonitrile) and  $^{13}\text{C}$ -zearalenone ( $^{13}\text{C}$ -ZEN, 25.5  $\mu\text{g}/\text{ml}$  in acetonitrile) were purchased from Romer Labs (Union, MO, USA). 3-acetyl- $\text{d}_3$ -deoxynivalenol solution (3-AcDON $\text{d}_3$ , 100  $\mu\text{g}/\text{ml}$  in acetonitrile) was purchased from Santa Cruz Biotechnology (Dallas, TX, USA). A combined 10  $\mu\text{g}/\text{ml}$  working solution of all mycotoxin standards was prepared in methanol every 6 months and stored in aliquots at  $-80^{\circ}\text{C}$ . Isotopically labelled standards were diluted to 10  $\mu\text{g}/\text{ml}$  for OTAd $_5$  in methanol and FB3 in acetonitrile, 4  $\mu\text{g}/\text{ml}$  for 3-AcDON $\text{d}_3$  and 1  $\mu\text{g}/\text{ml}$  for  $^{13}\text{C}$  ZEN in acetonitrile. 25 ng/ml concentration of OTAd $_5$  and FB3 was added immediately prior to LC-MS analysis while investigating different types of sample preparation techniques. The internal standards, 3-AcDON $\text{d}_3$  and  $^{13}\text{C}$  ZEN were used during final method validation at 10 ng/ml and 3 ng/ml final concentrations. During method validation, internal standards were used to monitor injection volume, signal stability and ionization matrix effects. For application of this final method to exposure studies, it is recommended to add internal standards to plasma prior to the extraction to also monitor extraction recovery in study samples as positive quality control.

### **2.2.3 Method development of sample preparation: comparison of LLE, SPE and protein precipitation methods**

#### **2.2.3.1 Protein precipitation**

300  $\mu\text{l}$  of acetonitrile was added to 100  $\mu\text{l}$  of plasma and mixed on vortex (Fisher Scientific Vortex Mixer) for 20 min. Samples were then centrifuged at  $25830\times g$ , (Thermo Fisher Scientific, Sorvall ST 16R centrifuge) for 10 min at  $4^{\circ}\text{C}$ . The 300  $\mu\text{l}$  of supernatant was aspirated into a new polypropylene extraction tube, evaporated to dryness using Speedvac (Labconco CentriVap 7812013) and reconstituted into 200  $\mu\text{l}$  of 20% methanol containing OTAd $_5$  and FB3 internal standards. This solution was transferred into polypropylene HPLC inserts for analysis.

#### **2.2.3.2 Three-step LLE procedure with ethyl acetate**

100  $\mu\text{l}$  of plasma and 150  $\mu\text{l}$  of ethyl acetate were vortexed for 20 min and centrifuged at  $25830\times g$ ,  $4^{\circ}\text{C}$  for 10 min. The organic layer (100  $\mu\text{l}$ ) was transferred into another centrifuge tube. Plasma

residues were re-extracted two more times using fresh portions of 150  $\mu$ l of ethyl acetate followed by vortexing, centrifugation and collection of the organic layers into the polypropylene collection tube. The collected organic phase (300  $\mu$ l) was evaporated to dryness using Speedvac, reconstituted into 200  $\mu$ l of 20% methanol containing internal standards, and transferred into polypropylene HPLC inserts for LC–MS analysis.

#### 2.2.3.3 Two-step LLE procedure with ethyl acetate

The same procedure as described for three-step LLE (Section 2.2.3.2) was used but only  $2 \times 150$   $\mu$ l portions of ethyl acetate were used.

#### 2.2.3.4 One step LLE procedure

100  $\mu$ l of plasma and 300  $\mu$ l of ethyl acetate were vortexed for 20 min and centrifuged at  $25830 \times g$ ,  $4^\circ\text{C}$  for 10 min. The collected organic layer (200  $\mu$ l) was transferred into a polypropylene centrifuge tube, evaporated to dryness using Speedvac, reconstituted into 20% methanol containing internal standards, and transferred into polypropylene HPLC inserts for LC–MS analysis.

#### 2.2.3.5 One-step LLE of acidified plasma with ethyl acetate or methyl tert-butyl ether (MTBE)

100  $\mu$ l of plasma was acidified with 1% (FA) to pH 4, and then extracted using ethyl acetate or methyl tert-butyl ether (MTBE) as described in one-step LLE extraction (Section 2.2.3.4).

#### 2.2.3.6 Complex four-step LLE with ethyl acetate, and sequential salt addition and acidification

Two-step LLE was performed as described in two-step LLE (Section 2.2.3.3), then  $\text{MgSO}_4$  (0.0241 g) was added to the plasma residue and extracted with a fresh portion of ethyl acetate (150  $\mu$ l) followed by vortexing, centrifugation and collection of the organic layer into the collection tube. After the third LLE step, FA (50  $\mu$ l) was added to the plasma residue and this was then extracted using a 150  $\mu$ l portion of ethyl acetate. The collected organic phase (400  $\mu$ l) was evaporated to dryness using Speedvac, reconstituted into 200  $\mu$ l of 20% methanol containing internal standards, and transferred into polypropylene HPLC inserts for LC–MS analysis.



### 2.2.3.7 HLB SPE procedure

Oasis HLB SPE (3 cc, 60 mg, average particle diameter 29.2  $\mu\text{m}$ , Waters, Massachusetts, USA) was performed as follows: (i) conditioning with 3 ml of methanol and 3 ml of  $\text{H}_2\text{O}$ , (ii) loading of 1 ml of plasma, (iii) washing of interferences with 1 ml of 5% methanol, and (iv) eluting mycotoxins with 1 ml of methanol. Collected eluents (700  $\mu\text{l}$ ) were then evaporated to dryness, reconstituted into 200  $\mu\text{l}$  of 20% methanol with internal standards, and transferred into HPLC inserts for LC–MS analysis. HLB SPE was chosen after preliminary comparison with  $\text{C}_{18}$  and SAX (Appendix A Supplementary Figure A1) because it provided the highest overall method recoveries across the analytes of interest.

### 2.2.3.8 Method comparison and selection of optimum sample preparation method

Recovery experiments were performed for each sample preparation technique in order to find an appropriate method with the highest process efficiency across different mycotoxin classes tested (Appendix A, Supplementary Figure A2). Blank plasma samples were spiked with 100 ng/ml of mycotoxins, incubated for an hour, and extracted according to the procedures described in Sections 2.2.3.1–2.2.3.7 ( $n = 3$  replicates). Blank plasma is the pooled plasma which does not contain any mycotoxins. The amount of analyte in each sample was determined using calibration curves prepared in reconstitution solvent (20% methanol) according to the formula  $\text{PE}\% = C_m/C_{th} * 100\%$ , where PE% is the process efficiency,  $C_m$  is the measured concentration in the injection solvent and  $C_{th}$  is theoretical concentration in injection solvent which includes the correction for differences in volumes transferred in specific procedures. This determination is equivalent to process efficiency as it includes the effects of both extraction recovery and matrix effects due to ionization suppression/enhancement.

In addition, ionization matrix effect was also evaluated for the best method from each sample preparation approach (Section 2.2.3). Blank plasma samples were extracted according to the procedures described in Sections 2.2.3.1, 2.2.3.2 and 2.2.3.7 ( $n = 3$ ), and then were spiked with 25 ng/ml ( $n = 3$ ) of mycotoxin mixture during the reconstitution step. Matrix effect was determined according to the formula  $\text{signal intensity}\% = A_{\text{plasma}}/A_{\text{std.}} * 100\%$ , where  $A_{\text{plasma}}$  is the measured peak area of a given mycotoxin in post-extracted spiked plasma, and  $A_{\text{std.}}$  is the measured peak area of the same mycotoxin in standard solution prepared at the same concentration in 20% methanol. The

values above 120% indicate significant ionization enhancement, while values below 80% indicate significant ionization suppression.

#### **2.2.4 Final optimized three-step LLE procedure with ethyl acetate used for method validation**

Final three-step LLE used for validation was modified as follows from the protocol used during method development. The collected organic volumes after each extraction step were changed to 70  $\mu$ l, 100  $\mu$ l and 200  $\mu$ l after the first, and second and third extraction steps, respectively. The reconstitution volume after evaporation was changed to 400  $\mu$ l to prevent early aging of the chromatographic column. Finally, the evaporation process was strictly time-controlled (320 min) in order to avoid over drying and achieve consistent recovery across different days.

#### **2.2.5 LC–MS analysis**

##### **2.2.5.1 LC–MS development**

Initial method development experiments compared the performance of core-shell Kinetex C<sub>18</sub> and PFP columns (2.6  $\mu$ m, 100 Å, 50  $\times$  2.1 mm, Phenomenex, Torrance, California, USA) in combination with various methanol and acetonitrile gradients in order to separate all mycotoxins of interest. The critical pair for this separation using both columns was found to be 3-AcDON and 15-AcDON, since the selected mass spectrometry method cannot discriminate isomers. The PFP column in combination with methanol provided good separation of all isomers, so it was selected for all further experiments. Next, the effect of mobile phase additives on mycotoxin signal intensities was investigated using PFP column and methanol gradient containing different additives (2 mM ammonium acetate, 0.1% FA or 0.1% AA). The effect of these additives on ionization in ESI(+) and ESI(–) was determined by comparing signal intensities obtained for high concentration mycotoxin standards and precision in order to find out which additive provided the highest signal intensity for given mycotoxins. Finally, for ESI(–), the concentration of the best additive (AA) was also optimized after testing 0.1%, 0.02% and 0.006% v/v AA. The final optimized conditions for LC–MS method are given in detail in Section 2.2.5.2 below.

### 2.2.5.2 Final validated LC–MS method

Chromatographic separation was performed using HPLC 1100 (Agilent Technologies, Santa Clara, CA, USA) with a Phenomenex Kinetex Pentafluorophenyl (PFP) column (2.6  $\mu\text{m}$ , 100  $\text{\AA}$ , 50  $\times$  2.1 mm, Torrance, California, USA) and a guard column (security guard ultra-cartridge for 2.1 mm ID columns) of the same type. The flow rate of 0.3 ml/min and the column temperature of 30°C (CERA Column Temperature controller for liquid chromatography heater 250, Cera Inc, Baldwin Park, California, USA) were used for all analyses. For positive electrospray ionization, the mobile phases A and B were water and methanol containing 0.1% AA (v/v). The following step gradient was used: 5% B for the first 1.0 min, increase to 50% B from 1.0 min to 3.0 min, keep isocratic at 50% B for 7 min, from 10 to 10.1 min increase to 70% B, from 10.1 to 17.5 min keep isocratic at 70% B, from 17.5 to 17.6 min increase to 98%, from 17.6 to 26.0 min keep isocratic at 98% B, and finally re-equilibrate the column at 5% B for 7 min. For negative electrospray ionization, the mobile phases A and B were water and methanol, both containing 0.02% AA (v/v). The step gradient conditions were 5% B for the first 1.0 min, increase to 50% B from 1.0 min to 3.0 min, keep isocratic conditions at 50% B for 7 min, from 10.0 to 10.1 min increase to 70% B, from 10.1 to 17.5 min keep isocratic at 70% B, from 17.5 to 17.6 min, increase to 98% B, from 17.6 up to 30.0 min keep isocratic at 98% B, and finally re-equilibrate the column at 5% B for 7 min. The washing step is longer in ESI(–) method because the reduction in the amount of acetic acid in the mobile phase increases the retention of many analytes by several minutes, so a longer wash step ensures any lipids are completely washed away before next injection. The injection volume for all analyses was 10  $\mu\text{l}$ .

High-resolution MS analysis was performed using LTQ Velos Orbitrap equipped with HESI electrospray ionization source (Thermo Scientific, San Jose, CA, USA). The following ESI(+) parameters were used: source voltage 4 kV, capillary temperature 275°C, source heater temperature 300°C, sheath gas flow 20, S-lens RF 62% and auxiliary gas flow 5. For ESI(–): source voltage 3 kV, capillary temperature 350°C, source heater temperature 300°C, sheath gas flow 20, S-lens RF 63% and auxiliary gas flow 10 were used. For both ESI( $\pm$ ), mass range 280–500 m/z, automatic gain control target  $1 \times 10^6$  ions, and resolution of 60,000 were used, except during development when mass range of 200–900 m/z was used.

All analytical batches included analysis of appropriate extraction (three-step LLE, described in Section 2.2.4) and solvent blanks (20% methanol), plasma calibration curves at the beginning and

end of the analytical batch, one solvent calibration curve and injection of quality control samples every 6–10 sample injections to ensure LC–MS stability throughout the run. Plasma calibration point with 5 ng/ml concentration was injected 4 times and used as a quality control sample during inter-day experiments. Mycotoxin standard solution with the concentration of 1.25 ng/ml prepared in injection solvent was injected 11 times and used as a quality control sample during intra-day experiments. The results of the quality control samples provided the basis of accepting or rejecting the run. Precision of the quality control replicate injections should not be more than 15%.

For data acquisition and processing, the Xcalibur software 2.7 SP1 was used. Mycotoxins were quantitated using the most intense ions from the full scan which were extracted with  $\pm 5$  ppm window. Mycotoxins that ionized efficiently in ESI(+) are aflatoxins and fumonisins with abundant protonated ions  $[M + H]^+$ , HT-2 with abundant ammonium adduct  $[M + NH_4]^+$ , and T-2 and 15-AcDON with abundant sodium adduct  $[M + Na]^+$ . Mycotoxins that exhibit better limits of detection in ESI(–) are type B trichothecenes including NIV, DON, FUS-X, and 3-AcDON producing abundant adducts with AA,  $[M + CH_3COO - H]^-$  and ZEN, ZAN,  $\beta$ -ZAL,  $\beta$ -ZOL,  $\alpha$ -ZAL,  $\alpha$ -ZOL demonstrating highly intense deprotonated molecular ion  $[M - H]^-$ . OTA is the only mycotoxin that gave similar intensities in both ionization modes with the (de)protonated molecular ion. Appendix A, Supplementary Table A1 summarizes the monoisotopic masses of the most intense ions and retention times of all mycotoxins.

### 2.2.6 Method validation

The final fully optimized method was validated according to the procedures described in FDA guidance for bioanalytical method validation.<sup>190</sup> The main parameters for validation were selectivity, linearity, absolute recovery, accuracy, precision, stability and LLOQ. Matrix-matched calibration curves were prepared each day for the quantification of mycotoxins in plasma in the range from 0.039 ng/ml to 10 ng/ml, except for NIV for which range was 3 $\times$  higher, 0.117 ng/ml to 30 ng/ml. Blank plasma was spiked with the combined mycotoxin standard to yield 10 ng/ml concentration of each mycotoxin, except for NIV at 30 ng/ml. Then, two-fold serial dilution with blank plasma was used to prepare eight more standard concentration levels, followed by mixing and incubation for 1 h at 4°C which allowed mycotoxins to equilibrate with plasma components. 4°C was required to prevent plasma composition changes caused by enzyme activity. The calibration curve samples were then treated with three-step LLE (Section 2.2.4) in the same way

as validation samples and analyzed using LC–MS. 1/x weighted linear regression was used for all mycotoxins to build calibration curves from LLOQ to upper limit of quantification (ULOQ) for each analyte. Internal standard, 3-AcDON<sub>3</sub> was used in ESI(+) for all mycotoxins, while 3-AcDON<sub>3</sub> and <sup>13</sup>C ZEN were used for early- and late-eluting ( $\alpha$ -ZOL, ZEN and ZAN) mycotoxins respectively in ESI(-). Absolute recovery was examined using three concentration levels: 0.5, 3 and 8 ng/ml (n = 3) for 16 mycotoxins, except for NIV where 9 and 24 ng/ml were used. For NIV, only two concentration levels were used because of higher LLOQ for this mycotoxin (3 ng/ml) and the expectation that NIV levels in real samples will not exceed 30 ng/ml. Therefore, two selected concentrations are sufficient to characterize method performance over narrow range of 3–30 ng/ml. For absolute recovery, blank plasma samples were spiked before extraction and analyzed against standard curves prepared using post-extracted spiked plasma. LLOQ, intra-day accuracy and precision were measured using validation samples (n = 6 replicates per concentration level) prepared by spiking blank plasma at seven concentration levels, 0.1, 0.2, 0.3, 0.5, 1, 3 and 10 ng/ml for all mycotoxins, except for NIV where 3× concentration levels were used (3 ng/ml, 9 ng/ml and 30 ng/ml), for the same reasons as described for recovery. Inter-day precision and accuracy were evaluated at the same concentration levels with one replicate per day (n = 5 days) measured against fresh plasma calibration curve prepared on that day. Inter- and intra-day precision was calculated using relative standard (RSD) formula for the concentrations determined from the calibration curves. Inter- and intra-day accuracy was calculated according to formula: accuracy =  $C_m/C_a \cdot 100\%$ , where  $C_m$  is measured concentration in validation sample and  $C_a$  is the actual value<sup>190</sup>. LLOQ was defined as the lowest concentration that meets minimum signal-to-noise ratio of 5 and the requirements for precision of  $\leq 20\%$  RSD and accuracy in the range of 80–120% based on inter- and intra-day runs. The selectivity of the method was investigated using human plasma samples from 10 different biological sources to ensure no interferences. The stability of plasma samples spiked at 0.5 ng/ml and 3 ng/ml for all mycotoxins except for 9 ng/ml NIV was evaluated under following conditions (n = 3 replicates per condition): autosampler at 4°C, freeze/thaw (3 cycles), 3 h and 6 h bench stability at room temperature.

## 2.3 Results and discussion

### 2.3.1 Development of a sensitive LC–MS method

The main objective of this study was to develop a sensitive and reliable LC–MS multi-mycotoxin assay to allow simultaneous detection and quantification of common toxicologically important mycotoxins and their metabolites frequently found in Canadian food supply and thus of possible interest for biomonitoring. In order to develop a LC–MS assay of suitable sensitivity for this application, method optimization included development of LC separation (Section 2.3.1.1), MS optimization (Section 2.3.1.2) and detailed comparison of sample preparation techniques (Section 2.3.2) for a total of 20 mycotoxins. The final optimized method was fully validated according to procedures described in FDA Bioanalytical Method Validation guidelines<sup>190</sup> for seventeen mycotoxins: AFB1, AFB2, AFG1, AFG2, ZEN,  $\alpha$ -ZOL,  $\beta$ -ZOL, ZAN,  $\alpha$ -ZAL,  $\beta$ -ZAL, T-2, HT-2, DON, NIV, 15-AcDON, 3-AcDON and FUS-X in human plasma. The proposed method is not suitable (i) for OTA, FB1 and FB2 due to poor extraction recovery by LLE shown in Supplementary Figure A9 and (ii) irreproducible retention time of FB1 and FB2 on PFP LC, which exceeded acceptance criteria for retention time variation during run of 2%.

#### 2.3.1.1 Development of LC separation

The LC–MS method development focused on the isomer separation and achieving low limits of detection by optimization of mobile phase additives. For LC separation of all mycotoxins and particularly isomers, different columns (C<sub>18</sub> and PFP), different solvents (methanol and acetonitrile), mobile phase modifiers (FA and AA), and gradients were manipulated to provide suitable separation. Achieving isomeric separation was important because tandem mass spectrometry was not used to distinguish isomers. It was found that the pentafluorophenyl column and methanol mobile phases provided the best separation of all mycotoxins and isomers, especially the separation of two isomeric compounds 15-AcDON and 3-AcDON which co-eluted when using acetonitrile-based mobile phases. The chromatographic separation of all mycotoxins is shown in Appendix A, Supplementary Figures A3 and A4. Isomers, including  $\alpha$ -ZAL and  $\beta$ -ZOL, and  $\alpha$ -ZOL,  $\beta$ -ZOL and ZAN are baseline separated except for 3-AcDON and 15-AcDON where a resolution of 0.7 is routinely obtained. In addition, 3-AcDON and 15-AcDON also show different ionization behaviour. 3-AcDON ionized better in ESI(–) whereas 15-AcDON preferentially

formed sodium adduct in ESI(+), permitting accurate quantitation. Our results of better chromatographic separation of these isomers on PFP versus C<sub>18</sub> column are similar to Breidbach<sup>206</sup> and Baker *et al.*<sup>207</sup> findings. In addition, Qi *et al.*<sup>208</sup> also applied PFP column for the separation of four aflatoxins and OTA.

During subsequent sample preparation method development and validation, the performance of both PFP and F5 columns was tested. The manufacturer describes the columns as having the same chemistry, but with a surface coverage of 2.4  $\mu\text{mol}/\text{m}^2$  for F5 versus 3.3  $\mu\text{mol}/\text{m}^2$  for PFP column. In our experiment, the selectivity of the two columns was considerably different, and F5 showed poor isomer separation even after gradient re-optimization. In addition, F5 showed build-up of triglycerides during long analytical batches which caused significant shifts in retention time of three mycotoxins ( $\alpha$ -ZOL, ZAN, and ZEN) and loss of chromatographic resolution between critical pair of  $\alpha$ -ZOL and ZAN when running long analytical batches (Appendix A, Supplementary Figure A5). Based on these results, F5 column is not recommended for this application, and PFP columns from other manufacturers should be carefully examined for similar issues if opting for PFP columns other than the recommended Kinetex PFP. These results are in agreement with Tamura *et al.*<sup>209</sup> who also found differences in isomer separation of selected mycotoxins when using PFP columns from different manufacturers.

### 2.3.1.2 Effect of mobile phase additives on ionization efficiency

The effect of additives (FA and AA) on ESI ionization efficiency was evaluated. The results showed that the intensity of 13 out of 15 tested mycotoxins increased from 1.4 x up to 26 x (for 3-AcDON) when using AA instead of FA (Appendix A, Supplementary Figure A6). No significant improvement was observed for NIV and T-2. Taking into account only mycotoxins for which ESI(-) gives better limits of detection, the average improvement obtained by using AA as additive was 4.5 x (not including 3-AcDON) showing it is important to use different mobile phases for positive and negative ESI analysis for this application. For the same mycotoxins, an additional improvement of signal intensity (ranging from 33% up to 89%) was achieved by decreasing AA concentration from 0.1% to 0.02% (v/v) in ESI(-) mode (Appendix A, Supplementary A Figure A7). Further decrease of AA concentration (0.02% versus 0.006%, v/v) showed an additional improvement of signal intensities ranging from 38% to 112%. However, 0.006% AA resulted in poor precision for all mycotoxins that form AA adduct (NIV, DON, FUS-X, and 3-AcDON). Area

RSD% of NIV, DON, FUS-X, and 3-AcDON (n = 6) were 28%, 51%, 46%, and 48%, respectively for 0.006% of AA versus 9%, 4%, 5%, and 4% for 0.02% of AA. In addition, the other mycotoxins detected in ESI(-) showed the same trend of poorer but still acceptable precision (range of RSD% was from 5 to 12% for 0.006% of AA versus 1–4% for 0.02% AA). Therefore, it is not recommended to decrease concentration of AA in mobile phase for mycotoxin analysis below 0.02% (v/v).

The influence of mobile phase additives on mycotoxin ionization efficiency has not been investigated in detail to the best of our knowledge. A variety of mobile phase additives are used for mycotoxin analysis, including FA, AA, ammonium formate, and ammonium acetate, but often only the final choice of additives is mentioned.<sup>75,114,152,210,211</sup> Among these studies, Huybrechts *et al.*<sup>119</sup> used 0.1% AA in ESI(-), and stated that both AA and acetate buffer mobile phases gave similar S/N ratios (similar sensitivity). Devreese *et al.*<sup>75</sup> used 0.1% AA and 0.01% AA for their multi-mycotoxin and ZEN class-specific methods in pig plasma samples, respectively and state that these modifiers provided the best sensitivity<sup>156</sup>, but the extent of improvement was not reported. Osteresch *et al.*<sup>136</sup> proposed the use of AA gradient and showed it provided better separation and S/N ratios than FA, but different gradients were tested for the two modifiers precluding direct side-by-side comparison. However, the potential of AA to increase signal intensity in ESI(-) was previously shown for other types of compounds. For example, Wu *et al.*<sup>212</sup> examined the effect of four mobile phase additives: formic, acetic, propionic, and n-butyric acids and their concentrations on the signal intensities of four androgen modulators without acidic functional groups in ESI(-). The maximum improvement of ionization efficiency (about 30%–50%) of four chosen compounds was obtained with 1 mM AA (equivalent to 0.006% v/v).<sup>212</sup> Zhang *et al.*<sup>213</sup> examined FA, AA, ammonium acetate, and ammonium fluoride and their concentrations on the ESI(-) ionization efficiency of 26 different standards and untargeted metabolomics of urine. The highest ionization efficiency was provided by 1 mM AA for 23 out of 26 standards and the highest metabolite coverage/intensity for untargeted metabolomics method. Although more fundamental research on this topic is needed, it is proposed that the observed good performance of AA for ESI(-) is due to a combination of factors including optimal pH of droplet environment (different than bulk pH), facilitating electrochemical reduction which in turn may improve droplet charging. High gas phase proton affinity of weak acid anions facilitate the deprotonation process



of analytes and sufficiently small molecular volume of the additive itself does not suppress analyte ionization.<sup>212,213</sup>

In summary, the final optimized LC–MS method uses a pentafluorophenyl column and the mobile phase containing water/methanol with 0.1% AA and water/methanol with 0.02% AA for ESI(+) and ESI(–), respectively to achieve the best possible limits of detection for all mycotoxins of interest.

### **2.3.2 Development of sample preparation method for multi-mycotoxin analysis**

Sample preparation is a crucial step for the development of this multi-class mycotoxin method. The mycotoxins of interest in this work are chemically diverse compounds with acidic, neutral and/or basic properties, and cover wide polarity scale (logP from –1.9 to 4.74).<sup>214–217</sup> High recovery was important for this application since mycotoxins are expected to be present in low concentrations (~pg/mL). In order to obtain high analyte recovery, good selectivity, and to minimize matrix effects in complex matrix such as plasma, several types of sample preparation techniques were initially investigated as summarized in Appendix A, Supplementary Figure A2. Among these, solvent precipitation with acetonitrile, Oasis HLB SPE, and LLE (ethyl acetate versus methyl tert-butyl ether with or without acidification and salting out) were selected for further detailed evaluation as described in Section 2.2.3.

The simplest procedure, protein precipitation with acetonitrile similar to the method proposed by Devreese *et al.*<sup>75</sup> for pig plasma, resulted in low process efficiencies of all aflatoxins (less than 45%). Matrix effects for aflatoxins ranged from 86-93% confirming that this is due to low extraction recovery (Figure 2.1a). Process efficiency below 80% was observed for NIV, 15-AcDON,  $\alpha$ -ZOL and ZAN, but matrix effect evaluation for these mycotoxins indicates that this is due to ionization suppression rather than poor extraction recovery (Figure 2.1a). Overall, our results for extraction recovery using protein precipitation matched well those of Devreese *et al.*<sup>75</sup>, after taking into account matrix effects except for AFB1. The difference in recovery observed for this mycotoxin may be due to different anticoagulant used (heparinized plasma versus citrated plasma), different species of plasma or the differences in chromatographic separation.

SPE methods, and especially Oasis HLB SPE, were successfully applied for the mycotoxin analysis in various matrices, such as aqueous environmental samples<sup>218</sup>, food<sup>219</sup> and urine samples<sup>38,45</sup>. The wide-spread application of Oasis HLB sorbent is explained by its capability to

retain different classes of mycotoxins, covering a wide range of polarity. However, this wide selectivity can also result in insufficient sample clean-up and/or requirement to extract highly hydrophobic compounds prior to SPE in order to increase the extraction efficiency of mycotoxins. For example, food supplement samples treated using combination of LLE with ethyl acetate and Oasis HLB SPE required removal of nonpolar compounds with hexane prior to SPE,<sup>219</sup> Solfrizzo *et al.*<sup>38</sup> developed a multi-analyte LC–MS/MS method for 7 mycotoxins in urine, which required two sequential SPEs, a multi-toxin immunoaffinity column and an Oasis HLB SPE, in order to get proper clean up, high recovery, and repeatability for all stated mycotoxins. The Oasis HLB SPE method (Figure 2.1a) developed in this work did not provide high process efficiencies of ZEN (21%) and its metabolites ( $\alpha$ -ZOL (8%) and  $\beta$ -ZOL (45%)), ZAN (10%), NIV (57%) and 15-AcDON (55%), OTA (16%), and AFB1 (69%) (Figure 2.1a). A matrix effect experiment (Figure 2.1b) showed significant suppression for: ZEN (57%) and  $\alpha$ -ZOL (17%),  $\beta$ -ZOL (46%), ZAN (32%), NIV (54%), 15-AcDON (29%), 3-AcDON (58%), FUS-X (76%),  $\beta$ -ZAL (78%), and  $\alpha$ -ZAL (71%). For majority of mycotoxins ionization suppression resulted in poor process efficiency, except for AFB1 and OTA where low extraction efficiency also played a role.

It should be noted that the SPE method presented here incorporates an enrichment step versus what was used for LLE, which significantly contributes to the observed ionization suppression. We also evaluated process efficiency for HLB SPE after 5x-dilution (without inclusion of evaporation/reconstitution step) to match LLE, and we still observed a low process efficiency for AFG2, AFG1, OTA,  $\alpha$ -ZOL, ZAN and ZEN. Further optimization of SPE wash and elution solvents may further improve the selectivity of SPE but was not further explored in this study as LLE provided an acceptable performance and lower cost per sample as discussed below.

To examine the recovery of mycotoxins using LLE, the selectivity of ethyl acetate versus methyl tert-butyl ether (MTBE) was first investigated. The results obtained showed that ethyl acetate provided a higher recovery for all mycotoxins of interest (Appendix A, Supplementary Figure A8b). The number of extraction steps required for complete recovery was investigated next (Appendix A, Supplementary Figure A9). Two-step LLE showed significant increase in process efficiency as expected theoretically, while third step provided noticeable gains in process efficiency for NIV, DON, FUS-X, 15-AcDON, HT-2 and T-2. Based on these results, the three-step LLE was selected. Considering the recovery of acidic mycotoxins was very low, the effect of plasma acidification prior to LLE was also investigated.

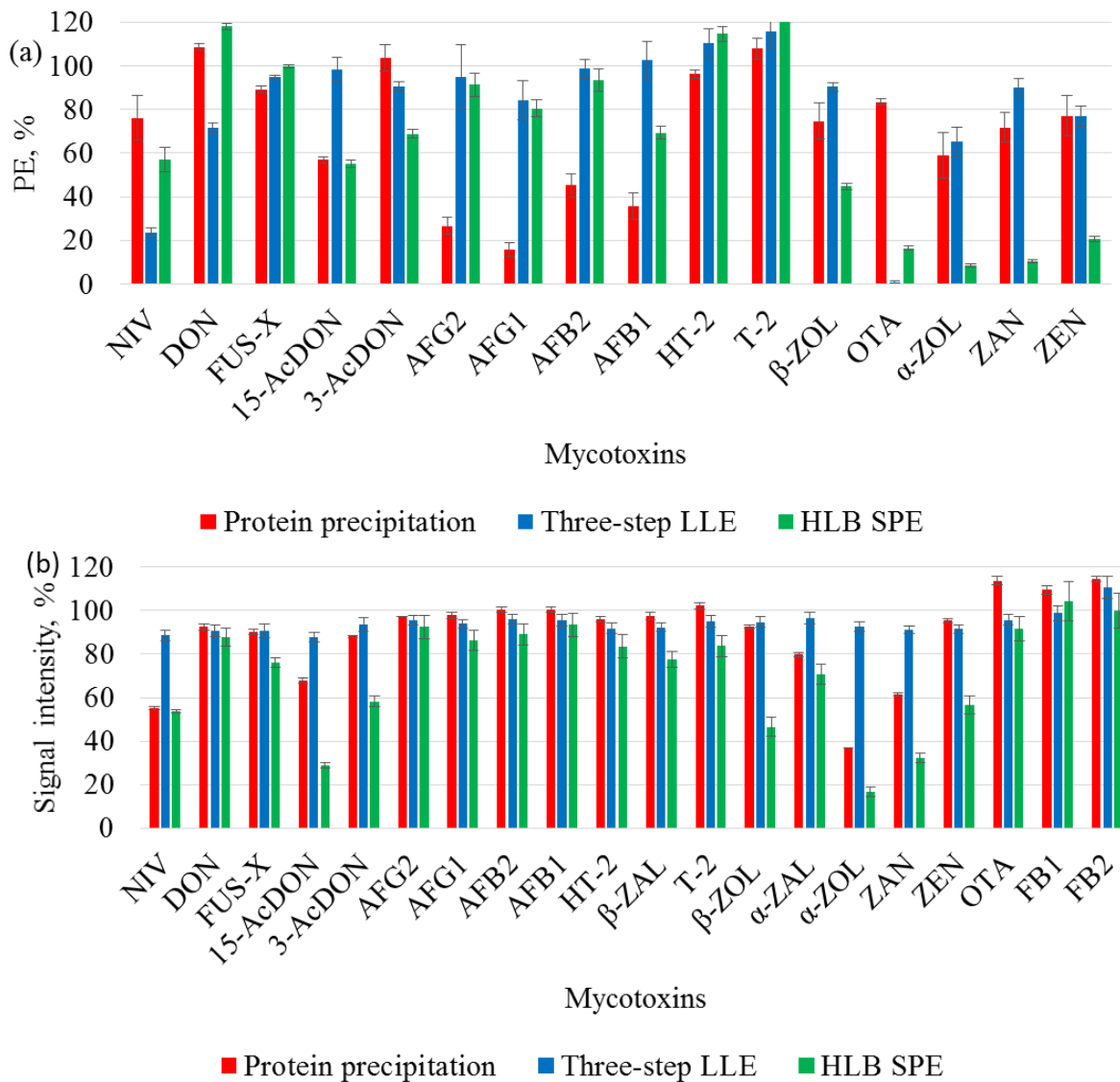


Figure 2.1. Comparison of (a) process efficiency (PE%) and (b) absolute matrix effects evaluated for mycotoxins in human plasma samples. Protein precipitation with acetonitrile, 3-step LLE with ethyl acetate, and Oasis HLB SPE were used for the evaluations of PE% and matrix effects.  $PE\% = C_m/C_{th} * 100\%$ ,  $C_m$  is the measured concentration in the injection solvent and  $C_{th}$  is theoretical concentration in injection solvent) and (b) absolute matrix effects observed for mycotoxins in human plasma using protein precipitation with acetonitrile, 3-step LLE with ethyl acetate, and Oasis HLB SPE. For (a) plasma ( $n = 3$ ) was spiked pre-extraction with 20 ng/ml of mycotoxins for LLE and SPE and 100 ng/ml for protein precipitation and analyzed against standard curve prepared in reconstitution solvent (20% methanol).  $\beta$ -ZAL and  $\alpha$ -ZAL standards were not available at the time experiment (a) was performed. For (b) extracted plasma ( $n = 3$ ) was spiked post-extraction with 25 ng/ml of mycotoxins; peak areas of mycotoxins in plasma were compared to the peak areas in solvent (20% MeOH) to estimate matrix effect. The results show mean values while error bars show standard deviation of three replicate determinations.

Considering pK<sub>a</sub> values of FB1 (pK<sub>a</sub> 3.16<sup>214</sup>), FB2 (pK<sub>a</sub> 3.16<sup>214</sup>) and OTA (pK<sub>a</sub> 4.2–4.4<sup>220</sup>), pre-spiked plasma samples were acidified with 1% of FA to a pH of 4 before one-step LLE to increase extraction efficiency. As expected, this enhanced the process efficiency of OTA (19.9%), FB1 (4.9%) and FB2 (8.9%), but unfortunately also significantly reduced the process efficiency of FUS-X, AFG1, AFB1, β-ZOL, T-2, HT-2, α-ZOL, ZAN and ZEN (Appendix A, Supplementary Figure A8a). In Appendix A, Supplementary Figure A10 shows that acidifying of plasma before or after two-step LLE results in improved process efficiency of acidic mycotoxins (OTA, FB1 and FB2) but lowers the process efficiency of all other mycotoxins because of matrix effects so lower pH values were not further explored. Finally, it was decided not to include a pH adjustment step in the final method.

Salting out effect was also investigated to improve the recovery for polar compounds, such as NIV. Addition of salts at high concentration can induce extraction of polar compounds from aqueous phase to organic one. Dissolved salt generates a combination of electrostatic repulsion and enhancement of the hydrophobic effect which disfavours water-solvated states of polar molecules forcing them to exit the aqueous phase. MgSO<sub>4</sub> was selected for this purpose based on the study by Song *et al.*<sup>114</sup> They investigated the influence of different salts on extraction efficiency of 12 mycotoxins using a salting-out assisted LLE that included addition of salt to urine samples before the extraction with ethyl acetate followed by addition of acetonitrile to the remaining sample. The highest process efficiency was achieved with MgSO<sub>4</sub> and it helped to improve process efficiency of all mycotoxins, especially polar mycotoxins such as NIV, DON, and FB1, for which the recovery increased from a few percent to almost 100%.<sup>114</sup> The use of MgSO<sub>4</sub> in our LLE method improved the process efficiency of the most polar mycotoxin NIV from 24% up to 34% (Appendix A, Supplementary Figure A10), but reduced process efficiency of all other mycotoxins. Sequential acidification followed by salt addition (Appendix A, Supplementary Figure A10) also did not result in acceptable recovery of both acidic and neutral/basic mycotoxins. Based on all these results, three step LLE using ethyl acetate without pH or salt adjustment was selected as the best LLE method for this application.

Tolosa *et al.*<sup>205</sup> and Escrivá *et al.*<sup>115</sup> also showed that ethyl acetate provided better extraction recovery than chloroform for various mycotoxins in plasma and urine samples, respectively using dispersive liquid–liquid microextraction format. Qi *et al.*<sup>208</sup> compared the extraction efficiency of ethyl acetate and toluene for four aflatoxins and OTA from snus and smokeless tobacco products,

whereas Belhassen *et al.*<sup>120</sup> used ethyl acetate for extraction of six zearanols from human urine samples with high recovery. Three type of sample preparation techniques, reversed phase SPE, LLE with chloroform and LLE with mixture of acidified acetonitrile and ethyl acetate, were also compared for the extraction of five aflatoxins and OTA from milk<sup>221</sup>. Both LLE methods resulted in better recovery than SPE, with the highest recovery provided by mixture of acidified acetonitrile and ethyl acetate.<sup>221</sup>

The results of all sample preparation techniques tested showed that there was no single method that could provide the process efficiency of all mycotoxins above 80% (Figure 2.1a). Figure 2.1 summarizes only the results of the three best methods from each technique; protein precipitation with ACN, three-step LLE with ethyl acetate, and Oasis HLB SPE. Based on the fact that three-step LLE showed no significant matrix effect for any of the mycotoxins and achieved recoveries above 80% for FUS-X, 15-AcDON, 3-AcDON, AFG2, AFG1, AB2, AFB1,  $\alpha$ -ZOL, ZAN, and ZEN mycotoxins, it was selected as the best method for this application. The presence of plasma compounds co-eluting with mycotoxins can enhance/suppress their signal intensities resulting in an inaccurate quantification, and effecting reproducibility and accuracy of the method. In addition, plasma samples without proper sample clean-up can cause early LC column aging. Therefore, the advantages of using more selective sample preparation methods such as LLE for this application are multi-fold. However, the chosen method provides unacceptably low recovery for OTA (0.6%), FB1 (0.7%), and FB2 (0.6%). Therefore, it is not recommended to monitor these analytes using the current method and OTA, FB1 and FB2 were excluded from method validation. A separate method that can provide high recovery and reduced matrix effect has to be developed for these analytes.

### **2.3.3 Results of method validation**

The primary goal of method validation is to assess the method performance for intended application. There is no specific validation guidance established for exposure monitoring studies, so the method performance in this study was evaluated using the procedures set by FDA for the evaluation of drugs and their metabolites in biological matrices using LC–MS, but slightly wider acceptance criteria of 80–120% accuracy and  $\leq 20\%$  RSD was applied for this biomonitoring method due to the measurement of very low concentrations of interest, close to instrumental LLOQ. The method validation was performed for 17 out of 20 mycotoxins; OTA and fumonisins were excluded based on their unacceptable recovery during method development. The main parameters

evaluated during method validation included: linearity, recovery, accuracy, precision, LLOQ, selectivity and stability.

Matrix-matched calibration curves were linear for all mycotoxins in the range of LLOQ to 10 ng/ml and LLOQ to 30 ng/ml for NIV with the average correlation coefficients in the range from 0.995 to 1.000. Mean absolute recoveries of 16 mycotoxins using the finalized method ranged from 74% to 113%, except for NIV (17%) (Appendix A, Supplementary Figure A11). The low absolute recovery of NIV led to higher LLOQ (3 ng/ml) than for other mycotoxins and necessitated higher spiking concentration levels for validation samples for NIV.

*Table 2.1. LOD and LLOQs of all mycotoxins and inter- and intra-day accuracy and precision obtained at LLOQ level. \*Analyte does not meet FDA requirements.*

Mycotoxin	LLOQ (ng/mL)	LLOQ (ng on-column)	ESI(-), intra-day		ESI(-), inter-day	
			Accuracy	RSD%	Accuracy	RSD%
β-ZAL	0.1	0.001	105.6	7.4	105.4	10.4
FUS-X	0.2	0.001	99.4	5.2	97.3	15.7
3-AcDON	0.2	0.001	88.4	8.3	97.1	16.7
β-ZOL	0.2	0.002	104.1	7.6	88.3	16.9
α-ZAL	0.2	0.002	100.7	6.7	84.2	11.7
DON	0.3	0.003	109.0	5.6	87.9	20.6
α-ZOL	0.5	0.005	146.0*	31.0*	91.4	15.4
ZEN	0.5	0.005	124.0*	6.5	86.5	11.8
ZAN	0.5	0.005	117.3	5.7	86.4	16.9
NIV	3	0.03	98.9	16.5	99.6	9.8
Mycotoxin	LLOQ (ng/ml)	LLOQ (ng)	ESI(+), intra-day		ESI(+), inter-day	
			Accuracy	RSD%	Accuracy	RSD%
15-AcDON	0.2	0.001	100.3	6.4	100.5	17.3
AFG2	0.2	0.002	102.9	6.1	89.6	11.4
AFG1	0.2	0.002	100.8	10.5	87.1	19.7
AB1	0.1	0.001	87.2	13.2	84.1	13.1
AFB2	0.2	0.001	96.2	9.1	86.0	14.7
HT-2	0.2	0.002	93.6	8.9	84.8	12.6
T-2	0.2	0.002	105.2	4.0	91.7	11.2

The LOD of the method was determined as the lowest concentration of mycotoxin that could be detected with a minimum signal-to-noise ratio of 3. The LLOQ of the method was determined based on the results of precision and accuracy obtained during intra- and inter-day experiments to meet the following requirements  $\leq 20\%$  RSD and the range of 80–120%,

respectively. Two compounds that did not meet the FDA requirements for LLOQ are  $\alpha$ -ZOL and ZEN. Their intra-day accuracy and precision were 146% for  $\alpha$ -ZOL with 31% RSD and 124% for ZEN with 6.5% RSD. The results obtained are summarized in Table 2.1.

The mean intra-day accuracy ranged from 85.8% to 116.4%, and intra-day precision ranged from 1.6% to 12.5% RSD for all the concentration levels higher than LLOQ except for  $\alpha$ -ZOL (Appendix A, Supplementary Figure A12). This meets the requirements of 80–120% accuracy and %RSD  $\leq$ 20% for 16 out of 17 mycotoxins.  $\alpha$ -ZOL showed poorer accuracy for 1 ng/ml (72.9% with 16.8% RSD). Inter-day accuracy and precision results are shown in Figure 2.2 and Appendix A, Supplementary Table A2. The mean accuracy ranged from 85.5% to 111.5%, while precision ranged from 2.7 to 17.7% RSD. In summary, intra- and inter-day accuracy and precision results show that this method performed well for the analysis of trace concentrations of mycotoxins, and that accuracy of 80–120% and precision of  $\leq$ 20% RSD can be achieved for all mycotoxins except for  $\alpha$ -ZOL at all concentration levels above LLOQ. The selectivity and detailed matrix effect experiments show that the poorer (and variable) precision and accuracy observed for  $\alpha$ -ZOL were primarily due to matrix effects and could not fully be compensated by using the  $^{13}\text{C}$ -labelled ZEN standard which elutes at different retention time (Appendix A, Supplementary Figure A13).

The selectivity experiment showed that there was a very intense co-eluting peak at m/z 277.1447 that can interfere with  $\alpha$ -ZOL and impact its accuracy/precision during the filling stage of the Orbitrap. The detailed investigation of absolute matrix effects in the same 10 individual plasma samples that were spiked at low mycotoxin concentrations (close to the LLOQ), show the influence of matrix on signal intensity (Figure 2.3). The experiment revealed that the zeranols could be prone to suppression in individual samples. All zeranols were suppressed more in female than male plasma samples, possibly due to suppression by female sex hormones which are structurally similar and expected to elute in the similar retention time window according to the LC-MS method developed by Capriotti et al.<sup>222</sup> Among all zeranols,  $\alpha$ -ZOL was the most affected by the plasma components, with signal intensity dropping to 29% (mean for female samples). The best solution to compensate and to monitor matrix effect for zeranols, and to have accurate quantification, especially for  $\alpha$ -ZOL, is to use a labelled internal standard for this analyte. Another option, in the absence of labelled standard, is to re-analyze  $\alpha$ -ZOL positive samples using a single-point standard addition to obtain more accurate concentrations of this mycotoxin, if required. A detailed study by Fabregat-Cabello *et al.*<sup>223</sup> compared different calibration approaches for mycotoxins in food and

feed, and found single-point standard addition is the most efficient option of accurate quantitation when an isotopically labelled internal standard is not available<sup>223</sup>. Finally, the observed matrix effects in some of the individual plasma samples will slightly impact the LOD of the method in individual samples for zeranol class of mycotoxins.

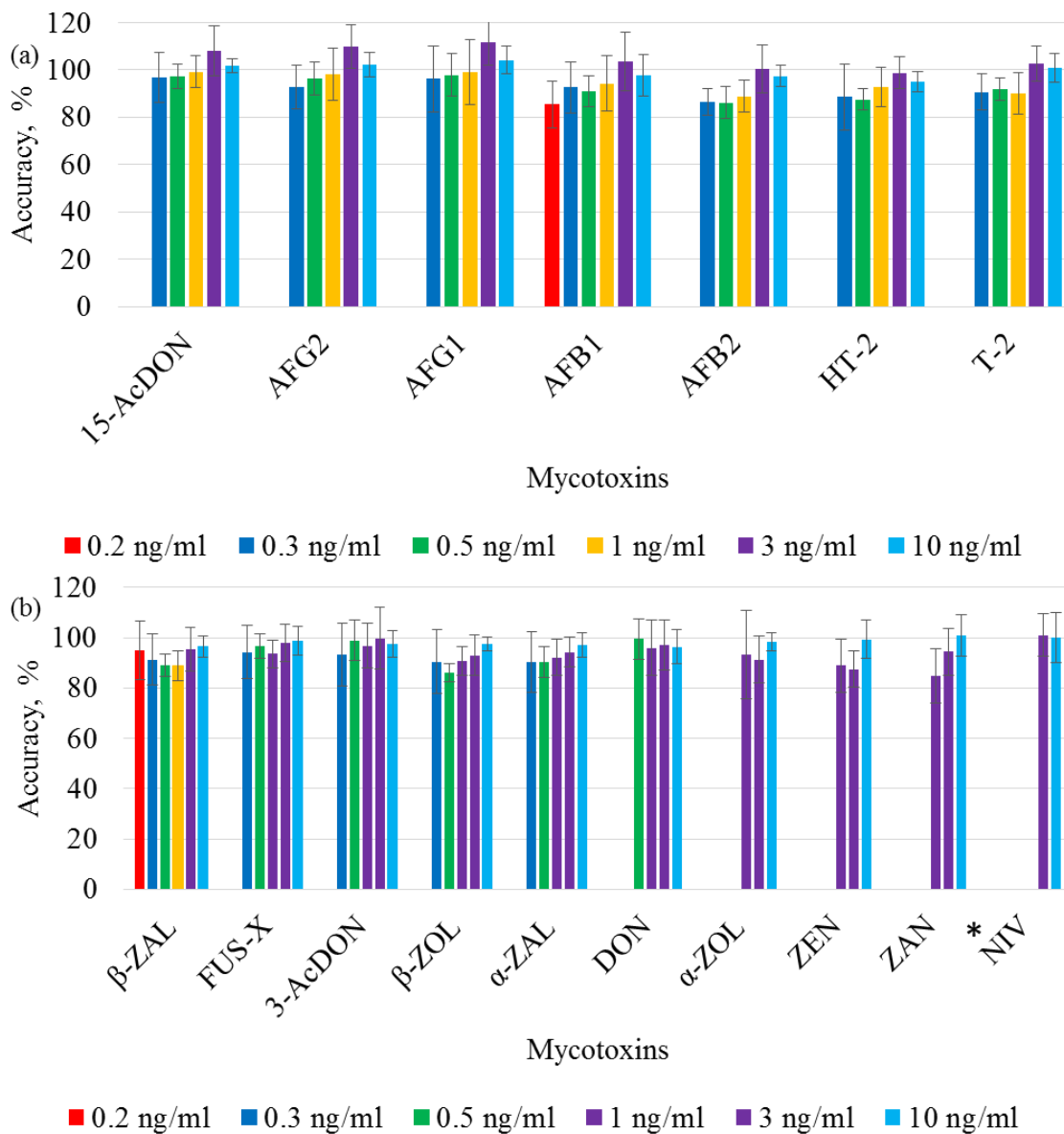


Figure 2.2. Inter-day accuracy and precision for mycotoxins detected in ESI(+) (a) and ESI(-) (b). y-axis shows mean accuracy, and standard deviation (n = 5) is shown as an error bar. Inter-day precision and accuracy determination was performed using 0.2, 0.3, 0.5, 1, 3, and 10 ng/ml validation plasma samples (n = 5 days), except for NIV where 3 x the stated concentrations were used (denoted with\*). Standard curve in plasma was prepared on each day to analyze validation samples. For each mycotoxin, all concentrations above its LLOQ are shown.



The highest impact will be for  $\alpha$ -ZOL, where 2–3 $\times$  higher LODs as well as LLOQs may be observed for the samples with severe matrix interference and suppression, while for other zeranols the effect on LOD or LLOQ will be slight to negligible. For other mycotoxin classes, Figure 2.3 shows that there were no significant absolute matrix effects detected across various individual samples. This confirms that the method will be able to provide highly accurate and precise results for these mycotoxins even if individual internal standards for each mycotoxin are not available.

The investigation of stability, namely, prepared extract stability on autosampler at 4°C for 96 h and stability during 3 freeze/thaw cycles showed that all analytes are stable at these conditions except DON for which a significant increase in recovery was observed for 96 h 0.5 ng/ml sample (Appendix A, Supplementary Figures A14 and 15). The 96 h stability shows that very long analytical batches, suitable for exposure monitoring studies, can be accommodated using the current method. However, tests of 3 h and 6 h bench stability of plasma samples at room temperature revealed that two compounds out of 17, AFG2 and AFG1 were not stable at these conditions (Appendix A, Supplementary Figure A14).

This result is in agreement with the study by Diaz *et al.*<sup>224</sup> They found that the AFG2 and AFG1 stability depends on temperature and composition of the solvent.<sup>224</sup> Huge losses of AFG2 and AFG1 were observed when they were dissolved in an organic solvent with any amount of water and kept for 24 h at 20°C. However, no significant decrease was noticed for AFG2 and AFG1 dissolved in a solution containing more than 20% of organic solvent and kept at 5°C. The evaluation of autosampler stability in this paper was performed using 20% organic solvent and showed similar stability of these compounds. For the purposes of this method, unacceptable benchtop stability of AFG1 and AFG2 in plasma means that plasma should be thawed on ice and processed immediately after thawing.

The method developed and validated in this work provides better sensitivity than the multi-class mycotoxin method proposed for pig plasma (2–10 ng/ml)<sup>75</sup> and analyte-specific methods proposed in the same work (0.5–5 ng/ml). In comparison to multi-mycotoxin method for dried serum spots, our assay provides better LLOQs for T-2, ZAN, ZEN and HT-2, similar LLOQ for AFG2 and slightly poorer LLOQs for other aflatoxins, but it should be noted that a S/N of 10 criteria was used for the determination of LLOQ without stringent accuracy/precision requirements applied in current study.<sup>136</sup> The LLOQs for aflatoxins in our work were 0.1 ng/ml for AFB1 and 0.2 ng/ml for the remaining aflatoxins. These results are better or similar to the class-specific

methods used for the direct measurement of aflatoxins in plasma or serum. For instance, reported LLOQs for aflatoxins using LC–MS/MS analysis ranged from 1 ng/ml for ethyl acetate LLE<sup>225</sup>, 0.21–0.43 ng/ml for dilute-and-shoot method by Cao *et al.*<sup>139</sup>, and 0.13–0.42 ng/ml for HLB SPE.<sup>226</sup>

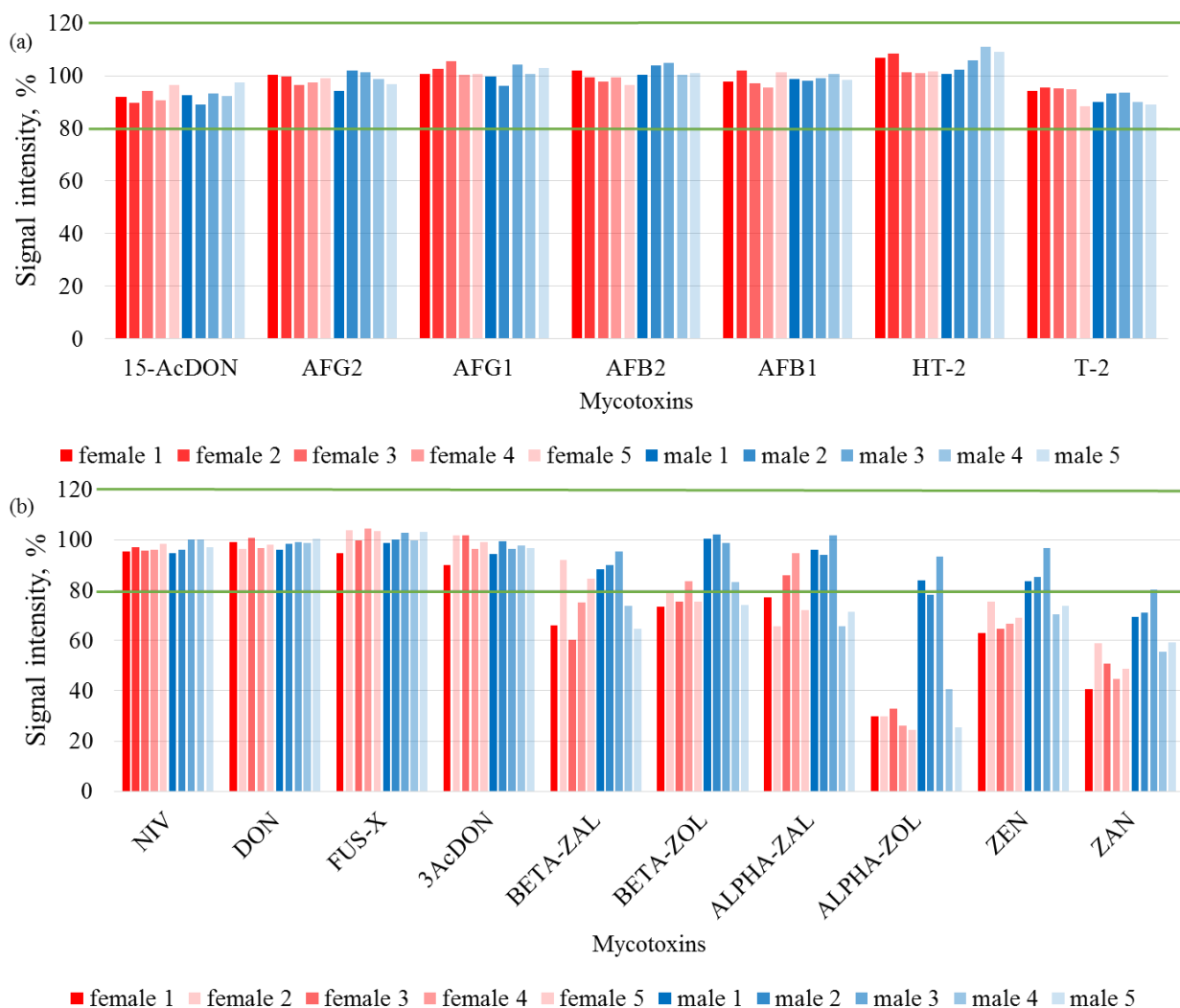


Figure 2.3. Investigation of absolute ionization matrix effect in 10 individual plasma samples using ESI(+) (a) and ESI(-) (b). Plasma samples were spiked with mycotoxin mixture to have concentration 0.3 ng/ml for 15-AcDON, AFB1, AFB2, AFG1, AFG2, HT-2, T-2, 3-ACDON, FUS-X,  $\beta$ -ZAN,  $\beta$ -ZOL,  $\alpha$ -ZAN, 1.5 ng/ml for DON,  $\alpha$ -ZOL, ZEN, ZAN and 9 ng/ml for NIV. The area of post-extraction spiked individual plasma was compared to the area of the standard solution prepared in 20% MeOH in order to determine absolute matrix effect.

It should be noted that all three of these studies used S/N ratio for LLOQ determination, while our study used the more stringent accuracy and precision requirements. Corcuera *et al.* obtained LLOQ of 2 ng/ml for AFB1 in combination with UHPLC with Post-column Fluorescence Derivatization (UHPLC-FLD) analysis using similar LLOQ criteria to our study.<sup>102</sup> For type A

trichothecenes, HT-2 and T-2, we established LLOQs of 0.2 ng/ml. This is significantly better than reported LLOQs in literature for animal plasma matrices which ranged from 1 ng/ml for pig plasma<sup>153</sup>, 2.5 ng/ml for chicken plasma<sup>153</sup> and 1–2 ng/ml for pig plasma.<sup>154</sup> Our results are comparable to analyte-specific method for AFB1 and T-2 where LLOQ of 0.05 ng/ml was obtained in rat plasma after protein precipitation and SPE and using S/N criterion of 10.<sup>150</sup> Type B trichothecenes had LLOQs of 0.2 ng/ml (3-AcDON and 15-AcDON) and 0.3 ng/ml (DON) in our study. In contrast, Broakert *et al.* reported LLOQs for 1–2 ng/ml for chicken plasma and 0.1–1 ng/ml for pig plasma for the same three analytes when using acetonitrile protein precipitation<sup>151</sup>, de Baere *et al.* reported 1 ng/ml for pig plasma (DON), 1.25 ng/ml for chicken plasma for DON when using a combination of protein precipitation and HLB SPE<sup>153</sup>, and Brezina *et al.* reported 0.45 ng/ml using HLB SPE for DON.<sup>152</sup> For other members of this family (NIV and FUS-X) we did not find any relevant literature for comparison. For the ZEN class, our LLOQs ranged from 0.1–0.5 ng/ml. Songsermsakul *et al.* reported 0.5–0.6 ng/ml for determination of this class in horse plasma<sup>155</sup>, whereas Brezina *et al.* reported LLOQs between 0.08–2.37 ng/ml using HLB SPE in pig serum.<sup>152</sup> In addition, LLOQs obtained for ZEN and its metabolites are better in current study than for analyte-specific method that relied on protein precipitation (0.2–5 ng/ml) in chicken and pig plasma<sup>156</sup>. Overall, the LLOQs for our multi-mycotoxin method compare well with class-specific methods previously reported in literature and provide similar or significantly better LLOQs while expanding the number of mycotoxins that can be evaluated. In addition, for many of the mycotoxins under study, this is first method developed for their measurement in human plasma.

For the mycotoxins included in current method, there is very limited data available on their concentrations and occurrence in plasma or serum. In a study of serum from 213 children, De Santis *et al.*<sup>137</sup> reported range from <LOD to 27.9 ng/ml for DON (19.5% positive), ZEN <LOD to 3.9 ng/ml (5.4% positive) and <LOD to 0.73 ng/ml for AFB1 (22.9% positive). Based on these reported concentrations, our method should be suitable for human biomonitoring studies and provides better LLOQs for two out of these three mycotoxins, while providing capability to simultaneously monitor additional 14 mycotoxins.

The simultaneous analysis is a critical aspect of this work. During biomonitoring studies, it is not known a priori which mycotoxins may be present. The availability of a method that can accurately measure large number of mycotoxins that commonly occur in the food supply reduces the cost of analysis per sample over methods that would focus only on a single mycotoxin. It allows

monitoring of large number of samples (hundreds or thousands) to identify sub-populations that may exceed recommended exposure guidelines. The use of high-resolution Orbitrap mass spectrometry and the extraction/separation methods which can accommodate mycotoxins of varying polarity, also permits the use of this method for screening of additional mycotoxin metabolites for later inclusion in the panel. These mycotoxin metabolites can be missed by targeted strategies relying on multiple reaction monitoring, and thus an underestimation of mycotoxin prevalence and concentrations can be reported. This has been illustrated well in recent studies on urine, where direct monitoring of urine samples for parent compounds resulted in low detection of positive study samples (0–8%) for ZEN and its metabolites, whereas inclusion of enzymatic hydrolysis and immunoaffinity cleanup step showed much higher prevalence across all studies ranging from 17 to 100% depending on geographic location and analyte.<sup>182</sup> In addition, high-resolution MS data can also be retrospectively examined for other mycotoxins that may become of particular health interest. The main disadvantages of high-resolution MS for this application are large file size, high cost of instrumentation and data analysis time required for retrospective analysis.

## 2.4 Conclusions

The goal of this study was to develop a sensitive and reliable LC–MS based multi-mycotoxin assay allowing simultaneous detection and quantification of common toxicologically important mycotoxins and their metabolites. The method was successfully developed and validated for 17 out of 20 initially stated mycotoxins, with 15 of these mycotoxins meeting accuracy and precision of 80–120% and  $\leq 20\%$  RSD at all concentrations tested including LLOQ. High sensitivity of the method was achieved through careful optimization of sample preparation technique, chromatographic separation, and mobile phase additive selection. With newer models of Orbitrap, additional shortening of analysis time and improved limits of detection can be anticipated. The cost per sample of the method was kept low by employing LLE and minimizing absolute matrix effects which permits the use of limited number of isotopically labelled internal standards for quality control purposes. This makes the proposed method cost-effective for implementation in large-scale population monitoring efforts. The main disadvantage of our method is that additional IS for  $\alpha$ -ZOL is highly desirable and should be incorporated in future studies whenever possible (or alternately, standard addition method should be used for  $\alpha$ -ZOL positive samples). Due to the use

of high-resolution MS, the method can also be used for screening of the presence of additional mycotoxins and their metabolites for future inclusion in the panel and to study mycotoxin metabolism in humans in more detail. It will also allow to study temporal and inter-individual differences of mycotoxin concentrations as insufficient data exists for the mycotoxins in our panel. To the best of our knowledge, this is the first LC–MS method for highly sensitive analysis and quantification of 17 mycotoxins in human plasma samples. The availability of this method opens up new and exciting opportunities for direct exposure monitoring of these common contaminants.

### **3. Characterization of Phase I and glucuronide Phase II metabolites of 17 mycotoxins using liquid chromatography – high-resolution mass spectrometry**

Chapter 3 was published in an article entitled “Characterization of Phase I and glucuronide Phase II metabolites of 17 mycotoxins using liquid chromatography—high-resolution mass spectrometry” authored by I. Slobodchikova, R. Sivakumar, S. Rahman and D. Vuckovic, in *Toxins* 2019, 11(8), 433.

#### **3.1 Introduction**

Mycotoxins are toxic chemically diverse secondary metabolites produced by filamentous fungi. Their structural diversity can give rise to several adverse effects in humans and animals, such as carcinogenicity, immunosuppression, teratogenicity, nephrotoxicity, and hepatotoxicity.<sup>2</sup> The contamination of food and feed supply with low levels of mycotoxins is widespread, and includes commodities such as wine, apple juice, cereals, milk, coffee beans, maize, nuts, dried fruits, and meat products.<sup>11,13,193,195,227,228</sup> For example, a worldwide survey of more than 19,000 cereal and oilseed samples found that 72% were contaminated with one or more mycotoxins: aflatoxins (26%), DON (56%), OTA (25%), fumonisins (54%), and ZEN (37%).<sup>8</sup> In agreement with these findings, the most recent surveys of Canadian food supply showed 59% and 75% of the tested samples had detectable levels of at least one mycotoxin, with the most frequent incidence of DON.<sup>9,11</sup> Many other studies to date have also confirmed the co-occurrence of multiple mycotoxins in food and feed samples<sup>5,8,229</sup>, which in turn may lead to synergistic or antagonistic effects. Currently, the assessment of human mycotoxin exposure is primarily modelled from the measured/estimated levels of mycotoxins in the various foods and the calculated daily average food intake of various food groups to estimate population exposure and introduce regulations for food monitoring when appropriate. However, an individual’s food consumption pattern depends on personal preferences. Thus, population-based food intake models can lead to the inaccurate estimation of human exposure to mycotoxins and, subsequently, higher health risk in some sub-populations. Vegetarian and non-vegetarian adult exposure to DON is one such example, whereby a recent U.K. study found  $\sim 2 \times$  higher mean level of DON in vegetarians than in non-vegetarians.<sup>48</sup> Furthermore, the exceeded recommended tolerable daily intakes (32%) were found only in

individuals belonging to the vegetarian group. Biomonitoring of adult and children urine samples in large-scale exposure studies also demonstrated that daily tolerable intake was exceeded for some mycotoxins.<sup>38,44,46</sup>

To address the limitations of food-based models, direct human biomonitoring of biological fluids is proposed as an alternative approach to assess health risk.<sup>38,44,46</sup> However, this approach currently has several limitations. It requires high-throughput, multi-mycotoxin methods that have very low limits-of-detection in complex biological matrices such as blood and urine. Secondly, metabolic pathways have not been investigated thoroughly for all mycotoxins and key metabolites have not yet been prioritized for inclusion in routine biomonitoring.<sup>230</sup> Consequently, most of the existing analytical LC-MS methods used for the assessment of human exposure focus only on the detection of parent compounds. This can lead to a significant underestimation of mycotoxin exposure. For example, a recent study of DON metabolism in humans confirmed the need for the inclusion of its metabolites in biomonitoring.<sup>54</sup> They showed that approximately 72.6% of total urinary DON was composed of its glucuronides, 15-Gluc-DON and 3-Gluc-DON and only 27.4% was present as free DON.<sup>54</sup> Thus, the measurement of DON only would underestimate DON exposure by ~4 ×. Other studies have also confirmed the importance of 15-Gluc-DON as a predominant glucuronide.<sup>46,231,232</sup> In general, biomonitoring methods should combine parent compounds and their predominant metabolite(s) in order to properly estimate exposure risk.<sup>168</sup>

Currently, most of the mycotoxin biomonitoring is performed using urine since it is non-invasive and accessible in relatively large volume. These methods can be divided into methods with and without  $\beta$ -glucuronidase treatment.  $\beta$ -glucuronidase catalyzes the hydrolysis of conjugated mycotoxins, such as sulfate and glucuronide conjugates. Thus, the use of enzymatic hydrolysis can provide an appropriate alternative to direct metabolite monitoring for at least those mycotoxins which are predominately metabolized to Phase II conjugated forms such as DON.<sup>54,87</sup> To date, such methods cover 7–11 mycotoxins.<sup>38,84,87,139</sup> The main disadvantages of  $\beta$ -glucuronidase treatment are: increases the cost per sample, requires longer processing time of about 16–18 h, and the additional step in sample preparation may give a rise to quantification errors. Multi-mycotoxin methods without  $\beta$ -glucuronidase treatment have been developed for 8–32 mycotoxins in urine<sup>44,115,117,119,137,202</sup>, and for 8–27 mycotoxins in blood, serum or plasma.<sup>136,137,139,233</sup> However, these methods often include no or limited direct monitoring of mycotoxin metabolites.

Due to their toxicity, *in vivo* data on mycotoxin metabolism in humans after exposure is rare, with few exceptions.<sup>54</sup> Animal models have been used more frequently, but the inter-species differences in mycotoxin metabolism should be taken into consideration.<sup>162,174,189</sup> *In vitro* human liver microsomal incubations have been used extensively in the metabolism studies of mycotoxins, for example to obtain metabolic profile of T-2 and HT-2 toxins<sup>162,189</sup>, or to study in detail the glucuronidation of the ZEN group.<sup>177,234,235</sup> Human liver microsomes contain a variety of enzymes that are involved in both Phase I and Phase II toxin metabolism and reaction conditions can be easily controlled to generate the needed quantity of metabolites. The examples of Phase I reactions are oxidation, reduction, dehalogenation, or hydrolysis and are catalyzed by several enzymes including cytochrome P450. Phase II reactions are conjugation reactions, for example with glucuronic acid, sulfate, glutathione, and/or amino acids. HRMS provides an excellent analytical platform for the characterization and investigation of mycotoxin metabolites and putative biomarkers for further human biomonitoring.<sup>168</sup> The combination of HRMS and metabolic software can greatly speed up and expand the ability to capture the broad spectrum of mycotoxin metabolites using both accurate-mass of full-scan MS and/or fragmentation mass spectral data (MS/MS or MS<sup>n</sup>). For instance, Yang *et al.* used HRMS to study T-2 and HT-2 metabolism in different species and identify main metabolic pathways and novel metabolites.<sup>162,189</sup> However, such single-analyte metabolism studies relied on a variety of analytical platforms and methods, thus hindering the creation of a comprehensive metabolite LC-MS library using a single analytical method and its further application in human biomonitoring. As such, it is of utmost importance to include mycotoxin metabolites in ongoing biomonitoring efforts and to use this information to prioritize the most observed mycotoxin metabolites that may contribute to under-estimation of exposure. To achieve this goal, the first step is to fully characterize and build a comprehensive LC-MS library of mycotoxin metabolites using a single well-characterized LC-MS method.

In this work we present *in vitro* metabolism studies of 17 mycotoxins detected in the Canadian food supply: AFB1, AFB2, AFG1, AFG2, ZEN,  $\alpha$ -ZOL,  $\beta$ -ZOL, ZAN,  $\alpha$ -ZAL,  $\beta$ -ZAL, T-2, HT-2, DON, NIV, 15-AcDON, 3-AcDON and FUS-X in order to characterize Phase I and glucuronide Phase II mycotoxin metabolites. Mycotoxin metabolites were generated *in vitro* using pooled human liver microsomes to build an extensive in-house library of these species, for which standard compounds are often not commercially available. The final in-house LC-MS library was built using a previously published validated method for sensitive quantitation of 17 mycotoxins in



plasma using LC-HRMS.<sup>233</sup> The use of this method allowed excellent chromatographic separation of many isomers and the optimized highly sensitive HRMS detection allowed detailed characterization of both known and novel metabolites.

## 3.2 Materials and methods

### 3.2.1 Chemicals

Water (H<sub>2</sub>O, LC-MS grade), methanol (MeOH), LC-MS grade), acetonitrile (MeCN, LC-MS grade), and acetic acid (AA, LC-MS grade) were purchased from Fisher Scientific (Ottawa, Ontario, Canada). Sodium chloride (NaCl), meets specifications of American Chemical Society grade (ACS),  $\geq 99.0\%$ ), sodium phosphate dibasic (Na<sub>2</sub>HPO<sub>4</sub>, ACS,  $\geq 99.0\%$ ), potassium phosphate monobasic (KH<sub>2</sub>PO<sub>4</sub>, ACS,  $\geq 99.0\%$ ), and magnesium chloride (MgCl<sub>2</sub>, anhydrous,  $\geq 98\%$ ),  $\beta$ -nicotinamide adenine dinucleotide 2'-phosphate reduced tetrasodium salt hydrate (NADPH,  $\geq 97\%$ ), uridine 5'-diphosphoglucuronic acid trisodium salt (UDPGA, 98–100%), alamethicin from *Trichoderma viride* ( $\geq 98\%$ , HPLC grade), and human microsomes from liver (pooled, CMV-negative, 20 mg/mL) were purchased from Sigma-Aldrich Canada (Oakville, Ontario, Canada). Potassium chloride (KCl, reagent grade, 99.0%) was purchased from BioShop Canada (Burlington, Ontario, Canada).

### 3.2.2 Mycotoxin standards

All mycotoxins were purchased from Sigma-Aldrich Canada, unless otherwise indicated. AFG1, T-2, HT-2,  $\alpha$ -ZAL,  $\beta$ -ZAL were purchased from Toronto Research Chemicals Inc. (Toronto, ON, Canada). Zearalenone was purchased from Cayman Chemicals (Ann Arbor, MI, USA). Individual standard stock solutions of all mycotoxins at 1 mg/ml concentration were prepared in methanol and kept at  $-80^{\circ}\text{C}$ .

### 3.2.3 Experimental design and microsomal incubations

The purpose of this work was to generate Phase I and Phase II (glucuronidation) metabolites of 17 mycotoxins using a standard *in vitro* microsomal incubation protocol. Each toxin was incubated individually with microsomes in the presence of NADPH for Phase I reactions. For Phase II glucuronidation reactions, UDPGA, alamethicin and MgCl<sub>2</sub> were also added. In all cases, the following controls were used in order to confirm product formation during enzymatic reaction: (i)

microsomal incubation without toxin added, (ii) microsomal incubation without co-factors added (iii), microsomal incubation without NADPH, but containing UDPGA, alamethicin and MgCl<sub>2</sub>, (iv) incubation with heated microsomes, and (v) standard solution of each toxin dissolved in PBS buffer. This experimental design is summarized in Figure 3.1.

PBS buffer (pH 7.4, 100 mM), 20 mM NADPH dissolved in 100 mM PBS buffer, 100 mM UDPGA in water, 5 mg/mL alamethicin in MeOH, 100 mM MgCl<sub>2</sub> in water and 200 µg/mL standard solution of each mycotoxin in MeCN were prepared before the start of microsomal incubations. Microsomes were thawed on ice. In an Eppendorf tube, 182 µL of PBS buffer, 2 µL of NADPH and 5 µL of microsomes were transferred for Phase I reactions. For phase II reactions, all of the reagents for Phase I reactions plus alamethicin, 10 µL of UDPGA and MgCl<sub>2</sub> were transferred. Microsomes were then pre-incubated for 5 min, followed by the addition of mycotoxin (final concentration of 1 µg/mL) and then the remaining amount of NADPH (10 µL). All samples were incubated for 1 h at 37°C, reactions were stopped by adding 200 µL of acetonitrile. Detailed description of test samples and controls is shown in Appendix B, Supplementary Table B1.

### 3.2.4 LC-HRMS analysis

All LC-MS measurements were performed according to the validated multi-mycotoxin method for 17 parent mycotoxins [29]. Briefly, the method combined HPLC 1100 (Agilent Technologies, Santa Clara, CA, USA) and reversed-phase chromatographic separation on pentafluorophenyl stationary phase and gradient elution using water and methanol containing 0.1% AA (v/v) for ESI(+), and 0.02% for ESI(-)<sup>233</sup>. The flow rate of 0.3 mL/min, the column temperature of 30°C, and 10 µL injection volume were used for all analyses. MS analysis was performed on LTQ Orbitrap Velos at 60,000 resolving power using the mass range of 200–700 m/z. In addition, MS<sup>n</sup> analysis with data-dependent acquisition (DDA) mode was used for the identification and elucidation of metabolite structures. In DDA mode, the three most intense ions from the full MS scan were selected for MS<sup>2</sup> fragmentation. MS<sup>2</sup> analysis used collision-induced dissociation (CID) and signal threshold: 5,000; normalized collision energy: 35; isolation width: 2 Da; activation time: 30 ms. MS<sup>3</sup> used targeted parent and product mass lists to trigger MS<sup>3</sup> for the selected ions of interest. MS<sup>3</sup> was performed with CID as activation type; minimal signal threshold: 5000; isolation width: 2 Da; activation time: 30 ms; normalized collision energy: 45. For AFB1 and its metabolites, MS<sup>2</sup> analysis used higher energy collisional dissociation (HCD) with signal threshold: 5000;

normalized collision energy: 35; isolation width: 2 Da; activation time: 0.1 ms, lock mass was used for ESI(-) and ESI(+).

Data was processed using Compound Discoverer 2.1 (ThermoFisher Scientific). Raw data files were uploaded to Compound Discoverer and analyzed using generic metabolism workflow. General settings in the workflow were mass tolerance, 5 ppm; signal threshold, 3; minimum peak intensity 10000. Parameters used to generate expected compounds were parent toxin structure, metabolic transformations for Phase I and II reactions, and preferred ions.

### 3.3 Results

Human liver microsomes are important and common tool for *in vitro* investigations of toxin metabolism because they express a variety of enzymes which are involved in Phase I metabolism such as microsomal cytochrome P450 (P450) and flavin-containing monooxygenases (FMO). These enzymes are responsible for the most common Phase I reactions, such as oxidation. Usually, toxins are converted to more polar compounds due to Phase I reactions. Phase II metabolism provides an additional mechanism to clear toxins from the body by adding water-soluble groups, such as glucuronic, methyl, sulfate and acetyl groups.<sup>159,168</sup> In this work, phase II glucuronidation reaction was chosen as a major human metabolic pathway of toxins in addition to Phase I metabolism. In total, 17 mycotoxins, such as trichothecene type A (T-2 and HT-2), trichothecene type B (NIV, FUS-X, DON, 3-AcDON and 15-AcDON), aflatoxins (AFB1, AFB2, AFG1, and AFG2) and ZEN group (ZEN,  $\alpha$ -ZOL,  $\beta$ -ZOL, ZAN,  $\alpha$ -ZAL, and  $\beta$ -ZAL) were incubated individually in the presence of human microsomes and 188 different fungal metabolites were characterized and detected. The analysis of all microsomal incubation samples was performed with HRMS (LTQ Orbitrap Velos) coupled with liquid chromatography in order to detect and identify the mycotoxin metabolites. Structural elucidation of metabolites was performed using data-dependent MS/MS acquisition and CID fragmentation technique. Metabolite characterization and data analysis was performed using Compound Discoverer software 2.1, which contains extensive libraries of common metabolic pathways and mass spectral libraries.

To confirm the enzymatic origin of metabolites, besides test samples for the Phase I and II, several controls were used as shown in Figure 3.1 and Appendix B, Supplementary Table B1: standard that contains toxin dissolved in PBS buffer, control without any co-factors, control without NADPH, but with UDPGA, and controls with previously heated microsomes (45°C) for

both Phase I and II samples. The mycotoxin standard control and the controls without cofactors were used to highlight and eliminate the metabolites that are not enzymatically produced from the final LC-MS library. Finally, the controls without toxin ensured that any endogenous species present in microsomes would not be misidentified as mycotoxin metabolites. The controls with pre-heated microsomes were included in the experiment to test the stability of microsomal enzymes. In heat-inactivated samples, the metabolic activity was changed, and the generation of metabolites was reduced during the Phase I metabolic reactions indicating that the responsible enzymes were sensitive to heat (Figure 3.2a). However, an opposite effect was observed in the phase II reactions, whereby an increased rate of glucuronidation was observed in all mycotoxin samples (Figure 3.2b). The deactivation of Phase I metabolism observed in our study matches the previously published work about enzyme stability.<sup>236,237</sup> In contrast, uridine 5'-diphosphoglucuronosyltransferases (UGTs), the key enzymes used in our phase II glucuronidation reactions, appear to be thermally stable enzymes<sup>238</sup>, and the heat-inactivation step was beneficial to generating additional glucuronide metabolites in sufficient quantities for detailed characterization.

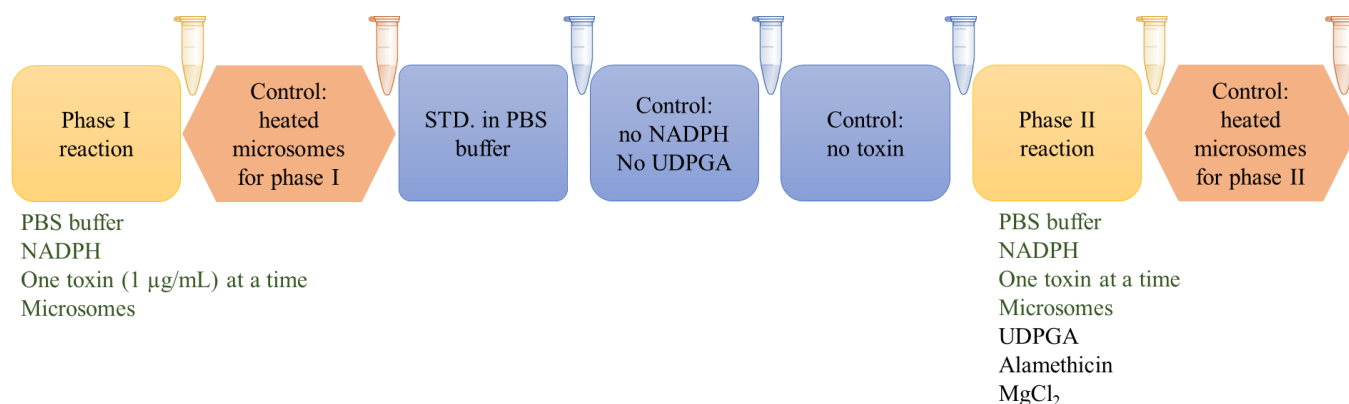


*Figure 3.1. Scheme of microsomal incubation experiment to generate Phase I and glucuronide Phase II metabolites.*

### 3.3.1 Trichothecene type A and B

#### 3.3.1.1 Trichothecene type A

The list of T-2 generated metabolites is shown in Appendix B, Supplementary Table B2. There were two main pathways for T-2 metabolites, hydrolysis, and oxidation in Phase I (Figure 3.3).

The chromatographic separation of T-2 and its metabolites is shown in Appendix B, Supplementary Figures B1 and B2. The identification of metabolites was performed by comparing  $[M+Na]^+$  product ion mass spectra of T-2 and its metabolites. The fragmentation pattern of T-2 showed some characteristic fragments, 387.2 m/z, 327.2 m/z and 267.2 m/z due to the loss of isovaleric acid ( $C_5H_{10}O_2$ , 102.1 Da) at position 8, and acetic acid ( $CH_3COOH$ ) at positions 15 or 4, respectively, (Appendix B, Supplementary Figure B3d). The extracted ion chromatogram of  $[M+Na]^+$  ion at 447.1989 m/z revealed two peaks at 7.93 min (447.1988, 0.22 ppm) and 8.22 min (447.1986, 0.67 ppm), indicating the presence of two metabolites that were 42.0 Da less than T-2 (Appendix B, Supplementary Figures B1 and B4a,b). The peak observed at 8.22 min was identified as HT-2, since it had the same RT and  $MS^2$  as the authentic standard of HT2. The second peak could be putatively identified as 15-deacetyl-T-2 (15-de-Ac-T-2). 15-de-Ac-T-2 had been previously observed as a metabolite of T-2 in Wistar rats.<sup>239</sup> Based on the structure of T-2, the possible loss of 42.0 Da can be due to the loss of the second acetyl group at position 15. Also, both metabolites had identical  $MS^2$  spectra with the typical losses of isovaleric side chain (102.1 Da) and acetic acid (60.0 Da) at fragments of 345.2 Da and 285.2 Da, respectively (Appendix B, Supplementary Table B2 and Figure B4a,b). There was also another ion at 405.1881 (0.74 ppm) m/z corresponding to a loss of two acetyl groups from T-2, but it was very low intensity ion, so further identification was not possible (Appendix B, Supplementary Table B2 and Figure B1). The literature reports two possible compounds with this mass, NEO and T-2 triol.<sup>154,239</sup>

The second pathway observed in Phase I reactions was oxidation of both T-2 and HT-2. The theoretical masses of  $[M+Na]^+$  ions of T-2 (505.2044) and HT-2 (463.1939) hydroxyl-metabolites were 16.0 Da higher than T-2 and HT-2, which confirmed the presence of additional oxygen in those compounds (Appendix B, Supplementary Table B2). There were three T-2 hydroxy metabolites observed at 6.54 min (505.2042, 0.40 ppm), 6.60 min 505.2041, 0.59 ppm), and 6.81 min (505.2043, 0.2 ppm), Appendix B, Supplementary Table B2 and Figure B2.

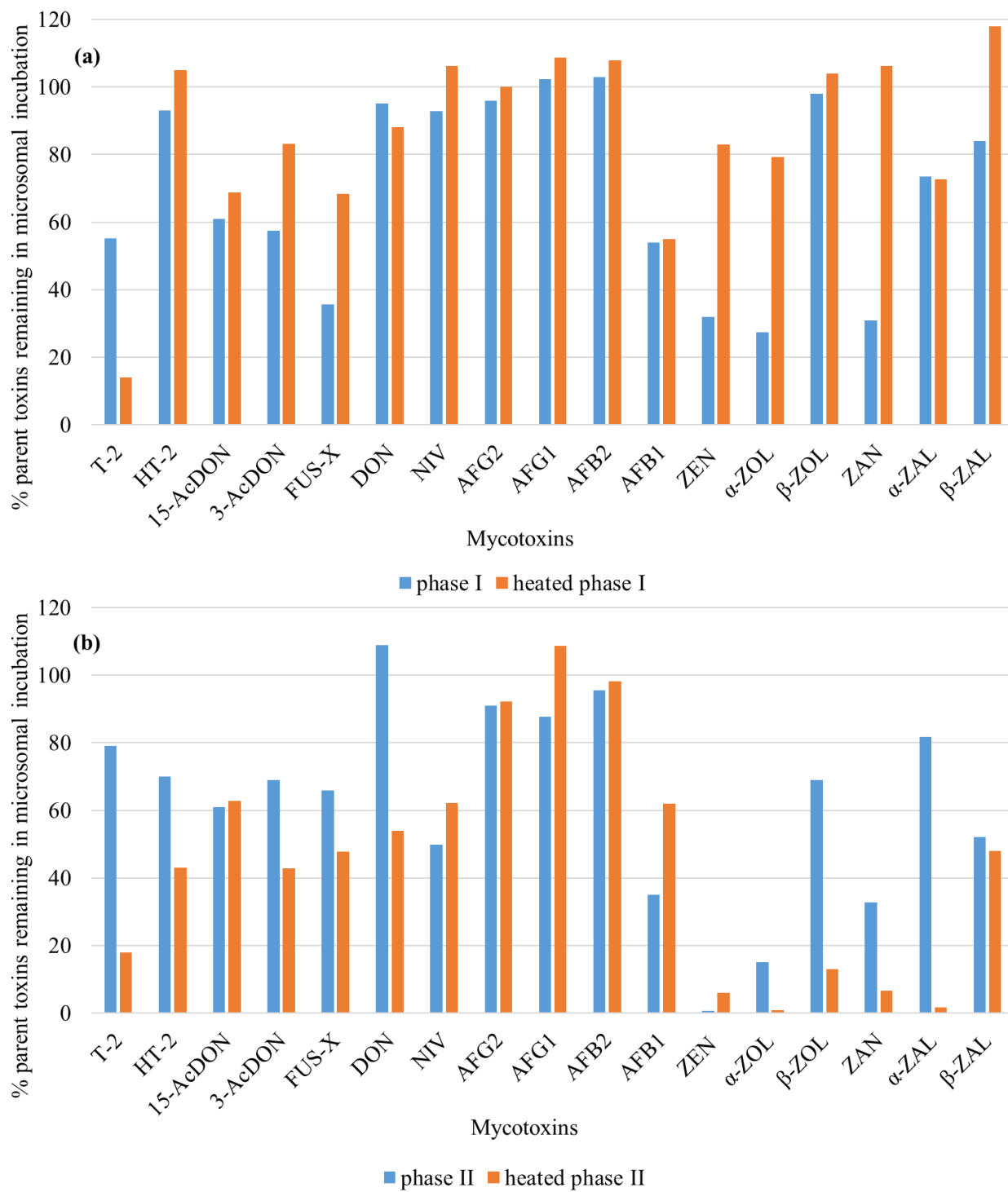


Figure 3.2. Comparison of the amount of parent toxins remaining after incubation in Phase I and heated Phase I (a) and Phase II and heated Phase II (b) microsomal incubation samples.

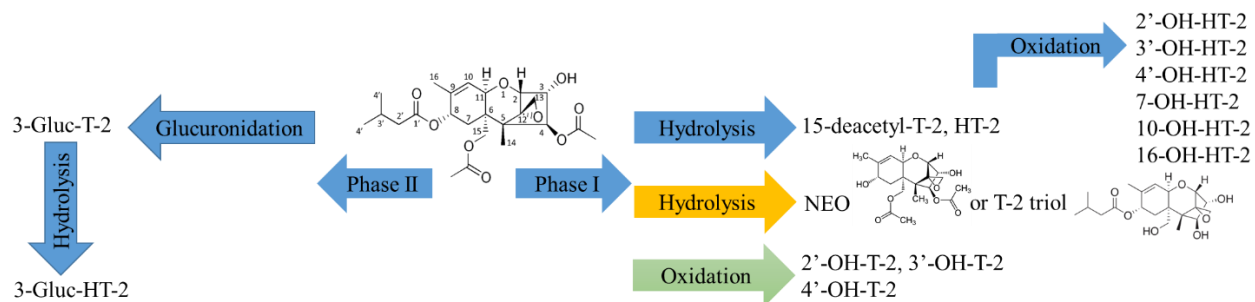


Figure 3.3. Microsomal biotransformation of T-2 in Phase I and Phase II reactions.

All three hydroxyl metabolites had similar MS<sup>2</sup> spectra, Appendix B, Supplementary Table B2 and Figure B3a–c). The position of hydroxyl group was identified by comparing [M+Na]<sup>+</sup> product ion spectra of the hydroxyl-metabolites and T-2. In MS<sup>2</sup> spectrum of hydroxyl metabolites there was a fragment with 387.2 m/z that could be generated as the loss of isovaleric acid side chain plus oxygen atom (C<sub>5</sub>H<sub>10</sub>O<sub>3</sub>, 118.1 Da). This fragment showed a 16.0 Da shift that indicated the position of hydroxyl group on the isovaleric side chain. Therefore, all three hydroxyl metabolites have OH group on isovaleric side at position 3', 4' or 2', (Appendix B, Supplementary Table B2 and Figure B3a–c). Hydroxy metabolites of HT-T-2 also had a 16.0 Da shift. The numbering of HT-2 metabolites was chosen to match numbering of the peaks described for HT-2 where incubation and detailed characterization was performed with HT-2. T-2 microsomal incubation samples had 5 out of 6 metabolites of these hydroxyl metabolites, but their intensity was ~4 × less than in HT-2 incubations, Appendix B, Supplementary Table B2 and Figure B2. Overall, only 26% of T-2 metabolized in Phase I reactions, with HT-2 as the predominant metabolite. The metabolism of T-2 has already been investigated by Yang *et al.* in farm animals and humans.<sup>162</sup> Our data are in agreement with their results, HT-2 is predominant metabolite of T-2. However, our study also generated two additional new hydroxyl metabolites of T-2. LC chromatographic separation of isomers using our pentafluorophenyl stationary phase and/or excellent limits of detection of the method may have facilitated the detection of these additional metabolites versus previous work. Furthermore, these newly detected metabolites are consistent with the available sites on T-2 for hydroxyl modifications.

In phase II reaction samples of T-2, there were two glucuronide forms, glucuronide of T-2 and HT-2 (Figure 3.3, Appendix B, Supplementary Table B2, and Figure B5). Different metabolic activity was observed in the phase II sample and heated control, about 79% and 18% of T-2 did not metabolize, respectively (Figure 3.2b). The most predominant glucuronide form was

glucuronide of HT-2 (51%) and only 8% T-2 glucuronide was present in the heated control. Their product ion mass spectra of  $[M+Na]^+$ , 665.2413 m/z (-0.43 ppm) and 623.2304 m/z (-0.96 ppm) showed the indicative loss for glucuronides, 176.0 Da and typical fragments, 489.2 m/z and 447.5 m/z of T-2 and HT-2 respectively, confirming the T-2 and HT-2 origin of glucuronides, Appendix B, Supplementary Table B2 and Figure B6a,b. Further comparison of the product ion spectra of  $[M+NH_4]^+$  (Appendix B, Supplementary Figure B6c) to literature spectra confirmed this glucuronide as 3-glucuronide-HT-2 (3-Gluc-HT-2) by the presence of fragment ions of 425.2 and 499.0 and their relative intensities to each other.<sup>154,162</sup> Ion with 499.0 m/z should be less intense than 425.2 m/z according to published data. According to the structure of T-2 and literature data there was only one possible glucuronide of T-2, 3-glucuronide-T-2 (3-Gluc-T-2).<sup>240</sup>

The generated metabolites of HT-2 are presented in Appendix B, Supplementary Table B3. HT-2 is a main metabolite of T-2 and has hydroxyl group at position 4 instead of acetyl group. Two pathways were observed in Phase I reactions, hydrolysis, and oxidation. The chromatographic separation of HT-2 and its metabolites is shown in Appendix B, Supplementary Figures B7 and B8. Two hydrolysis products were observed as shown in Appendix B, Supplementary Table B3 and Figure B7. The extracted ion of  $[M+Na]^+$  at m/z 363.1413 (0.28 ppm) shows the 84.1 Da mass difference from HT-2  $[M+Na]^+$  ion, which can be attributed to the loss of isovaleric group at position 8 and the addition of OH group. The first peak at 3.56 min can be putatively identified as 4-deacetyl-neosolaniol (4-de-Ac-NEO) which has OH group instead of isovaleric group. The product ion spectrum of the first peak has fragments with mass of 345.1 Da and 303.1 Da that confirm the water loss and further loss of acetic acid which were also found in the product ion spectra of HT-2, Appendix B, Supplementary Table B3. The  $[M+Na]^+$  ion at m/z 463.1939 was 16.0 Da higher than HT-2  $[M+Na]^+$  ion, m/z 447.1989, and confirmed the hydroxylation pathway, Appendix B, Supplementary Table B3. The extracted ion chromatogram displayed 6 peaks with the same m/z 463.1936 (0.65 ppm) at 5.67 min, 5.77 min, 5.95 min, 6.11 min, 6.21 min and 8.23 min, Appendix B, Supplementary Figure B8. The first two peaks at RTs of 5.67 min and 5.77 min have similar product ion spectra, containing an indicative fragment ion at m/z 345.5 and 345.2, respectively, Appendix B, Supplementary Table B3 and Figure B9a,b. These ions were generated as the loss of isovaleric side chain ( $C_5H_{10}O_2$ ) plus oxygen atom resulting in the neutral loss of 118.1 Da. The presence of these fragments confirmed the position of hydroxyl group at isovaleric side chain either at position 3' or 4'. 3' and 4'-hydroxy-HT-2 metabolites were observed in human and



animals, respectively, by Yang *et al.*<sup>162</sup> The third peak at 5.95 min was a very low intensity, and its product ion spectra were similar to the previous peaks (Appendix B, Supplementary Figure B9c), assuming that OH is present at isovaleric group at position 2'. For the next three peaks, the loss of 102.1 Da results in an ion fragment with  $m/z$  361.2 Da, so it indicates that the isovaleric side chain is not changed, Appendix B, Supplementary Table B3 and Figure B9d–f. Therefore, the position of OH group can be found at the position 7, 10 or 16 carbon atoms. However, the product mass spectra are similar, so further identification is not possible. Overall, six hydroxyl metabolites were also detected by Yang *et al.*, but only four of their metabolites were observed in human liver microsomes<sup>189</sup>. Additionally, two peaks at RT of 5.44 min and 6.55 min were observed with the mass of 405.1880 (0.99 ppm) which corresponds to 42.0 Da difference from the parent compound (HT-2) which could indicate the loss of acyl group at position 15, Appendix B, Supplementary Table B3. However, their product ion mass spectra showed similar losses to HT-2. Based on the fragments at 303.2  $m/z$  and 345.2  $m/z$  which were generated as the loss of isovaleric acid (102 Da) and acetic acid (60 Da) respectively it was concluded that the main structure is not changed, and from the known metabolites it was not possible to propose putative structures. Overall, our data are similar to the previous metabolism studies done by Yang *et al.*<sup>189</sup>, confirming hydroxylation as the major pathway of HT-2.

In phase II reaction samples of HT-2, the 3-glucuronide of HT-2 was generated as described when discussing the observed T-2 metabolites.

### 3.3.1.2 Trichothecene type B

The common Phase I pathways of type B trichothecenes are de-acetylation for 3/15-AcDON and FUS-X and de-epoxidation for DON (Figure 3.4) and NIV. Microsomal biotransformation of DON is summarized in Figure 3.4 as an example representative for this family. Chromatographic separation and MS<sup>2</sup> spectra of 3/15-AcDON, FUS-X, DON, NIV and their metabolites are shown in Appendix B, Supplementary Tables B4–B8 and Figures B10–B21. In Phase I, all metabolites were generated non-enzymatically—all these metabolites were observed not only in the Phase I sample, but also in controls without NADPH and in heat-inactivated controls. The examples of non-enzymatic reactions included the removal of acetyl group in 3-AcDON converting into DON and DOM-1, 15-AcDON into DON, FUS-X into NIV, DON into DOM-1, and NIV converted into de-epoxy-nivalenol (DNIV), Appendix B, Supplementary Tables B4–B8. 1% of 15-AcDON and

50% of 3-AcDON was converted into DON, whereas 54% of FUS-X was converted into NIV. Only 5% of NIV was converted into DNIV and less than 1% of DON to DNIV. Higher deacetylation rate of 3-AcDON than 15-AcDON had already been demonstrated in literature.<sup>241</sup> In our studies, these metabolites were clearly of non-enzymatic origin; however, other studies have also shown that 3-AcDON can be metabolized to DON (78%) during incubation with human feces.<sup>242</sup>

During Phase II incubations, type B trichothecenes generated 3- and 15-Gluc-DON (1%), shown in Figure 3.4, Gluc-3-AcDON (11%), and Gluc-15-AcDON (1%) (Appendix B, Supplementary Table B4–B8 and Figures B10–B15, B17–B21), whereas heated samples generated 3- and 15-Gluc-DON (2%), 41% of Gluc-3-AcDON and 2% of Gluc-15-AcDON. However, to observe the glucuronidation of NIV (<1%) and FUS-X (<1%), it was necessary to increase the mycotoxin concentration x10 and incubation time (20 h), and they were only observed in heated samples (Appendix B, Supplementary Figures B18 and B20). The identifications of glucuronides were based on the product ion spectra of  $[M-H]^-$  for Gluc-FUS-X (529.1561, 0.32 ppm), Gluc-NIV (487.1457, 0.23 ppm), 3- and 15-Gluc-DON (471.1508, 0 ppm), and Gluc-3-AcDON (513.1614, 0.19 ppm) and  $[M+Na]^+$  for Gluc-15-AcDON (537.1575, 0.74 ppm), Appendix B, Supplementary Tables B4–B8.

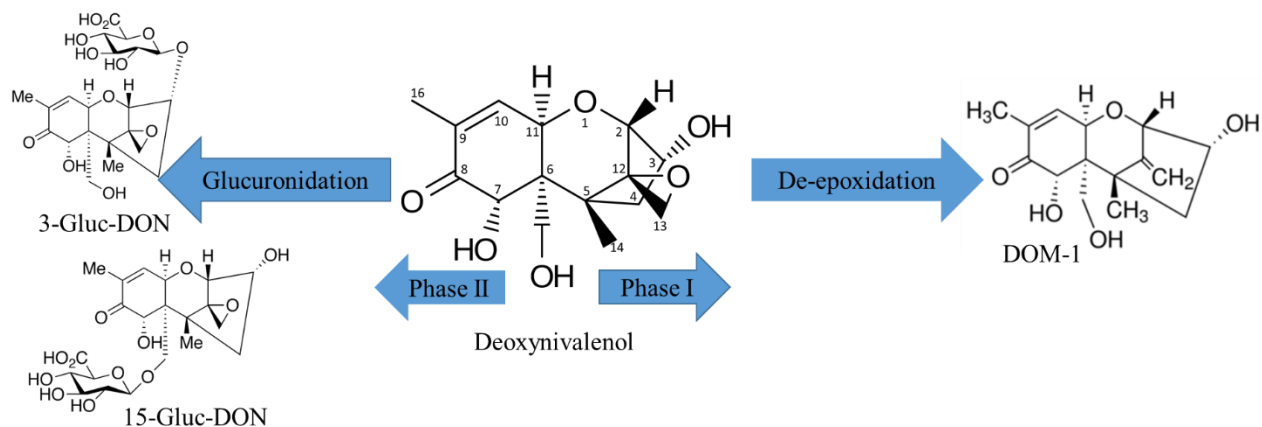


Figure 3.4. Microsomal biotransformation of DON in Phase I and II reactions.

It is interesting to note that all glucuronides in ESI(-) generated only  $[M-H]^-$  and not  $[M+HAc-H]^-$  as their parent mycotoxins. Some mycotoxins, like DON (2 forms), FUS-X (2 forms), and NIV (3 forms), could have more than one glucuronic form based on their structures. In our experiment, we possibly observed two glucuronides of DON based on two distinctive product mass spectra, 3 and 15-Gluc-DON. However, the peaks were not fully resolved and MS<sup>2</sup> spectra could be a mixture of the two, Appendix B, Supplementary Figures B14 and B17. According to the literature, the first

peak can be assigned as 3-Gluc-DON and the second as 15-Gluc-DON.<sup>232</sup> MS<sup>2</sup> spectrum of the first peak has intense fragment of 441.1 m/z that can happen due to the loss of CH<sub>2</sub>O at position 15 when it is not glucuronidated, Appendix B, Supplementary Figure B17. The partial chromatographic separation of 3-Gluc-DON and 15-Gluc-DON shows that the predominant form is 15-Gluc-DON. FUS-X glucuronide showed only one chromatographic peak as shown in Appendix B, Supplementary Figure B18. Previously, FUS-X glucuronides were not reported either in animal or human samples (Appendix B, Supplementary Figure B19). NIV glucuronides showed two not fully resolved peaks, assuming that there are at least two glucuronic forms present, Appendix B, Supplementary Figure B20. Only one MS<sup>2</sup> spectrum was obtained for the second peak, Appendix B, Supplementary Figure B21b. However, previous studies of NIV metabolism in rats exhibited only one 3-glucuronide-NIV and DNIV<sup>243</sup>. De-epoxidation of DON also was observed in both human and animals.<sup>54,244,245</sup> In contrast to rat metabolism studies, NIV incubation with human feces showed no de-epoxydated metabolites.<sup>242</sup> To the best of our knowledge, NIV glucuronides have not been previously observed in human samples, possibly due to the low extent of glucuronidation and/or poor limits of detection for the polar NIV and its metabolites using most LC-MS methods. The human exposure studies to DON revealed that the predominant species were 15-Gluc-DON (49%), then free DON (27%), and 3-Gluc-DON (14%) in urine and proposed to use them as biomarkers of DON exposure.<sup>54</sup> Despite trichothecene type B mycotoxins, including DON, being extensively studied, we found new metabolites, showing the importance of these detailed incubation studies and the need to build more systematic libraries of mycotoxin metabolites.

### 3.3.2 Aflatoxins

AFB1 microsomal biotransformations included the following three types of reactions: oxidative (hydroxylation, epoxidation), reductive (keto-reduction), and hydrolytic (hydrolysis) in Phase I, as summarized in Figure 3.5 and Appendix B, Supplementary Table B9. AFB1 generated various metabolites, including AFM1 (3%), AFBO (<1%), AFB1-diol (<1%), and minor metabolites, AFP1 (<1%), ((H2)+(O))-AFB1 (<1%), and AFL (<1%). The chromatographic separation of AFB1 and its metabolites is shown in Appendix B, Supplementary Figure B22. All metabolites were identified based on their MS1 and comparison of their MS<sup>2</sup> spectra to the literature data as described in Appendix B, Supplementary Table B9. Two hydroxy-metabolites at m/z 329.0651 (1.8 ppm) showed shift of 16.0 Da versus [M+H]<sup>+</sup> ion of AFB1 at 313.0707 (0 ppm), thus

confirming the presence of additional oxygen in those compounds, Appendix B, Supplementary Table B9 and Figure B23a,b. The first peak at RT of 5.03 min was identified as AFBO based on the fact of in-source AFB1-diol formation, Appendix B, Supplementary Figures B22 and B23e. AFBO was previously described as a non-stable compound that reacts with water to form AFB1-diol.<sup>246,247</sup> The second peak at RT 6.32 min was identified as hydroxy-metabolite, AFM1. The identification of this hydroxy metabolite was performed by comparing its product ion mass spectra (Appendix B, Supplementary Figure B23b) to the published one.<sup>248</sup> The main distinctive fragment ion of AFM1 is 273.0757 m/z, which can be present only in AFM1 and not in its isomer AFQ1 based on the previously published work by Walton *et al.*<sup>249</sup> Also, fragment ions of 273.1 Da and 259.0 Da observed in our product ion spectra were chosen as quantifier and qualifier ion for AFM1 in other published papers.<sup>221,248,250</sup> Finally, MS<sup>2</sup> of AFM1 is similar to product mass spectra obtained by Everley *et al.*<sup>248</sup> [M+H]<sup>+</sup> ion at m/z 347.0760 (0.23 ppm) was 34.0 mass units greater than AFB1, Appendix B, Supplementary Table B9 and Figure B23c,d. This difference indicated the presence of two hydroxyl groups, whereas the presence of two chromatographic peaks indicates the presence of two isomers as shown in Appendix B, Supplementary Figure B22. Their MS<sup>2</sup> spectra exhibited the intense water loss fragment, 329.0650 (3.3 ppm) and 329.0653 (2.1 ppm) for the first and the second peaks, which confirms the presence of hydroxyl groups, Appendix B, Supplementary Figure B23c,d. Additionally, both peaks showed the loss of two water molecules that yielded fragments, 311.0545 (3.5 ppm) and 311.0549 (2.3 ppm), Appendix B, Supplementary Figure B23c,d. The first peak can be identified as AFB1-diol with hydroxyl groups at positions 8 and 9. Its product mass spectra fragments, 283.0597 (38%) and 329.0650 (100%), have similar intensity as shown by Walton *et al.*, namely, 329.1 (100%) and 283.0 (32%).<sup>249</sup> The identification of O-demethylated products with theoretical mass of [M+H]<sup>+</sup> ion at 299.0550 m/z resulted in two chromatographic peaks at 7.05 min (299.0549, 0.33 ppm) and 7.31 min (299.0549, 0.33 ppm), Appendix B, Supplementary Table B9 and Figure B22. Both peaks had similar product ion mass spectra, Appendix B, Supplementary Figure B24. Based on the comparison of fragment ions 271.0602 Da and 299.0554 Da (Appendix B, Supplementary Figure B24) observed in their product ion mass spectra to the literature data, it was possible to determine these peaks as AFP1 and its isomer.<sup>249</sup> Two metabolites of keto-reduction pathway with measured m/z 337.0682 (0 ppm) of [M+Na]<sup>+</sup> ion at 8.60 min and 7.66 min were putatively identified as AFL and its isomer, respectively, since they were found at trace level, Appendix B, Supplementary Table B9 and Figure

B22. The conversion of AFB1 to AFL was previously confirmed using *in vitro* studies of placental human microsomal proteins.<sup>251</sup> One more type of reduction reaction with the further oxidation resulted in metabolites (+H<sub>2</sub>)+(O)-AFB1 with m/z 331.0812 (0 ppm) of [M+H]<sup>+</sup> ion at and RT at 5.45 min, Appendix B, Supplementary Table B9 and Figures B22 and B23f. This metabolite definitely has AFB1 origin, since its product mass spectrum has the same fragments, 285.0757 m/z and 313.0705 m/z as AFB1 (Appendix B, Supplementary Figure B23). The loss of H<sub>2</sub>O (18.0106, 0 ppm) in product ion mass spectra confirmed the OH group in this molecule. Dohnal *et al.* reviewed aflatoxin metabolism and concluded that besides the interspecies differences there were also regional, inter-individual differences.<sup>252</sup> The main urinary metabolite of AFB1 was AFM1, which was observed in Brazilian volunteers.<sup>166</sup> Also, AFM1 was found in Italian adult urine samples<sup>45</sup> and Italian children urine and serum samples.<sup>137</sup> However, AFQ1 was found as the most predominant form of aflatoxins in Chinese urinary and fecal samples.<sup>167</sup> Also, previously it was shown that different enzymes are responsible for the conversion of AFB1 to AFQ1 and AFM1.<sup>253,254</sup>

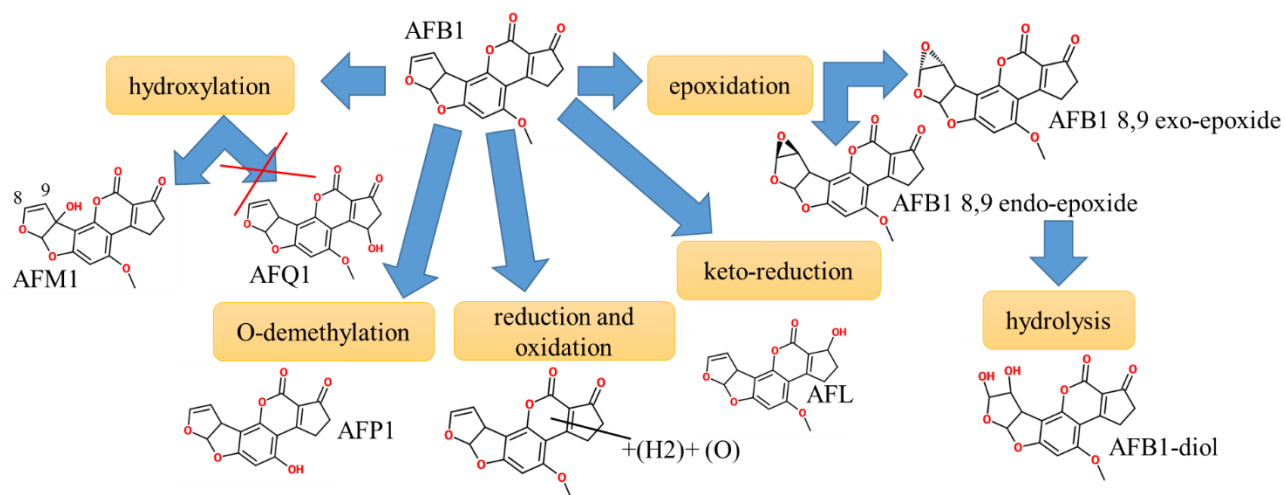


Figure 3.5. Microsomal biotransformations of AFB1 in Phase I reactions.

The remaining aflatoxins, AFG1, AFB2 and AFG2 were unstable during the experiment and produced non-enzymatic hydroxyl metabolites. AFG1, AFB2, AFG2 and their metabolites are summarized in Appendix B, Supplementary Tables B10–B12. The stability of aflatoxins in plasma at room temperature was evaluated and it was shown that AFG1 and AFG2 were not stable in plasma for more than 3 h.<sup>233</sup> Another stability study demonstrated the dependence of aflatoxin stability on the temperature and the composition of the solvent.<sup>224</sup> One hydroxy metabolite with enzymatic origin was observed corresponding to the hydroxy-metabolite of AFG1, [M+H]<sup>+</sup> ion at

m/z 345.0604 (0.3 ppm), Appendix B, Supplementary Table B11. MS<sup>2</sup> spectra of AFG1 and its hydroxyl metabolite are shown in Appendix B, Supplementary Figure B25a,b. This AFG1 hydroxy metabolite can be putatively identified as aflatoxin GM1 (AFGM1) metabolite<sup>255</sup>; however, this metabolite, to our knowledge, had not been previously found in human samples. Studies of the prevalence of different aflatoxins in Egyptian infant blood and urine samples performed by Hatem *et al.* did not confirm its presence.<sup>256</sup> To our knowledge, there were no *in vitro* metabolism studies performed for AFG1 or AFG2. In our experiment, four non-enzymatic hydroxy metabolites of AFG2 (Appendix B, Supplementary Table B12) were observed with 347.0761 m/z, at least two of them could be aflatoxin GM2 (AFGM2) and aflatoxin G2A (AFG2A) as mentioned in the previous review paper.<sup>254</sup> Product mass spectrum of AFG2 is shown in Appendix B, Supplementary Figure B26. AFB2 was converted non-enzymatically to three hydroxy metabolites with 331.0813 m/z (Appendix B, Supplementary Table B10). Product mass spectra of AFB2 and its hydroxyl metabolites are shown in Appendix B, Supplementary Figure B27a–c. Putatively, they can be identified as previously mentioned aflatoxin M2 (AFM2), aflatoxin Q2 (AFQ2), and aflatoxin B2A (AFB2A).<sup>254,257</sup> Roebuck *et al.* performed *in vitro* metabolism studies of AFB2 which showed the presence of trace levels of AFQ2, aflatoxin P2 (AFP2) and either AFM1 or AFM2 in human samples.<sup>258</sup> In Phase II, no glucuronides for any aflatoxins were generated.

### 3.3.3 Group of zearalenone

Microsomal biotransformation of ZEN is summarized in Figure 3.6 as an example representative for this family. The ZEN group, ZEN,  $\alpha$ -ZOL,  $\beta$ -ZOL, ZAN,  $\alpha$ -ZAL, and  $\beta$ -ZAL, was metabolized most extensively out of all chosen mycotoxin groups, resulting in total of 133 metabolites (Figure 3.7, Appendix B, Supplementary Tables B13–B18). The most predominant Phase I metabolic pathway for this class of mycotoxins is oxidation. There were seven types of oxidation reactions, desaturation with oxidation  $(-(H_4) + (O))$ , desaturation with oxidation  $(-(H_2) + (O))$ , oxidation  $(+(O))$ , reduction with oxidation  $(+(H_2) + (O))$ , oxidation  $(+(O_2))$ , and desaturation with oxidation  $(-(H_2) + (O_2))$  and  $(-(H_4) + (O_2))$ . Among these oxidation  $(+(O))$  reactions resulted in the formation of the highest number of metabolites for ZEN, 9 metabolites,  $\alpha$ -ZAL (4),  $\beta$ -ZAL (8),  $\alpha$ -ZOL (8),  $\beta$ -ZOL (7), except ZAN for which the reduction with oxidation  $(+(H_2) + (O))$  resulted in the highest number of metabolites (8), as shown in Table 3.1. Also, the total pattern number of oxidized metabolites of ZEN and its two metabolites,  $\alpha$ -ZOL and  $\beta$ -ZOL differed from ZAN and its two metabolites,  $\alpha$ -ZAL and  $\beta$ -ZAL. ZAN metabolized the most extensively and resulted in 22

metabolites, but ZEN had only 12 metabolites.  $\alpha$ -ZOL (15) had more oxidized metabolites than  $\beta$ -ZOL (8), but  $\alpha$ -ZAL (10) had less than  $\beta$ -ZAL (15). According to the percentage of metabolized parent toxin in Phase I reactions, ZEN (27%), ZAN (66%),  $\alpha$ -ZAL (29%),  $\beta$ -ZAL (23%),  $\alpha$ -ZOL (70%), and  $\beta$ -ZOL (7%), this metabolic pathway is not predominant, except for ZEN and  $\alpha$ -ZOL. Presumably, differences in epimer metabolic pathways can be explained by stereoselective specificity of cytochrome P450 enzymes which are known to be responsible for the differences in metabolism of drug and toxin isomers, especially enantiomers.<sup>259</sup> The metabolism of ZEN has already been investigated by Yang *et al.*<sup>174</sup>, and they reported a variety of ZEN oxidized metabolites. Also, ZEN,  $\alpha$ -ZAL and ZAN oxidized metabolites were reported in other studies<sup>260,261</sup>, but there were no metabolism studies performed for  $\alpha$ -ZOL,  $\beta$ -ZOL and  $\beta$ -ZAL. Based on the present results, the glucuronidation pathway is the predominant metabolic pathway for almost all the group of zearalenones. Based on the literature *in vitro* and *in vivo* studies glucuronidation was a major ZEN metabolic route in rats, humans and pigs.<sup>174,179,262</sup> In this experiment, the majority of ZAN (93%), ZEN (99%),  $\beta$ -ZAL(64%),  $\beta$ -ZOL (51%), and  $\alpha$ -ZOL (88%) was converted into glucuronides, except for  $\alpha$ -ZAL where conversion was 36% (Figure 3.7).

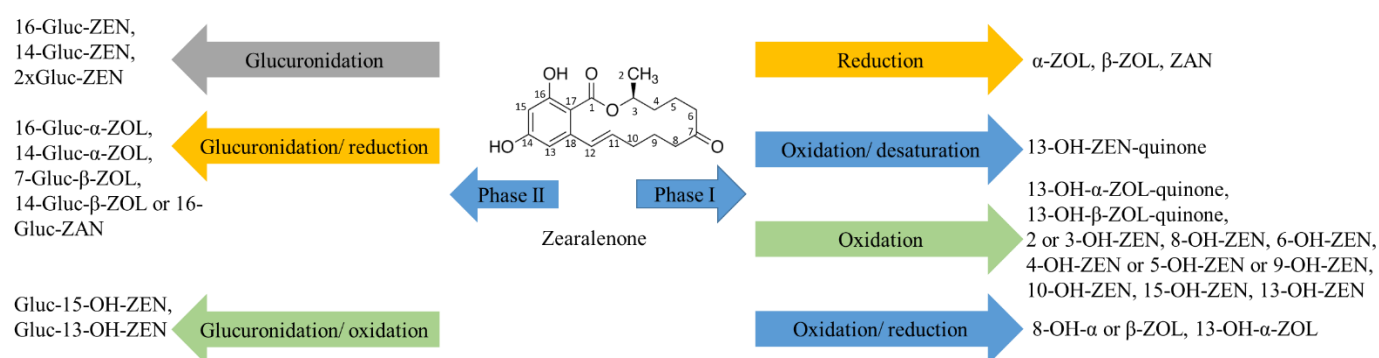


Figure 3.6. Microsomal biotransformation of ZEN in Phase I and II reactions.

The identifications of both Phase I and II reaction products were based on the comparison MS<sup>2</sup> spectra to literature data and/or analysis of MS<sup>2</sup> spectra. Phase II reactions resulted in various glucuronide forms of the parent toxin, its metabolites of Phase I reactions, and double glucuronide forms (denoted as 2 × Gluc). The numbers of observed glucuronide forms for each mycotoxin from ZEN group are summarized in Table 3.2. Common glucuronide forms of parent toxins were glucuronides at position C-14 or C-16 for ZEN and ZAN and at additional position C-7 for  $\alpha$ -ZOL,  $\beta$ -ZOL,  $\alpha$ -ZAL and  $\beta$ -ZAL. These glucuronides were previously generated by Stevenson *et al.*<sup>234</sup>, and their studies are in accordance with ours. Among the most predominant glucuronides were

glucuronides of parent toxins at position C-14, ZEN (86%), ZAN (73%),  $\alpha$ -ZOL (72%),  $\beta$ -ZOL (27%),  $\alpha$ -ZAL (23%) and  $\beta$ -ZAL (45%). The sum of parent glucuronides of ZEN group composed 91% for ZEN, 74% for ZAN, 86% for  $\alpha$ -ZOL, 49% for  $\beta$ -ZOL, 33% for  $\alpha$ -ZAL and 62%  $\beta$ -ZAL as shown in Figure 3.7. The glucuronides of oxidized metabolites and double glucuronides were only minor products, 19% for ZAN, 3% for  $\alpha$ -ZAL, 2% for  $\beta$ -ZAL, 8% for ZEN, 2% for  $\alpha$ -ZOL, 2% for  $\beta$ -ZOL. Yang *et al.* have already reported ZEN glucuronides of oxidized metabolites and di-glucuronide forms.<sup>263</sup> Overall, ZAN was the most metabolized toxin in Phase II and resulted in 24 glucuronides.  $\beta$ -ZOL and  $\beta$ -ZAL were least metabolized toxins and each generated only seven glucuronic forms. Comparing Phase II reaction samples to heated controls, it was noticed that the glucuronidation process was more efficient in heated samples (45°C) vs. Phase II reaction samples, except for ZAN.

Table 3.1. Summary of Phase I oxidation metabolites observed for ZEN group.

Mycotoxin	Oxidation Reactions and Number of Metabolites, (n)							$\Sigma$ n
	Desaturation, oxidation, -(H4) +(O)	Desaturation, oxidation, -(H2) +(O)	Oxidation +(O)	Reduction, oxidation, +(H2) +(O)	Oxidation, +(O2)	Desaturation oxidation, -(H2) +(O2)	Oxidation, -(H4) +(O2)	
ZEN	0	1	9(75%)	2	0	0	0	12
$\alpha$ -ZOL	1	6	8(53%)	0	0	0	0	15
$\beta$ -ZOL	1	1	7(88%)	0	0	0	0	8
ZAN	0	1	5(23%)	8(36%)	6(27%)	2	0	22
$\alpha$ -ZAL	1	3	4(40%)	0	0	1	1	10
$\beta$ -ZAL	1	4	8(53%)	0	0	1	1	15

Table 3.2. Number of glucuronides observed in ZEN group.

Mycotoxins	Total Number of Glucuronides
ZEN	10
$\alpha$ -ZOL	10
$\beta$ -ZOL	7
ZAN	24
$\alpha$ -ZAL	10
$\beta$ -ZAL	7



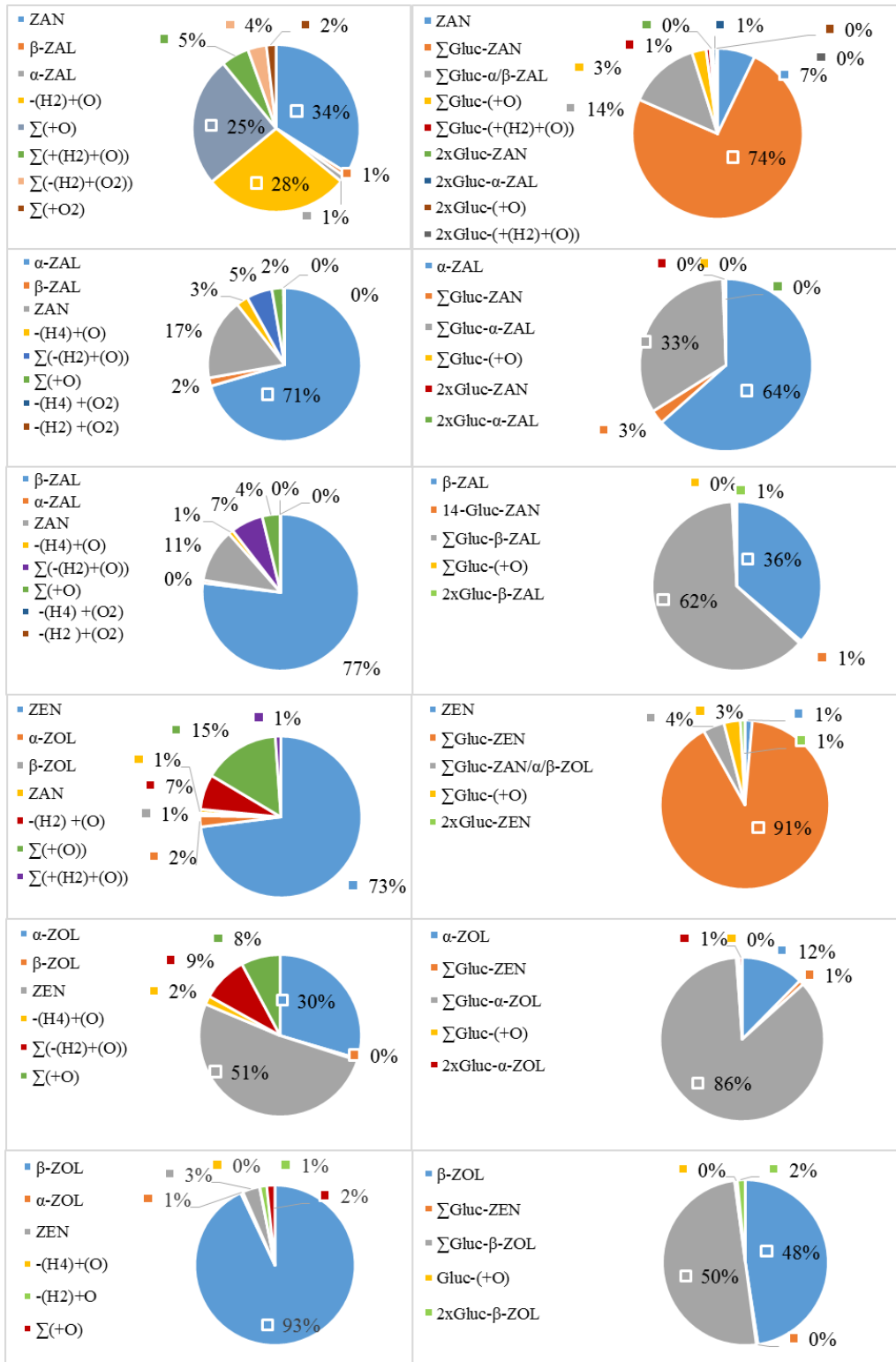


Figure 3.7. Summary of Phase I and Phase II metabolism of ZEN group.

### 3.4 Conclusions

In conclusion, the newly generated LC-MS library containing 188 metabolites represents the most comprehensive resource of human mycotoxin metabolites that can be analyzed using a single LC-MS method. The *in vitro* microsomal incubation workflow used in this work was able to successfully generate metabolites from hydrolysis, oxidation, de-epoxidation, epoxidation, demethylation, reduction and glucuronidation pathways as summarized in Table 3.3. The excellent limits-of-detection and isomer separation capability of our LC-MS method allowed us to characterize for the first time 100 metabolites that had not been previously reported in the literature, to the best of our knowledge. Among the known Phase I and Phase II metabolites of 17 mycotoxins that were the focus of this study, only four metabolites—AFQ1, aflatoxin P2 (AFP2), Gluc-4-HT-2, Gluc-3-4-de-acetyl-neosolaniol—could not be generated using our microsomal incubation workflow. The remaining 88 known metabolites were successfully generated, thus showing the power of our workflow and high-confidence identification capability. Table 3.4 summarizes the main subclasses of the newly characterized metabolites in this study.

Table 3.3. Summary of metabolic pathways of 17 mycotoxins.

Mycotoxins	Hydrolysis	Oxidation	De-Epoxidation	Epoxidation	Demethylation	Reduction	Glucuronidation
T-2	✓	✓					✓
HT-2	✓	✓					✓
3-AcDON	✓						✓
15-AcDON	✓						✓
FUS-X	✓						✓
DON			✓				✓
NIV			✓				✓
AFB1	✓	✓		✓	✓	✓	
AFB2		✓					
AFG1		✓					
AFG2		✓					
ZEN		✓					✓
α-ZOL		✓					✓
β-ZOL		✓					✓
ZAN		✓					✓
α-ZAL		✓					✓
β-ZAL		✓					✓

Table 3.4. Comparison of expected metabolites known in literature and metabolites generated in this assay.

<b>Mycotoxin</b>	<b>Expected Metabolites</b>	<b>Missing Metabolites</b>	<b>LC-MS Library</b>	<b>New Metabolites</b>
T-2	Phase I metabolites: HT-2, 15-deacetyl-T-2 (15-de-Ac-T-2), 3'-OH-T-2, NEO, T-2 triol, 3'-OH-HT-2, T-2 triol, Glucuronides: Gluc-3-T-2	NONE	Phase I metabolites: HT-2, 15-de-Ac-T-2, 3'-OH-T-2 and its two isomers, NEO, or T-2 triol, 3'-OH-HT-2, Glucuronides: Gluc-3-T-2	Two isomers of 3'-OH-T-2, 4 isomers of 3'-OH-HT-2
HT-2	Phase I metabolites: 4-de-Ac-NEO, 3'-OH-HT-2, 4'-OH-HT-2 7-OH-HT-2 and its isomer, 10-OH-HT-2, Glucuronides: Gluc-3-HT-2, Gluc-4-HT-2, Gluc-3-4-de-Ac-NEO	Gluc-4-HT-2, Gluc-3-4-de-Ac-NEO	Phase I metabolites: 4-de-Ac-NEO and its isomer, 3'-OH-HT-2, 4'-OH-HT-2 and its isomer 3 OH-T-2 metabolites at 7 or 10 or 16-OH-HT-2 Two unknown metabolites Glucuronides: Gluc-3-HT-2	4-de-Ac-NEO isomer
3-AcDON	Phase I metabolites: DON Glucuronides: Gluc-3-AcDON	NONE	Phase I metabolites: DON Glucuronides: Gluc-3-AcDON	NONE
15-AcDON	Phase I metabolites: DON Glucuronides: Gluc-15-AcDON	NONE	Phase I metabolites: DON Glucuronides: Gluc-15-AcDON	NONE

<b>Mycotoxin</b>	<b>Expected Metabolites</b>	<b>Missing Metabolites</b>	<b>LC-MS Library</b>	<b>New Metabolites</b>
FUS-X	Phase I metabolites: NIV	NONE	Phase I metabolites: NIV Glucuronides: Gluc-FUS-X	Gluc-FUS-X
DON	Phase I metabolites: De-epoxy-DON (DOM-1) Glucuronides: Gluc-15-DON, Gluc-3-DON	NONE	Phase I metabolites: NIV, DOM-1 and its two isomers, Glucuronides: Gluc-15-DON, Gluc-3-DON	NIV, isomers of DOM-1
NIV	Phase I metabolites: De-epoxy-NIV (DENIV), Glucuronides: Gluc-3-NIV	NONE	Phase I metabolites: DENIV and its two isomers Glucuronides: Two Gluc-NIVs	Gluc-NIV
AFB1	Phase I metabolites: AFM1, AFQ1, AFBO, AFP1, AFL, AFB1-diol Glucuronides: NO	AFQ1	Phase I metabolites: AFM1, AFBO, AFP1 and its isomer, AFL and its isomer, AFB1-diol and its isomer, ((H <sub>2</sub> )+(O)-AFB1 Glucuronides: NO	((H <sub>2</sub> )+(O)-AFB1
AFB2	Phase I metabolites: AFM2, AFQ2, AB2A, AFP2 Glucuronides: NO	AFP2	Phase I metabolites: AFM2, AFQ2 and AFB2A Glucuronides: NO	NONE
AFG1	Phase I metabolites: AFGM1 Glucuronides: NO	NONE	Phase I metabolites: AFGM1 Glucuronides: NO	NONE

<b>Mycotoxin</b>	<b>Expected Metabolites</b>	<b>Missing Metabolites</b>	<b>LC-MS Library</b>	<b>New Metabolites</b>
AFG2	Phase I metabolites: AFGM2, AFG2A Glucuronides: NO	NONE	Phase I metabolites: AFGM2, AFG2A Glucuronides: NO	NONE
ZEN	Phase I metabolites: (-H <sub>2</sub> )+(O))- ZEN, (+O))-ZEN, (+H <sub>2</sub> )+(O))- ZEN Glucuronides: Gluc-16-ZEN, Gluc-14-ZEN, Gluc-(+O)- ZEN, 2xGluc-ZEN	NONE	Phase I metabolites: (-H <sub>2</sub> )+(O))- ZEN, (+O))-ZEN, (+H <sub>2</sub> )+(O))- ZEN Glucuronides: Gluc-16-ZEN, Gluc-14-ZEN, Gluc-(+O)- ZEN, 2xGluc-ZEN	NONE
α-ZOL	Phase I metabolites: (-H <sub>4</sub> )+(O))- α- ZOL (-H <sub>2</sub> )+(O))- α- ZOL (+O)- α-ZOL Glucuronides: Gluc-16- α- ZOL, Gluc-14- α-ZOL, Gluc-7- α-ZOL	NONE	Phase I metabolites: (-H <sub>4</sub> )+(O))- α- ZOL (-H <sub>2</sub> )+(O))- α- ZOL (+O)- α-ZOL Glucuronides: Gluc-16- α- ZOL, Gluc-14- α-ZOL, Gluc-7- α-ZOL, Gluc-(+O)- α- ZOL, 2xGluc- α-ZOL	Gluc-(+O)- α- ZOL, (2xGluc)- α- ZOL

<b>Mycotoxin</b>	<b>Expected Metabolites</b>	<b>Missing Metabolites</b>	<b>LC-MS Library</b>	<b>New Metabolites</b>
$\beta$ -ZOL	Phase I metabolites: NO Glucuronides: Gluc-16- $\beta$ -ZOL, Gluc-14- $\beta$ -ZOL, Gluc-7- $\beta$ -ZOL,	NONE	Phase I metabolites: (-(H <sub>4</sub> )+(O))- $\beta$ -ZOL (-(H <sub>2</sub> )+(O))- $\beta$ -ZOL (+O)- $\beta$ -ZOL Glucuronides: Gluc-16- $\beta$ -ZOL, Gluc-14- $\beta$ -ZOL, Gluc-7- $\beta$ -ZOL, Gluc-(+O)- $\beta$ -ZOL, 2xGluc- $\beta$ -ZOL	(-(H <sub>4</sub> )+(O))- $\beta$ -ZOL (-(H <sub>2</sub> )+(O))- $\beta$ -ZOL (+O)- $\beta$ -ZOL Gluc-(+O)- $\beta$ -ZOL, (2xGluc)- $\beta$ -ZOL
ZAN	Phase I metabolites: NO Glucuronides: Gluc-16- ZAN, Gluc-14-ZAN	NONE	Phase I metabolites: (-(H <sub>2</sub> )+(O))-ZAN, (+O))-ZAN, (+H <sub>2</sub> )+(O))-ZAN, (+O <sub>2</sub> ))-ZAN, (-H <sub>2</sub> )+(O <sub>2</sub> ))-ZAN Glucuronides: Gluc-16- ZAN, Gluc-14-ZAN, Gluc-(+O)-ZAN, 2xGluc- ZAN, Gluc-(+H <sub>2</sub> )+(O))-ZAN, 2xGluc-(+O)-ZAN, 2xGluc-(+H <sub>2</sub> )+(O))-ZAN	Gluc-(+O)-ZAN, (2xGluc)- ZAN, Gluc-(+H <sub>2</sub> )+(O))-ZAN, (2xGluc)-(+O)-ZAN, (2xGluc)-(+H <sub>2</sub> )+(O))-ZAN

<b>Mycotoxin</b>	<b>Expected Metabolites</b>	<b>Missing Metabolites</b>	<b>LC-MS Library</b>	<b>New Metabolites</b>
$\alpha$ -ZAL	Phase I metabolites: (-H <sub>4</sub> )+(O)- $\alpha$ -ZAL (-H <sub>2</sub> )+(O)- $\alpha$ -ZAL (+O)- $\alpha$ -ZAL (-H <sub>4</sub> )+(O <sub>2</sub> )- $\alpha$ -ZAL (-H <sub>2</sub> )+(O <sub>2</sub> )- $\alpha$ -ZAL Glucuronides: Gluc-16- $\alpha$ -ZAL, Gluc-14- $\alpha$ -ZAL, Gluc-7- $\alpha$ -ZAL,	NONE	Phase I metabolites: (-H <sub>4</sub> )+(O)- $\alpha$ -ZAL (-H <sub>2</sub> )+(O)- $\alpha$ -ZAL (+O)- $\alpha$ -ZAL (-H <sub>4</sub> )+(O <sub>2</sub> )- $\alpha$ -ZAL (-H <sub>2</sub> )+(O <sub>2</sub> )- $\alpha$ -ZAL Glucuronides: Gluc-16- $\alpha$ -ZAL, Gluc-14- $\alpha$ -ZAL, Gluc-7- $\alpha$ -ZAL, Gluc-(+O)- $\alpha$ -ZAL 2xGluc- $\alpha$ -ZAL	Gluc-(+O)- $\alpha$ -ZAL (2xGluc)- $\alpha$ -ZAL
$\beta$ -ZAL	Phase I metabolites: NO Glucuronides: Gluc-16- $\beta$ -ZAL, Gluc-14- $\beta$ -ZAL, Gluc-7- $\beta$ -ZAL	NONE	Phase I metabolites: (-H <sub>4</sub> )+(O)- $\beta$ -ZAL (-H <sub>2</sub> )+(O)- $\beta$ -ZAL (+O)- $\beta$ -ZAL (-H <sub>4</sub> )+(O <sub>2</sub> )- $\beta$ -ZAL (-H <sub>2</sub> )+(O <sub>2</sub> )- $\beta$ -ZAL Glucuronides: Gluc-16- $\beta$ -ZAL, Gluc-14- $\beta$ -ZAL, Gluc-7- $\beta$ -ZAL, Gluc-(+O)- $\beta$ -ZAL, 2xGluc- $\beta$ -ZAL	(-H <sub>4</sub> )+(O)- $\beta$ -ZAL (-H <sub>2</sub> )+(O)- $\beta$ -ZAL (+O)- $\beta$ -ZAL (-H <sub>4</sub> )+(O <sub>2</sub> )- $\beta$ -ZAL (-H <sub>2</sub> )+(O <sub>2</sub> )- $\beta$ -ZAL Gluc-(+O)- $\beta$ -ZAL, (2xGluc)- $\beta$ -ZAL

To ensure the high confidence of our library identifications we used three key strategies: (i) incubation with one mycotoxin at a time to properly assign the origin of metabolites to a given parent mycotoxin, (ii) extensive controls to eliminate endogenous biomolecules present in microsomes, impurities in standards and metabolites that could be generated non-enzymatically,

and (iii) MS/MS comparison to the published literature spectra when available and to the parent compounds since the generated metabolites share many of the same structural features as the parent compounds. In the absence of authentic standards for all these metabolites, our identifications are putative. In the future, this new LC-MS library will be used during biomonitoring studies to characterize which of these metabolites may be observed in various biological samples *in vivo* and to provide semi-quantitative information on their concentrations using parent calibration curves. This relevant subset of metabolites then can be synthesized for further confirmation of identity and full quantification. Additionally, the clarification of some metabolite structures that remain ambiguous in our library (e.g., exact position of hydroxyl groups in several ZEN metabolites) can be improved in future work by the application of isotopically labeled standards, as was previously demonstrated in the literature<sup>261,264</sup>, or through synthesis of authentic standards.



## **4. Development and validation of polarity-switching liquid chromatography high-resolution mass spectrometry method for ochratoxins, fumonisins and enniatins in human plasma**

### **4.1 Introduction**

Filamentous fungi, from genera such as *Fusarium*, *Aspergillus*, and *Penicillium* can produce toxic secondary metabolites, called mycotoxins.<sup>56,265</sup> Mycotoxin toxicity poses an important human health issue, as mycotoxins may contribute to the development of a number of diseases, such as kidney diseases, oesophageal and liver cancer and immunosuppression.<sup>27,266–268</sup> In addition, human health risk can be augmented by combined exposure to multiple mycotoxins at the same time, if a given combination of mycotoxins leads to additive or synergetic effects.<sup>23,269–271</sup>

Filamentous fungi are important pathogen of the crop plants, and can grow at pre- and post- harvest or storage period.<sup>2,272</sup> Thus, up to 60-80% of crops worldwide are estimated to be contaminated with detectable levels of mycotoxins.<sup>4</sup> Emerging mycotoxins have recently been detected in food and feed samples.<sup>17,273</sup> In addition, climate change can increase the rate of fungi ingress, in turn enhancing the mycotoxin levels in various foods.<sup>13,17,274</sup>

There are three routes of exposure to mycotoxins: ingestion, dermal contact or inhalation<sup>84</sup>, and the intake of contaminated food is considered to be the main route of exposure.<sup>275</sup> To minimize mycotoxin exposure, current regulations for mycotoxins establish maximum levels of some mycotoxins in various foods and feed. These are regulatory limits established on models based on the estimation of daily food intake. However, this may generate inaccurate health risk evaluation or prediction. Different types of diet (plant-based-diet or meat-based-diet) and food preferences can lead to various consumption of food types, deviating from population-based models built for risk assessment and resulting in different amount of ingested mycotoxins.<sup>275</sup> In addition, factors such as age, gender, and individual metabolism can impact the fate and half-lives of mycotoxins once ingested. Human biomonitoring can more accurately estimate an individual's exposure than the approaches based on the daily food intake. In fact, several biomonitoring studies of mycotoxins in urine demonstrated that the established maximum levels of mycotoxins were exceeded. For example, the most frequently detected mycotoxin, DON, exceeded tolerable daily intakes in urine in 33% of samples from Austria, 8.1% of samples from Spain, in 6% of samples from Germany,

40% of samples from Italy, 16 to 69% of samples from Belgium, and 1.3% of samples from Sweden.<sup>44–47,123,232</sup> For OTA, 94% of tested urine samples from Italy and 1% of samples from Belgium exceeded tolerable daily intakes levels.<sup>45,46</sup> Methods covering one or few analytes in human blood have been reported for OTA<sup>135</sup>, emerging mycotoxins<sup>121</sup>, and CIT.<sup>141</sup> Thus, the development of highly sensitive and low-cost biomonitoring approaches for large-scale population screening is important to complement regulatory efforts to ensure safety of food and feed. In addition, human biomonitoring is appropriate for the measurement of any type of exposure routes.

Human biomonitoring can be performed using urine, blood-derived products, milk, feces, and hair. Currently, mycotoxin exposure is evaluated predominantly using urine because it requires non-invasive sampling and can be easily collected in a large amount. Urine reflects dietary exposure to mycotoxins with fast urinary clearance. LC-MS methods for one mycotoxin or single mycotoxin class are widely employed. Several immunoaffinity methods covering 4 to 9 mycotoxins were developed and applied for the evaluation of mycotoxin exposure in urine.<sup>45,59,84,276</sup> Generic sample preparation, dilute-and-shoot and filtration, has been successfully used to increase mycotoxin coverage to 15 and 32 mycotoxins, respectively<sup>119,202</sup>. However, these generic sample preparation methods with poor sample clean-up typically result in unacceptable matrix effects impacting the reliability of the measurement.<sup>114,119</sup> Sample preparation methods that provide improved sample clean-up in turn compromise mycotoxin coverage. For example, LLE methods in combination with LC-MS were developed for 12 mycotoxins<sup>114</sup>, or LLE followed by SAX SPE for 18 mycotoxins.<sup>117</sup> Enzymatic hydrolysis with  $\beta$ -glucuronidase is also often used before urine sample preparation to release conjugated metabolites of mycotoxins, thus measuring the total concentration of a given mycotoxin and its conjugates.<sup>45,59,276,277</sup> Enzyme hydrolysis is necessary for the improved detection of mycotoxins which extensively excreted via urine in the conjugated forms. OTA and its metabolite, OT $\alpha$  require  $\beta$ -glucuronidase treatment as it was reported by Solfrizzo *et al.*, Klapac *et al.*, Muñoz *et al.*<sup>38,99,185</sup> Direct measurements of conjugated and other mycotoxin metabolites is not often preferred in multi-mycotoxin LC-MS methods due to the lack of commercial standards and their different physicochemical properties.<sup>54,175,278</sup>

The exposure to multiple mycotoxins at the same time has been documented and requires appropriate LC-MS methods enabling determination of multiple mycotoxins in a single analytical run<sup>165</sup>. However, common toxicologically important mycotoxins belong to different mycotoxin classes with diverse chemical properties which hinder the development of a single LC-MS method.

For example, methods for the determination of OTA and/or its hydroxyl metabolite was developed in human blood-derived samples.<sup>134,135,137</sup> There are single-analyte methods for analysis of CIT and/or its hydroxyl metabolite<sup>138,141</sup> and group of emerging mycotoxins<sup>121</sup>. Fumonisin-class and FB1-specific methods were developed and validated for chicken plasma and pig plasma.<sup>279</sup> Overall, the usage of class-specific or one mycotoxin methods may be too expensive and time-consuming to implement for biomonitoring especially when multiple mycotoxin classes are of interest.

In addition, all multi-mycotoxin LC-MS methods must balance maximum mycotoxin coverage, matrix effect and sensitivity. Achieving LLOQs at pg/ml level is one of the critical requirement, since mycotoxins are routinely present at sub ng/ml levels in biofluids.<sup>80,280</sup> However, many existing methods do not achieve such LLOQs, for example, LC-MS method was developed and validated for the determination of 24 mycotoxins, including emerging mycotoxins, OTA, aflatoxins, trichothecenes in chicken and pig plasma which resulted in 1-2 ng/ml LLOQ of pig plasma and 1-5 ng/ml LLOQ for chicken plasma only, and fumonisins were not included because of low recovery.<sup>279</sup>

Three multi-mycotoxin methods were developed for human blood-derived samples using universal sample preparation techniques, protein precipitation and DBS/DSS.<sup>64,136,139</sup> They mostly focused on achieving the widest mycotoxin coverage, 11, 27 and 28 mycotoxins, respectively. However, three methods suffer from unacceptable matrix effects, 28%-125%, 13%-939%, 60%-140%, respectively.<sup>64,136,139</sup> The presence of significant ionization suppression impacts achievable LLOQ and makes obtaining sub ng/mL LLOQ difficult or impossible to achieve. For example, 27-mycotoxin method developed for blood and serum had wide ranges of LLOQs, 0.005-5 ng/ml and 0.05-5 ng/ml in blood and serum, respectively.<sup>136</sup> Significant matrix effects can also affect the accurate quantitation when isotopically labeled standards are not available for all mycotoxins and lead to underestimation/overestimation of exposure. Isotopically-labelled standards are not always available and are expensive, thus increasing the cost of analysis drastically for multi-mycotoxin biomonitoring methods. Commonly, LC-MS methods designed for mycotoxin exposure studies use few or no isotopically labeled standards.<sup>64,136,137,139</sup>

Therefore, the goal of this study is to develop a multi-class LC-MS method with negligible absolute matrix effects for all mycotoxins and sub ng/mL LLOQ levels in human plasma to complement our existing 17-mycotoxin fully validated method.<sup>233</sup> This new method includes the

fumonisin (FB1 and FB2), ochratoxins (OTA, CIT and OT $\alpha$ ) and emerging mycotoxins of interest (ENNA, ENNA1, ENNB, ENNB1 and BEA) which could not be accurately measured by the first method due to irreproducible retention, poor recovery and solubility issues, respectively. There is no method that could cover this set of mycotoxins reported in literature today.

## **4.2 Materials and methods**

### **4.2.1 Chemicals**

LC–MS grade water, methanol, acetonitrile and 2-propanol, HPLC grade methyl tert-butyl ether (MTBE), acetic acid (AA, Optima<sup>R</sup> LC/MS) and formic acid (FA, Optima<sup>R</sup> LC/MS) were purchased from Fisher Scientific (Ottawa, Ontario, Canada). Pooled human plasma with sodium citrate as anti-coagulant was purchased from Bioreclamation Inc. (Baltimore, MD, USA). Ammonium formate (for mass spectrometry) and ammonium acetate (for mass spectrometry) were purchased from Sigma-Aldrich Canada (Oakville, Ontario, Canada).

### **4.2.2 Mycotoxin standards**

Ochratoxin A-d<sub>5</sub> (OTAd<sub>5</sub>) was purchased from Toronto Research Chemicals Inc. (Toronto, ON, Canada). FB1, FB2 and BEA were purchased from Cayman Chemicals (Ann Arbor, MI, USA). Fumonisin B3 (50  $\mu$ g/ml in 50% acetonitrile) and OT $\alpha$  (10  $\mu$ g/ml in 50% acetonitrile) were purchased from Romer Labs (Union, MO, USA). CIT, OTA, ENNA, ENNA1, ENNB, ENNB1 were purchased from Sigma-Aldrich Canada (Oakville, Ontario, Canada). A combined 10  $\mu$ g/ml working solution of all mycotoxin standards except for OT $\alpha$  was prepared in methanol and stored in aliquots at  $-80^{\circ}\text{C}$ . A combined 1  $\mu$ g/ml internal standard solution of OTAd<sub>5</sub> and FB3 was prepared in methanol and stored in aliquots at  $-80^{\circ}\text{C}$ . 10 ng/ml of OTAd<sub>5</sub> and FB3 was added immediately prior to LC–MS analysis during the investigation of sample preparation techniques. In all validation experiments, internal standards (10 ng/ml) were added pre-extraction to thawed plasma before protein precipitation in order to monitor injection volume, signal stability, recovery and ionization matrix effects.

## 4.2.3 Sample preparation method development

### 4.2.3.1 Effect of solvent composition on recovery and reconstitution

#### 4.2.3.1.1 Protein precipitation with methanol and reconstitution in methanol

To 100  $\mu\text{l}$  of plasma, 300  $\mu\text{l}$  of cold methanol was added and mixed on vortex (Fisher Scientific Vortex Mixer) for 20 min. Samples were then centrifuged at  $25830\times g$ , (Thermo Fisher Scientific, Sorvall ST 16R centrifuge) for 10 min at  $4^{\circ}\text{C}$ . The 300  $\mu\text{l}$  of supernatant was aspirated into a new polypropylene extraction tube, evaporated to dryness using Speedvac (Labconco CentriVap 7812013) and reconstituted into 200  $\mu\text{l}$  of 40% methanol containing 10 ng/mL OTAd<sub>5</sub> and FB3 internal standards by mixing on vortex for 20 min. The samples were then centrifuged at  $25830\times g$ , (Thermo Fisher Scientific, Sorvall ST 16R centrifuge) for 10 min at  $4^{\circ}\text{C}$ . This solution was transferred into polypropylene HPLC inserts for analysis.

#### 4.2.3.1.2 Protein precipitation with methanol and reconstitution in acetonitrile

The same procedure as described in Section 4.2.3.1.1 was followed but the samples were reconstituted into 200  $\mu\text{l}$  of 40% acetonitrile containing 10 ng/mL OTAd<sub>5</sub> and FB3.

#### 4.2.3.1.3 Protein precipitation with acetonitrile and reconstitution in acetonitrile

To 100  $\mu\text{l}$  of plasma, 300  $\mu\text{l}$  of cold acetonitrile was added and mixed on vortex for 20 min. Samples were then centrifuged at  $25830\times g$  for 10 min at  $4^{\circ}\text{C}$ . The 300  $\mu\text{l}$  of supernatant was aspirated into a new polypropylene extraction tube, evaporated to dryness using Speedvac (Labconco CentriVap 7812013) and reconstituted into 200  $\mu\text{l}$  of 40% acetonitrile containing OTAd<sub>5</sub> and FB3 internal standards by mixing on vortex for 20 min. Samples were centrifuged at  $25830\times g$  for 10 min at  $4^{\circ}\text{C}$ , and the resulting supernatant was transferred into polypropylene HPLC inserts for analysis.

#### 4.2.3.1.4 Protein precipitation with acetonitrile and reconstitution in methanol

The same procedure for protein precipitation as described in the section 4.2.3.1.3 was used but the sample were reconstituted using 200  $\mu\text{l}$  of 40% methanol containing 10 ng/mL OTAd<sub>5</sub> and FB3 internal standards.

#### 4.2.3.1.5 Comparison of four protein precipitation protocols and selection of optimal solvent

The objective of this experiment was to find an appropriate solvent for protein precipitation and reconstitution. Plasma samples, confirmed not to contain any detectable levels of mycotoxins, were spiked with 100 ng/ml of OT $\alpha$ , CIT, OTA, FB1, FB2 and BEA, incubated for 30 min and extracted according to the procedures described in the sections 4.2.3.1.1- 4.2.3.1.4 (n = 3 replicates). The amount of analyte in each sample was determined using calibration curves prepared in the appropriate reconstitution solvents (40% methanol or 40% acetonitrile). Process efficiency was calculated according to the formula  $PE\% = C_m/C_{th} * 100\%$ , where PE% is the process efficiency,  $C_m$  is the measured concentration in the extracted samples and  $C_{th}$  is theoretical concentration. This determination includes the effects of both extraction recovery and matrix effects due to ionization suppression/enhancement.

#### 4.2.3.2 Comparison of protein precipitation and combined protein precipitation - LLE methods

##### 4.2.3.2.1 Protein precipitation with methanol without evaporation/reconstitution step

To 100  $\mu$ l of plasma, 300  $\mu$ l of cold methanol was added and mixed on vortex for 20 min. Samples were then centrifuged at 25830 $\times$ g for 10 min at 4°C. The 100  $\mu$ l of supernatant was aspirated into a new polypropylene extraction tube, and then, 25  $\mu$ l of water containing OTAd<sub>5</sub> and FB3 was added to supernatant. This solution was transferred into polypropylene HPLC inserts for analysis.

##### 4.2.3.2.2 Combined MTBE LLE- protein precipitation with methanol

To 200  $\mu$ l of plasma, 600  $\mu$ l of MTBE was added and mixed on vortex for 20 min. Samples were then centrifuged at 25830 $\times$ g for 10 min at 4°C. The 100  $\mu$ l of aqueous phase was aspirated into a new polypropylene extraction tube to which 300  $\mu$ l of methanol was then added to perform protein precipitation according to the procedure in Section 4.2.3.2.1.

##### 4.2.3.2.3 Combined hexane-LLE - protein precipitation with methanol

To 200 µl of plasma, 600 µl of hexane was added and mixed on vortex for 20 min. Samples were then centrifuged at 25830×g for 10 min at 4°C. The 100 µl of aqueous phase was aspirated into a new polypropylene extraction tube to which 300 µl of methanol was then added to perform protein precipitation according to the procedure in Section 4.2.3.2.1.

#### 4.2.3.2.4 Evaluation of recovery using sample preparation protocols described in Sections 4.2.3.2.1-4.2.3.2.3

The goal of this experiment was to evaluate the effect of additional clean-up of plasma samples, preferably to remove lipids while keeping high recovery of mycotoxins. Plasma containing no detectable levels of mycotoxins of interest, was spiked with 100 ng/ml of mycotoxins (OT $\alpha$ , CIT, OTA, FB1, FB2, ENNA, ENNA1, ENNB, ENNB1 and BEA) pre-extraction, incubated for 30 min and then processed according to the procedures described in Sections 4.2.3.2.1-4.2.3.2.3 (n = 3 replicates). The recovery of analytes in each sample was determined using post-spiked reference samples. To prepare these samples, plasma was processed with respective sample preparation procedures outlined in Sections 4.2.3.2.1-4.2.3.2.3 and then spiked with 20 ng/ml immediately prior to LC-MS analysis. This spiked concentration corresponds to the mycotoxin concentration at the time of injection, assuming quantitative recovery at all steps and taking into account all volume corrections throughout the procedures. Recovery was calculated according to the formula  $RE\% = A_{\text{pre-spiked}}/A_{\text{post-spiked}} * 100\%$ , where RE% is the recovery,  $A_{\text{pre-spiked}}$  is the measured area in pre-spiked samples in the injection solvent and  $A_{\text{post-spiked}}$  is the measured area in post-spiked samples in the injection solvent. This determination is equivalent to extraction recovery.<sup>281</sup>

#### **4.2.4 Final protein precipitation with subsequent acidification used for the method validation**

To 100 µl of plasma, 300 µl of methanol was added and mixed on vortex for 3 min. Samples are kept at -80°C for 20 min. Samples were then centrifuged at 25830×g for 20 min at 4°C. The 200 µl of supernatant was aspirated into a new polypropylene extraction tube, to which 50 µl of 1% FA (v/v) was added, mixed for 1 min, and then centrifuged at 25830×g for 10 min at 4°C. This solution was transferred into polypropylene HPLC inserts for analysis.

#### **4.2.5 Evaluation of recovery and matrix effects using final protein precipitation with subsequent acidification**

Recovery and matrix effects were evaluated using final protein precipitation with subsequent acidification described in Section 4.2.4 using 10 individual lots of plasma. The evaluation of recovery and matrix effects was performed according to Matuszewski *et al.*<sup>281</sup> Three sets of samples were prepared. First set, pre-spiked samples, used plasma samples from 10 different individuals (five females and five males) which were spiked with mycotoxin mixture (7 ng/ml) and internal standards (OTAd<sub>5</sub> and FB3, concentration 10 ng/ml) and then extracted using final protein precipitation with subsequent acidification (Section 4.2.4). The second set, post-spiked samples, used the same lots of individual plasma which was extracted first and then spiked with mycotoxin mixture (1.4 ng/ml) and internal standards (OTAd<sub>5</sub> and FB3, concentration 10 ng/ml) before transferring to LC-MS inserts. The third set was the 1.4 ng/ml mycotoxin standard prepared in injection solvent 60% containing 1% FA and 10 ng/ml OTAd<sub>5</sub> and FB3. Finally, the recovery was evaluated as described in Section 4.2.3.2.4 Matrix effect was evaluated by formula  $\text{intensity}\% = \frac{A_{\text{post-spiked}}}{A_{\text{std.}}} * 100\%$ , where  $A_{\text{post-spiked}}$  is the measured peak area of a given mycotoxin in post-extracted spiked plasma, and  $A_{\text{std.}}$  is the measured peak area of the same mycotoxin in standard solution prepared at the same concentration the injection solvent.

#### **4.2.6 LC-HRMS analysis**

##### **4.2.6.1 LC–MS development**

Initial method development experiments compared the performance of several columns, including core-shell Kinetex C<sub>18</sub> (2.6 μm, 100 Å, 50 × 2.1 mm, Phenomenex, Torrance, California, USA) and Biphenyl column (1.7 μm, 100 Å, 100 mm x 2.1 mm, Phenomenex), ZORBAX Eclipse Plus C<sub>18</sub> (1.8 μm, 100 Å, 100 × 2.1 mm, Agilent Technologies, Santa Clara, CA, USA) and Waters CORTECS T3 column (120Å, 1.6 μm, 2.1 mm x 100 mm, Waters, Milford, MA, USA) in combination with various water/methanol mobile phase gradients in order to separate all mycotoxins of interest and allow polarity switching for different time segments of LC run. The critical separation pairs were between OTA and FB2 and/or FB3, and CIT and FB1. Waters CORTECS T3 column provided good separation and peak shape of all mycotoxins of interest, so it was selected for all further experiments.



Next, the effect of mobile phase additives on mycotoxin signal intensities was investigated using methanol gradient containing different additives (2 mM ammonium acetate, 2 mM ammonium formate, 0.05% FA (v/v) and 0.05% AA (v/v)). The effect of these additives on ionization in ESI(+) and ESI(-) was determined by comparing signal intensities obtained for high concentration mycotoxin standard in order to find best additive for this application. Finally, water/methanol mobile phase gradient was replaced with water/methanol/isopropanol gradient to ensure effective elution of lipids. This choice forced the re-evaluation of mobile phase additives, (FA vs. AA). The effect of concentration of mobile phase additives (0.02% vs. 0.05% v/v) was also evaluated. The final optimized conditions for LC-MS method are given in detail in Section 4.2.6.3.

#### 4.2.6.2 Evaluation of injection solvent composition

Several experiments were performed to find an appropriate injection solvent for the selected mycotoxins. The composition of injection solvent (40%, 60% and 80% methanol) and type of injection inserts (polypropylene plastic versus glass inserts) were evaluated systematically in order to ensure good solubility for all mycotoxins, adequate LC peak shape and prevent non-specific adsorption losses.

All samples were prepared from one stock solution (10 µg/ml mycotoxin mixture dissolved in methanol), from which two 100 ng/ml standards in 40% methanol and 60% methanol, respectively were prepared. Then, 100 ng/ml mixtures in 40% methanol or 60% methanol were diluted to 20 ng/ml with the same solvent. After dilution, 100 µl of 20 ng/ml in 40% methanol was transferred to LC-MS vial with plastic insert (control\_40) or to LC-MS vial with glass insert (condition#1\_40). For condition2\_40, adsorption experiment was added, whereby 100 µl of 20 ng/ml mycotoxin standard in 40% methanol was kept in an Eppendorf tube for 20 min then transferred to another Eppendorf tube for 20 min and procedure was repeated for total of 5 times before it was transferred to LC-MS vial with glass insert. After dilution, 100 µl of 20 ng/ml standard in 60% methanol was transferred to LC-MS vial with plastic insert (condition3\_40). The scheme of the experiment is shown in Figure 4.1a (Experiment #1). Based on the results of this experiment, Experiment #2 was also performed as shown in Figure 4.1b.

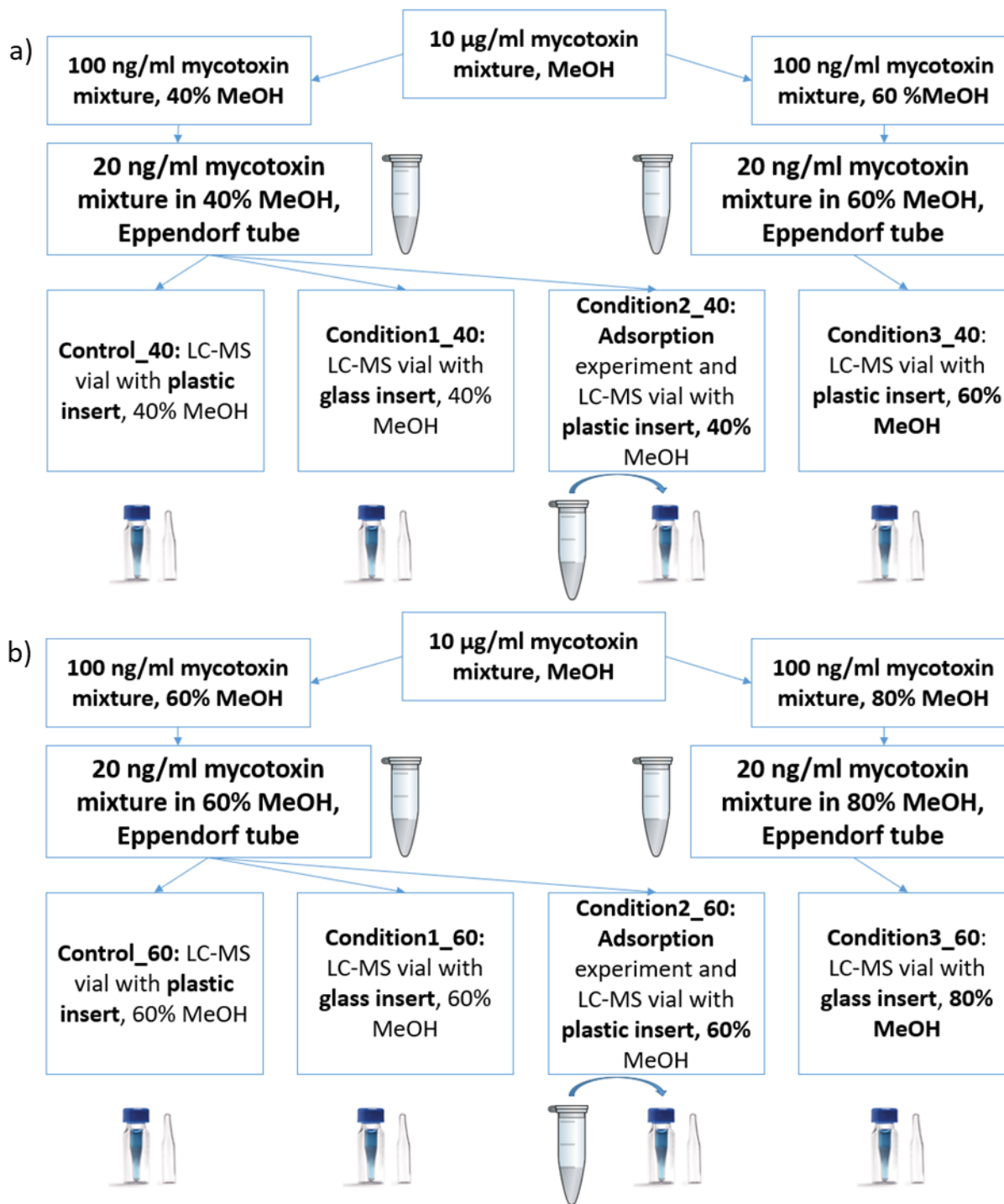


Figure 4.1. The scheme of experiment #1 (a) and experiment #2 (b) for the evaluation of the mycotoxin solubility and adsorption.

All samples were prepared from one stock solution (10 µg/ml mycotoxin mixture dissolved in methanol) from which two 100 ng/ml standards in 60% and 80% methanol were diluted to 20 ng/ml with the same solvent. After dilution, 100 µl of 20 ng/ml in 60% methanol was transferred

to LC-MS vial with plastic insert (control\_60) or to LC-MS vial with glass insert (condition1\_60). For condition2\_60, the adsorption experiment was performed first, 100  $\mu$ l of 20 ng/ml in 60% methanol was kept in an Eppendorf tube for 20 min then transferred to another Eppendorf tube and procedure was repeated for 5 times before it was transferred to LC-MS vial with glass insert. 100  $\mu$ l of 20 ng/ml in 80% methanol LC-MS vial with glass insert (condition3\_60). The scheme of the experiment is shown in Figure 4.1b (Experiment #2). Injection solvent composition of 60% methanol was selected as satisfactory choice for all mycotoxins. Furthermore, 1% FA (v/v) was added to injection solvent in order to prevent signal intensity drift of fumonisins across long analytical run.

#### 4.2.6.3 Final LC–MS method

Chromatographic separation was performed using UHPLC 1290 (Agilent Technologies) with Waters CORTECS T3 Column (120 $\text{\AA}$ , 1.6  $\mu$ m, 2.1 mm x 100 mm), guard column (CORTECS T3 VanGuard Pre-column, 120 $\text{\AA}$ , 1.6  $\mu$ m, 2.1 mm x 5 mm) and column in-line filter (0.2  $\mu$ m, ACQUITY UPLC™ BEH, Waters). The flow rate of 0.3 ml/min and the column temperature of 40°C were used for all analyses. The mobile phases A, water/methanol (60%/40%, v/v) and B, isopropanol/methanol (90%/10% v/v), containing 0.02% (v/v) AA were used for the final method. The following step gradient was used: increase from 0% to 5% B for the first 1.0 min, increase from 5% B to 13% B from 1.0 min to 2.0 min, increase from 13% B to 19% B for the next two minutes, keep isocratic at 19% B from 4.0 min to 6.0 min, from 6.1 min to 13 min increase from 30% to 60% B, from 13.1 to 18 min keep isocratic at 90% B, and finally re-equilibrate the column at 0% B for 6 min. Injection volume was 10  $\mu$ l.

High-resolution MS analysis was performed using Agilent QTOF 6545 (Agilent Technologies, Santa Clara, CA, USA). The following MS parameters were used: acquisition rate 2 spectra/s, gas temperature 195°C, drying gas 13 L/min, nebulizer 30 psi, sheath gas temperature 325°C, sheath gas flow 12 L/min, capillary voltage 3500 V and mass range 100 to 1000 m/z. Nozzle voltage 2000 V in ESI(-) and nozzle voltage 1250 V in ESI(+) were used in the method. LC-MS method was divided into five-time segments with ESI mode and fragmentor voltages specified in Table 4.1. For internal calibration, ESI(-) and ESI(+) used the following calibrant masses: 119.03632 m/z (purine), 980.016375 m/z (HP-0921, acetic adduct) and 121.050873

(purine), 922.009798 (HP-0921), respectively. Data acquisition was controlled by Mass Hunter software version 10.00.

*Table 4.1. MS settings, time segments, ionization mode and fragmentor voltage.*

Time segment, min	Ionization mode	Fragmentor voltage, V
0	ESI(-)	160
3.2	ESI(-)	235
4.2	ESI(+)	245
5.7	ESI(-)	200
6.8	ESI(-)	245

#### 4.2.6.4 Data analysis

Data analysis was performed using Agilent Mass Hunter software (TOF Qualitative Analysis 10.0 and TOF Quantitative Analysis 10.0). Mycotoxins were quantitated using the most intense ions which were extracted with  $\pm 10$  ppm window. For fumonisins, the most abundant protonated ions  $[M + H]^+$  were used. For enniatins and BEA, the most abundant sodium adduct  $[M + Na]^+$  in ESI(+) was used. For OT $\alpha$ , CIT and OTA, the most abundant deprotonated ion  $[M - H]^-$  in ESI(-) was used for quantitation.

#### 4.2.6.5 Calibration curve during method development

For the quantification of mycotoxins in plasma, matrix-matched calibrations were prepared in the range of 0.039 ng/ml to 20 ng/ml during method development. Pooled plasma containing no detectable levels of mycotoxins of interest was spiked with combined mycotoxin standard to yield 20 ng/ml concentration of each mycotoxin. Nine more concentration levels were generated using two-fold serial dilution with plasma. All spiked calibration samples were incubated on ice for 30 min prior to extraction using procedure described in Section 4.2.3.2.1. All calibration curves were built using 1/x weighted linear regression.

#### 4.2.6.6 Matrix-matched calibration curves and estimation of LLOQ using intra-day accuracy and precision validation experiment

Matrix-matched calibration curves were prepared for the quantification of mycotoxins in plasma during validation experiments, as described in Section 4.2.6.5. The final extraction procedure

described in Section 4.2.4 was used. Three intra-day experiments were performed. The first experiment used matrix-matched calibration curves, ranging from 0.075 ng/ml to 19.2 ng/ml for OTA, ENNB, ENNB1, from 0.1 ng/ml to 25.6 ng/ml for CIT, from 0.25 ng/ml to 32 ng/ml for ENNA, ENNA1, BEA, FB1, FB2 and OT $\alpha$ , as shown in Supplementary Table C3. Matrix-matched calibration curves for the second and third intra-day experiments ranging from 0.08 ng/ml to 20.00 ng/ml and from 0.16 ng/ml to 20 ng/ml, respectively, as shown in Supplementary Table C4.

Plasma was spiked with combined mycotoxin standard to yield 19.2 ng/ml for OTA, ENNB, ENNB1, 25.6 ng/ml for CIT 32.0 ng/ml for ENNA, ENNA1, BEA, FB1, FB2 and OT $\alpha$  ng/ml concentrations for the first experiment. For the second and third experiments, plasma was spiked with combined mycotoxin standard to yield 20 ng/ml concentration for each mycotoxin. Then, two-fold serial dilution with blank plasma was used to prepare 8, 9 and 7 additional standard concentration levels for the first, second, third experiments, respectively, followed by mixing and incubation for 30 min at on ice. For the first and the second intra-day experiment, validation samples (n=6) were prepared as discussed in Section 4.3.3 and Tables 4.4 and 4.5. For the third intra-day experiment, validation samples (n = 6 replicates per concentration level) were prepared by spiking plasma at eight concentration levels, 0.2, 0.3, 0.45, 0.625, 1.25, 4, 8 and 16 ng/ml for all mycotoxins. All validation samples were extracted using procedure in Section 4.2.4. samples. All validation and calibration samples were analyzed using developed LC–MS method.

## **4.3 Results and discussion**

### **4.3.1 Development of a sensitive LC-HRMS method**

The objective of this study was to develop a highly sensitive LC-MS method for 10 mycotoxins covering ochratoxins, fumonisins and enniatin mycotoxin classes. The method should enable accurate quantitation of 10 mycotoxins at sub ng/ml levels in plasma samples, while minimizing matrix effects to allow the use of one or few isotopically-labelled internal standards. To develop this method, the optimization of sample preparation, LC separation and MS parameters were all investigated in detail. In addition, the influence of injection solvent composition on analyte solubility and method robustness was investigated.

#### 4.3.1.1 Development of LC separation

LC-MS method development focused on achieving adequate mycotoxin separation to allow polarity switching in different time segments of LC method and on achieving good peak shape for all mycotoxins which included both polar and highly hydrophobic species. Different stationary phases, such as biphenyl and C<sub>18</sub> were investigated. The best separation was achieved with Waters CORTECS T3 column C<sub>18</sub> column (1.6 μm, 120Å, 2.1 mm x 100 mm). This separation allowed switching of ESI polarity to ESI(-) mode for the time segments where OTα, CIT and OTA eluted, without adversely impacting the detection of the remaining mycotoxins using ESI(+). The separation of all 10 mycotoxins obtained with water/methanol mobile phase is shown in Appendix C, Supplementary Figure C1.

When this LC-MS method was used in combination with protein precipitation, lipid build-up was observed on the column (Appendix C, Supplementary Figure C2). The results showed that hydrophobic matrix components, such as lipids were not completely washed away before next injection. To address this issue isopropanol was added to mobile phase to help remove any triglyceride build-up from the column. After switch to isopropanol, gradient was also modified accordingly to keep the separation of mycotoxins as required for time-segmented polarity switching. The final LC separation requires 24 min/injection and is shown in Figure 4.2. Similarly, to the first developed method, this method also can be expanded to add the relevant metabolites of the mycotoxins of interest. It is the most likely that the method will work well for emerging mycotoxin metabolites, which should all elute in the last time segment. The CIT hydroxyl metabolite also can be added to the method, which should ionize similar to CIT in ESI(-) and be detected in the first time segment. However, the time-segmented polarity switching can be a limiting factor for the addition of fumonisin metabolites, since they will be more polar than the parent toxins. They can elute in the time segment where ESI(-) is used which is not the preferred mode of fumonisin ionization. Similar to fumonisin metabolites, the OTA hydroxyl metabolite can also elute in the time segment with ESI(+) instead of ESI(-). In addition, the capability of this method to separate metabolite isomers would have to be evaluated.

In published papers for plasma multi-class mycotoxin methods C<sub>18</sub> is one of the often used columns that can provide suitable separation of hydrophobic structurally different compounds.<sup>64,134,137,139,140</sup>

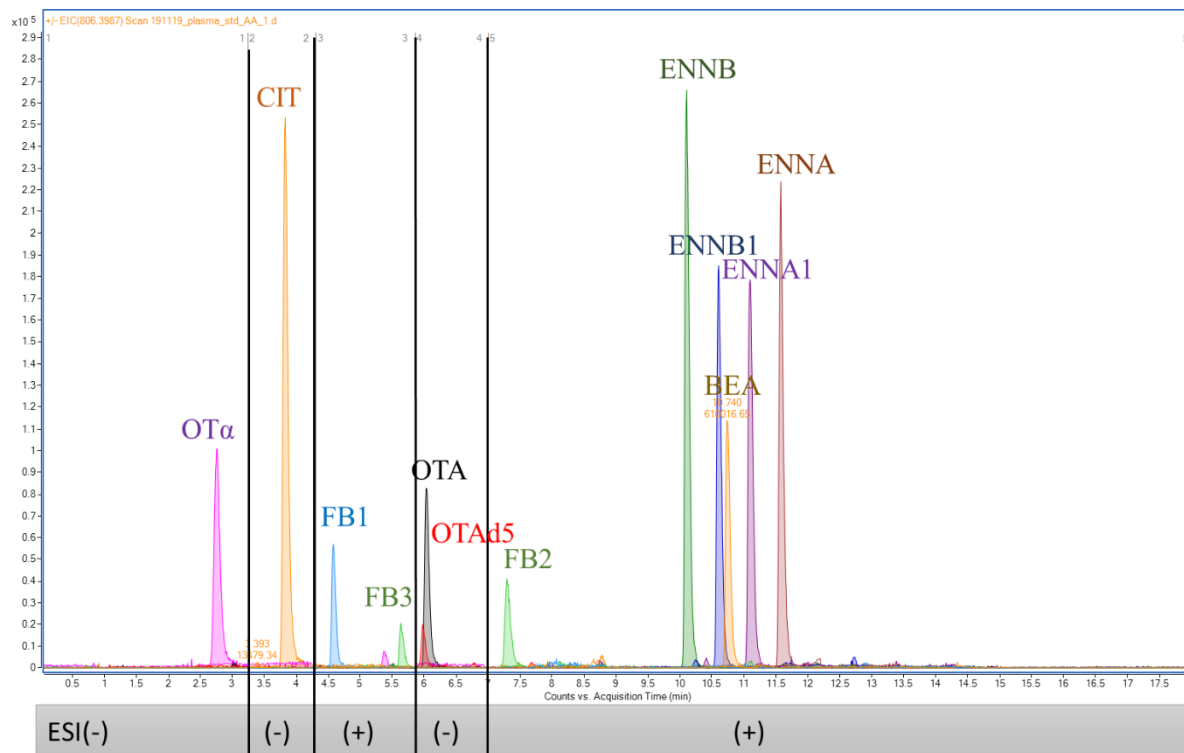


Figure 4.2. Chromatographic separation of all mycotoxins obtained using optimized Cortecs T3 C<sub>18</sub> LC method and methanol/water/isopropanol/0.02% AA mobile phase. The results are shown for 20 ng/mL mycotoxin plasma standard in 60% methanol with 1% FA. Mycotoxins are shown in the ESI modes where maximum signal intensity was obtained, which is the same mode used for mycotoxin quantitation.

No published methods that covered the exact same 10 mycotoxins. The multi-mycotoxin method developed by Osteresch *et al.* covered nine out of our 10 mycotoxins, except for FB2 and uses HPLC C<sub>18</sub> column combined with water/acetonitrile mobile phase.<sup>136</sup> Lauwers *et al.* compared the performance of four different RP columns, Hypersil Gold (1.9 μm, 50 mm × 2.1 mm), Zorbax Eclipse C18 (1.8 μm, 50 mm × 2.1 mm), Acquity BEH-C<sub>18</sub> (1.7 μm, 50 mm × 2.1 mm), and Acquity HSS-T3 (1.8 μm, 100 mm × 2.1 mm) for the separation of 24 mycotoxins which included emerging mycotoxins and OTA.<sup>279</sup> The best mycotoxin separation was achieved with Acquity HSS-T3 column and water/ methanol mobile phase.<sup>279</sup> Cao *et al.* developed multi-mycotoxin method for FB1, FB2, CIT, OTA, aflatoxins, patulin and sterigmatocystin using Kinetex C<sub>18</sub> column and water/ acetonitrile mobile phase.<sup>139</sup> To the best of my best knowledge, none of the reported methods used isopropanol for the detection of mycotoxins in blood-derived samples in order to prevent the column build-up caused by endogenous compounds in samples. In

addition, there are two mycotoxin methods with fast polarity switching in food poultry samples<sup>282,283</sup> but this is the first that time-segmented polarity switching was used for multi-mycotoxin detection in any samples.

#### 4.3.1.2 Effect of mobile phase additives on ionization efficiency

In Chapter 2, it was clearly shown that mobile phase additives can drastically increase ionization efficiency and significantly influence the limits of detection. In addition, enniatins and BEA are prone to generating multiple adduct ions, such as ammonium or sodium adduct ions in ESI(+), as shown in Appendix C Supplementary Figure C3. To address this issue, a number of publications use ammonium formate and ammonium acetate mobile phases to promote reproducible ammonium adduct formation over other forms.<sup>75,121,153,284</sup> In addition, ammonium adduct is easier to fragment than sodium, thus resulting in better LLOQs since tandem mass spectrometry is often used for mycotoxin analysis.<sup>75,279</sup> On the other hand, fumonisins also better ionize in ESI(+), but they do not generate adducts. Their most intense ion is a protonated ion.<sup>75,285</sup> OTA and CIT deprotonated ions were detected by Devreese *et al.* pig plasma Blazkewicz *et al.* human plasma methods, respectively<sup>75,138</sup>, while Osteresch *et al.* human blood and serum method for OTA, OT $\alpha$  and CIT and Cao *et al.* plasma for OTA and CIT produced protonated ions.<sup>136,139</sup>

For this method, both ESI(+) and ESI(-) were required to achieve the best sensitivity for the analytes of interest. Polarity-switching was thus investigated to see if it can provide optimum sensitivity for various analytes, while increasing overall throughput. The use of ammonium salts may decrease signal intensity in ESI(-), whereas the use of acetic acid which promotes ESI(-) may in turn decrease LLOQs for enniatins to unacceptable levels. Thus, to investigate the effect of mobile phase additives on time-segmented polarity switching method, four mobile phase additives: ammonium acetate, ammonium formate, FA and AA, were investigated. The results obtained are shown in Figure 4.3. However, the results demonstrated that combination ESI(-) and ESI(+) in a single analytical run was challenging. FA was the best compromise between all additives when using methanol mobile phases, as shown in Figure 4.3. Ammonium acetate and ammonium formate were suitable only for emerging mycotoxins and significantly decreased fumonisin signal intensities.



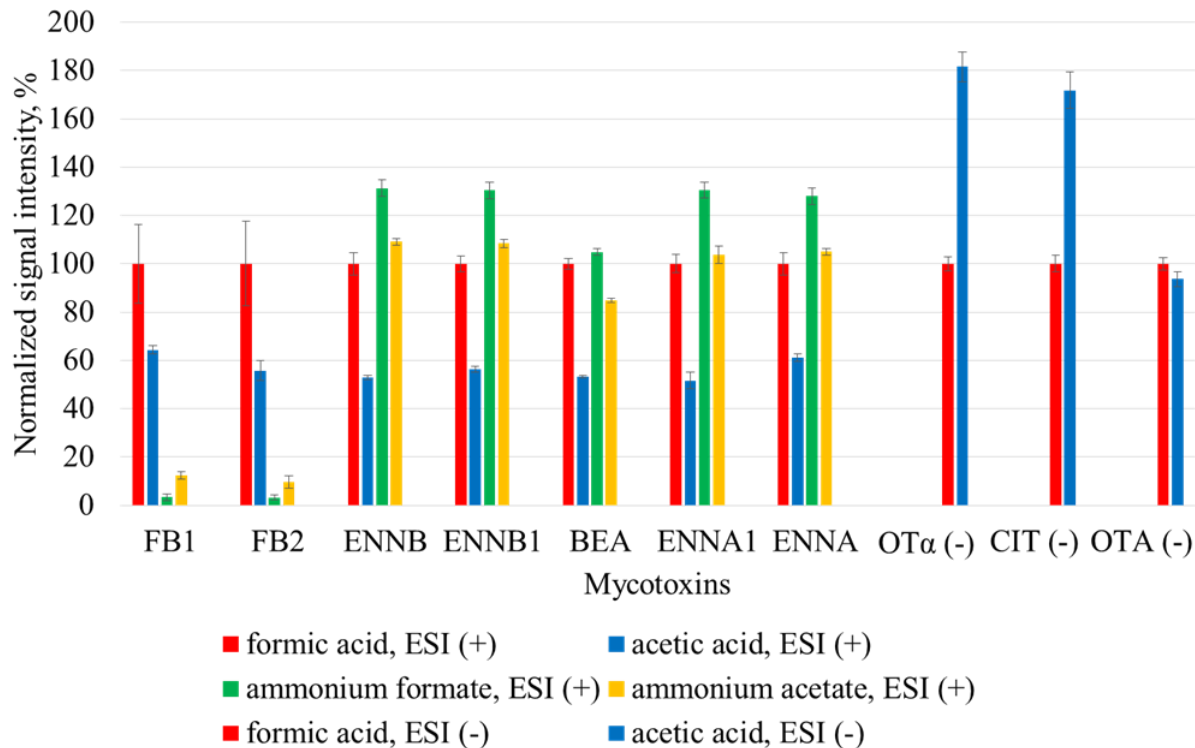


Figure 4.3. Evaluation of signal intensities of mycotoxins using different mobile phase additives. FB1, FB2, ENNB, ENNB1, BEA, ENNA, and ENNA were detected in ESI(+) and OT $\alpha$ , CIT and OTA were in ESI(-). The signal intensities (expressed as peak area) of mycotoxins obtained with 0.05% (8 mM) acetic acid, 2 mM ammonium acetate and 2 mM ammonium formate were normalized to the signal intensity obtained with 0.05% (13 mM) formic acid in mobile phase. The results are shown for 10 ng/mL mycotoxin standard (n=3) in 40% methanol. The separation was performed using water/methanol mobile phase. Mycotoxins were detected as protonated ions for fumonisins, deprotonated ions for ochratoxins and ammonium adducts for emerging mycotoxins.

Acetic acid performed well for OT $\alpha$  and CIT but was less efficient for fumonisins and emerging mycotoxins. After switching methanol mobile phase to isopropanol, the effects of two additives (AA and FA) and their concentration (0.02% vs. 0.05% v/v) were further evaluated using matrix-matched calibration curves in plasma in order to evaluate the effect of additives on LOD and S/N ratios in complex matrix. The best performance was observed with 0.02% AA (Appendix C, Supplementary Figures C4-8), as indicated by the ability to detect low concentration standards and the highest signal intensities obtained with 0.02% AA. Thus, 0.02% AA was selected for all further work. This observation is in agreement with our previous findings for ESI(-)<sup>233</sup>.

#### 4.3.1.3 Optimization of MS parameters for time-segmented polarity-switching method

In order to reduce the MS analysis time per sample, time-segmented polarity switching method was used to measure 10 mycotoxins of interest. This approach required sufficient separation of critical pairs that require different ESI modes. The same values for MS settings, including drying gas and sheath temperature in both ESI(-) and ESI(+) were used to ensure stable electrospray. However, since method sensitivity was critically important for this application, MS settings such as fragmentor voltage were investigated from 50 to 250 V to obtain the highest signal intensities for each mycotoxin. The findings demonstrated that signal intensity of three mycotoxins detected in ESI(-) drastically depended on the fragmentor voltage and optimum individual values were set for these analytes (Appendix C Supplementary Figures from C9 to C12 ). All fumonisins and emerging mycotoxins detected in ESI(+) had high signal intensities at 245 V fragmentor value. Final fragmentor values are shown in Table. 4.1 according to the time segments.

The other settings that were investigated were the calibration parameters of the instrument. This instrument can be calibrated at two mass ranges, 50-1700 m/z and 50-750 m/z. Mycotoxin monoisotopic masses of the most intense ion ranged from 249.0763 m/z to 806.3987 m/z (Appendix C Supplementary Table C1), so both mass ranges can be used for this method. The comparison of signal intensities was performed at three concentration levels in spiked plasma, 0.3 ng/ml, 2.5 ng/ml and 20 ng/ml for all mycotoxins, except for OT $\alpha$  (only 2.5 ng/mL and 20 ng/mL). Using 50-750 m/z calibration mass range, signal intensities for OT $\alpha$ , CIT and OTA increased by 60% (Appendix C Supplementary Figure C13). For the remaining mycotoxins, there was no significant change in signal intensities observed. Thus, the narrow mass range was chosen, 50-750 m/z.

Next, high resolution mode (4 GHz) vs. extended dynamic range mode (2 GHz) of QTOF was examined using plasma calibration curves, ranging from 0.039 ng/ml to 20 ng/ml. All results are summarized in Appendix C Supplementary Figures C14-18. High resolution mode (4 GHz) acquire data at the apex of the mass peak more heavily than at the shoulders providing narrower and better resolution peaks vs. extended dynamic range mode (2 GHz). Resolving power ranged from 19000 to 31000 and 17000 to 25000 for ESI(+) and ESI(-), respectively, for high resolution mode (4 GHz). While extended dynamic range mode (2 GHz) resolving power ranged from 10000 to 22000 for ESI(+) and from 10000 to 20000 and ESI(-). Based on the results, high resolution mode (4 GHz) gave better sensitivity for all mycotoxins compared to the extended dynamic range

mode (2 GHz) and was chosen for the final method settings. Our findings are in agreement with Jensen *et al.*<sup>286</sup> They investigated the effect of four resolving power settings (17500, 35000, 70000 and 140000) using HRMS, Q-Exactive Orbitrap, at three different mycotoxin concentration levels in feed samples.<sup>286</sup> The resolving power of 17500 resulted in a wide range of mass accuracies, even more than 10 ppm<sup>286</sup> Therefore, masses that had more than  $\pm 5$ ppm error would not be detected at  $\pm 5$ ppm extraction window and generate false negatives.<sup>286</sup> In order to extract at  $\pm 5$ ppm mass window minimal 35000 resolving power was necessary.<sup>286</sup> However, some complex samples required 70000 resolving power to enable the separation of mycotoxins from interfering ions at low concentration levels.<sup>286</sup> In sum, the insufficient resolving power of HRMS can result in poor mass accuracy and poor selectivity at trace concentrations.

Acquisition rate is MS parameter that defines how many spectra are acquired per second. Acquisition rates and time influence the signal intensity and the number of acquired scans across the peak. Signal intensities of mycotoxins were first compared at 1 spectra per second, 3 spectra per second and 6 spectra per second. However, at 1 spectra per second FB2 was not observed, presumably because of insufficient scans across the peak, whereas at 6 spectra per second OT $\alpha$  and CIT were not observed due to the low intensities. The final optimization thus compared the performance of 3 and 2 spectra per second (Appendix C Supplementary Figure C19 and Supplementary Table C2). The acquisition rate of 2 spectra per second increased signal intensities of mycotoxins by 43-56% while still providing acceptable scan numbers ranging from 15 to 42 points across the peak, thus allowing accurate quantification. This setting was selected for all subsequent experiments.

#### 4.3.1.4 Selection of injection solvent

Injection solvent composition was critical for this method since the method combines mycotoxins with different properties. Our initial work showed that hydrophobic compounds, such as OTA and BEA gave higher signal intensity in 40% methanol vs. 20% methanol.<sup>233</sup> Thus, the starting composition of injection solution was 40% methanol for this new method, which also matched closely to the initial LC conditions (45% B, methanol mobile phase). Further experiment evaluated the injection solvent composition in terms of analyte solubility, peak shape of early-eluting compounds and signal stability over the analytical run. The evaluation of signal stability over the analytical run demonstrated that fumonisin and emerging mycotoxin signal intensities

continuously decreased over time. For example, 20 ng/ml mycotoxin standard prepared in 40% methanol and injected as a quality control sample every 3 or 4 injections, systematic drift was observed over time (Appendix C Supplementary Figure C20). It was hypothesized that this can happen due to solubility issues and/or non-specific adsorption effects. To investigate this hypothesis, different compositions, 40%, 60% and 80% methanol, and plastic and glass inserts were investigated using the experimental scheme shown in Figures 4.1 and 4.2. In addition, to check the losses due to adsorption, the experiments described in Section 4.2.6.2 were performed. As expected, based on the solvent injection strength, the experiments showed that the early-eluting mycotoxins, CIT and OT $\alpha$ , peak shape depended on the solvent composition. The best shape was obtained with 40% methanol, 60% methanol showed some peak shape deterioration but was still acceptable, whereas unacceptable peak shape was obtained with 80% methanol (Appendix C Supplementary Figure C21). The remaining mycotoxins showed good peak shape across all injection solvent compositions tested. Overall, 60% methanol is good compromise for all mycotoxins.

Furthermore, mycotoxin signal intensities were compared in injection solvents (40%, 60% and 80% methanol) and type of injection inserts (polypropylene plastic versus glass inserts) in order to ensure good solubility for all mycotoxins (Figure 4.4 and Figure 4.5). 40% methanol composition in plastic inserts showed solubility issues for FB1, FB2, ENNB, BEA, ENNB1, ENNA and ENNA1 vs. glass inserts (Figure 4.4). The intensities are not dependent on the type of inserts when methanol composition is held above 60% for OT $\alpha$ , CIT, FB1, and OTA, additional signal increments, from 8% to 79%, were observed for FB2, ENNB, BEA, ENNA1 and ENNA vs. 40% methanol composition in glass inserts (Figure 4.4). Figure 4.5 shows that 80% methanol composition is slightly better in terms of signal intensity (additional 9-21% increment) than 60% for all emerging mycotoxins and OTA. Additionally, Figure 4.5 demonstrates that the mycotoxin intensities are not dependent on the type of inserts for all mycotoxins dissolved in 60% methanol.

The evidence of non-specific adsorption was demonstrated in Eppendorf tubes and plastic insets for BEA, ENNA and ENNA1, when 40% methanol was used (Figure 4.4). This adsorption experiment was then repeated with 60% methanol, and no adsorptive losses were observed, except for ENNB1 (Figure 4.5).

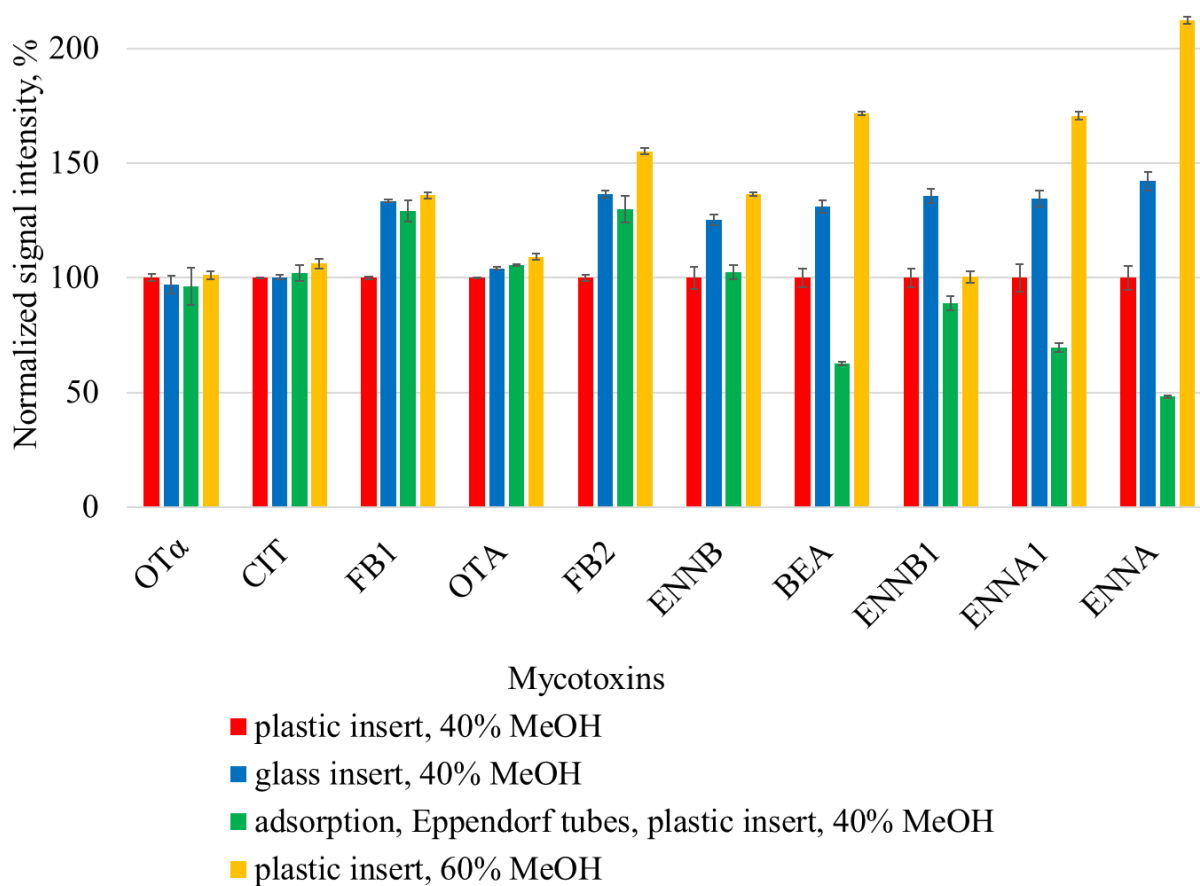


Figure 4.4. Evaluation of non-specific adsorption using plastic and glass inserts and different injection solvent compositions, 40% and 60% methanol,  $n=3$ . ■ - 20 ng/mL standard mycotoxin solution in 40% methanol transferred into plastic inserts for LC-MS analysis, ■ - 20 ng/mL standard mycotoxin solution in 40% methanol transferred into glass inserts for LC-MS analysis, ■ - adsorption experiment then 20 ng/mL standard mycotoxin solution in 40% methanol transferred into plastic inserts for LC-MS analysis. ■ - standard mycotoxin solution in 60% methanol transferred into plastic inserts for LC-MS analysis.

ENNB1 signal intensity dropped to 73% in 60% methanol, but this value was considered as outlier because signal intensity of 89% was observed in 40% methanol (Figure 4.4). In sum, 60% methanol is good compromise for all mycotoxins considering mycotoxin solubility, non-specific adsorptive losses, and peak shapes for early-eluting polar mycotoxins.

Next, the stability of signal intensity was re-evaluated using standard solutions prepared in 60% methanol, however, fumonisin signal intensities still showed systematic decrease in signal intensity over time (Appendix C Supplementary Figure C22), indicating that additional modification to the method was needed.

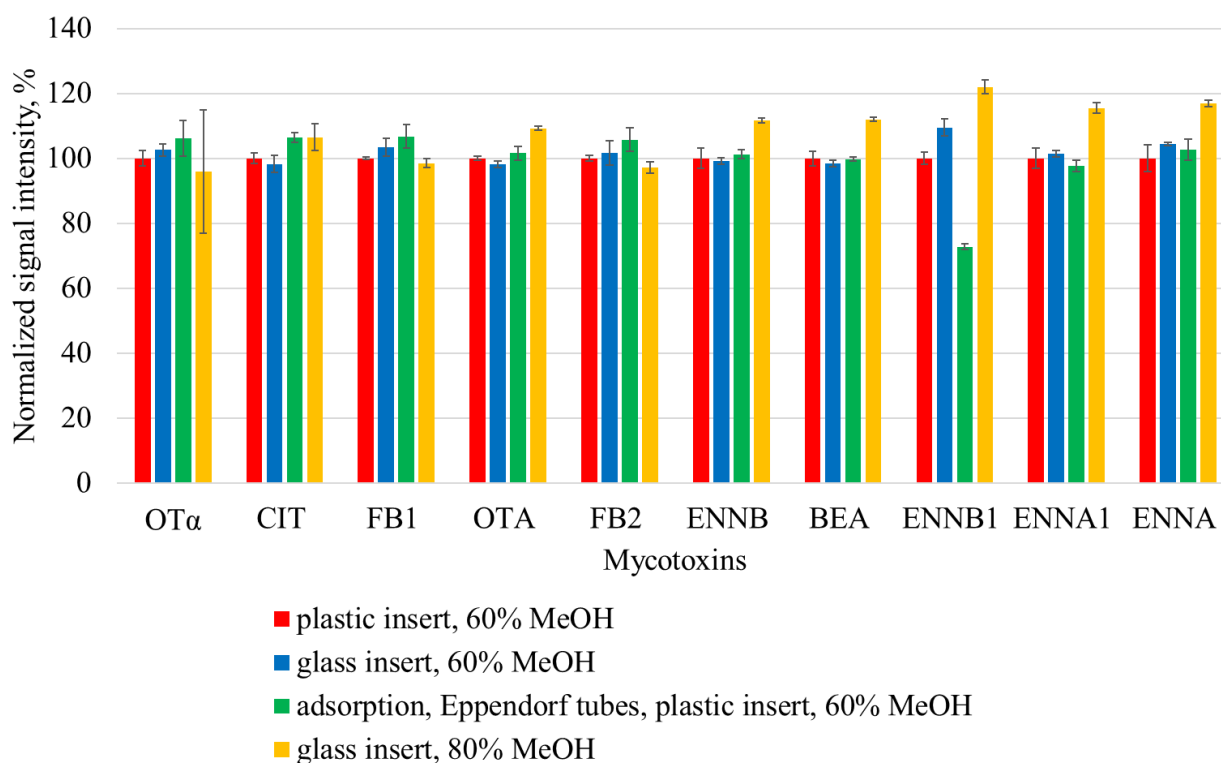


Figure 4.5. Evaluation of non-specific adsorption using plastic and glass inserts and different injection solvent compositions, 40% and 60% methanol, n=3. ■ - 20 ng/mL standard mycotoxin solution in 60% methanol transferred into plastic inserts for LC-MS analysis, ■ - 20 ng/mL standard mycotoxin solution in 60% methanol transferred into glass inserts for LC-MS analysis, ■ - adsorption experiment then 20 ng/mL standard mycotoxin solution in 60% methanol transferred into plastic inserts for LC-MS analysis, ■ - standard mycotoxin solution in 80% methanol transferred into plastic inserts for LC-MS analysis.

Since fumonisins are acidic compounds, the addition of 1% of FA to injection solvent was examined. The summary of the signal intensity results over time is shown in Appendix C Supplementary Figure C23. The addition of 1% FA to 60% methanol resolved the issue of drifting signal intensity of fumonisins and did not adversely affect the rest of mycotoxins. This was selected as the final injection solvent composition. To the best of our knowledge, this is the first extensive evaluation of injection solution composition to ensure accurate quantitation and minimize losses due to non-specific adsorption for multi-mycotoxin methods. The importance of this parameter during method development should not be under-estimated.

#### 4.3.1.5 Development of sample preparation method for 10 mycotoxins

Sample preparation is a key step for the development of multi-mycotoxin LC-MS methods. Sample preparation is a critical determinant of method sensitivity and accurate quantitation of mycotoxins. Mycotoxins combined in this method have different chemical and physical properties. Fumonisin and ochratoxins are acidic compounds, emerging mycotoxins are basic compounds. Their logPs also vary, from 0.81-4.61 for ochratoxins, -0.67-0.72 for fumonisins and 4.96-7.27 for emerging mycotoxins using ChemAxon prediction algorithm. Ochratoxins and fumonisins are polyketide-derived compounds, whereas emerging mycotoxins are depsipeptides, Figure 1.1. For this reason, a simple generic sample preparation technique of organic solvent protein precipitation was chosen for this application in order to provide high analyte recovery. In addition, evaluation of sample preparation techniques for the method #1 showed that OTA, FB1 and FB2 were not extracted with LLE (ethyl acetate) with PE% > 70% even when acidification was used and HLB Oasis may lead to the high cost per samples<sup>233</sup>. Acetonitrile and methanol were first evaluated as protein precipitation and reconstitution solvents for OT $\alpha$ , CIT, OTA, FB1, FB2 and BEA. According to PEs% summarized in Figure 4.6, methanol provided the best PEs% (85.8-102.4%) for all compounds when used as a solvent for both protein precipitation and reconstitution. When acetonitrile was used for reconstitution, it resulted in low PEs%, 18.1%, 34.7% and 12.2% for OT $\alpha$ , CIT and BEA, respectively, demonstrating that acetonitrile does not sufficiently solubilize these mycotoxins. Similar results were observed when acetonitrile protein precipitation samples were reconstituted into acetonitrile. PEs% were 20.7%, 36.4% and 13.5% for OT $\alpha$ , CIT and BEA, respectively. However, PEs% were 85.0%, 97.2% and 89.9% for OT $\alpha$ , CIT and BEA, respectively, when acetonitrile protein precipitation samples were reconstituted into methanol. Acetonitrile is not an appropriate solvent for protein precipitation for fumonisins, since acetonitrile protein precipitation samples reconstituted in acetonitrile had low PEs%, 27.0% and 37.9% for FB1 and FB2, respectively. Similar results were obtained with acetonitrile protein precipitation samples reconstituted in methanol, 11.1% and 22.9% for FB1 and FB2, respectively. This effect was not observed for methanol protein precipitation samples. Organic solvent protein precipitation can effectively remove most of the proteins from blood-derived products, such as plasma and serum.

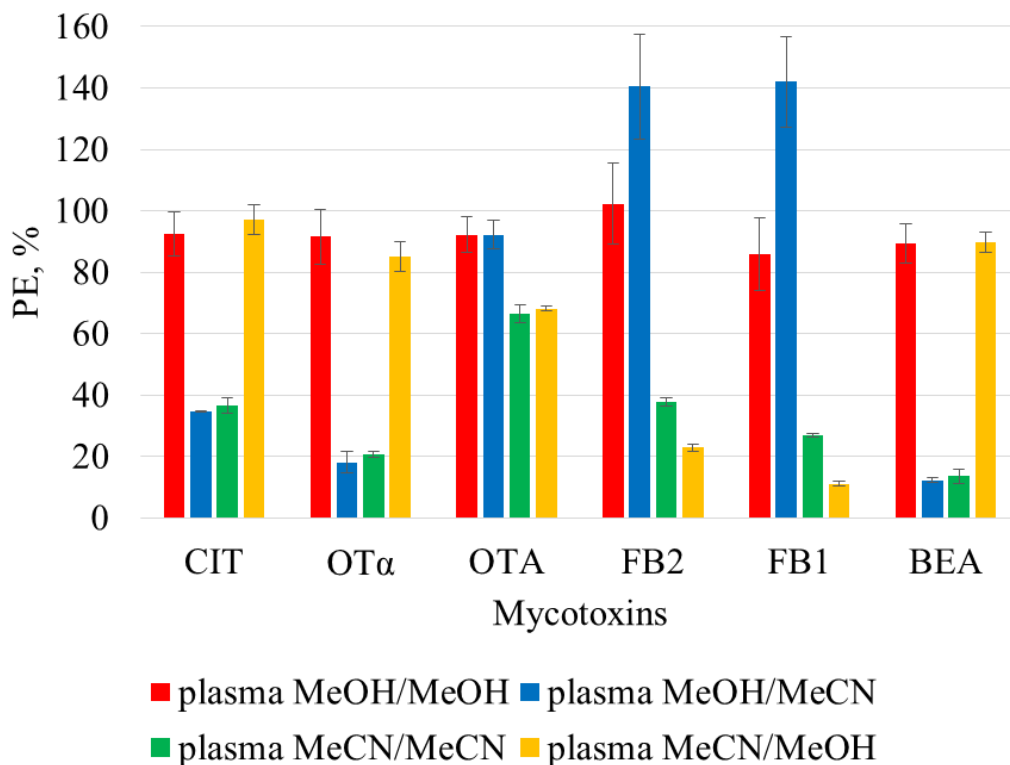


Figure 4.6. Evaluation of PEs% using different precipitation and reconstitution solvents, methanol and acetonitrile,  $n=3$ . The results are shown for plasma spiked with 100 ng/mL of mycotoxins ■ - extracted with methanol and reconstituted into 40% methanol, ■ - extracted with methanol and reconstituted into 40% acetonitrile, ■ - extracted with acetonitrile and reconstituted into 40% acetonitrile, ■ - extracted with acetonitrile and reconstituted into 40% methanol.

Protein removal efficiencies were found to be >90% for both methanol and acetonitrile<sup>287</sup>. For this multi-mycotoxin method, it is prioritized to have negligible matrix effects as isotopically-labelled internal standards for all analytes of interest are not available. Plasma after protein precipitation can still have high content of lipids and other endogenous compounds that can interfere with mycotoxin analysis. Thus, additional clean-up steps to remove lipids, such as LLE with hexane and MTBE, were evaluated. The recoveries of all mycotoxins using protein precipitation with methanol and combined LLE-protein precipitation methods are shown in Figure 4.7. The addition of both MTBE and hexane LLE sample clean-up resulted in low recoveries of ENNs and BEA, ranging from 0% to 11.2%. Further application of LLE clean-up was discontinued for this reason. Finally, matrix effects were evaluated for protein precipitation with methanol and found to be negligible (80-120%) for all mycotoxins, as shown in Figure 4.8.



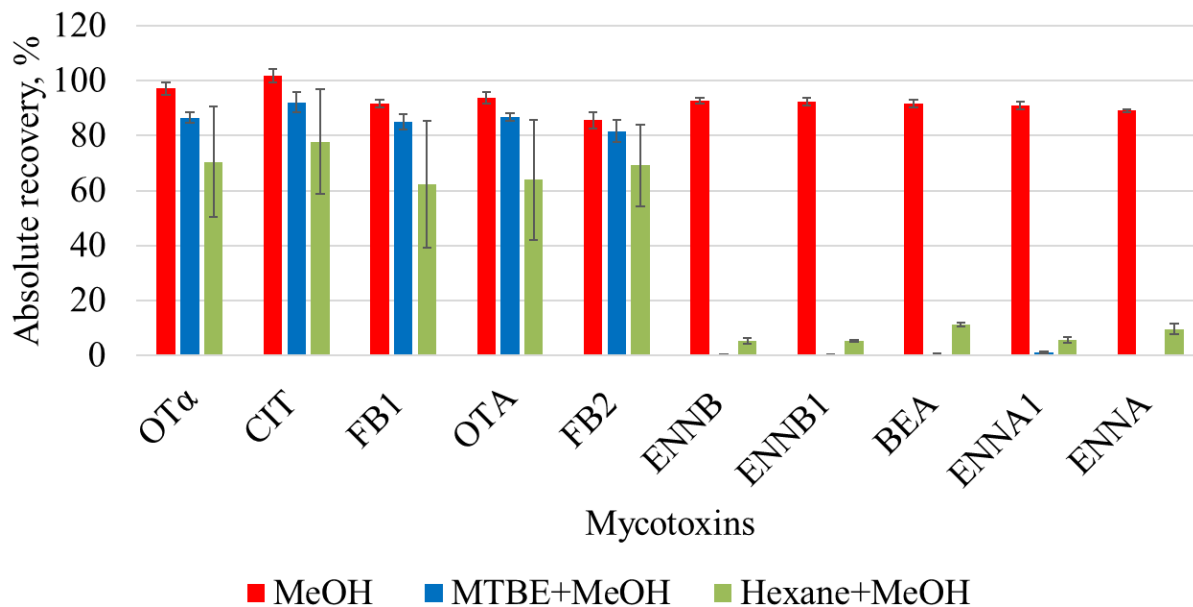


Figure 4.7. Evaluation of absolute extraction recoveries using different sample preparation methods. ■ - protein precipitation with methanol, ■ - LLE extraction with MTBE followed by protein precipitation with methanol, ■ - LLE extraction with hexane followed by protein precipitation with methanol. The results are shown for plasma spiked with 100 ng/mL mycotoxins, n=3.

Sample preparation protocol, Section 4.2.3.2.1, was changed to protocol described in Section 4.2.4. The first change was increasing the time of centrifugation, from 10 to 20 min to ensure an effective sedimentation of precipitated proteins. 10-min centrifugation was found to cause increasing LC pressure during method development indicating protein-binding on the column. A second centrifugation step was also added when injection solvent composition was changed to contain formic acid. Acids can cause additional protein precipitation, and small amount of precipitation was observed in samples after adding FA and centrifugation. However, even after these two changes, increases in column pressure were still observed after long analytical runs. To address this issue, methanol was kept at 4°C before adding to plasma, mixing time was reduced to 3 min, and samples were kept at -80°C for 20 minutes. According to Sarafian *et al.* freezing temperatures maximize protein precipitation.<sup>288</sup> During evaluation of long analytical run of 200 samples, the column pressure still increased slightly but this precipitate formation affected only guard column. Thus, in-line filter was added prior to guard column to prevent frequent guard replacement.

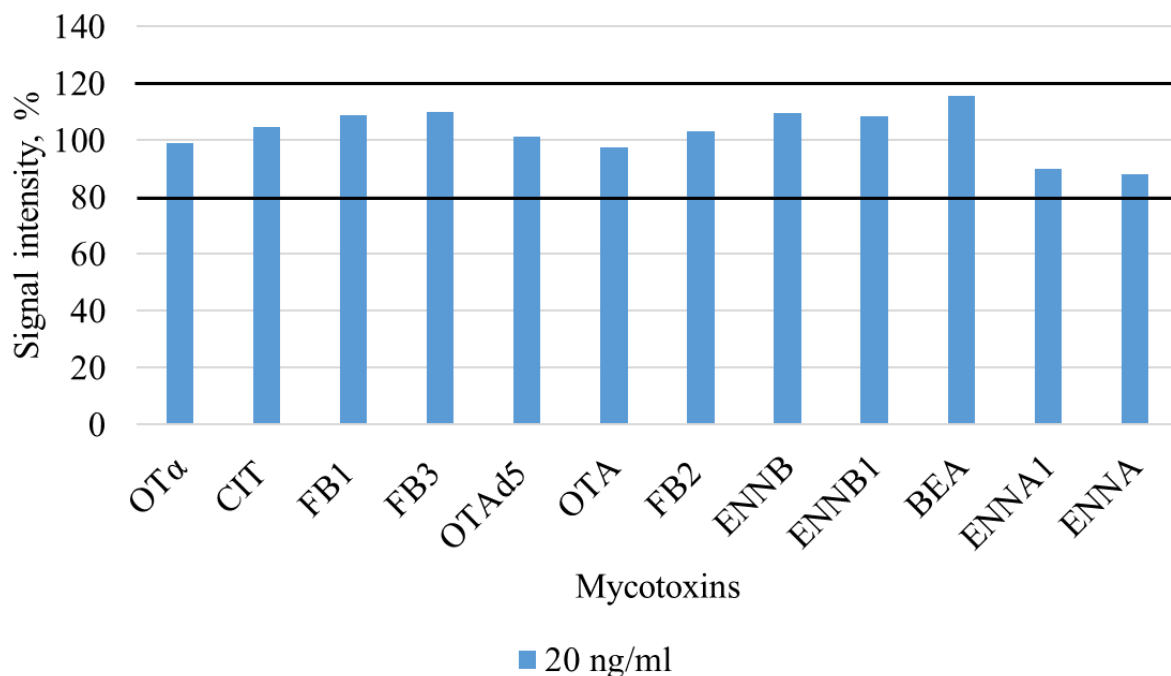


Figure 4.8. Evaluation of matrix effects using protein precipitation with methanol. The results are shown for pooled plasma spiked with 20 ng/mL mycotoxins,  $n=3$ .

#### 4.3.2 Evaluation of method accuracy and precision

Validation is the process to determine method performance parameters, including precision, accuracy, LLOQ, LOD, linearity, recovery, selectivity, and stability. Thus, validation results can be used to estimate the method reliability and determination whether method is suitable for its intended use. Currently, there is no guidance for the validation of biomonitoring LC-MS methods, so FDA Bioanalytical Method Validation Guideline procedures were selected for this purpose.<sup>190</sup> According to FDA guidelines, method accuracy and precision should meet 85-115% accuracy and  $\leq 15\%$  RSD for precision for all levels except for LLOQ where 80-120% accuracy and  $\leq 20\%$  RSD for precision are acceptable. Considering biomonitoring methods are applied for ultra-trace analysis of very low levels of xenobiotics, we consider method performance to be acceptable if 80-120% accuracy and  $\leq 20\%$  RSD are met across all levels.

During method evaluation, intra-day accuracy and precision experiments were performed three times. The first experiment used matrix-matched calibration curves, ranging from 0.075 to 19.2 ng/ml for OTA, ENNB, ENNB1, from 0.10 to 25.6 ng/ml for CIT, and from 0.25 to 32.0

ng/ml for ENNA, ENNA1, BEA, FB1, FB2 and OT $\alpha$ . Validation samples (n=6) spiked with different concentrations of mycotoxins of interest were prepared using the same procedures as calibration curves at concentrations shown in Table 4.2. Figure 4.9 shows the results of the first intra-day accuracy and precision experiment. This experiment demonstrated that both LOQ 1 and LOQ 2 levels of OT $\alpha$  (216.2% and 221.5%), CIT (149.2% and 122.2%), FB1 (134.3%, and 147.7%), OTA (69.6% and 46.4%), BEA (203.5% and 169.7%), ENNA1 (186.2% and 152.1%), ENNA (157.0% and 150.5%) and ENNB (62.5% for LOQ 2) did not pass criteria for accuracy (within 20% of nominal concentration). Precision criteria did not meet acceptance of  $\leq 20\%$  RSD for CIT (21.9%, 22.4%), OTA (117.0%, 109.2%), FB2 (24.8% only for LOQ 1) and ENNB (30.3% for LOQ 2). In addition, accuracy values of OT $\alpha$  (168.5%, 170.0% for low 1, low 2, respectively), ENNB (64.6% and 74.6% for low 1 and low 2), BEA (125.0% for low 2) and ENNA (124.0% for low 2) were unacceptable. Furthermore, OTA showed poor precision (25.6% and 44.5% RSD for low 1 and low 2). These results demonstrated unacceptable method performance and experiment was repeated to test additional concentration levels.

*Table 4.2. Validation sample concentrations prepared to evaluate method accuracy and precision in the first intra-day experiment.*

<b>Level</b>	<b>OT<math>\alpha</math></b>	<b>CIT</b>	<b>FB1</b>	<b>OTA</b>	<b>FB2</b>	<b>ENNB</b>	<b>ENNB1</b>	<b>BEA</b>	<b>ENNA1</b>	<b>ENNA</b>
	<b>Concentration, ng/ml</b>									
LOQ 1	0.50	0.10	0.63	0.08	0.63	0.15	0.15	0.25	0.25	0.25
LOQ 2	0.63	0.13	0.78	0.10	0.78	0.19	0.19	0.31	0.31	0.31
LOW 1	1.50	0.30	1.88	0.24	1.88	0.45	0.45	0.75	0.75	0.75
LOW 2	1.88	0.38	2.34	0.30	2.34	0.56	0.56	0.93	0.93	0.93
MEDIUM	3.33	2.67	3.33	2.00	3.33	2.00	2.00	3.33	3.33	3.33
HIGH	18.3	14.7	18.3	11.0	18.3	11.0	11.0	18.3	18.3	18.3

Considering that the accuracy and precision of several mycotoxins in the first experiment did not meet requirements, the validation samples were modified and prepared as summarized in Table 4.3. Three higher concentration levels were set as low (3.5 ng/ml), medium (8 ng/ml) and high (16 ng/ml) for all mycotoxins. Three possible LLOQ concentrations, LOQ 1, LOQ 2, and LOQ 3 were varied for mycotoxins, considering the results from method development and first intra-day validation experiment.

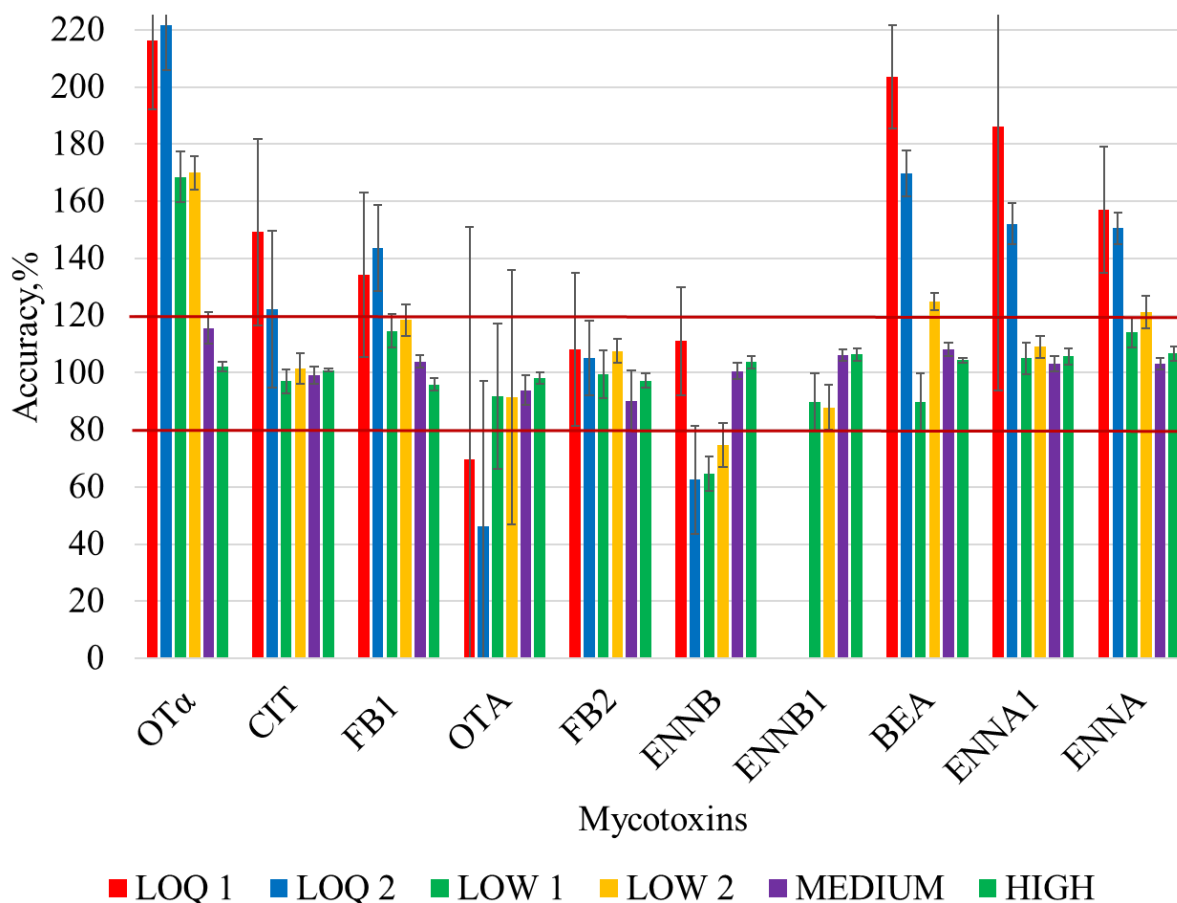


Figure 4.9. Summary of intra-day accuracy and precision results obtained in the first experiment. y-axis shows mean accuracy, and standard deviation ( $n = 6$ ) is shown as error bar. Intra-day precision and accuracy determination was performed using validation plasma samples shown in Table 4.2. and appropriate matrix-matched calibration curves. Red lines show acceptable accuracy which is set at 80% to 120%.

Matrix-matched calibration curves were prepared at equal concentration levels for all mycotoxins, ranging from 0.08 to 20.0 ng/ml. Figure 4.10 summarizes the results of the second intra-day validation experiment. Overall, all validation samples at low, medium, and high concentration levels passed precision and accuracy criteria, showing acceptable method performance above 3.5 ng/ml. Among three potential LLOQ levels, at least one LLOQ level met precision and accuracy requirements, except for CIT and ENNB1. CIT was not observed in any LLOQ samples whereas ENNB1 accuracy exceeded acceptance of 120% in all three LLOQ levels tested.

Table 4.3. Validation sample concentrations prepared to evaluate method accuracy and precision in the second experiment.

Level	OT $\alpha$	CIT	FB1	OTA	FB2	ENNB	ENNB1	BEA	ENNA1	ENNA
	Concentration, ng/ml									
LOQ 1	0.63	0.10	0.63	0.10	0.63	0.15	0.15	0.25	0.25	0.25
LOQ 2	1.25	0.20	1.25	0.20	1.25	0.30	0.30	0.50	0.50	0.50
LOQ 3	1.88	0.30	1.88	0.30	1.88	0.45	0.45	0.75	0.75	0.75
LOW	3.50	3.50	3.50	3.50	3.50	3.50	3.50	3.50	3.50	3.50
MEDIUM	8.00	8.00	8.00	8.00	8.00	8.00	8.00	8.00	8.00	8.00
HIGH	16.0	16.0	16.0	16.0	16.0	16.0	16.0	16.0	16.0	16.0

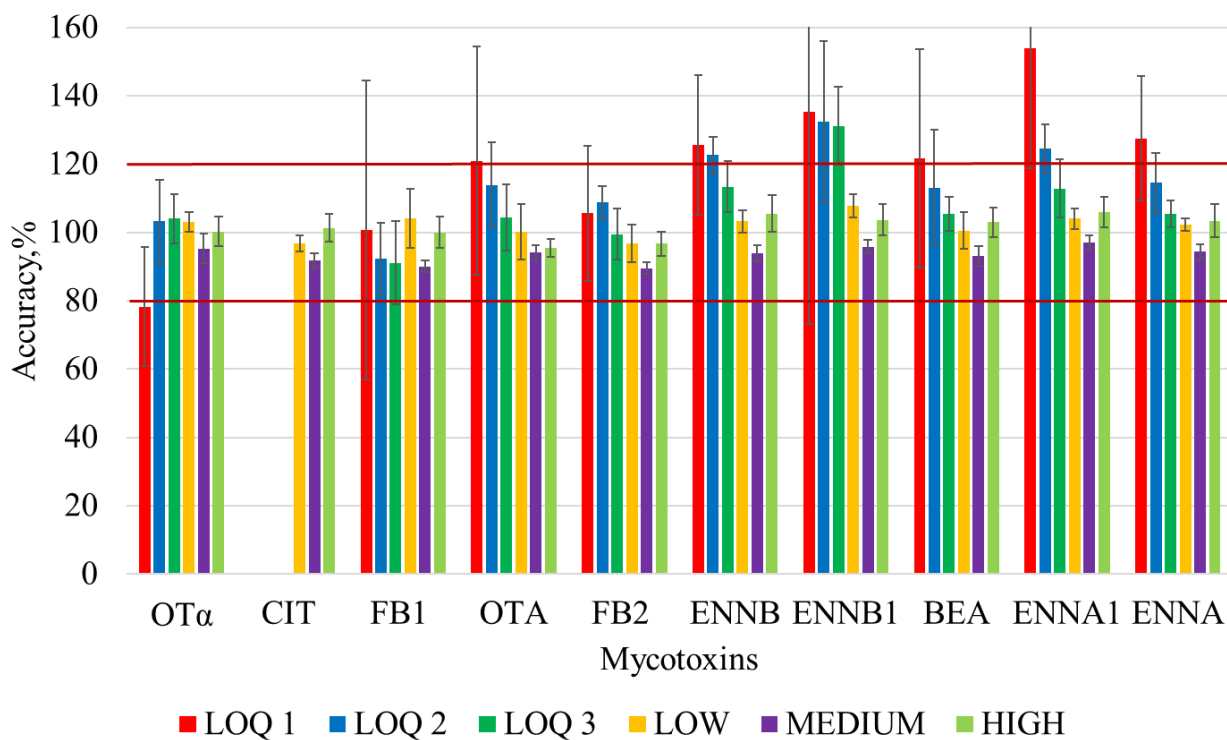


Figure 4.10. Summary of intra-day accuracy and precision results obtained in the second experiment. y-axis shows mean accuracy, and standard deviation ( $n = 6$ ) is shown as error bar. Intra-day precision and accuracy determination was performed using validation plasma samples shown in Table 4.3. and appropriate matrix-matched calibration curves. Red lines show acceptable accuracy which is set at 80% to 120%.

The results of first and second intra-day experiments did not show good agreement, so a third intra-day experiment was performed. Matrix-matched calibration curves were prepared in the range of 0.16 to 20 ng/ml for all mycotoxins. Considering unexpected results obtained with CIT and ENNB1, concentrations for validation samples were changed. Three concentrations at low (4.00 ng/ml), medium (8.00 ng/ml) and high (16.0 ng/ml) levels were prepared for all mycotoxins. Additional possible LLOQ levels were prepared for all mycotoxins to help refine LLOQ determination: LOQ 1 (0.20 ng/ml), LOQ 2 (0.30 ng/ml), LOQ 3 (0.45 ng/ml), LOQ 4 (0.65 ng/ml) and LOQ 5 (1.25 ng/ml) as shown in Table 4.4. The accuracy and precision results obtained for the third experiment are shown in Figure 4.11. All low, medium, and high validation samples met accuracy and precision requirements which agreed well with the results from second experiment. However, unexpectedly mycotoxins spiked at LLOQ concentrations from 0.20 ng/ml to 0.63 ng/ml were not detected in validation samples. At 1.25 ng/ml concentration level, only OT $\alpha$ , CIT and OTA met requirements. These results showed poor agreement with both first and second experiment, indicating significant issues with the reliability of the method. Table 4.5 summarizes LLOQs obtained across three experiments for all mycotoxins of interest.

*Table 4.4. Validation sample concentrations prepared to evaluate method accuracy and precision in the third experiment.*

<b>Level</b>	<b>Concentration, ng/ml</b>
LOQ 1	0.20
LOQ 2	0.30
LOQ 3	0.45
LOQ 4	0.63
LOQ 5	1.25
LOW	4.00
MEDIUM	8.00
HIGH	16.0

Several possible reasons for this disagreement between results were investigated. The matrix-matched calibration curves for all mycotoxins across three experiments were compared by calculating slope RSDs, 27.3-54.5%, which showed variability between three calibration curves (Table 4.6). Internal standard RSDs across the three experiments showed %RSD values of 3.2-7.9% across all validation samples within a given experiment indicating no issues with the

extraction process (Table 4.7). Additionally, internal standard signals over intra-day experiment shown in Appendix C Supplementary Figure C24 demonstrated signal stability during the run.

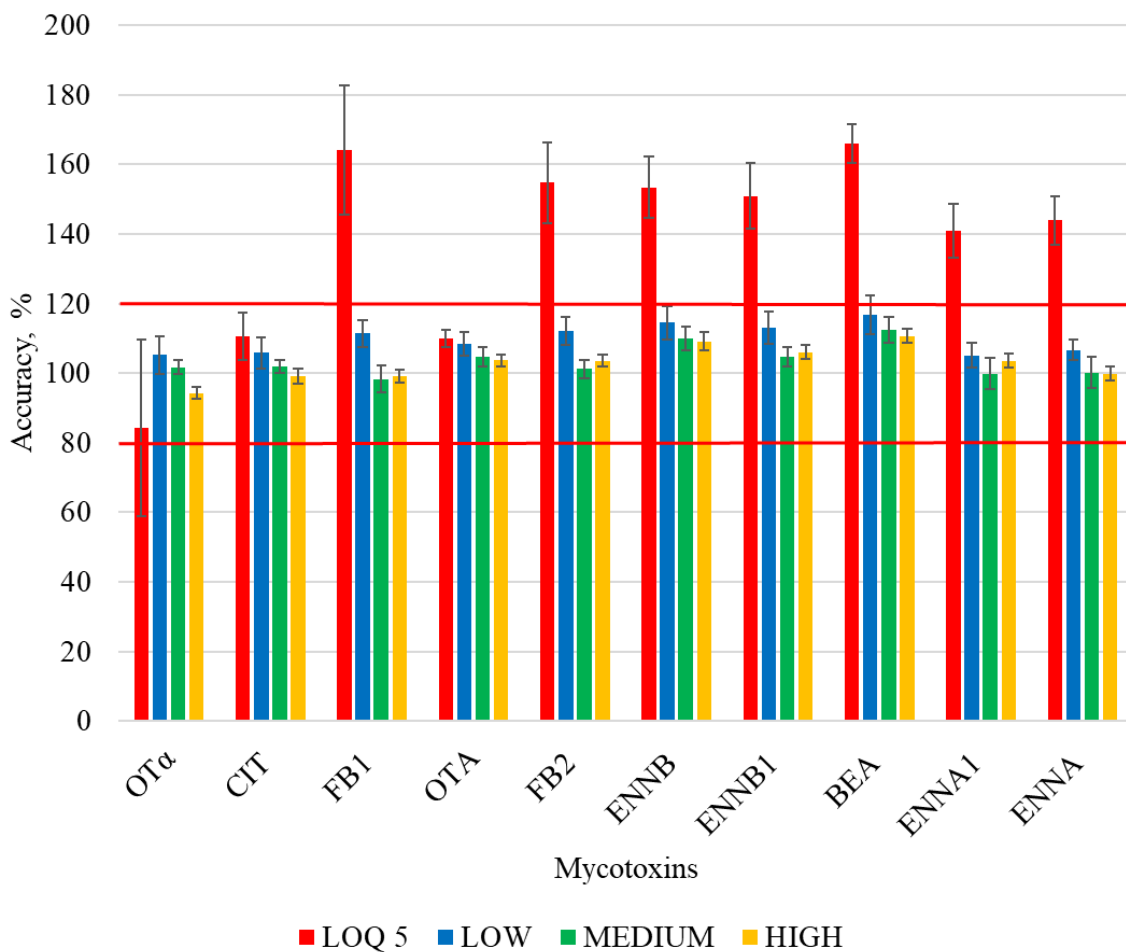


Figure 4.11. Summary of intra-day accuracy and precision results obtained in the third experiment. y-axis shows mean accuracy, and standard deviation ( $n = 6$ ) is shown as error bar. Intra-day precision and accuracy determination was performed using validation plasma samples shown in Table 4.4 and appropriate matrix-matched calibration curves. Red lines show acceptable accuracy which is set at 80% to 120%.

Mycotoxin areas were normalized to internal standard areas, and calibration curves were re-calculated using the ratio of mycotoxin areas to internal standard area. OT $\alpha$ , CIT and OTA areas were normalized to OTAd<sub>5</sub> internal standard, while the rest mycotoxin areas to FB3 internal standard. Finally, the calculated slope RSDs were improved and ranged from 3.1% to 17.6% for all mycotoxins, except for OT $\alpha$  (75.7%) and CIT (43.3%) as shown in Table 4.8, showing that

internal standard does not compensate variability in this time segments and not appropriate for these compounds.

Table 4.5. Summary of LLOQ values obtained for three intra-day accuracy and precision experiments. LLOQ was set as the lowest concentration that meets 80-120% accuracy and  $\leq 20\%$  RSD (n=6 replicates)

LLOQ	OT $\alpha$	CIT	FB1	OTA	FB2	ENNB	ENNB1	BEA	ENNA1	ENNA
	<b>Concentration, ng/ml</b>									
Experiment 1	3.33	0.30	1.88	2.00	0.78	2.00	0.45	0.75	0.75	0.75
Experiment 2	1.25	3.50	1.25	0.20	0.63	0.45	3.50	0.50	0.75	0.50
Experiment 3	4.00	1.25	4.00	1.25	4.00	4.00	4.00	4.00	4.00	4.00

Table 4.6. Summary of matrix-matched calibration curves for all mycotoxins across three experiments. The calibration curve is a plot of the instrumental responses versus concentrations (ng/ml), linear regression using a 1/x weighting factor.

Mycotoxin	Calibration Experiment 1	Calibration Experiment 2	Calibration Experiment 3	% RSD of slopes (n=3)
OT $\alpha$	Y=17095*x+3603	Y=24099*x-2005	Y=47987*x-495	54.5
CIT	Y=52079*x+892	Y=29912*x-3915	Y=37742*x+1488	28.2
FB1	Y=9392*x+2106	Y=6959*x+2834	Y=15800*x+5982	42.6
OTA	Y=17737*x+4244	Y=14567*x+3034	Y=36806*x+8177	52.2
FB2	Y=10346*x-482	Y=6889*x+129	Y=15159*x+3312	38.5
ENNB	Y=52713*x-1889	Y=30942*x+918	Y=63416*x+2438	33.8
ENNB1	Y=32068*x-3292	Y=16815*x-555	Y=37742*x+1488	37.5
BEA	Y=20301*x-3140	Y=14598*x+224	Y=28777*x-1894	33.6
ENNA1	Y=32515*x-8617	Y=23067*x-1641	Y=52490*x-12335	41.7
ENNA	Y=30969*x-3589	Y=22301*x-176	Y=39134*x-5669	27.3

Table 4.7. Internal standard mean peak area and %RSD across all three experiments.



Internal standard	Experiment 1		Experiment 2		Experiment 3	
	Mean peak area	%RSD	Mean peak area	%RSD	Mean peak area	%RSD
FB3	107053	6.0	76210	7.1	178799	7.9
OTAd <sub>5</sub>	157095	5.5	140641	5.4	425253	3.2

Table 4.8. Summary of matrix-matched calibration curves for all mycotoxins across three experiments normalized to internal standards. <sup>a</sup>Normalized to OTAd<sub>5</sub>, <sup>b</sup>normalized to FB3.

Mycotoxin	Calibration Experiment 1	Calibration Experiment 2	Calibration Experiment 3	% RSD of slopes (n=3)
OTα <sup>a</sup>	$y=4.68*x-0.002$	$y=1.64*x-0.02$	$y=1.19*x-0.04$	75.7
CIT <sup>a</sup>	$y=3.07*x-0.01$	$y=2.02*x-0.03$	$y=1.25*x-0.01$	43.3
FB1 <sup>b</sup>	$y=0.86*x-0.01$	$y=0.90*x-0.01$	$y=0.98*x-0.02$	6.8
OTA <sup>a</sup>	$y=1.07*x+0.08$	$y=1.00*x+0.01$	$y=0.91*x+0.02$	8.2
FB2 <sup>b</sup>	$y=0.90*x-0.02$	$y=0.85*x-0.01$	$y=0.93*x-0.02$	5.4
ENNB <sup>b</sup>	$y=4.71*x-0.03$	$y=3.80*x-0.04$	$y=3.77*x-0.03$	13.1
ENNB1 <sup>b</sup>	$y=2.85*x-0.03$	$y=2.05*x-0.02$	$y=2.25*x-0.02$	17.6
BEA <sup>b</sup>	$y=1.81*x-0.03$	$y=1.79*x-0.02$	$y=1.71*x-0.03$	3.1
ENNA1 <sup>b</sup>	$y=2.87*x-0.05$	$y=2.80*x-0.03$	$y=3.06*x-0.06$	4.7
ENNA <sup>b</sup>	$y=2.76*x-0.03$	$y=2.72*x-0.03$	$y=2.30*x-0.05$	9.7

Table 4.9. Quality control (QC) standard sample %RSD across three experiments.

QC	%RSD Experiment 1	%RSD Experiment 2	%RSD Experiment 3
OTα	4.7	8.6	3.9
CIT	4.6	2.8	6.7
FB1	4.9	6.1	2.0
OTA	4.0	4.3	3.6
FB2	4.4	6.1	7.1
ENNB	4.1	1.3	2.2
ENNB1	4.2	2.9	1.7
BEA	4.9	3.2	1.9
ENNA1	4.4	4.3	2.2
ENNA	4.7	3.9	1.9

QC samples injected throughout the sequence were extremely stable as shown in Table 4.9. This eliminates LC-MS drift as contributing factor to the observed results. In prior studies using this QTOF instrument, we noticed poor mass accuracy at low concentration levels, so this factor was investigated but was found not to explain the observed results. For example, widening extraction window to  $\pm 50$  ppm for third experiment did not enable detection of lower concentration of mycotoxins. Next, the total ion current chromatograms of validation samples across three experiments were compared with similar concentrations as shown in Appendix C, Supplementary Figure C25. The total ion current chromatograms of the experiments 1 and 2 differ from the total ion current chromatogram of experiment 3. The same trend was observed in the total ion current chromatograms of standard solutions and blank samples (60% methanol with 1% FA) across three experiments. Additionally, base peaks were extracted, the comparison of the ion masses showed similarity and did not reveal the reason resulting in the different total ion current chromatograms, further investigation is necessary. The impact of noise on LLOQ determination was also investigated. Extracted ion chromatograms of similar concentration across three experiments for OT $\alpha$ , OTA, FB2 and ENNA were investigated, and S/Ns were compared, Appendix C, Supplementary Figures C26-C29. However, differences in terms of S/N ratio were not observed. The comparison of protonated ion, ammonium and sodium adducts of emerging mycotoxins showed the variable ionization pattern in all three experiments Appendix C, Supplementary Figure C30. If the percentage of adduct formations varies across samples or days perhaps it also contributes to the discussed results. Additionally, RSD%s were calculated for 6 replicates of validation samples (4 ng/ml), experiment 3, using the sum of ammonium and sodium areas and only the area of sodium ion, Appendix C, Supplementary Table C5. The results of calculations demonstrated that precision improved up to 2.5x when RSD%s were calculated as sum of areas.

In conclusion, the evaluation of three experiments showed that the LC-MS method was not reproducible, at levels below 4 ng/ml and requires further modifications. Possibly that the method can not provide suitable selectivity at low concentration levels and thus can not have the ability to discriminate mycotoxins from other co-eluting compounds requiring additional clean-up and enrichment. To address this limitation, selective pre-concentration and purification can be performed by using solid phase extraction which can improve simultaneously sensitivity and selectivity. A number of mycotoxin studies has already used solid phase extractions demonstrating sub ng/ml LLOQs levels.<sup>278,289</sup> The other way to improve method performance is to change HRMS

for tandem mass spectrometry. The comparison of the analytical characteristics of QQQ 6410B and QTOF 6545 showed that QTOF 6545 had about 5x worse sensitivity and worse precision.<sup>290</sup> They declared that both instruments enabled to perform quantitative analyses, however, interference-free environment would be preferable for QTOF 6545.<sup>290</sup>

#### **4.3.3 Evaluation of recovery and matrix effects of finalized method using 10 individual lots of plasma**

The absolute recoveries and matrix effects in individual plasma samples were evaluated. The results of this experiment are shown in Figure 4.12. Matrix effects exceeding 80-120% acceptance criteria were observed for fumonisins (134.8% to 167.8%), OT $\alpha$  (77.5% to 92.6%), ENNB (69.7% to 79.4%) and ENNA (69.3% to 79.2%). For fumonisins, internal standard FB3 shows the same ionization trends and can be used to correct for these matrix effects. Ionization pattern of emerging mycotoxins were evaluated in 10 lots of plasma, Appendix C, Supplementary Figures C31. Results demonstrated that sodium ions were the most intense. Ammonium adduct areas were the most variable across 10 lots of plasma and needed mobile phase additives to be controlled. The comparison of signal intensities of protonated ions, ammonium and sodium adducts shown in Supplementary Figures C32-C34 demonstrated that sodium signal intensities were less variable than ammonium signal intensities, and that is why it was used for evaluation of matrix effect and recovery. Additionally, the sum areas of protonated, ammonium, and sodium adducts showed that variability increased in ENNB and ENNA1 comparing to sodium adduct areas across 10 lots of plasma, Supplementary Figures C34 and C35. For accurate quantitation of ENNB and ENNA, either additional internal standards or additional sample clean-up are needed to address the observed ion suppression.

The extraction recovery for individual plasma lots ranged from 86.6% to 127.7%. No sex-specific effects were observed. However, the observed matrix effect for several mycotoxins in different lots of plasma show that protein precipitation does not provide sufficient clean-up of the samples for this multi-mycotoxin method.

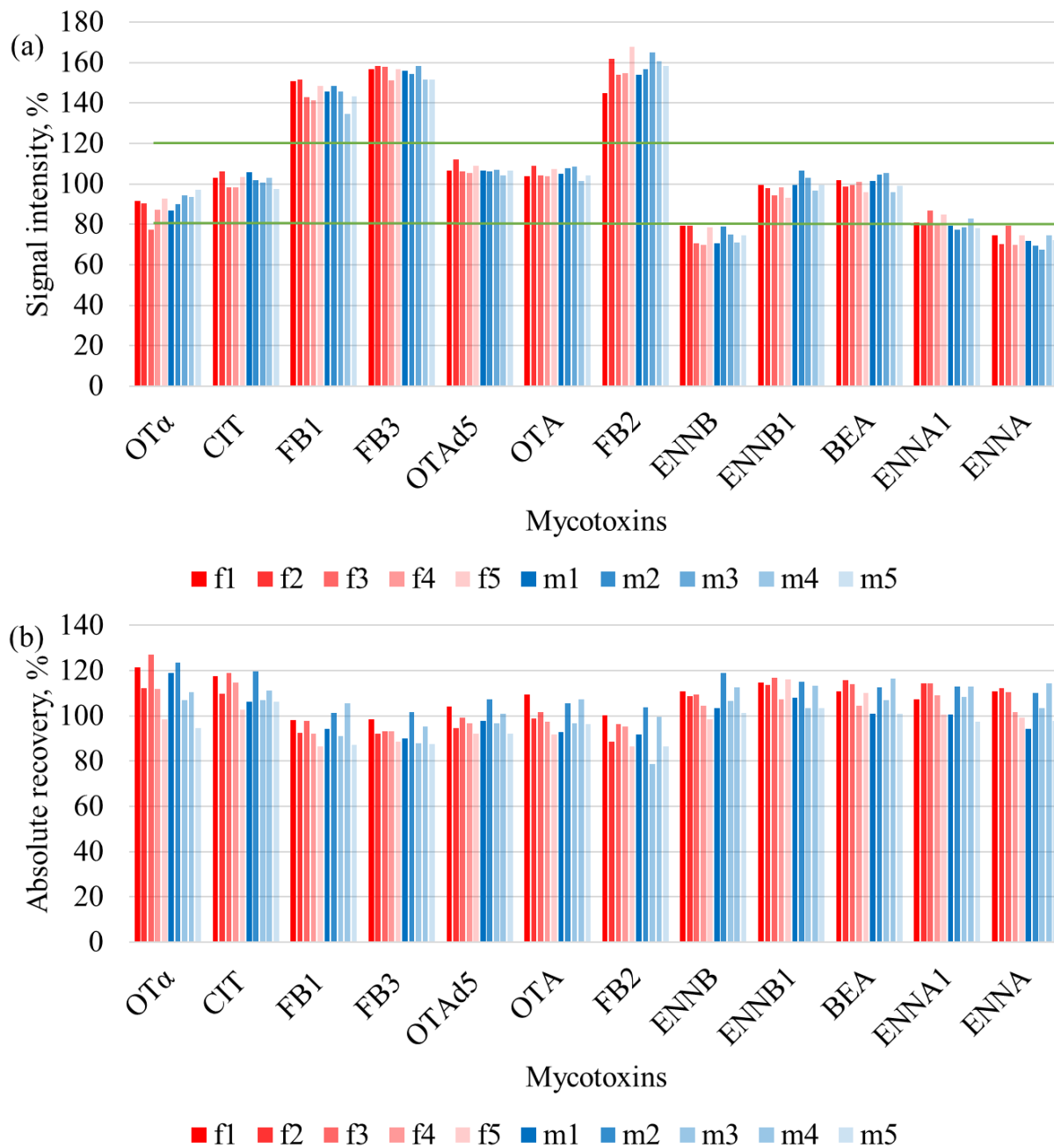


Figure 4.12. Evaluation of absolute ionization matrix effects (a) and absolute recoveries (b), obtained for 10 individual plasma samples spiked at 1.4 ng/ml and 7 ng/ml, respectively, (n=1 replicate per plasma lot). Results were obtained as described in Section 4.2.5. 10 individual plasma samples were 5 female and 5 male samples.

#### 4.3.4 Comparison of current method to literature methods

Current developed method has poor LLOQs compared to the literature as summarized in Table 4.10. Fumonisin LLOQs are comparable to the literature, whereas the LLOQs of ochratoxins and emerging mycotoxins are better in literature. For example, OTA LLOQs from literature ranged from 0.005 ng/ml to 10 ng/ml, CIT from 0.021 ng/ml to 0.25 ng/ml, fumonisins from 0.16 ng/ml to 10 ng/ml, emerging mycotoxin LLOQs from 0.005 ng/ml to 1.5 ng/ml. There is no method that could cover the same 10 mycotoxins in human and animal blood-derived products that could be easily adopted to our purposes. Method developed by Osteresch *et al.* could analysis nine of our mycotoxins, except FB2, using dried serum spots and dried blood spots with the following acetonitrile extraction.<sup>136</sup> The method has LLOQs ranged from 0.005-0.25 ng/ml, however, their method suffers from matrix effects that ranged from 46 to 842% for these mycotoxins.<sup>136</sup> Devreese *et al.* developed multi-mycotoxin method for FB1 and OTA based on protein precipitation with acetonitrile (1:3, v/v).<sup>75</sup> However, they could only obtain 2 ng/ml LLOQs for FB1 and OTA.<sup>75</sup> They had acceptable matrix effects 87.9% for OTA and 98.8% for FB.<sup>75</sup> Cao *et al.* method contained three out our mycotoxins, FB1, FB2 and OTA.<sup>139</sup> Using enzymatic treatment with the following protein precipitation with acidified acetonitrile (1:4, v/v), LLOQs ranged from 0.44 to 0.92 ng/ml, matrix effects were acceptable for FB1 (80%) and OTA (100%), but not for FB2 (60%).<sup>139</sup> Recently developed multi-mycotoxin method for 24 mycotoxins in pig and chicken plasma based on the usage of protein precipitation with acetonitrile (1:3, v/v) or additional removal of phospholipids, respectively.<sup>279</sup> LLOQs was 1 ng/ml for OTA and emerging mycotoxins and matrix effects ranged from 45.5-135.5%.<sup>279</sup> There are a few a single or class-specific methods for OTA (0.15 ng/ml), CIT (0.15 ng/ml, 0.07 ng/ml) and emerging mycotoxins (0.2-0.04 ng/ml) that uses different instruments and sample preparation, including immunoaffinity clean-up.<sup>121,135,138,141</sup> Serrano *et al.* obtained LLOQs and process efficiency ranging from 0.02-0.04 ng/ml and 99.7-109.5%, respectively, in human plasma due to the usage of graphitized carbon black sorbents for the clean-up of human plasma.<sup>121</sup> Korn *et al.* compared two sample preparation techniques, LLE with the following immunoaffinity clean-up and dispersive solid-phase extraction for the OTA analysis in human blood-derived products.<sup>135</sup>

Table 4.10. Comparison of our method and class-specific and multi-class method LLOQs.

Mycotoxin class	Our method	Other published <b>class-specific methods</b> and <b>multi-class methods</b>		
	LLOQ, ng/ml	LLOQ, ng/ml	Matrix	Author
OTA OT $\alpha$ CIT	0.20-2.00 1.25-4.00 0.30-3.50	0.15 (CIT) 0.15 (CIT) 0.07 (OTA) 0.021 (OTA) 0.5 (OTA) 0.16 (OTA) 2 (OTA) 0.05-0.25/ 0.05-0.25 0.5 (OTA) 0.1-0.2 1/1 (OTA) 10 (OTA)	Human plasma Human serum Human blood Human blood Human serum Human serum Pig plasma Human serum/blood Human plasma Human plasma Pig/chicken plasma Fish plasma	Blazkewicz <i>et al.</i> <sup>138</sup> Ali <i>et al.</i> <sup>141</sup> Korn <i>et al.</i> <sup>135</sup> Cramer <i>et al.</i> <sup>134</sup> Ritieni <i>et al.</i> <sup>140</sup> De Santis <i>et al.</i> <sup>137</sup> Devreese <i>et al.</i> <sup>75</sup> Osteresch <i>et al.</i> <sup>136</sup> Cao <i>et al.</i> <sup>139</sup> Fan <i>et al.</i> <sup>64</sup> Lauwers <i>et al.</i> <sup>279</sup> Tolosa <i>et al.</i> <sup>205</sup>
FB1 FB2	1.25-4.00 0.63-4.00	0.16 (FB1) 2 (FB1) 2.5/ 2.5 (FB1) 0.5 0.5 (FB1) 8-10	Human serum Pig plasma Human serum/ blood Human plasma Human plasma Fish plasma	De Santis <i>et al.</i> <sup>137</sup> Devreese <i>et al.</i> <sup>75</sup> Osteresch <i>et al.</i> <sup>136</sup> Cao <i>et al.</i> <sup>139</sup> Fan <i>et al.</i> <sup>64</sup> Tolosa <i>et al.</i> <sup>205</sup>
ENNB ENNB1 BEA ENNA1 ENNA	0.45-4.00 0.45-4.00 0.5-4.00 0.75-4.00 0.5-4.00	0.02 – 0.04 0.01-0.05/ 0.005-0.05 1/1 1-1.5	Human plasma Human serum/ blood Pig/chicken plasma Fish plasma	Serrano <i>et al.</i> <sup>121</sup> Osteresch <i>et al.</i> <sup>136</sup> Lauwers <i>et al.</i> <sup>279</sup> Tolosa <i>et al.</i> <sup>205</sup>

They obtained similar LLOQs for both methods, 0.07 ng/ml and 0.08 ng/ml for immunoaffinity and dispersive solid-phase extraction, respectively, without reporting matrix effects<sup>135</sup>. Blazkewicz *et al.* used enzymatic treatment with the following protein precipitation with acetonitrile (1:1, v/v) for CIT analysis in human plasma.<sup>138</sup> Their method LLOQ was 0.15 ng/ml, unfortunately matrix effect was not reported.<sup>138</sup> Literature demonstrated that different sample preparation methods were applied for mycotoxin analysis, the frequently used technique are protein precipitation which not always provide simultaneously good LLOQ levels and negligible matrix effects.

ENNB1, BEA, ENNA1 and ENNA were not detected in human blood-derived samples to the best of my knowledge. In two studies, the presence of these mycotoxins was verified in human blood-derived samples, but they were not detected.<sup>121,136</sup> The rest of mycotoxins, FB1, CIT, OTA, OT $\alpha$ , and ENNB, were previously detected in either blood, or serum, or plasma, as shown in Table 4.11. The mean concentrations of mycotoxins were at sub ng/ml levels, except for OTA value of 1.2 ng/ml which was detected in plasma from China. The mean observed concentrations of FB1 and ochratoxins were 0.09 ng/ml to 1.2 ng/ml. ENNB was observed in two studies with similar mean levels, 0.0367 ng/ml and 0.0481 ng/ml.<sup>136,280</sup> The summarized measured levels of mycotoxins clearly demonstrate that the developed LC-MS method should have LLOQs at sub ng/ml levels.

*Table 4.11. Mean measured concentrations of FB1, CIT, OTA, OT $\alpha$ , ENNB in human blood-derived samples, and the rest mycotoxins were not observed.*

<b>Mycotoxins</b>	<b>Mean concentration in blood-derived samples, ng/ml</b>	<b>Reference</b>
FB1	0.756	64
CIT	0.36	141
OTA	1.20	64
	0.71	135
	0.756	280
	0.25	66
OT $\alpha$	0.09	66
	0.96	66
ENNB	0.0367	136
	0.0481	280

#### **4.4 Conclusion and future work for LC-HRMS method for 10 mycotoxins**

In order to develop LC-MS method with good LLOQs, further enrichment and clean-up steps, or/and the usage of tandem mass spectrometry will be needed to improve the method before proceeding with full validation. However, to find the suitable additional sample preparation step can take time. Solid-phase extraction should be first considered as a candidate to address this limitation. It can provide both enrichment and clean-up steps, however, it will increase time and cost per sample. For, example, Serrano *et al.* used SPE (graphitized carbon black sorbent) as sample preparation for emerging mycotoxin analysis in human plasma, to reduce matrix effect

that was evaluated as a part of process efficiency (100%-110%), to increase mycotoxin recoveries (76%–103%) and to remove matrix interferences.<sup>121</sup> De Baere *et al.* developed method for fumonisins in chicken plasma using Oasis® Ostro™ 96-well plate to remove proteins and phospholipid.<sup>291</sup> This method had recoveries more than 80% and matrix effects ranged from 112.5–127.1%.<sup>291</sup> Oasis® Ostro™ 96-well plate was also applied by Lauwers *et al.* for chicken plasma in multi-mycotoxin method.<sup>279</sup> OTA ENNA1, ENNA, ENNB1, ENNB1 and BEA recoveries ranged from 66.2% to 90.9%, while matrix effects ranged from 73.9% to 135.5% chicken plasma samples.<sup>279</sup> There are several published methods that used C<sub>18</sub> SPE for the OTA extraction in human blood-derived products, reporting recoveries > 85%.<sup>53,292,293</sup> Based on the mycotoxin chemistry and the developed chromatographic conditions using C<sub>18</sub> column and methanol mobile phase, the rational choice of SPE to improve LLOQs can be C<sub>18</sub> sorbents. Knowing chromatographic elution times of mycotoxins, it will be easy to develop C<sub>18</sub> SPE method which will allow to concentrate and to purify mycotoxins from plasma samples. By sequentially increasing solvent polarity, acidic mycotoxins will be fractionated from polar compounds and compounds with intermediate polarity, then emerging mycotoxins can be selectively isolated from highly hydrophobic compounds, such as triglycerides. In addition to complex sample preparation tandem mass spectrometry can be also considered to improve LLOQs, since it provides additional selectivity and sensitivity by improving S/N ratio, however, the method would be difficult to adopt for metabolite characterization and screening. Recently the performance of QQQ low resolution, Agilent QQQ 6410B, and high resolution, Agilent QTOF 6540, mass spectrometry was compared using analysis of amino acids.<sup>290</sup> The quantification range of compounds was 3 to 5 orders of magnitude better for QQQ than for QTOF.<sup>290</sup> Precision with QQQ was below 5% for most compounds tested whereas the RSDs from 5 to 20% was observed by the QTOF detection for all compounds.<sup>290</sup> Overall, authors concluded that both platforms can be used for the accurate quantifications, however, QQQ provides compound quantifications with the highest precision, while QTOF performance is still acceptable with benefits to perform analysis of unknown compounds.<sup>290</sup>



## 5. Conclusions and future work

### 5.1 Conclusions

Mycotoxin contamination is a well-known global issue that demands accurate, sensitive and validated mycotoxin methods for the assessment of human exposure to mycotoxins. In this thesis, two multi-mycotoxin LC-MS methods were successfully developed for 27 mycotoxins and their metabolites in human plasma. The first method used high-resolution mass spectrometry (LTQ Velos Orbitrap) coupled to RP liquid chromatography to measure 17 mycotoxins (NIV, DON, FUS-X, 3-AcDON, 15-AcDON, T-2, HT-2, AFB1, AFB2, AFG1, AFG2, ZEN,  $\alpha$ -ZOL,  $\beta$ -ZOL, ZAN,  $\alpha$ -ZAL and  $\beta$ -ZAL). The application of core-shell Kinetex PFP column allowed successful separation of all isomeric and isobaric compounds, including  $\alpha$ -ZOL,  $\beta$ -ZOL, and ZAN, 3-AcDON and 15-AcDON, and  $\alpha$ -ZAL and  $\beta$ -ZAL. In order to achieve good method sensitivity, several sample preparation techniques were evaluated, including solid-phase extraction, liquid-liquid extraction and protein precipitation. The recovery and matrix effects of the best three methods, including protein precipitation with acetonitrile, SPE Oasis HLB and three-step-LLE with ethyl acetate were systematically compared. Three-step-LLE with ethyl acetate was chosen because of optimal method recovery, > 70% for 16 mycotoxins, except for NIV (24%) and negligible matrix effects. Out of the three methods only three-step-LLE had matrix effect in the range 80% to 120% across all 17 mycotoxins, in order to provide accurate quantification of mycotoxins in the absence of individual isotopically-labelled standards for each mycotoxin. In addition to the extensive clean-up achieved with the selected LLE method, good method sensitivity was also achieved due to novel discovery of the effect of acetic acid on ionization efficiency. Acetic acid increased signal intensity of the mycotoxins in the range of 1.4x up to 26x compared to formic acid. Further evaluation of three concentrations of acetic acid, 0.1%, 0.02% and 0.006% (v/v) on signal intensity in ESI(-) showed that the most preferable concentration of acetic acid among those tested is 0.02% to ensure effective ionization while maintaining good method precision. This was an important finding which extended beyond my own research, and was found to enhance ionization of lipids as well.<sup>294</sup>

The final method was validated according to the procedure described in Section 2.2.6. Method LLOQs ranged from 0.1-0.5 ng/ml, except for NIV for which LLOQ of 3 ng/ml was achieved due to its low extraction efficiency (Table 5.1). Overall, the LLOQs of our multi-

mycotoxin method are similar or better than the LLOQs of both class-specific and multi-class methods previously reported in literature, as shown in Table 5.1.

Finally, mean intra-day accuracy ranged from 85.8% to 116.4%, and intra-day precision (n=6) ranged from 1.6% to 12.5% RSD for all mycotoxins except for  $\alpha$ -ZOL for which mean accuracy ranged from 72.9% to 97.2%. Inter-day accuracy and precision were 85.6% to 111.5% and 2.7 to 15.6% RSD respectively. The method outperformed other multi-mycotoxin methods available in literature in terms of successfully addressing absolute matrix effects. However, the current routinely-used procedures to evaluate matrix effects may not detect all issues. Our more extensive evaluation of different individual lots of human plasma showed gender-specific differences in individual lots of plasma for some analytes of ZEN group. This issue was not detected using pooled plasma lots using routine procedure, thus showing the critical importance of more in-depth evaluation of matrix effects as part of method validation.

The LLE pentafluorophenyl LC-HRMS method did not perform well for fumonisin and ochratoxin classes of mycotoxins due to low extraction recovery with ethyl acetate and irreproducible retention time for fumonisins. To address this limitation, a second high-resolution mass spectrometry method was developed using polarity-switching ESI on an Agilent QTOF 6545 coupled to ultra-high performance liquid chromatography with a Cortecs T3 C<sub>18</sub> column. This method was developed for 10 mycotoxins, including fumonisins (FB1 and FB2), ochratoxins (OTA, CIT and OT $\alpha$ ) and emerging mycotoxins (ENNA, ENNA1, ENNB, ENNB1 and BEA). The key advantage of the Cortecs T3 C<sub>18</sub> column for this application was effective chromatographic separation of all mycotoxins that allowed to use polarity-switching which drastically reduced the LC analysis time and enabled accurate determination of 10 mycotoxins in one analytical run. Method recoveries ranged from 86.6% to 127.7%. Matrix effects were in the range of 69.3% to 167.8%, with only fumonisins, ENNB and ENNA matrix effects exceeding the acceptable range of 80-120%. Method LLOQs were in the range of 0.3-4 ng/ml. Sub ng/ml LLOQs were not obtained for all mycotoxins, therefore, further method modifications were required to make the method relevant for biomonitoring analysis. This second method also used a universal sample preparation technique, protein precipitation with methanol that made the method high-throughput, cost and labor-effective.

The first multi-mycotoxin methods surpass current methods for accurate mycotoxin quantification in human plasma based on their negligible matrix effects. The novelty of both

methods is the successful application of high-resolution mass spectrometry that is still rare in mycotoxin quantitative analysis for any complex matrices, including food and feed samples, but especially for human and animal biofluid biomonitoring. High-resolution mass spectrometry has key advantages over low resolution mass spectrometry. For example, it allows easily to add new emerging mycotoxins or metabolites to the analytical method if they have similar physicochemical properties and it is suitable for retrospective data analysis without the need to repeat the analysis. It is a versatile tool that can be used and adopted for other applications, including metabolism studies or toxicity studies.

Although the mycotoxin metabolism has been studied in detail in different species, these efforts relied on many different analytical approaches. Standards for many of these metabolites are also not commercially available. Furthermore, human metabolites of some mycotoxins, such as FUS-X, NIV,  $\alpha$ -ZOL,  $\beta$ -ZOL, ZAN,  $\alpha$ -ZAL,  $\beta$ -ZOL, have not been studied in detail. To address these limitations and to examine the capability of our validated biomonitoring method to be expanded for the measurements of mycotoxin metabolites, human liver microsomal incubations were performed on each individual mycotoxin of interest with focus on Phase I and glucuronidation Phase II metabolism using the first LC-HRMS method. Data-dependent acquisition in combination with collision-induced dissociation or higher energy collisional dissociation was used to ensure adequate fragmentation, which can further facilitate studies of mycotoxin metabolite structures, including positional isomer characterization. The separation capability of the PFP stationary phase enabled the detection and identification of several isomeric compounds, such as hydroxyl metabolites of the ZEN group, T-2, HT-2, AFB1 and glucuronides of ZEN group. In total, 188 metabolites were characterized and used to build the LC-MS library, including 100 metabolites reported for the first time. This represents the most comprehensive LC-MS library of human mycotoxin metabolites built to date and shows the capability of the developed methods for further expansion to ensure exposure is not under-estimated.

## **5.2 Future work**

The thesis successfully addressed some of the key limitations in mycotoxin biomonitoring by providing a new set of workflows and an extensive LC-MS library to this field of research. However, some future work remains to be done.

Table 5.1. Comparison of LLOQs obtained in our method presented in Chapter 2 and published methods.

Mycotoxin class	Our method	Other published <b>class-specific methods</b> and <b>multi-class methods</b>		
	LLOQ, ng/ml	LLOQ, ng/ml	Matrix	Author
<b>Aflatoxins: AFB1, AFB2, AFG1, and AFG2</b>	0.1 – 0.2	1 0.13-0.42 0.05 (AFB1) 1 0.03 (AFB1) 2 (AFB1) 0.05-0.125/ 0.02 – 0.125 0.25-0.43 0.1-0.2	Human serum Human serum Rat plasma Human serum Human serum Pig plasma Human serum/blood Human plasma Human plasma	Santini <i>et al.</i> <sup>225</sup> Chen <i>et al.</i> <sup>226</sup> Han <i>et al.</i> <sup>150</sup> Ritieni <i>et al.</i> <sup>140</sup> De Santis <i>et al.</i> <sup>137</sup> Devreese <i>et al.</i> <sup>75</sup> Osteresch <i>et al.</i> <sup>136</sup> Cao <i>et al.</i> <sup>139</sup> Fan <i>et al.</i> <sup>64</sup>
<b>Trichothecenes type A: T-2 and HT-2</b>	0.2	1 and 2.5 1-2 0.05 (T-2) 2 and 5 0.1 and 5/ 1 and 5 0.1-0.5	Pig and chicken plasma Pig plasma Rat plasma Pig plasma Human serum/blood Human plasma	De Baere <i>et al.</i> <sup>153</sup> Sun <i>et al.</i> <sup>154</sup> Han <i>et al.</i> <sup>150</sup> Devreese <i>et al.</i> <sup>75</sup> Osteresch <i>et al.</i> <sup>136</sup> Fan <i>et al.</i> <sup>64</sup>
<b>Trichothecenes type B: 3-AcDON, 15-AcDON and DON</b>	0.2 – 0.3	0.1-1 and 1-2 1 and 1.25 (DON) 0.45 (DON) 1.4 (DON) 10 (DON) 1 (DON) 1	Pig and chicken plasma Pig and chicken plasma Pig serum Human serum Pig plasma Human serum/blood Human plasma	Broekaert <i>et al.</i> <sup>151</sup> Baere <i>et al.</i> <sup>153</sup> Brezina <i>et al.</i> <sup>152</sup> De Santis <i>et al.</i> <sup>137</sup> Devreese <i>et al.</i> <sup>75</sup> Osteresch <i>et al.</i> <sup>136</sup> Fan <i>et al.</i> <sup>64</sup>

Mycotoxin class	Our method	Other published <b>class-specific methods</b> and <b>multi-class methods</b>		
	LLOQ, ng/ml	LLOQ, ng/ml	Matrix	Author
<b>Zearalenone and its metabolites</b>	0.1 – 0.5	0.5-0.6 0.08 -2.37 0.2- 1/ 1-5 1.6 5 1 0.1-0.5	Horse plasma Pig serum Pig and chicken plasma Human serum Pig plasma Human serum Human plasma	Songsermsakul <i>et al.</i> <sup>155</sup> Brezina <i>et al.</i> <sup>152</sup> De Baere <i>et al.</i> <sup>156</sup> De Santis <i>et al.</i> <sup>137</sup> Devreese <i>et al.</i> <sup>75</sup> Osteresch <i>et al.</i> [7] Fan <i>et al.</i> <sup>64</sup>

First of all, LLOQs must be improved for the method presented in Chapter 4 by adding an enrichment step or a sample clean-up step as a part of sample preparation procedure and/or or using other instruments such as a triple quadrupole mass spectrometer. In the future, the second multi-mycotoxin method should be validated for human plasma samples. Then, these two multi-mycotoxin LC-MS methods should be further adapted and validated for urine samples. It is important to have methods for both urine and plasma samples in order to estimate accurately both long-term and short-term exposure for mycotoxins with different half-lives.

Currently, the mycotoxin metabolite LC-MS library is not completed yet for all possible mycotoxin metabolites. My metabolism studies focused on the generation of Phase I metabolites and glucuronide metabolites of 17 mycotoxins, but the library can be expanded to other Phase II conjugated forms, such as sulfates and glutathione conjugates. In addition, the metabolites of fumonisins, ochratoxins and emerging mycotoxins should also be generated and included into LC-MS library. This established library will be useful beyond plasma biomonitoring, for biological matrices such as, urine, breast milk, feces and other matrices of interest, and can facilitate studies on mycotoxin fate and exposure in long-term.

HRMS and good chromatographic separations have played a key role to characterize and identify mycotoxin metabolites.

HRMS allows to perform simultaneous analysis of hundreds of metabolite species due to the capability of full scan acquisition combined with fragmentation spectra that greatly facilitate structural elucidation. In addition, as shown in this work, efficient chromatographic separations enable the analysis of isomeric and isobaric compounds, in order to reduce the number of LC-MS methods required for monitoring of mycotoxins and their metabolites. Currently, mycotoxin metabolism studies are usually performed for a single mycotoxin so that different mass spectrometers and columns have been used. For example, Phase I metabolites and glucuronides of HT-2 and T-2 were generated by Yang *et al.* using Water QTOF coupled to UHPLC with Acquity HSS T3 and Acquity BEH RP18 columns, respectively.<sup>162,189</sup> DON and its metabolites in human urine were analyzed by Waters Quattro XEVO TQS mass spectrometer and UHPLC with Acquity UPLC HSS T3 column.<sup>54</sup> A 6500 QTrap mass spectrometer (Sciex) with UHPLC (Agilent) and Kinetex Biphenyl column were used for the identification of ZEN group glucuronides.<sup>179</sup>

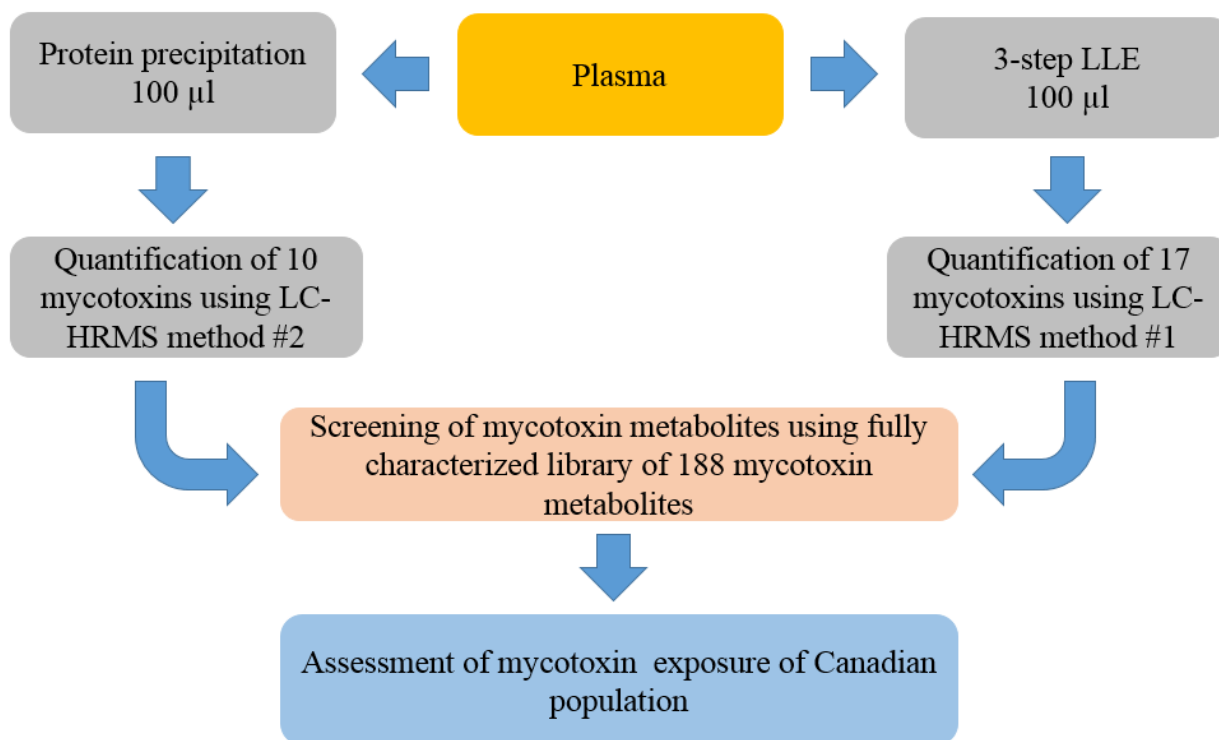


Figure 5.1. The workflow for LC-HRMS monitoring of 215 mycotoxins and their metabolites to enable extensive exposure studies.

In contrast my research showed that a single multi-class method for 17 mycotoxins can be expanded for the first time to monitor 188 additional metabolites, thus making it more amenable for large-scale population screening.

The two LC-MS methods developed in these studies require only 200 µl of plasma for mycotoxin analysis, as shown in Figure 5.1. They can accurately measure exposure to 27 mycotoxins of interest but can also be used to screen for the presence of more than 188 metabolites in large-scale exposure studies. These results will in turn allow the prioritization of which metabolites should be included in routine mycotoxin monitoring and may further be validated as biomarkers. Large-scale biomonitoring studies of Canadian population will address a critical gap in our knowledge. In these studies, mycotoxin exposure can be evaluated in different sub-population groups according to gender, age, geographical area and eating preferences. Finally, prevalent mycotoxins and most frequently co-occurring mycotoxins can be identified in Canadian blood samples, to prioritize the mycotoxin combinations to study for future long-term chronic toxicity assessments. With this information additional toxicity studies examining the effect of low-dose simultaneous exposure to multiple mycotoxins can be designed to best mimic the real-life scenario. Human biomonitoring is an important tool for health risk assessment which should be performed routinely and be used together with existing food regulations. In addition, this work fits well within the broader field of exposomics and provides new highly-relevant mycotoxin metabolite libraries to this research.

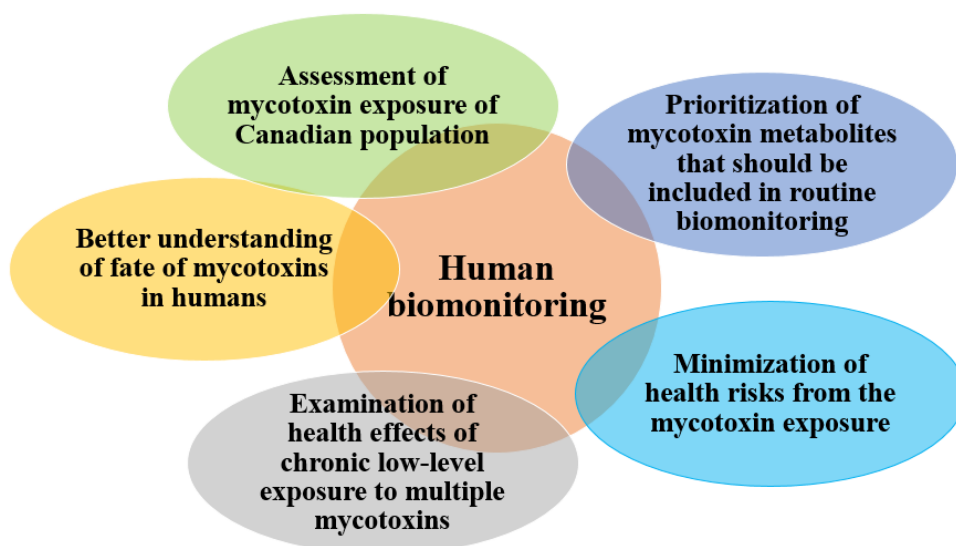


Figure 5.2. Current and future research objectives to enable mycotoxin human biomonitoring.

The first comprehensive mycotoxin data set will also allow to verify if the Canadian population is protected by current mycotoxin regulations or whether additional more stringent measures are required for any of the monitored mycotoxins. Figure 5.2 describes key research areas that are facilitated by more powerful biomonitoring methods.

Climate change impact on the mycotoxin occurrence attracted significant attention in the last decades. It can influence the presence and frequency of mycotoxin contamination, and food security. Verheecke-Vaessen *et al.* showed that environmental factors, such as temperature, affected *Fusarium* growth.<sup>295</sup> In this study, the examination of the temperatures (20°C, 25°C and 30°C) showed that T-2 and HT-2 production was higher at 20°C and 25°C than at 30°C.<sup>295</sup> Moretti *et al.* summarized and reported that climate change can effect on the growth of filamentous fungi, such as *Aspergillus*, *Fusarium* and *Penicillium* which in turn are responsible for the production of toxicologically important mycotoxins (aflatoxins, fumonisins, ochratoxins, trichothecenes, and zearalenones).<sup>296</sup> For example, heat and drought regions usually experience greater aflatoxin prevalence than cooler regions.<sup>296</sup> The occurrence of OTA increased at hot temperatures (around 30°C) and high humidity, while fumonisins prefer variable weather conditions when dry weather is followed by warm and humid weather.<sup>297</sup> However, moderate warm weather favors production of DON.<sup>296</sup> Paterson *et al.* also predicts that global warming may accelerate the growth of high temperature species, such as *Aspergillus flavus* and mycotoxin, such as aflatoxins.<sup>297</sup> Given that climate fluctuations affect the occurrence of mycotoxins, and mycotoxins have preferred weather conditions for their production, biomonitoring is necessary to ensure the protection of population against the potential hazards of mycotoxins in a time of a changing climate.



## References

- (1) Pleadin, J.; Frece, J.; Markov, K. Mycotoxins in Food and Feed. *Adv. Food Nutr. Res.* **2019**, *89*, 297–345. <https://doi.org/10.1016/bs.afnr.2019.02.007>.
- (2) Alshannaq, A.; Yu, J. Occurrence, Toxicity, and Analysis of Major Mycotoxins in Food. *Int. J. Environ. Res. Public Health* **2017**, *14* (6), 632. <https://doi.org/10.3390/ijerph14060632>.
- (3) Berthiller, F.; Crews, C.; Dall'Asta, C.; De Saeger, S.; Haesaert, G.; Karlovsky, P.; Oswald, I. P.; Seefelder, W.; Speijers, G.; Stroka, J. Masked Mycotoxins: A Review. *Mol. Nutr. Food Res.* **2013**, *57* (1), 165–186. <https://doi.org/10.1002/mnfr.201100764>.
- (4) Eskola, M.; Kos, G.; Elliott, C. T.; Hajšlová, J.; Mayar, S.; Krska, R. Worldwide Contamination of Food-Crops with Mycotoxins: Validity of the Widely Cited 'FAO Estimate' of 25%. *Crit. Rev. Food Sci. Nutr.* **2019**, *59* (1), 1–17. <https://doi.org/10.1080/10408398.2019.1658570>.
- (5) Smith, M.; Madec, S.; Coton, E.; Hymery, N. Natural Co-Occurrence of Mycotoxins in Foods and Feeds and Their in Vitro Combined Toxicological Effects. *Toxins (Basel)*. **2016**, *94* (8), 1–36. <https://doi.org/10.3390/toxins8040094>.
- (6) García-Moraleja, A.; Font, G.; Mañes, J.; Ferrer, E. Development of a New Method for the Simultaneous Determination of 21 Mycotoxins in Coffee Beverages by Liquid Chromatography Tandem Mass Spectrometry. *Food Res. Int.* **2015**, *72*, 247–255. <https://doi.org/10.1016/j.foodres.2015.02.030>.
- (7) Zöllner, P.; Mayer-Helm, B. Trace Mycotoxin Analysis in Complex Biological and Food Matrices by Liquid Chromatography-Atmospheric Pressure Ionisation Mass Spectrometry. *J. Chromatogr. A* **2006**, *1136* (2), 123–169. <https://doi.org/10.1016/j.chroma.2006.09.055>.
- (8) Schatzmayr, G.; Streit, E. Global Occurrence of Mycotoxins in the Food and Feed Chain: Facts and Figures. *World Mycotoxin J.* **2013**, *6* (3), 213–222. <https://doi.org/10.3920/WMJ2013.1572>.

- (9) Canadian Food Inspection Agency. 2013-2015 Multi-Mycotoxin Analysis in Selected Foods. Ottawa, ON, Canada, 2016.
- (10) RG-8 Regulatory Guidance: Contaminants in Feed (formerly RG-1, Chapter 7), Section 1: Mycotoxins in Livestock Feed, Canadian Food Inspection Agency (CFIA), Ottawa, ON, Canada <https://www.inspection.gc.ca/animals/feeds/regulatory-guidance/rg-8/eng/1347383943203/1347384015909?chap=1> (accessed Oct 30, 2019).
- (11) Roscoe, V.; Lombaert, G. ; Huzel, V.; Neumann, G.; Melietio, J.; Kitchen, D.; Kotello, S.; Krakalovich, T.; Trelka, R.; Scott, P. M. Mycotoxins in Breakfast Cereals from the Canadian Retail Market: A 3-Year Survey. *Food Addit. Contam. Part A. Chem. Anal. Control. Expo. Risk Assess.* **2008**, *25* (3), 347–355.  
<https://doi.org/10.1080/02652030701551826>.
- (12) Tam, J.; Pantazopoulos, P.; Scott, P. M.; Moisey, J.; Dabeka, R. W.; Richard, I. D. K. Application of Isotope Dilution Mass Spectrometry: Determination of Ochratoxin A in the Canadian Total Diet Study. *Food Addit. Contam. Part A. Chem. Anal. Control. Expo. Risk Assess.* **2011**, *28* (6), 754–761. <https://doi.org/10.1080/19440049.2010.504750>.
- (13) Turcotte, A.-M.; Scott, P. M. Ochratoxin A in Cocoa and Chocolate Sampled in Canada. *Food Addit. Contam. Part A* **2011**, *28* (6), 762–766.  
<https://doi.org/10.1080/19440049.2010.508796>.
- (14) Canadian Food Inspection Agency. 2010-2011 Fumonisin in Corn Products. Ottawa, ON, Canada, 2011.
- (15) Canadian Food Inspection Agency. Aflatoxins in Selected Corn Products, Nuts, Nut Products, Raisins, Cocoa Powder, Chili Powder and Paprika - April 1, 2012 to March 31, 2013. Ottawa, ON, Canada, 2013.
- (16) Canadian Food Inspection Agency. Aflatoxins in Selected Spices, Oilseeds, Rice and Rice Products – April 1, 2015 to March 31, 2016. Ottawa, ON, Canada, 2016.
- (17) Tittlemier, S. A.; Roscoe, M.; Trelka, R.; Gaba, D.; Chan, J. M.; Patrick, S. K.; Sulyok, M.; Krska, R.; Mckendry, T.; Gra, T. Fusarium Damage in Small Cereal Grains from Western Canada. 2. Occurrence of Fusarium Toxins and Their Source Organisms in Durum Wheat Harvested in 2010. *J. Agric. Food Chem.* **2013**, *61* (23), 5438–5448.

- <https://doi.org/10.1021/jf400652e>.
- (18) Bennett, J. W.; Klich, M. Mycotoxins. *Clin. Microbiol. Rev.* **2003**, *16* (3), 497–516.  
<https://doi.org/10.1128/CMR.16.3.497>.
- (19) Liew, W. P. P.; Mohd-Redzwan, S. Mycotoxin: Its Impact on Gut Health and Microbiota. *Front. Cell. Infect. Microbiol.* **2018**, *8* (60). <https://doi.org/10.3389/fcimb.2018.00060>.
- (20) Adhikari, M.; Negi, B.; Kaushik, N.; Adhikari, A. T-2 Mycotoxin: Toxicological Effects and Decontamination Strategies. *Oncotarget* **2017**, *8* (20), 33933–33952.  
<https://doi.org/10.18632/oncotarget.15422>.
- (21) Peraica, M.; Radić, B.; Lucić, A.; Pavlović, M. Toxic Effects of Mycotoxins in Humans. *Bull. World Health Organ.* **1999**, *77* (9), 754–766.
- (22) McKean, C.; Tang, L.; Tang, M.; Billam, M.; Wang, Z.; Theodorakis, C. W.; Kendall, R. J.; Wang, J. S. Comparative Acute and Combinative Toxicity of Aflatoxin B1 and Fumonisin B1 in Animals and Human Cells. *Food Chem. Toxicol.* **2006**, *44* (6), 868–876.  
<https://doi.org/10.1016/j.fct.2005.11.011>.
- (23) Creppy, E. E.; Chiarappa, P.; Baudrimont, I.; Borracci, P.; Moukha, S.; Carratù, M. R. Synergistic Effects of Fumonisin B1 and Ochratoxin A: Are in Vitro Cytotoxicity Data Predictive of in Vivo Acute Toxicity? *Toxicology* **2004**, *201*, 115–123.  
<https://doi.org/10.1016/j.tox.2004.04.008>.
- (24) Saini, S. S.; Kaur, A. Aflatoxin B1 : Toxicity , Characteristics and Analysis : Mini Review. *Glob. Adv. Res. J. Chem. Mater. Sci.* **2012**, *1* (4), 63–70.
- (25) <http://www.t3db.ca/toxins/T3D3668>, accessed date 20191005.
- (26) Ostry, V.; Malir, F.; Toman, J.; Grosse, Y. Mycotoxins as Human Carcinogens—the IARC Monographs Classification. *Mycotoxin Res.* **2017**, *33* (1), 65–73.  
<https://doi.org/10.1007/s12550-016-0265-7>.
- (27) Liu, Y.; Wu, F. Global Burden of Aflatoxin-Induced Hepatocellular Carcinoma: A Risk Assessment. *Environ. Health Perspect.* **2010**, *118* (6), 818–824.  
<https://doi.org/10.1289/ehp.0901388>.
- (28) Ahlberg, S.; Randolph, D.; Okoth, S. Aflatoxin Binders in Foods for Human

- Consumption—Can This Be Promoted Safely and Ethically? Sara. *Toxins (Basel)*. **2019**, *11* (7), 410. <https://doi.org/10.3390/toxins11070410>.
- (29) Anzai, N.; Jutabha, P.; Endou, H. Molecular Mechanism of Ochratoxin A Transport in the Kidney. *Toxins (Basel)*. **2010**, *2* (6), 1381–1398. <https://doi.org/10.3390/toxins2061381>.
- (30) Malir, F.; Ostry, V.; Pfohl-leszkowicz, A.; Malir, J.; Toman, J. Ochratoxin A : 50 Years of Research. 12–15. <https://doi.org/10.3390/toxins8070191>.
- (31) Wang, S. K.; Wang, T. T.; Huang, G. L.; Shi, R. F.; Yang, L. G.; Sun, G. J. Stimulation of the Proliferation of Human Normal Esophageal Epithelial Cells by Fumonisin B1 and Its Mechanism. *Exp. Ther. Med.* **2013**, *7* (1), 55–60. <https://doi.org/10.3892/etm.2013.1364>.
- (32) Missmer, S.; Suarez, L.; Felkner, M.; Wang, E.; Merrill, A. H.; Rothman, K. J.; Hendricks, K. Exposure to Fumonisin and the Occurrence of Neural Tube Defects along the Texas-Mexico Border. *Environ. Health Perspect.* **2006**, *114* (2), 237–241. <https://doi.org/10.1289/ehp.8221>.
- (33) Wu, Q. H.; Wang, X.; Yang, W.; Nüssler, A. K.; Xiong, L. Y.; Kuča, K.; Dohnal, V.; Zhang, X. J.; Yuan, Z. H. Oxidative Stress-Mediated Cytotoxicity and Metabolism of T-2 Toxin and Deoxynivalenol in Animals and Humans: An Update. *Arch. Toxicol.* **2014**, *88* (7), 1309–1326. <https://doi.org/10.1007/s00204-014-1280-0>.
- (34) Kuciel-Lisieska, G.; Obremski, K.; Stelmachow, J.; Gajęcka, M.; Zielonka, Ł.; JAKIMIUK, E.; Gajęcki, M. Presence of Zearalenone in Blood Plasma in Women with Neoplastic Lesions in the Mammary Gland. *Bull. Vet. Inst. Pulawy* **2008**, *52* (2), 671–674.
- (35) Fleck, S. C.; Hildebrand, A. A.; Müller, E.; Pfeiffer, E.; Metzler, M. Genotoxicity and Inactivation of Catechol Metabolites of the Mycotoxin Zearalenone. *Mycotoxin Res.* **2012**, *28* (4), 267–273. <https://doi.org/10.1007/s12550-012-0143-x>.
- (36) Qin, X.; Cao, M.; Lai, F.; Yang, F.; Ge, W.; Zhang, X.; Cheng, S.; Sun, X.; Qin, G.; Shen, W.; Li, L. Oxidative Stress Induced by Zearalenone in Porcine Granulosa Cells and Its Rescue by Curcumin In Vitro. *PLoS One* **2015**, *10* (6), e0127551. <https://doi.org/10.1371/journal.pone.0127551>.
- (37) Kuiper-Goodman, T.; Hilts, C.; Billiard, S. M.; Kiparissis, Y.; Richard, I. D. K.; Hayward, S. Health Risk Assessment of Ochratoxin A for All Age-Sex Strata in a Market Economy.

- Food Addit. Contam. Part A. Chem. Anal. Control. Expo. Risk Assess.* **2010**, 27 (2), 212–240. <https://doi.org/10.1080/02652030903013278>.
- (38) Solfrizzo, M.; Gambacorta, L.; Lattanzio, V. M. T.; Powers, S.; Visconti, A. Simultaneous LC-MS/MS Determination of Aflatoxin M 1, Ochratoxin A, Deoxynivalenol, de-Epoxydeoxynivalenol,  $\alpha$  and  $\beta$ -Zearalenols and Fumonisin B 1 in Urine as a Multi-Biomarker Method to Assess Exposure to Mycotoxins. *Anal. Bioanal. Chem.* **2011**, 401 (9), 2831–2841. <https://doi.org/10.1007/s00216-011-5354-z>.
- (39) Kongkapan, J.; Giorgi, M.; Poapolathep, S.; Isariyodom, S.; Poapolathep, A. Toxicokinetics and Tissue Distribution of Nivalenol in Broiler Chickens. *Toxicon* **2016**, 111 (1), 31–36. <https://doi.org/10.1016/j.toxicon.2015.12.013>.
- (40) Steinkellner, H.; Binaglia, M.; Dall'Asta, C.; Gutleb, A. C.; Metzler, M.; Oswald, I. P.; Parent-Massin, D.; Alexander, J. Combined Hazard Assessment of Mycotoxins and Their Modified Forms Applying Relative Potency Factors: Zearalenone and T2/HT2 Toxin. *Food Chem. Toxicol.* **2019**, 131, 110599. <https://doi.org/10.1016/j.fct.2019.110599>.
- (41) Tittlemier, S. A.; Blagden, R.; Chan, J.; Roscoe, M.; Pleskach, K. A Multi-Year Survey of Mycotoxins and Ergosterol in Canadian Oats. *Mycotoxin Res.* **2020**, 36 (1), 103–114. <https://doi.org/10.1007/s12550-019-00373-9>.
- (42) Tittlemier, S. A.; Blagden, R.; Chan, J.; Gaba, D.; Mckendry, T.; Pleskach, K.; Roscoe, M. Fusarium and Alternaria Mycotoxins Present in Canadian Wheat and Durum Harvest Samples. *Can. J. Plant Pathol.* **2019**, 41 (3), 403–414. <https://doi.org/10.1080/07060661.2019.1592784>.
- (43) Edwards, S. G. Impact of Agronomic and Climatic Factors on the Mycotoxin Content of Harvested Oats in the United Kingdom. *Food Addit. Contam. - Part A Chem. Anal. Control. Expo. Risk Assess.* **2017**, 34 (12), 2230–2241. <https://doi.org/10.1080/19440049.2017.1372639>.
- (44) Rodríguez-Carrasco, Y.; Moltó, J. C.; Mañes, J.; Berrada, H. Exposure Assessment Approach through Mycotoxin / Creatinine Ratio Evaluation in Urine by GC – MS / MS. *Food Chem. Toxicol.* **2014**, 72, 69–75. <https://doi.org/10.1016/j.fct.2014.07.014>.
- (45) Solfrizzo, M.; Gambacorta, L.; Visconti, A. Assessment of Multi-Mycotoxin Exposure in

- Southern Italy by Urinary Multi-Biomarker Determination. *Toxins (Basel)*. **2014**, *6* (2), 523–538. <https://doi.org/10.3390/toxins6020523>.
- (46) Heyndrickx, E.; Sioen, I.; Huybrechts, B.; Callebaut, A.; De Henauw, S.; De Saeger, S. Human Biomonitoring of Multiple Mycotoxins in the Belgian Population: Results of the BIOMYCO Study. *Environ. Int.* **2015**, *84*, 82–89. <https://doi.org/10.1016/j.envint.2015.06.011>.
- (47) Mitropoulou, A.; Gambacorta, L.; Lemming, E.; Solfrizzo, M.; Olsen, M. Extended Evaluation of Urinary Multi-Biomarker Analyses of Mycotoxins in Swedish Adults and Children. *World Mycotoxin J.* **2018**, *11* (4), 647–659. <https://doi.org/10.3920/WMJ2018.2313>.
- (48) Wells, L.; Hardie, L.; Williams, C.; White, K.; Liu, Y.; De Santis, B.; Debegnach, F.; Moretti, G.; Greetham, S.; Brera, C.; Papageorgiou, M.; Thatcher, N. J.; Rigby, A.; Atkin, S. L.; Sathyapalan, T. Deoxynivalenol Biomarkers in the Urine of UK Vegetarians. *Toxins (Basel)*. **2017**, *9* (7), 196. <https://doi.org/10.3390/toxins9070196>.
- (49) Lee, H. J.; Ryu, D. Worldwide Occurrence of Mycotoxins in Cereals and Cereal-Derived Food Products: Public Health Perspectives of Their Co-Occurrence. *J. Agric. Food Chem.* **2017**, *65* (33), 7034–7051. <https://doi.org/10.1021/acs.jafc.6b04847>.
- (50) Karlovsky, P.; Suman, M.; Berthiller, F.; De Meester, J.; Eisenbrand, G.; Perrin, I.; Oswald, I. P.; Speijers, G.; Chiodini, A.; Recker, T.; Dussort, P. Impact of Food Processing and Detoxification Treatments on Mycotoxin Contamination. *Mycotoxin Res.* **2016**, *32* (4), 179–205. <https://doi.org/10.1007/s12550-016-0257-7>.
- (51) Sakuma, H.; Watanabe, Y.; Furusawa, H.; Yoshinari, T.; Akashi, H.; Kawakami, H.; Saito, S.; Sugita-Konishi, Y. Estimated Dietary Exposure to Mycotoxins after Taking into Account the Cooking of Staple Foods in Japan. *Toxins (Basel)*. **2013**, *5* (5), 1032–1042. <https://doi.org/10.3390/toxins5051032>.
- (52) Copetti, M. V.; Iamanaka, B. T.; Nester, M. A.; Efraim, P.; Taniwaki, M. H. Occurrence of Ochratoxin A in Cocoa By-Products and Determination of Its Reduction during Chocolate Manufacture. *Food Chem.* **2013**, *136* (1), 100–104. <https://doi.org/10.1016/j.foodchem.2012.07.093>.

- (53) Scottt, P. M.; Kanhere, S. R.; Lau, B. P. -Y.; Levvis, D. a.; Hayward, S.; Ryan, J. J.; Kuiper-Goodman, T. Survey of Canadian Human Blood Plasma for Ochratoxin A. *Food Addit. Contam.* **1998**, *15* (5), 555–562. <https://doi.org/10.1080/02652039809374681>.
- (54) Vidal, A.; Claeys, L.; Mengelers, M.; Vanhoorne, V.; Vervaet, C.; Huybrechts, B.; De Saeger, S.; De Boevre, M. Humans Significantly Metabolize and Excrete the Mycotoxin Deoxynivalenol and Its Modified Form Deoxynivalenol-3-Glucoside within 24 Hours. *Sci. Rep.* **2018**, *8* (1), 1–11. <https://doi.org/10.1038/s41598-018-23526-9>.
- (55) Viegas, S.; Assunção, R.; Martins, C.; Nunes, C.; Osteresch, B.; Twarużek, M.; Kosicki, R.; Grajewski, J.; Ribeiro, E.; Viegas, C. Occupational Exposure to Mycotoxins in Swine Production: Environmental and Biological Monitoring Approaches. *Toxins (Basel)*. **2019**, *11* (2). <https://doi.org/10.3390/toxins11020078>.
- (56) Egbuta, M. A.; Mwanza, M.; Babalola, O. O. Health Risks Associated with Exposure to Filamentous Fungi. *Int. J. Environ. Res. Public Health* **2017**, *14* (7), 14–17. <https://doi.org/10.3390/ijerph14070719>.
- (57) Liang, B.; Du, X. J.; Li, P.; Sun, C. C.; Wang, S. Investigation of Citrinin and Pigment Biosynthesis Mechanisms in *Monascus Purpureus* by Transcriptomic Analysis. *Front. Microbiol.* **2018**, *9*, 1374. <https://doi.org/10.3389/fmicb.2018.01374>.
- (58) Shi, H.; Schwab, W.; Yu, P. Natural Occurrence and Co-Contamination of Twelve Mycotoxins in Industry-Submitted Cool-Season Cereal Grains Grown under a Low Heat Unit Climate Condition. *Toxins (Basel)*. **2019**, *11* (3), 160. <https://doi.org/10.3390/toxins11030160>.
- (59) Wallin, S.; Gambacorta, L.; Kotova, N.; Warensjö Lemming, E.; Nälsén, C.; Solfrizzo, M.; Olsen, M. Biomonitoring of Concurrent Mycotoxin Exposure among Adults in Sweden through Urinary Multi-Biomarker Analysis. *Food Chem. Toxicol.* **2015**, *83*, 133–139. <https://doi.org/10.1016/j.fct.2015.05.023>.
- (60) Sobral, M. M. C.; Faria, M. A.; Cunha, S. C.; Ferreira, I. M. P. L. V. O. Toxicological Interactions between Mycotoxins from Ubiquitous Fungi: Impact on Hepatic and Intestinal Human Epithelial Cells. *Chemosphere* **2018**, *202*, 538–548. <https://doi.org/10.1016/j.chemosphere.2018.03.122>.

- (61) Mwanza, M.; Kametler, L.; Bonai, A.; Rajli, V.; Kovacs, M.; Dutton, M. F. The Cytotoxic Effect of Fumonisin B1 and Ochratoxin A on Human and Pig Lymphocytes Using the Methyl Thiazol Tetrazolium (MTT) Assay. *Mycotoxin Res.* **2009**, *25* (4), 233–238. <https://doi.org/10.1007/s12550-009-0033-z>.
- (62) De Ruyck, K.; Huybrechts, I.; Yang, S.; Arcella, D.; Claeys, L.; Abbeddou, S.; De Keyzer, W.; De Vries, J.; Ocke, M.; Ruprich, J.; De Boevre, M.; De Saeger, S. Mycotoxin Exposure Assessments in a Multi-Center European Validation Study by 24-Hour Dietary Recall and Biological Fluid Sampling. *Environ. Int.* **2020**, *137*, 105539. <https://doi.org/10.1016/j.envint.2020.105539>.
- (63) Souto, P. C. M. C.; Jager, A. V.; Tonin, F. G.; Petta, T.; Di Gregório, M. C.; Cossalter, A. M.; Pinton, P.; Oswald, I. P.; Rottinghaus, G. E.; Oliveira, C. A. F. Determination of Fumonisin B1 Levels in Body Fluids and Hair from Piglets Fed Fumonisin B1-Contaminated Diets. *Food Chem. Toxicol.* **2017**, *108*, 1–9. <https://doi.org/10.1016/j.fct.2017.07.036>.
- (64) Fan, K.; Xu, J.; Jiang, K.; Liu, X.; Meng, J.; Di Mavungu, J. D.; Guo, W.; Zhang, Z.; Jing, J.; Li, H.; Yao, B.; Li, H.; Zhao, Z.; Han, Z. Determination of Multiple Mycotoxins in Paired Plasma and Urine Samples to Assess Human Exposure in Nanjing, China. *Environ. Pollut.* **2019**, *248*, 865–873. <https://doi.org/10.1016/j.envpol.2019.02.091>.
- (65) Warensjö Lemming, E.; Montano Montes, A.; Schmidt, J.; Cramer, B.; Humpf, H. U.; Moraes, L.; Olsen, M. Mycotoxins in Blood and Urine of Swedish Adolescents—Possible Associations to Food Intake and Other Background Characteristics. *Mycotoxin Res.* **2020**, *36* (2), 193–206. <https://doi.org/10.1007/s12550-019-00381-9>.
- (66) Muñoz, K.; Blaszkewicz, M.; Degen, G. H. Simultaneous Analysis of Ochratoxin A and Its Major Metabolite Ochratoxin Alpha in Plasma and Urine for an Advanced Biomonitoring of the Mycotoxin. *J. Chromatogr. B Anal. Technol. Biomed. Life Sci.* **2010**, *878* (27), 2623–2629. <https://doi.org/10.1016/j.jchromb.2009.11.044>.
- (67) Rose, C.; Parker, A.; Jefferson, B.; Cartmell, E. The Characterization of Feces and Urine: A Review of the Literature to Inform Advanced Treatment Technology. *Crit. Rev. Environ. Sci. Technol.* **2015**, *45* (17), 1827–1879.



<https://doi.org/10.1080/10643389.2014.1000761>.

- (68) Bi, H.; Guo, Z.; Jia, X.; Liu, H.; Ma, L.; Xue, L. The Key Points in the Pre-Analytical Procedures of Blood and Urine Samples in Metabolomics Studies. *Metabolomics* **2020**, *16* (6), 1–15. <https://doi.org/10.1007/s11306-020-01666-2>.
- (69) Calafat, A. M. Contemporary Issues in Exposure Assessment Using Biomonitoring. *Curr. Epidemiol. Reports* **2016**, *3* (2), 145–153. <https://doi.org/10.1007/s40471-016-0075-7>.
- (70) Devreese, M.; Croubels, S.; De Baere, S.; Gehring, R.; Antonissen, G. Comparative Toxicokinetics and Plasma Protein Binding of Ochratoxin A in Four Avian Species. *J. Agric. Food Chem.* **2018**, *66* (9), 2129–2135. <https://doi.org/10.1021/acs.jafc.7b06048>.
- (71) Scholl, P. F.; Mcoy, L.; Kensler, T. W.; Groopman, J. D. Quantitative Analysis and Chronic Dosimetry of the Aflatoxin B1 Plasma Albumin Adduct Lys-AFB1 in Rats by Isotope Dilution Mass Spectrometry. *Chem. Res. Toxicol.* **2006**, *19* (1), 44–49. <https://doi.org/10.1021/tx020089h>.
- (72) Studer-Rohr, I.; Schlatter, J.; Dietrich, D. R. Kinetic Parameters and Intraindividual Fluctuations of Ochratoxin A Plasma Levels in Humans. *Arch. Toxicol.* **2000**, *74* (9), 499–510. <https://doi.org/10.1007/s002040000157>.
- (73) Schertz, H.; Kluess, J.; Frahm, J.; Schatzmayr, D.; Dohnal, I.; Bichl, G.; Schwartz-Zimmermann, H.; Breves, G.; Dänicke, S. Oral and Intravenous Fumonisin Exposure in Pigs—a Single-Dose Treatment Experiment Evaluating Toxicokinetics and Detoxification. *Toxins (Basel)*. **2018**, *10* (4), 1–23. <https://doi.org/10.3390/toxins10040150>.
- (74) Saint-Cyr, M. J.; Perrin-Guyomard, A.; Manceau, J.; Houée, P.; Delmas, J. M.; Rolland, J. G.; Laurentie, M. Risk Assessment of Deoxynivalenol by Revisiting Its Bioavailability in Pig and Rat Models to Establish Which Is More Suitable. *Toxins (Basel)*. **2015**, *7* (12), 5167–5181. <https://doi.org/10.3390/toxins7124873>.
- (75) Devreese, M.; De Baere, S.; De Backer, P.; Croubels, S. Quantitative Determination of Several Toxicological Important Mycotoxins in Pig Plasma Using Multi-Mycotoxin and Analyte-Specific High Performance Liquid Chromatography-Tandem Mass Spectrometric Methods. *J. Chromatogr. A* **2012**, *1257*, 74–80.

<https://doi.org/10.1016/j.chroma.2012.08.008>.

- (76) Coulombe, R. A.; Sharma, R. P. Clearance and Excretion of Intratracheally and Orally Administered Aflatoxin B1 in the Rat. *Food Chem. Toxicol.* **1985**, *23* (9), 827–830.
- (77) Pestka, J. J.; Clark, E. S.; Schwartz-zimmermann, H. E.; Berthiller, F. Sex Is a Determinant for Deoxynivalenol Metabolism and Elimination in the Mouse. *Toxins (Basel)*. **2017**, *9* (8), 240. <https://doi.org/10.3390/toxins9080240>.
- (78) Gambacorta, S.; Solfrizzo, H.; Visconti, A.; Powers, S.; Cossalter, A. M.; Pinton, P.; Oswald, I. P. Validation Study on Urinary Biomarkers of Exposure for Aflatoxin B1, Ochratoxin A, Fumonisin B1, Deoxynivalenol and Zearalenone in Piglets. *World Mycotoxin J.* **2013**, *6* (3), 299–308.
- (79) Sexton, K.; Needham, L.; Pirkle, J. Human Biomonitoring of Environmental Chemicals. *Am. Sci.* **2004**, *92* (1), 38. <https://doi.org/10.1511/2004.45.921>.
- (80) Escrivá, L.; Font, G.; Manyes, L.; Berrada, H. Studies on the Presence of Mycotoxins in Biological Samples: An Overview. *Toxins* **2017**, *9* (8), 251. <https://doi.org/10.3390/toxins9080251>.
- (81) Berthiller, F.; Brera, C.; Iha, M. H.; Krska, R.; Lattanzio, V. M. T.; MacDonald, S.; Malone, R. J.; Maragos, C.; Solfrizzo, M.; Stranska-Zachariasova, M.; Stroka, J.; Tittlemier, S. A. Developments in Mycotoxin Analysis: An Update for 2015-2016. *World Mycotoxin J.* **2017**, *10* (1), 5–29. <https://doi.org/10.3920/WMJ2016.2138>.
- (82) Heyndrickx, E.; Sioen, I.; Bellemans, M.; De Maeyer, M.; Callebaut, A.; De Henauw, S.; De Saeger, S. Assessment of Mycotoxin Exposure in the Belgian Population Using Biomarkers: Aim, Design and Methods of the BIOMYCO Study. *Food Addit. Contam. - Part A* **2014**, *31* (5), 924–931. <https://doi.org/https://doi.org/10.1080/19440049.2014.900192>.
- (83) Gerding, J.; Cramer, B.; Humpf, H. U. Determination of Mycotoxin Exposure in Germany Using an LC-MS/MS Multibiomarker Approach. *Mol. Nutr. Food Res.* **2014**, *58* (12), 2358–2368. <https://doi.org/10.1002/mnfr.201400406>.
- (84) Föllmann, W.; Ali, N.; Blaszkewicz, M.; Degen, G. H. Biomonitoring of Mycotoxins in Urine: Pilot Study in Mill Workers. *J. Toxicol. Environ. Health. A* **2016**, *79* (22–23),

- 1015–1025. <https://doi.org/10.1080/15287394.2016.1219540>.
- (85) Cigić, I. K.; Prosen, H. An Overview of Conventional and Emerging Analytical Methods for the Determination of Mycotoxins. *Int. J. Mol. Sci.* **2009**, *10* (1), 62–115. <https://doi.org/10.3390/ijms10010062>.
- (86) András, N.; Helenkár, A.; Záray, G.; Vasánits, A.; Molnár-Perl, I. Derivatization and Fragmentation Pattern Analysis of Natural and Synthetic Steroids, as Their Trimethylsilyl (Oxime) Ether Derivatives by Gas Chromatography Mass Spectrometry: Analysis of Dissolved Steroids in Wastewater Samples. *J. Chromatogr. A* **2011**, *1218* (14), 1878–1890. <https://doi.org/10.1016/j.chroma.2011.01.051>.
- (87) Rodríguez-Carrasco, Y.; Moltó, J. C.; Mañes, J.; Berrada, H. Development of Microextraction Techniques in Combination with GC–MS/MS for the Determination of Mycotoxins and Metabolites in Human Urine. *J. Sep. Sci.* **2017**, *40* (7), 1572–1582. <https://doi.org/10.1002/jssc.201601131>.
- (88) Echarte, J. M.; Fernández, D. C.; Chiacchio, C. A.; Torres Leedham, V. M. Comparison of a Validated LC/MS/MS Method with a Validated GC/MS Method for the Analysis of Zeranol and Its Related Mycotoxin Residues in Bovine Urine Samples Collected during Argentina’s Residue Monitoring Control Program (2005-2012). *J. AOAC Int.* **2014**, *97* (5), 1470–1475. <https://doi.org/10.5740/jaoacint.13-283>.
- (89) Ali, N.; Blaszkewicz, M.; Hossain, K.; Degen, G. H. Determination of Aflatoxin M1 in Urine Samples Indicates Frequent Dietary Exposure to Aflatoxin B1 in the Bangladeshi Population. *Int. J. Hyg. Environ. Health* **2017**, *220* (2), 271–281. <https://doi.org/10.1016/j.ijheh.2016.11.002>.
- (90) Sánchez, E. M.; Diaz, G. J. Frequency and Levels of Aflatoxin M1 in Urine of Children in Bogota, Colombia. *Mycotoxin Res.* **2019**, *35* (3), 271–278. <https://doi.org/10.1007/s12550-019-00355-x>.
- (91) Soh, J. H.; Lin, Y.; Rana, S.; Ying, J. Y.; Stevens, M. M. Colorimetric Detection of Small Molecules in Complex Matrixes via Target-Mediated Growth of Aptamer-Functionalized Gold Nanoparticles. *Anal. Chem.* **2015**, *87* (15), 7644–7652. <https://doi.org/10.1021/acs.analchem.5b00875>.

- (92) Dohnal, V.; Dvořák, V.; Malíř, F.; Ostrý, V.; Roubal, T. A Comparison of ELISA and HPLC Methods for Determination of Ochratoxin A in Human Blood Serum in the Czech Republic. *Food Chem. Toxicol.* **2013**, *62*, 427–431.  
<https://doi.org/10.1016/j.fct.2013.09.010>.
- (93) Josephs, R. D.; Schuhmacher, R.; Krska, R. International Interlaboratory Study for the Determination of the Fusarium Mycotoxins Zearalenone and Deoxynivalenol in Agricultural Commodities. *Food Addit. Contam.* **2001**, *18* (5), 417–430.  
<https://doi.org/10.1080/02652030120332>.
- (94) Cavaliere, C.; D'Ascenzo, G.; Foglia, P.; Pastorini, E.; Samperi, R.; Laganà, A. Determination of Type B Trichothecenes and Macrocyclic Lactone Mycotoxins in Field Contaminated Maize. *Food Chem.* **2005**, *92* (3), 559–568.  
<https://doi.org/10.1016/j.foodchem.2004.10.008>.
- (95) Tangni, E. K.; Motte, J. C.; Callebaut, A.; Pussemier, L. Cross-Reactivity of Antibodies in Some Commercial Deoxynivalenol Test Kits against Some Fusariotoxins. *J. Agric. Food Chem.* **2010**, *58* (24), 12625–12633. <https://doi.org/10.1021/jf103025e>.
- (96) Turner, N. W.; Bramhmbhatt, H.; Szabo-Vezse, M.; Poma, A.; Coker, R.; Piletsky, S. A. Analytical Methods for Determination of Mycotoxins: An Update (2009-2014). *Anal. Chim. Acta* **2015**, *901*, 12–33. <https://doi.org/10.1016/j.aca.2015.10.013>.
- (97) Kos, J.; Hajnal, E. J.; Jajić, I.; Krstović, S.; Mastilović, J.; Šarić, B.; Jovanov, P. Comparison of ELISA, HPLC-FLD and HPLC-MS/MS Methods for Determination of Aflatoxin M1 in Natural Contaminated Milk Samples. *Acta Chim. Slov.* **2016**, *63* (4), 747–756. <https://doi.org/10.17344/acsi.2016.2451>.
- (98) Duarte, S. C.; Alves, M. R.; Pena, A.; Lino, C. M. Determinants of Ochratoxin A Exposure-A One Year Follow-up Study of Urine Levels. *Int. J. Hyg. Environ. Health* **2012**, *215* (3), 360–367. <https://doi.org/10.1016/j.ijheh.2011.12.001>.
- (99) Klapac, T.; Šarkanj, B.; Banjari, I.; Strelec, I. Urinary Ochratoxin A and Ochratoxin Alpha in Pregnant Women. *Food Chem. Toxicol.* **2012**, *50* (12), 4487–4492.  
<https://doi.org/10.1016/j.fct.2012.09.030>.
- (100) Muscarella, M.; Iammarino, M.; Nardiello, D.; Palermo, C.; Centonze, D. Determination

- of Deoxynivalenol and Nivalenol by Liquid Chromatography and Fluorimetric Detection with On-Line Chemical Post-Column Derivatization. *Talanta* **2012**, *97*, 145–149. <https://doi.org/10.1016/j.talanta.2012.04.009>.
- (101) Milićević, D.; Jurić, V.; Stefanović, S.; Baltić, T.; Janković, S. Evaluation and Validation of Two Chromatographic Methods (HPLC-Fluorescence and LC-MS/MS) for the Determination and Confirmation of Ochratoxin A in Pig Tissues. *Arch. Environ. Contam. Toxicol.* **2010**, *58* (4), 1074–1081. <https://doi.org/10.1007/s00244-009-9436-2>.
- (102) Corcuera, L. A.; Ibáñez-Vea, M.; Vettorazzi, A.; González-Peñas, E.; Cerain, A. L. de. Validation of a UHPLC-FLD Analytical Method for the Simultaneous Quantification of Aflatoxin B1 and Ochratoxin a in Rat Plasma, Liver and Kidney. *J. Chromatogr. B Anal. Technol. Biomed. Life Sci.* **2011**, *879* (26), 2733–2740. <https://doi.org/10.1016/j.jchromb.2011.07.039>.
- (103) Sun, L.; Zhao, Q. Direct Fluorescence Anisotropy Approach for Aflatoxin B1 Detection and Affinity Binding Study by Using Single Tetramethylrhodamine Labeled Aptamer. *Talanta* **2018**, *189*, 442–450. <https://doi.org/10.1016/j.talanta.2018.07.036>.
- (104) Beheshti-Marnani, A.; Hatefi-Mehrijardi, A.; Es'haghi, Z. A Sensitive Biosensing Method for Detecting of Ultra-Trace Amounts of AFB1 Based on “Aptamer/Reduced Graphene Oxide” Nano-Bio Interaction. *Colloids Surfaces B Biointerfaces* **2019**, *175*, 98–105. <https://doi.org/10.1016/j.colsurfb.2018.11.087>.
- (105) Jiang, K.; Nie, D.; Huang, Q.; Fan, K.; Tang, Z.; Wu, Y.; Han, Z. Thin-Layer MoS<sub>2</sub> and Thionin Composite-Based Electrochemical Sensing Platform for Rapid and Sensitive Detection of Zearalenone in Human Biofluids. *Biosens. Bioelectron.* **2019**, *130* (November 2018), 322–329. <https://doi.org/10.1016/j.bios.2019.02.003>.
- (106) Schwartzbord, J.; Severe, L.; Brown, D. Detection of Trace Aflatoxin M1 in Human Urine Using a Commercial ELISA Followed by HPLC. *Biomarkers* **2017**, *22* (1), 1–4. <https://doi.org/10.1080/1354750X.2016.1203998>.
- (107) Ali, N.; Hossain, K.; Blaszkewicz, M.; Rahman, M.; Mohanto, N. C.; Alim, A.; Degen, G. H. Occurrence of Aflatoxin M1 in Urines from Rural and Urban Adult Cohorts in Bangladesh. *Arch. Toxicol.* **2016**, *90* (7), 1749–1755. <https://doi.org/10.1007/s00204-015->

1601-y.

- (108) Brewer, J. H.; Thrasher, J. D.; Straus, D. C.; Madison, R. A.; Hooper, D. Detection of Mycotoxins in Patients with Chronic Fatigue Syndrome. *Toxins (Basel)*. **2013**, *5* (4), 605–617. <https://doi.org/10.3390/toxins5040605>.
- (109) Asci, A.; Durmaz, E.; Erkekoglu, P.; Pasli, D.; Bircan, I.; Kocer-Gumusel, B. Urinary Zearalenone Levels in Girls with Premature Thelarche and Idiopathic Central Precocious Puberty. *Minerva Pediatr*. **2014**, *66* (6), 571–578.
- (110) McMillan, A.; Renaud, J. B.; Burgess, K. M. N.; Orimadegun, A. E.; Akinyinka, O. O.; Allen, S. J.; Miller, J. D.; Reid, G.; Sumarah, M. W. Aflatoxin Exposure in Nigerian Children with Severe Acute Malnutrition. *Food Chem. Toxicol*. **2018**, *111*, 356–362. <https://doi.org/10.1016/j.fct.2017.11.030>.
- (111) Akdemir, C.; Ulker, O. C.; Basaran, A.; Ozkaya, S.; Karakaya, A. Estimation of Ochratoxin A in Some Turkish Populations: An Analysis in Urine as a Simple, Sensitive and Reliable Biomarker. *Food Chem. Toxicol*. **2010**, *48* (3), 877–882. <https://doi.org/10.1016/j.fct.2009.12.026>.
- (112) Ali, N.; Blaszkewicz, M.; Manirujjaman, M.; Degen, G. H. Biomonitoring of Concurrent Exposure to Ochratoxin A and Citrinin in Pregnant Women in Bangladesh. *Mycotoxin Res*. **2016**, *32* (3), 163–172. <https://doi.org/10.1007/s12550-016-0251-0>.
- (113) Coronel, M. B.; Marin, S.; Tarragó, M.; Cano-Sancho, G.; Ramos, A. J.; Sanchis, V. Ochratoxin A and Its Metabolite Ochratoxin Alpha in Urine and Assessment of the Exposure of Inhabitants of Lleida, Spain. *Food Chem. Toxicol*. **2011**, *49* (6), 1436–1442. <https://doi.org/10.1016/j.fct.2011.03.039>.
- (114) Song, S.; Ediage, E. N.; Wu, A.; De Saeger, S. Development and Application of Salting-out Assisted Liquid/Liquid Extraction for Multi-Mycotoxin Biomarkers Analysis in Pig Urine with High Performance Liquid Chromatography/Tandem Mass Spectrometry. *J. Chromatogr. A* **2013**, *1292*, 111–120. <https://doi.org/10.1016/j.chroma.2012.10.071>.
- (115) Escrivá, L.; Manyes, L.; Font, G.; Berrada, H. Mycotoxin Analysis of Human Urine by LC-MS/MS: A Comparative Extraction Study. *Toxins (Basel)*. **2017**, *9* (10), 330. <https://doi.org/10.3390/toxins9100330>.

- (116) Malachová, A.; Stránská, M.; Václavíková, M.; Elliott, C. T.; Black, C.; Meneely, J.; Haj, J.; Ezekiel, C. N.; Schuhmacher, R.; Krska, R. Advanced LC – MS-Based Methods to Study the Co-Occurrence and Metabolization of Multiple Mycotoxins in Cereals and Cereal-Based Food. *Anal. Bioanal. Chem.* **2018**, *410*, 801–825. <https://doi.org/10.1007/s00216-017-0750-7>.
- (117) Ediage, E. N.; Di Mavungu, J. D.; Song, S.; Wu, A.; Van Peteghem, C.; De Saeger, S. A Direct Assessment of Mycotoxin Biomarkers in Human Urine Samples by Liquid Chromatography Tandem Mass Spectrometry. *Anal. Chim. Acta* **2012**, *741*, 58–69. <https://doi.org/10.1016/j.aca.2012.06.038>.
- (118) Tittlemier, S. A.; Cramer, B.; Dall’Asta, C.; Iha, M. H.; Lattanzio, V. M. T.; Malone, R. J.; Maragos, C.; Solfrizzo, M.; Stranska-Zachariasova, M.; Stroka, J. Developments in Mycotoxin Analysis: An Update for 2017-2018. *World Mycotoxin J.* **2019**, *12* (1), 3–29. <https://doi.org/10.3920/WMJ2018.2398>.
- (119) Huybrechts, B.; Martins, J. C.; Debongnie, P.; Uhlig, S.; Callebaut, A. Fast and Sensitive LC–MS/MS Method Measuring Human Mycotoxin Exposure Using Biomarkers in Urine. *Arch. Toxicol.* **2015**, *89* (11), 1993–2005. <https://doi.org/10.1007/s00204-014-1358-8>.
- (120) Belhassen, H.; Jiménez-Díaz, I.; Ghali, R.; Ghorbel, H.; Molina-Molina, J. M.; Olea, N.; Hedili, A. Validation of a UHPLC-MS/MS Method for Quantification of Zearalenone,  $\alpha$ -Zearalenol,  $\beta$ -Zearalenol,  $\alpha$ -Zearalanol,  $\beta$ -Zearalanol and Zearalanone in Human Urine. *J. Chromatogr. B* **2014**, *962*, 68–74. <https://doi.org/10.1016/j.jchromb.2014.05.019>.
- (121) Serrano, A. B.; Capriotti, A. L.; Cavaliere, C.; Piovesana, S.; Samperi, R.; Ventura, S.; Laganà, A. Development of a Rapid LC-MS/MS Method for the Determination of Emerging Fusarium Mycotoxins Enniatins and Beauvericin in Human Biological Fluids. *Toxins (Basel)*. **2015**, *7* (9), 3554–3571. <https://doi.org/10.3390/toxins7093554>.
- (122) Warth, B.; Sulyok, M.; Berthiller, F.; Schuhmacher, R.; Fruhmann, P.; Hametner, C.; Adam, G.; Fröhlich, J.; Krska, R. Direct Quantification of Deoxynivalenol Glucuronide in Human Urine as Biomarker of Exposure to the Fusarium Mycotoxin Deoxynivalenol. *Anal. Bioanal. Chem.* **2011**, *401* (1), 195–200. <https://doi.org/10.1007/s00216-011-5095-z>.
- (123) Gerding, J.; Ali, N.; Schwartzbord, J.; Cramer, B.; Brown, D. L.; Degen, G. H.; Humpf,

- H.-U. A Comparative Study of the Human Urinary Mycotoxin Excretion Patterns in Bangladesh, Germany, and Haiti Using a Rapid and Sensitive LC-MS/MS Approach. *Mycotoxin Res.* **2015**, *31* (3), 127–136. <https://doi.org/10.1007/s12550-015-0223-9>.
- (124) Seetha, A.; Monyo, E. S.; Tsusaka, T. W.; Msere, H. W.; Madinda, F.; Chilunjika, T.; Sichone, E.; Mbughi, D.; Chilima, B.; Matumba, L. Aflatoxin-Lysine Adducts in Blood Serum of the Malawian Rural Population and Aflatoxin Contamination in Foods (Groundnuts, Maize) in the Corresponding Areas. *Mycotoxin Res.* **2018**, *34* (3), 195–204. <https://doi.org/10.1007/s12550-018-0314-5>.
- (125) Viegas, S.; Veiga, L.; Figueiredo, P.; Almeida, A.; Carolino, E.; Viegas, C. Assessment of Workers' Exposure to Aflatoxin B1 in a Portuguese Waste Industry. *Ann. Occup. Hyg.* **2015**, *59* (2), 173–181. <https://doi.org/10.1093/annhyg/meu082>.
- (126) Williams, J. H.; Phillips, T. D.; Jolly, P. E.; Stiles, J. K.; Jolly, C. M.; Aggarwal, D. Human Aflatoxicosis in Developing Countries: A Review of Toxicology, Exposure, Potential Health Consequences, and Interventions. *Am. Soc. Clin. Nutr.* **2004**, *80* (5), 1106–1122. <https://doi.org/10.1093/ajcn/80.5.1106>.
- (127) Obuseh, F.; Jolly, P. E.; Kulczycki, A.; Ehiri, J.; Waterbor, J.; Desmond, R.; Preko, P. O.; Jiang, Y.; Piyathilake, C. J. Aflatoxin Levels, Plasma Vitamins A and E Concentrations, and Their Association with HIV and Hepatitis B Virus Infections in Ghanaians: A Cross-Sectional Study. *J. Int. AIDS Soc.* **2011**, *14* (1), 53. <https://doi.org/10.1186/1758-2652-14-53>.
- (128) Lai, H.; Mo, X.; Yang, Y.; He, K.; Xiao, J.; Liu, C.; Chen, J.; Lin, Y. Association between Aflatoxin B1 Occupational Airway Exposure and Risk of Hepatocellular Carcinoma: A Case-Control Study. *Tumor Biol.* **2014**, *35* (10), 9577–9584. <https://doi.org/10.1007/s13277-014-2231-3>.
- (129) Sompunga, P.; Pruksametanan, N.; Rangnoi, K.; Choowongkomon, K.; Yamabhai, M. Generation of Human and Rabbit Recombinant Antibodies for the Detection of Zearalenone by Phage Display Antibody Technology. *Talanta* **2019**, *201*, 397–405. <https://doi.org/10.1016/j.talanta.2019.04.034>.
- (130) Coronel, M. B.; Sanchis, V.; Ramos, A. J.; Marin, S. Ochratoxin A in Adult Population of



- Lleida, Spain: Presence in Blood Plasma and Consumption in Different Regions and Seasons. *Food Chem. Toxicol.* **2011**, *49* (10), 2697–2705.  
<https://doi.org/10.1016/j.fct.2011.07.045>.
- (131) Aslam, M.; Hassan Rivzi, A. S.; Beg, A. E.; Blaszkewicz, M.; Golka, K.; Degen, G. H. Analysis of Ochratoxin a Blood Levels in Bladder Cancer Cases and Healthy Persons from Pakistan. *J. Toxicol. Environ. Heal. - Part A* **2012**, *75* (19–20), 1776–1784.  
<https://doi.org/10.1080/15287394.2012.707602>.
- (132) Ali, N.; Blaszkewicz, M.; Manirujjaman, M.; Perveen, R.; Nahid, A. Al; Mahmood, S.; Rahman, M.; Hossain, K.; Degen, G. H. Biomonitoring of Ochratoxin A in Blood Plasma and Exposure Assessment of Adult Students in Bangladesh. *Mol. Nutr. Food Res.* **2014**, *58* (11), 2219–2225. <https://doi.org/10.1002/mnfr.201400403>.
- (133) Choe, S.; In, S.; Jeon, Y.; Choi, H.; Kim, S. Identification of Trichothecene-Type Mycotoxins in Toxic Mushroom *Podostroma Cornu-Damae* and Biological Specimens from a Fatal Case by LC–QTOF/MS. *Forensic Sci. Int.* **2018**, *291*, 234–244.  
<https://doi.org/10.1016/j.forsciint.2018.08.043>.
- (134) Cramer, B.; Osteresch, B.; Munoz, K. A.; Hillmann, H.; Sibrowski, W.; Humpf, H. U. Biomonitoring Using Dried Blood Spots: Detection of Ochratoxin A and Its Degradation Product 2’R-Ochratoxin A in Blood from Coffee Drinkers. *Mol. Nutr. Food Res.* **2015**, *59* (9), 1837–1843. <https://doi.org/10.1002/mnfr.201500220>.
- (135) Korn, M.; Frank, O.; Hofmann, T.; Rychlik, M. Development of Stable Isotope Dilution Assays for Ochratoxin A in Blood Samples. *Anal. Biochem.* **2011**, *419* (2), 88–94.  
<https://doi.org/10.1016/j.ab.2011.08.032>.
- (136) Osteresch, B.; Viegas, S.; Cramer, B.; Humpf, H. U. Multi-Mycotoxin Analysis Using Dried Blood Spots and Dried Serum Spots. *Anal. Bioanal. Chem.* **2017**, *409* (13), 3369–3382. <https://doi.org/10.1007/s00216-017-0279-9>.
- (137) De Santis, B.; Raggi, M. E.; Moretti, G.; Facchiano, F.; Mezzelani, A.; Villa, L.; Bonfanti, A.; Campioni, A.; Rossi, S.; Camposeo, S.; Soricelli, S.; Moracci, G.; Debegnach, F.; Gregori, E.; Ciceri, F.; Milanese, L.; Marabotti, A.; Brera, C. Study on the Association among Mycotoxins and Other Variables in Children with Autism. *Toxins (Basel)*. **2017**, *9*

- (7), 1–20. <https://doi.org/10.3390/toxins9070203>.
- (138) Blaszkewicz, M.; Muñoz, K.; Degen, G. H. Methods for Analysis of Citrinin in Human Blood and Urine. *Arch. Toxicol.* **2013**, *87* (6), 1087–1094. <https://doi.org/10.1007/s00204-013-1010-z>.
- (139) Cao, X.; Li, X.; Li, J.; Niu, Y.; Shi, L.; Fang, Z.; Zhang, T. Quantitative Determination of Carcinogenic Mycotoxins in Human and Animal Biological Matrices and Animal-Derived Foods Using Multi-Mycotoxin and Analyte-Specific High Performance Liquid Chromatography-Tandem Mass Spectrometric Methods. *J. Chromatogr. B* **2018**, *1073*, 191–200. <https://doi.org/10.1016/j.jchromb.2017.10.006>.
- (140) Ritieni, A.; Santini, Antonello Mussap, M.; Ferracane, R.; Bosco, P.; Gazzolo, D.; Galvano, F. Simultaneous Determination of Mycotoxins in Biological Fluids by LC-MS/MS. *Front. Biosci.* **2010**, *2*, 151–158. <https://doi.org/10.2741/e77>.
- (141) Ali, N.; Hossain, K.; Degan, G. Blood Plasma Biomarkers of Citrinin and Ochratoxin A Exposure in Young Adults in Bangladesh. *Mycotoxin Res.* **2018**, *34*, 59–67. <https://doi.org/10.1007/s12550-017-0299-5>.
- (142) Dettmer, K.; Aronov, P. a; Hammock, B. D. Mass Spectrometry-Based Metabolomics. *Mass Spectrom. Rev.* **2007**, *26* (1), 51–78. <https://doi.org/10.1002/mas.20108>.
- (143) Bruce, S. J.; Tavazzi, I.; Parisod, V.; Rezzi, S.; Kochhar, S.; Guy, P. A. Investigation of Human Blood Plasma Sample Preparation for Performing Metabolomics Using Ultrahigh Performance Liquid Chromatography/Mass Spectrometry. *Anal. Chem.* **2009**, *81* (9), 3285–3296. <https://doi.org/10.1021/ac8024569>.
- (144) Poór, M.; Bálint, M.; Hetényi, C.; Gődér, B.; Kunsági-Máté, S.; Kőszegi, T.; Lemli, B. Investigation of Non-Covalent Interactions of Aflatoxins (B1, B2, G1, G2, and M1) with Serum Albumin. *Toxins (Basel)*. **2017**, *9* (11), 1–12. <https://doi.org/10.3390/toxins9110339>.
- (145) Faisal, Z.; Lemli, B.; Szerencsés, D.; Kunsági-Máté, S.; Bálint, M.; Hetényi, C.; Kuzma, M.; Mayer, M.; Poór, M. Interactions of Zearalenone and Its Reduced Metabolites  $\alpha$ -Zearalenol and  $\beta$ -Zearalenol with Serum Albumins: Species Differences, Binding Sites, and Thermodynamics. *Mycotoxin Res.* **2018**, *34* (4), 269–278.

- <https://doi.org/10.1007/s12550-018-0321-6>.
- (146) Kőszegi, T.; Poór, M. Ochratoxin a: Molecular Interactions, Mechanisms of Toxicity and Prevention at the Molecular Level. *Toxins (Basel)*. **2016**, *8* (4), 1–25.  
<https://doi.org/10.3390/toxins8040111>.
- (147) Sintov, A.; Bialer, M.; Yagen, B. Pharmacokinetics and Protein Binding of Trichothecene Mycotoxins, T-2 Toxin and HT-2 Toxin, in Dogs. *Toxicon* **1988**, *26* (2), 153–160.  
[https://doi.org/10.1016/0041-0101\(88\)90167-5](https://doi.org/10.1016/0041-0101(88)90167-5).
- (148) Poór, M.; Lemli, B.; Bálint, M.; Hetényi, C.; Sali, N.; Kőszegi, T.; Kunsági-Máté, S. Interaction of Citrinin with Human Serum Albumin. *Toxins (Basel)*. **2015**, *7* (12), 5155–5166. <https://doi.org/10.3390/toxins7124871>.
- (149) Li, Y.; Wang, H.; Jia, B.; Liu, C.; Liu, K.; Qi, Y.; Hu, Z. Study of the Interaction of Deoxynivalenol with Human Serum Albumin by Spectroscopic Technique and Molecular Modelling. *Food Addit. Contam. - Part A Chem. Anal. Control. Expo. Risk Assess.* **2013**, *30* (2), 356–364. <https://doi.org/10.1080/19440049.2012.742573>.
- (150) Han, Z.; Zhao, Z.; Song, S.; Liu, G.; Shi, J.; Zhang, J.; Liao, Y.; Zhang, D.; Wu, Y.; De Saeger, S.; Wu, A. Establishment of an Isotope Dilution LC-MS/MS Method Revealing Kinetics and Distribution of Co-Occurring Mycotoxins in Rats. *Anal. Methods* **2012**, *4* (11), 3708. <https://doi.org/10.1039/c2ay25891a>.
- (151) Broekaert, N.; Devreese, M.; De Mil, T.; Fraeyman, S.; De Baere, S.; De Saeger, S.; De Backer, P.; Croubels, S. Development and Validation of an LC-MS/MS Method for the Toxicokinetic Study of Deoxynivalenol and Its Acetylated Derivatives in Chicken and Pig Plasma. *J. Chromatogr. B Anal. Technol. Biomed. Life Sci.* **2014**, *971*, 43–51.  
<https://doi.org/10.1016/j.jchromb.2014.09.012>.
- (152) Brezina, U.; Valenta, H.; Rempe, I.; Kersten, S.; Humpf, H. U.; Dänicke, S. Development of a Liquid Chromatography Tandem Mass Spectrometry Method for the Simultaneous Determination of Zearalenone, Deoxynivalenol and Their Metabolites in Pig Serum. *Mycotoxin Res.* **2014**, *30*, 171–186. <https://doi.org/10.1007/s12550-014-0200-8>.
- (153) De Baere, S.; Goossens, J.; Osselaere, A.; Devreese, M.; Vandenbroucke, V.; De Backer, P.; Croubels, S. Quantitative Determination of T-2 Toxin, HT-2 Toxin, Deoxynivalenol

- and Deepoxy-Deoxynivalenol in Animal Body Fluids Using LC-MS/MS Detection. *J. Chromatogr. B Anal. Technol. Biomed. Life Sci.* **2011**, 879 (24), 2403–2415.  
<https://doi.org/10.1016/j.jchromb.2011.06.036>.
- (154) Sun, Y.; Zhang, G.; Zhao, H.; Zheng, J.; Hu, F.; Fang, B. Liquid Chromatography-Tandem Mass Spectrometry Method for Toxicokinetics, Tissue Distribution, and Excretion Studies of T-2 Toxin and Its Major Metabolites in Pigs. *J. Chromatogr. B Anal. Technol. Biomed. Life Sci.* **2014**, 958, 75–82.  
<https://doi.org/10.1016/j.jchromb.2014.03.010>.
- (155) Songsermsakul, P.; Sontag, G.; Cichna-Markl, M.; Zentek, J.; Razzazi-Fazeli, E. Determination of Zearalenone and Its Metabolites in Urine, Plasma and Faeces of Horses by HPLC-APCI-MS. *J. Chromatogr. B Anal. Technol. Biomed. Life Sci.* **2006**, 843 (2), 252–261. <https://doi.org/10.1016/j.jchromb.2006.06.012>.
- (156) De Baere, S.; Osselaere, A.; Devreese, M.; Vanhaecke, L.; De Backer, P.; Croubels, S. Development of a Liquid-Chromatography Tandem Mass Spectrometry Chromatography High-Resolution Mass Spectrometry Method for the Quantitative Determination of Zearalenone and Its Major Metabolites in Chicken and Pig Plasma. *Anal. Chim. Acta* **2012**, 756, 37–48. <https://doi.org/10.1016/j.aca.2012.10.027>.
- (157) Wermuth, C. G. *Biotransformations Leading to Toxic Metabolites: Chemical Aspects*; 2008. <https://doi.org/10.1016/B978-0-12-417205-0.00025-0>.
- (158) Wu, Q.; Dohnal, V.; Huang, L.; Kuca, K.; Wang, X.; Chen, G.; Yuan, Z. Metabolic Pathways of Ochratoxin A. *Curr. Drug Metab.* **2011**, 12 (1), 1–10.  
<https://doi.org/10.2174/138920011794520026>.
- (159) Wen, J.; Mu, P.; Deng, Y. Mycotoxins: Cytotoxicity and Biotransformation in Animal Cells. *Toxicol. Res. (Camb)*. **2016**, 5 (2), 377–387. <https://doi.org/10.1039/c5tx00293a>.
- (160) Bryła, M.; Waskiewicz, A.; Ksieniewicz-Wozniak, E.; Szymczyk, E.; Jedrzejczak, R. Modified Fusarium Mycotoxins in Cereals and Their Products—Metabolism, Occurrence, and Toxicity: An Updated Review. *Molecules* **2018**, 23 (4), 1–34.  
<https://doi.org/10.3390/molecules23040963>.
- (161) Hughes, W. *Essentials of Environmental Toxicology*; 1996.

- (162) Yang, S.; De Boevre, M.; Zhang, H.; De Ruyck, K.; Sun, F.; Zhang, J.; Jin, Y.; Li, Y.; Wang, Z.; Zhang, S.; Zhou, J.; Li, Y.; De Saeger, S. Metabolism of T-2 Toxin in Farm Animals and Human In Vitro and in Chickens In Vivo Using Ultra High-Performance Liquid Chromatography- Quadrupole/Time-of-Flight Hybrid Mass Spectrometry Along with Online Hydrogen/Deuterium Exchange Technique. *J. Agric. Food Chem.* **2017**, *65* (33), 7217–7227. <https://doi.org/10.1021/acs.jafc.7b02575>.
- (163) Astashkina, A.; Mann, B.; Grainger, D. W. A Critical Evaluation of in Vitro Cell Culture Models for High-Throughput Drug Screening and Toxicity. *Pharmacol. Ther.* **2012**, *134* (1), 82–106. <https://doi.org/10.1016/j.pharmthera.2012.01.001>.
- (164) Rougée, L. R. A.; Richmond, R. H.; Collier, A. C. Natural Variations in Xenobiotic-Metabolizing Enzymes: Developing Tools for Coral Monitoring. *Coral Reefs* **2014**, *33* (2), 523–535. <https://doi.org/10.1007/s00338-014-1136-3>.
- (165) Warth, B.; Sulyok, M.; Krska, R. LC-MS/MS-Based Multibiomarker Approaches for the Assessment of Human Exposure to Mycotoxins. *Anal. Bioanal. Chem.* **2013**, *405* (17), 5687–5695. <https://doi.org/10.1007/s00216-013-7011-1>.
- (166) Jager, A. V.; Tonin, F. G.; Souto, P. C. M. C.; Privatti, R. T.; Oliveira, C. A. F. Determination of Urinary Biomarkers for Assessment of Short-Term Human Exposure to Aflatoxins in São Paulo, Brazil. *Toxins (Basel)*. **2014**, *6* (7), 1996–2007. <https://doi.org/10.3390/toxins6071996>.
- (167) Mykkänen, H.; Zhu, H.; Salminen, E.; Juvonen, R. O.; Ling, W.; Ma, J.; Polychronaki, N.; Kemiläinen, H.; Mykkänen, O.; Salminen, S.; El-Nezami, H. Fecal and Urinary Excretion of Aflatoxin B1 Metabolites (AFQ1, AFM1 and AFB-N7-Guanine) in Young Chinese Males. *Int. J. Cancer* **2005**, *115* (6), 879–884. <https://doi.org/10.1002/ijc.20951>.
- (168) Vidal, A.; Mengelers, M.; Yang, S.; De Saeger, S.; De Boevre, M. Mycotoxin Biomarkers of Exposure: A Comprehensive Review. *Compr. Rev. Food Sci. Food Saf.* **2018**, *17* (5), 1127–1155. <https://doi.org/10.1111/1541-4337.12367>.
- (169) Warth, B.; Del Favero, G.; Wiesenberger, G.; Puntischer, H.; Woelflingseder, L.; Fruhmann, P.; Sarkanj, B.; Krska, R.; Schuhmacher, R.; Adam, G.; Marko, D. Identification of a Novel Human Deoxynivalenol Metabolite Enhancing Proliferation of

- Intestinal and Urinary Bladder Cells. *Sci. Rep.* **2016**, *6* (January), 1–10.  
<https://doi.org/10.1038/srep33854>.
- (170) Itäaho, K.; Court, M. H.; Uutela, P.; Kostianen, R.; Radomska-Pandya, A.; Finel, M. Dopamine Is a Low-Affinity and High-Specificity Substrate for the Human UDP-Glucuronosyltransferase 1A10. *Drug Metab. Dispos.* **2009**, *37* (4), 768–775.  
<https://doi.org/10.1124/dmd.108.025692>.
- (171) Leung, A. W. Y.; Backstrom, I.; Bally, M. B. Sulfonation, an Underexploited Area: From Skeletal Development to Infectious Diseases and Cancer. *Oncotarget* **2016**, *7* (34), 55811–55827. <https://doi.org/10.18632/oncotarget.10046>.
- (172) Williams, R. T. Species Variations in the Pathways of Drug Metabolism. *Environ. Health Perspect.* **1978**, *22*, 133–138. <https://doi.org/10.2307/3428562>.
- (173) Slovak, J. .; Mealey, K.; Court, M. . Comparative Metabolism of Mycophenolic Acid by Glucuronic Acid and Glucose Conjugation in Human, Dog, and Cat Liver Microsomes. *J. Vet. Pharmacol. Ther.* **2017**, *40* (2), 123–129.  
<https://doi.org/10.1016/j.physbeh.2017.03.040>.
- (174) Yang, S.; Zhang, H.; Sun, F.; De Ruyck, K.; Zhang, J.; Jin, Y.; Li, Y.; Wang, Z.; Zhang, S.; De Saeger, S.; Zhou, J.; Li, Y.; De Boevre, M. Metabolic Profile of Zearalenone in Liver Microsomes from Different Species and Its in Vivo Metabolism in Rats and Chickens Using Ultra High-Pressure Liquid Chromatography-Quadrupole/Time-of-Flight Mass Spectrometry. *J. Agric. Food Chem.* **2017**, *65* (51), 11292–11303.  
<https://doi.org/10.1021/acs.jafc.7b04663>.
- (175) Warth, B.; Sulyok, M.; Berthiller, F.; Schuhmacher, R.; Krska, R. New Insights into the Human Metabolism of the Fusarium Mycotoxins Deoxynivalenol and Zearalenone. *Toxicol. Lett.* **2013**, *220* (1), 88–94. <https://doi.org/10.1016/j.toxlet.2013.04.012>.
- (176) Pfeiffer, E.; Kommer, A.; Dempe, J. S.; Hildebrand, A. A.; Metzler, M. Absorption and Metabolism of the Mycotoxin Zearalenone and the Growth Promotor Zeranol in Caco-2 Cells in Vitro. *Mol. Nutr. Food Res.* **2011**, *55* (4), 560–567.  
<https://doi.org/10.1002/mnfr.201000381>.
- (177) Pfeiffer, E.; Hildebrand, A.; Mikula, H.; Metzler, M. Glucuronidation of Zearalenone ,

- Zeranol and Four Metabolites in Vitro: Formation of Glucuronides by Various Microsomes and Human UDP-Glucuronosyltransferase Isoforms. *Mol. Nutr. Food Res.* **2010**, *54* (10), 1468–1476. <https://doi.org/10.1002/mnfr.200900524>.
- (178) Wu, B.; Basu, S.; Meng, S.; Wang, X.; Zhang, S.; Hu, M. Regioselective Sulfation and Glucuronidation of Phenolics: Insights into the Structural Basis of Conjugation. *Curr. Drug Metab.* **2008**, *12* (9), 900–916. <https://doi.org/10.1038/jid.2014.371>.
- (179) Binder, S. B.; Schwartz-Zimmermann, H. E.; Varga, E.; Bichl, G.; Michlmayr, H.; Adam, G.; Berthiller, F. Metabolism of Zearalenone and Its Major Modified Forms in Pigs. *Toxins (Basel)*. **2017**, *9* (2), 1–15. <https://doi.org/10.3390/toxins9020056>.
- (180) Martins, C.; Vidal, A.; De Boevre, M.; De Saeger, S.; Nunes, C.; Torres, D.; Goios, A.; Lopes, C.; Assunção, R.; Alvito, P. Exposure Assessment of Portuguese Population to Multiple Mycotoxins: The Human Biomonitoring Approach. *Int. J. Hyg. Environ. Health* **2019**, *222* (6), 913–925. <https://doi.org/10.1016/j.ijheh.2019.06.010>.
- (181) Mukherjee, D.; Royce, S. G.; Alexander, J. A. Physiologically-Based Toxicokinetic Modeling of Zearalenone and Its Metabolites: Application to the Jersey Girl Study. *PLoS One* **2014**, *9* (12), 1–30. <https://doi.org/10.1371/journal.pone.0113632>.
- (182) Mally, A.; Solfrizzo, M.; Degen, G. H. Biomonitoring of the Mycotoxin Zearalenone: Current State-of-the Art and Application to Human Exposure Assessment. *Arch. Toxicol.* **2016**, *90* (6), 1281–1292. <https://doi.org/10.1007/s00204-016-1704-0>.
- (183) Ivanova, L.; Fæste, C. K.; Uhlig, S. In Vitro Phase I Metabolism of the Depsipeptide Enniatin B. *Anal. Bioanal. Chem.* **2011**, *400* (9), 2889–2901. <https://doi.org/10.1007/s00216-011-4964-9>.
- (184) Fraeyman, S.; Devreese, M.; Antonissen, G.; De Baere, S.; Rychlik, M.; Croubels, S. Comparative Oral Bioavailability, Toxicokinetics, and Biotransformation of Enniatin B1 and Enniatin B in Broiler Chickens. *J. Agric. Food Chem.* **2016**, *64* (38), 7259–7264. <https://doi.org/10.1021/acs.jafc.6b02913>.
- (185) Muñoz, K.; Cramer, B.; Dopstadt, J.; Humpf, H. U.; Degen, G. H. Evidence of Ochratoxin A Conjugates in Urine Samples from Infants and Adults. *Mycotoxin Res.* **2017**, *33* (1), 39–47. <https://doi.org/10.1007/s12550-016-0261-y>.

- (186) Ali, N.; Blaszkewicz, M.; Degen, G. H. Occurrence of the Mycotoxin Citrinin and Its Metabolite Dihydrocitrinone in Urines of German Adults. *Arch. Toxicol.* **2015**, *89* (4), 573–578. <https://doi.org/10.1007/s00204-014-1363-y>.
- (187) Ali, N.; Blaszkewicz, M.; Alim, A.; Hossain, K.; Degen, G. H. Urinary Biomarkers of Ochratoxin A and Citrinin Exposure in Two Bangladeshi Cohorts: Follow-up Study on Regional and Seasonal Influences. *Arch. Toxicol.* **2016**, *90* (11), 2683–2697. <https://doi.org/10.1007/s00204-015-1654-y>.
- (188) Osselaere, A.; Devreese, M.; Goossens, J.; Vandebroucke, V.; De Baere, S.; De Backer, P.; Croubels, S. Toxicokinetic Study and Absolute Oral Bioavailability of Deoxynivalenol, T-2 Toxin and Zearalenone in Broiler Chickens. *Food Chem. Toxicol.* **2013**, *51* (1), 350–355. <https://doi.org/10.1016/j.fct.2012.10.006>.
- (189) Yang, S.; DE Boevre, M.; Li, Y.; De Saeger, S. The Toxicokinetics of HT-2 Toxin in Rats and Its Metabolic Profile in Livestock and Human Liver Microsomes. *J. Agric. Food Chem.* **2018**, *66* (30), 8160–8168. <https://doi.org/10.1021/acs.jafc.8b02893>.
- (190) Food and Drug Administration. *Draft Guidance for Industry Bioanalytical Method Validation*; 2013. <https://doi.org/http://www.labcompliance.de/documents/FDA/FDA-Others/Laboratory/f-507-bioanalytical-4252fnl.pdf>.
- (191) Capriotti, A. L.; Caruso, G.; Cavaliere, C.; Foglia, P.; Samperi, R.; Laganà, A. Multiclass Mycotoxin Analysis in Food, Environmental and Biological Matrices with Chromatography/Mass Spectrometry. *Mass Spectrom. Rev.* **2012**, *31* (4), 466–503.
- (192) Fromme, H.; Gareis, M.; Völkel, W.; Gottschalk, C. Overall Internal Exposure to Mycotoxins and Their Occurrence in Occupational and Residential Settings - An Overview. *Int. J. Hyg. Environ. Health* **2016**, *219* (2), 143–165. <https://doi.org/10.1016/j.ijheh.2015.11.004>.
- (193) Lombaert, G. A.; Pellaers, P.; Roscoe, V.; Mankotia, M.; Neil, R.; Scott, P. M. Mycotoxins in Infant Cereal Foods from the Canadian Retail Market. *Food Addit. Contam.* **2003**, *20* (5), 494–504. <https://doi.org/10.1080/0265203031000094645>.
- (194) Lombaert, G.; Pellaers, P.; Neumann, G.; Kitchen, D.; Huzel, V.; Trelka, R.; Kotello, S.; Scott, P. M. Ochratoxin A in Dried Vine Fruits on the Canadian Retail Market. *Food*



- Addit. Contam.* **2004**, *21* (6), 578–585. <https://doi.org/10.1080/02652030410001687681>.
- (195) Ng, L.; Mankotia, M.; Pantazopoulos, P.; Neil, R. J.; Scott, P. M. Ochratoxin A in Wine and Grape Juice Sold in Canada. *Food Addit. Contam.* **2004**, *21* (10), 971–981. <https://doi.org/10.1080/02652030400000653>.
- (196) Tran, S. T.; Smith, T. K.; Girgis, G. N. A Survey of Free and Conjugated Deoxynivalenol in the 2008 Corn Crop in Ontario, Canada. *J. Sci. Food Agric.* **2012**, *92* (1), 37–41. <https://doi.org/10.1002/jsfa.4674>.
- (197) Märtlbauer, E.; Usleber, E.; Dietrich, R.; Schneider, E. Ochratoxin A in Human Blood Serum - Retrospective Long-Term Data. *Mycotoxin Res.* **2009**, *25*, 175–186. <https://doi.org/10.1007/s12550-009-0025-z>.
- (198) Turner, N. W.; Subrahmanyam, S.; Piletsky, S. A. Analytical Methods for Determination of Mycotoxins: A Review. *Anal. Chim. Acta* **2009**, *632* (2), 168–180. <https://doi.org/https://doi.org/10.1016/j.aca.2008.11.010>.
- (199) Ali, N.; Muñoz, K.; Degen, G. H. Ochratoxin A and Its Metabolites in Urines of German Adults—An Assessment of Variables in Biomarker Analysis. *Toxicol. Lett.* **2017**, *275* (April), 19–26. <https://doi.org/https://doi.org/10.1016/j.toxlet.2017.04.013>.
- (200) Scroll, P. F.; Groopman, J. D. Long-Term Stability of Human Aflatoxin B1 Albumin Adducts Assessed by Isotope Dilution Mass Spectrometry and High-Performance Liquid Chromatography-Fluorescence. *Cancer Epidemiol Biomarkers Prev* **2008**, *17* (6), 1436–1439. <https://doi.org/10.1158/1055-9965.EPI-07-2926.Long>.
- (201) Shephard, G.; Thiel, P.; Sydenham, E. Initial Studies on the Toxicokinetics of Fumonisin B1 in Rats. *Food Chem. Toxicol.* **1992**, *30* (4), 277–279. [https://doi.org/https://doi.org/10.1016/0278-6915\(92\)90004-5](https://doi.org/https://doi.org/10.1016/0278-6915(92)90004-5).
- (202) Warth, B.; Sulyok, M.; Fruhmann, P.; Mikula, H.; Berthiller, F.; Schuhmacher, R.; Hametner, C.; Abia, W. A.; Adam, G.; Fröhlich, J.; Krska, R. Development and Validation of a Rapid Multi-Biomarker Liquid Chromatography/Tandem Mass Spectrometry Method to Assess Human Exposure to Mycotoxins. *Rapid Commun. Mass Spectrom.* **2012**, *26* (13), 1533–1540. <https://doi.org/10.1002/rcm.6255>.
- (203) Rubert, J.; León, N.; Sáez, C.; Martins, C. P. B.; Godula, M.; Yusà, V.; Mañes, J.;

- Soriano, J. M.; Soler, C. Evaluation of Mycotoxins and Their Metabolites in Human Breast Milk Using Liquid Chromatography Coupled to High Resolution Mass Spectrometry. *Anal. Chim. Acta* **2014**, *820*, 39–46.  
<https://doi.org/10.1016/j.aca.2014.02.009>.
- (204) Zhao, Z.; Liu, N.; Yang, L.; Deng, Y.; Wang, J.; Song, S.; Lin, S.; Wu, A.; Zhou, Z.; Hou, J. Multi-Mycotoxin Analysis of Animal Feed and Animal-Derived Food Using LC-MS/MS System with Timed and Highly Selective Reaction Monitoring. *Anal. Bioanal. Chem.* **2015**, *407* (24), 7359–7368. <https://doi.org/10.1007/s00216-015-8898-5>.
- (205) Tolosa, J.; Font, G.; Mañes, J.; Ferrer, E. Multimycotoxin Analysis in Water and Fish Plasma by Liquid Chromatography-Tandem Mass Spectrometry. *Chemosphere* **2016**, *145*, 402–408. <https://doi.org/10.1016/j.chemosphere.2015.11.085>.
- (206) Breidbach, A. The Impact of Superficially Porous Particles and New Stationary-Phase Chemistries on the LC-MS Determination of Mycotoxins in Food and Feed. *LC GC* **2016**, *34* (4), 10–14.
- (207) Baker, D.; Titman, C.; Loftus, N.; Horner, J. Multi-Residue Analysis of 18 Regulated Mycotoxins by LC-MS / MS ASMS 2017. In *ASMS 2017 TP-185*; 2017; pp 1–8.
- (208) Qi, D.; Fei, T.; Liu, H.; Yao, H.; Wu, D.; Liu, B. Development of Multiple Heart-Cutting Two-Dimensional Liquid Chromatography Coupled to Quadrupole-Orbitrap High Resolution Mass Spectrometry for Simultaneous Determination of Aflatoxin B1, B2, G1, G2, and Ochratoxin A in Snus, a Smokeless Tobacco Product. *J. Agric. Food Chem.* **2017**, *65* (45), 9923–9929. <https://doi.org/10.1021/acs.jafc.7b04329>.
- (209) Tamura, M.; Mochizuki, N.; Nagatomi, Y.; Harayama, K.; Toriba, A.; Hayakawa, K. A Method for Simultaneous Determination of 20 Fusarium Toxins in Cereals by High-Resolution Liquid Chromatography-Orbitrap Mass Spectrometry with a Pentafluorophenyl Column. *Toxins (Basel)*. **2015**, *7* (5), 1664–1682.  
<https://doi.org/10.3390/toxins7051664>.
- (210) De Santis, B.; Debegnach, F.; Gregori, E.; Russo, S.; Marchegiani, F.; Moracci, G.; Brera, C. Development of a LC-MS/MS Method for the Multi-Mycotoxin Determination in Composite Cereal-Based Samples. *Toxins (Basel)*. **2017**, *9* (5), 169.

- <https://doi.org/10.3390/toxins9050169>.
- (211) Soleimany, F.; Jinap, S.; Abas, F. Determination of Mycotoxins in Cereals by Liquid Chromatography Tandem Mass Spectrometry. *Food Chem.* **2012**, *130* (4), 1055–1060. <https://doi.org/10.1016/j.foodchem.2011.07.131>.
- (212) Wu, Z.; Gao, W.; Phelps, M. A.; Wu, D.; Miller, D. D.; Dalton, J. T. Favorable Effects of Weak Acids on Negative-Ion Electrospray Ionization Mass Spectrometry. *Changes* **2004**, *76* (3), 839–847. <https://doi.org/10.1016/j.biotechadv.2011.08.021>.Secreted.
- (213) Zhang, X.; Clausen, M. R.; Zhao, X.; Zheng, H.; Bertram, H. C. Enhancing the Power of Liquid Chromatography-Mass Spectrometry-Based Urine Metabolomics in Negative Ion Mode by Optimization of the Additive. *Anal. Chem.* **2012**, *84* (18), 7785–7792. <https://doi.org/10.1021/ac3013835>.
- (214) [Http://www.hmdb.ca/](http://www.hmdb.ca/). “HMDB: The Human Metabolome Database”, <http://www.hmdb.ca/> Data accessed 2017/08/02.
- (215) Wishart, D. S.; Tzur, D.; Knox, C.; Eisner, R.; Guo, A. C.; Young, N.; Cheng, D.; Jewell, K.; Arndt, D.; Sawhney, S.; Fung, C.; Nikolai, L.; Lewis, M.; Coutouly, M. A.; Forsythe, I.; Tang, P.; Shrivastava, S.; Jeroncic, K.; Stothard, P.; Amegbey, G.; Block, D.; Hau, D. D.; Wagner, J.; Miniaci, J.; Clements, M.; Gebremedhin, M.; Guo, N.; Zhang, Y.; Duggan, G. E.; MacInnis, G. D.; Weljie, A. M.; Dowlatabadi, R.; Bamforth, F.; Clive, D.; Greiner, R.; Li, L.; Marrie, T.; Sykes, B. D.; Vogel, H. J.; Querengesser, L. HMDB: The Human Metabolome Database. *Nucleic Acids Res.* **2007**, *35* (SUPPL. 1), 521–526. <https://doi.org/10.1093/nar/gkl923>.
- (216) Lim, E.; Pon, A.; Djoumbou, Y.; Knox, C.; Shrivastava, S.; Guo, A. C.; Neveu, V.; Wishart, D. S. T3DB: A Comprehensively Annotated Database of Common Toxins and Their Targets. *Nucleic Acids Res.* **2009**, *38* (SUPPL.1), 781–786. <https://doi.org/10.1093/nar/gkp934>.
- (217) “The Toxin and Toxin Target Database (T3DB)”, <http://www.t3db.ca/>, data accessed 2017/08/02.
- (218) Schenzel, J.; Schwarzenbach, R. P.; Bucheli, T. D. Multi-Residue Screening Method to Quantify Mycotoxins in Aqueous Environmental Samples. *J. Agric. Food Chem.* **2010**, *58*

- (21), 11207–11217. <https://doi.org/10.1021/jf102737q>.
- (219) Diana Di Mavungu, J.; Monbaliu, S.; Scippo, M.-L.; Maghuin-Rogister, G.; Schneider, Y.-J.; Larondelle, Y.; Callebaut, A.; Robbens, J.; Van Peteghem, C.; De Saeger, S. LC-MS/MS Multi-Analyte Method for Mycotoxin Determination in Food Supplements. *Food Addit. Contam. Part A. Chem. Anal. Control. Expo. Risk Assess.* **2009**, *26* (6), 885–895. <https://doi.org/10.1080/02652030902774649>.
- (220) Anil, E.; Alkis, I. M. Ochratoxin A and Brewing Technology: A Review. *J. Inst. Brew.* **2010**, *116* (1), 23–32. <https://doi.org/10.1002/j.2050-0416.2010.tb00394.x>.
- (221) Andrade, P. D.; Gomas da Silva, J. L.; Caldas, E. D. Simultaneous Analysis of Aflatoxins B1, B2, G1, G2, M1 and Ochratoxin A in Breast Milk by High-Performance Liquid Chromatography/Fluorescence after Liquid-Liquid Extraction with Low Temperature Purification (LLE-LTP). *J. Chromatogr. A* **2013**, *1304*, 61–68. <https://doi.org/10.1016/j.chroma.2013.06.049>.
- (222) Capriotti, A. L.; Cavaliere, C.; Piovesana, S.; Stampacchiacchiere, S.; Samperi, R.; Ventura, S.; Laganà, A. Simultaneous Determination of Naturally Occurring Estrogens and Mycoestrogens in Milk by Ultrahigh-Performance Liquid Chromatography-Tandem Mass Spectrometry Analysis. *J. Agric. Food Chem.* **2015**, *63* (40), 8940–8946. <https://doi.org/10.1021/acs.jafc.5b02815>.
- (223) Fabregat-Cabello, N.; Zomer, P.; Sancho, J. V.; Roig-Navarro, A. F.; Mol, H. G. . Comparison of Approaches to Deal with Matrix Effects in LC-MS/MS Based Determinations of Mycotoxins in Food and Feed. *World Mycotoxin J.* **2016**, *9* (2), 149–161. <https://doi.org/10.3920/WMJ2014.1872>.
- (224) Diaz, G. J.; Cepeda, S. M.; Martos., P. A. Stability of Aflatoxins in Solution. *J. AOAC Int.* **2012**, *95* (4), 1084–1088. <https://doi.org/10.5740/jaoacint.11-017>.
- (225) Santini, A.; Ferracane, R.; Meca, G.; Ritieni, A. Comparison and Improvement of the Existing Methods for the Determination of Aflatoxins in Human Serum by LC-MS/MS. *Anal. Methods* **2010**, *2* (7), 884. <https://doi.org/10.1039/b9ay00316a>.
- (226) Chen, Z.-Y.; Ying, S.; Liu, J.-H.; Zhan, P.-P.; Zhao, Y.-G. PRiME Pass-through Cleanup for the Fast Determination of Aflatoxins in Human Serum by Using LC-MS/MS. *Anal.*

- Methods* **2016**, 8 (7), 1457–1462. <https://doi.org/10.1039/C5AY03099D>.
- (227) Kolakowski, B.; O'Rourke, S. M.; Bietlot, H. P.; Kurz, K.; Aweryn, B. Ochratoxin A Concentrations in a Variety of Grain-Based and Non – Grain-Based Foods on the Canadian Retail Market from 2009 to 2014. *J. Food Prot.* **2016**, 79 (12), 2143–2159. <https://doi.org/10.4315/0362-028X.JFP-16-051>.
- (228) Hooker, D. C.; Schaafsma, A. W. Agronomic and Environmental Impacts on Concentrations of Deoxynivalenol and Fumonisin B1 in Corn across Ontario. *Can. J. Plant Pathol.* **2005**, 27 (April), 347–356. <https://doi.org/10.1080/07060660509507232>.
- (229) Serrano, A. B.; Font, G.; Ruiz, M. J.; Ferrer, E. Co-Occurrence and Risk Assessment of Mycotoxins in Food and Diet from Mediterranean Area. *Food Chem.* **2012**, 135 (2), 423–429. <https://doi.org/10.1016/j.foodchem.2012.03.064>.
- (230) Turner, P. C.; Burley, V. J.; Rothwell, J. A.; White, K. L. M.; Cade, J. E.; Wild, C. P. Deoxynivalenol: Rationale for Development and Application of a Urinary Biomarker. *Food Addit. Contam. - Part A Chem. Anal. Control. Expo. Risk Assess.* **2008**, 25 (7), 864–871. <https://doi.org/10.1080/02652030801895040>.
- (231) Maul, R.; Warth, B.; Kant, J. S.; Schebb, N. H.; Krska, R.; Koch, M.; Sulyok, M. Investigation of the Hepatic Glucuronidation Pattern of the Fusarium Mycotoxin Deoxynivalenol in Various Species. *Chem. Res. Toxicol.* **2012**, 25 (12), 2715–2717. <https://doi.org/10.1021/tx300348x>.
- (232) Warth, B.; Sulyok, M.; Fruhmann, P.; Berthiller, F.; Schuhmacher, R.; Hametner, C.; Adam, G.; Fröhlich, J.; Krska, R. Assessment of Human Deoxynivalenol Exposure Using an LC-MS/MS Based Biomarker Method. *Toxicol. Lett.* **2012**, 211 (1), 85–90. <https://doi.org/10.1016/j.toxlet.2012.02.023>.
- (233) Slobodchikova, I.; Vuckovic, D. Liquid Chromatography – High Resolution Mass Spectrometry Method for Monitoring of 17 Mycotoxins in Human Plasma for Exposure Studies. *J. Chromatogr. A* **2018**, 1548, 51–63. <https://doi.org/10.1016/j.chroma.2018.03.030>.
- (234) Stevenson, D. E.; Hansen, R. P.; Loader, J. I.; Jensen, D. J.; Cooney, J. M.; Wilkins, A. L.; Miles, C. O. Preparative Enzymatic Synthesis of Glucuronides of Zearalenone and Five of

- Its Metabolites. *J. Agric. Food Chem.* **2008**, *56* (11), 4032–4038.
- (235) Frizzell, C.; Uhlig, S.; Miles, C. O.; Verhaegen, S.; Elliott, C. T.; Eriksen, G. S.; Sørli, M.; Ropstad, E.; Connolly, L. Biotransformation of Zearalenone and Zearalenols to Their Major Glucuronide Metabolites Reduces Estrogenic Activity. *Toxicol. Vitro.* **2015**, *29* (3), 575–581. <https://doi.org/10.1016/j.tiv.2015.01.006>.
- (236) Yanni, S. .; Annaert, P. P.; Augustijns, P.; Bridges, A.; Gao, Y.; Daniel, K.; Thakker, D. R. Role of Flavin-Containing Monooxygenase in Oxidative Metabolism of Voriconazole by Human Liver Microsomes. *Drug Metab. Dispos.* **2009**, *36* (6), 1119–1125. <https://doi.org/10.1124/dmd.107.019646.Role>.
- (237) Grothusen, A.; Hardt, J.; Bräutigam, L.; Lang, D.; Böcker, R. A Convenient Method to Discriminate between Cytochrome P450 Enzymes and Flavin Containing Monooxygenases in Human Liver Microsomes. *Arch. Toxicol.* **1996**, *71* (1–2), 64–71. <https://doi.org/10.1007/s002040050359>.
- (238) Fujiwara, R.; Nakajima, M.; Yamamoto, T.; Nagao, H.; Yokoi, T. In Silico and in Vitro Approaches to Elucidate the Thermal Stability of Human UDP-Glucuronosyltransferase UGT 1A9. *Drug Metab. Pharmacokinet.* **2009**, *24* (3), 235–244. <https://doi.org/10.2133/dmpk.24.235>.
- (239) Yang, S.; Li, Y.; Cao, X.; Hu, D.; Wang, Z.; Wang, Y.; Shen, J.; Zhang, S. Metabolic Pathways of T-2 Toxin in in Vivo and in Vitro Systems of Wistar Rats. *J. Agric. Food Chem.* **2013**, *61* (40), 9734–9743. <https://doi.org/10.1021/jf4012054>.
- (240) Welsch, T.; Humpf, H. U. HT-2 Toxin 4-Glucuronide as New T-2 Toxin Metabolite: Enzymatic Synthesis, Analysis, and Species Specific Formation of T-2 and HT-2 Toxin Glucuronides by Rat, Mouse, Pig, and Human Liver Microsomes. *J. Agric. Food Chem.* **2012**, *60* (40), 10170–10178. <https://doi.org/10.1021/jf302571y>.
- (241) Ajandouz, E. H.; Berdah, S.; Moutardier, V.; Bege, T.; Birnbaum, D. J.; Perrier, J.; Pasquale, E. Di; Maresca, M. Hydrolytic Fate of 3/15-Acetyldeoxynivalenol in Humans: Specific Deacetylation by the Small Intestine and Liver Revealed Using in Vitro and Ex Vivo Approaches. *Toxins (Basel)*. **2016**, *8* (8), 232. <https://doi.org/10.3390/toxins8080232>.

- (242) Eriksen, G. S.; Pettersson, H. Lack of De-Epoxidation of Type B Trichothecenes in Incubates with Human Faeces. *Food Addit. Contam.* **2003**, *20* (6), 579–582. <https://doi.org/10.1080/0265203031000102573>.
- (243) Schwartz-Zimmermann, H. E.; Binder, S. B.; Hametner, C.; Miró-Abella, E.; Schwarz, C.; Michlmayr, H.; Reiterer, N.; Labudova, S.; Adam, G.; Berthiller, F. Metabolism of Nivalenol and Nivalenol-3-Glucoside in Rats. *Toxicol. Lett.* **2019**, *306* (15 May 2019), 43–52. <https://doi.org/10.1016/j.toxlet.2019.02.006>.
- (244) Gratz, S. W.; Duncan, G.; Richardson, A. J. The Human Fecal Microbiota Metabolizes Deoxynivalenol and Deoxynivalenol-3-Glucoside and May Be Responsible for Urinary. *Appl. Environ. Microbiol.* **2013**, *79* (6), 1821–1825. <https://doi.org/10.1128/AEM.02987-12>.
- (245) Brezina, U.; Rempe, I.; Kersten, S.; Valenta, H.; Humpf, H. U.; Dänicke, S. Diagnosis of Intoxications of Piglets Fed with Fusarium Toxin-Contaminated Maize by the Analysis of Mycotoxin Residues in Serum, Liquor and Urine with LC-MS/MS. *Arch. Anim. Nutr.* **2014**, *68* (6), 425–447. <https://doi.org/10.1080/1745039X.2014.973227>.
- (246) Guengerich, F. P.; Arneson, K. O.; Williams, K. M.; Deng, Z.; Harris, T. M. Reaction of Aflatoxin B1 Oxidation Products with Lysine. *Chem. Res. Toxicol.* **2002**, *15* (6), 780–792. <https://doi.org/10.1021/tx010156s>.
- (247) Johnson, W. W.; Guengerich, F. P. Reaction of Aflatoxin B1 Exo-8,9-Epoxy with DNA: Kinetic Analysis of Covalent Binding and DNA-Induced Hydrolysis. *Proc. Natl. Acad. Sci. U. S. A.* **1997**, *94* (12), 6121–6125. <https://doi.org/10.1073/pnas.94.12.6121>.
- (248) Everley, R. A.; Ciner, F. L.; Zhang, D.; Scholl, P. F.; Groopman, J. D.; Croley, T. R. Measurement of Aflatoxin and Aflatoxin Metabolites in Urine by Liquid Chromatography-Tandem Mass Spectrometry. *J. Anal. Toxicol.* **2007**, *31* (3), 150–156. <https://doi.org/10.1093/jat/31.3.150>.
- (249) Walton, M.; Egnér, P.; Scholl, P. F.; Walker, J.; Kensler, T. W.; Groopman, J. D. Liquid Chromatography Electrospray-Mass Spectrometry of Urinary Aflatoxin Biomarkers: Characterization and Application to Dosimetry and Chemoprevention in Rats. *Chem. Res. Toxicol.* **2001**, *14* (7), 919–926. <https://doi.org/10.1021/tx010063a>.

- (250) Fan, S.; Li, Q.; Sun, L.; Du, Y.; Xia, J.; Zhang, Y. Simultaneous Determination of Aflatoxin B 1 and M 1 in Milk, Fresh Milk and Milk Powder by LC-MS/MS Utilising Online Turbulent Flow Chromatography. *Food Addit. Contam. Part A* **2015**, *32* (7), 1175–1184. <https://doi.org/10.1080/19440049.2015.1048311>.
- (251) Leppänen, J. M.; Partanen, H. A.; Vähäkangas, K. H.; Woodhouse, H. J.; Myllynen, P. K.; El-Nezami, H. S. Aflatoxin B1 Transfer and Metabolism in Human Placenta. *Toxicol. Sci.* **2009**, *113* (1), 216–225. <https://doi.org/10.1093/toxsci/kfp257>.
- (252) Dohnal, V.; Wu, Q.; Kuc, K. Metabolism of Aflatoxins : Key Enzymes and Interindividual as Well as Interspecies Differences. *Arch. Toxicol.* **2014**, *88* (9), 1635–1644. <https://doi.org/10.1007/s00204-014-1312-9>.
- (253) Gallagher, E. P.; Wienkers, L. C.; Stapleton, P. L.; Kunze, K. L.; Eaton, D. L. Role of Human Microsomal and Human Complementary DNA-Expressed Cytochromes P4501A2 and P4503A4 in the Bioactivation of Aflatoxin B11. *Cancer Res.* **1994**, *54* (1), 101–108.
- (254) Wild, C. P.; Turner, P. C. The Toxicology of Aflatoxins as a Basis for Public Health Decisions. *Mutagenesis* **2002**, *17* (6), 471–481. <https://doi.org/10.1093/mutage/17.6.471>.
- (255) Bbosa, G. S.; Kitya, D.; Lubega, A.; Ogwal-Okeng, J.; Anokbonggo, William W. Kyegombe, D. B. Review of the Biological and Health Effects of Aflatoxins on Body Organs and Body Systems. *Aflatoxins - Recent Adv. Futur. Prospect.* **2013**, *12*, 239–265. <https://doi.org/10.5772/51201>.
- (256) Hatem, N. L.; Hassab, H. M. A.; Abd Al-Rahman, E. M.; El-Deeb, S. A.; El-Sayed Ahmed, R. L. Prevalence of Afl Atoxins in Blood and Urine of Egyptian Infants with Protein – Energy Malnutrition. *Food Nutr. Bull.* **2005**, *26* (1), 49–56.
- (257) Leong, Y. H.; Latiff, A. A.; Ahmad, N. I.; Rosma, A. Exposure Measurement of Aflatoxins and Aflatoxin Metabolites in Human Body Fluids. A Short Review. *Mycotoxin Res.* **2012**, *28* (2), 79–87. <https://doi.org/10.1007/s12550-012-0129-8>.
- (258) Roebuck, B. D.; Siegel, W. G.; Wogan, G. N. In Vitro Metabolism of Aflatoxin B2 by Animal and Human Liver. *Cancer Res.* **1978**, *38* (April), 999–1002.
- (259) Li, D.; Huang, X.; Han, K.; Zhan, C. G. Catalytic Mechanism of Cytochrome P450 for 5'-Hydroxylation of Nicotine: Fundamental Reaction Pathways and Stereoselectivity. *J. Am.*



- Chem. Soc.* **2011**, *133* (19), 7416–7427. <https://doi.org/10.1021/ja111657j>.
- (260) Bravin, F.; Duca, R. C.; Balaguer, P.; Delaforge, M. In Vitro Cytochrome P450 Formation of a Mono-Hydroxylated Metabolite of Zearalenone Exhibiting Estrogenic Activities: Possible Occurrence of This Metabolite in Vivo. *Int. J. Mol. Sci.* **2009**, *10* (4), 1824–1837. <https://doi.org/10.3390/ijms10041824>.
- (261) Hildebrand, A.; Pfeiffer, E.; Metzler, M. Aromatic Hydroxylation and Catechol Formation: A Novel Metabolic Pathway of the Growth Promotor Zeranone. *Toxicol. Lett.* **2010**, *192* (3), 379–386. <https://doi.org/10.1016/j.toxlet.2009.11.014>.
- (262) Ueberschär, K.; Brezina, U.; Dänicke, S. Zearalenone (ZEN) and ZEN Metabolites in Feed, Urine and Bile of Sows: Analysis, Determination of the Metabolic Profile and Evaluation of the Binding Forms. *Landbauforsch. Volkenrode* **2016**, *2016* (66), 21–28. <https://doi.org/10.3220/LBF1462863902000>.
- (263) Yang, S.; Zhang, H.; Zhang, J.; Li, Y.; Jin, Y.; Zhang, S.; De Saeger, S.; Li, Y.; Sun, F.; De Boevre, M. Deglucosylation of Zearalenone-14-Glucoside in Animals and Human Liver Leads to Underestimation of Exposure to Zearalenone in Humans. *Arch. Toxicol.* **2018**, *92* (9), 2779–2791. <https://doi.org/10.1007/s00204-018-2267-z>.
- (264) Kluger, B.; Bueschl, C.; Neumann, N.; Stückler, R.; Doppler, M.; Chassy, A. W.; Waterhouse, A. L.; Rechthaler, J.; Kamleitner, N.; Thallinger, G. G.; Adam, G.; Krska, R.; Schuhmacher, R. Untargeted Profiling of Tracer-Derived Metabolites Using Stable Isotopic Labeling and Fast Polarity-Switching LC-ESI-HRMS. *Anal. Chem.* **2014**, *86* (23), 11533–11537. <https://doi.org/10.1021/ac503290j>.
- (265) Zain, M. E. Impact of Mycotoxins on Humans and Animals. *J. Saudi Chem. Soc.* **2011**, *15* (2), 129–144. <https://doi.org/10.1016/j.jscs.2010.06.006>.
- (266) Reddy, L.; Bhoola, K. Ochratoxins-Food Contaminants: Impact on Human Health. *Toxins (Basel)*. **2010**, *2*, 771–779. <https://doi.org/10.3390/toxins2040771>.
- (267) Wild, C. P.; Gong, Y. Y. Mycotoxins and Human Disease: A Largely Ignored Global Health Issue. *Carcinogenesis* **2009**, *31* (1), 71–82. <https://doi.org/10.1093/carcin/bgp264>.
- (268) Bezerra da Rocha, M.; Francisco Da Chagas, O.; Feitosa Maia, Fábio Florindo Guedes, M.; Rondina, D. Mycotoxins and Their Effects on Human and Animal Health. *Food*

- Control* **2014**, *36* (1), 159–165. <https://doi.org/10.1016/j.foodcont.2013.08.021>.
- (269) Vejdovszky, K.; Hahn, K.; Braun, D.; Warth, B.; Marko, D. Synergistic Estrogenic Effects of Fusarium and Alternaria Mycotoxins in Vitro. *Arch. Toxicol.* **2017**, *91* (3), 1447–1460. <https://doi.org/10.1007/s00204-016-1795-7>.
- (270) Schulz, M.; Schumann, L.; Rottkord, U.; Humpf, H.; Gekle, M.; Schwerdt, G. Synergistic Action of the Nephrotoxic Mycotoxins Ochratoxin A and Citrinin at Nanomolar Concentrations in Human Proximal Tubule-Derived Cells. *Toxicol. Lett.* **2018**, *291*, 149–157. <https://doi.org/10.1016/j.toxlet.2018.04.014>.
- (271) Li, Y.; Zhang, B.; He, X.; Cheng, W.-H.; Xu, W.; Luo, Y.; Liang, R.; Luo, H.; Huang, K. Analysis of Individual and Combined Effects of Ochratoxin A and Zearalenone on HepG2 and KK-1 Cells with Mathematical Models. *Toxins (Basel)*. **2014**, *6*, 1177–1192. <https://doi.org/10.3390/toxins6041177>.
- (272) Meyer, V.; Andersen, M. R.; Brakhage, A. A.; Braus, G. H.; Caddick, M. X.; Cairns, T. C.; de Vries, R. P.; Haarmann, T.; Hansen, K.; Hertz-Fowler, C.; Krappmann, S.; Mortensen, U. H.; Peñalva, M. A.; Ram, A. F. J.; Head, R. M. Current Challenges of Research on Filamentous Fungi in Relation to Human Welfare and a Sustainable Bio-Economy: A White Paper. *Fungal Biol. Biotechnol.* **2016**, *3* (1), 1–17. <https://doi.org/10.1186/s40694-016-0024-8>.
- (273) de Lourdes Mendes de Souza, M.; Sulyok, M.; Freitas-Silva, O.; Costa, S. S.; Brabet, C.; Machinski Junior, M.; Sekiyama, B. L.; Vargas, E. A.; Krska, R.; Schuhmacher, R. Cooccurrence of Mycotoxins in Maize and Poultry Feeds from Brazil by Liquid Chromatography/Tandem Mass Spectrometry. *Sci. World J. J.* **2013**, *2013*, 427369. <https://doi.org/10.1155/2013/427369>.
- (274) Prella, A.; Spadaro, D.; Denca, A.; Garibaldi, A.; Gullino, M. L. Comparison of Clean-up Methods for Ochratoxin a on Wine, Beer, Roasted Coffee and Chili Commercialized in Italy. *Toxins (Basel)*. **2013**, *5* (10), 1827–1844. <https://doi.org/10.3390/toxins5101827>.
- (275) Omotayo, O. P.; Omotayo, A. O.; Mwanza, M.; Babalola, O. O. Prevalence of Mycotoxins and Their Consequences on Human Health. *Toxicol. Res.* **2019**, *35* (1), 1–7. <https://doi.org/10.5487/TR.2019.35.1.001>.

- (276) Shephard, G. S.; Burger, H. M.; Gambacorta, L.; Gong, Y. Y.; Krska, R.; Rheeder, J. P.; Solfrizzo, M.; Srey, C.; Sulyok, M.; Visconti, A.; Warth, B.; van der Westhuizen, L. Multiple Mycotoxin Exposure Determined by Urinary Biomarkers in Rural Subsistence Farmers in the Former Transkei, South Africa. *Food Chem. Toxicol.* **2013**, *62*, 217–225. <https://doi.org/10.1016/j.fct.2013.08.040>.
- (277) Ali, N.; Degen, G. H. Urinary Biomarkers of Exposure to the Mycoestrogen Zearalenone and Its Modified Forms in German Adults. *Arch. Toxicol.* **2018**, *92* (8), 2691–2700. <https://doi.org/10.1007/s00204-018-2261-5>.
- (278) Šarkanj, B.; Ezekiel, C. N.; Turner, P. C.; Abia, W. A.; Rychlik, M.; Krska, R.; Sulyok, M.; Warth, B. Ultra-Sensitive, Stable Isotope Assisted Quantification of Multiple Urinary Mycotoxin Exposure Biomarkers. *Anal. Chim. Acta* **2018**, *1019*, 84–92. <https://doi.org/10.1016/j.aca.2018.02.036>.
- (279) Lauwers, M.; De Baere, S.; Letor, B.; Rychlik, M.; Croubels, S.; Devreese, M. Multi LC-MS/MS and LC-HRMS Methods for Determination of 24 Mycotoxins Including Major Phase I and II Biomarker Metabolites in Biological Matrices from Pigs and Broiler Chickens. *Toxins (Basel)*. **2019**, *11* (3), 171. <https://doi.org/10.3390/toxins11030171>.
- (280) Viegas, S. Enniatin B and Ochratoxin A in the Blood Serum of Workers from the Waste Management Setting. *Mycotoxin Res.* **2018**, *34* (2), 85–90.
- (281) Matuszewski, B. K.; Constanzer, M. L.; Chavez-Eng, C. M. Strategies for the Assessment of Matrix Effect in Quantitative Bioanalytical Methods Based on HPLC-MS/MS. *Anal. Chem.* **2003**, *75* (13), 3019–3030. <https://doi.org/10.1021/ac020361s>.
- (282) Varga, E.; Glauner, T.; K?ppen, R.; Mayer, K.; Sulyok, M.; Schuhmacher, R.; Krska, R.; Berthiller, F. Stable Isotope Dilution Assay for the Accurate Determination of Mycotoxins in Maize by UHPLC-MS/MS. *Anal. Bioanal. Chem.* **2012**, *402* (9), 2675–2686. <https://doi.org/10.1007/s00216-012-5757-5>.
- (283) Paoloni, A.; Solfrizzo, M.; Bibi, R.; Pecorelli, I. Development and Validation of LC-MS/MS Method for the Determination of Ochratoxin A and Its Metabolite Ochratoxin  $\alpha$  in Poultry Tissues and Eggs. *J. Environ. Sci. Heal. - Part B Pestic. Food Contam. Agric. Wastes* **2018**, *53* (5), 327–333. <https://doi.org/10.1080/03601234.2018.1431455>.

- (284) Nathanail, A. V.; Varga, E.; Meng-reiterer, J.; Bueschl, C.; Michlmayr, H.; Malachova, A.; Fruhmann, P.; Jestoi, M.; Peltonen, K.; Adam, G.; Lemmens, M.; Schuhmacher, R.; Berthiller, F. Metabolism of the Fusarium Mycotoxins T - 2 Toxin and HT - 2 Toxin in Wheat. *J. Agric. Food Chem.* **2015**, *63* (35), 7862–7872.  
<https://doi.org/10.1021/acs.jafc.5b02697>.
- (285) Li, C.; Wu, Y. L.; Yang, T.; Huang-Fu, W. G. Rapid Determination of Fumonisin B1 and B2 in Corn by Liquid Chromatography-Tandem Mass Spectrometry with Ultrasonic Extraction. *J. Chromatogr. Sci.* **2012**, *50* (1), 57–63.  
<https://doi.org/10.1093/chromsci/bmr009>.
- (286) Jensen, T.; De Boevre, M.; Preußke, N.; De Saeger, S.; Birr, T.; Verreet, J. A.; Sönnichsen, F. D. Evaluation of High-Resolution Mass Spectrometry for the Quantitative Analysis of Mycotoxins in Complex Feed Matrices. *Toxins (Basel)*. **2019**, *11* (9), 531.  
<https://doi.org/10.3390/toxins11090531>.
- (287) Polson, C.; Sarkar, P.; Incledon, B.; Raguvaran, V.; Grant, R. Optimization of Protein Precipitation Based upon Effectiveness of Protein Removal and Ionization Effect in Liquid Chromatography-Tandem Mass Spectrometry. *J. Chromatogr. B Anal. Technol. Biomed. Life Sci.* **2003**, *785* (2), 263–275. [https://doi.org/10.1016/S1570-0232\(02\)00914-5](https://doi.org/10.1016/S1570-0232(02)00914-5).
- (288) Sarafian, M. H.; Gaudin, M.; Lewis, M. R.; Martin, F. P.; Holmes, E.; Nicholson, J. K.; Dumas, M. E. Objective Set of Criteria for Optimization of Sample Preparation Procedures for Ultra-High Throughput Untargeted Blood Plasma Lipid Profiling by Ultra Performance Liquid Chromatography-Mass Spectrometry. *Anal. Chem.* **2014**, *86*, 5766–5774. <https://doi.org/10.1021/ac500317c>.
- (289) Sun, D.; Li, C.; Zhou, S.; Zhao, Y.; Gong, Y.; Gong, Z.; Wu, Y. Determination of Trace Zearalenone and Its Metabolites in Human Serum by a High-Throughput UPLC-MS/MS Analysis. *Appl. Sci.* **2019**, *9* (4), 741. <https://doi.org/10.3390/app9040741>.
- (290) Feith, A.; Teleki, A.; Graf, M.; Favilli, L.; Takors, R. Hilic-Enabled<sup>13</sup>C Metabolomics Strategies: Comparing Quantitative Precision and Spectral Accuracy of Qtof High- and Qqq Low-Resolution Mass Spectrometry. *Metabolites* **2019**, *9* (4), 63.

<https://doi.org/10.3390/metabo9040063>.

- (291) De Baere, S.; Croubels, S.; Novak, B.; Bichl, G.; Antonissen, G. Development and Validation of a UPLC-MS/MS and UPLC-HR-MS Method for the Determination of Fumonisin B1 and Its Hydrolysed Metabolites and Fumonisin B2 in Broiler Chicken Plasma. *Toxins (Basel)*. **2018**, *10* (2), 4–7. <https://doi.org/10.3390/toxins10020062>.
- (292) Hmaissia Khelifa, K.; Ghali, R.; Mazigh, C.; Aouni, Z.; Machgoul, S.; Hedhili, A. Ochratoxin A Levels in Human Serum and Foods from Nephropathy Patients in Tunisia: Where Are You Now? *Exp. Toxicol. Pathol.* **2012**, *64* (5), 509–512. <https://doi.org/10.1016/j.etp.2010.11.006>.
- (293) Muñoz, K.; Vega, M.; Rios, G.; Muñoz, S.; Madariaga, R. Preliminary Study of Ochratoxin A in Human Plasma in Agricultural Zones of Chile and Its Relation to Food Consumption. *Food Chem. Toxicol.* **2006**, *44* (11), 1884–1889. <https://doi.org/10.1016/j.fct.2006.06.008>.
- (294) Monnin, C.; Ramrup, P.; Daigle-Young, C.; Vuckovic, D. Improving Negative Liquid Chromatography/Electrospray Ionization Mass Spectrometry Lipidomic Analysis of Human Plasma Using Acetic Acid as a Mobile-Phase Additive. *Rapid Commun. Mass Spectrom.* **2018**, *32* (3), 201–211. <https://doi.org/10.1002/rcm.8024>.
- (295) Verheecke-Vaessen, C.; Diez-Gutierrez, L.; Renaud, J.; Sumarah, M.; Medina, A.; Magan, N. Interacting Climate Change Environmental Factors Effects on *Fusarium Langsethiae* Growth, Expression of Tri Genes and T-2/HT-2 Mycotoxin Production on Oat-Based Media and in Stored Oats. *Fungal Biol.* **2019**, *123* (8), 618–624. <https://doi.org/10.1016/j.funbio.2019.04.008>.
- (296) Moretti, A.; Pascale, M.; Logrieco, A. F. Mycotoxin Risks under a Climate Change Scenario in Europe. *Trends Food Sci. Technol.* **2019**, *84*, 38–40. <https://doi.org/10.1016/j.tifs.2018.03.008>.
- (297) Paterson, R. R. M.; Lima, N. Further Mycotoxin Effects from Climate Change. *Food Res. Int.* **2011**, *44* (9), 2555–2566. <https://doi.org/10.1016/j.foodres.2011.05.038>.

## **Appendix A**

Supplementary Information for Chapter 2

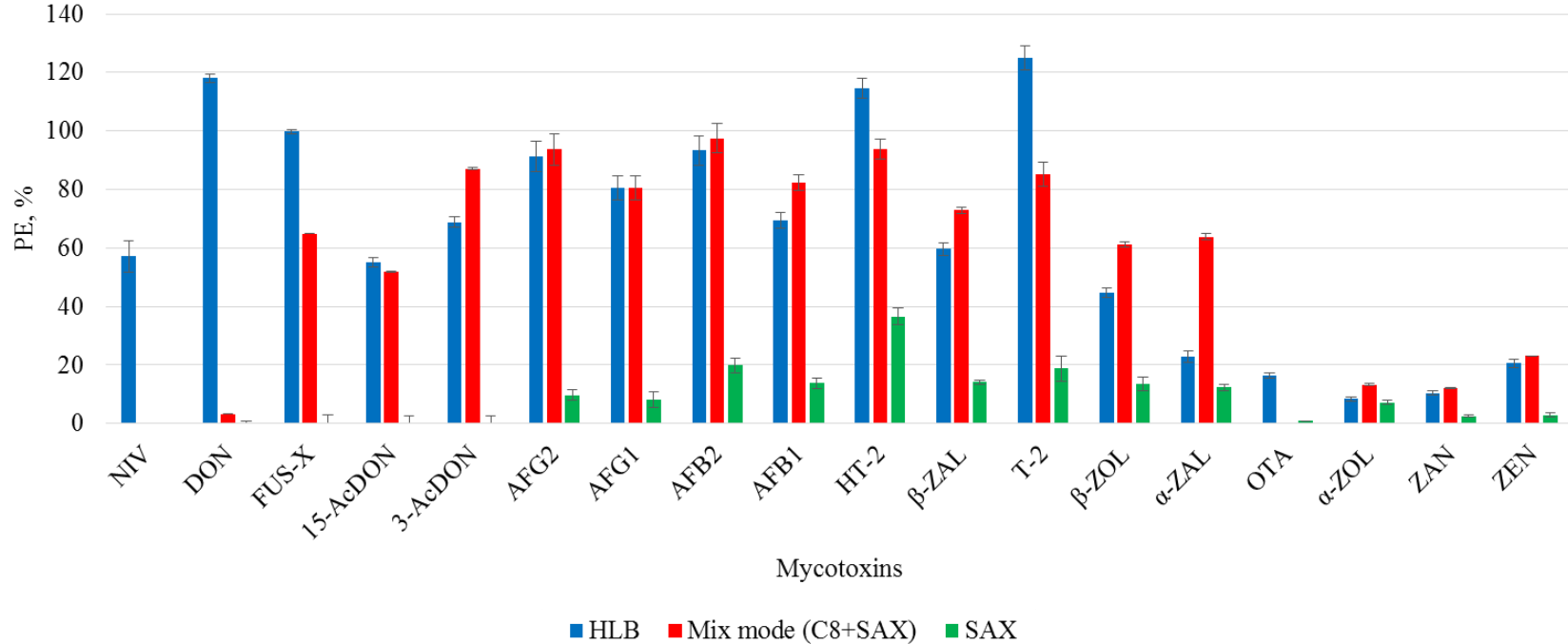
Supplementary Table A1. Monoisotopic masses of the most intense ions and retention times of all mycotoxins and internal standards.

<b>Mycotoxin in ESI(+)</b>	<b>The most intense ion</b>	<b>Theoretical monoisotopic m/z</b>	<b>RT, min</b>
15-AcDON	[M+Na] <sup>+</sup>	361.1258	5.46
AFG2	[M+H] <sup>+</sup>	331.0812	6.71
AFG1	[M+H] <sup>+</sup>	329.0656	7.14
AFB2	[M+H] <sup>+</sup>	315.0863	7.52
AFB1	[M+H] <sup>+</sup>	313.0707	8.07
HT-2	[M+NH <sub>4</sub> ] <sup>+</sup>	442.2435	8.15
T-2	[M+Na] <sup>+</sup>	489.2095	12.19
3-AcDONd <sub>3</sub>	[M+Na] <sup>+</sup>	364.1446	5.61
OTA	[M+H] <sup>+</sup>	404.0896	13.06
FB1	[M+H] <sup>+</sup>	722.3958	15.37
FB2	[M+H] <sup>+</sup>	706.4009	19.60
FB3	[M+H] <sup>+</sup>	706.4009	18.23
OTAd <sub>5</sub>	[M+H] <sup>+</sup>	409.1215	13.06
<b>Mycotoxin in ESI(-)</b>	<b>The most intense ion</b>	<b>Theoretical monoisotopic m/z</b>	<b>RT, min</b>
NIV	[M+CH <sub>3</sub> COO-H] <sup>-</sup>	371.1348	1.90
DON	[M+CH <sub>3</sub> COO-H] <sup>-</sup>	355.1399	3.95
FUS-X	[M+CH <sub>3</sub> COO-H] <sup>-</sup>	413.1454	4.93
3-AcDON	[M+CH <sub>3</sub> COO-H] <sup>-</sup>	397.1505	5.61
β-ZAL	[M-H] <sup>-</sup>	321.1707	12.01
β-ZOL	[M-H] <sup>-</sup>	319.1551	12.57
α-ZAL	[M-H] <sup>-</sup>	321.1707	13.09
α-ZOL	[M-H] <sup>-</sup>	319.1551	13.50
ZEN	[M-H] <sup>-</sup>	317.1394	13.81
ZAN	[M-H] <sup>-</sup>	319.1551	13.88
3-AcDONd <sub>3</sub>	[M+CH <sub>3</sub> COO-H] <sup>-</sup>	400.1692	5.62
<sup>13</sup> C-ZEN	[M-H] <sup>-</sup>	335.1993	13.80

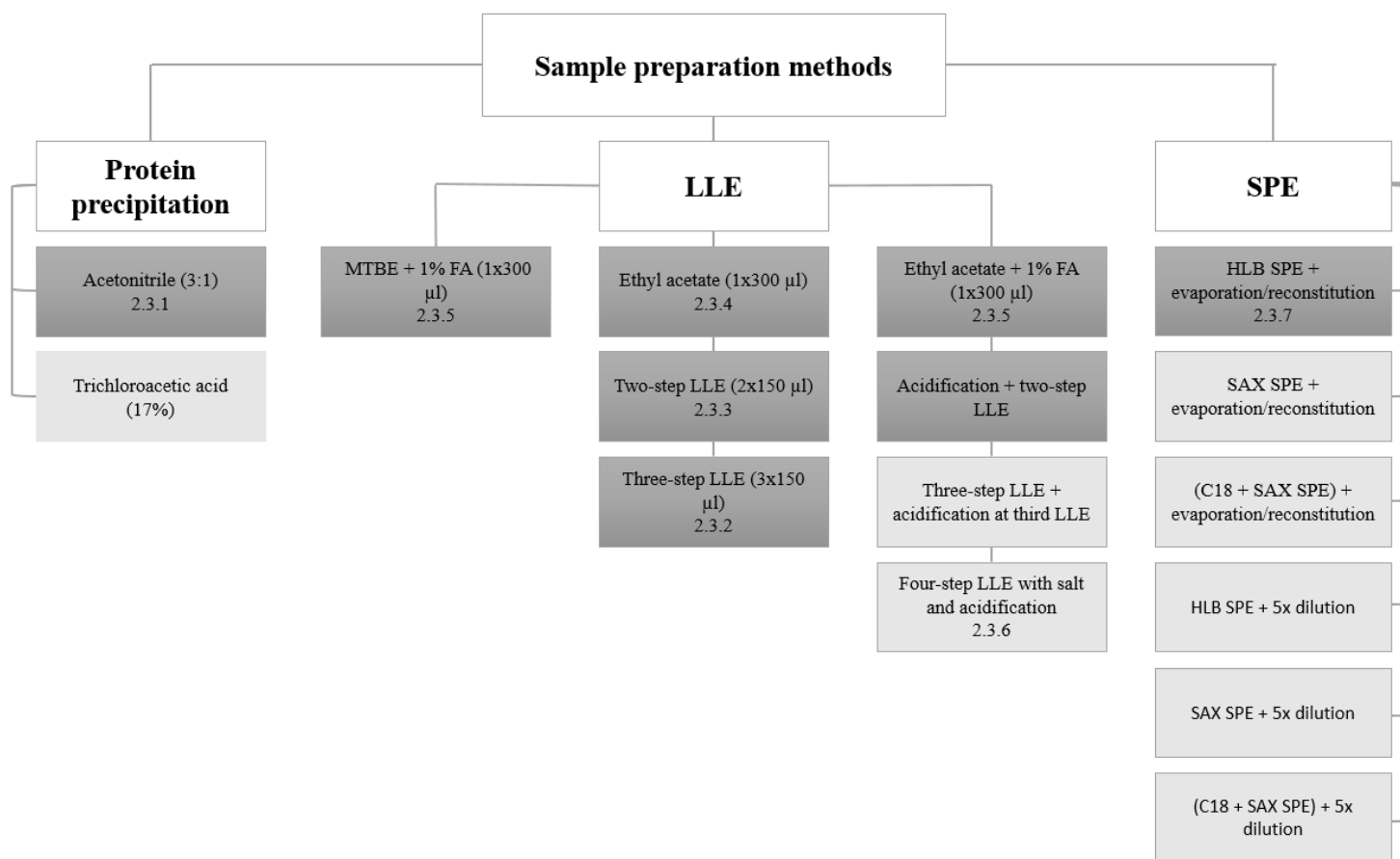
Supplementary Table A2. Inter-day accuracy and precision for mycotoxins detected in ESI(+) and ESI(-). Determination was performed using 0.2, 0.3, 0.5, 1, 3 and 10 ng/ml (n=6 days), except for NIV. all NIV concentration levels were 3x the stated concentrations. Only results above LLOQ are shown. Standard curve in plasma in the range of LLOQ to 10 ng/ml, except for NIV (LLOQ to 30 ng/ml), was prepared to analyze validation samples. \*Analyte does not meet FDA requirements.

ESI(+) and ESI(-), Inter-day accuracy and precision												
Mycotoxins	0.2 ng/ml		0.3 ng/ml		0.5 ng/ml		1 ng/ml		3 ng/ml		10 ng/ml	
	Accuracy (%)	RSD %	Accuracy (%)	RSD %	Accuracy (%)	RSD %	Accuracy (%)	RSD %	Accuracy (%)	RSD %	Accuracy (%)	RSD %
15-AcDON	N/A	N/A	96.8	11.1	97.2	5.3	99.2	6.8	108.0	9.7	101.6	2.8
AFG2	N/A	N/A	92.7	10.1	96.4	7.4	98.2	11.3	109.8	8.4	102.1	5.1
AFG1	N/A	N/A	96.3	14.5	97.9	9.1	99.0	13.9	111.5	8.4	104.1	5.5
AFB1	85.5	11.6	92.6	11.3	91.1	6.6	94.3	11.2	103.6	10.6	97.8	8.1
AFB2	N/A	N/A	86.5	6.6	86.1	7.9	88.8	7.5	100.5	10.2	97.4	4.6
HT-2	N/A	N/A	88.5	15.6*	87.5	5.2	92.7	9.0	98.8	6.9	94.9	4.6
T-2	N/A	N/A	90.7	8.6	91.9	5.3	90.2	9.7	102.4	7.2	100.9	5.8
$\beta$ -ZAL	95.0	12.2	91.4	10.9	89.0	5.1	88.9	6.7	95.3	9.1	96.6	4.4
FUS-X	N/A	N/A	94.2	11.2	96.7	5.2	93.6	5.9	98.1	7.5	98.8	5.9
3-AcDON	N/A	N/A	93.2	13.3	98.9	8.3	96.8	9.1	99.8	12.4	97.5	5.5
$\beta$ -ZOL	N/A	N/A	90.4	14.0	86.1	4.1	90.8	6.3	93.0	8.7	97.5	2.7
$\alpha$ -ZAL	N/A	N/A	90.3	13.3	90.3	6.9	92.2	8.0	94.3	6.3	97.1	5.2
DON	N/A	N/A	N/A	N/A	99.4	8.0	96.0	11.6	97.0	10.2	96.4	6.9
$\alpha$ -ZOL	N/A	N/A	N/A	N/A	N/A	N/A	93.4	18.9*	91.3	10.1	98.5	3.6
ZEN	N/A	N/A	N/A	N/A	N/A	N/A	88.9	12.0	87.5	8.3	99.3	7.7
ZAN	N/A	N/A	N/A	N/A	N/A	N/A	84.7	12.7	94.4	9.9	101.0	8.1
NIV	N/A	N/A	N/A	N/A	N/A	N/A	N/A	N/A	101.1	8.3	100.0	10.1

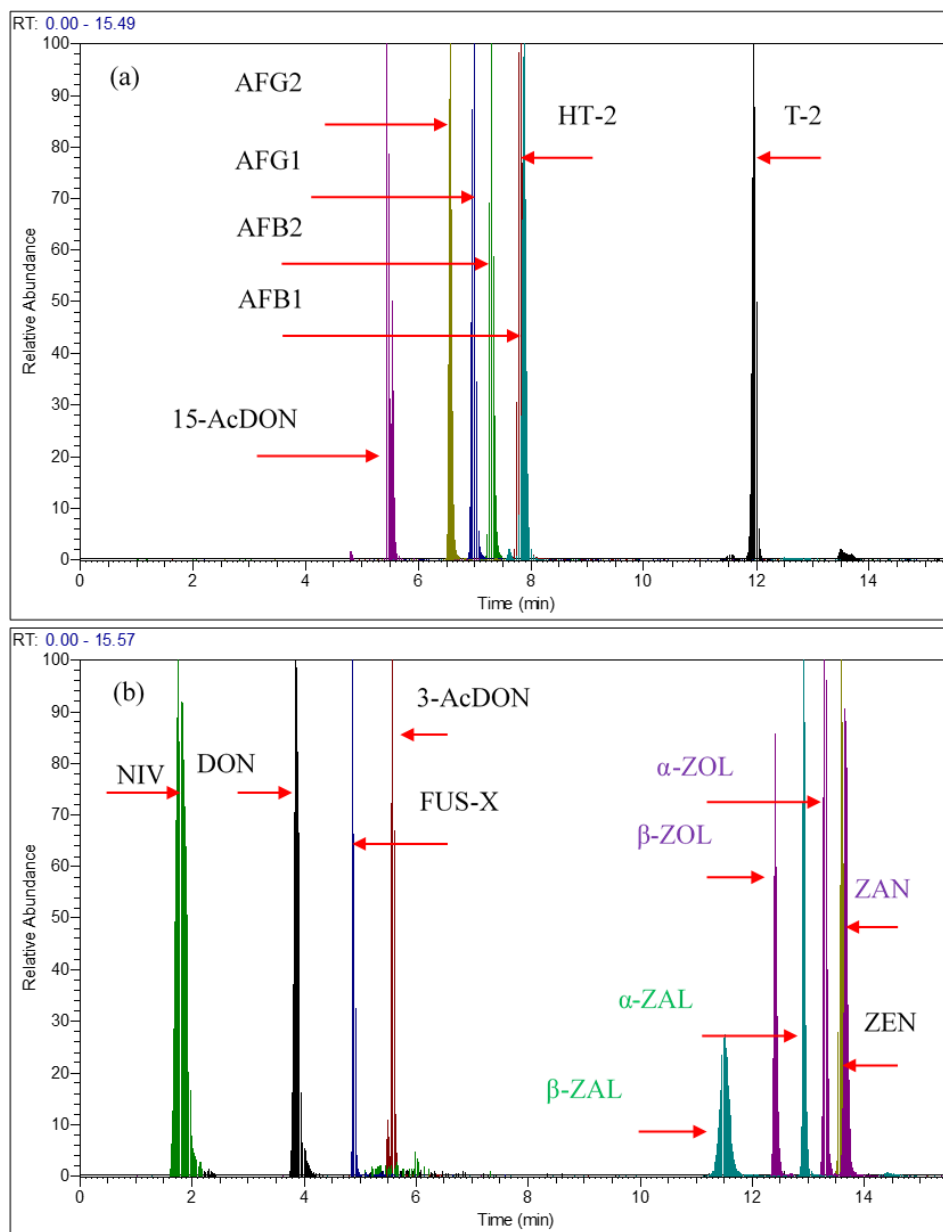




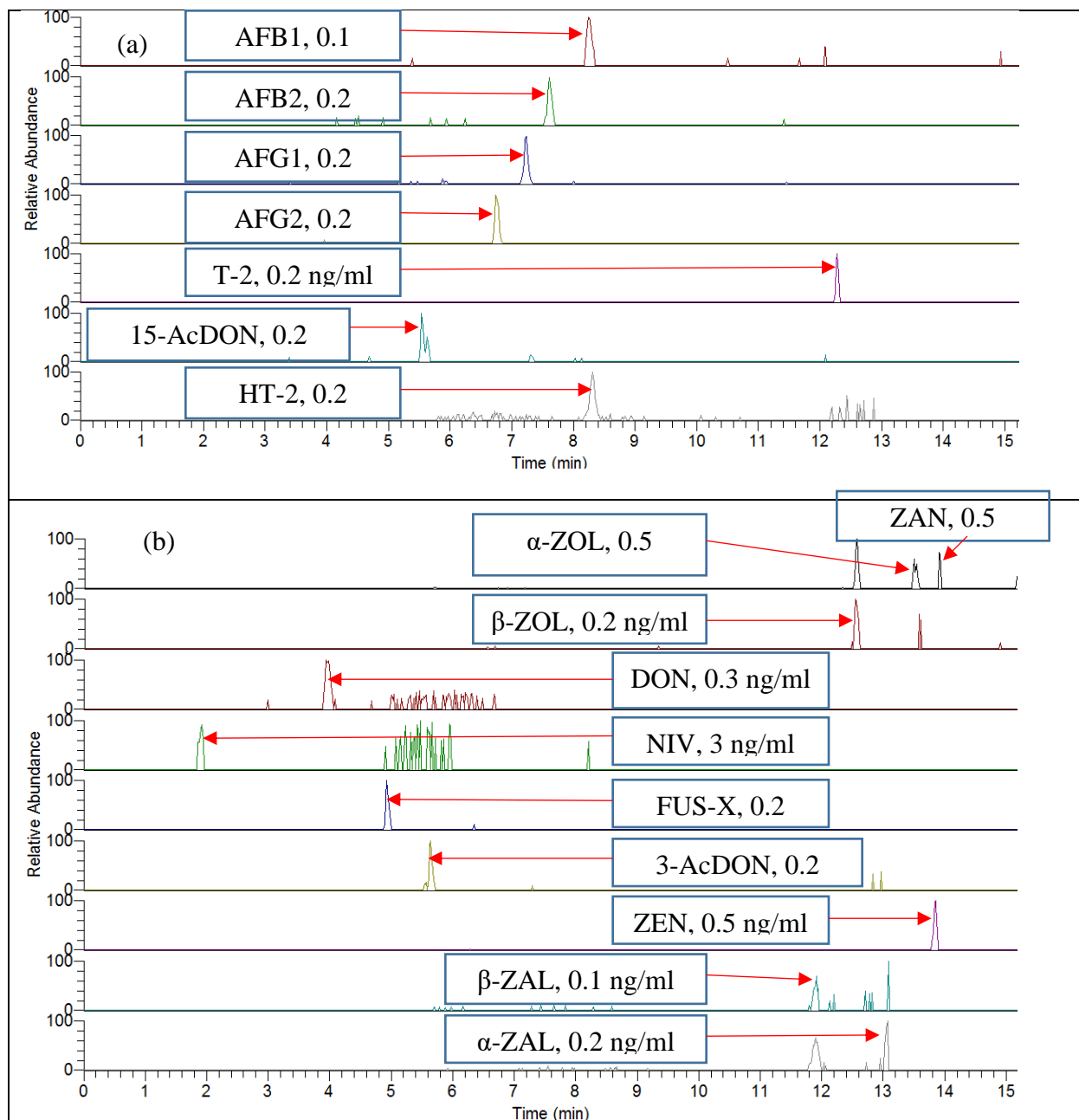
Supplementary Figure A1. The comparison of the process efficiencies (PE%) for the mycotoxins in human plasma using different sample preparation techniques.  $PE\% = C_m/C_{th} \cdot 100\%$ ,  $C_m$  is the measured concentration in the injection solvent and  $C_{th}$  is theoretical concentration in injection solvent) using three SPEs sorbents, such as Oasis HLB SPE, Mix mode and SAX. Plasma ( $n = 3$ ) was spiked pre-extraction with 20 ng/ml of mycotoxins SPEs and analyzed against standard curve prepared in reconstitution solvent (20% methanol).  $\beta$ -ZAL and  $\alpha$ -ZAL standards were not available at the time experiment was performed. The results show mean values while error bars show standard deviation of three replicate determinations.



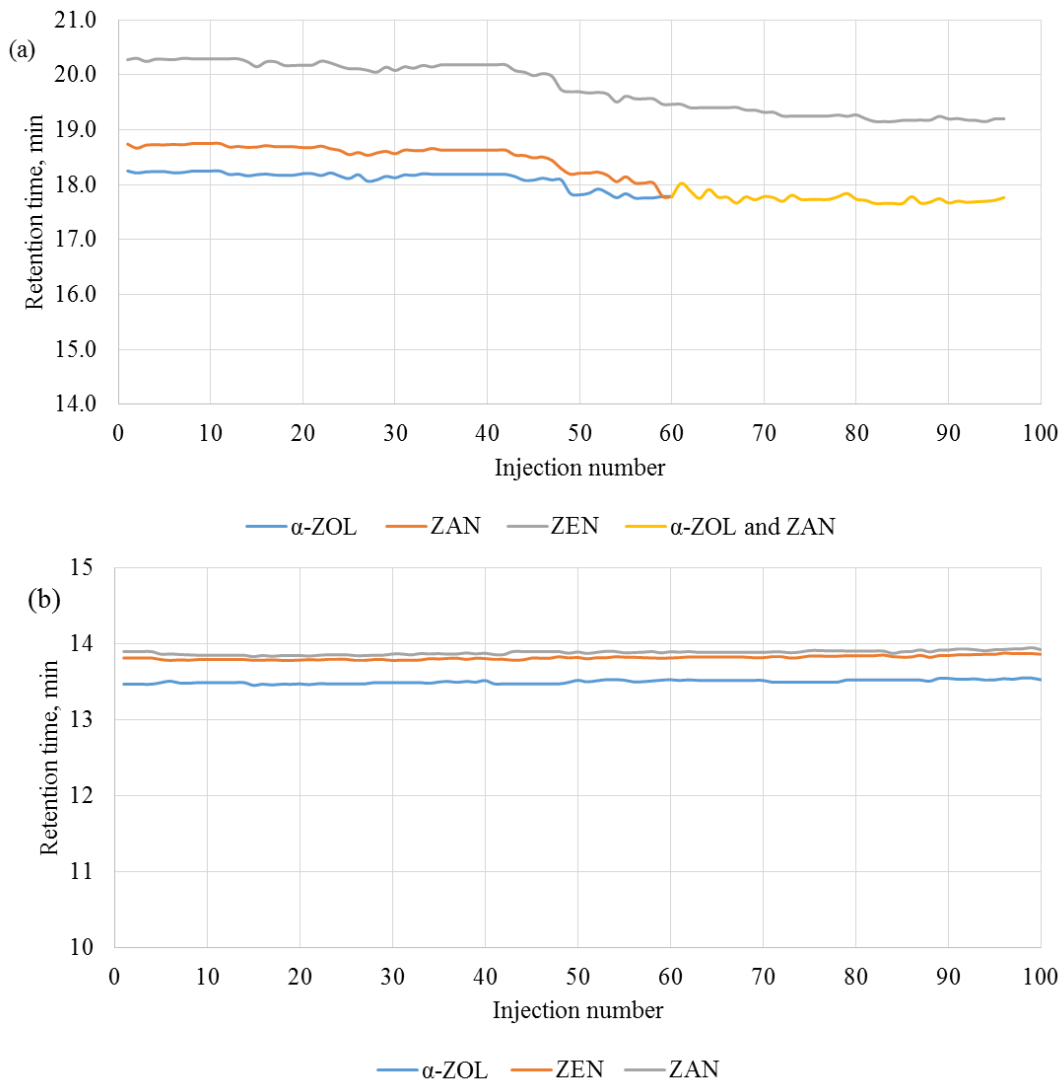
*Supplementary Figure A2. Overview of sample preparation methods tested during method development. Dark gray boxes represent methods described in Section 2.2.3 in the main text with section numbers specified below. Light gray boxes represent methods that were also evaluated during initial method development that were not included for the final optimization.*



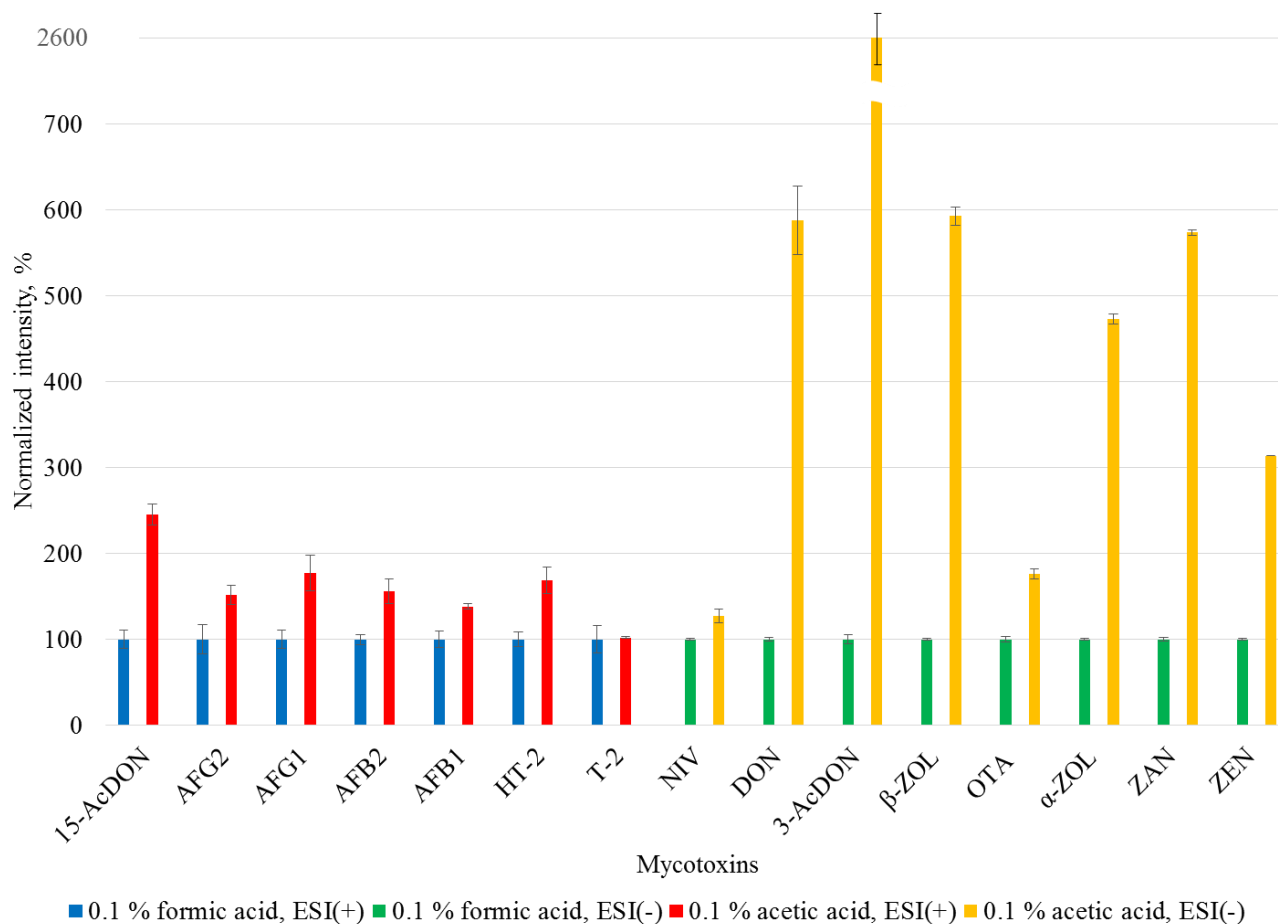
Supplementary Figure A3. Chromatographic separation of all mycotoxins obtained using optimized PFP LC method using (a) ESI(+) and (b) ESI(-). The results are shown for 10 ng/mL mycotoxin standard in 20% methanol. Mycotoxins are shown in the ESI mode where maximum signal intensity was obtained, which is the same mode used for mycotoxin quantitation. OTA, FB1 and FB2 had retention times of 13.06 min, 15.37 min and 19.60 min, respectively using this method, but are omitted since they were not included in the final validated method.



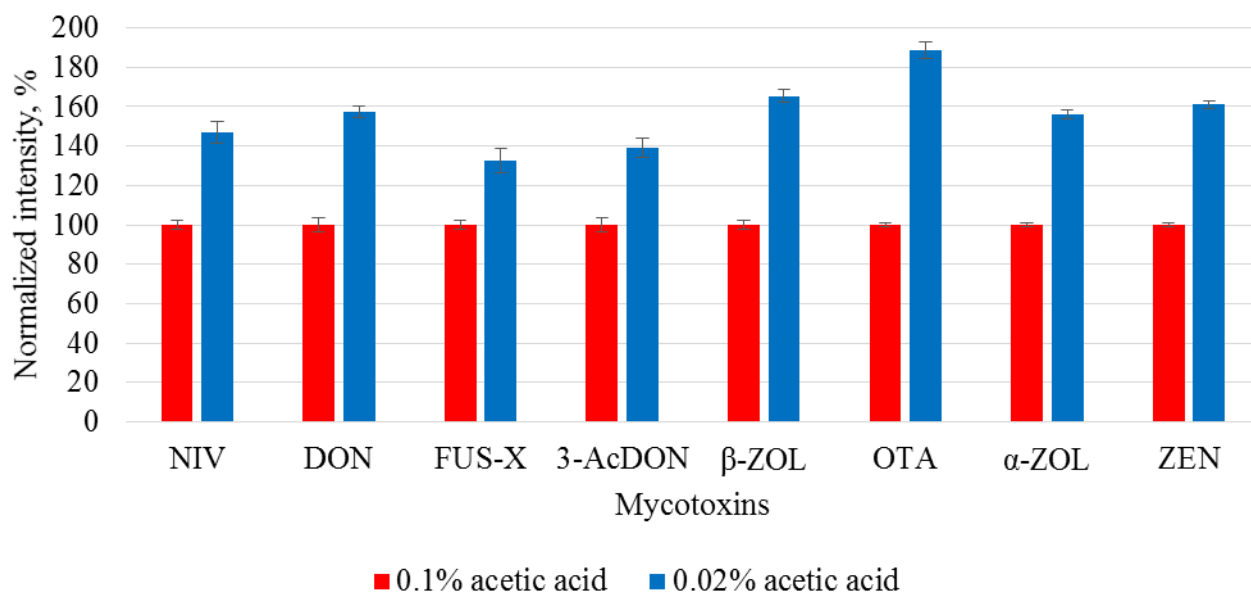
Supplementary Figure A4. Extracted ion chromatograms of all mycotoxins obtained using optimized PFP LC method using (a) ESI(+) and (b) ESI(-). The results are shown for human plasma samples spiked with mycotoxins at LLOQ levels, ranging from 0.1 ng/mL to 3 ng/mL as indicated in heading. Mycotoxins are shown in the ESI mode where maximum signal intensity was obtained, which is the same mode used for mycotoxin quantitation.



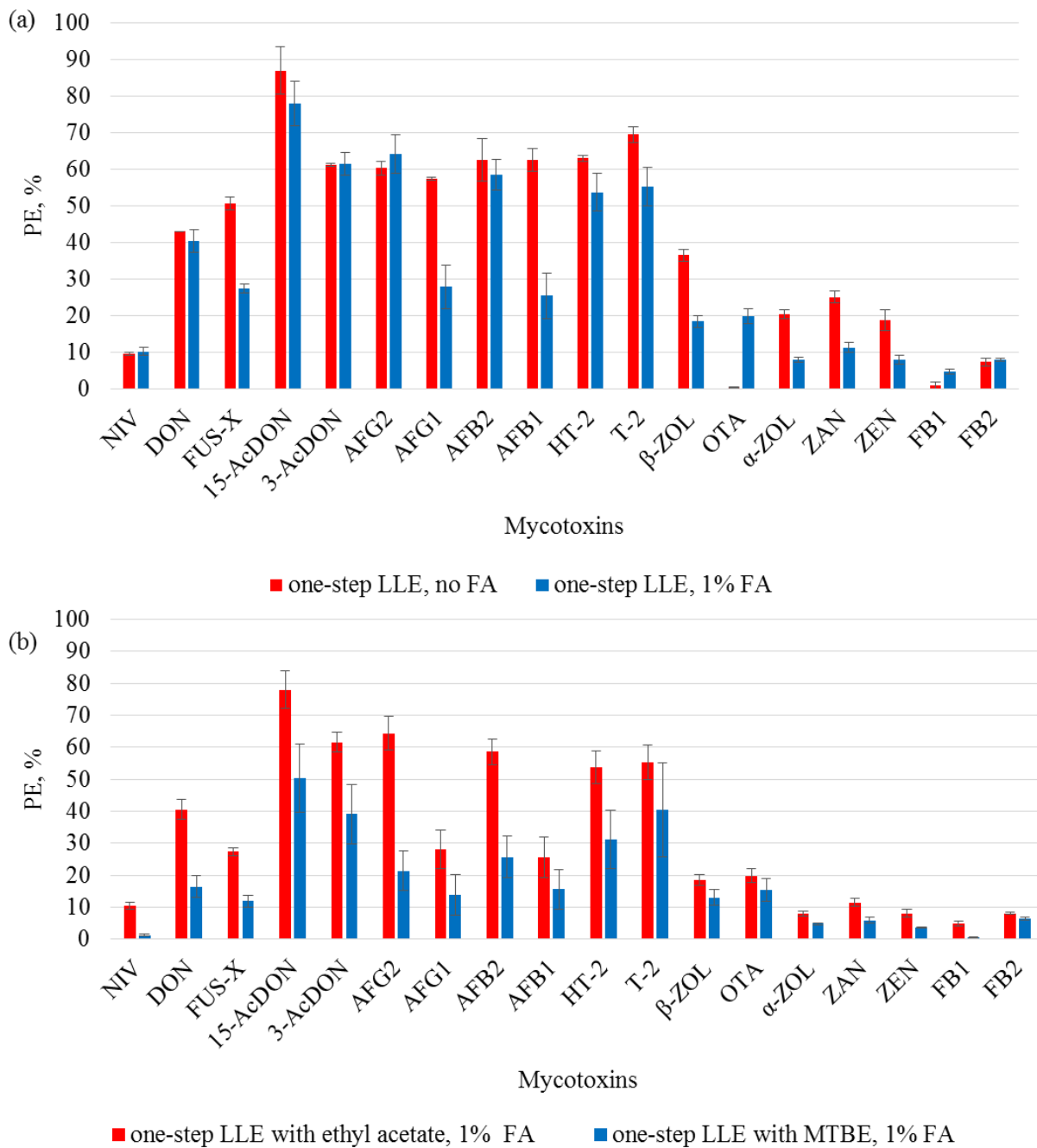
Supplementary Figure A5. Retention time stability of  $\alpha$ -ZOL, ZAN, and ZEN on F5 (a) and PFP (b) columns over long analytical run. Retention times are shown for on F5 and PFP columns. RSD% of retention time for  $\alpha$ -ZOL, ZAN, and ZEN on F5 and PFP columns, respectively, 1.2 and 0.2; 2.4 and 0.2; 2.2 and 0.2. Retention time of ZEN,  $\alpha$ -ZOL and ZAN systematically decreases over long analytical batch and results in co-elution of  $\alpha$ -ZOL and ZAN on F5 column. On PFP, their retention times are stable, and no loss of chromatographic resolution is observed. Details for PFP separation are given in main text. For F5 separation, the same mobile phase composition was used with the following gradient: 5% B for the first 1.0 min, increase to 53% B from 1.0 min to 2.0 min, increase to 56% from 2 to 18 min, from 18.00 to 18.10 min increase to 95%, keep isocratic conditions at 95% B for 4.9 min, and finally re-equilibrate the column at 5% B for 6 min.



*Supplementary Figure A6. Effect of different additives, formic (0.1% v/v) and acetic acid (0.1% v/v) in mobile phase, on signal intensity of mycotoxins in ESI(+) and ESI(-). The signal intensity (expressed as peak area) of mycotoxins obtained with 0.1% acetic acid was normalized to the signal intensity obtained with 0.1% formic acid in mobile phase. The results are shown for 100 ng/mL mycotoxin standard (n=3). FUS-X,  $\alpha$ -ZAL, and  $\beta$ -ZOL are not included because their standards were not available at the time of this experiment.*

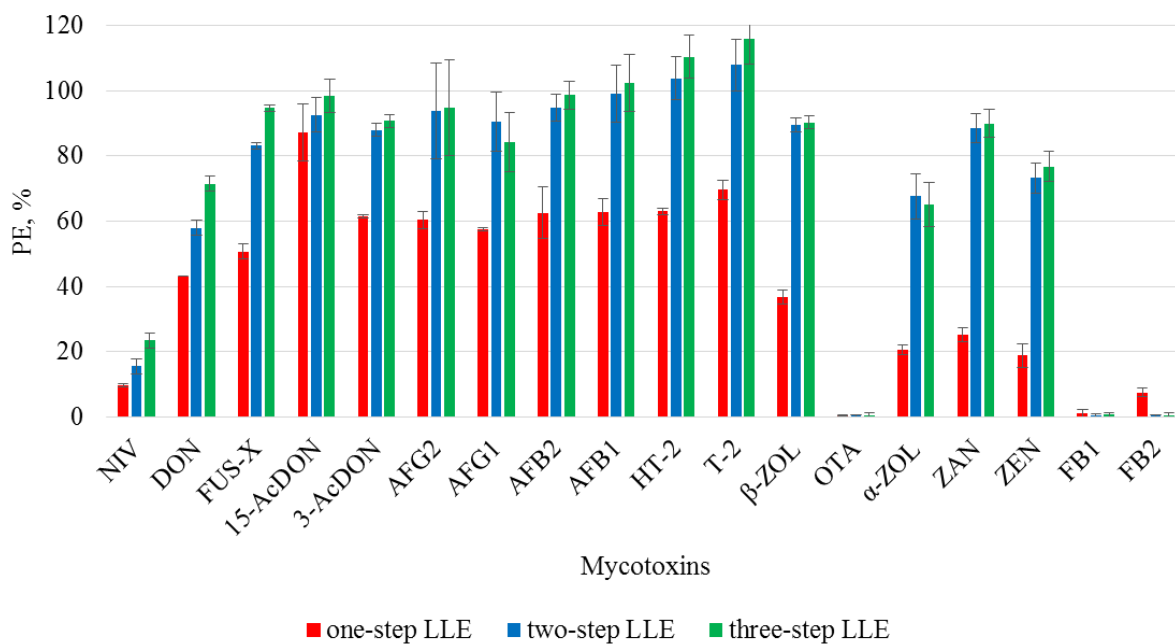


*Supplementary Figure A7. Effect of acetic acid concentration on signal intensity of 100 ng/mL mycotoxin standard (n=3) in ESI(-) mode. The signal intensity (expressed as peak area) of mycotoxins observed using 0.02% (v/v) acetic acid was normalized to the signal intensity obtained using 0.1% (v/v) acetic acid concentration in mobile phase. The results are shown only for mycotoxins that ionize better in ESI(-).*

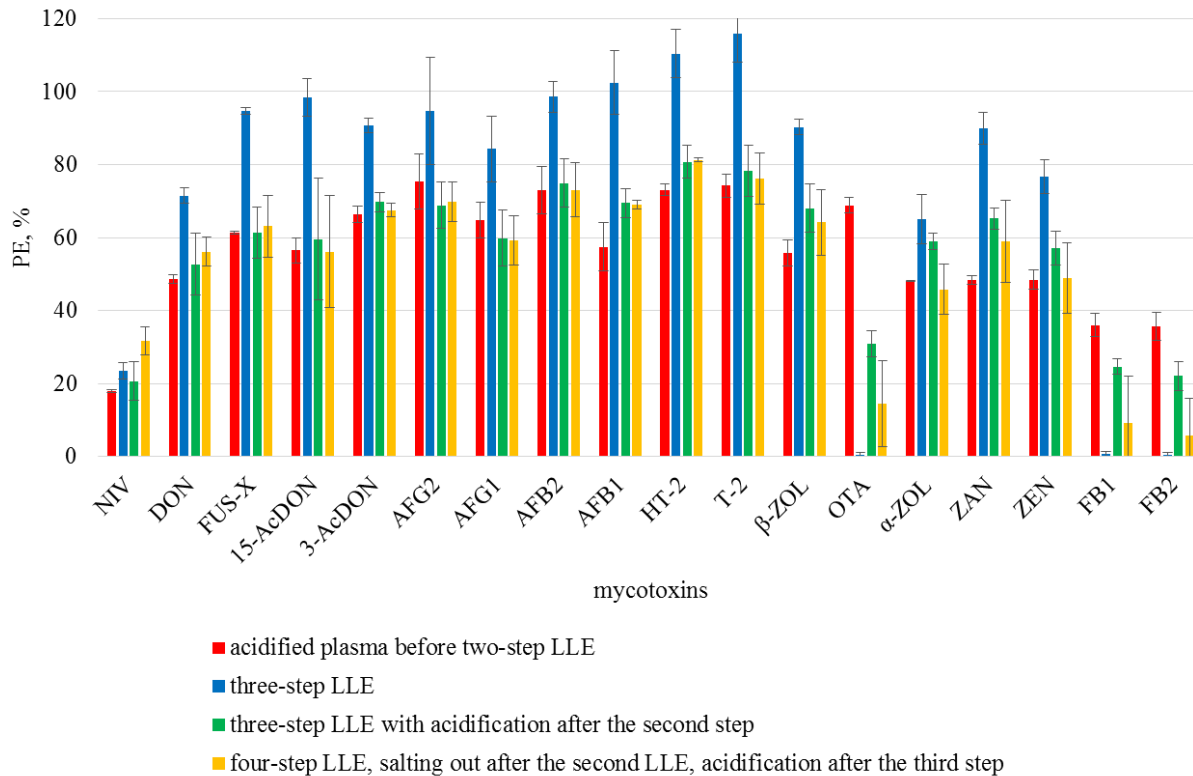


Supplementary Figure A8. Effect of sample pH (a) and solvent selection (b) on the process efficiency of mycotoxins using LLE. Effect of plasma acidification using 1% FA (pH 4) on one step-LLE with ethyl acetate (a). Comparison of extraction efficiency of ethyl acetate and methyl tert-butyl ether (MTBE) using one-step LLE on plasma previously acidified with 1% FA (pH 4) (b). Process efficiency results are shown for plasma samples spiked with 400 ng/mL mycotoxin concentration before extraction ( $n=3$ ) and analyzed against standard curve prepared in solvent (20% MeOH).

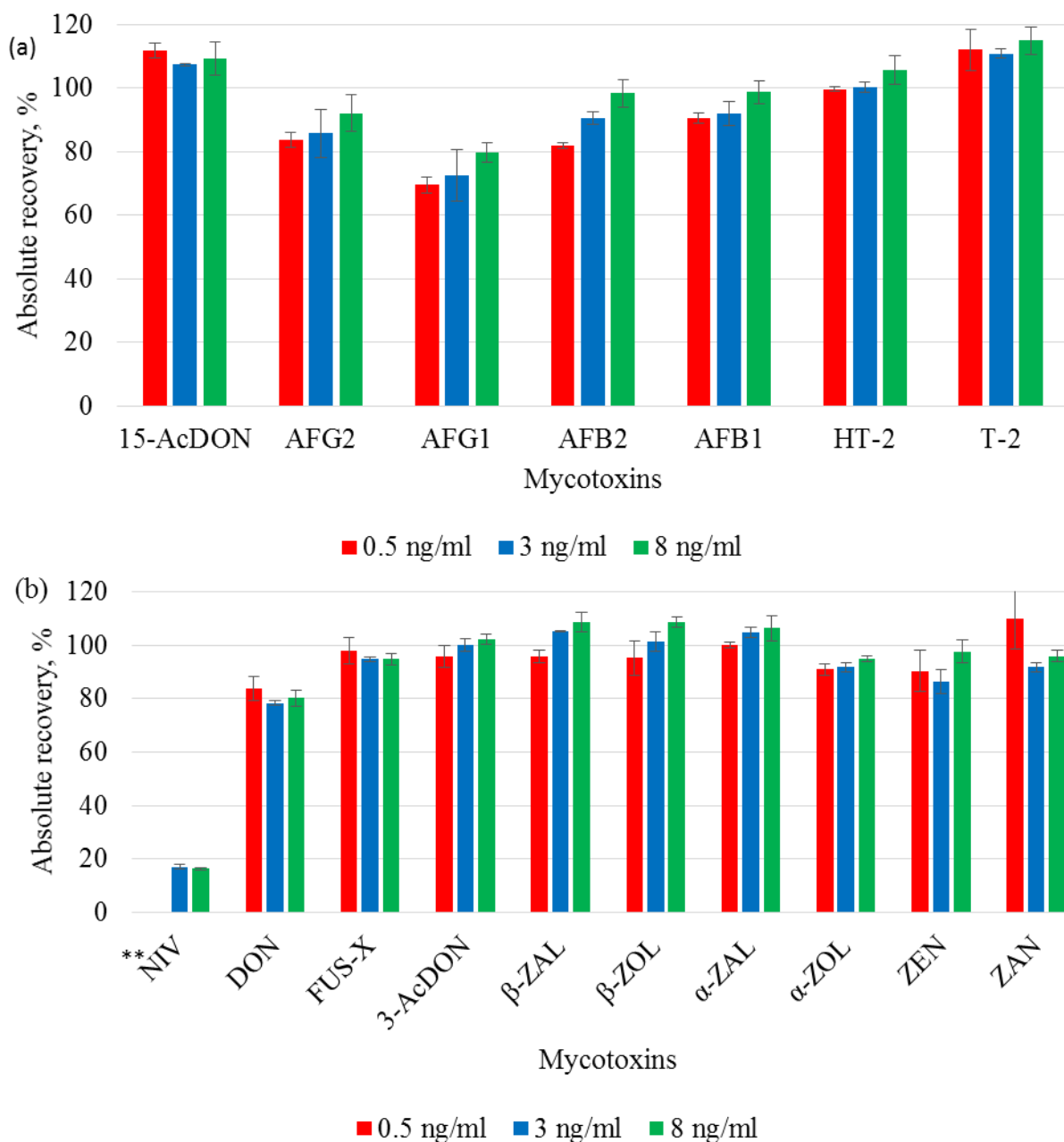




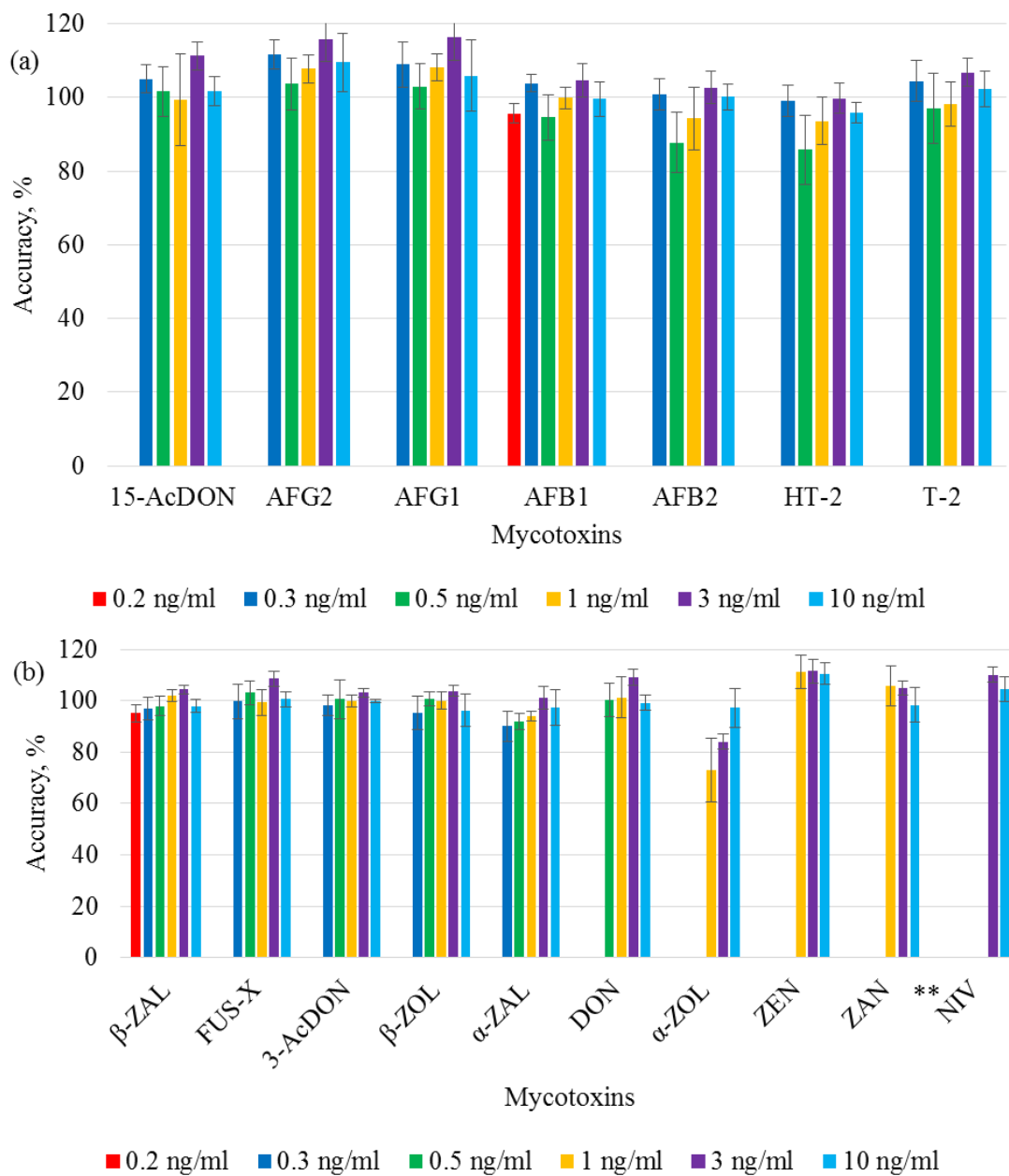
*Supplementary Figure A9. Effect of multi-step extraction with ethyl acetate on the process efficiency of mycotoxins. LLE was performed using 1x 300 µl or 2x 150 µl or 3x 150 µl portions of ethyl acetate on plasma samples spiked with 400 ng/mL mycotoxin concentration before extraction (n=3) and analysed against standard curve prepared in solvent (20% MeOH).*



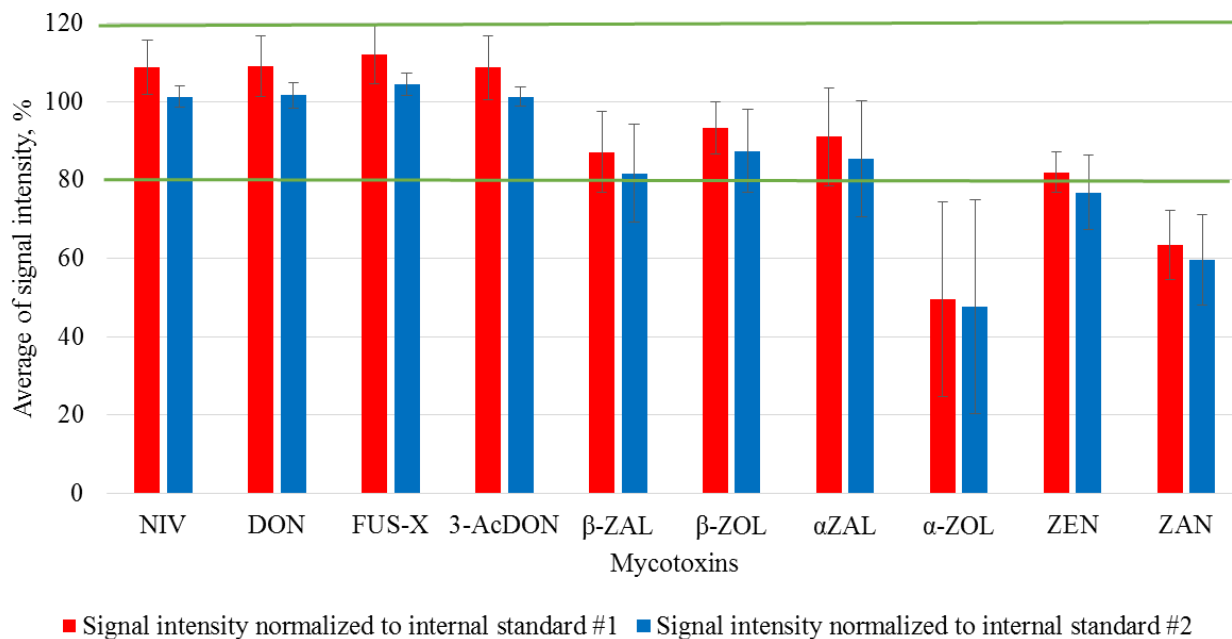
*Supplementary Figure A10. Effect of salting out and acidification on the process efficiency of mycotoxins using multi-step LLE with ethyl acetate. Results are shown for plasma samples spiked with 400 ng/mL mycotoxin (n=3) before extraction and analysed against standard curve in solvent (20% MeOH). ■ - pre-spiked plasma was acidified with 20 µl of FA (pH 2) and then two-step LLE with ethyl acetate was performed (2x150 µl); ■ - three-step LLE without acidification or salting out; ■ - two-step LLE (2x150 µl of ethyl acetate) with pre-spiked plasma, then 40 µl of FA (pH 2) was added followed by LLE (1x 150 µl of ethyl acetate); ■ - two-step LLE was done with pre-spiked plasma, then MgSO<sub>4</sub> was added with followed by LLE (1x 150 µl of ethyl acetate), and finally acid was added followed by fourth step of LLE (1x 150 µl of ethyl acetate).*



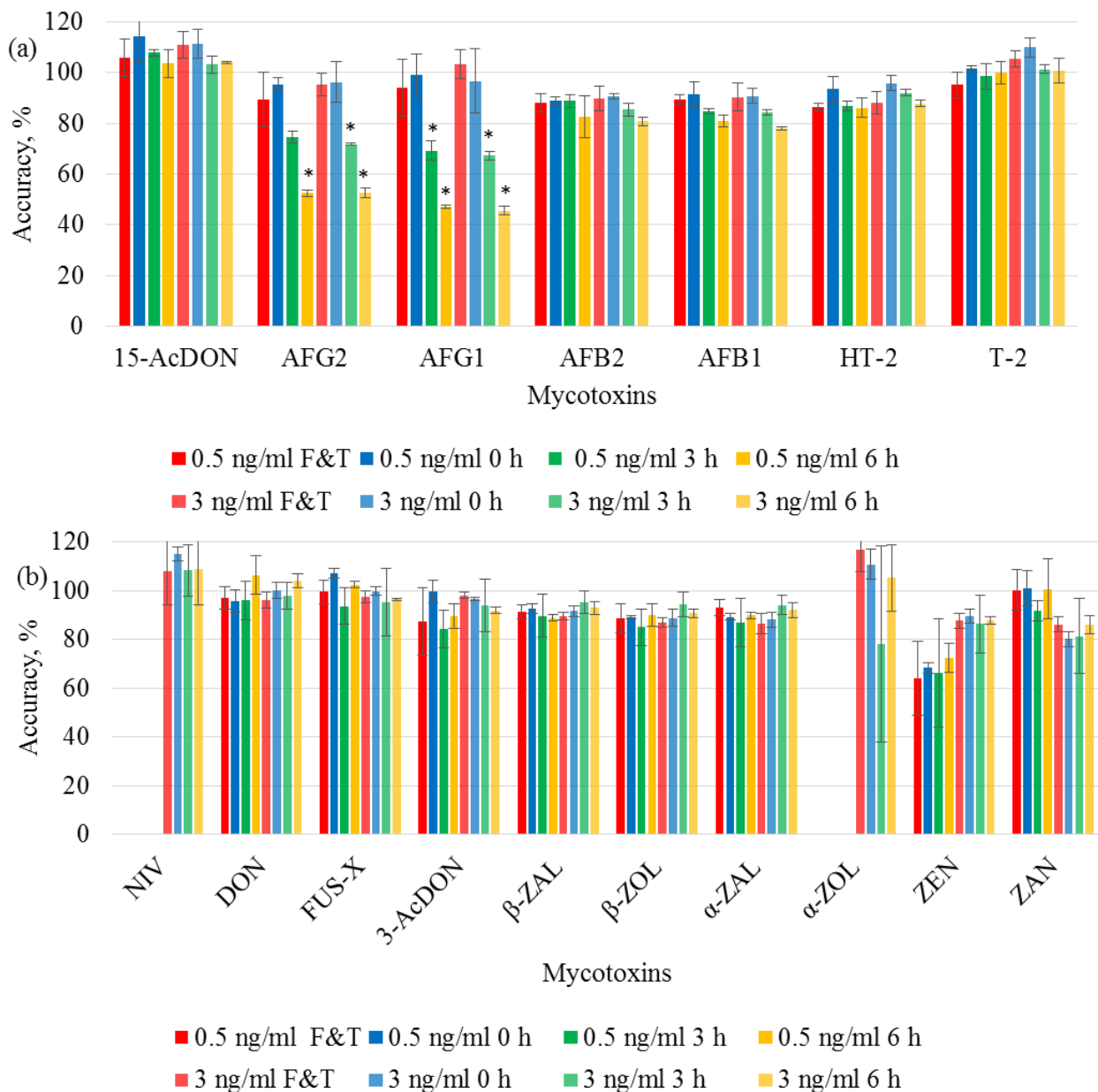
*Supplementary Figure A11. Investigation of absolute mycotoxin recovery in plasma samples using ESI(+) (a) and ESI(-) (b). Plasma was spiked with mycotoxin mixture at three concentration levels: 0.5 ng/ml, 3 ng/ml, and 8 ng/ml (n=3), except \*\*NIV for which levels were 3x, and processed using three-step LLE with ethyl acetate. The samples were analyzed against standard curve prepared in post-extraction spiked plasma in the range of LLOQ to 10 ng/ml for all mycotoxins except for NIV where 3x range (LLOQ to 30 ng/ml) was used.*



Supplementary Figure A12. Intra-day accuracy and precision for mycotoxins detected in ESI(+) (a) and ESI(-) (b). Y-axis shows mean accuracy (n=6), and error bars show standard deviation of the measurement. Determination was performed using 0.2, 0.3, 0.5, 1, 3 and 10 ng/ml (n=6), except for NIV. \*\*All NIV concentration levels were 3x the stated concentrations. Only results above LLOQ are shown. Standard curve in plasma in the range of LLOQ to 10 ng/ml, except for NIV (LLOQ to 30 ng/ml), was prepared to analyze validation samples.

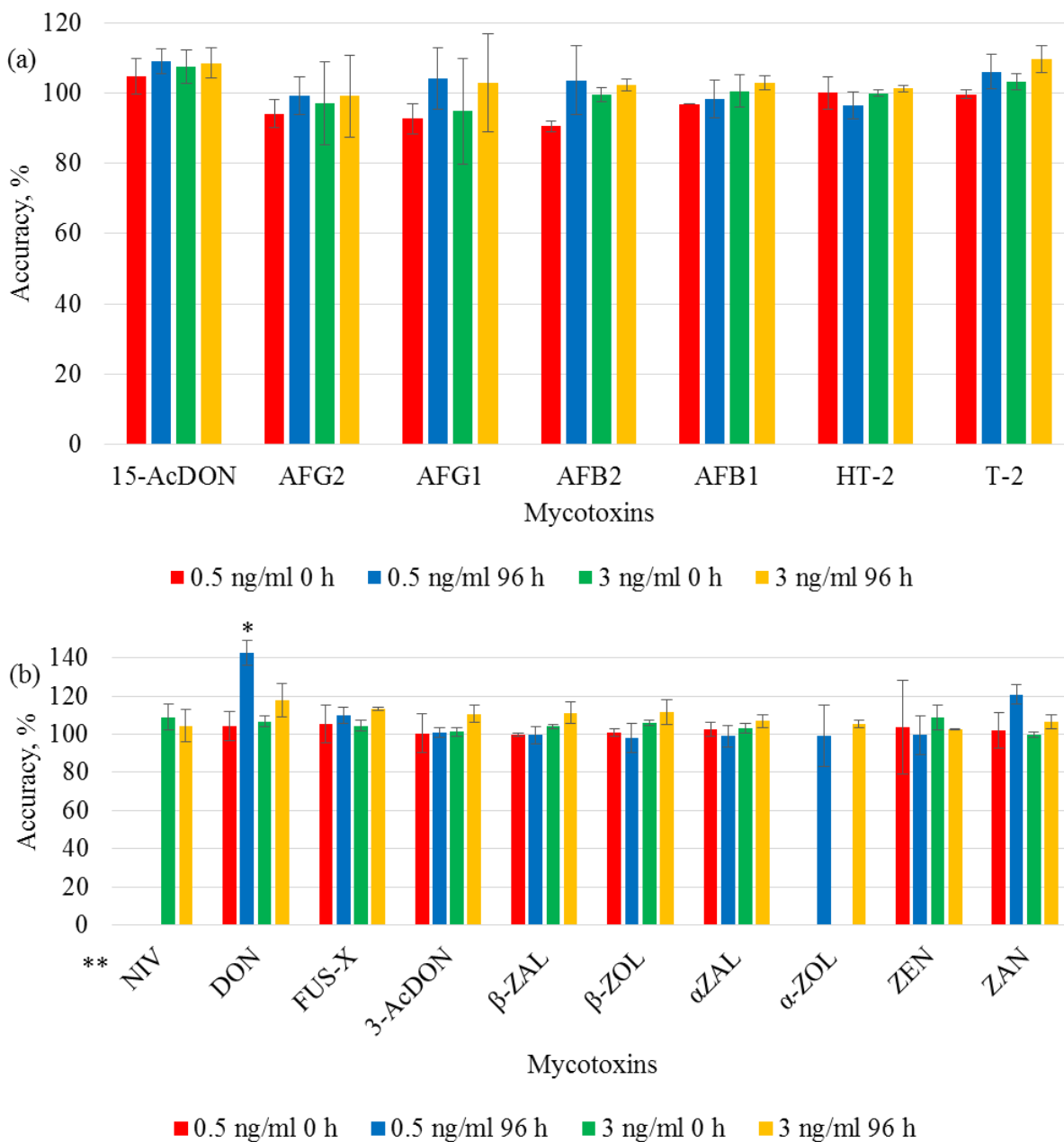


*Supplementary Figure A13. Effect of using two internal standards. Internal standard #1 –  $^{13}\text{C}$ -ZEN and internal standard #2 – 3-AcDON<sub>3</sub>, on compensating for matrix effects in 10 individual plasma samples using ESI(-). Individual plasma samples were spiked post-extraction at 0.3 ng/ml for 3-ACDON, FUS-X,  $\beta$ -ZAN,  $\beta$ -ZOL,  $\alpha$ -ZAN, 1.5 ng/ml for DON,  $\alpha$ -ZOL, ZEN, ZAN and 9 ng/ml for NIV. The area of post-extraction spiked individual plasma was compared to the area of the standard solution prepared in 20% MeOH, after correction with the stated internal standard, in order to determine absolute matrix effect. Green lines show the acceptance criteria for no significant matrix effects, 80-120%.*



Supplementary Figure A14. Evaluation of mycotoxin stability in ESI(+) (a) and in ESI(-) (b). Freeze/ thaw (3 cycles) stability, abbreviation – F&T; 3 hour and 6 hour bench stability of plasma samples, abbreviation – 3 h and 6 h. Stability was evaluated at two concentrations, 0.5 ng/ml (n=3) and 3 ng/ml (n=3), except \*\*NIV for which the level was 9 ng/ml. Fresh calibration curve in plasma was prepared with the reference samples, abbreviation – 0 h (n=3) to analyse 3 hour and 6 hour bench stability of plasma samples. \*The student's t-test was performed to compare stability condition against appropriate 0 h sample: \* denotes statistically significant result AFG2 (3 h 0.5 ng/ml, p value = 0.0005), AFG2 (6 h 0.5 ng/ml, p value =  $1.5 \times 10^{-05}$ ), AFG2 (3 h 3 ng/ml, p value = 0.0063), AFG2 (6 h 3 ng/ml, p value = 0.0008); AFG1 (3 h 0.5 ng/ml, p value = 0.0046), AFG1 (6 h 0.5 ng/ml, p value = 0.0004), AFG1 (3 h 3 ng/ml, p value = 0.0158), AFG1 (6 h 3 ng/ml, p value = 0.0022).  $\alpha$ -ZOL 3h 3 ng/ml evaluation has an outlier that resulted in poor repeatability for this analyte. Column aging eventually causes complete co-elution of 277.1447

*m/z interference with  $\alpha$ -ZOL. This occurred during analysis of 0.5 ng/mL  $\alpha$ -ZOL samples, and changing the column resolved the problem as shown in Figure A13 for 96 hour stability.*



Supplementary Figure A15. Evaluation of mycotoxin stability in autosampler in ESI(+) (a) and ESI(-) (b). Stability was evaluated at two concentrations, 0.5 and 3 ng/ml (n=3), except \*\*NIV for which the level was 9 ng/ml. Samples were prepared with calibration curve in plasma and analysed on the same day (0 h, ■ and ■). Then, samples were kept for 4 days in autosampler at 4°C and re-analysed on fourth day (96 h, ■ and ■) against a freshly-made calibration curve in plasma. \*The student's t-test was performed to compare 96 h stability against 0 h: \* denotes statistically significant result DON (96 h 0.5 ng/ml, p value = 0.002). Column aging eventually causes complete co-elution of 277.1447 m/z interference with  $\alpha$ -ZOL. This occurred during 0 h stability run so  $\alpha$ -ZOL could not be properly quantitated due to severe suppression. Changing the column for 96 h run, allowed the quantification of  $\alpha$ -ZOL.



## Appendix B

Supplementary Information for Chapter 3

Supplementary Table B1. Microsomal incubation protocol for Phase I and II reactions. \*Heated microsomes at T 45°C for 30 min.

Phase I reaction							
Sample type	Mycotoxin volume, $\mu\text{L}$	Microsome volume, $\mu\text{L}$	NADPH volume, $\mu\text{L}$		PBS buffer volume, $\mu\text{L}$		
Test	1	5	12		182		
Control 1	0	5	12		182		
Control 2	1	5	0		194		
Control 3	1	5 *	12		182		
Control 4	1	0	0		199		
Phase II reaction							
Sample type	Mycotoxin volume, $\mu\text{L}$	Microsome volume, $\mu\text{L}$	NADPH volume, $\mu\text{L}$	UDPGA volume, $\mu\text{L}$	Alamethecin volume, $\mu\text{L}$	MgCl <sub>2</sub> volume, $\mu\text{L}$	PBS buffer volume, $\mu\text{L}$
Test	1	5	12	10	1	10	183
Control 5	0	5	12	10	1	10	184
Control 6	1	5	0	10	1	10	195
Control 7	1	5 *	12	10	1	10	183

Supplementary Table B2. T-2 and its metabolites generated in Phase I and Phase II. They detected in ESI(+), as CID product ion spectra of  $[M+Na]^+$ , unless otherwise specified fragments with intensity >10% are shown in the table, \*fragmentation pattern are shown for  $[M+NH_4]^+$  ions.

T-2 Phase I metabolites								
Name	RT, min	Measured m/z	Theoretical m/z	ppm	Fragments, CID	Formula	Transformation	Comments
T-2	12.23	489.2092	489.2095	0.61	245.2(10), 327.2(37), 387.2(100)	$C_{24}H_{34}O_9$	parent	
Peak 1-447	7.93	447.1988	447.1989	0.22	285.2(21), 345.2(100)	$C_{22}H_{32}O_8$	-( $C_2H_2O$ )	Non enzymatic, 15-deacetyl-T-2
Peak 2-447	8.22	447.1986	447.1989	0.67	285.2(20), 345.2(100)	$C_{22}H_{32}O_8$	-( $C_2H_2O$ )	Non enzymatic, HT-2
Peak 1-505	6.54	505.2042	505.2044	0.40	327.2(27), 387.2(100)	$C_{24}H_{34}O_{10}$	+(O)	2'-OH-T-2 or 3'-OH-T-2 or 4'-OH-T-2
Peak 2-505	6.60	505.2041	505.2044	0.59	327.2(22), 387.2(100)	$C_{24}H_{34}O_{10}$	+(O)	2'-OH-T-2 or 3'-OH-T-2 or 4'-OH-T-2
Peak 3-505	6.81	505.2043	505.2044	0.20	327.2(10), 387.4(100)	$C_{24}H_{34}O_{10}$	+(O)	2'-OH-T-2 or 3'-OH-T-2 or 4'-OH-T-2
Peak 1-463	5.68	463.1936	463.1939	0.65	285.1(16), 345.2(100), 446.0(12)	$C_{22}H_{32}O_9$	-( $C_2H_2$ )	3' or 4'- Hydroxy-HT-2
Peak 2-463	5.76	463.1938	463.1939	0.22	345.43(100)	$C_{22}H_{32}O_9$	-( $C_2H_2$ )	3' or 4'- Hydroxy-HT-2

Name	RT, min	Measured m/z	Theoretical m/z	ppm	Fragments, CID	Formula	Transformation	Comments
Peak 3-463	5.94	463.1938	463.1939	0.22	No MS2	C <sub>22</sub> H <sub>32</sub> O <sub>9</sub>	-(C <sub>2</sub> H <sub>2</sub> )	2'-OH-T-2
Peak 4-463	6.12	463.1937	463.1939	0.43	No MS2	C <sub>22</sub> H <sub>32</sub> O <sub>9</sub>	-(C <sub>2</sub> H <sub>2</sub> )	Low intensity, 7-OH-HT-2 10-OH-HT-2 16-OH-HT-2
Peak 5-463	6.21	463.1936	463.1939	0.65	301.2(21), 361.2(100), 381.0(20), 434.0(10), 446.0(26)	C <sub>22</sub> H <sub>32</sub> O <sub>9</sub>	-(C <sub>2</sub> H <sub>2</sub> )	7-OH-HT-2 or 10-OH-HT-2 or 16-OH-HT-2
Peak 1-405	6.55	405.1881	405.1884	0.74	No MS2	C <sub>19</sub> H <sub>26</sub> O <sub>8</sub>	-(C <sub>5</sub> H <sub>8</sub> O)	Low intensity, NEO or T-triol
<b>T-2 Phase II metabolites</b>								
Name	RT, min	Measured m/z	Theoretical m/z	ppm	Fragments, CID	Formula	Transformation	Comments
Gluc-T-2	8.88	665.2413	665.2416	0.43	489.2 100	C <sub>30</sub> H <sub>42</sub> O <sub>15</sub>	+(C <sub>6</sub> H <sub>8</sub> O <sub>6</sub> )	
Gluc-HT-2	6.91	623.2304	623.2310	0.96	263.2(13) 425.2(6) 443.0(35) 499.2(3) 601.0(100)* and 447.5(100)	C <sub>28</sub> H <sub>40</sub> O <sub>14</sub>	+(C <sub>4</sub> H <sub>6</sub> O <sub>5</sub> )	HT-2 3-glucuronide

Supplementary Table B3. HT-2 and its metabolites, detected in ESI(+), as  $[M+Na]^+$  ions. Unless otherwise specified fragments with intensity >10% are shown in the table. \* Intensities of fragments are more than 40% shown only; \*\* fragments with intensity >19% are shown.

HT-2 Phase I metabolites								
Name	RT, min	Measured m/z	Theoretical m/z	ppm	Fragments, CID	Formula	Transformation	Comments
HT-2	8.22	447.1986	447.1989		285.2(13), 345.3(100)	C <sub>22</sub> H <sub>32</sub> O <sub>8</sub>	parent	
Peak 1-463	5.67	463.1936	463.1939	0.65	285.2(10), 345.5(100)	C <sub>22</sub> H <sub>32</sub> O <sub>9</sub>	+(O)	3' or 4'-Hydroxy-HT-2
Peak 2-463	5.77	463.1936	463.1939	0.65	285.2(14), 345.2(100)	C <sub>22</sub> H <sub>32</sub> O <sub>9</sub>	+(O)	3' or 4'-Hydroxy-HT-2
Peak 3-463	5.95	463.1936	463.1939	0.65	285.3(19), 345.2(100), 431.2(19), 445.2(79), 446.1(35), 454.4(20), 457.4(25), 463.2(32)**	C <sub>22</sub> H <sub>32</sub> O <sub>9</sub>	+(O)	Low intensity
Peak 4-463	6.11	463.1936	463.1939	0.65	301.1(31), 361.2(100), 445.2(15)	C <sub>22</sub> H <sub>32</sub> O <sub>9</sub>	+(O)	
Peak 5-463	6.21	463.1936	463.1939	0.65	301.2(24), 361.2(100)	C <sub>22</sub> H <sub>32</sub> O <sub>9</sub>	+(O)	

Name	RT, min	Measured m/z	Theoretical m/z	ppm	Fragments, CID	Formula	Transformation	Comments
Peak 6-463	8.23	463.1936	463.1939	0.65	301.2(30), 345.3(11), 361.2(100), 403.2(85), 421.2(17), 445.2(17)	C <sub>22</sub> H <sub>32</sub> O <sub>9</sub>	+(O)	Low intensity peak
Peak 1-405	5.44	405.1880	405.1884	0.99	303.2(100), 323.1(17), 325.3 (59), 345.2(19), 360.5(10), 387.2(42), 395.4(14), 396.1(19), 396.8(11)	C <sub>20</sub> H <sub>30</sub> O <sub>7</sub>	-(C <sub>2</sub> H <sub>2</sub> O)	Low intensity peak
Peak 2-405	6.55	405.1880	405.1884	0.99	303.2(100), 323.1(36), 345.1(27), 361.2(10), 373.4(19), 387.2(36), 395.6(26), 396.5(23), 404.9(12)	C <sub>20</sub> H <sub>30</sub> O <sub>7</sub>	-(C <sub>2</sub> H <sub>2</sub> O)	Low intensity peak
Peak 1-363	3.58	363.1413	363.1414	0.28	303.1(100), 345.2(11)	C <sub>17</sub> H <sub>24</sub> O <sub>7</sub>	-(C <sub>5</sub> H <sub>8</sub> O)	4-de-Ac-NEO

Name	RT, min	Measured m/z	Theoretical m/z	ppm	Fragments, CID	Formula	Transformation	Comments
Peak 2-363	4.87	363.1413	363.1414	0.28	305.3(100), 363.2(37)	C <sub>17</sub> H <sub>24</sub> O <sub>7</sub>	-(C <sub>5</sub> H <sub>8</sub> O)	

Supplementary Table B4. Metabolites of 3-AcDON generated in Phase I and Phase II. The metabolites detected in ESI(-), as  $[M+CH_3COO-H]^-$  ions, except for Gluc-3-AcDON which was detected as  $[M-H]^-$  ion. Unless otherwise specified fragments with intensity >10% are shown in the table.

3-AcDON Phase I and II metabolites								
Name	RT, min	Measured m/z	Theoretical m/z	ppm	Fragments, CID	Formula	Transformation	Comments
3-AcDON	5.67	397.1497	397.1505	2.01	307.2(11), 337.2(100)	C <sub>17</sub> H <sub>22</sub> O <sub>7</sub>	parent	
DON	3.96	355.1394	355.1399	1.41	265.1(19), 295.1(100)	C <sub>15</sub> H <sub>20</sub> O <sub>6</sub>	-(C <sub>2</sub> H <sub>2</sub> O)	Non-enzymatic
Peak 1-339	4.24	339.1448	339.1449	0.29	No MS2	C <sub>15</sub> H <sub>20</sub> O <sub>5</sub>	-(C <sub>2</sub> H <sub>2</sub> O <sub>2</sub> )	Non-enzymatic
Gluc-3-AcDON	5.13	513.1613	513.1613	0	175.0(35), 191.0(26), 193.0(69), 203.1(15), 217.0(11), 229.1(10), 247.1(29), 265.2(14), 289.2(10), 307.2(100), 337.2(14), 453.1(65), 471.1(62), 495.1(66)	C <sub>23</sub> H <sub>30</sub> O <sub>13</sub>	+(C <sub>6</sub> H <sub>8</sub> O <sub>6</sub> )	Gluc-3-AcDON



Supplementary Table B5. Metabolites of 15-AcDON generated in Phase I and Phase II. Metabolites detected in ESI(+), as  $[M+Na]^+$  ions of 15-AcDON and Gluc-15-AcDON, except for DON which was detected as  $[M+H]^+$  ion. Unless otherwise specified fragments with intensity >10% are shown in the table.

15-AcDON Phase I and II metabolites								
Name	RT, min	Measured m/z	Theoretical m/z	ppm	Fragments, CID	Formula	Transformation	Comments
15-AcDON	5.57	361.1258	361.1258	0	158.1(32), 159.2(90), 165.1(15), 167.1(14), 217.2(31), 283.2(10), 289.0(15), 301.1(100), 311.3(11), 325.4(19), 329.3(38), 343.3(82), 344.4(24)	C <sub>17</sub> H <sub>22</sub> O <sub>7</sub>	parent	
DON	3.96	297.1330	297.1333	1.01	NO MS2	C <sub>17</sub> H <sub>12</sub> O <sub>8</sub>	-(C <sub>2</sub> H <sub>2</sub> O)	Non-enzymatic
Gluc-15-AcDON	5.20	537.1575	537.1579	0.74	361.47(100)	C <sub>23</sub> H <sub>30</sub> O <sub>13</sub>	+(C <sub>6</sub> H <sub>8</sub> O <sub>6</sub> )	

Supplementary Table B6. Metabolites of DON generated in Phase I and Phase II. Metabolites detected in ESI(-), as  $[M+CH_3COO-H]^-$  ions, except for Gluc-DON which was detected as  $[M-H]^-$  ion. Unless otherwise specified fragments with intensity >10% are shown in the table.

DON Phase I and II metabolites								
Name	RT, min	Measured m/z	Theoretical m/z	ppm	Fragments, CID	Formula	Transformation	Comments
DON	3.96	355.1393	355.1399	1.67	265.1(21), 295.1(100)	C <sub>15</sub> H <sub>20</sub> O <sub>6</sub>	parent	
NIV	1.97	371.1348	371.1348	0	304.4(100)	C <sub>15</sub> H <sub>20</sub> O <sub>7</sub>	+(O)	Non-enzymatic
peak 1-339	4.11	339.1449	339.1449	0	249.1(13), 279.1(100)	C <sub>15</sub> H <sub>20</sub> O <sub>5</sub>	-(O)	Non-enzymatic, DOM-1
Peak 2-339	4.69	339.1449	339.1449	0	231.2(14), 249.1(100), 256.9(65), 261.2(14), 279.1(55), 321.2(24), 329.6(13)	C <sub>15</sub> H <sub>20</sub> O <sub>5</sub>	-(O)	Non-enzymatic, DOM-1 isomer
Peak 3-339	5.08	339.1448	339.1449	0.29	No MS2	C <sub>15</sub> H <sub>20</sub> O <sub>5</sub>	-(O)	Non-enzymatic, Low intensity peak, DOM-1 isomer
Peak 4-339	5.33	339.1449	339.1449	0	163.1(11), 231.1(13), 249.4(100)	C <sub>15</sub> H <sub>20</sub> O <sub>5</sub>	-(O)	Non-enzymatic, DOM-1 isomer
Gluc-DON Peak 1	3.48	471.1508	471.1508	0	193.0(84), 265.1(50) 300.15(86), 341.11(69) 389.0(72), 410.9(81) 441.1(72), 443.9(77) 453.0(100)*	C <sub>21</sub> H <sub>28</sub> O <sub>12</sub>	+(C <sub>6</sub> H <sub>8</sub> O <sub>6</sub> )	Peaks are nor resolved, 3 -Gluc-DON

Name	RT, min	Measured m/z	Theoretical m/z	ppm	Fragments, CID	Formula	Transformation	Comments
Gluc-DON Peak 2	3.48	471.1508	471.1508	0	193.1(12), 265.2(15) 300.1(40), 322.8(17) 323.5(33), 341.2(25) 389.0(16), 422.7(100) 423.6(14), 441.3(16) 453.1(29), 461.8(16)	C <sub>21</sub> H <sub>28</sub> O <sub>12</sub>	+(C <sub>6</sub> H <sub>8</sub> O <sub>6</sub> )	Peaks are not resolved, 15-Gluc- DON

Supplementary Table B7. Metabolites of FUS-X generated in Phase I and Phase II. Metabolites detected in ESI(-), as  $[M+CH_3COO-H]^-$  ions, except for Gluc-FUS-X which was detected as  $[M-H]^-$  ion. Unless otherwise specified fragments with intensity >10% are shown in the table.

FUS-X Phase I and II metabolites								
Name	RT, min	Measured m/z	Theoretical m/z	ppm	Fragments, CID	Formula	Transformation	Comments
FUS-X	4.93	413.1448	413.1454	1.33	353.3(100)	$C_{17}H_{22}O_8$	parent	
NIV	1.97	371.1347	371.1348	0.27	304.3(100.0)	$C_{15}H_{20}O_7$	-( $C_2H_2O$ )	Non-enzymatic
Gluc-FUS-X	4.62	529.1561	529.1563	0.38	245.1(12), 426.1(34), 448.1(20), 469.1(100), 470.1(20), 487.2(34), 499.1(10), 510.8(20)	$C_{23}H_{30}O_{14}$	+( $C_6H_8O_6$ )	

Supplementary Table B8. Metabolites of NIV generated in Phase I and Phase II. Metabolites detected in ESI(-), as  $[M+CH_3COO-H]^-$  ions, except for Gluc-NIV which was detected as  $[M-H]^-$  ion. Unless otherwise specified fragments with intensity >10% are shown in the table.

NIV Phase I and II metabolites								
Name	RT, min	Measured m/z	Theoretical m/z	ppm	Fragments, CID	Formula	Transformation	Comments
NIV	1.97	371.1343	371.1348	1.35	304.33(100.0)	C <sub>15</sub> H <sub>20</sub> O <sub>7</sub>	-(C <sub>2</sub> H <sub>2</sub> O)	
Peak 1-355	2.5	355.1396	355.1398	0.56	217.07(44), 265.12(33), 273(11), 295.09(100)	C <sub>15</sub> H <sub>20</sub> O <sub>6</sub>	-(O)	Non-enzymatic, DNIV
Peak 2-355	2.96	355.1396	355.1398	0.56	No MS2	C <sub>15</sub> H <sub>20</sub> O <sub>6</sub>	-(O)	Non-enzymatic, DNIV isomer
Peak 3-355	4.28	355.1396	355.1398	0.56	No MS2	C <sub>15</sub> H <sub>20</sub> O <sub>6</sub>	-(O)	Non-enzymatic, DNIV isomer
Gluc-NIV	1.29	487.1458	487.1457	0.18	NO MS2	C <sub>21</sub> H <sub>28</sub> O <sub>13</sub>	+(C <sub>6</sub> H <sub>8</sub> O <sub>6</sub> )	
Gluc-NIV	1.56	487.1456	487.1457	0.23	352.94(100), 404.86(83), 418.91(56), 426.87(96), 468.96(60)	C <sub>21</sub> H <sub>28</sub> O <sub>13</sub>	+(C <sub>6</sub> H <sub>8</sub> O <sub>6</sub> )	

Supplementary Table B9. AFB1 and its metabolites of Phase I reactions. Metabolites detected in ESI(+), as  $[M+H]^+$  ions and  $[M+Na]^+$  ions for AFL. Unless otherwise specified fragments with intensity >10% are shown in the table.

AFB1 Phase I metabolites								
Name	RT, min	Measured m/z	Theoretical m/z	ppm	Fragments, HCD	Formula	Transformation	Comments
AFB1	8.10	313.0707	313.0707	0	285.0756(15), 313.0703(100)	C <sub>17</sub> H <sub>12</sub> O <sub>6</sub>	N/A	Parent
Peak 1-329	5.03	329.0655	329.0661	1.8	206.0571(19), 283.0597(11), 301.0703(16), 311.0547(22), 329.0649(100)	C <sub>17</sub> H <sub>12</sub> O <sub>7</sub>	+(O)	AFBO
Peak 2-329	6.32	329.0655	329.0661	1.8	259.0600(20), 273.0757(45), 301.0704(29), 311.0548(12), 329.0651(100)	C <sub>17</sub> H <sub>12</sub> O <sub>7</sub>	+(O)	AFM1
Peak 1-347	5.63	347.0760	347.0761	0.23	259.0598(13), 273.0755(78), 283.0597(38), 287.0546(14), 289.0703(26), 301.0701(98), 311.0546(21), 329.0650(100), 347.0546(25)	C <sub>17</sub> H <sub>14</sub> O <sub>8</sub>	+(H <sub>2</sub> )+(O <sub>2</sub> )	AFB1- diol/isomers
Name	RT, min	Measured m/z	Theoretical m/z	ppm	Fragments, HCD	Formula	Transformation	Comments

Peak 2-347	5.99	347.0761	347.0761	0	273.0757(18), 283.0599(83), 287.0548(18), 301.0705(79), 311.0549(10), 329.0653(100), 347.0759(11)	C <sub>17</sub> H <sub>14</sub> O <sub>8</sub>	+(H <sub>2</sub> )+(O <sub>2</sub> )	AFB1-diol/isomers
Peak 1-299	7.05	299.0549	299.0550	0.3	271.0605(41), 299.0435(11) 299.0554(100)	C <sub>16</sub> H <sub>10</sub> O <sub>6</sub>	-(CH <sub>2</sub> )	Low intensity
Peak 2-299	7.31	299.0549	299.0550	0.3	271.0602(11), 299.0550(100)	C <sub>16</sub> H <sub>10</sub> O <sub>6</sub>	-(CH <sub>2</sub> )	AFP1
Peak 1-337	7.66	337.0682	337.0682*	0	No MS2	C <sub>17</sub> H <sub>14</sub> O <sub>6</sub>	+(H <sub>2</sub> )	AFL isomer, low intensity
Peak 2-337	8.60	337.0682	337.0682*	0	No MS2	C <sub>17</sub> H <sub>14</sub> O <sub>6</sub>	+(H <sub>2</sub> )	AFL
Peak 1-331	5.45	331.0812	331.0812	0	219.0651(10), 229.0858(10), 243.0651(42), 257.0807(33), 271.0600(16), 285.0757(71), 287.0912(12), 313.0705(100)	C <sub>17</sub> H <sub>14</sub> O <sub>7</sub>	+(H <sub>2</sub> )+(O)	The rest peak are non-enzymatic

Supplementary Table B10. AFB2 and its metabolites of Phase I reactions. Metabolites detected in ESI(+), as  $[M+H]^+$  ions. Unless otherwise specified fragments with intensity >10% are shown in the table.

AFB2 Phase I metabolites								
Name	RT, min	Measured m/z	Theoretical m/z	ppm	Fragments, CID	Formula	Transformation	Comments
AFB2	7.53	315.0864	315.0863	0.32	259.1(24), 273.1(11), 285.2(10), 287.2(100), 288.2(12), 297.1(44)	C <sub>17</sub> H <sub>14</sub> O <sub>6</sub>	parent	
Peak 1-329	4.77	331.0811	331.0813	0.60	No MS2	C <sub>17</sub> H <sub>14</sub> O <sub>7</sub>	+(O)	Low intensity peak, non-enzymatic, AFM2
Peak 2-329	5.92	331.0812	331.0813	0.30	191.0(20), 273.1(17), 285.1(19), 303.1(31), 313.1(100), 314.1(17)	C <sub>17</sub> H <sub>14</sub> O <sub>7</sub>	+(O)	Non-enzymatic, AFQ2
Peak 3-329	6.73	331.0812	331.0813	0.30	285.1(14), 303.2(27), 313.1(100), 314.1(17)	C <sub>17</sub> H <sub>14</sub> O <sub>7</sub>	+(O)	Non-enzymatic, AB2A



Supplementary Table B11. AFG1 and its metabolite (OH-AFG1). Metabolites detected in ESI(+), as  $[M+H]^+$  ions. Unless otherwise specified fragments with intensity >10% are shown in the table.

AFG1 Phase I metabolites								
Name	RT, min	Measured m/z	Theoretical m/z	ppm	Fragments, CID	Formula	Transformation	Comments
AFG1	7.08	329.0656	329.0656	0	243.1(11), 283.1(10), 301.2(20), 311.1(100), 312.1(10)	C <sub>17</sub> H <sub>12</sub> O <sub>7</sub>	N/A	
Peak 1-345	5.89	345.0604	345.0605	0.3	273.2(19), 275.1(15), 289.2(36), 299.1(11), 303.2(22), 317.2(100)	C <sub>17</sub> H <sub>12</sub> O <sub>8</sub>	+(O)	AFGM1

Supplementary Table B12. AFG2 and its metabolites of Phase I reactions. Metabolites detected in ESI(+), as  $[M+H]^+$  ions. Unless otherwise specified fragments with intensity >10% are shown in the table.

AFG2 Phase I metabolites								
Name	RT, min	Measured m/z	Theoretical m/z	ppm	Fragments, CID	Formula	Transformation	Comments
AFG2	6.73	331.0814	331.0813	0.30	303.2(13), 313.4(100)	C <sub>17</sub> H <sub>14</sub> O <sub>7</sub>	parent	
Peak 1-347	5.47	347.0760	347.0761	0.29	No MS2	C <sub>17</sub> H <sub>14</sub> O <sub>8</sub>	+(O)	Low intensity peak, non-enzymatic
Peak 2-347	5.55	347.0760	347.0761	0.29	No MS2	C <sub>17</sub> H <sub>14</sub> O <sub>8</sub>	+(O)	Low intensity peak, non-enzymatic
Peak 3-347	5.67	347.0760	347.0761	0.29	No MS2	C <sub>17</sub> H <sub>14</sub> O <sub>8</sub>	+(O)	Low intensity peak, non-enzymatic, AFGM2
Peak 4-347	5.87	347.0760	347.0761	0.29	No MS2	C <sub>17</sub> H <sub>14</sub> O <sub>8</sub>	+(O)	Low intensity peak, non-enzymatic, AFG2A

Supplementary Table B13. Metabolites of ZEN generated in Phase I and Phase II. Metabolites detected in ESI(-), as  $[M-H]^-$  ions. Unless otherwise specified fragments with intensity >10% are shown in the table.

ZEN Phase I metabolites								
Name	RT, min	M-H measured	M-H theoretical	ppm	Fragments, CID	Formula	Transformation	Comment
ZEN-main	13.52	317.1394	317.1394	0	149.1(10), 175.1(10), 273.5(100), 299.4(80)	C <sub>18</sub> H <sub>22</sub> O <sub>5</sub>	parent	
ZEN-MINOR	13.15	317.1394	317.1394	0	149.1(22), 161.1(10), 175.1(15), 203.1(30), 273.2(90), 299.2(100)	C <sub>18</sub> H <sub>22</sub> O <sub>5</sub>	N/A	isomer
β-ZOL	12.30	319.1547	319.1545	0.6	275.2(100), 287.8(10), 299.1(25), 301.1(70)	C <sub>18</sub> H <sub>24</sub> O <sub>5</sub>	+(H <sub>2</sub> )	
ZAN	13.27	319.1544	319.1545	0.3	205.1(10), 275.4(100), 301.1(20)	C <sub>18</sub> H <sub>24</sub> O <sub>5</sub>	+(H <sub>2</sub> )	
α-ZOL	13.48	319.1550	319.1545	1.6	No ms2	C <sub>18</sub> H <sub>24</sub> O <sub>5</sub>	+(H <sub>2</sub> )	
Peak 1-331	8.69	331.1186	331.1182	1.2	202.1(40), 287.2(80), 303.1(100), 312.2(60)	C <sub>18</sub> H <sub>20</sub> O <sub>6</sub>	-(H <sub>2</sub> )+(O)	13-OH-ZEN-quinone
Peak 1-335	7.53	335.1500	335.1495	1.5	211.0(30), 253.0(50), 291.2(100), 315.0(70), 317.1(100)	C <sub>18</sub> H <sub>24</sub> O <sub>6</sub>	+(H <sub>2</sub> )+(O)	8-OH-α or β-ZOL
Peak 2-335	12.23	335.1496	335.1495	0.3	No ms2	C <sub>18</sub> H <sub>24</sub> O <sub>6</sub>	+(H <sub>2</sub> )+(O)	13-OH-α-ZOL
Peak 1-333	8.11	333.1342	333.1338	1.2	289.1(80), 305.2(100), 315.1(40)	C <sub>18</sub> H <sub>22</sub> O <sub>6</sub>	+(O)	α or β-OH-ZOL-quinone
Peak 2-333	8.71	333.1340	333.1338	0.6	288.2(70), 289.2(100), 304.2(90), 315.1(30)	C <sub>18</sub> H <sub>22</sub> O <sub>6</sub>	+(O)	α or β-OH-ZOL-quinone

Name	RT, min	M-H measured	M-H theoretical	ppm	Fragments, CID	Formula	Transformation	Comment
Peak 3-333	8.87	333.1341	333.1338	0.9	No ms2	C <sub>18</sub> H <sub>22</sub> O <sub>6</sub>	+(O)	2 or 3-OH-ZEN
Peak 4-333	9.38	333.1342	333.1338	1.2	250.1(20), 289.1(100), 315.1(80)	C <sub>18</sub> H <sub>22</sub> O <sub>6</sub>	+(O)	6 or 8-OH-ZEN
Peak 5-333	10.96	333.1341	333.1338	0.9	216.1(15), 289.2(100), 314.3(60), 315.2(60)	C <sub>18</sub> H <sub>22</sub> O <sub>6</sub>	+(O)	6 or 8-OH-ZEN
Peak 6-333	11.52	333.1341	333.1338	0.9	191.0(60), 289.2(90), 314.3(100), 315.2(90)	C <sub>18</sub> H <sub>22</sub> O <sub>6</sub>	+(O)	4-OH-ZEN or 5-OH-ZEN or 9-OH-ZEN
Peak 7-333	12.22	333.1342	333.1338	1.2	289.3(20), 315.5(100)	C <sub>18</sub> H <sub>22</sub> O <sub>6</sub>	+(O)	10-OH-ZEN
Peak 8-333	12.51	333.134	333.1338	0.6	175.1(15), 203.1(30), 289.2(50), 315.4(100)	C <sub>18</sub> H <sub>22</sub> O <sub>6</sub>	+(O)	15-OH-ZEN
Peak 9-333	12.62	333.1342	333.1338	1.2	No ms2	C <sub>18</sub> H <sub>22</sub> O <sub>6</sub>	+(O)	13-OH-ZEN
<b>ZEN Phase II metabolites</b>								
Name	RT, min	M-H measured	M-H theoretical	ppm	Fragments, CID	Formula	Transformation	Comment
Peak 1-493	5.82	493.1714	493.1710	0.8	175.0(15), 317.2(100), 410.9(10), 449.2(31), 475.0(11)	C <sub>24</sub> H <sub>30</sub> O <sub>11</sub>	+(C <sub>6</sub> H <sub>8</sub> O <sub>6</sub> )	16-Gluc-ZEN
Peak 2-493	7.20	493.1714	493.1710	0.8	175.0(20), 317.2(100)	C <sub>24</sub> H <sub>30</sub> O <sub>11</sub>	+(C <sub>6</sub> H <sub>8</sub> O <sub>6</sub> )	14-Gluc-ZEN
Peak 3-493	12.22	493.1714	493.1710	0.8	174.9(20), 316.3(15), 317.2(100), 411.0(25), 433.0(14), 473.0(15), 474.3(17), 475.1(17)	C <sub>24</sub> H <sub>30</sub> O <sub>11</sub>	+(C <sub>6</sub> H <sub>8</sub> O <sub>6</sub> )	Shallow peak

Name	RT, min	M-H measured	M-H theoretical	ppm	Fragments, CID	Formula	Transformation	Comment
Peak 1-495	5.57	495.1869	495.1866	0.6	175.1(20), 319.2(100), 397.0(10), 413.11(90), 413.9(10), 433.2(10), 434.9(46), 440.1(12), 463.1(18), 473.6(16), 477.1(58), 478.0(26), 479.0(10,) 485.8(38), 486.5(10)	C <sub>24</sub> H <sub>32</sub> O <sub>11</sub>	+(C <sub>6</sub> H <sub>10</sub> O <sub>6</sub> )	16-Gluc-β-ZOL
Peak 2-495	5.89	495.18697	495.1866	0.7	175.0(18), 317.2(10), 319.2(100), 331.1(10), 397.1(32), 413.0(78), 433.1(10), 433.9(30), 451.1(24), 454.7(14), 464.2(10), 465.2(20), 475.0(10), 476.9(65), 477.9(10) 486.1(25)	C <sub>24</sub> H <sub>32</sub> O <sub>11</sub>	+(C <sub>6</sub> H <sub>10</sub> O <sub>6</sub> )	14-Gluc-β-ZOL or 16-Gluc-ZAN,
Peak 3-495	7.31	495.1858	495.1866	1.6	175.0(42), 176.0(10), 317.2(40), 318.2(82), 319.2(100)	C <sub>24</sub> H <sub>32</sub> O <sub>11</sub>	+(C <sub>6</sub> H <sub>10</sub> O <sub>6</sub> )	14-Gluc-α-ZOL
Peak 4-495	12.22	495.1866	495.1866	0.0	319.2(25), 413.0(22), 435.0(10), 451.2(100), 475.0(16), 477.2(17)	C <sub>24</sub> H <sub>32</sub> O <sub>11</sub>	+(C <sub>6</sub> H <sub>10</sub> O <sub>6</sub> )	7-Gluc-α-ZOL
Peak 1-509	6.43	509.1662	509.1659	0.6	175.0(10), 333.2(100), 427.0(10), 490.9(10)	C <sub>24</sub> H <sub>30</sub> O <sub>12</sub>	+(C <sub>6</sub> H <sub>8</sub> O <sub>7</sub> )	Gluc-15-OH-ZEN
Peak 2-509	7.54	509.1660	509.1659	0.2	332.4(10), 333.2(100), 491.1(12)	C <sub>24</sub> H <sub>30</sub> O <sub>12</sub>	+(C <sub>6</sub> H <sub>8</sub> O <sub>7</sub> )	Gluc-13-OH-ZEN
Peak 1-669	5.28	669.2035	669.2031	0.6	493.1(100)	C <sub>24</sub> H <sub>30</sub> O <sub>12</sub>	+(C <sub>12</sub> H <sub>16</sub> O <sub>12</sub> )	2xGluc-ZEN

Supplementary Table B14. Metabolites of  $\alpha$ -ZOL generated in Phase I and Phase II. Metabolites detected in ESI(-), as  $[M-H]^-$  ions. Unless otherwise specified fragments with intensity >10% are shown in the table.

$\alpha$ -ZOL Phase I metabolite								
Name	RT, min	M-H measured	M-H theoretical	ppm	Fragments, CID	Formula	Transformation	Comment
$\alpha$ -ZOL	13.63	319.1549	319.1545	1.3	257.2(4), 275.6(100), 301.5(80)	C <sub>18</sub> H <sub>24</sub> O <sub>5</sub>	parent	
$\beta$ -ZOL	12.41	319.1549	319.1545	1.3	275.5(100), 301.2(35)	C <sub>18</sub> H <sub>24</sub> O <sub>5</sub>	isomer	Non enzymatic
One more isomer	13.01	319.1549	319.1545	1.3	275.5(100), 301.2(10)	C <sub>18</sub> H <sub>24</sub> O <sub>5</sub>	isomer	Non enzymatic
ZEN	13.67	317.1394	317.1394	0	149.1(11), 175.1(10), 261.2(5), 273.5(100), 299.4(80)	C <sub>18</sub> H <sub>22</sub> O <sub>5</sub>	-(H <sub>2</sub> )	
Peak 1-331	9.05	331.1186	331.1182	1.2	287.2 (70), 303.2(100), 312.3(10), 313.2(15)	C <sub>18</sub> H <sub>20</sub> O <sub>6</sub>	-(H <sub>4</sub> )+(O)	
Peak 1-333	8.36 main	333.1343	333.1338	1.5	261.3(12), 289.3(68), 305.2(100), 315.2(10)	C <sub>18</sub> H <sub>22</sub> O <sub>6</sub>	-(H <sub>2</sub> )+(O)	
Peak 2-333	9.69	333.1342	333.1338	1.2	No ms2	C <sub>18</sub> H <sub>22</sub> O <sub>6</sub>	-(H <sub>2</sub> )+(O)	
Peak 3-333	11.94	333.1343	333.1338	1.5	190.0 (10), 191.0(82), 201.0(10), 219.1(10), 261.1(26), 289.2(100), 305.2(13), 314.2(20), 315.2(45)	C <sub>18</sub> H <sub>22</sub> O <sub>6</sub>	-(H <sub>2</sub> )+(O)	
Peak 4-333	12.33	333.1342	333.1338	1.2	191.0(40), 197.1(10), 271.3(10), 289.2(35), 313.1(12), 314.3(11), 315.2(100)	C <sub>18</sub> H <sub>22</sub> O <sub>6</sub>	-(H <sub>2</sub> )+(O)	

Name	RT, min	M-H measured	M-H theoretical	ppm	Fragments, CID	Formula	Transformation	Comment
Peak 5-333	12.63	333.1343	333.1338	1.5	175.1(18), 191.1(24), 203.0(28), 216.1(13), 271.24(20), 289.2(100), 313.1(21), 314.2(24), 315.2(95)	C <sub>18</sub> H <sub>22</sub> O <sub>6</sub>	-(H <sub>2</sub> )+(O)	
Peak 6-333	12.72	333.1341	333.1338	0.9	No ms2	C <sub>18</sub> H <sub>22</sub> O <sub>6</sub>	-(H <sub>2</sub> )+(O)	
Peak 1-335	7.70	335.1499	335.1495	1.2	No ms2	C <sub>18</sub> H <sub>24</sub> O <sub>6</sub>	+(O)	
Peak 2-335	9.33	335.1499	335.1495	1.2	No ms2	C <sub>18</sub> H <sub>24</sub> O <sub>6</sub>	+(O)	
Peak 3-335	11.31	335.1498	335.1495	0.9	161.0(14), 163.0(18), 190.0(18), 235.2(10), 273.2(22), 291.2(100), 317.2(52)	C <sub>18</sub> H <sub>24</sub> O <sub>6</sub>	+(O)	
Peak 4-335	11.86	335.1499	335.1495	1.2	190.0(30), 203.1(10), 219.1(10), 291.2(100), 292.2(15), 307.2(12), 317.2(20)	C <sub>18</sub> H <sub>24</sub> O <sub>6</sub>	+(O)	
Peak 5-335	12.34	335.1498	335.1495	0.9	163.1(10), 175.1(11), 189.1(34), 273.2(19), 291.2(100), 299.2(19), 315.0(14), 317.2(82)	C <sub>18</sub> H <sub>24</sub> O <sub>6</sub>	+(O)	
Peak 6-335	12.44	335.1499	335.1495	1.2	175.0(84), 179.1(24), 190.0(10), 247.2(10), 273.23(24), 291.2(80), 317.2(100)	C <sub>18</sub> H <sub>24</sub> O <sub>6</sub>	+(O)	
Peak 7-335	12.71	335.1498	335.1495	0.9	No ms2	C <sub>18</sub> H <sub>24</sub> O <sub>6</sub>	+(O)	

Name	RT, min	M-H measured	M-H theoretical	ppm	Fragments, CID	Formula	Transformation	Comment
Peak 8-335	13.18	335.1500	335.1495	1.5	175.0(40), 207.1(22), 247.2(22), 299.2(16), 317.3(100)	C <sub>18</sub> H <sub>24</sub> O <sub>6</sub>	+(O)	
<b><i>α</i>-ZOL Phase II metabolite</b>								
Name	RT, min	M-H measured	M-H theoretical	ppm	Fragments, CID	Formula	Transformation	Comment
Peak 1-493	5.95	493.1714	493.1710	0.8	No MS2	C <sub>24</sub> H <sub>30</sub> O <sub>11</sub>	+(C <sub>6</sub> H <sub>6</sub> O <sub>6</sub> )	Gluc-ZEN
Peak 2-493	7.44	493.1721	493.1710	2.2	175.0(22), 317.2(100), 411.1(10)	C <sub>24</sub> H <sub>30</sub> O <sub>11</sub>	+(C <sub>6</sub> H <sub>6</sub> O <sub>6</sub> )	Gluc-ZEN
Peak 1-495	5.66	495.1870	495.1866	0.8	175.1(20), 319.2(100), 451.2(36), 477.2(12)	C <sub>24</sub> H <sub>32</sub> O <sub>11</sub>	+(C <sub>6</sub> H <sub>8</sub> O <sub>6</sub> )	16-Gluc- <i>α</i> -ZOL
Peak 2-495	7.53	495.1871	495.1866	1.0	175.0(32), 319.2(100)	C <sub>24</sub> H <sub>32</sub> O <sub>11</sub>	+(C <sub>6</sub> H <sub>8</sub> O <sub>6</sub> )	14-Gluc- <i>α</i> -ZOL
Peak 3-495	12.37	495.1869	495.1866	0.6	451.5(100)	C <sub>24</sub> H <sub>32</sub> O <sub>11</sub>	+(C <sub>6</sub> H <sub>8</sub> O <sub>6</sub> )	7-Gluc- <i>α</i> -ZOL
Peak 1-511	6.01	511.1819	511.1816	0.6	No ms2	C <sub>24</sub> H <sub>32</sub> O <sub>12</sub>	+(C <sub>6</sub> H <sub>8</sub> O <sub>7</sub> )	Gluc-(+O)
Peak 2-511	6.51	511.1819	511.1816	0.6	No ms2	C <sub>24</sub> H <sub>32</sub> O <sub>12</sub>	+(C <sub>6</sub> H <sub>8</sub> O <sub>7</sub> )	Gluc-(+O)
Name	RT, min	M-H measured	M-H theoretical	ppm	Fragments, CID	Formula	Transformation	Comment
Peak 3-511	7.63	511.1814	511.1816	0.4	335.2(100), 493.2(11)	C <sub>24</sub> H <sub>32</sub> O <sub>12</sub>	+(C <sub>6</sub> H <sub>8</sub> O <sub>7</sub> )	Gluc-(+O)
Peak 4-511	8.94	511.1820	511.1816	0.8	175.1(16), 192.2(28), 317.3(18), 335.3(100), 347.1(57), 393.3(11), 397.0(10), 429.1(49), 451.0(14), 467.09(39), 493.1(34)	C <sub>24</sub> H <sub>32</sub> O <sub>12</sub>	+(C <sub>6</sub> H <sub>8</sub> O <sub>7</sub> )	Gluc-(+O)



<b>Name</b>	<b>RT, min</b>	<b>M-H measured</b>	<b>M-H theoretical</b>	<b>ppm</b>	<b>Fragments, CID</b>	<b>Formula</b>	<b>Transformation</b>	<b>Comment</b>
Peak 1- 671	5.31	671.2191	671.2187	0.6	495.2(100)	C <sub>30</sub> H <sub>40</sub> O <sub>17</sub>	+C <sub>12</sub> H <sub>16</sub> O <sub>12</sub>	di-Gluc- $\alpha$ - ZAL

Supplementary Table B15. Metabolites of  $\beta$ -ZOL generated in Phase I and Phase II. Metabolites detected in ESI(-), as  $[M-H]^-$  ions. Unless otherwise specified fragments with intensity >10% are shown in the table.

<b><math>\beta</math>-ZOL Phase II metabolite</b>								
Name	RT, min	M-H measured	M-H theoretical	ppm	Fragments, CID	Formula	Transformation	Comment
$\beta$ -ZOL	12.42	319.1547	319.1545	0.6	275.2(100), 301.5(80)	$C_{18}H_{24}O_5$	parent	
$\alpha$ -ZOL	13.62	319.1552	319.1545	2.2	274.3(24), 275.5(100), 300.2(12), 301.2(26)	$C_{18}H_{24}O_5$	isomer	Non-enzymatic
ZEN	13.67	317.1396	317.1394	0.6	149.1(11), 175.1(10), 273.46(100), 299.38(85)	$C_{18}H_{22}O_5$	-(H <sub>2</sub> )	
Peak 1-335	7.55	335.1499	335.1495	1.2	190.0(28), 291.2(100), 292.2(11), 307.2(10), 317.2(15)	$C_{18}H_{24}O_6$	+(O)	
Peak 2-335	8.68	335.1499	335.1495	1.2	175.0(100), 273.2(10), 291.2(15), 317.2(15)	$C_{18}H_{24}O_6$	+(O)	Only in heated
Peak 3-335	8.90	335.1499	335.1495	1.2	No ms2	$C_{18}H_{24}O_6$	+(O)	
Peak 4-335	11.64	335.1499	335.1495	1.2	175.0(100), 273.2(10), 291.2(30), 315.1(10), 317.2(24)	$C_{18}H_{24}O_6$	+(O)	
Peak 5-335	12.03	335.1499	335.1495	1.2	No ms2	$C_{18}H_{24}O_6$	+(O)	
Peak 6-335	12.17	335.1499	335.1495	1.2	193.1 (40), 273.3(15), 291.2(35), 315.07(10), 317.3(100)	$C_{18}H_{24}O_6$	+(O)	
Peak 7-335	12.35	335.1499	335.1495	1.2	No ms2	$C_{18}H_{24}O_6$	+(O)	
Peak 1-333	8.43	333.1343	333.1338	1.5	261.2(15), 289.2(73), 305.2(100), 315.2(12)	$C_{18}H_{22}O_6$	-(H <sub>2</sub> )+(O)	

Name	RT, min	M-H measured	M-H theoretical	ppm	Fragments, CID	Formula	Transformation	Comment
Peak 1-331	9.16	331.1186	331.1182	1.2	No ms2	C <sub>18</sub> H <sub>20</sub> O <sub>6</sub>	-(H <sub>4</sub> )+(O)	
<b>β-ZOL Phase II metabolite</b>								
Name	RT	M-H measured	M-H theoretical	ppm	Fragments, CID	Formula	Transformation	Comment
Peak 1-495	5.57	495.1871	495.1866	1.0	175.0(20), 319.2(100), 451.3(27), 477.2(10)	C <sub>24</sub> H <sub>32</sub> O <sub>11</sub>	+(C <sub>6</sub> H <sub>8</sub> O <sub>6</sub> )	16-Gluc-β-ZOL
Peak 2-495	6.00	495.1871	495.1866	1.0	175.0(28), 319.2(100), 451.3(14)	C <sub>24</sub> H <sub>32</sub> O <sub>11</sub>	+(C <sub>6</sub> H <sub>8</sub> O <sub>6</sub> )	14-Gluc-β-ZOL
Peak 3-495	8.96	495.1871	495.1866	1.0	407.3(11), 451.3(100), 477.2(15)	C <sub>24</sub> H <sub>32</sub> O <sub>11</sub>	+(C <sub>6</sub> H <sub>8</sub> O <sub>6</sub> )	7-Gluc-β-ZOL
Peak 1-493	5.96	493.1718	493.1710	1.6	No ms2	C <sub>24</sub> H <sub>30</sub> O <sub>11</sub>	+(C <sub>6</sub> H <sub>6</sub> O <sub>6</sub> )	
Peak 2-493	7.59	493.1714	493.1710	0.8	175.0(23), 317.2(100), 411.0(22), 432.92(10)	C <sub>24</sub> H <sub>30</sub> O <sub>11</sub>	+(C <sub>6</sub> H <sub>6</sub> O <sub>6</sub> )	
Peak 1-511	5.86	511.1819	511.1816	0.6	335.4(100)	C <sub>24</sub> H <sub>32</sub> O <sub>12</sub>	+(C <sub>6</sub> H <sub>8</sub> O <sub>7</sub> )	
Peak 1-671	5.15	671.2191	671.2187	0.6	495.4(100)	C <sub>30</sub> H <sub>40</sub> O <sub>17</sub>	+(C <sub>12</sub> H <sub>16</sub> O <sub>12</sub> )	di-Gluc-β-ZOL

Supplementary Table B16. Metabolites of ZAN generated in Phase I and Phase II. Metabolites detected in ESI(-), as  $[M-H]^-$  ions. Unless otherwise specified fragments with intensity >10% are shown in the table.

ZAN Phase I metabolites								
Name	RT, min	M-H measured	M-H theoretical	ppm	Fragments, CID	Formula	Transformation	Comment
ZAN	13.35	319.1545	319.1545	0.0	205.2(26), 275.5(100), 301.5(70)	C <sub>18</sub> H <sub>24</sub> O <sub>5</sub>	parent	
β-ZAL	11.33	321.1707	321.1702	1.6	277.5(100), 303.2(20)	C <sub>18</sub> H <sub>26</sub> O <sub>5</sub>	+(H <sub>2</sub> )	
α-ZAL	12.92	321.1707	321.1702	1.6	277.6(100), 303.5(86)	C <sub>18</sub> H <sub>26</sub> O <sub>5</sub>	+(H <sub>2</sub> )	
Peak 1-333	9.14	333.1341	333.1338	0.9	289.5(92), 305.5(100), 315.2(12)	C <sub>18</sub> H <sub>22</sub> O <sub>6</sub>	-(H <sub>2</sub> )+(O)	
Peak 1-335	8.69	335.1497	335.1495	0.6	291.2(30), 307.5(100)	C <sub>18</sub> H <sub>24</sub> O <sub>6</sub>	+(O)	
Peak 2-335	9.06	335.1497	335.1495	0.6	290.3(38), 291.2(34), 306.4(100), 307.2(18), 317.2(16)	C <sub>18</sub> H <sub>24</sub> O <sub>6</sub>	+(O)	
Peak 3-335	9.41	335.1497	335.1495	0.6	290.4(10), 291.5(100), 306.2(12), 317.2(12)	C <sub>18</sub> H <sub>24</sub> O <sub>6</sub>	+(O)	
Peak 4-335	11.05	335.1498	335.1495	0.9	291.2(45), 317.2(100)	C <sub>18</sub> H <sub>24</sub> O <sub>6</sub>	+(O)	
Peak 5-335	12.11	335.1498	335.1495	0.9	193.1(12), 221.1(10), 273.2(14), 291.2(100), 307.2(14), 317.18(85)	C <sub>18</sub> H <sub>24</sub> O <sub>6</sub>	+(O)	
Peak 1-337	6.47	337.1656	337.1651	1.5	No MS2	C <sub>18</sub> H <sub>26</sub> O <sub>6</sub>	+(H <sub>2</sub> )+(O)	
Peak 2-337	6.83	337.1656	337.1651	1.5	177.1(14), 231.2(12), 275.2(24), 293.2(100) 319.2(16)	C <sub>18</sub> H <sub>26</sub> O <sub>6</sub>	+(H <sub>2</sub> )+(O)	

Name	RT, min	M-H measured	M-H theoretical	ppm	Fragments, CID	Formula	Transformation	Comment
Peak 3-337	7.45	337.1655	337.1651	1.2	No MS2	C <sub>18</sub> H <sub>26</sub> O <sub>6</sub>	+(H <sub>2</sub> )+(O)	
Peak 4-337	7.65	337.1656	337.1651	1.5	No MS2	C <sub>18</sub> H <sub>26</sub> O <sub>6</sub>	+(H <sub>2</sub> )+(O)	
Peak 5-337	9.78	337.1656	337.1651	1.5	177.1(10), 231.1(8), 275.2(14), 293.4(100), 319.2(10)	C <sub>18</sub> H <sub>26</sub> O <sub>6</sub>	+(H <sub>2</sub> )+(O)	
Peak 6-337	10.31	337.1656	337.1651	1.5	No MS2	C <sub>18</sub> H <sub>26</sub> O <sub>6</sub>	+(H <sub>2</sub> )+(O)	
Peak 7-337	11.74 main	337.1656	337.1651	1.5	177.0(16), 275.2(22), 293.3(100) 319.22(20)	C <sub>18</sub> H <sub>26</sub> O <sub>6</sub>	+(H <sub>2</sub> )+(O)	
Peak 8-337	12.20	337.1653	337.1651	0.6	No MS2	C <sub>18</sub> H <sub>26</sub> O <sub>6</sub>	+(H <sub>2</sub> )+(O)	
Peak 1-349	6.44	349.1291	349.1287	1.1	No MS2	C <sub>18</sub> H <sub>22</sub> O <sub>7</sub>	+(H <sub>2</sub> )+(O)	
Peak 2-349	6.86	349.1291	349.1287	1.1	163.0(20), 177.0(45), 179.1(15), 191.1(48), 217.1(44), 235.1(70), 261.2(11), 267.1(10), 277.2(22), 287.2(41), 303.2(11), 305.2(100), 321.2(98), 330.4(16), 331.2(68), 339.7(10)	C <sub>18</sub> H <sub>22</sub> O <sub>7</sub>	-(H <sub>2</sub> )+(O <sub>2</sub> )	
Peak 1-351	6.34	351.1447	351.1444	0.9	No MS2	C <sub>18</sub> H <sub>24</sub> O <sub>7</sub>	+(O <sub>2</sub> )	

Name	RT, min	M-H measured	M-H theoretical	ppm	Fragments, CID	Formula	Transformation	Comment
Peak 2-351	6.79	351.1447	351.1444	0.9	191.0(10), 205.0(14), 269.0(15), 279.2(20), 289.2(11), 307.2(100), 323.2(70), 333.1(32)	C <sub>18</sub> H <sub>24</sub> O <sub>7</sub>	+(O <sub>2</sub> )	
Peak 3-351	7.15	351.1447	351.1444	0.9	No MS2	C <sub>18</sub> H <sub>24</sub> O <sub>7</sub>	+(O <sub>2</sub> )	
Peak 4-351	7.62	351.1448	351.1444	1.1	219.1(18), 307.3(28), 333.2(100)	C <sub>18</sub> H <sub>24</sub> O <sub>7</sub>	+(O <sub>2</sub> )	
Peak 5-351	8.28	351.1448	351.1444	1.1	289.2(24), 307.3(100), 333.2(68)	C <sub>18</sub> H <sub>24</sub> O <sub>7</sub>	+(O <sub>2</sub> )	
Peak 6-351	9.06	351.1447	351.1444	0.9	269.0(10), 289.2(15), 307.3(40), 315.3(16), 333.3(100)	C <sub>18</sub> H <sub>24</sub> O <sub>7</sub>	+(O <sub>2</sub> )	Low intensity peak
<b>ZAN Phase II metabolites</b>								
Fragments	Formula	Transformation	Comment	ppm	Fragments, CID	Formula	Transformation	Comment
Peak 1-497	5.70	497.2026	497.2023	0.6	175.0(25), 321.2(100), 453.2(30), 479.1(15)	C <sub>24</sub> H <sub>34</sub> O <sub>11</sub>	+(C <sub>6</sub> H <sub>10</sub> O <sub>6</sub> )	
Peak 2-497	5.90	497.2025	497.2023	0.4	175.0(50), 321.2(100), 452.2(10)	C <sub>24</sub> H <sub>34</sub> O <sub>11</sub>	+(C <sub>6</sub> H <sub>10</sub> O <sub>6</sub> )	
Peak 3-497	6.53	497.2026	497.2023	0.6	175.0(40), 321.2(100)	C <sub>24</sub> H <sub>34</sub> O <sub>11</sub>	+(C <sub>6</sub> H <sub>10</sub> O <sub>6</sub> )	
Peak 4-497	10.25	497.2025	497.2023	0.4	321.2(10), 415.2(10), 453.2(100), 479.2(24)	C <sub>24</sub> H <sub>34</sub> O <sub>11</sub>	+(C <sub>6</sub> H <sub>10</sub> O <sub>6</sub> )	
Peak 1-495	5.96	495.1872	495.1866	1.2	175.0(20), 319.2(100), 451.2(28), 477.2(10)	C <sub>24</sub> H <sub>32</sub> O <sub>11</sub>	+(C <sub>6</sub> H <sub>8</sub> O <sub>6</sub> )	
Peak 2-495	7.18	495.1869	495.1866	0.6	175.0(30), 319.2(100), 477.2(5)	C <sub>24</sub> H <sub>32</sub> O <sub>11</sub>	+(C <sub>6</sub> H <sub>8</sub> O <sub>6</sub> )	

Name	RT, min	M-H measured	M-H theoretical	ppm	Fragments, CID	Formula	Transformation	Comment
Peak 1-513	5.07	513.1975	513.1972	0.6	No MS2	C <sub>24</sub> H <sub>34</sub> O <sub>12</sub>	+(C <sub>6</sub> H <sub>10</sub> O <sub>7</sub> )	
Peak 2-513	5.55	513.1974	513.1972	0.4	No MS2	C <sub>24</sub> H <sub>34</sub> O <sub>12</sub>	+(C <sub>6</sub> H <sub>10</sub> O <sub>7</sub> )	
Peak 3-513	5.90	513.1973	513.1972	0.2	175.0(20), 337.2(100)	C <sub>24</sub> H <sub>34</sub> O <sub>12</sub>	+(C <sub>6</sub> H <sub>10</sub> O <sub>7</sub> )	
Peak 4-513	8.12	513.1974	513.1972	0.4	No MS2	C <sub>24</sub> H <sub>34</sub> O <sub>12</sub>	+(C <sub>6</sub> H <sub>10</sub> O <sub>7</sub> )	
Peak 5-513	8.45	513.1974	513.1972	0.4	175.0(2), 337.2(100), 469.2(40), 495.2(15),	C <sub>24</sub> H <sub>34</sub> O <sub>12</sub>	+(C <sub>6</sub> H <sub>10</sub> O <sub>7</sub> )	
Peak 1-511	5.31	511.1818	511.1816	0.4	No MS2	C <sub>24</sub> H <sub>32</sub> O <sub>12</sub>	+(C <sub>6</sub> H <sub>8</sub> O <sub>7</sub> )	
Peak 2-511	5.58	511.1818	511.1816	0.4	No MS2	C <sub>24</sub> H <sub>32</sub> O <sub>12</sub>	+(C <sub>6</sub> H <sub>8</sub> O <sub>7</sub> )	
Peak 3-511	5.98	511.1818	511.1816	0.4	175.0(20), 335.2(100), 493.2(10)	C <sub>24</sub> H <sub>32</sub> O <sub>12</sub>	+(C <sub>6</sub> H <sub>8</sub> O <sub>7</sub> )	
Peak 4-511	6.50	511.1818	511.1816	0.4	335.2(100)	C <sub>24</sub> H <sub>32</sub> O <sub>12</sub>	+(C <sub>6</sub> H <sub>8</sub> O <sub>7</sub> )	
Peak 5-511	6.55	511.1814	511.1816	0.4	335.2(100)	C <sub>24</sub> H <sub>32</sub> O <sub>12</sub>	+(C <sub>6</sub> H <sub>8</sub> O <sub>7</sub> )	
Peak 6-511	9.41	511.1819	511.1816	0.6	335.2(100), 493.2(10)	C <sub>24</sub> H <sub>32</sub> O <sub>12</sub>	+(C <sub>6</sub> H <sub>8</sub> O <sub>7</sub> )	
Peak 1-671	5.80	671.2189	671.2187	0.3	495.4(100)	C <sub>30</sub> H <sub>40</sub> O <sub>17</sub>	+(C <sub>12</sub> H <sub>16</sub> O <sub>12</sub> )	di-Gluc-ZAN
Peak 1-673	5.39	673.2344	673.2344	0	497.4(100)	C <sub>30</sub> H <sub>42</sub> O <sub>17</sub>	+(C <sub>12</sub> H <sub>18</sub> O <sub>12</sub> )	di-Gluc- $\alpha$ -ZAL

<b>Name</b>	<b>RT, min</b>	<b>M-H measured</b>	<b>M-H theoretical</b>	<b>ppm</b>	<b>Fragments, CID</b>	<b>Formula</b>	<b>Transformation</b>	<b>Comment</b>
Peak 1-687	5.16	687.2139	687.2136	0.44	No MS2	C <sub>30</sub> H <sub>40</sub> O <sub>18</sub>	+(C <sub>12</sub> H <sub>16</sub> O <sub>13</sub> )	di-Gluc-(+O))
Peak 2-687	6.17	687.2139	687.2136	0.44	No MS2	C <sub>30</sub> H <sub>40</sub> O <sub>18</sub>	+(C <sub>12</sub> H <sub>16</sub> O <sub>13</sub> )	di-Gluc-(+O))
Peak 1-689	5.07	689.2296	689.2293	0.4	No MS2	C <sub>30</sub> H <sub>42</sub> O <sub>18</sub>	+(C <sub>12</sub> H <sub>18</sub> O <sub>13</sub> )	di-Gluc-(+(H2)+(O))
Peak 2-689	5.69	689.2296	689.2293	0.4	No MS2	C <sub>30</sub> H <sub>42</sub> O <sub>18</sub>	+(C <sub>12</sub> H <sub>18</sub> O <sub>13</sub> )	di-Gluc-(+(H2)+(O))



Supplementary Table B17. Metabolites of  $\alpha$ -ZAL generated in Phase I and Phase II. Metabolites detected in ESI(-), as  $[M-H]^-$  ions. Unless otherwise specified fragments with intensity >10% are shown in the table.

$\alpha$ -ZAL Phase I metabolite								
Name	RT, min	M-H measured	M-H theoretical	ppm	Fragments, CID	Formula	Transformation	Comment
$\alpha$ -ZAL	12.91	321.1704	321.1702	0.6	277.5(100), 303.5(85)	C <sub>18</sub> H <sub>26</sub> O <sub>5</sub>	parent	
$\beta$ -ZAL	11.33	321.1707	321.1702	1.6	277.5(100), 303.2(20)	C <sub>18</sub> H <sub>26</sub> O <sub>5</sub>	isomer	Non enzymatic
ZAN	13.34	319.15460	319.1545	0.3	205.2(19), 275.5(100), 301.2(25)	C <sub>18</sub> H <sub>24</sub> O <sub>5</sub>	-(H <sub>2</sub> )	
Peak 1-333	9.18	333.1344	333.1338	1.8	289.2(80), 305.2(100), 315.1(20)	C <sub>18</sub> H <sub>22</sub> O <sub>6</sub>	-(H <sub>4</sub> )+(O)	
Peak 1-335	8.74	335.1499	335.1495	1.2	263.3(10), 291.3(75), 307.5(100), 317.8(15)	C <sub>18</sub> H <sub>24</sub> O <sub>6</sub>	-(H <sub>2</sub> )+(O)	
Peak 2-335	11.11	335.1499	335.1495	1.2	291.2(50), 307.2(15), 315.1(12), 317.2(100)	C <sub>18</sub> H <sub>24</sub> O <sub>6</sub>	-(H <sub>2</sub> )+(O)	
Peak 3-335	12.11	335.1499	335.1495	1.2	291.5(100), 317.5(75)	C <sub>18</sub> H <sub>24</sub> O <sub>6</sub>	-(H <sub>2</sub> )+(O)	
Peak 1-337	6.83	337.1657	337.1651	1.8	177.1(15), 231.1(10), 275.2(20), 293.2(100), 319.2(20)	C <sub>18</sub> H <sub>26</sub> O <sub>6</sub>	+O	found only in heated
Peak 2-337	10.34	337.1657	337.1651	1.8	293.4(100), 319.2(27)	C <sub>18</sub> H <sub>26</sub> O <sub>6</sub>	+O	found only in heated
Peak 3-337	11.75	337.1657	337.1651	1.8	177.1(15), 255.2(10), 275.2(20), 293.2(100), 319.2(24)	C <sub>18</sub> H <sub>26</sub> O <sub>6</sub>	+O	
Peak 4-337	12.21	337.1657	337.1651	1.8	177.1(6), 221.1(14), 293.5(100), 318.3(10), 319.2(20)	C <sub>18</sub> H <sub>26</sub> O <sub>6</sub>	+O	

Name	RT, min	M-H measured	M-H theoretical	ppm	Fragments, CID	Formula	Transformation	Comment
Peak 1-349	6.85	349.1293	349.1287	1.7	No MS2	C <sub>18</sub> H <sub>22</sub> O <sub>7</sub>	-(H <sub>4</sub> ) +(O <sub>2</sub> )	
Peak 1-351	6.78	351.1449	351.1444	1.4	No MS2	C <sub>18</sub> H <sub>24</sub> O <sub>7</sub>	-(H <sub>2</sub> ) +(O <sub>2</sub> )	
<b><i>α</i>-ZAL Phase II metabolite</b>								
Name	RT, min	M-H measured	M-H theoretical	ppm	Fragments, CID	Formula	Transformation	Comment
Peak 1-497	5.70	497.2027	497.2023	0.8	175.0(25), 321.2(100), 453.2(25), 479.2(10)	C <sub>24</sub> H <sub>34</sub> O <sub>11</sub>	+(C <sub>6</sub> H <sub>8</sub> O <sub>6</sub> )	May be 16-Gluc-β-ZAL
Peak 2-497	5.89	497.2026	497.2023	0.6	175.0(40), 321.2(100), 441.2(14), 453.20(15), 479.1(20)	C <sub>24</sub> H <sub>34</sub> O <sub>11</sub>	+(C <sub>6</sub> H <sub>8</sub> O <sub>6</sub> )	Then it is 16-Gluc-α-ZAL
Peak 3-497	6.56	497.2026	497.2023	0.6	175.0(35), 321.2(100)	C <sub>24</sub> H <sub>34</sub> O <sub>11</sub>	+(C <sub>6</sub> H <sub>8</sub> O <sub>6</sub> )	14-Gluc-α-ZAL
Peak 4-497	10.19	497.2026	497.2023	0.6	453.3(100), 479.2(15)	C <sub>24</sub> H <sub>34</sub> O <sub>11</sub>	+(C <sub>6</sub> H <sub>8</sub> O <sub>6</sub> )	7-Gluc-α-ZAL
Peak 5-497	12.10	497.2026	497.2023	0.6	321.2(10), 453.5(100), 479.2(30), 498.3(10)	C <sub>24</sub> H <sub>34</sub> O <sub>11</sub>	+(C <sub>6</sub> H <sub>8</sub> O <sub>6</sub> )	Shallow peak
Peak 1-495	5.94	495.1871	495.1866	1.0	No MS2	C <sub>24</sub> H <sub>32</sub> O <sub>11</sub>	+(C <sub>6</sub> H <sub>6</sub> O <sub>6</sub> )	16-Gluc-ZAN
Peak 2-495	7.34*	495.1871	495.1866	1.0	175.0(30), 319.2(100), 413.1(15), 477.1(14)	C <sub>24</sub> H <sub>32</sub> O <sub>11</sub>	+(C <sub>6</sub> H <sub>6</sub> O <sub>6</sub> )	14-Gluc-ZAN
Peak 1 to 3 - 511	5.99, 7.39, 9.36	511.1819	511.1816	0.6	No MS2, low intensity	C <sub>24</sub> H <sub>32</sub> O <sub>12</sub>	+(C <sub>6</sub> H <sub>6</sub> O <sub>7</sub> )	Gluc+(O)-(H <sub>2</sub> )
Peak 1-513	5.08	513.1975	513.1972	0.6	No MS2	C <sub>24</sub> H <sub>34</sub> O <sub>12</sub>	+(C <sub>6</sub> H <sub>6</sub> O <sub>7</sub> )	Gluc+(O)

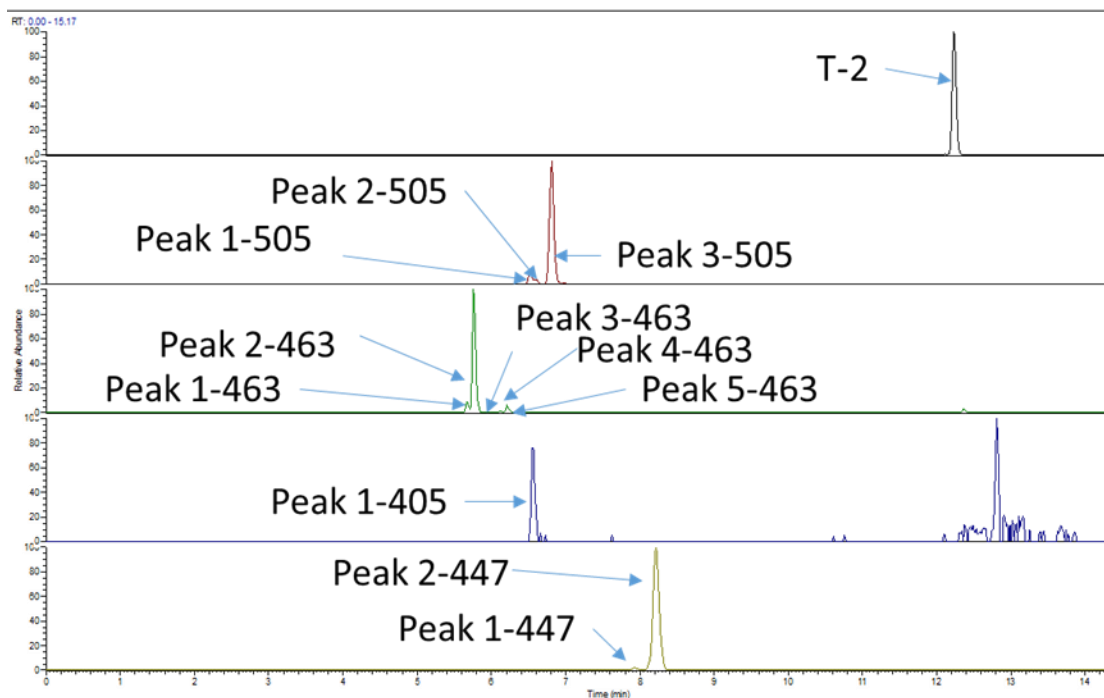
<b>Name</b>	<b>RT, min</b>	<b>M-H measured</b>	<b>M-H theoretical</b>	<b>ppm</b>	<b>Fragments, CID</b>	<b>Formula</b>	<b>Transformation</b>	<b>Comment</b>
Peak 2-513	5.89 - 6.1	513.1975	513.1972	0.6	No MS2	C <sub>24</sub> H <sub>34</sub> O <sub>12</sub>	+(C <sub>6</sub> H <sub>6</sub> O <sub>7</sub> )	Gluc+(O)
Peak 3-513	8.45	513.1975	513.1972	0.6	337.2(100), 469.2(28), 495.1(15)	C <sub>24</sub> H <sub>34</sub> O <sub>12</sub>	+(C <sub>6</sub> H <sub>6</sub> O <sub>7</sub> )	Gluc+(O)
Peak 1-671	5.72	671.2192	671.2187	0.7	No ms2, low intensity peak	C <sub>30</sub> H <sub>40</sub> O <sub>17</sub>	+(C <sub>12</sub> H <sub>14</sub> O <sub>12</sub> )	di-Gluc-ZAN
Peak 1-673	5.38	673.2345	673.2344	0.1	497.4(100)	C <sub>30</sub> H <sub>42</sub> O <sub>17</sub>	+(C <sub>12</sub> H <sub>16</sub> O <sub>12</sub> )	di-Gluc- $\alpha$ -ZAL

Supplementary Table B18. Metabolites of  $\beta$ -ZAL generated in Phase I and Phase II. Metabolites detected in ESI(-), as  $[M-H]^-$  ions. Unless otherwise specified fragments with intensity >10% are shown in the table.

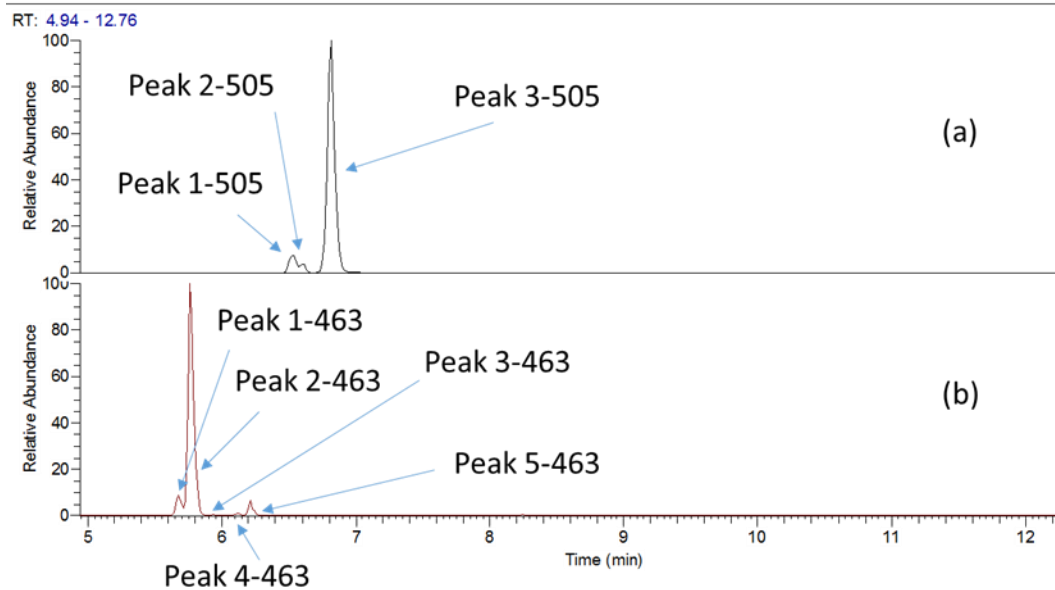
<b><math>\beta</math>-ZAL Phase I metabolites</b>								
Name	RT, min	M-H measured	M-H theoretical	ppm	Fragments, CID	Formula	Transformation	Comment
$\beta$ -ZAL	11.48	321.1748	321.1702		277.5(100), 293.3(4), 303.4(60)	C <sub>18</sub> H <sub>26</sub> O <sub>5</sub>	parent	
$\alpha$ -ZAL	12.94	321.1707	321.1702	1.6	277.6(100), 303.2(35)	C <sub>18</sub> H <sub>26</sub> O <sub>5</sub>	isomer	
ZAN	13.39	319.1549	319.1545	1.3	205.2(25), 275.5(100), 301.4(75)	C <sub>18</sub> H <sub>24</sub> O <sub>5</sub>	-(H <sub>2</sub> )	
Peak1-333	9.17	333.1343	333.1338	1.5	289.2(85), 305.2(100), 315.1(28)	C <sub>18</sub> H <sub>22</sub> O <sub>6</sub>	-(H <sub>4</sub> )+(O)	13-OH-ZAN quinone
Peak 1-335	7.89	335.1499	335.1495	1.2	123.1(12), 175.1(22), 219.1(20), 253.0(30), 273.3(15), 291.2(100), 303.1(18), 307.2(20), 315.2(35), 317.1(40)	C <sub>18</sub> H <sub>24</sub> O <sub>6</sub>	-(H <sub>2</sub> )+(O)	
Peak 2-335	8.78	335.1499	335.1495	1.2	263.2(12), 291.2(85), 307.2(100), 317.2(20)	C <sub>18</sub> H <sub>24</sub> O <sub>6</sub>	-(H <sub>2</sub> )+(O)	13-OH- $\alpha$ -ZAL quinone
Peak 3-335	11.16	335.1498	335.1495	0.9	211.0(10), 253.0(22), 291.2(65), 292.2(10), 307.29(24), 315.1(24), 317.2(100), 318.2(10)	C <sub>18</sub> H <sub>24</sub> O <sub>6</sub>	-(H <sub>2</sub> )+(O)	15-OH-ZAN
Peak 4-335	12.13	335.1499	335.1495	1.2	291.5(100), 317.5(98)	C <sub>18</sub> H <sub>24</sub> O <sub>6</sub>	-(H <sub>2</sub> )+(O)	13-OH-ZAN
Peak 1-337	5.78	337.1656	337.1651	1.5	No MS2	C <sub>18</sub> H <sub>26</sub> O <sub>6</sub>	+(O)	

Name	RT, min	M-H measured	M-H theoretical	ppm	Fragments, CID	Formula	Transformation	Comment
Peak 2-337	6.49	337.1656	337.1651	1.5	177.1(12), 221.1(30), 275.2(15), 293.2(100), 319.2(20)	C <sub>18</sub> H <sub>26</sub> O <sub>6</sub>	+(O)	
Peak 3-337	7.50	337.1656	337.1651	1.5	177.1(19), 255.2(15), 275.2(23), 293.2(100), 319.19(15)	C <sub>18</sub> H <sub>26</sub> O <sub>6</sub>	+(O)	
Peak 4-337	7.67	337.1656	337.1651	1.5	293.5(100), 319.3(30)	C <sub>18</sub> H <sub>26</sub> O <sub>6</sub>	+(O)	
Peak 5-337	8.13	337.1656	337.1651	1.5	No MS2	C <sub>18</sub> H <sub>26</sub> O <sub>6</sub>	+(O)	
Peak 6-337	9.25	337.1655	337.1651	1.2	221.1(15), 293.5(100), 319.2(22)	C <sub>18</sub> H <sub>26</sub> O <sub>6</sub>	+(O)	
Peak 7-337	9.88	337.1655	337.1651	1.2	No MS2	C <sub>18</sub> H <sub>26</sub> O <sub>6</sub>	+(O)	
Peak 8-337	11.88	337.1655	337.1651	1.2	No MS2	C <sub>18</sub> H <sub>26</sub> O <sub>6</sub>	+(O)	
Peak 1-349	6.83	349.1292	349.1287	1.4	No MS2	C <sub>18</sub> H <sub>26</sub> O <sub>6</sub>	-(H <sub>4</sub> ) +(O <sub>2</sub> )	
Peak 1-351	6.74	351.1449	351.1444	1.4	No MS2	C <sub>18</sub> H <sub>26</sub> O <sub>6</sub>	-(H <sub>2</sub> ) +(O <sub>2</sub> )	
<b>β-ZAL Phase II metabolites</b>								
Name	RT, min	M-H measured	M-H theoretical	ppm	Fragments, CID	Formula	Transformation	Comment
Peak 1-497	5.67	497.2027	497.2023	0.8	175.0(30), 321.3(100), 453.3(30), 479.2(10)	C <sub>24</sub> H <sub>34</sub> O <sub>11</sub>	+(C <sub>6</sub> H <sub>8</sub> O <sub>6</sub> )	16-Gluc-β-ZAL
Peak 2-497	5.86	497.2027	497.2023	0.8	175.0(42), 321.3(100)	C <sub>24</sub> H <sub>34</sub> O <sub>11</sub>	+(C <sub>6</sub> H <sub>8</sub> O <sub>6</sub> )	14-Gluc-β-ZAL
Peak 3-497	7.67	497.2028	497.2023	1.0	321.2(18), 403.2(14), 409.3(22), 453.2(100), 479.2(42)	C <sub>24</sub> H <sub>34</sub> O <sub>11</sub>	+(C <sub>6</sub> H <sub>8</sub> O <sub>6</sub> )	7-Gluc-β-ZAL

Peak 1-495	7.31	495.1871	495.1866	1.0	No MS2	C <sub>24</sub> H <sub>32</sub> O <sub>11</sub>	+(C <sub>6</sub> H <sub>6</sub> O <sub>6</sub> )	14-Gluc-ZAN
Peak 1-513	5.71	513.1975	513.1972	0.6	No MS2	C <sub>24</sub> H <sub>34</sub> O <sub>12</sub>	+(C <sub>6</sub> H <sub>8</sub> O <sub>7</sub> )	Gluc+(O)
Peak 2-513	6.29	513.1976	513.1972	0.8	337.2(100), 495.2(12)	C <sub>24</sub> H <sub>34</sub> O <sub>12</sub>	+(C <sub>6</sub> H <sub>8</sub> O <sub>7</sub> )	Gluc+(O)
Peak 1-673	5.42	673.2342	673.2344	0.3	497.2(100)	C <sub>30</sub> H <sub>42</sub> O <sub>17</sub>	+(C <sub>12</sub> H <sub>16</sub> O <sub>12</sub> )	di-Gluc-β-ZAL

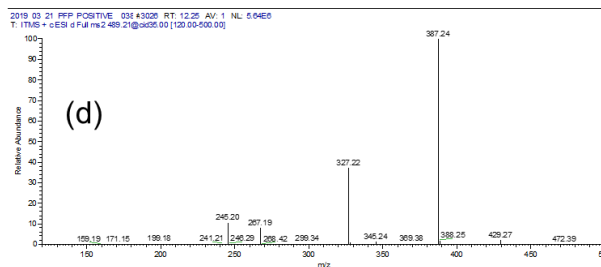
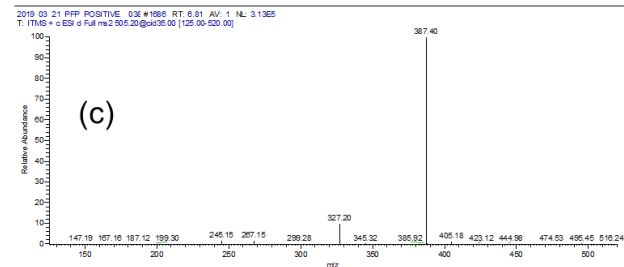
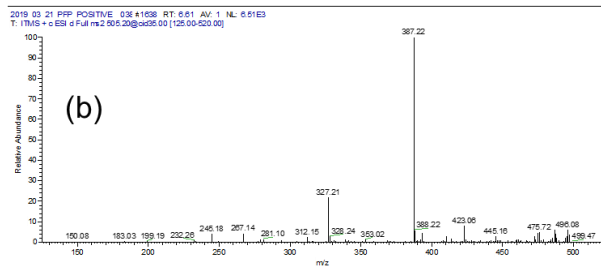
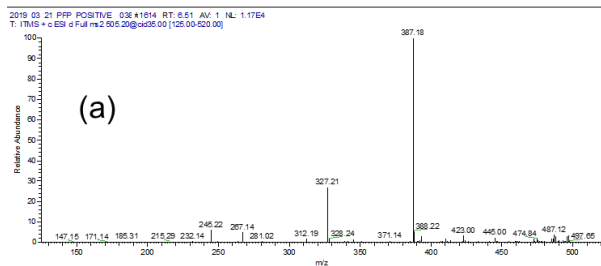


*Supplementary Figure B1. Chromatographic separation of T-2 and its metabolites. Extracted ion chromatogram of peak 1-505 to peak 3-505 with 505.2044 m/z, peak 1-463 to peak 5-463 with 463.1939 m/z peak, peak 1-405 with 405.1884 m/z, peak 1-447 and peak 2-447 with 447.1989 m/z detected in ESI(+), as  $[M+Na]^+$  ions are shown.*

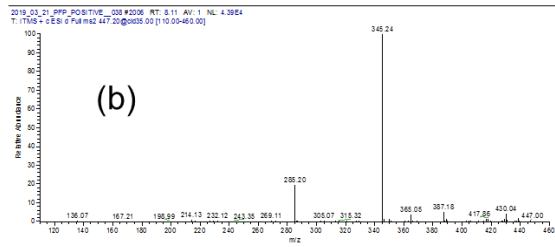
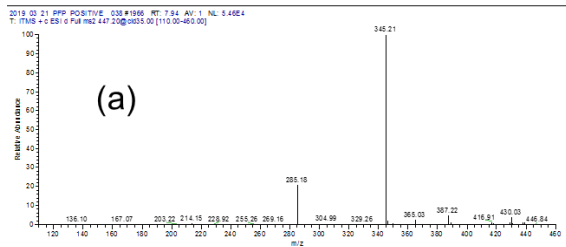


*Supplementary Figure B2. Extracted ion chromatograms of T-2 hydroxyl metabolites. Zooming into extracted ion chromatogram of T-2 (505.2044 m/z) and HT-2 (463.1938 m/z) hydroxyl metabolites detected in ESI(+), as  $[M+Na]^+$  ions are shown. Panel (a) shows T-2 hydroxyl metabolites, panel (b) shows HT-2 hydroxyl metabolites.*

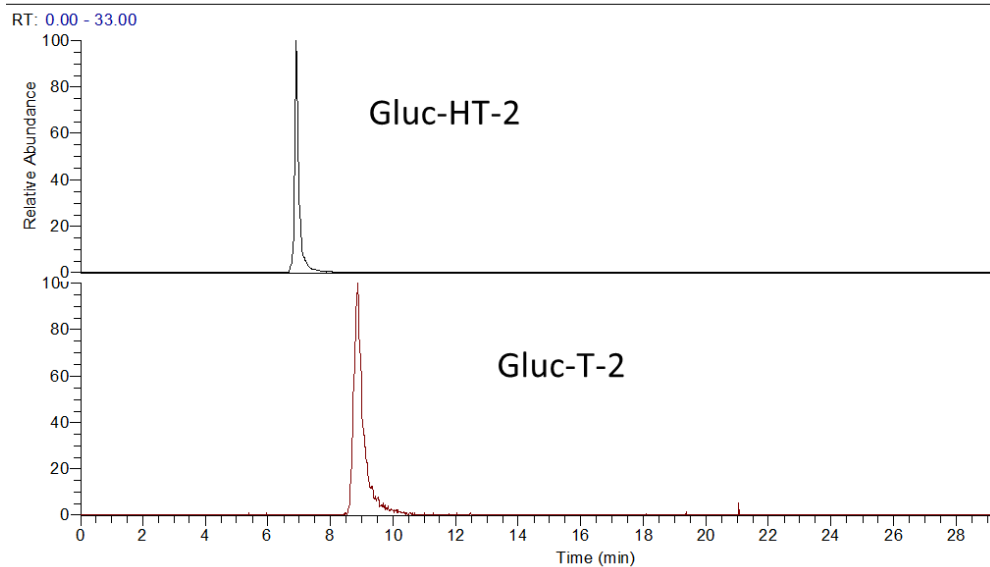




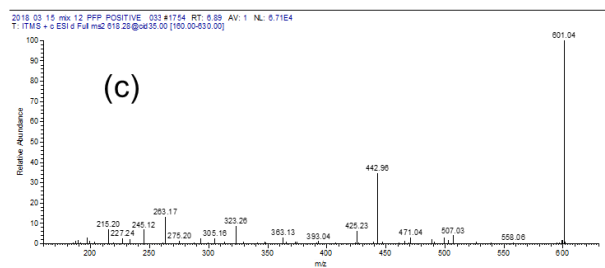
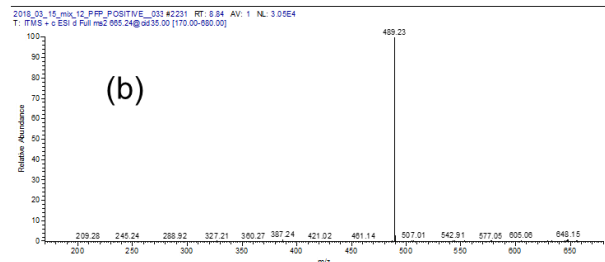
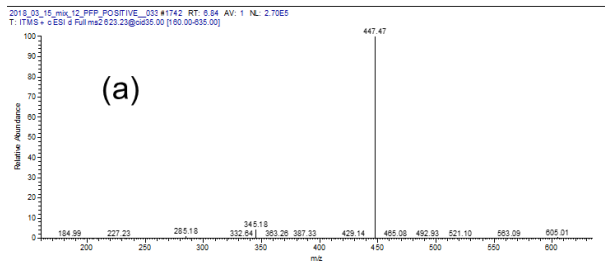
Supplementary Figure B3. Product ion spectra of T-2 hydroxy metabolites. The hydroxy metabolites at 505.2044 m/z, peak 1-505 (a), peak 2-505 (b), peak 3-505 (c) and at 489.2095, T-2 (d), detected in ESI(+), as  $[M+Na]^+$  ions.



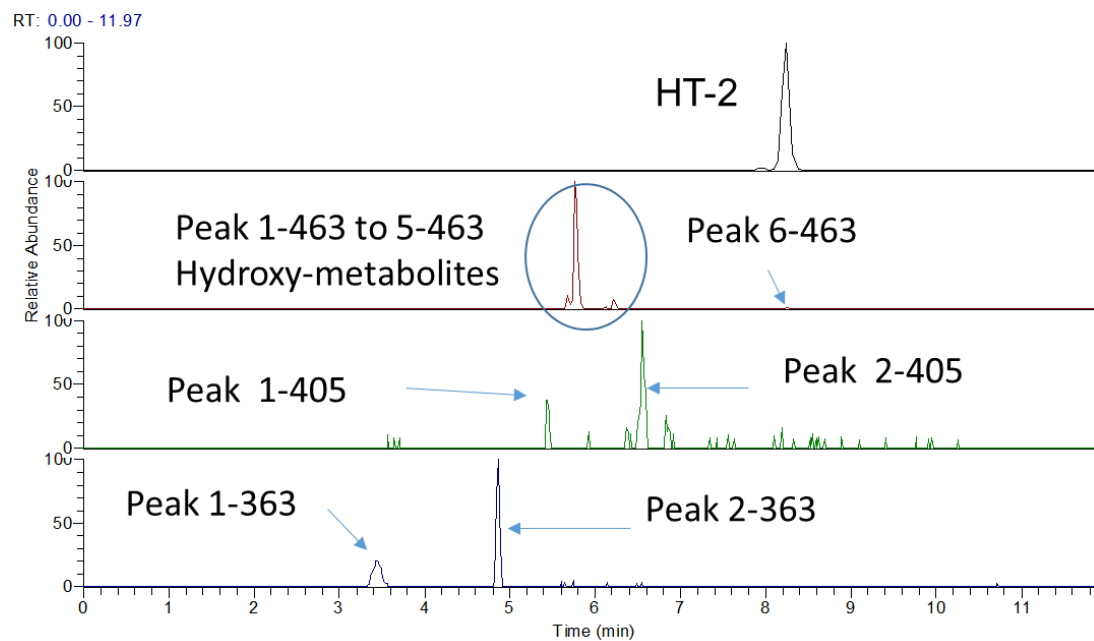
Supplementary Figure B4. Product ion mass spectra of the T-2 hydrolyzed metabolites. The peak 1-447 (a) and peak 2-447 (b). Peak 1-447 was tentatively identified as 15-deacetyl-T-2 and the peak 2-447 was identified as HT-2, detected in ESI(+), as  $[M+Na]^+$  ions.



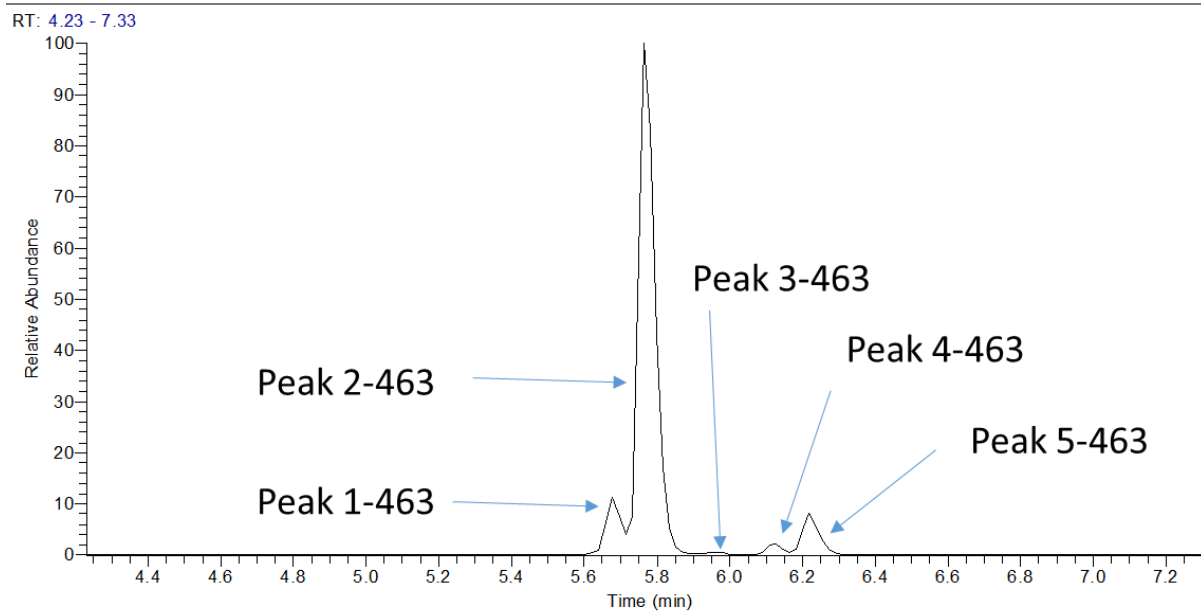
*Supplementary Figure B5. Chromatographic separation of T-2 and HT-2 glucuronides. Extracted ion chromatogram of T-2 and HT-2 glucuronides (665.2416 m/z, Gluc-T-2, and 623.2310 m/z, Gluc-HT-2) in ESI(+), detected as  $[M+Na]^+$  ions.*



Supplementary Figure B6. Product ion spectra of T-2 and HT-2 glucuronides. HT-2 glucuronide (a) at 623.2310  $m/z$  and T-2 glucuronide (b) at 665.2416  $m/z$  detected in ESI(+), as  $[M+Na]^+$ , HT-2 glucuronide (c) at 618.2756  $m/z$ , detected in ESI(+), as  $[M+NH_4]^+$  ions.

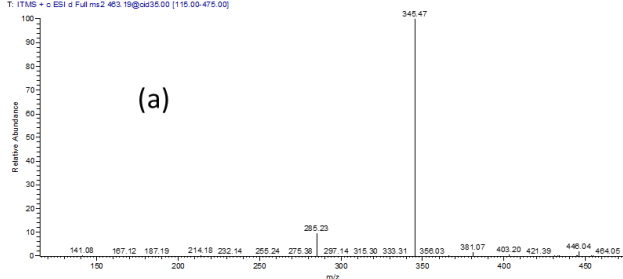


*Supplementary Figure B7. Chromatographic separation of HT-2 and its metabolites. Extracted ion chromatogram of peak 1-463 to peak 5-463 (463.1939 m/z), peak 1-405 and peak 2-405 (405.1884 m/z), peak 1-363 and peak 2-363 (363.1414 m/z) in ESI(+), detected as  $[M+Na]^+$  ions.*

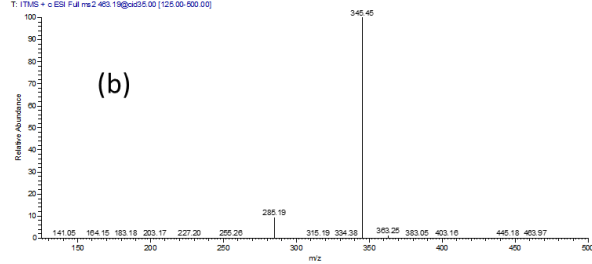


*Supplementary Figure B8. Extracted ion chromatogram of HT-2 hydroxyl-metabolites. Zooming into extracted ion chromatogram of HT-2 hydroxyl-metabolites (463.1939 m/z, peak 1-463 to 5-463).*

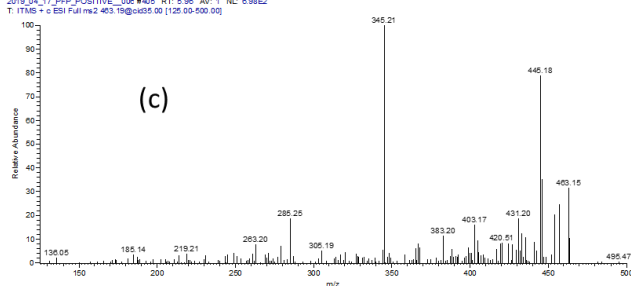
2019\_04\_21\_PFP\_POSITIVE\_001#1274 RT: 5.67 AV: 1 NL: 1.21E5  
T: ITMS + e ESI Full m/z 463.19@cs05.00 [115.00-500.00]



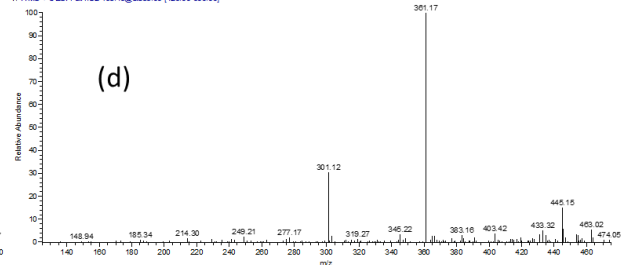
2019\_04\_17\_PFP\_POSITIVE\_001#393 RT: 5.78 AV: 1 NL: 1.81E5  
T: ITMS + e ESI Full m/z 463.19@cs05.00 [125.00-500.00]



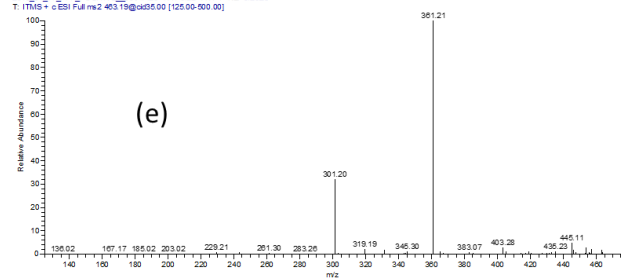
2019\_04\_17\_PFP\_POSITIVE\_001#406 RT: 5.96 AV: 1 NL: 6.98E2  
T: ITMS + e ESI Full m/z 463.19@cs05.00 [125.00-500.00]



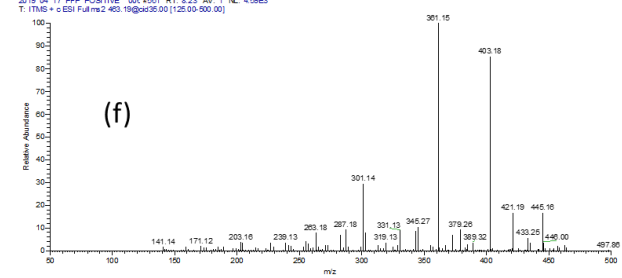
2019\_04\_17\_PFP\_POSITIVE\_001#417 RT: 6.13 AV: 1 NL: 2.12E3  
T: ITMS + e ESI Full m/z 463.19@cs05.00 [125.00-500.00]



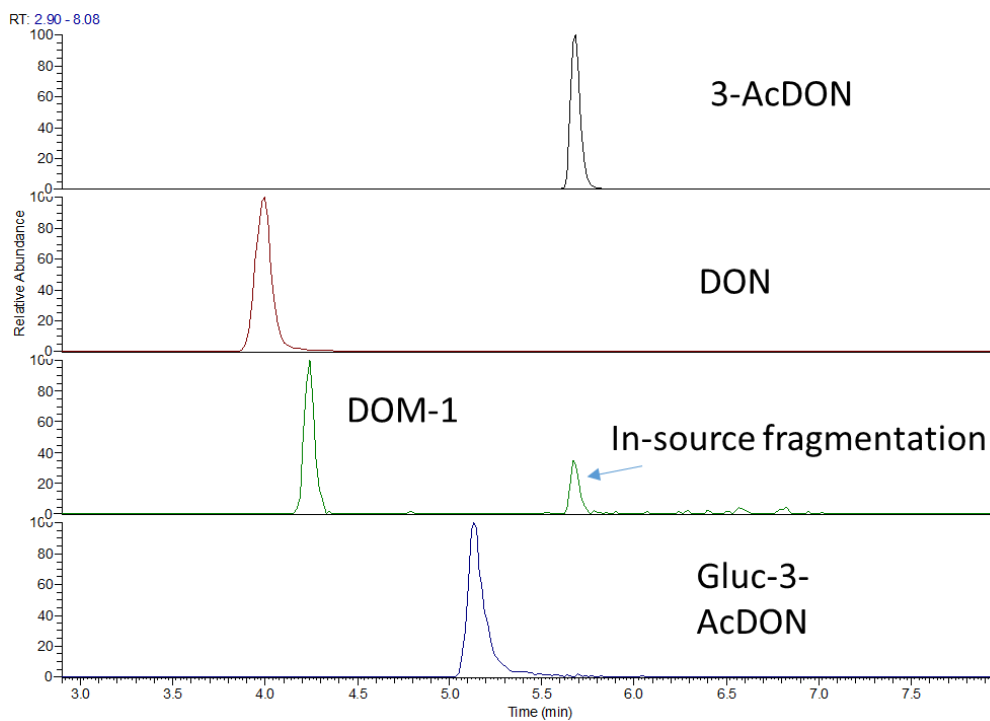
2019\_04\_17\_PFP\_POSITIVE\_001#423 RT: 6.22 AV: 1 NL: 8.20E3  
T: ITMS + e ESI Full m/z 463.19@cs05.00 [125.00-500.00]



2019\_04\_17\_PFP\_POSITIVE\_001#561 RT: 8.23 AV: 1 NL: 4.59E3  
T: ITMS + e ESI Full m/z 463.19@cs05.00 [125.00-500.00]

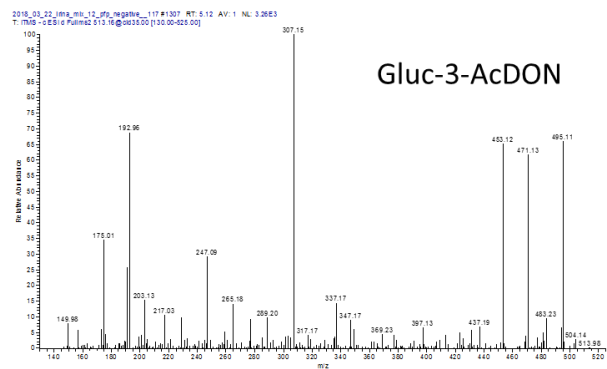
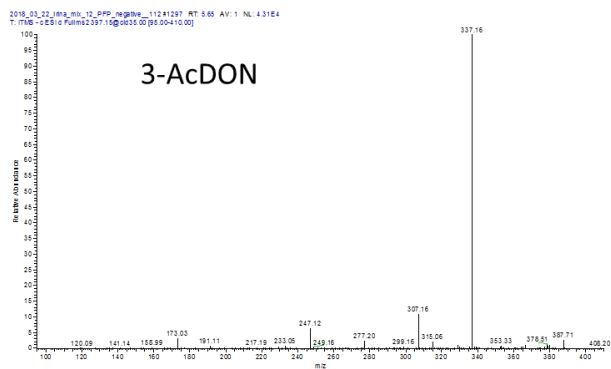


*Supplementary Figure B9. Product ion mass spectra of HT-2 hydroxy metabolites. Peak 1-463 (a), peak 2-463 (b), peak 3-463 (c), peak 4-463 (d), peak 5-463 (e), peak 6-463 (f) at 463.1939 m/z, detected in ESI(+), as  $[M+Na]^+$  ions.*

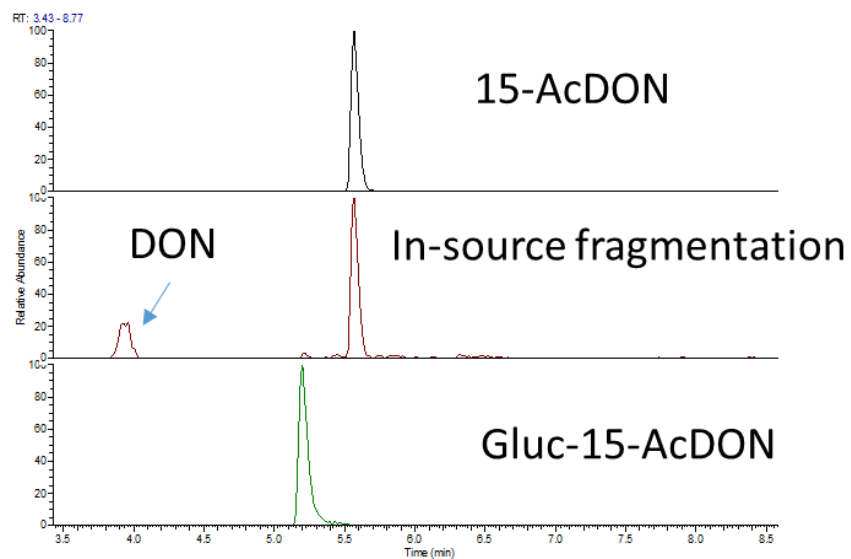


Supplementary Figure B10. Chromatographic separation of 3-AcDON and its metabolites. Extracted ion chromatogram of 3-AcDON (397.1505  $m/z$ ) and its metabolites (355.1399  $m/z$ , DON, 339.1448  $m/z$ , DOM-1, and 513.1613  $m/z$ , Gluc-3-AcDON) in ESI(-), detected as  $[M+CH_3COO-H]^-$  ions for all except for Gluc-3-AcDON ( $[M-H]^-$ ).



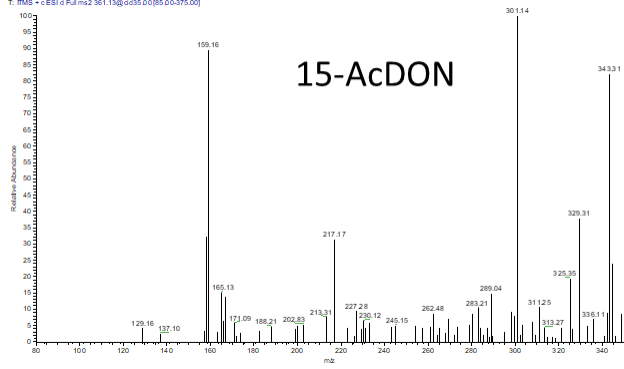


*Supplementary Figure B11. Product ion mass spectra of 3-AcDON and its glucuronide. 3-AcDON and its glucuronide (397.1505 m/z) and its glucuronide (513.1613 m/z), detected in ESI(-), as  $[M+CH_3COO-H]^-$  and Gluc-3-AcDON ( $[M-H]^-$ ) ions, respectively. The other metabolites of 3-AcDON, including DON and DOM-1 is shown in the Supplementary Figure B15 and B17, respectively.*

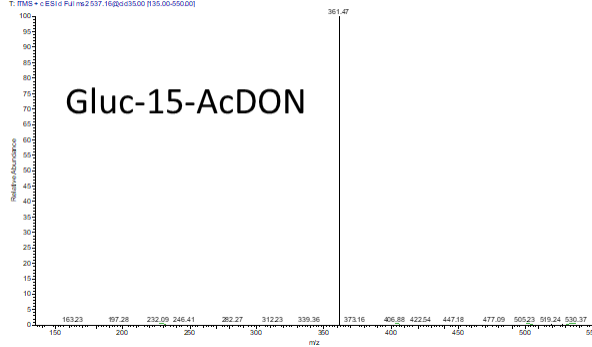


*Supplementary Figure B12. Chromatographic separation of 15-AcDON and its metabolites. Extracted ion chromatogram of 15-DON (297.1333 m/z), and Gluc-15-AcDON (537.1579 m/z) in ESI(+), detected as  $[M+Na]^+$  ions.*

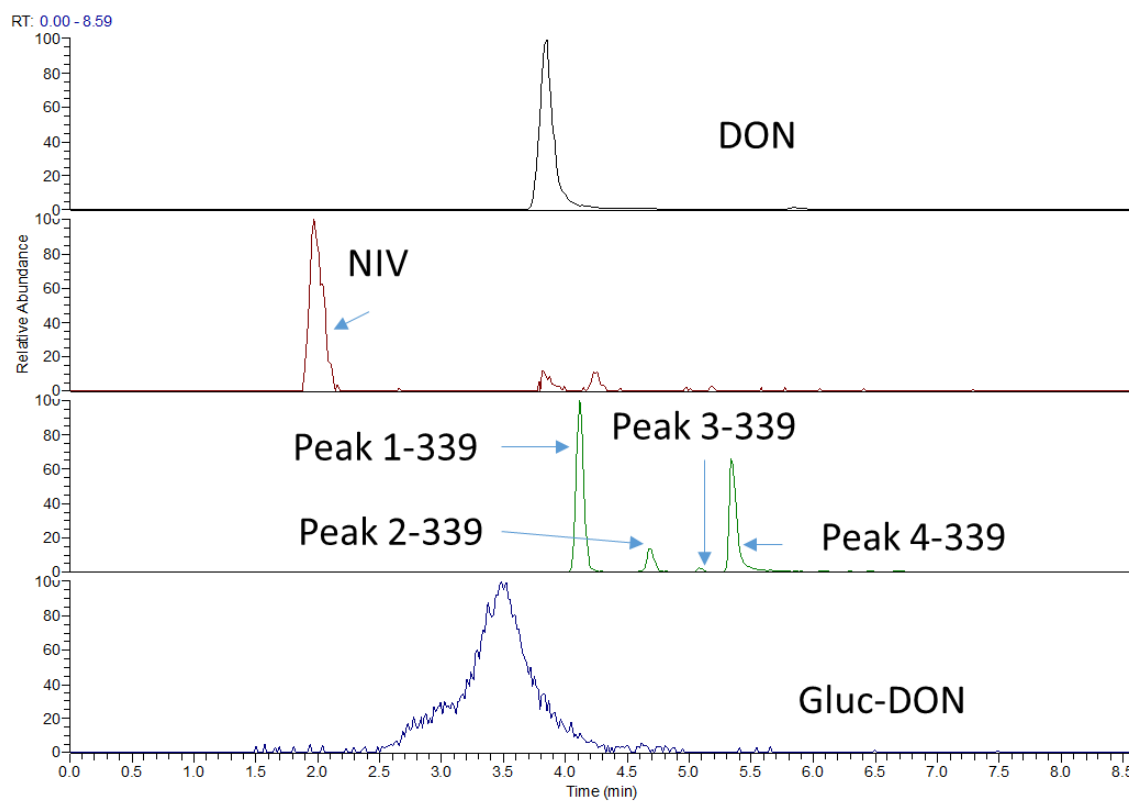
2018 03 15 15 mix 12 PEP POSITIVE 056 #1383 RT: 5.54 AV: 1 NL: 9.6762  
T: PMS - ESI+ FullMS2 361.15600000000000



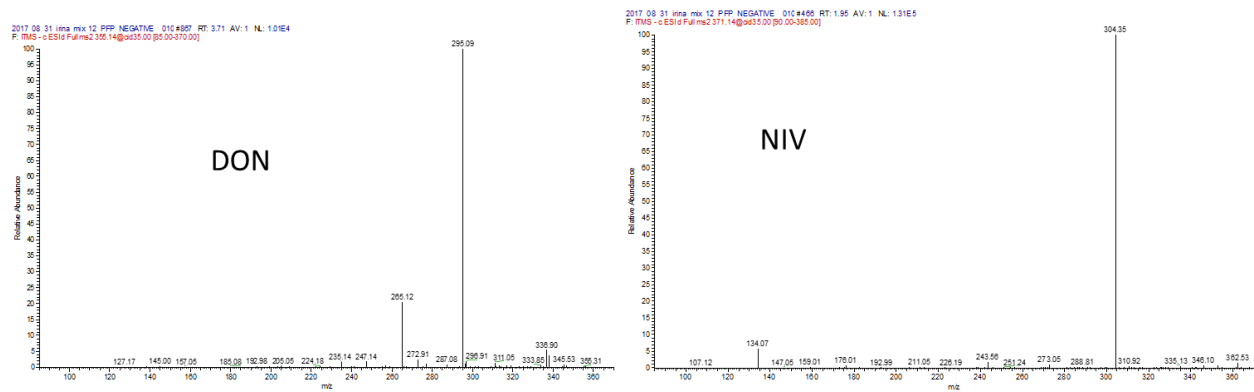
2018 03 15 15 mix 12 PEP POSITIVE 056 #1390 RT: 5.20 AV: 1 NL: 1.5465  
T: PMS - ESI+ FullMS2 537.15600000000000



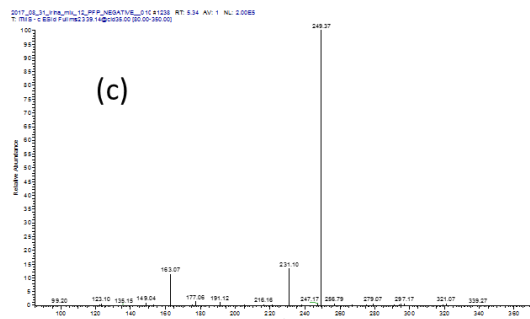
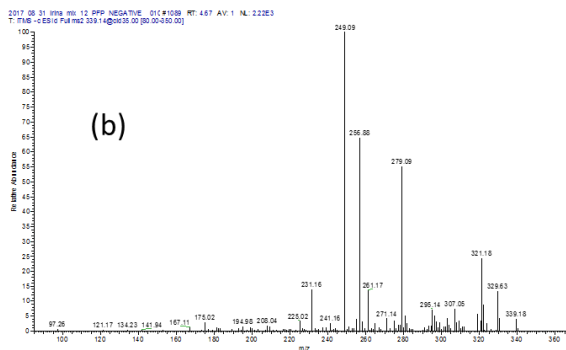
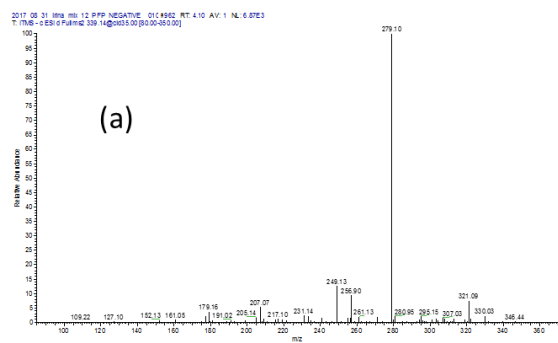
Supplementary Figure B13. Product mass spectra of 15-AcDON and its glucuronide. 15-AcDON (361.1258 m/z) and its glucuronide (537.1579 m/z), detected in ESI(+) as  $[M+Na]^+$  ions.



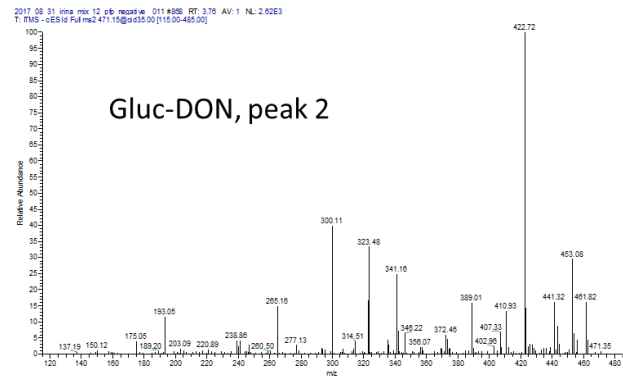
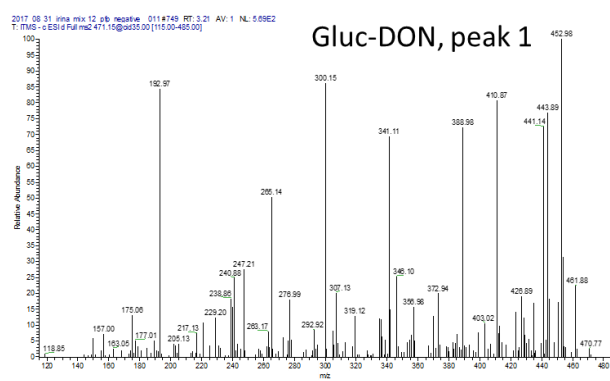
*Supplementary Figure B14. Chromatographic separation of DON and its metabolites. Extracted ion chromatogram of DON and NIV (371.1348 m/z), peak 1-339 to peak 4-339 (339.1449 m/z), and Gluc-DON (471.1508 m/z) in ESI(-), detected as  $[M+CH_3COO-H]^-$  ions for all except for Gluc-DON ( $[M-H]^-$ ).*



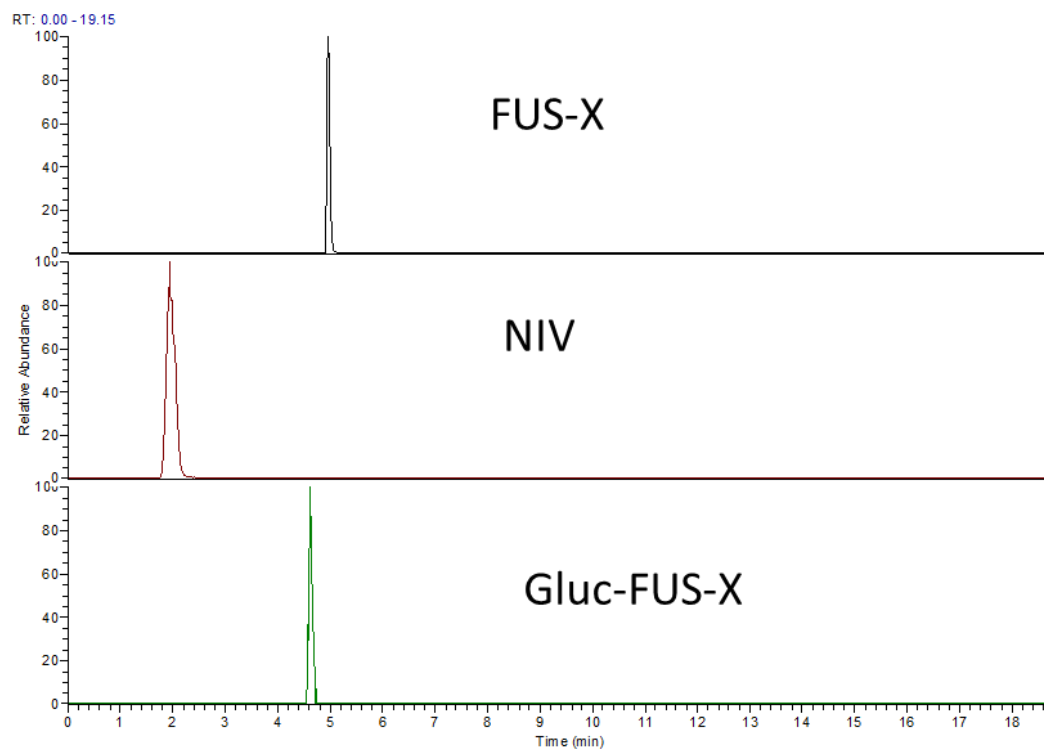
Supplementary Figure B15. Product mass spectra of DON and NIV. DON (355.1399  $m/z$ ) and NIV (371.1348  $m/z$ ) detected in ESI(-), as  $[M+CH_3COO-H]^-$  ions.



Supplementary Figure B16. Product ion mass spectra of DON Phase I metabolites. De-epoxy-deoxynivalenol at 339.1348 m/z, detected in ESI(-), as  $[M+CH_3COO-H]^-$  ions. Peak 1-339 (a) was observed as Phase I metabolite of DON and 3-AcDON, peak 2-339 (b) and peak 4-339 (c) were observed as Phase I metabolite of DON only.

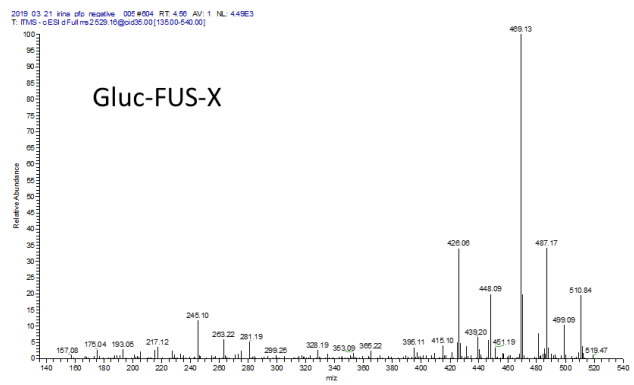
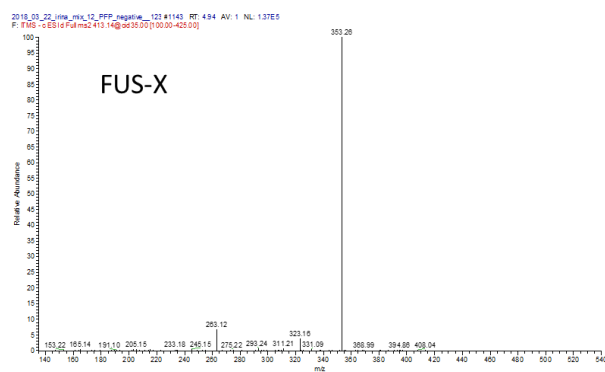


Supplementary Figure B17. Product mass spectra of DON glucuronides. DON glucuronides (471.1508 m/z), detected in ESI(-), as  $[M-H]^-$  ions.

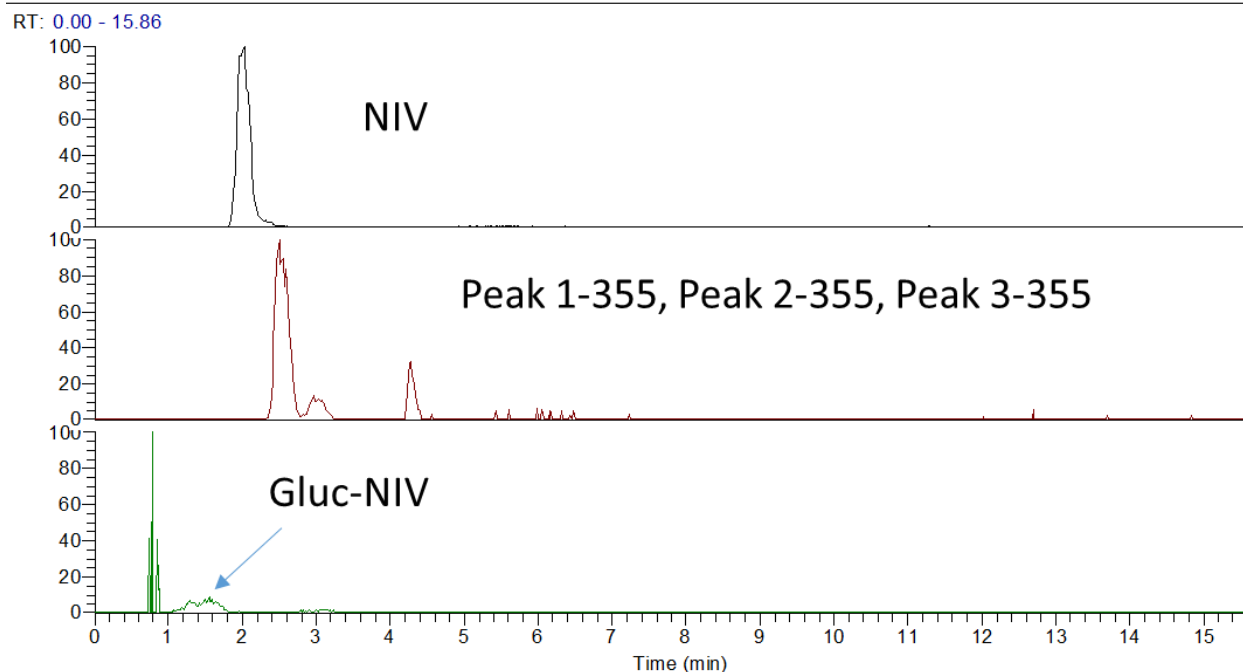


Supplementary Figure B18. Extracted ion chromatogram of FUS-X and its metabolites. FUS-X (413.1454  $m/z$ ) and its metabolites (371.1348  $m/z$ , NIV, and 529.1563  $m/z$ , Gluc-FUS-X) in ESI(-), detected as  $[M+CH_3COO-H]^-$  ions for all except for Gluc-FUS-X ( $[M-H]^-$ ).

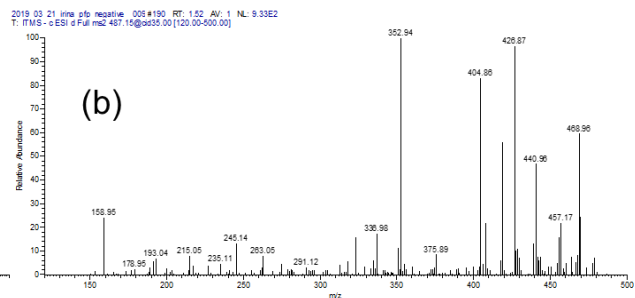
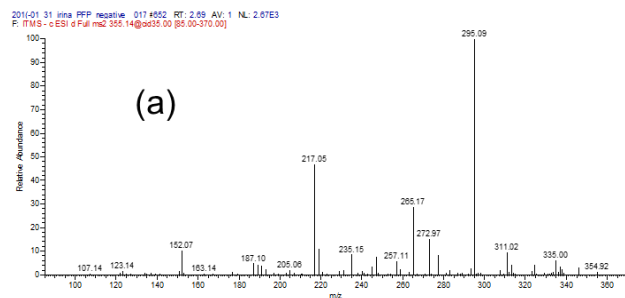




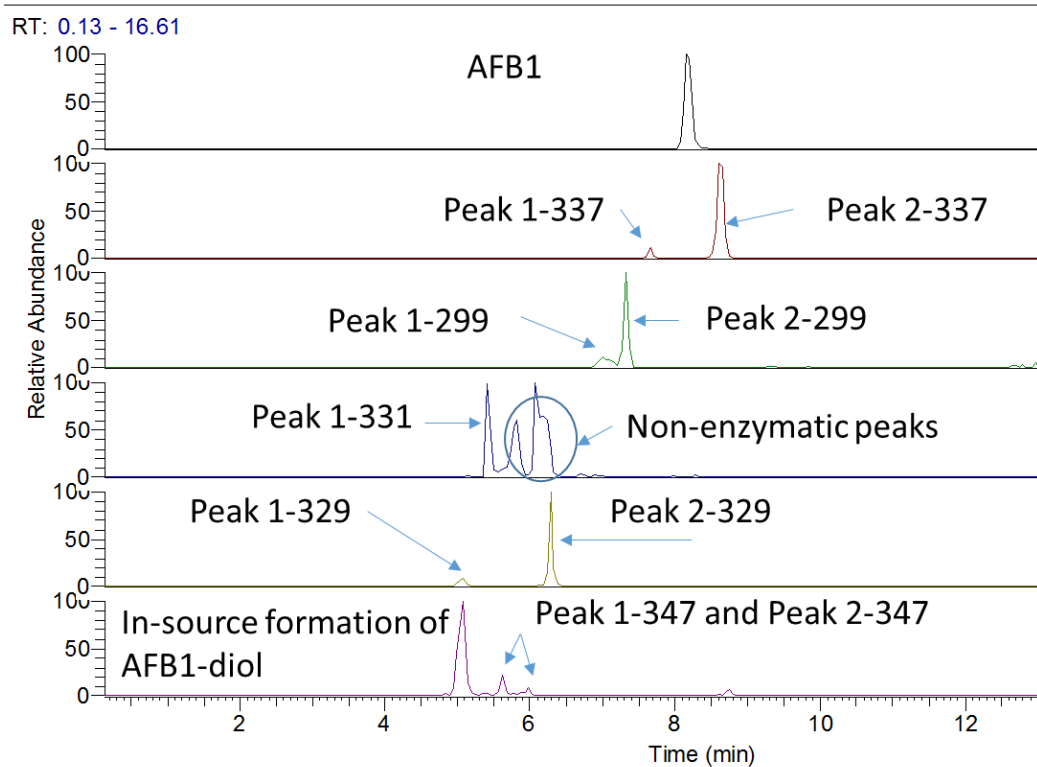
*Supplementary Figure B19. Product ion mass spectra of FUS-X and its glucuronide. FUS-x at 413.1454 m/z and its glucuronide at 529.1563 m/z, detected in ESI(-), as  $[M+CH_3COO-H]^-$  and Gluc-3-AcDON ( $[M-H]^-$ ) ions, respectively. NIV mass spectrum which also was one of FUS-X metabolite was shown in the Supplementary Figure B15.*



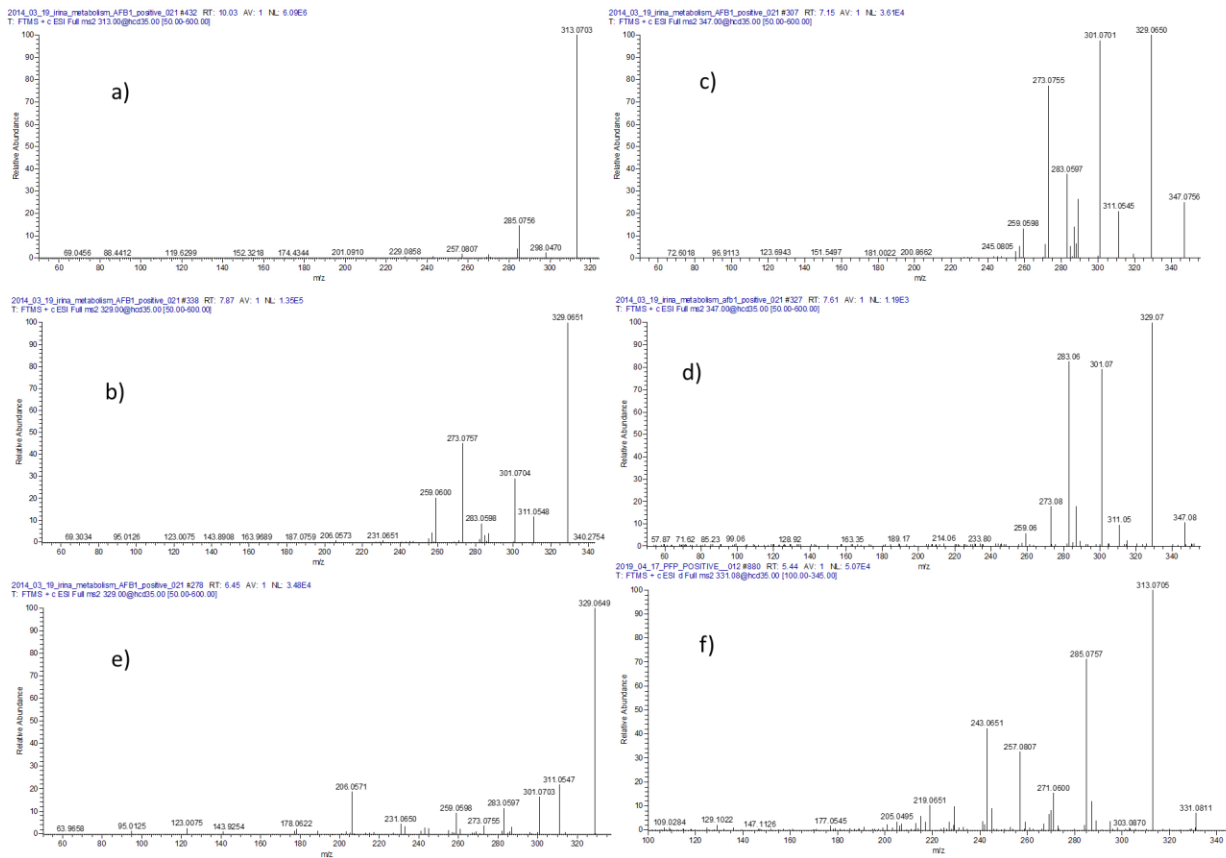
*Supplementary Figure B20. Extracted ion chromatogram of NIV and its metabolites. NIV, de-epoxy-metabolite (355.1398 m/z, peak 1-355) and its isomers (355.1398 m/z, peak 2-355, peak 3-355) and its glucuronides (487.1457 m/z) in ESI(-), NIV and de-epoxy-metabolite were detected as  $[M+CH_3COO-H]^-$  ions and glucuronides as  $[M-H]^-$  ion.*



*Supplementary Figure B21. Product ion mass spectra of NIV metabolites. De-epoxy-nivalenol, peak 1-355 (a) at 355.1398 m/z and NIV glucuronide (b) at 487.1458 m/z, detected in ESI(-), as  $[M-H]^-$  and  $[M+CH_3COO-H]^-$  ions, respectively. NIV mass spectrum was shown in the Supplementary Figure B15.*

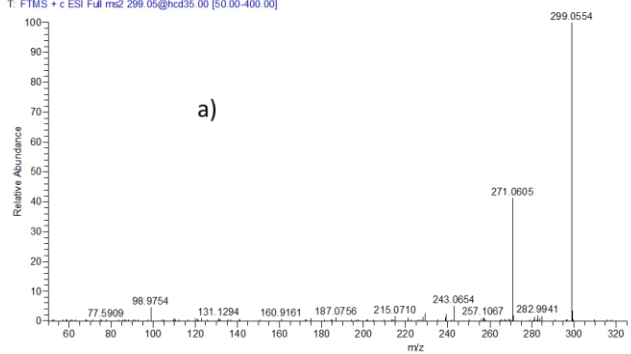


Supplementary Figure B22. Chromatographic separation of AFB1 metabolites. Extracted ion chromatogram of AFB1 (313.0707 m/z), 337.0682 m/z (peak 1-337 and peak 2-337), 299.0550 m/z (peak 1-299 and peak 2-299), 331.0812 m/z (peak 1-331), 329.0661 m/z (peak 1-329, AFBO, and peak 2-329, AFM1), 347.0761 m/z (peak 1-347 and peak 2-347) detected in ESI(+).

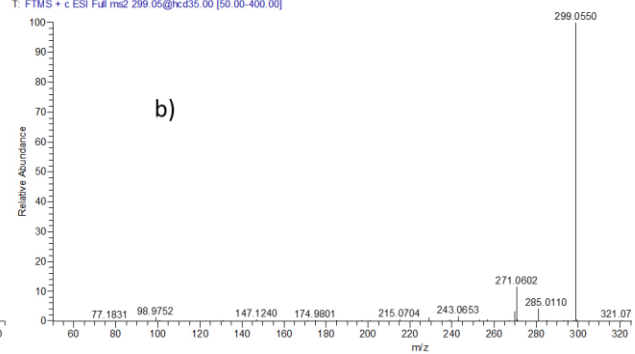


Supplementary Figure B23. Product mass spectra of AFB1 and its metabolites. AFB1(a), AFM1, peak 2-329 (b); AFB-diol, peak 1 (c); AFB-diol, peak 2 (d); AFB-8,9-endo/exo-epoxide (AFBO), peak 1-329 (e); peak 1-331 (f), detected in ESI(+), as  $[M+H]^+$  ions.

2019\_04\_17\_PFP\_POSITIVE\_011 #473 RT: 6.92 AV: 1 NL: 5.37E3  
T: FTMS + c ESI Full ms2 299 05@hcd35.00 [50.00-400.00]

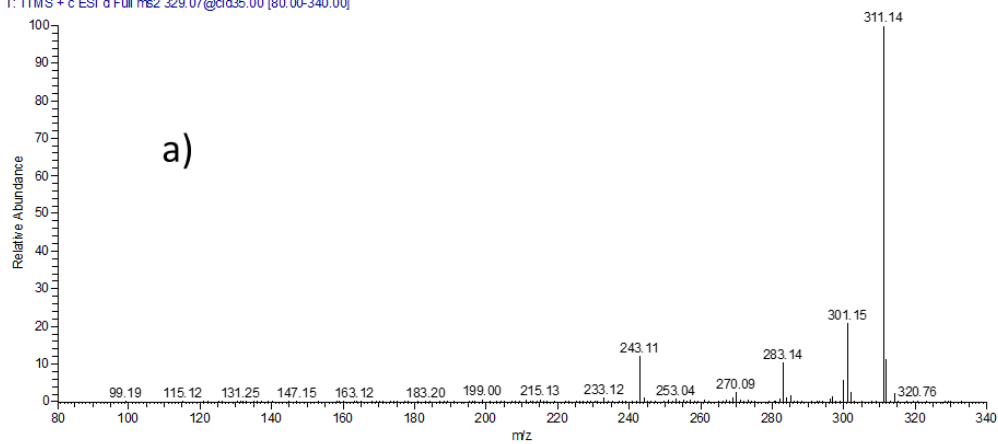


2019\_04\_17\_PFP\_POSITIVE\_011 #497 RT: 7.27 AV: 1 NL: 2.23E4  
T: FTMS + c ESI Full ms2 299 05@hcd35.00 [50.00-400.00]

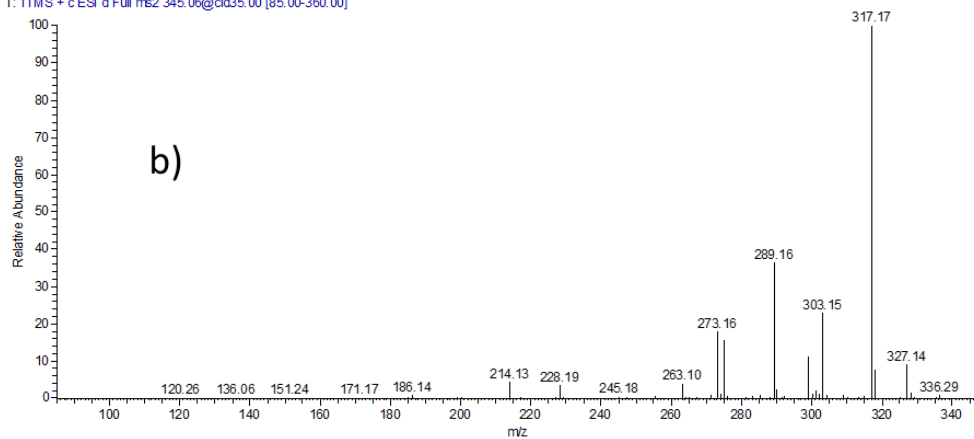


Supplementary Figure B24. Product mass spectra of AFB1 O-demethylated metabolites. Peak 1-299 (a) and peak 2-299 (b), detected in ESI(+), as  $[M+H]^+$  ions, identified as AFP1 and its isomer.

2018\_03\_15\_mix\_12\_PFP\_POSITIVE\_036#1750 RT: 6.97 AV: 1 NL: 5.71E4  
T: ITMS + c ESI d Full ms2 329.07@cid35.00 [80.00-340.00]

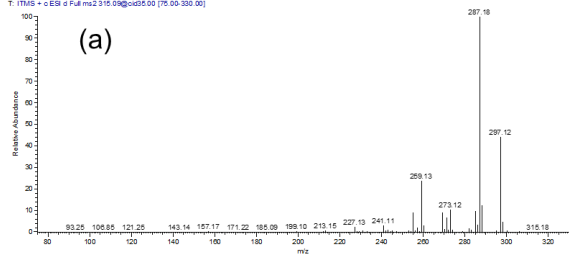


2018\_03\_15\_mix\_12\_PFP\_POSITIVE\_036#1496 RT: 5.91 AV: 1 NL: 4.54E4  
T: ITMS + c ESI d Full ms2 345.06@cid35.00 [85.00-360.00]

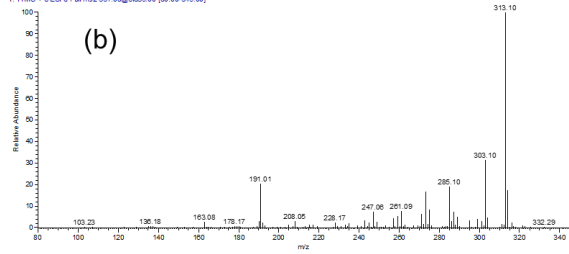


Supplementary Figure B25. Product mass spectra of AFG1 and its hydroxyl metabolite. AFG1 (a) at 329.0656 m/z and its hydroxyl metabolite peak 1-345 (b), detected in ESI(+), as  $[M+H]^+$  ions.

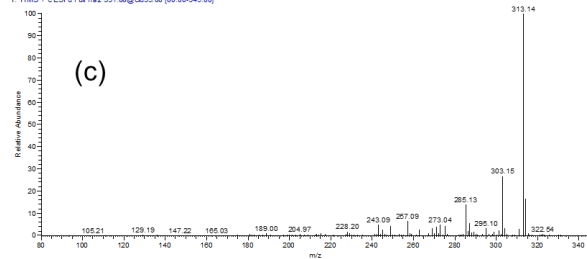
2019\_01\_31\_PFP\_POSITIVE\_011#1802 RT: 7.42 AV: 1 NL: 7.71E4  
T: ITMS = eESI of Full ms2 315.09@ac35.00 (16.00-30.00)



2019\_01\_31\_PFP\_POSITIVE\_011#1404 RT: 0.99 AV: 1 NL: 2.17E4  
T: ITMS = eESI of Full ms2 331.09@ac35.00 (30.00-34.00)



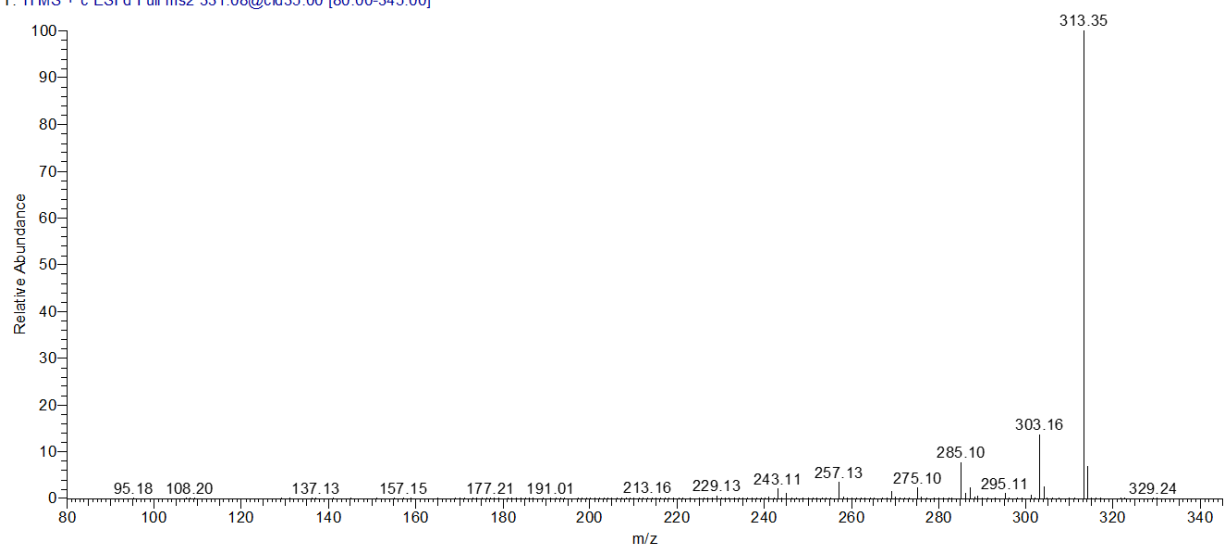
2019\_01\_31\_PFP\_POSITIVE\_011#1655 RT: 6.72 AV: 1 NL: 1.93E4  
T: ITMS = eESI of Full ms2 331.09@ac35.00 (30.00-34.00)



Supplementary Figure B26. Product mass spectra of AFB2 and its hydroxyl metabolites. AFB2 (a) at 315.0863 m/z and its hydroxyl metabolites at 331.0813, peak 2-331 (b) and peak 3-331 (c), detected in ESI(+), as  $[M+H]^+$  ions.



2019\_01\_31\_PFP\_POSITIVE\_005#1666 RT: 6.67 AV: 1 NL: 1.08E6  
T: ITMS + c ESI d Full ms2 331.08@cid35.00 [80.00-345.00]



*Supplementary Figure B27. Product mass spectra of AFG2. AFG2 at 331.0813 m/z, detected in ESI(+), as [M+H]<sup>+</sup> ion.*

## Appendix C

Supplementary Information for Chapter 4

*Supplementary Table C1. Monoisotopic masses of the most intense ions and retention times of all mycotoxins and internal standards.*

<b>Mycotoxin in ESI(-)</b>	<b>The most intense ion</b>	<b>Monoisotopic mass, m/z</b>	<b>RT, min</b>
OT $\alpha$	[M-H] <sup>-</sup>	255.0060	2.72
CIT	[M-H] <sup>-</sup>	249.0763	3.79
OTA	[M-H] <sup>-</sup>	402.0750	5.96
OTAd <sub>5</sub>	[M-H] <sup>-</sup>	407.1058	5.90
<b>Mycotoxin in ESI(+)</b>	<b>The most intense ion</b>	<b>Monoisotopic mass, m/z</b>	<b>RT, min</b>
FB1	[M+H] <sup>+</sup>	722.3958	4.54
FB2	[M+H] <sup>+</sup>	706.4009	7.18
ENNB	[M+Na] <sup>+</sup>	662.3987	10.10
ENNB1	[M+Na] <sup>+</sup>	676.4143	10.62
BEA	[M+Na] <sup>+</sup>	806.3987	10.75
ENNA	[M+Na] <sup>+</sup>	704.4456	11.10
ENNA1	[M+Na] <sup>+</sup>	690.4300	11.59
FB3	[M+H] <sup>+</sup>	706.4009	5.57

*Supplementary Table C2. Comparison of S/N ratio and the number of points per peak at two MS settings, 2 scans/s and 3 scans/s. Results are shown for pre-spiked plasma samples with 20 ng/ml mycotoxin mixture.*

<b>Mycotoxins</b>	<b>2 scans/s</b>		<b>3 scans/s</b>	
	<b>S/N</b>	<b>Points/peak</b>	<b>S/N</b>	<b>Points/peak</b>
OT $\alpha$	43	34	56	53
CIT	343	19	343	33
OTA	216	42	309	51
FB1	103	15	93	22
FB2	578	20	678	33
ENNB	1246	19	1357	34
ENNB1	886	19	867	30
BEA	857	24	905	38
ENNA	512	20	725	31
ENNA1	224	19	256	29
FB3	402	16	253	24

*Supplementary Table C3. Concentrations of matrix-matched calibration curves prepared for the first intra-day accuracy and precision experiment.*

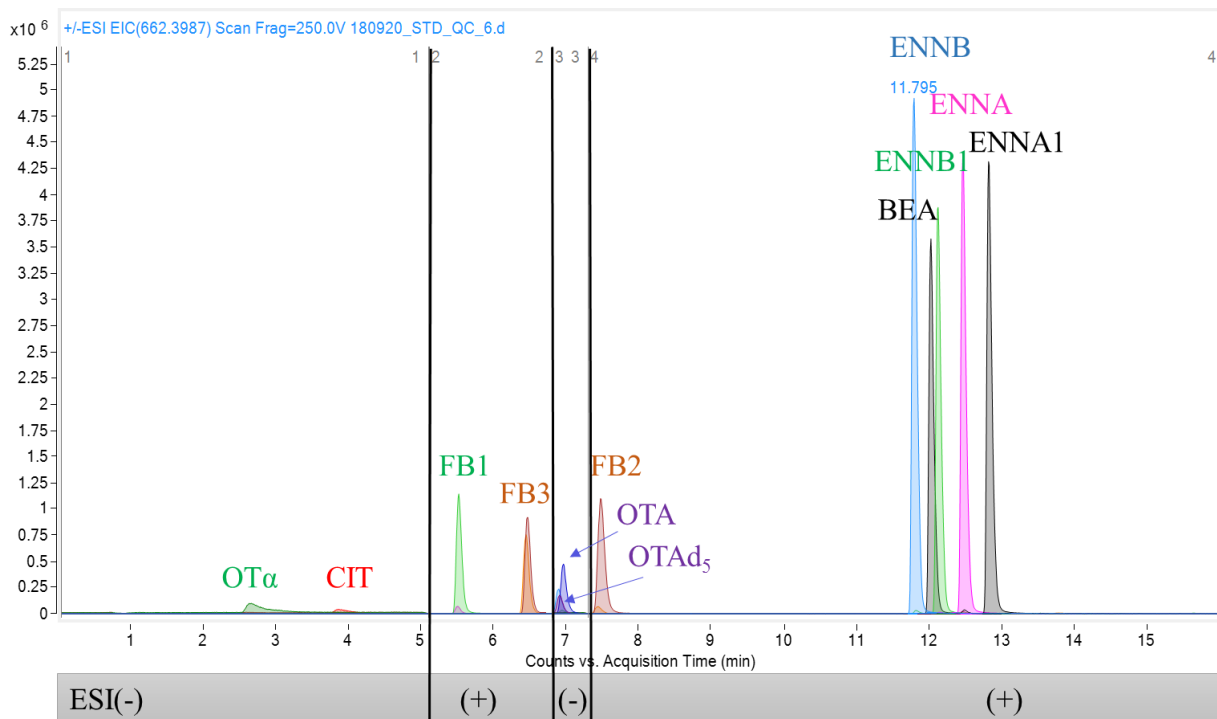
<b>Level</b>	<b>OTA, ENNB, B1</b>	<b>CIT</b>	<b>ENNA, A1, BEA, FB1, B2, OT<math>\alpha</math></b>
	<b>Concentration, ng/ml</b>		
1	19.2	25.6	32
2	9.6	12.8	16
3	4.8	6.4	8
4	2.4	3.2	4
5	1.2	1.6	2
6	0.6	0.8	1
7	0.3	0.4	0.5
8	0.15	0.2	0.25
9	0.075	0.1	-

*Supplementary Table C4. Concentrations of matrix-matched calibration curves for all mycotoxins prepared for the second intra-day accuracy and precision experiment.*

<b>Level</b>	<b>Concentration, ng/ml</b>
1	0.08
2	0.16
3	0.31
4	0.63
5	1.25
6	2.50
7	5.00
8	10.0
9	20.0

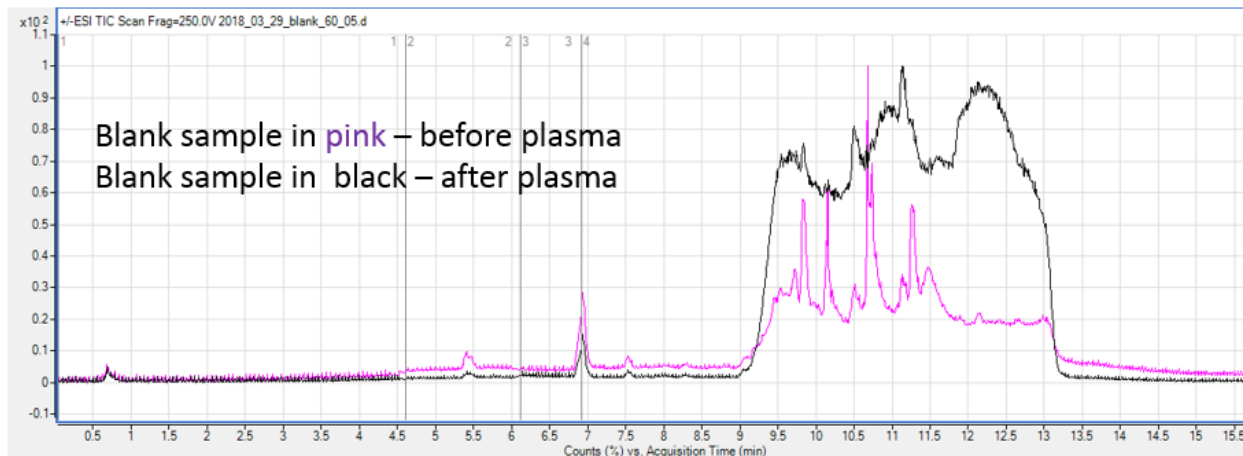
Supplementary Table C5. Evaluation of RSD% using validation samples for the experiment 3, low concentration, 4 ng/ml. The first column represents the sum of ammonium and sodium ion areas for each mycotoxin and the second column is the sodium ion area.

	<b>ENNB</b>	<b>ENNB (Na)</b>	<b>ENNB</b>	<b>ENNB1 (Na)</b>	<b>BEA</b>	<b>BEA (Na)</b>	<b>ENNA1</b>	<b>ENNA1 (Na)</b>	<b>ENNA</b>	<b>ENNA (Na)</b>
	$\Sigma$ Area	Area	$\Sigma$ Area	Area	$\Sigma$ Area	Area	$\Sigma$ Area	Area	$\Sigma$ Area	Area
LOW 6	501382	342024	354265	196974	269079	160707	397298	262819	276323	180718
LOW 5	520999	342761	359896	205266	273887	159599	396243	251562	270710	180709
LOW 4	500246	329721	339414	190581	271055	155931	361962	233639	261203	163532
LOW 3	465045	303990	367583	224019	264621	165636	399325	265466	260465	160863
LOW 1	525032	330736	355965	188747	255778	147603	397630	240786	260899	167454
LOW 2	525032	324405	362151	193057	263649	149610	379970	229874	268471	171043
Mean	506290	329847	355425	201118	266884	157895	390492	250854	265920	170655
Stdev	23154	15688	10318	14343	7066	6718	15987	13738	7218	9476
RSD%	4.6	4.8	2.9	7.1	2.6	4.3	4.1	5.5	2.7	5.6

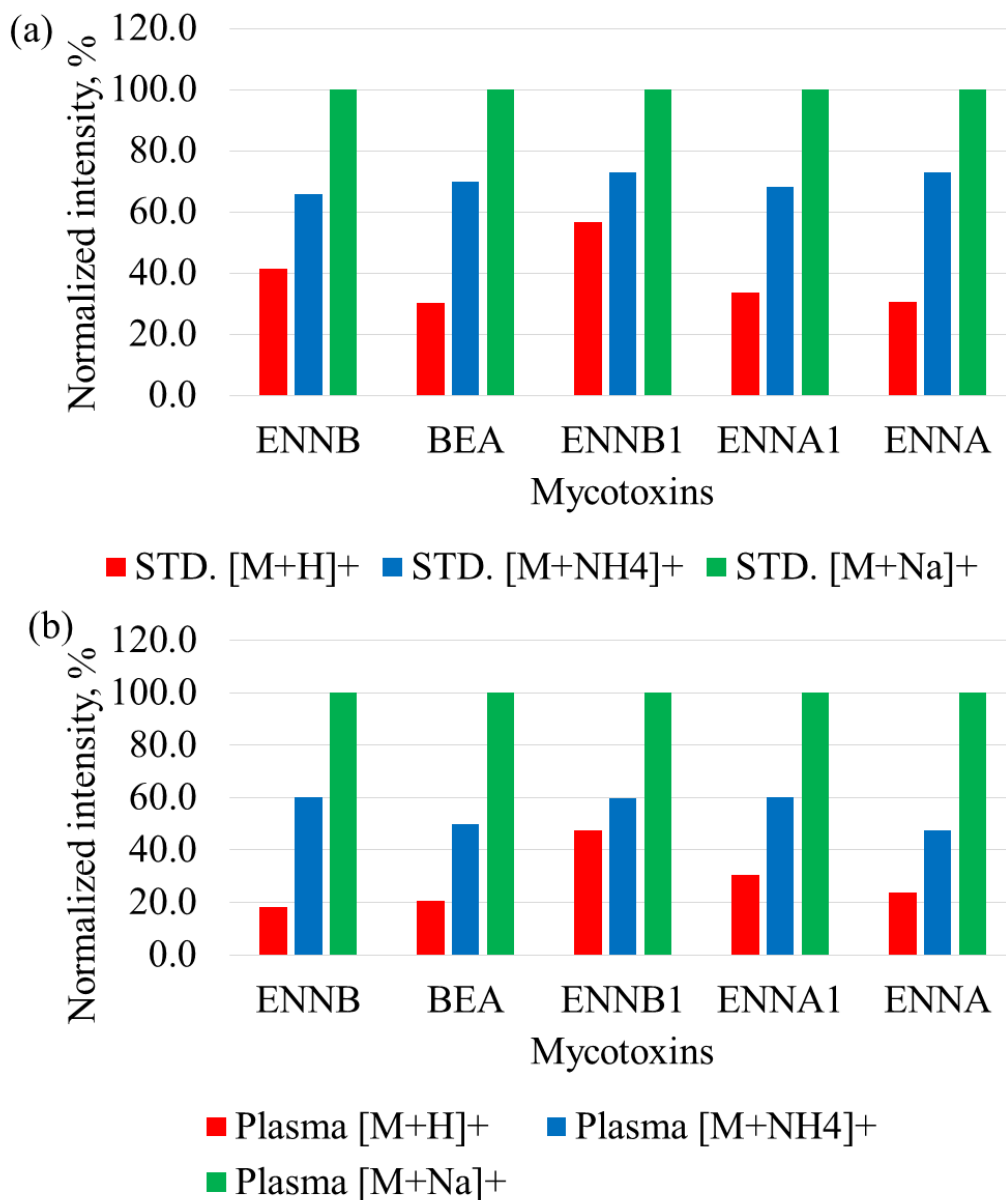


Supplementary Figure C1. Chromatographic separation of all mycotoxins. Optimized Cortecs T3 C<sub>18</sub> LC method uses methanol/water/0.05% FA mobile phase. The results are shown for 20 ng/mL mycotoxin plasma standard in 60% methanol with 1% FA. Mycotoxins are shown in the ESI modes where maximum signal intensity was obtained, which is the same mode used for mycotoxin quantitation.

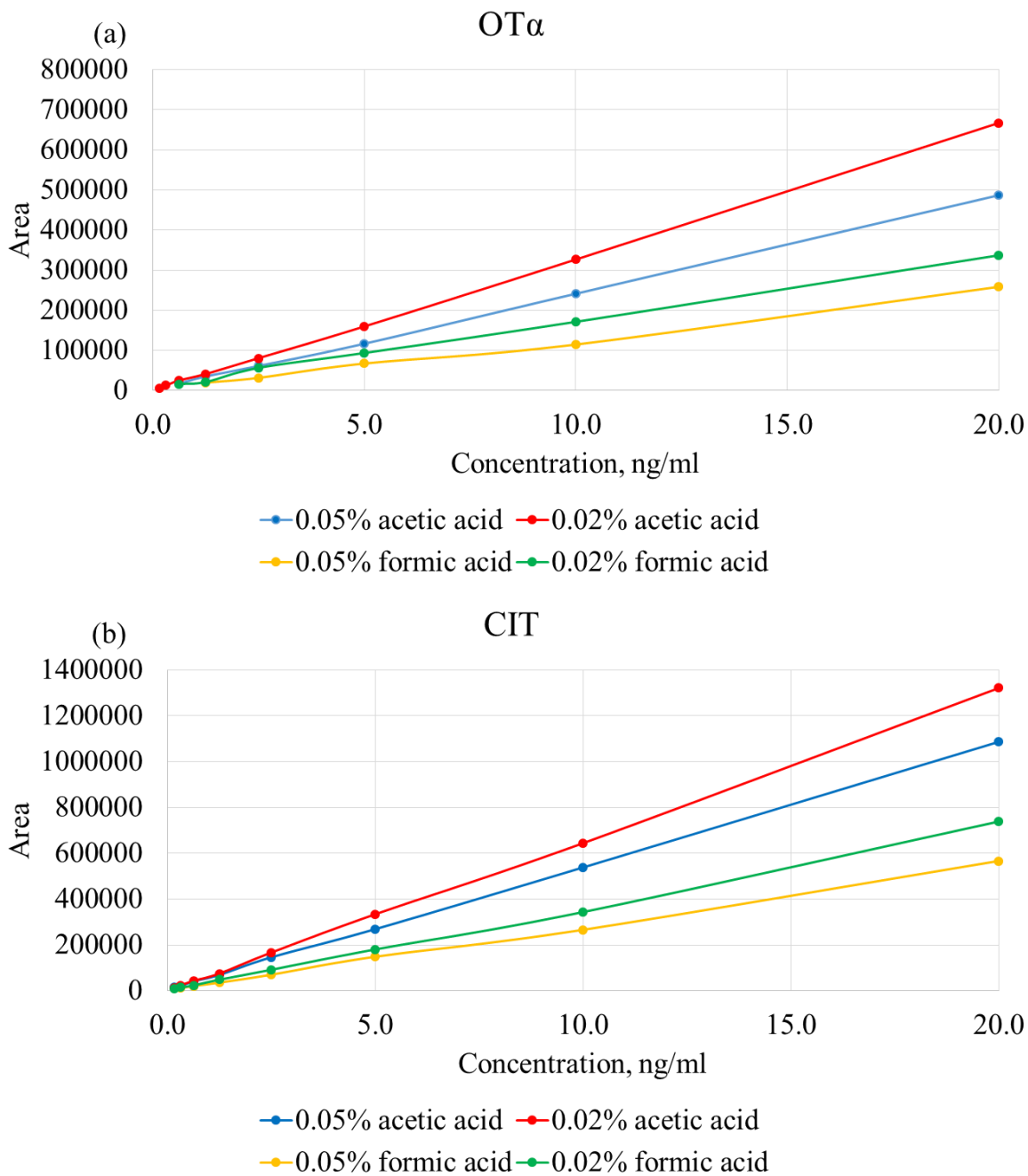




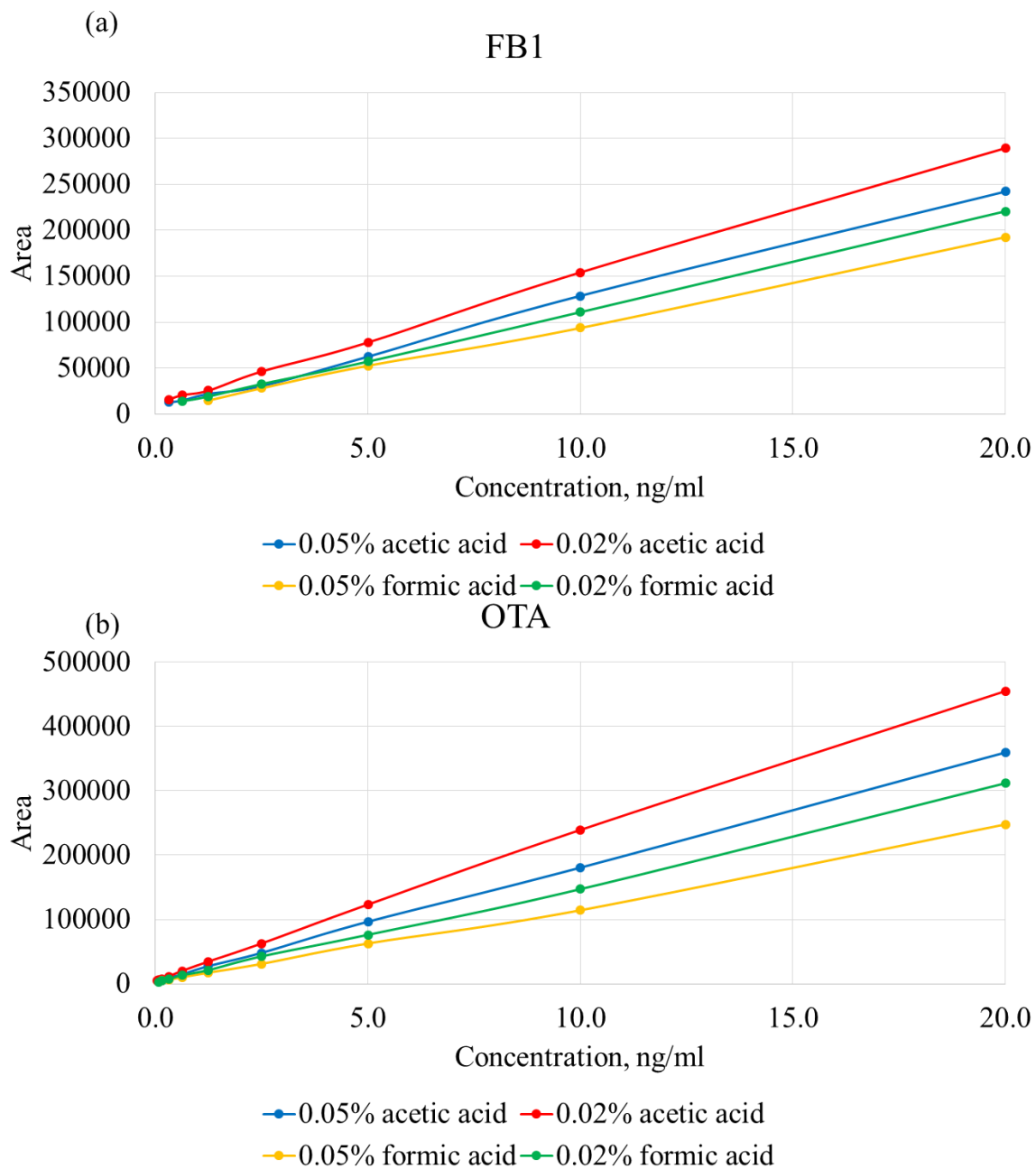
*Supplementary Figure C2. Total ion chromatograms of the blank samples. Blank sample (60% methanol) in pink injected immediately before plasma sample and blank sample (60% methanol) in black injected immediately after plasma sample reveal column build-up and incomplete elution of hydrophobic components present in plasma samples.*



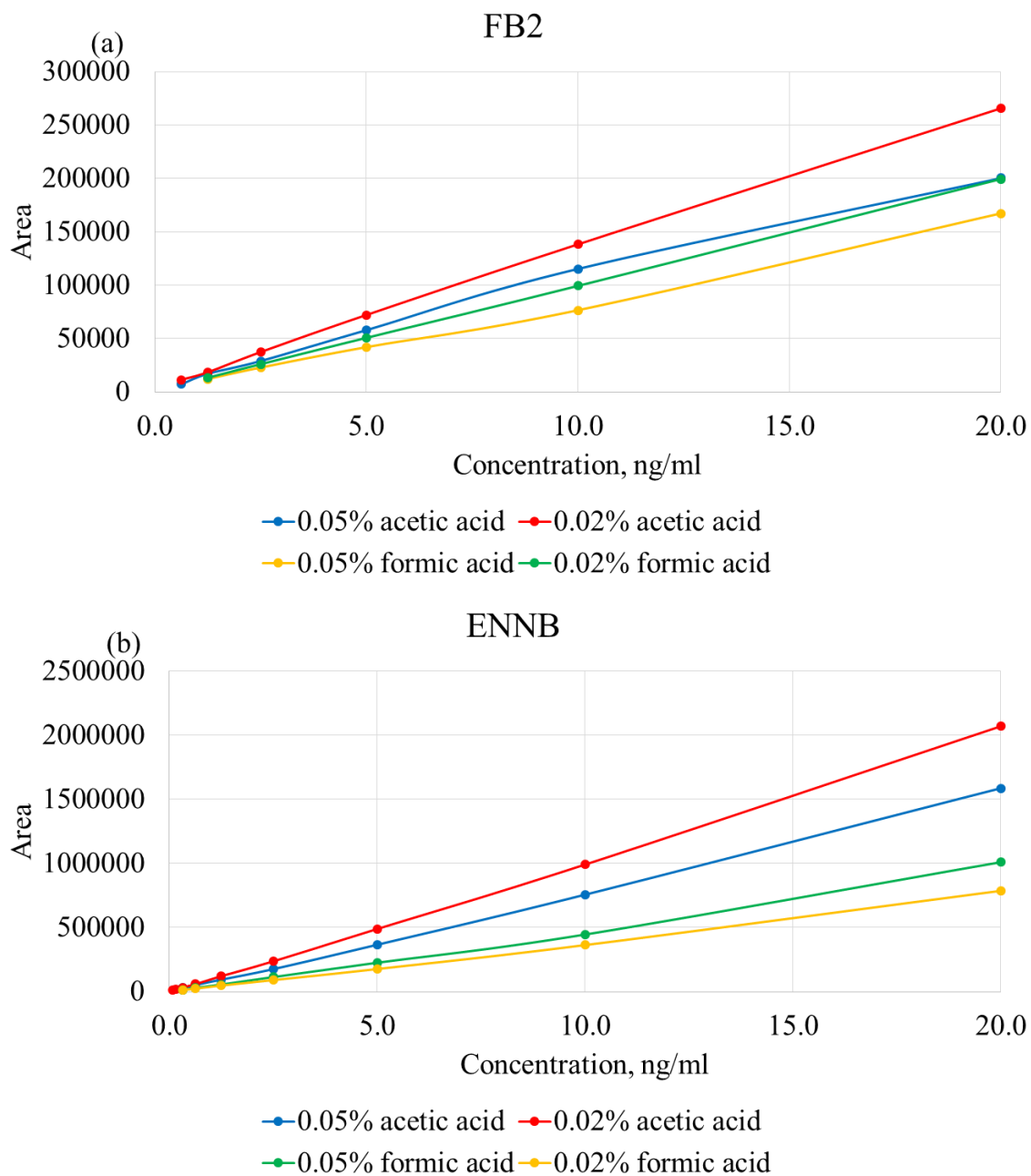
*Supplementary Figure C3. Ionization patterns of emerging mycotoxins. Standard mycotoxin mixture (4 ng/ml) (a) and plasma sample pre-spiked at 20 ng/ml (b) analysed using water/methanol/isopropanol mobile phase. The signal intensities (expressed as peak area) of protonated and ammonium ions were normalized to the signal intensities obtained using sodium ions.*



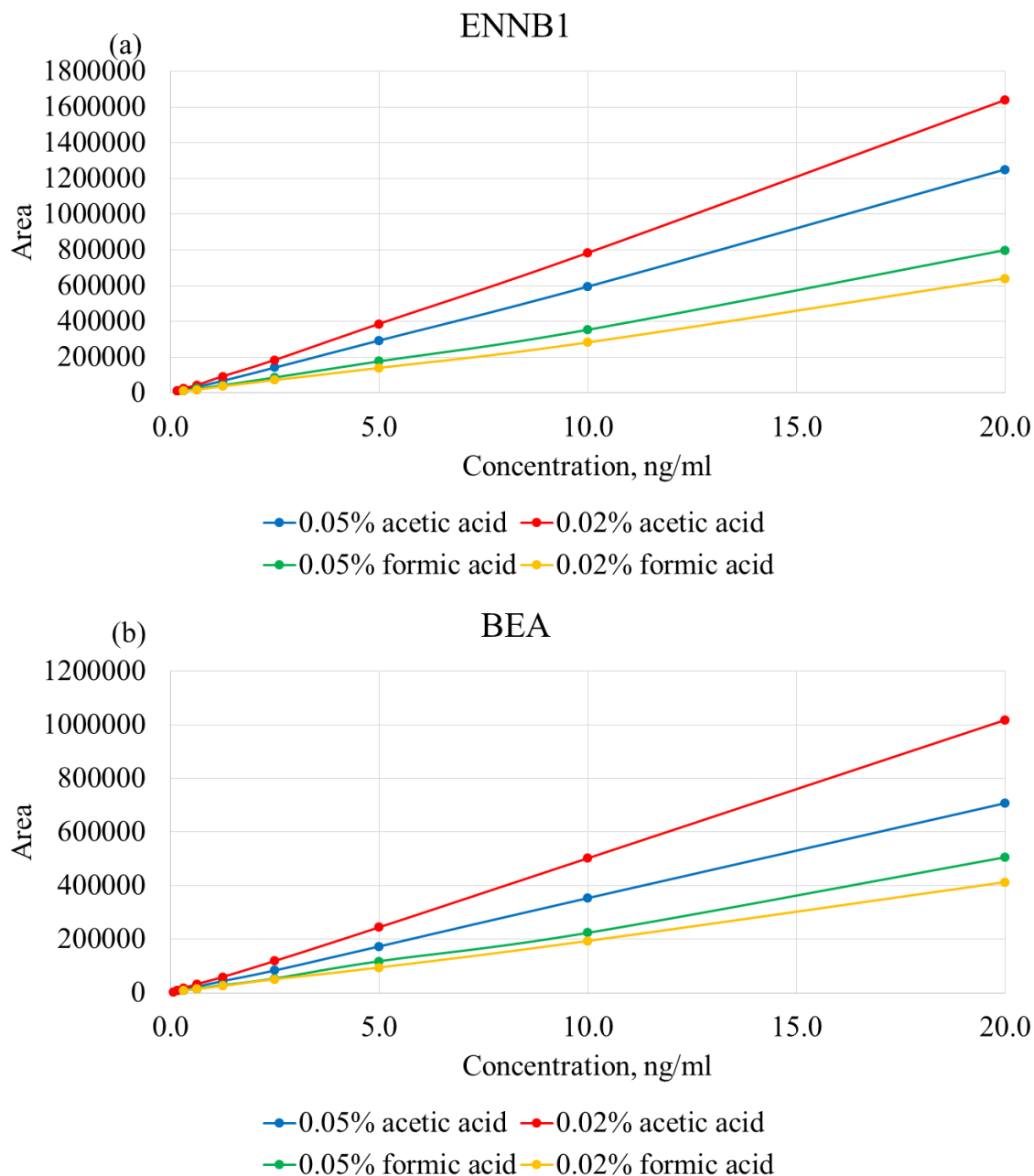
Supplementary Figure C4. Comparison of four calibration curves of OT $\alpha$  (a) and CIT (b). The calibration curves in plasma using different mobile phase additives, 0.05% AA, 0.02% AA, 0.05% FA and 0.02% FA. Overlaid calibration curves were replotted using peak area to compare ionization trends.



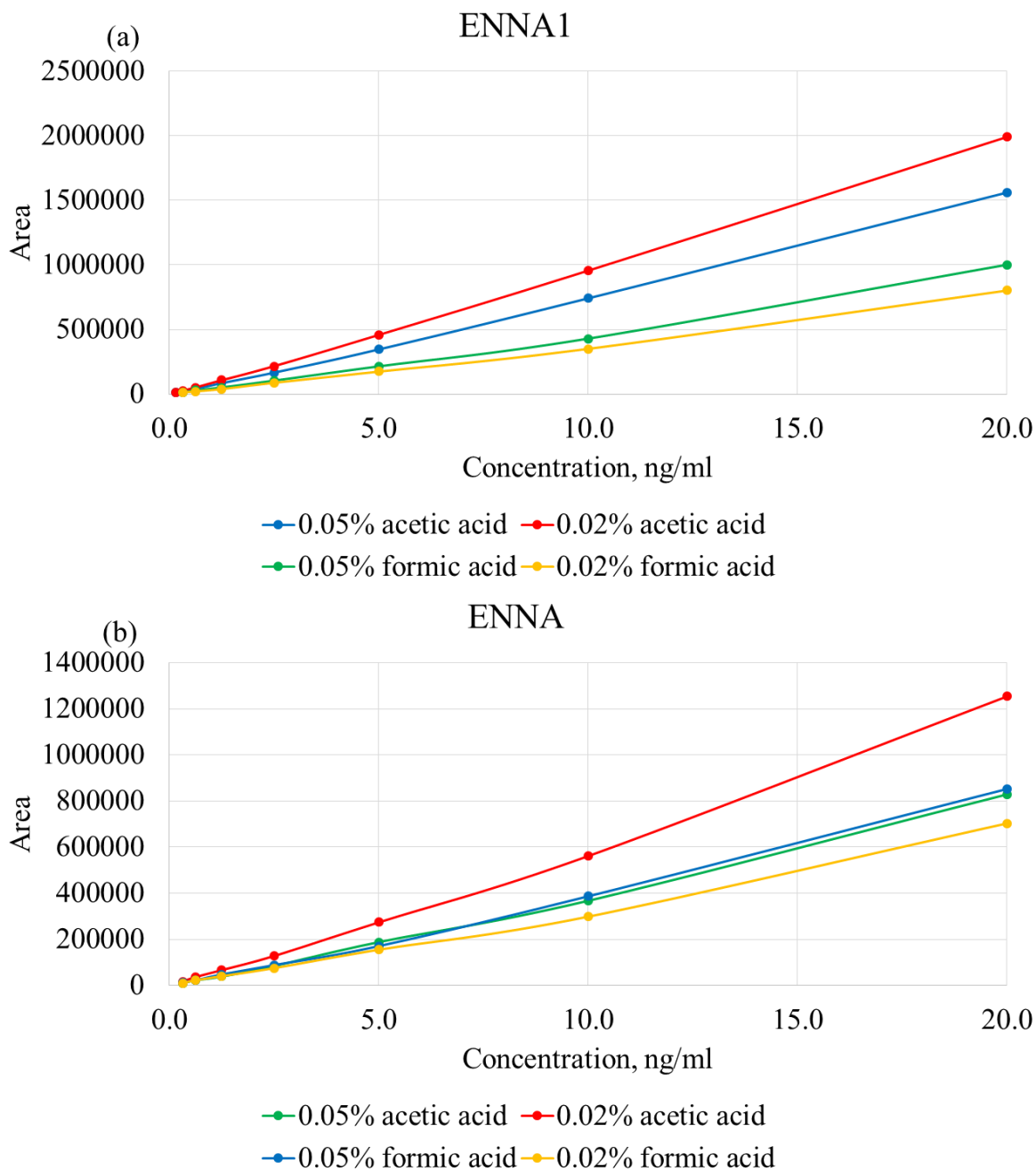
Supplementary Figure C5. Comparison of four calibration curves of FB1 (a) and OTA (b). The calibration curves in plasma using different mobile phase additives, 0.05% AA, 0.02% AA, 0.05% FA and 0.02% FA. Overlaid calibration curves were replotted using peak area to compare ionization trends.



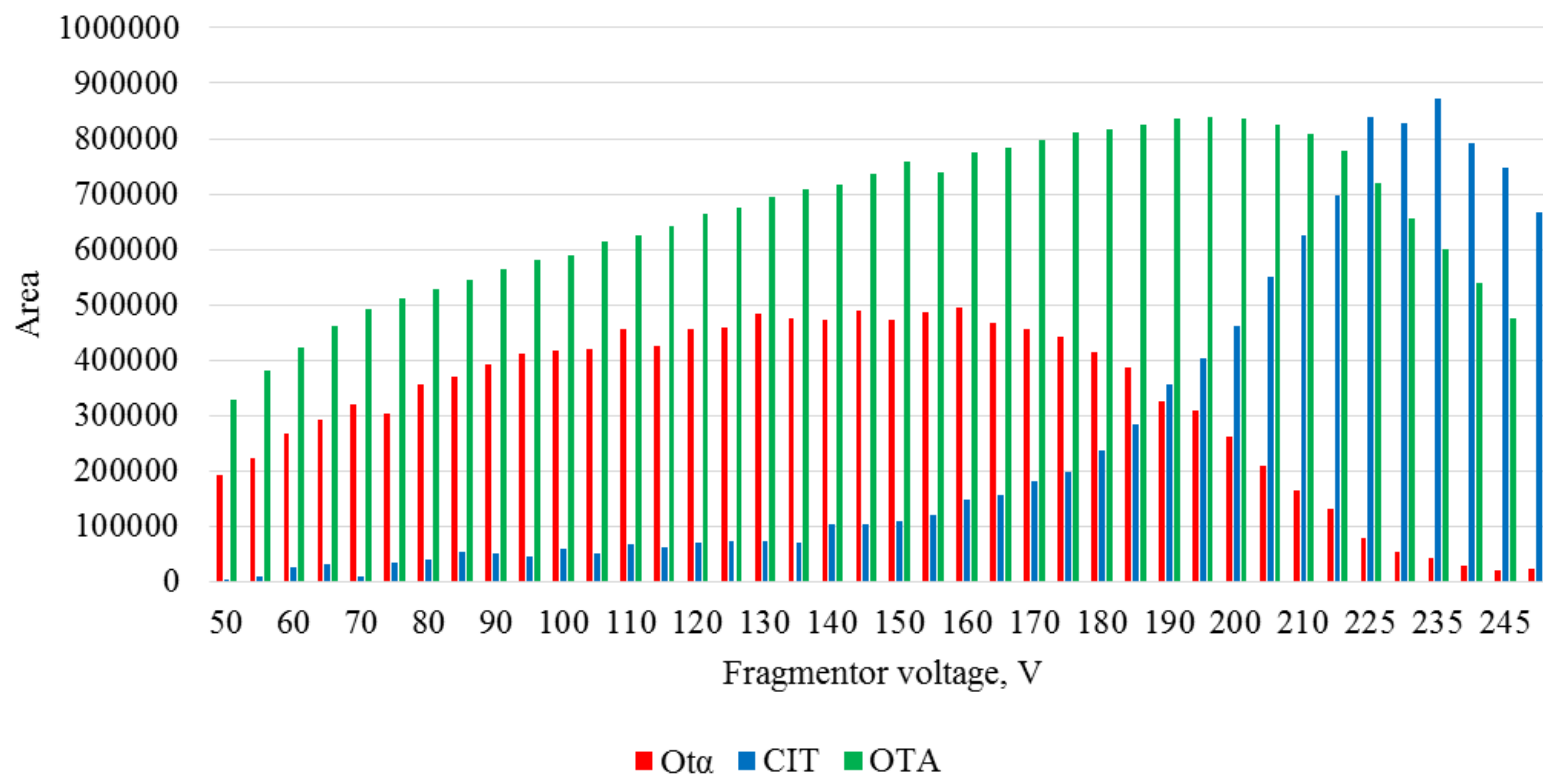
Supplementary Figure C6. Comparison of four calibration curves of FB2 (a) and ENNB (b). The calibration curves in plasma using different mobile phase additives, 0.05% AA, 0.02% AA, 0.05% FA and 0.02% FA. Overlaid calibration curves were replotted using peak area to compare ionization trends.



Supplementary Figure C7. Comparison of four calibration curves of ENNB1 (a) and BEA (b). The calibration curves in plasma using different mobile phase additives, 0.05% AA, 0.02% AA, 0.05% FA and 0.02% FA. Overlaid calibration curves were replotted using peak area to compare ionization trends.

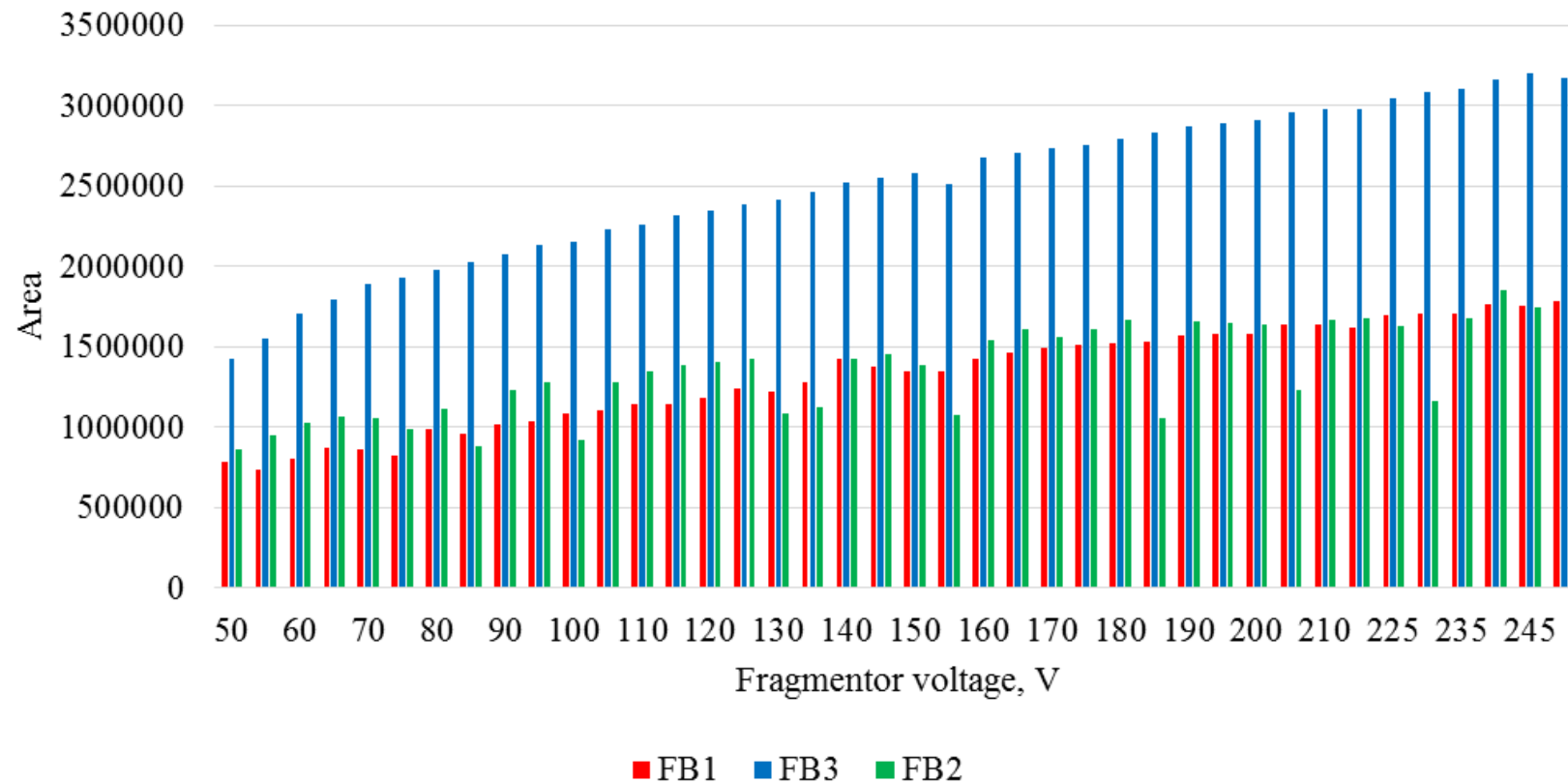


Supplementary Figure C8. Comparison of four calibration curves of ENNA1 (a) and ENNA (b). The calibration curves in plasma using different mobile phase additives, 0.05% AA, 0.02% AA, 0.05% FA and 0.02% FA. Overlaid calibration curves were replotted using peak area to compare ionization trends.

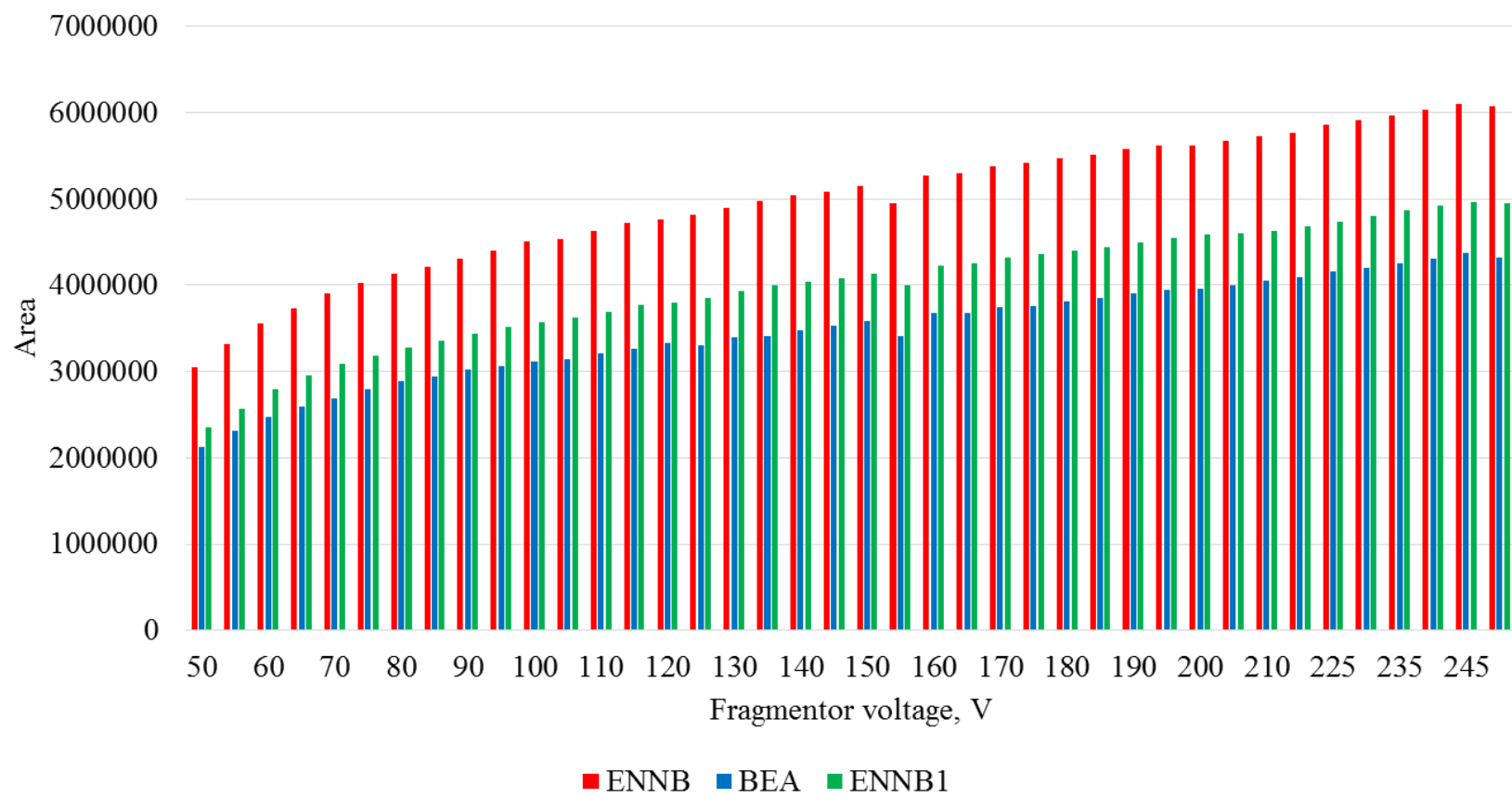


Supplementary Figure C9. Evaluation of Ota, CIT and OTA signal intensities at different fragmentor values (from 50 to 250 V). The results are shown for Ota, CIT and OTA 20 ng/mL mycotoxin standard (n=1) in 60% methanol with 1% FA.

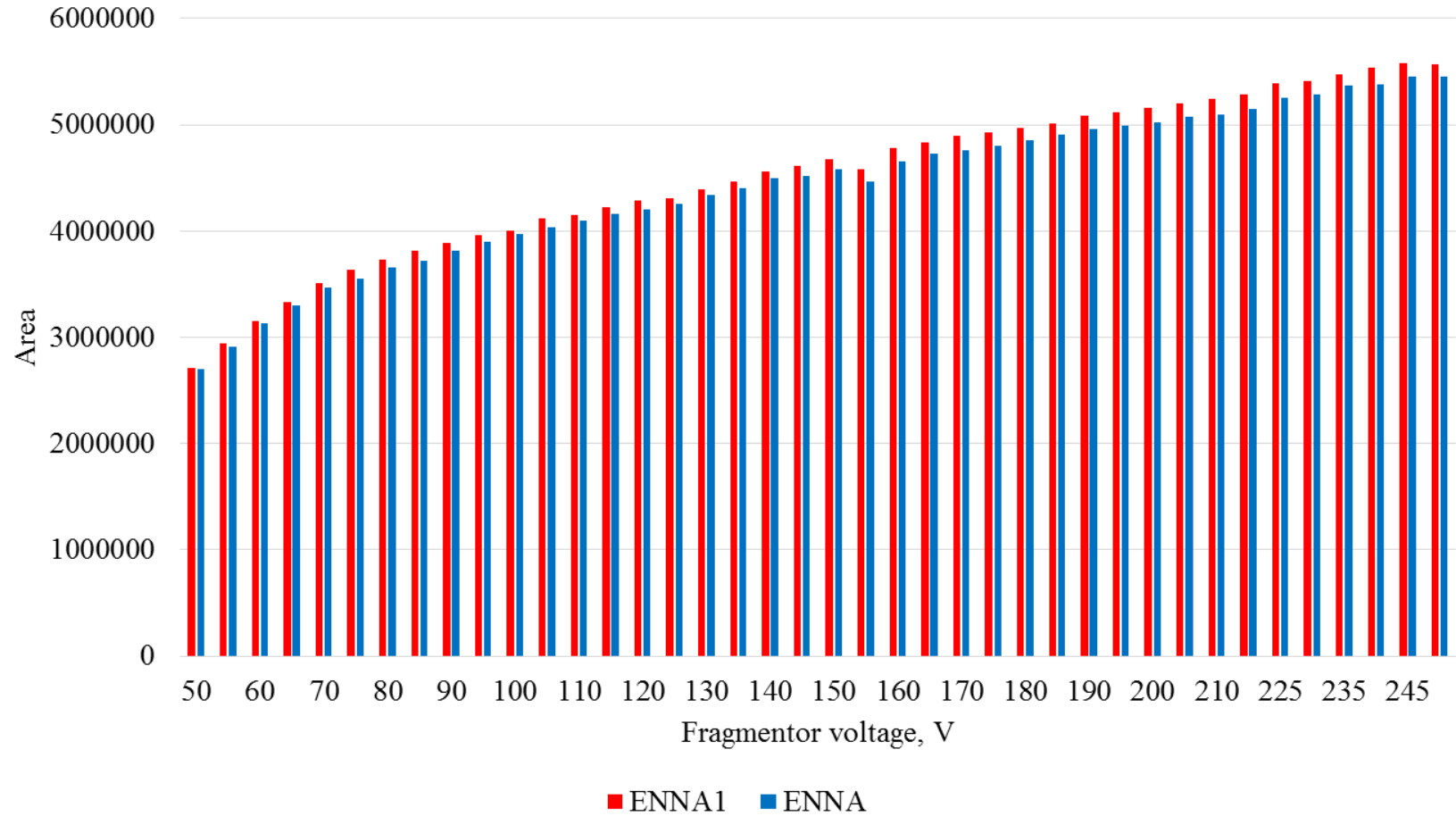




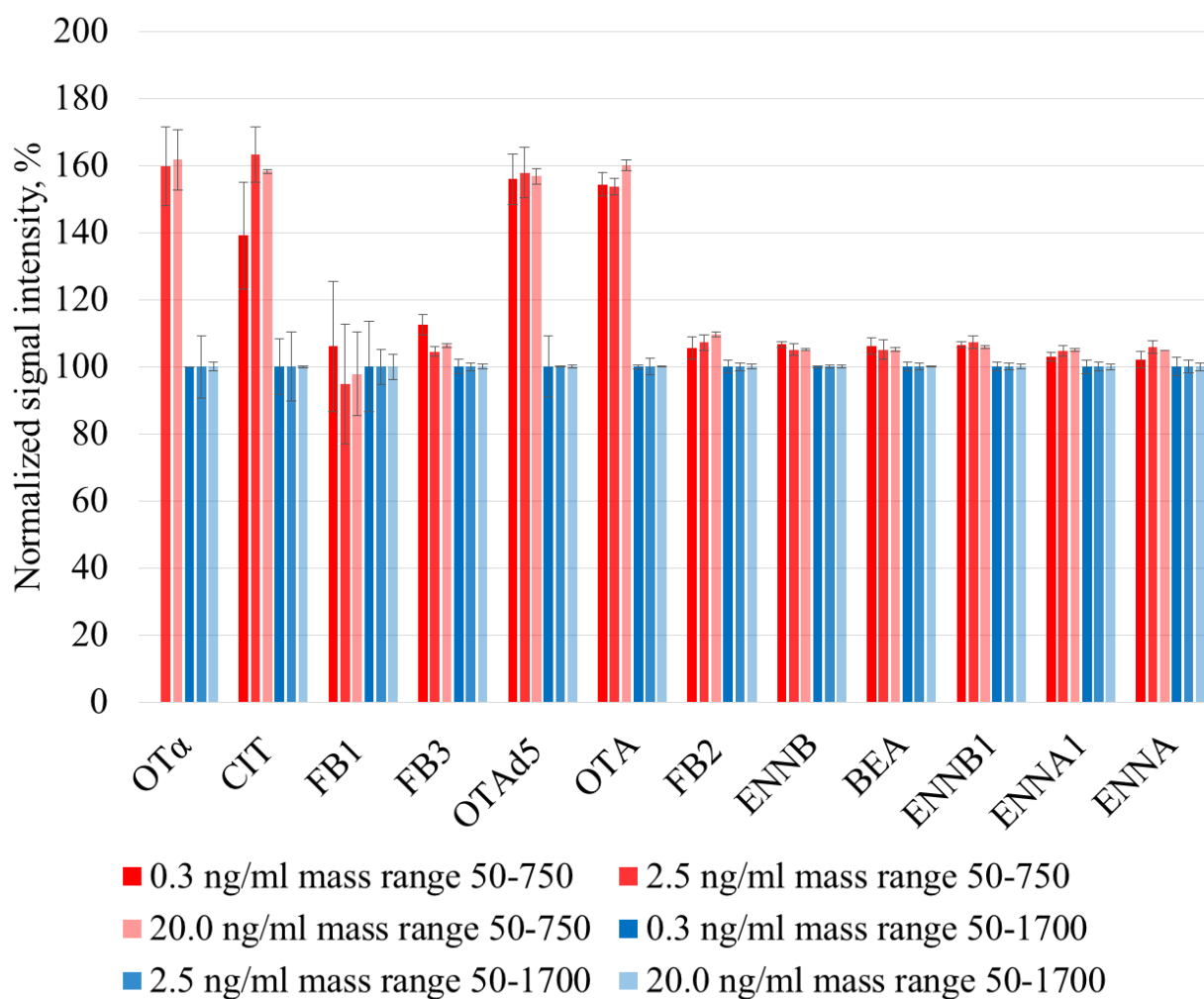
Supplementary Figure C10. Evaluation of FB1, FB2 and FB3 signal intensities at different fragmentor values (from 50 to 250 V). The results are shown for FB1, FB2 and FB3 20 ng/mL mycotoxin standard (n=1) in 60% methanol with 1% FA.



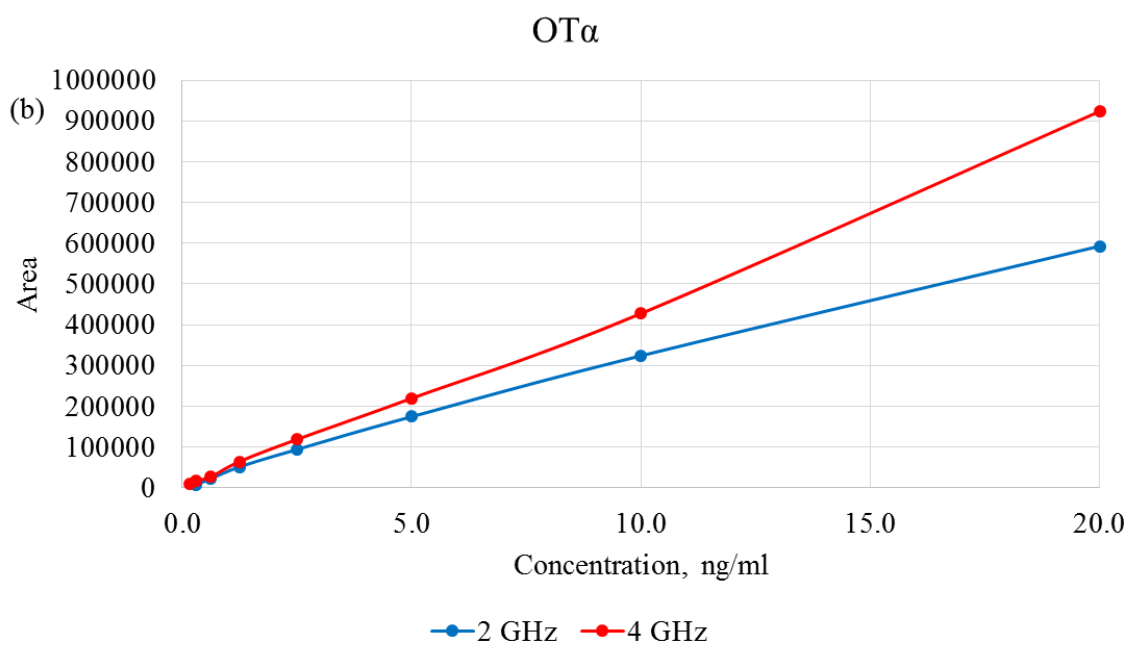
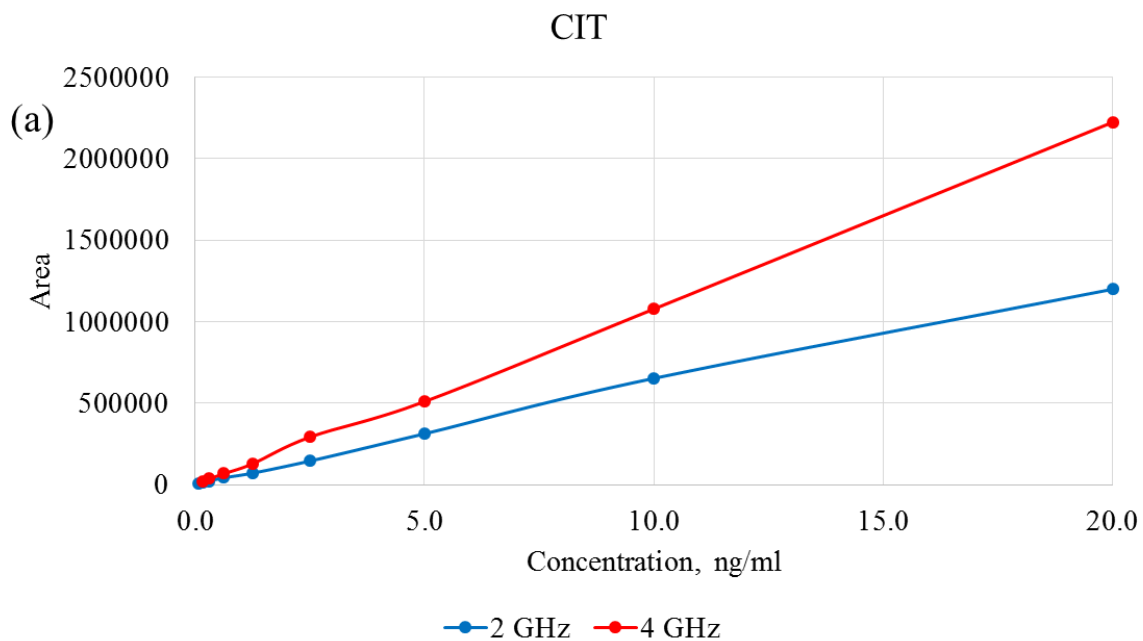
Supplementary Figure C11. Evaluation of ENNB, BEA and ENNB1 signal intensities at different fragmentor values (from 50 to 250 V). The results are shown for ENNB, BEA and ENNB1 20 ng/mL mycotoxin standard (n=1) in 60% methanol with 1% FA.



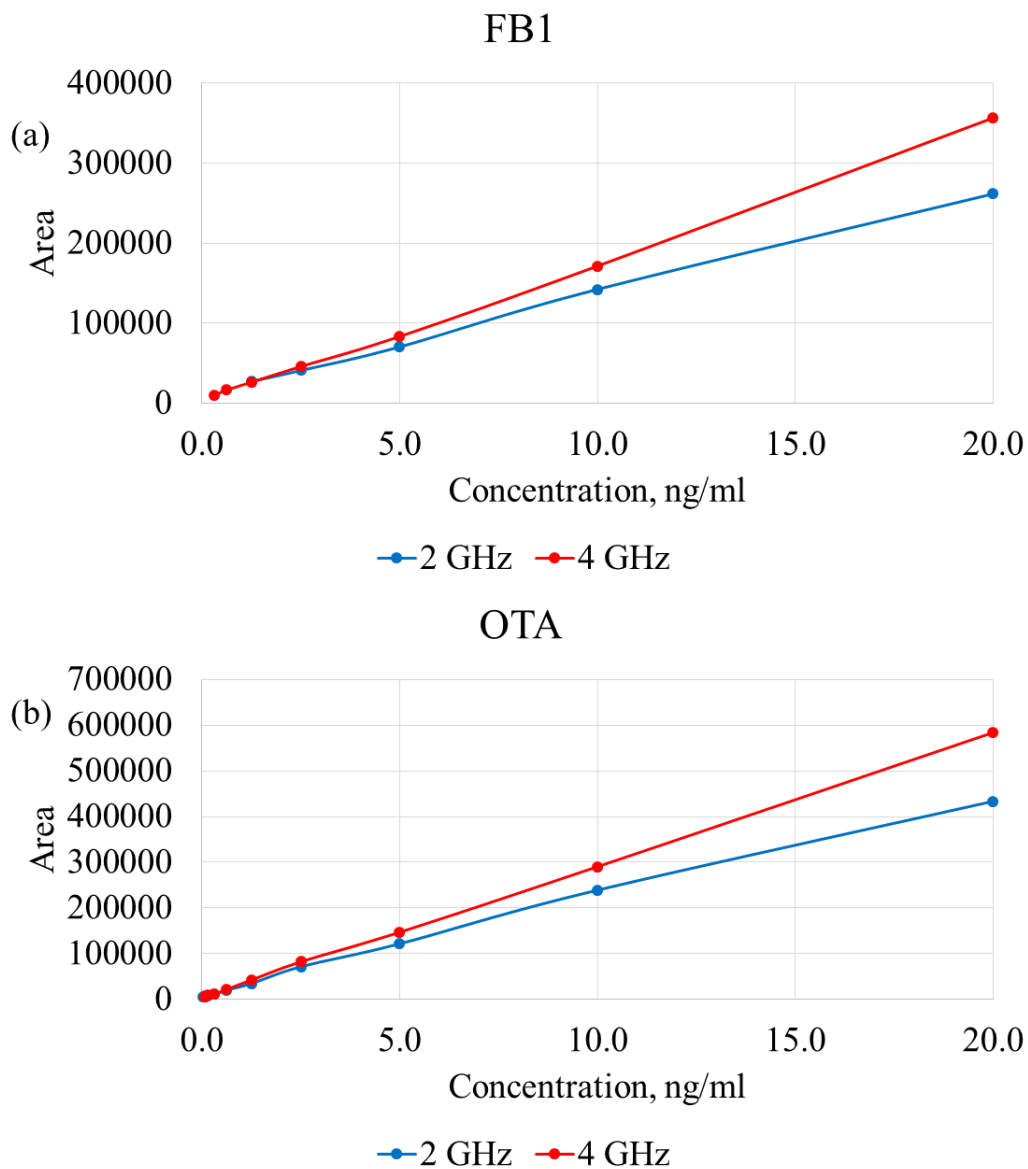
Supplementary Figure C12. Evaluation of ENNA1 and ENNA signal intensities at different fragmentor values (from 50 to 250 V). The results are shown for ENNA1, and ENNA 20 ng/mL mycotoxin standard (n=1) in 60% methanol with 1% FA.



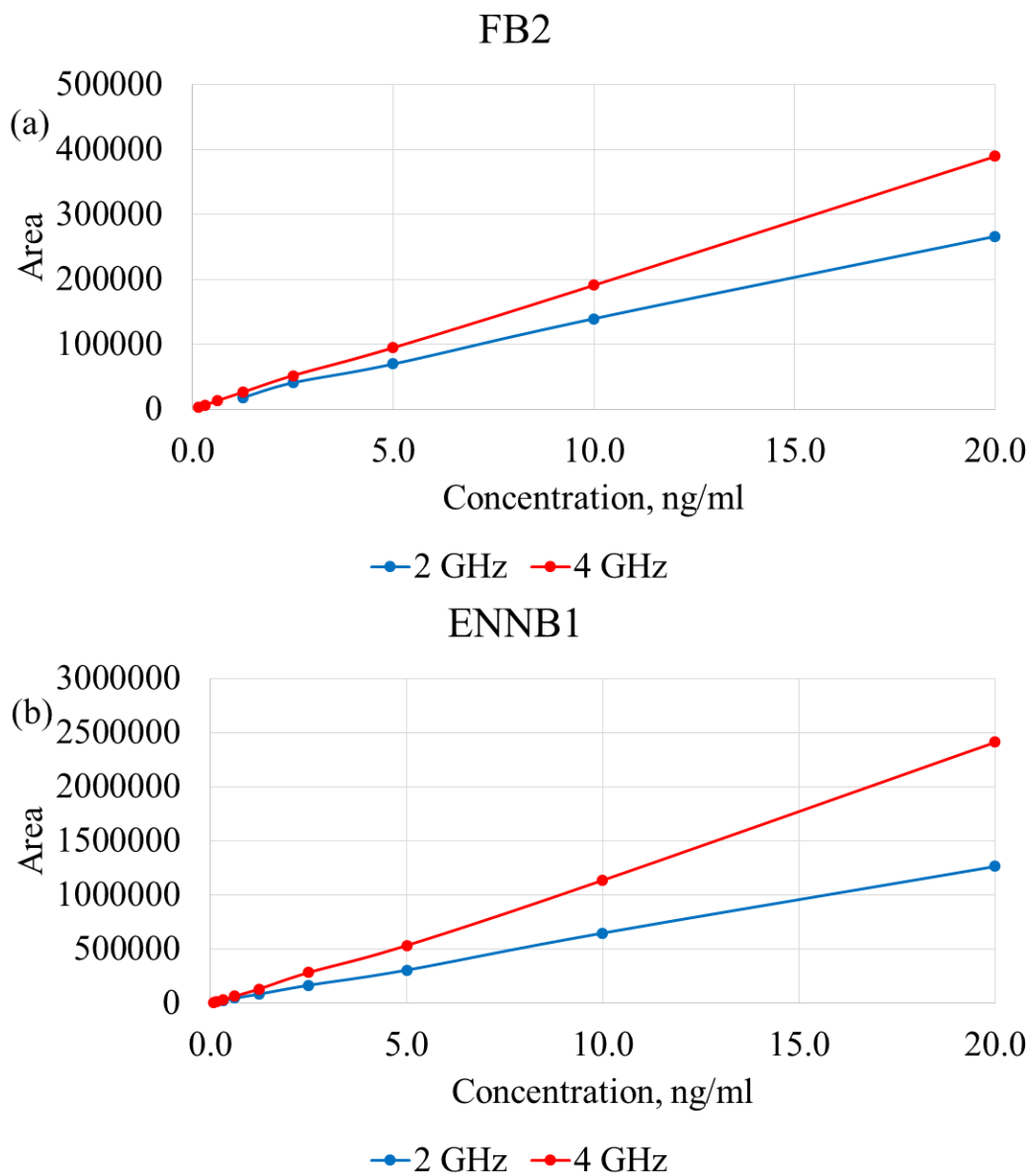
Supplementary Figure C13. Evaluation of signal intensities of mycotoxins at different calibration instrument mass ranges (50-1700 and 50-750  $m/z$ ). The signal intensities (expressed as peak area) of mycotoxins obtained with the calibration mass range of 50-750  $m/z$  were normalized to the signal intensity obtained with the calibration mass range of 50-1700  $m/z$ . The results are shown for three concentration levels in spiked plasma, 20 ng/mL, 2.5 ng/mL and 0.3 ng/mL ( $n=3$ ) for all mycotoxins, except for OT $\alpha$  (only 20 ng/mL and 2.5 ng/mL).



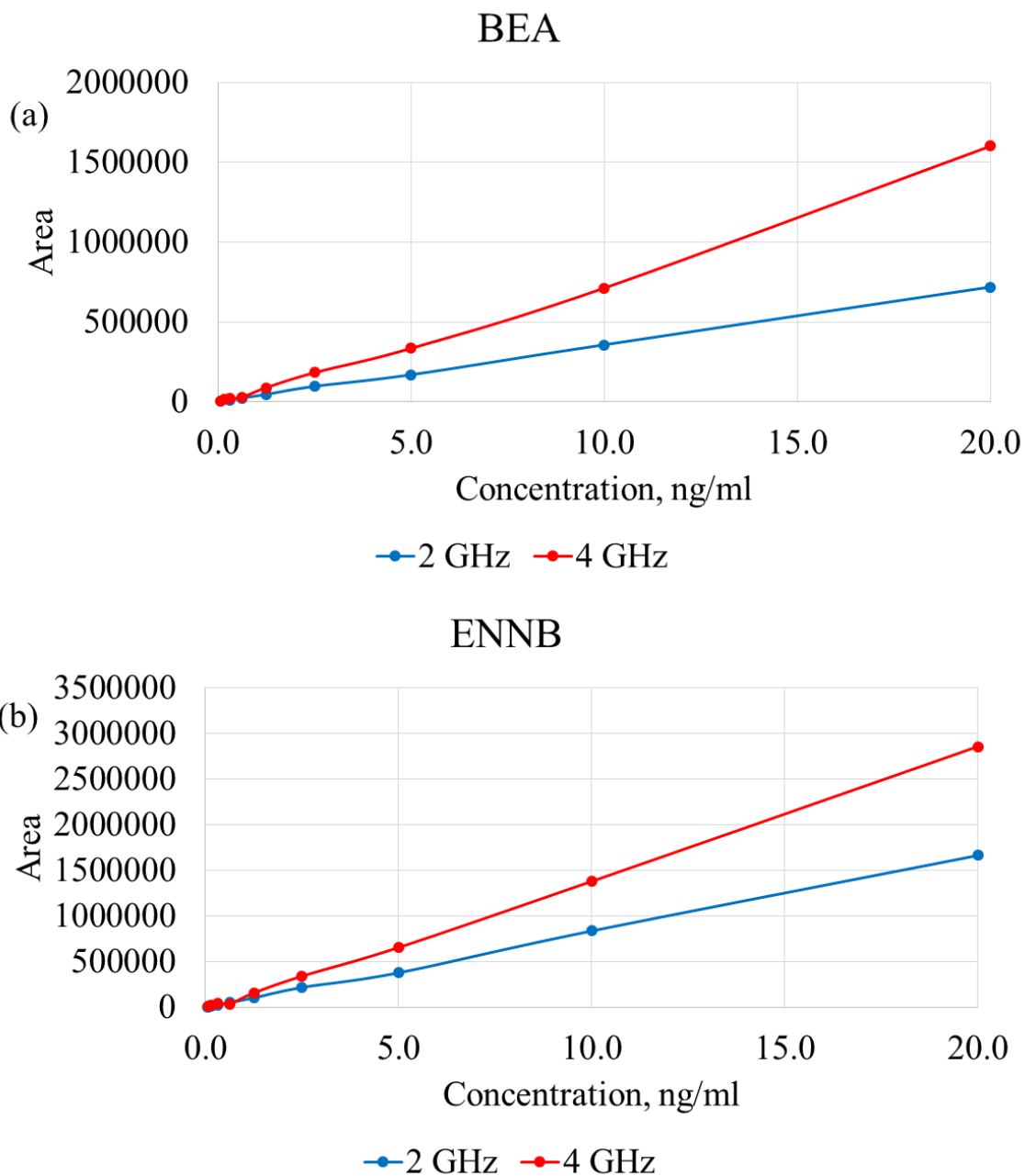
*Supplementary Figure C14. Comparison of two calibration curves of (a) CIT and (b) OT $\alpha$  in plasma using extended dynamic range mode (2 GHz) vs. high resolution mode (4 GHz). Overlaid calibration curves were replotted using peak area to see trends in signal intensity clearly.*



*Supplementary Figure C15. Comparison of two calibration curves of (a) FB1 and (b) OTA in plasma using extended dynamic range mode (2 GHz) vs. high resolution mode (4 GHz). Overlaid calibration curves were replotted using peak area to see trends in signal intensity clearly.*

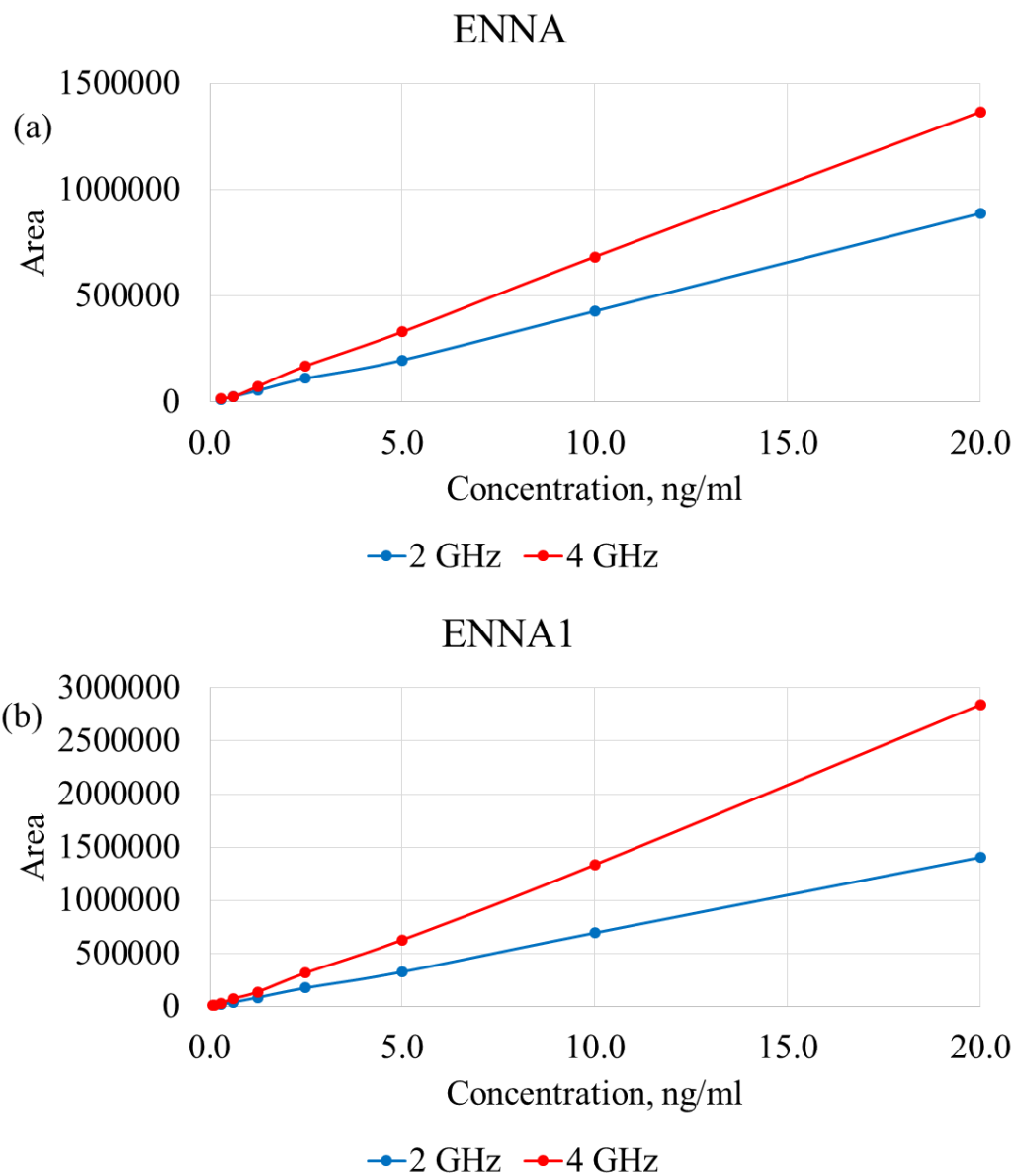


*Supplementary Figure C16. Comparison of two calibration curves of (a) FB2 and (b) ENNB1 in plasma using extended dynamic range mode (2 GHz) vs. high resolution mode (4 GHz). Overlaid calibration curves were replotted using peak area to see trends in signal intensity clearly.*

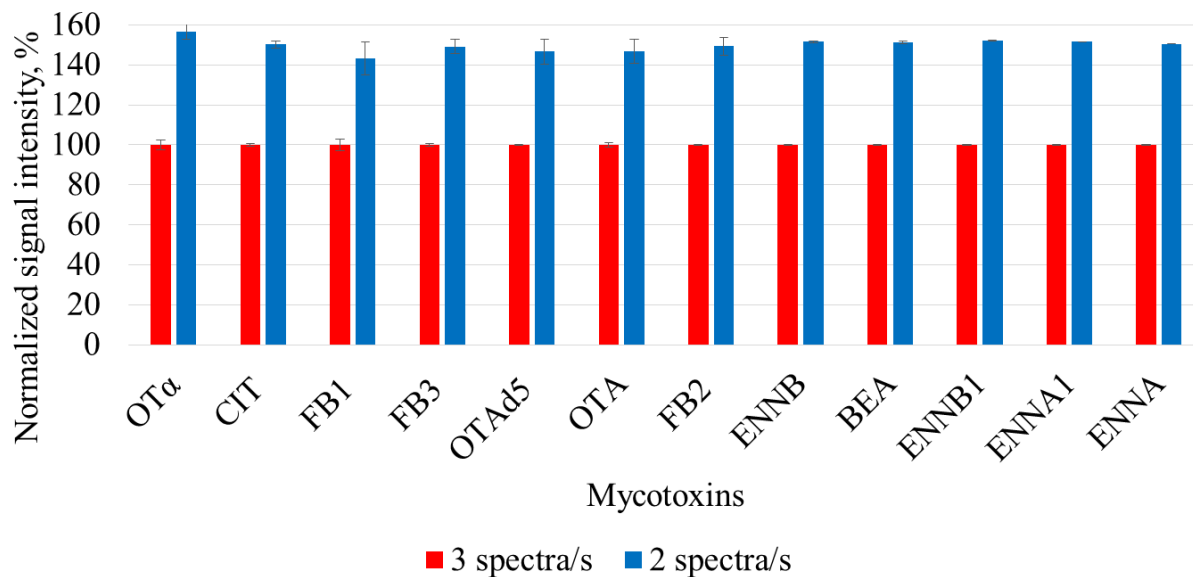


*Supplementary Figure C17. Comparison of two calibration curves of (a) BEA and (b) ENNB in plasma using extended dynamic range mode (2 GHz) vs. high resolution mode (4 GHz). Overlaid calibration curves were replotted using peak area to see trends in signal intensity clearly.*

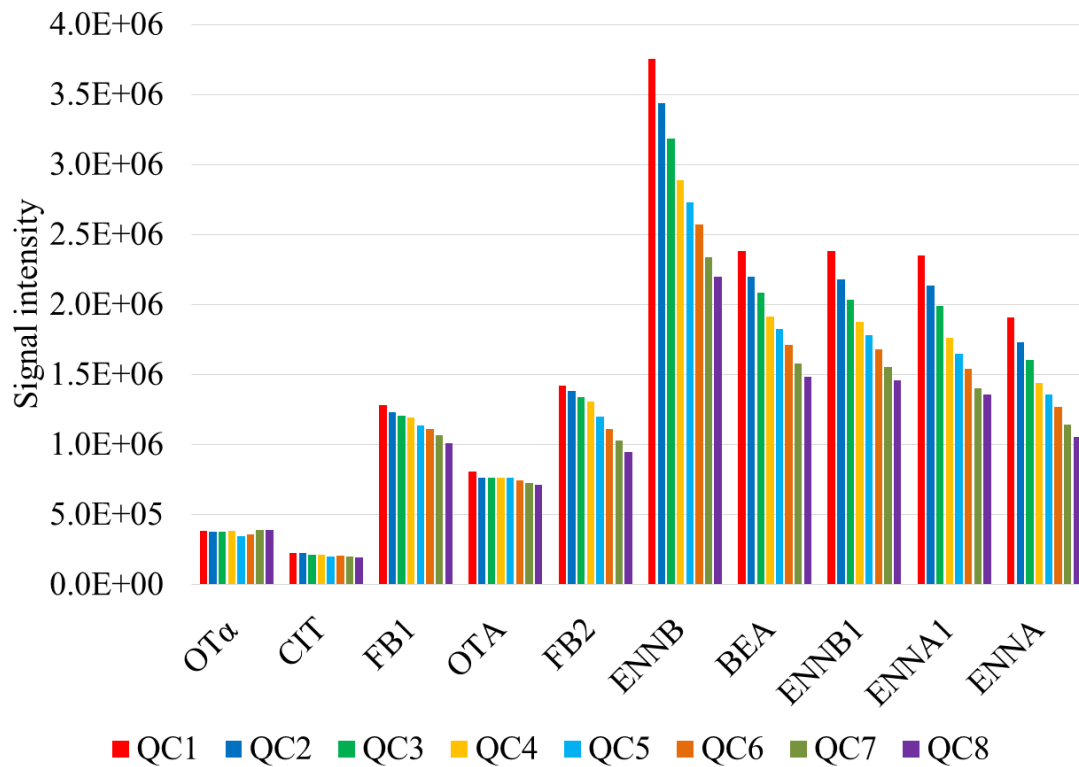




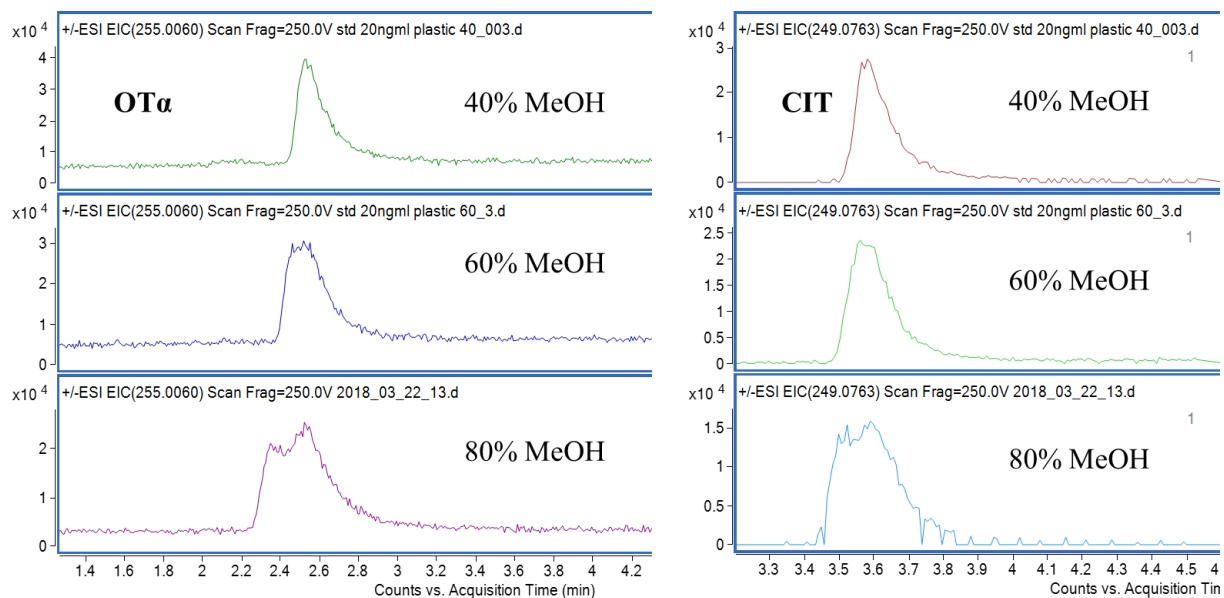
Supplementary Figure C18. Comparison of two calibration curves of (a) ENNA and (b) ENNA1 in plasma using extended dynamic range mode (2 GHz) vs. high resolution mode (4 GHz). Overlaid calibration curves were replotted using peak area to see trends in signal intensity clearly.



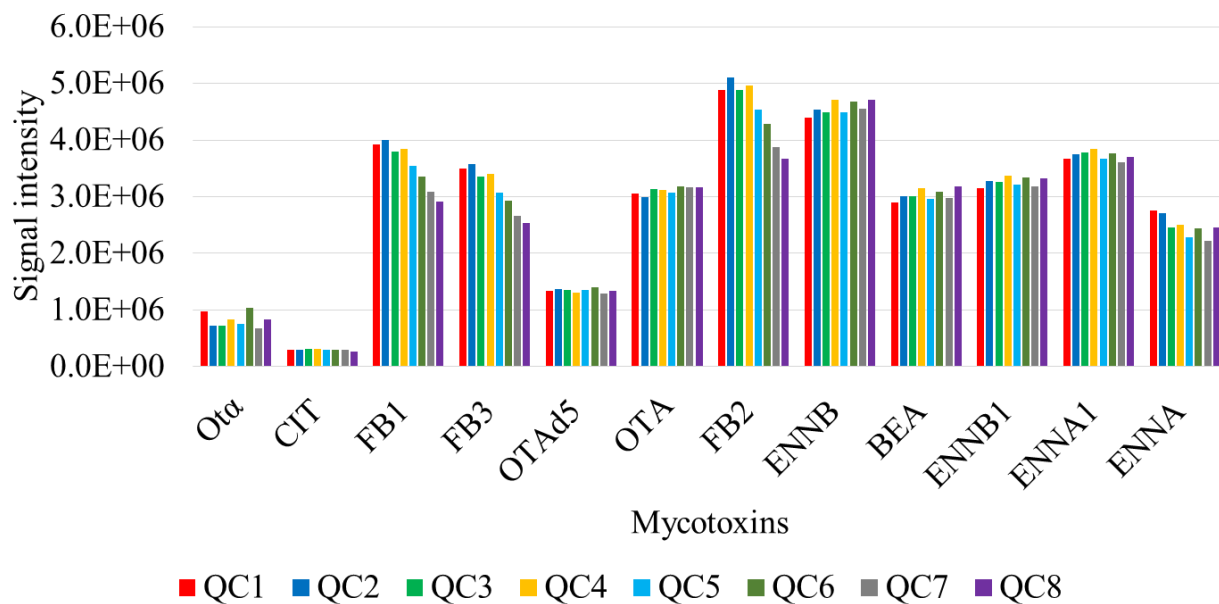
*Supplementary Figure C19. Evaluation of signal intensities of mycotoxins using different acquisition rate time, 3 and 2 spectra per second. The signal intensities (expressed as peak area) of mycotoxins obtained with 2 spectra per second were normalized to the signal intensity obtained with 3 spectra per second. The results are shown for the standard mycotoxin mixture solution of 20 ng/mL concentration.*



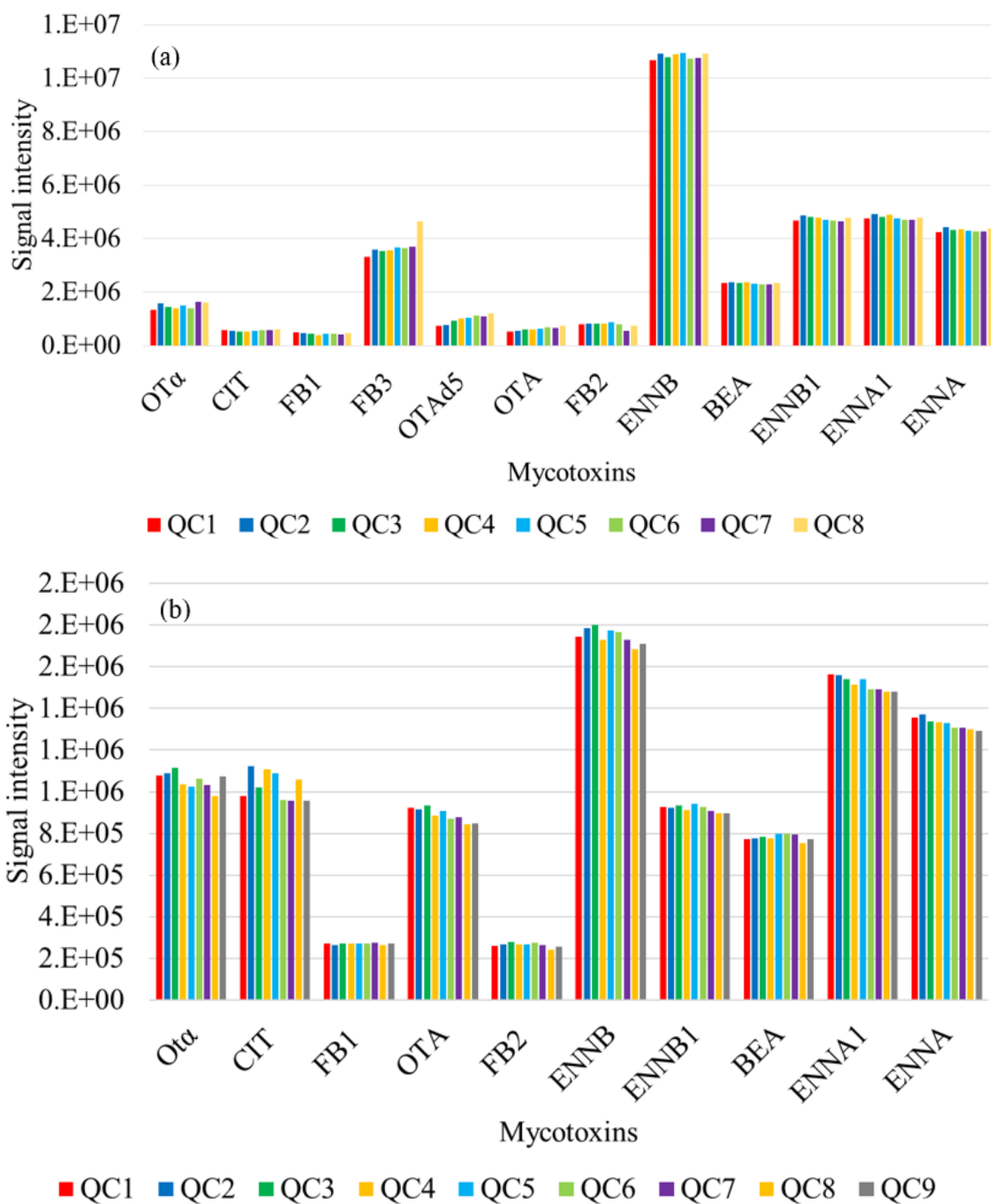
Supplementary Figure C20. Evaluation of signal stability during the analytical run. QC stands for quality control samples, 20 ng/ml mycotoxin standard in 40% methanol transferred into plastic inserts. The time elapsed between injections QC1 to QC8 was 13.4 hours.



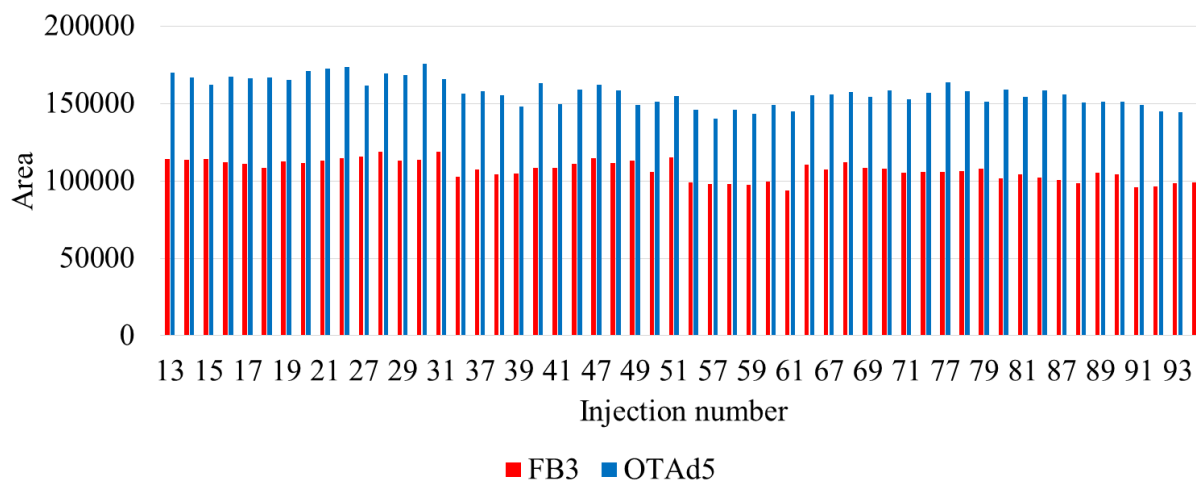
*Supplementary Figure C21. Comparison of peak shapes of OTα and CIT in different solvents, 40%, 60% and 80% methanol. Results obtained using standard solution prepared at 20 ng/ml.*



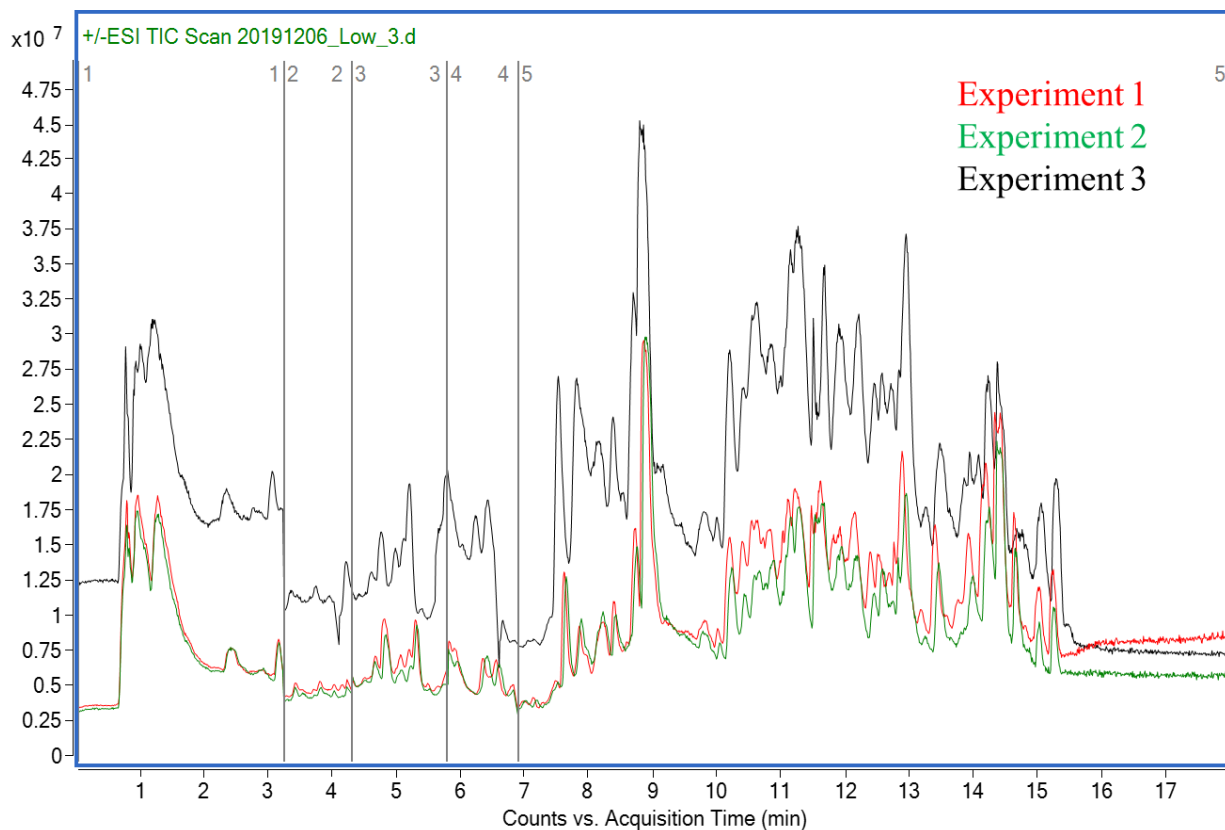
Supplementary Figure C22. Evaluation of signal stability during the analytical run. QC stands for quality control samples, 20 ng/ml mycotoxin standard in 60% methanol. The time elapsed between injections QC1 to QC8 was 15.0 hours.



Supplementary Figure C23. Evaluation of signal stability during the analytical run. QC stands for quality control samples. The results are shown for QC samples that represent the standard mycotoxin mixture solution of 20 ng/ml (a) and 4 ng/ml (b) concentrations in 60% methanol with 1% FA. The time elapsed between injections injection QC1 to QC8 elapsed 6 hours for (a) QC1 to QC9 elapsed time 28 hours for (b).

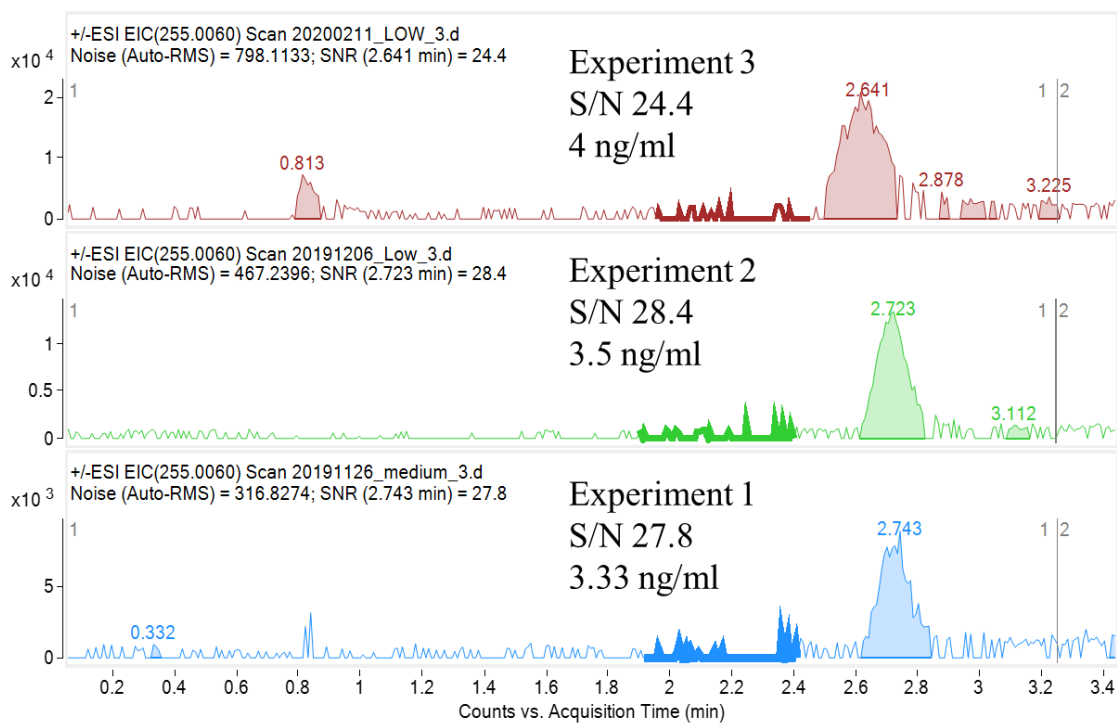


*Supplementary Figure C24. Internal standard areas of FB3 and OTAd5 over long analytical run. Results are for experiment 1, including the matrix-matched calibration curve and validation samples.*

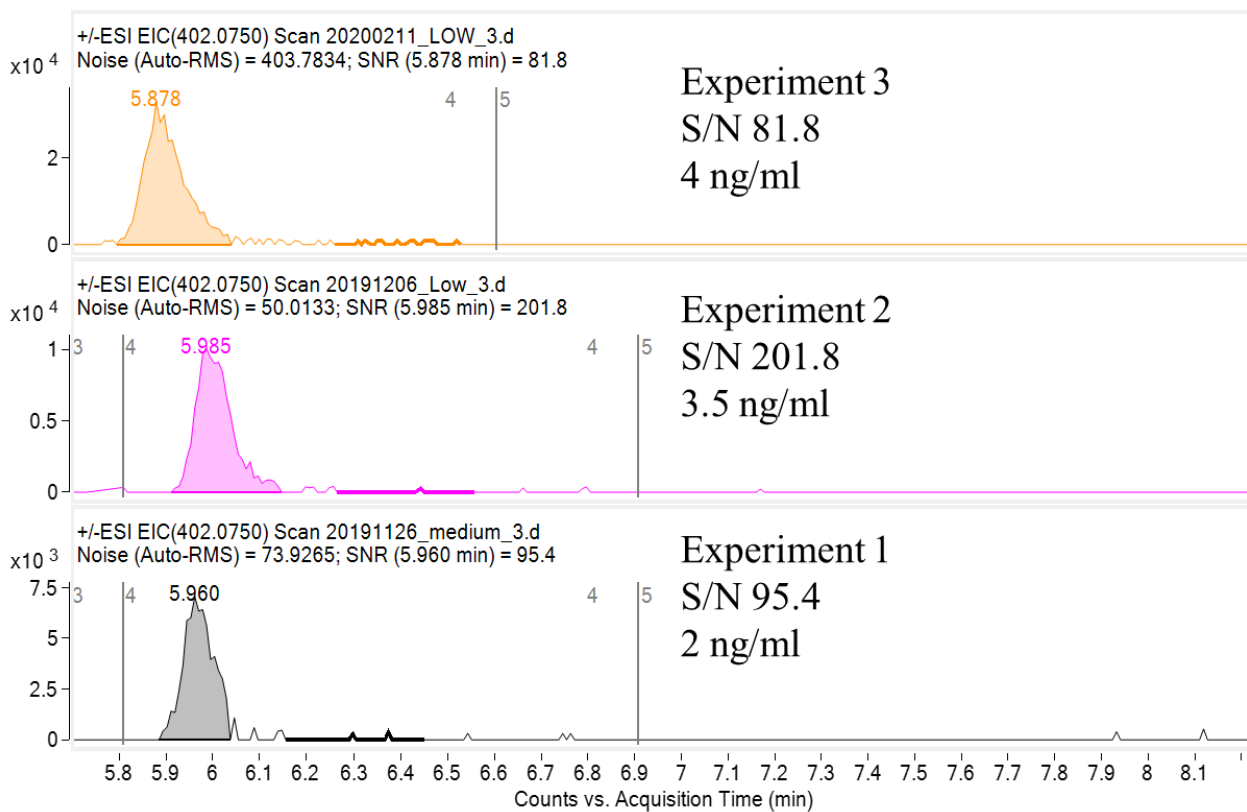


*Supplementary Figure C25. TICs of validation samples. Experiment 1 (red, mycotoxin concentrations from 2 ng/ml to 3.33 ng/ml, experiment 2 (green, mycotoxin concentrations 3.5 ng/ml), and experiment 3 (black, mycotoxin concentrations 4 ng/ml).*

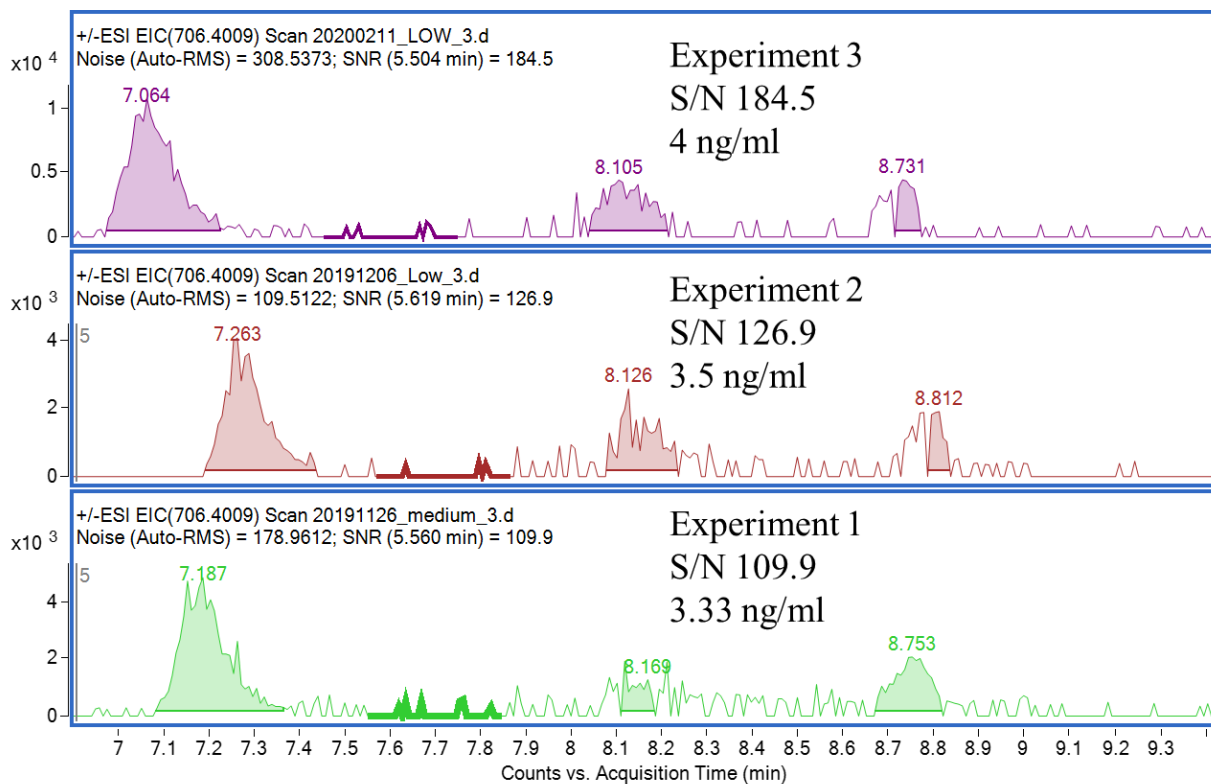




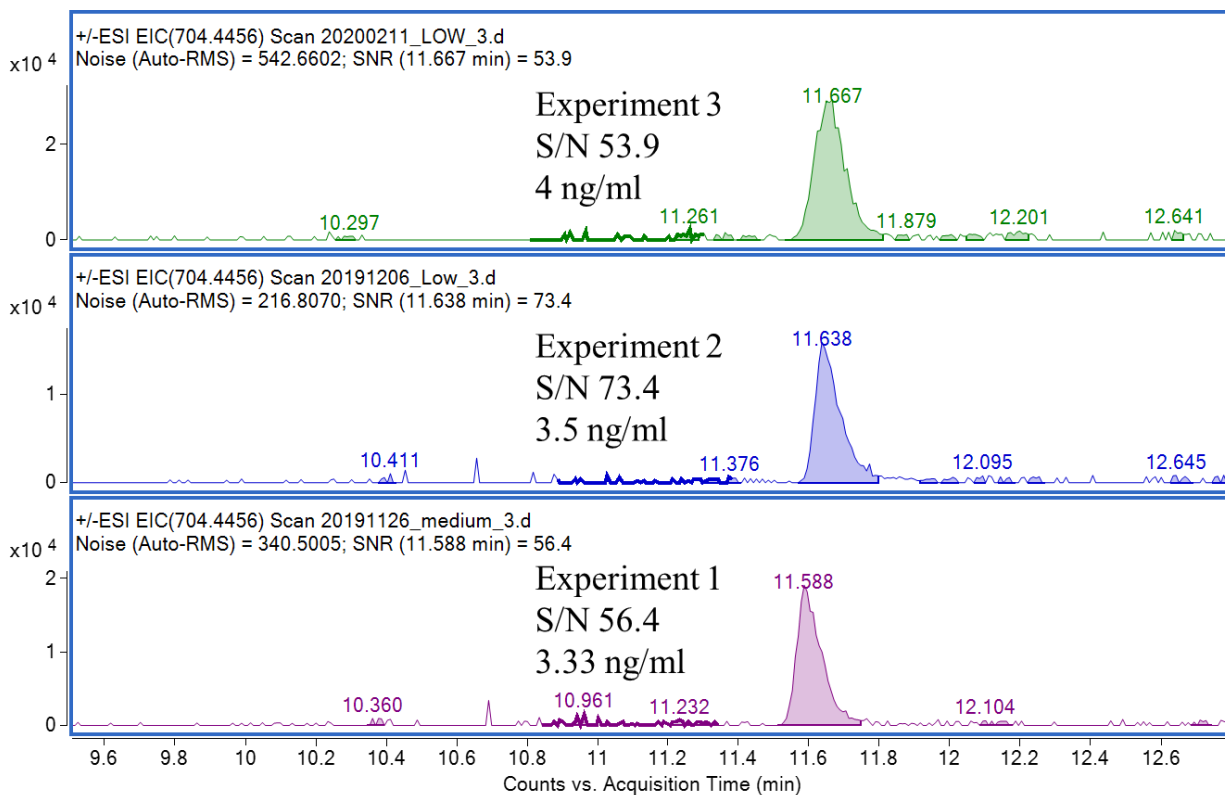
*Supplementary Figure C26. Extracted ion chromatogram of OT $\alpha$  and S/N determination. A bold segment on EICs in experiment 1, 2 and 3 shows the region for the determination of noise.*



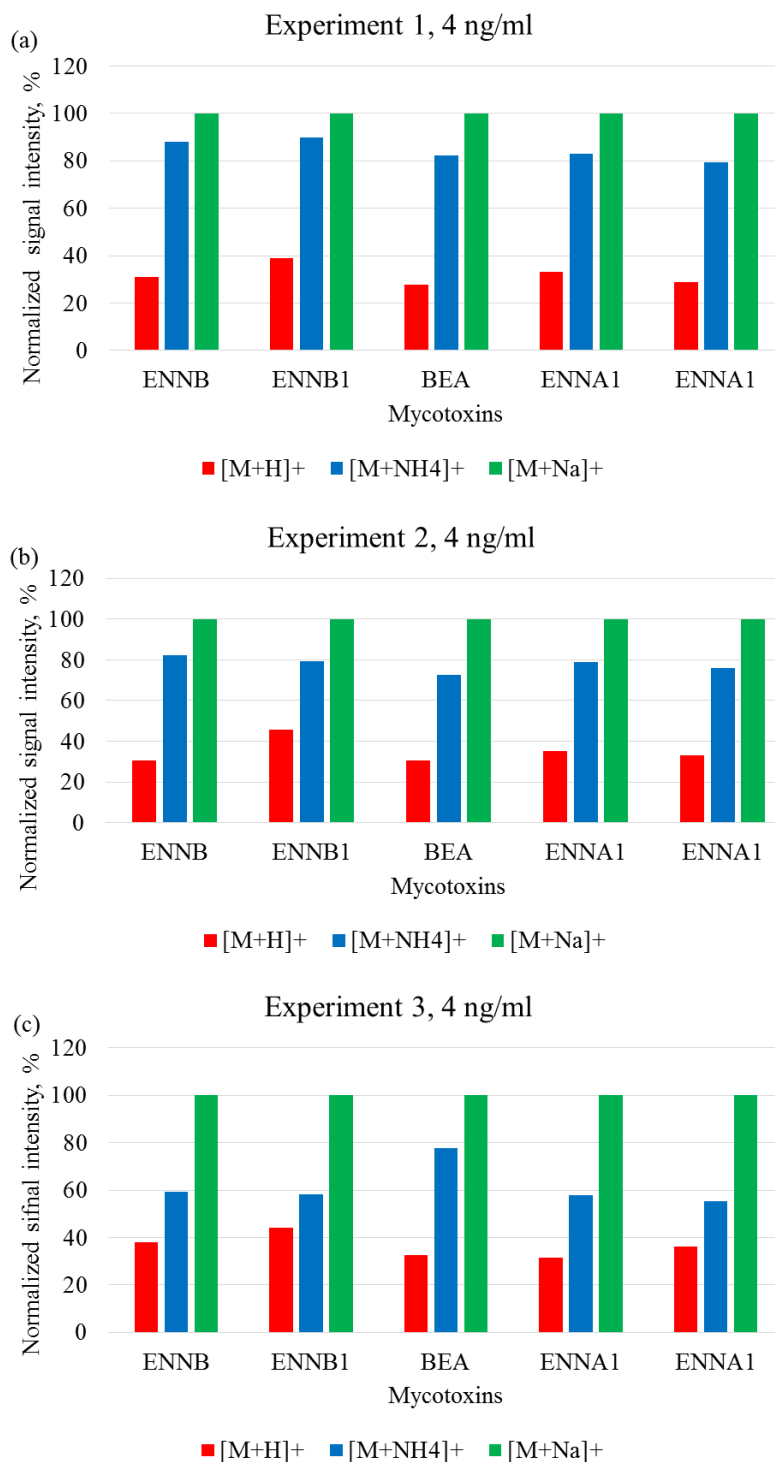
*Supplementary Figure C27. Extracted ion chromatogram of OTA and S/N determination. A bold segment on EICs in experiment 1, 2 and 3 shows the region for the determination of noise.*



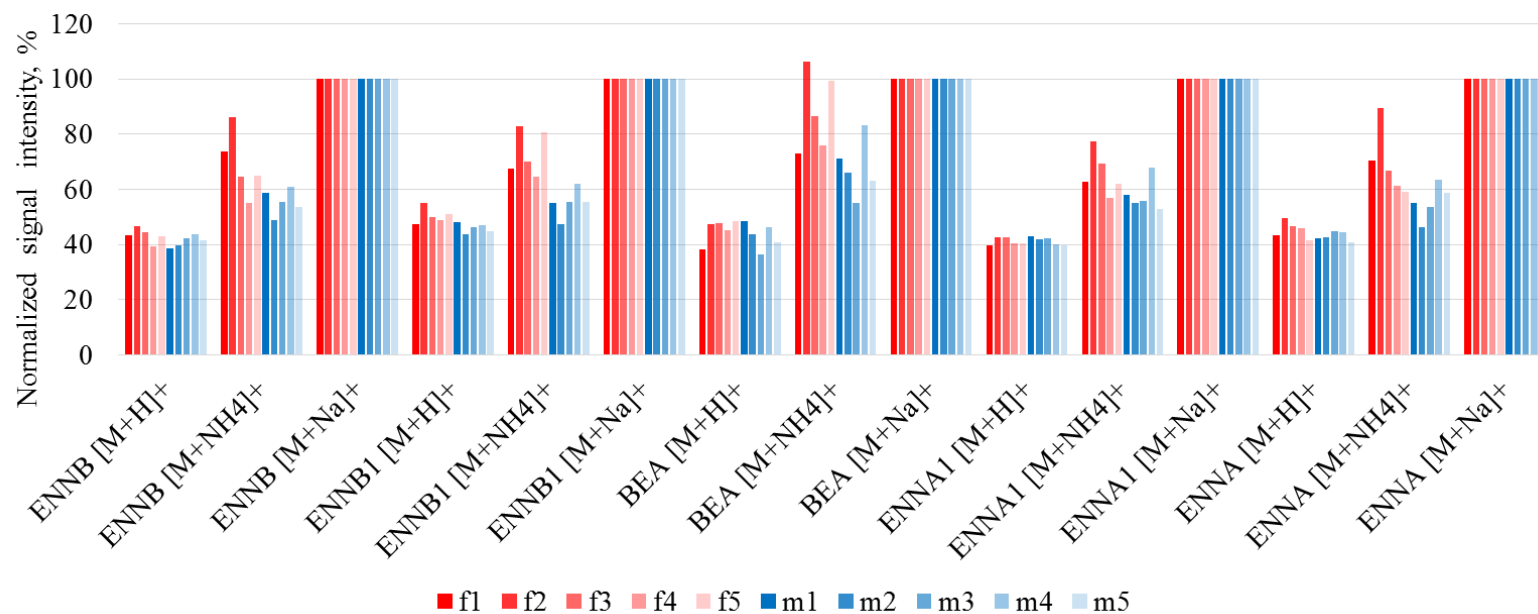
Supplementary Figure C28. Extracted ion chromatogram of FB2 and S/N determination. A bold segment on EICs in experiment 1, 2 and 3 shows the region for the determination of noise, S/N is determined for peak at 7.1 min.



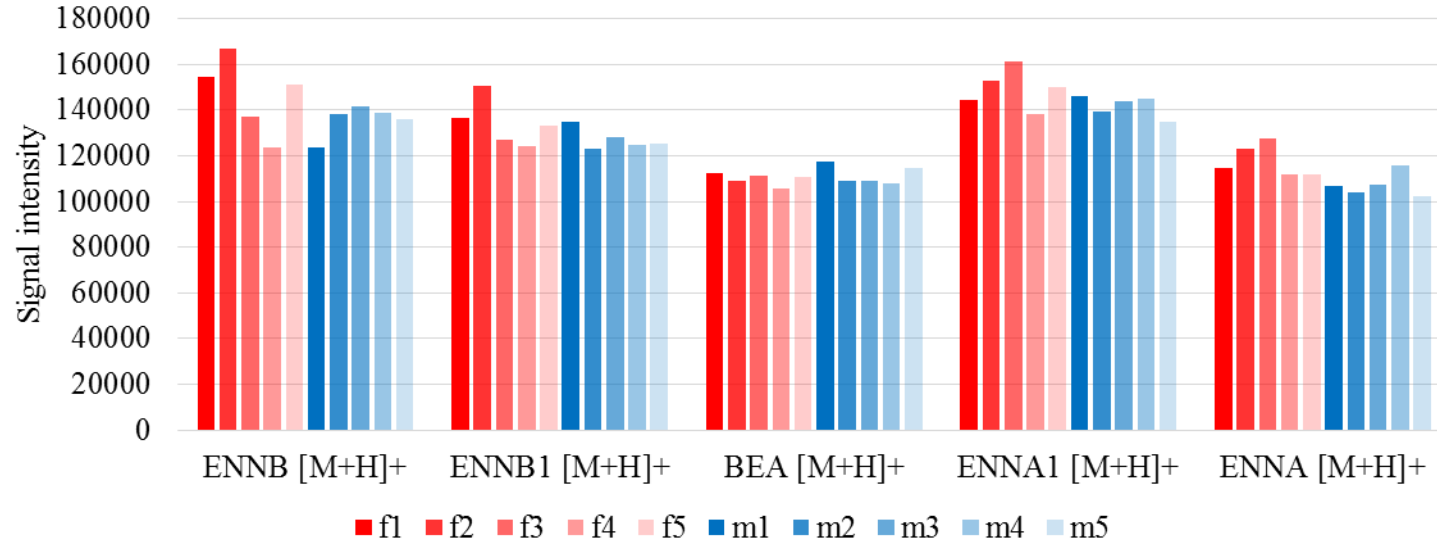
Supplementary Figure C29. Extracted ion chromatogram of ENNA and S/N determination. A bold segment on EICs in experiment 1, 2 and 3 shows the region for the determination of noise.



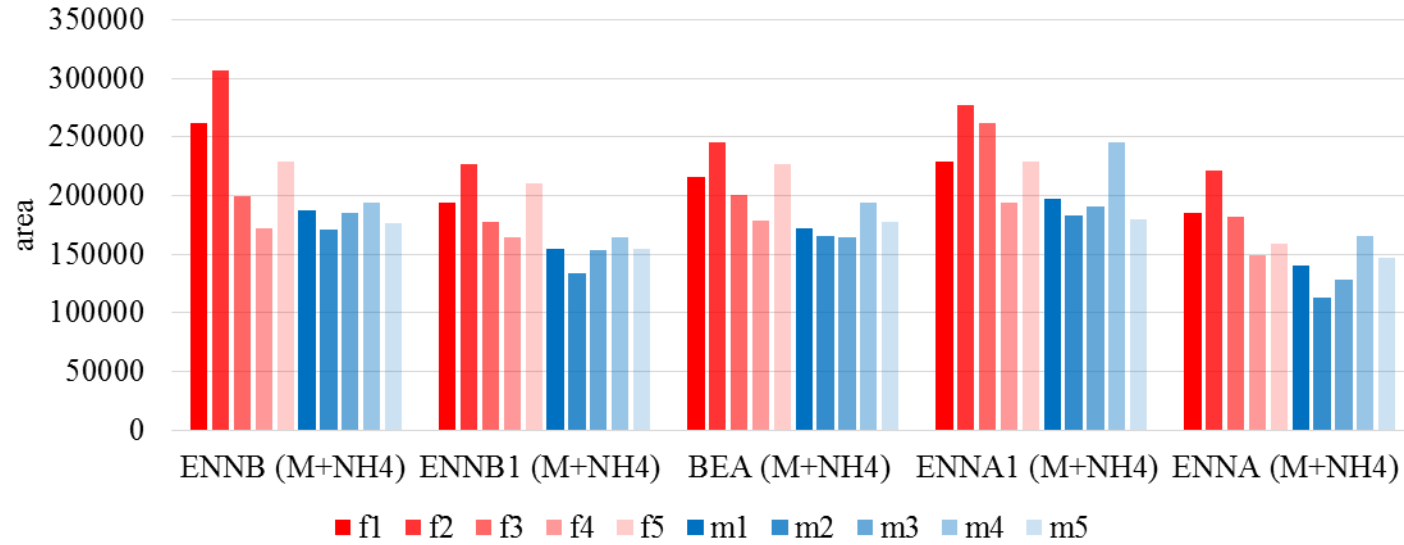
Supplementary Figure C30. Ionization patterns of emerging mycotoxins are shown for (a) experiment 1, (b) experiment 2 and (c) experiment 3. The signal intensities (expressed as peak area) of protonated and ammonium ions were normalized to the signal intensities obtained using sodium ions. Results were shown for 4 ng/ml standard solution mixture.



*Supplementary Figure C31. Ionization patterns of emerging mycotoxins are shown for 10 individual lots of plasma. The signal intensities (expressed as peak area) of protonated and ammonium ions were normalized to the signal intensities obtained using sodium ions. Results are shown for post-spiked plasma samples, 1.4 ng/ml concentration.*

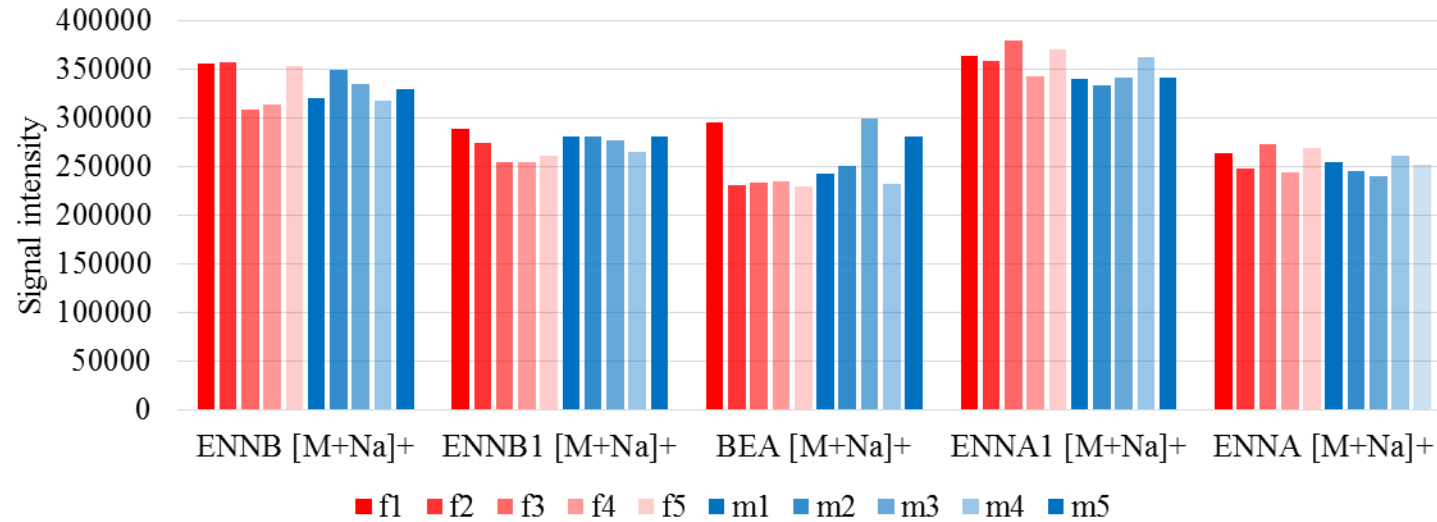


Supplementary Figure C32. Signal intensities (expressed as peak area) of the protonated ions of emerging mycotoxins are shown for 10 individual lots of plasma. Results are shown for post-spiked plasma samples, 1.4 ng/ml concentration.

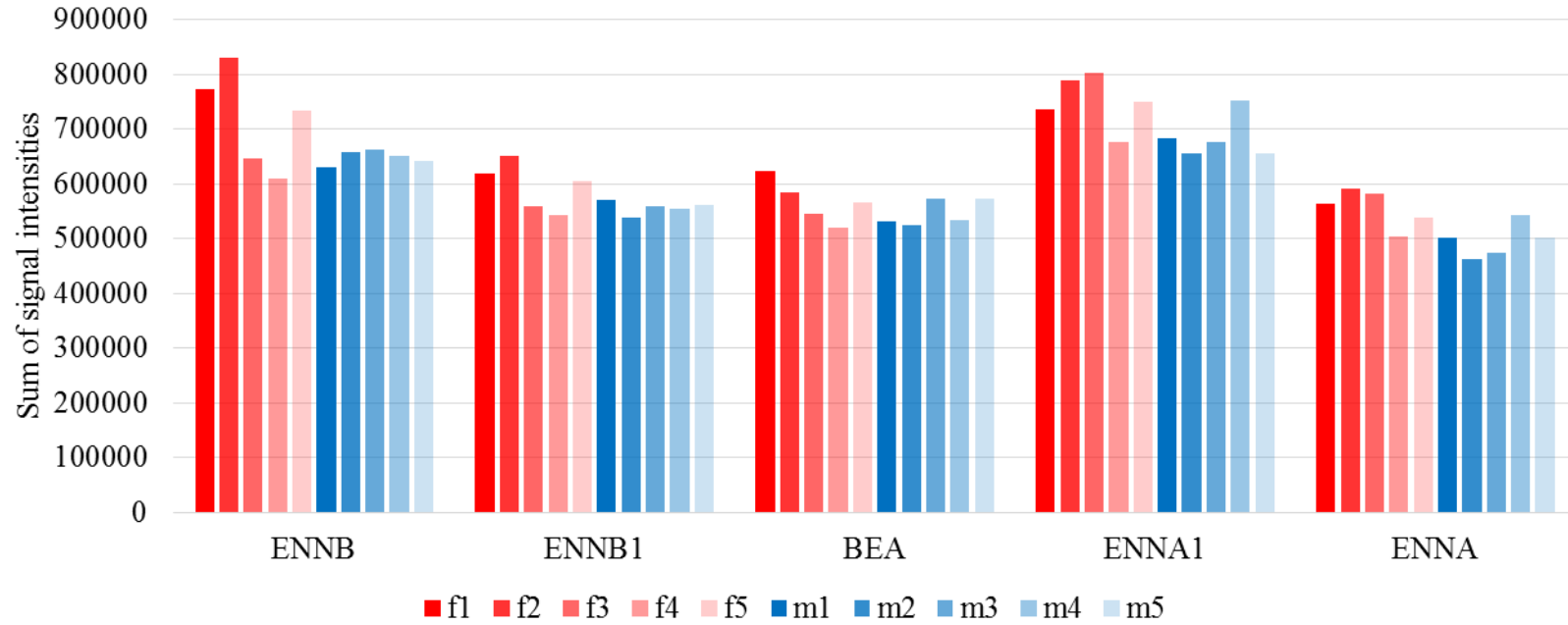


*Supplementary Figure C33. Signal intensities (expressed as peak area) of the ammonium ions of emerging mycotoxins are shown for 10 individual lots of plasma. Results are shown for post-spiked plasma samples, 1.4 ng/ml concentration.*





Supplementary Figure C34. Signal intensities (expressed as peak area) of the sodium ions of emerging mycotoxins are shown for 10 individual lots of plasma. Results are shown for post-spiked plasma samples, 1.4 ng/ml concentration.



*Supplementary Figure C35. Sum of signal intensities (expressed as peak area) of the protonated, ammonium ions and sodium ions of emerging mycotoxins. Results are shown for 10 individual lots of plasma. Results are shown for post-spiked plasma samples, 1.4 ng/ml concentration.*